

Enteral feeding interventions for optimal fetal and neonatal health

Citation for published version (APA):

de Lange, I. H. (2022). *Enteral feeding interventions for optimal fetal and neonatal health: towards novel preventive strategies for necrotizing enterocolitis*. [Doctoral Thesis, Maastricht University]. Ridderprint. <https://doi.org/10.26481/dis.20220419il>

Document status and date:

Published: 01/01/2022

DOI:

[10.26481/dis.20220419il](https://doi.org/10.26481/dis.20220419il)

Document Version:

Publisher's PDF, also known as Version of record

Please check the document version of this publication:

- A submitted manuscript is the version of the article upon submission and before peer-review. There can be important differences between the submitted version and the official published version of record. People interested in the research are advised to contact the author for the final version of the publication, or visit the DOI to the publisher's website.
- The final author version and the galley proof are versions of the publication after peer review.
- The final published version features the final layout of the paper including the volume, issue and page numbers.

[Link to publication](#)

General rights

Copyright and moral rights for the publications made accessible in the public portal are retained by the authors and/or other copyright owners and it is a condition of accessing publications that users recognise and abide by the legal requirements associated with these rights.

- Users may download and print one copy of any publication from the public portal for the purpose of private study or research.
- You may not further distribute the material or use it for any profit-making activity or commercial gain
- You may freely distribute the URL identifying the publication in the public portal.

If the publication is distributed under the terms of Article 25fa of the Dutch Copyright Act, indicated by the "Taverne" license above, please follow below link for the End User Agreement:

www.umlib.nl/taverne-license

Take down policy

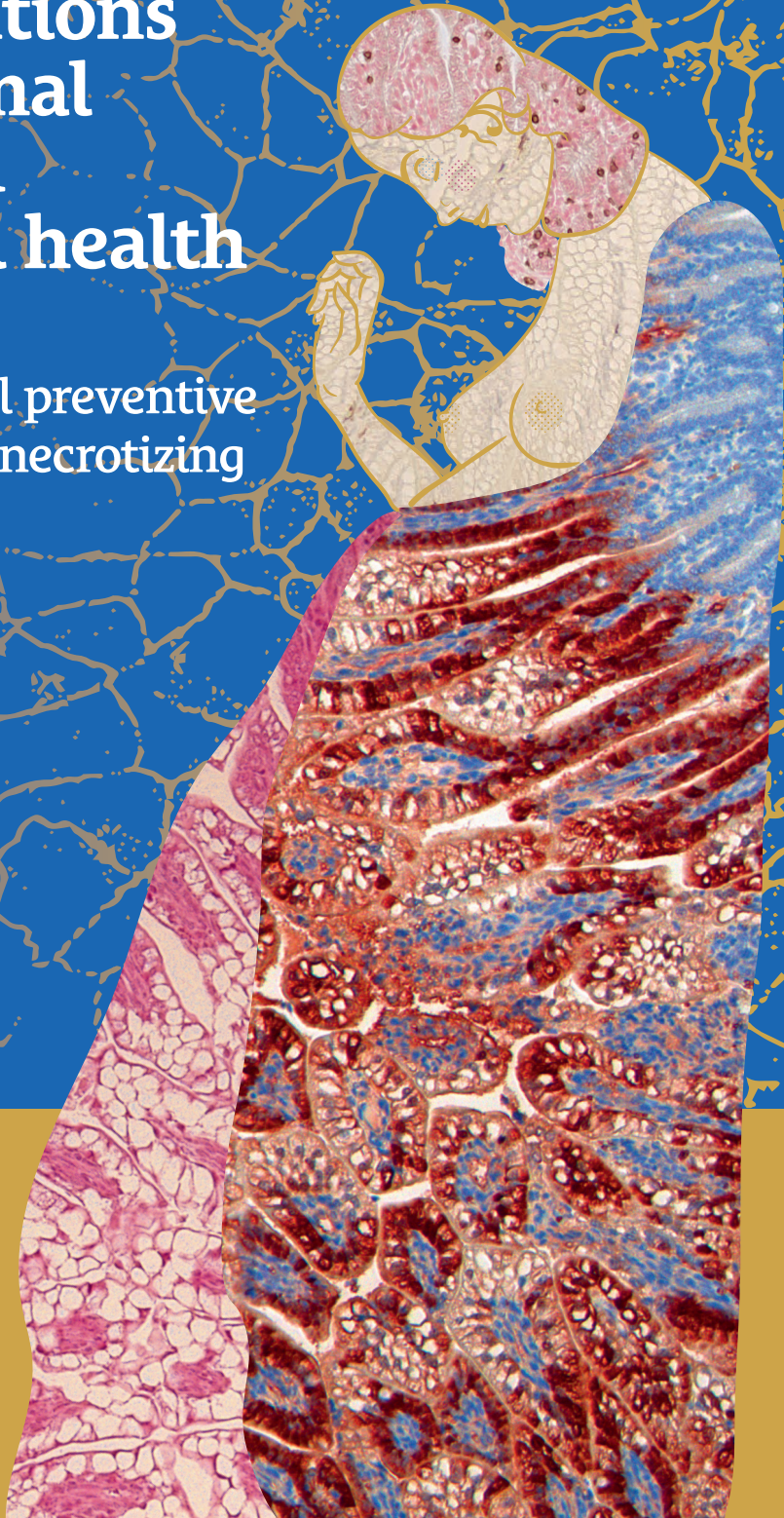
If you believe that this document breaches copyright please contact us at:

repository@maastrichtuniversity.nl

providing details and we will investigate your claim.

Enteral feeding interventions for optimal fetal and neonatal health

Towards novel preventive strategies for necrotizing enterocolitis



Ilse H. de Lange

**Enteral feeding interventions
for optimal fetal and neonatal health**

Towards novel preventive strategies for necrotizing enterocolitis

Copyright © Ilse H. de Lange, Maastricht 2022

All rights reserved. No part of this thesis may be reproduced or distributed in any form or by any means, without the prior written permission of the author or the publisher.

Layout: Tiny Wouters

Cover design: Peter van Drongelen | www.grafischenvoornix.nl

Printing: Ridderprint | www.ridderprint.nl

ISBN: 978-94-6458-173-7

Enteral feeding interventions for optimal fetal and neonatal health

Towards novel preventive strategies for necrotizing enterocolitis

PROEFSCHRIFT

ter verkrijging van
de graad van doctor aan de Universiteit Maastricht,
op gezag van de Rector Magnificus, prof. dr. Pamela Habibović,
volgens het besluit van het College van Decanen,
in het openbaar te verdedigen
op dinsdag 19 april 2022 om 10.00 uur

door

Ilse Hilligje de Lange

Promotores

Dr. T.G.A.M. Wolfs

Prof. dr. W.G. van Gemert

Copromotor

Dr. J.P.M. Derikx, Amsterdam Universitair Medisch Centrum

Beoordelingscommissie

Prof. dr. G.J.A. Driessen (voorzitter)

Prof. dr. D.M.A.E. Jonkers

Prof. dr. T. Plösch, Rijksuniversiteit Groningen

Prof. dr. A.M.W.J. Schols

Prof. dr. D. Tibboel, Erasmus Medisch Centrum Rotterdam

voor mijn moeder

en alle andere moeders

Table of contents

Chapter 1	General introduction	9
Part I	Enteral nutritional interventions and NEC: the current state of evidence	37
Chapter 2	Enteral feeding interventions in the prevention of necrotizing enterocolitis: a systematic review of experimental and clinical studies	39
Part II	Understanding NEC pathophysiology: ENS alterations during chorioamnionitis and NEC	191
Chapter 3	Chorioamnionitis induces enteric nervous system injury: effects of timing and inflammation in the ovine fetus	193
Chapter 4	Chronic intra-uterine <i>Ureaplasma parvum</i> infection induces injury of the enteric nervous system in ovine fetuses	209
Chapter 5	Alterations of the enteric nervous system and intestinal motility in a mouse model of necrotizing enterocolitis	229
Part III	Understanding NEC pathophysiology: mucus barrier alterations during chorioamnionitis and NEC	251
Chapter 6	Intestinal goblet cell loss during chorioamnionitis in fetal lambs: mechanistic insights and postnatal implications	253
Chapter 7	Antenatal <i>Ureaplasma parvum</i> infection induces ovine small intestinal goblet cell abnormalities: a strong link with NEC pathology	275
Part IV	Towards better strategies for the prevention of NEC with enteral feeding interventions	301
Chapter 8	Protection of the ovine fetal gut against <i>Ureaplasma</i> -induced chorioamnionitis: a potential role for plant sterols	303
Chapter 9	Hypoxia-driven changes in a human intestinal organoid model and the protective effects of hydrolyzed whey	331

Part V	Conclusions, perspectives and impact	375
Chapter 10	Summary and general discussion	377
Chapter 11	Scientific and societal impact	397
Addendum		405
	Nederlandse samenvatting	407
	Abbreviations	415
	Dankwoord	421
	List of publications	429
	Curriculum vitae	431

Chapter 1

General introduction

Preterm birth: a considerable concern

Around 10% of children are born preterm (i.e., before 37 weeks of gestational age [GA]), which translates to a global figure of approximately 15 million neonates each year¹. Of these preterm infants, approximately 5% are born extremely premature (<28 weeks GA), 15% severely premature (28-31 weeks GA) and 20% moderately preterm (32-33 weeks GA)². The remaining 60% of preterm births (34-36 weeks GA) are considered near-term². Approximately 70% of preterm births follow spontaneous onset of labor with intact membranes or preterm premature rupture of membranes (PPROM)² and these births are collectively referred to as spontaneous preterm birth. The remaining 30% of premature births are the consequence of medically induced labor or caesarian section for maternal or fetal indications such as (pre-)eclampsia or intrauterine growth retardation². Importantly, despite gradually improving survival, premature birth remains the leading cause of neonatal mortality and mortality below 5 years of age^{1,3}. Moreover, it causes considerable short-term and long-term morbidity³ and is associated with extensive health care costs and societal costs, in particular in case of extremely and severely premature neonates^{1,3,4}.

Chorioamnionitis, intra-uterine inflammation and FIRS

A major cause for spontaneous preterm birth is chorioamnionitis^{2,5}. Chorioamnionitis is an inflammatory process in the fetal membranes (i.e., chorion and amnion) that is characterized by an influx of inflammatory cells that migrate from the decidua (mucosal lining of the uterus, maternal tissue) towards the chorion and amnion^{6,7}. Chorioamnionitis is most often caused by bacteria originating from the lower genital tract of the mother that ascend to the fetal membranes^{7,8}. Besides reaching the fetal membranes, microorganisms can enter the amniotic fluid, the umbilical cord, and, in severe cases, the choriodecidual space (maternal-fetal interface) and placenta⁵, thereby causing intra-amniotic (IA) infection, funisitis and villitis respectively⁶. Direct microbial invasion of the amniotic cavity or release of inflammatory mediators from infected chorion and amnion may provoke an IA inflammatory response that is mainly driven by cells in the chorion and amnion, fetal skin cells and cells from the umbilical cord⁶. This IA pro-inflammatory response is characterized by increased levels of various pro-inflammatory cytokines, such as IL1, TNF α , IL6 and IL8, and elevated numbers of inflammatory cells in the amniotic fluid^{6,9}. Inflammatory cytokines and chemokines that are involved in IA inflammation stimulate production of prostaglandins in the decidua, which together with migrated inflammatory cells, promotes the secretion of matrix metalloproteinases from placenta and fetal membranes, which in turn results in ripening of the cervix and weakening or even rupture of the fetal membranes¹⁰. In conjunction with stimulation of uterine contractions by the increased levels of prostaglandins, this can lead to preterm labor¹⁰. Although chorioamnionitis can give rise to maternal signs and symptoms such as fever, tachycardia, uterine tenderness, leukocytosis, and foul-smelling amniotic fluid (together called clinical chorioamnionitis), it is frequently clinically silent^{6,11}. Hence, chorioamnionitis is often not recognized until preterm birth and histological examination of the placenta and fetal membranes (histological chorioamnionitis)^{6,12}. Risk factors for chorioamnionitis include PPRM, prolonged labor,

nulliparity, alcohol and tobacco use, bacterial vaginosis, group B streptococcus colonization and chorioamnionitis in a previous pregnancy^{8,13}.

Microbial invasion of the amniotic fluid and/or intrauterine inflammation can ultimately lead to fetal invasion and inflammation, as the fetus is exposed to the contaminated amniotic fluid via skin, pulmonary tract, gastrointestinal tract and mucosal membranes in the middle ear and conjunctiva^{6,11}. This may cause inflammation of fetal tissues, such as the gastrointestinal tract, and a systemic inflammatory reaction in the fetus called Fetal Inflammatory Response Syndrome (FIRS)^{6,11}. FIRS is defined as increased fetal plasma concentrations of IL6 (>11 pg/mL) and regarded as the fetal equivalent of the systemic inflammatory response syndrome (SIRS) in adults^{14,15}.

The prevalence of clinical and histological chorioamnionitis, intrauterine infection (e.g., positive chorioamniotic tissue culture or amniotic fluid culture), intrauterine inflammation (increased amniotic fluid IL6 concentrations), and FIRS are inversely related to the GA at time of delivery^{5,8,10,16-19}. During pathological examination of the placenta, histological chorioamnionitis is observed in ~30-70% of spontaneous preterm births^{8,17,18}, and around 20-60% of preterm births following spontaneous labor with intact membranes is associated with intrauterine infection or inflammation^{5,16,17}. Importantly, only about half of the patients with IA inflammation had a positive amniotic fluid culture, which suggests an underestimation of intra-uterine inflammation when only culture results are considered¹⁷. The prevalence of FIRS is ~30-35% in pregnancies complicated by preterm labor with intact membranes, PPRM or other risk factors of bacterial infection such as chorioamnionitis^{20,21}. Last, in a cross sectional study, prevalence of FIRS in infants with a positive amniotic fluid culture was 69%, while this was 12% in infants with a negative amniotic fluid culture²².

Ureaplasma spp.: the main culprits in chorioamnionitis

A broad range of microorganisms including bacteria, viruses, and—to a lesser extent—fungi and yeast have been implicated in chorioamnionitis²³. Of these microorganisms, *Ureaplasma* spp. are most commonly detected in the amniotic fluid and placenta of women with chorioamnionitis, funisitis and preterm delivery¹⁰. *Ureaplasma* spp. are part of the family of *Mycoplasmataceae* and are for their energy supply dependent on hydrolysis of urea by their urease enzyme¹⁰. They do not have a cell wall and range in size from 100 nm to 1 μm ¹⁰. *Ureaplasma* spp. consist of two species (*Ureaplasma parvum* [UP] and *Ureaplasma urealyticum* [UU]), which contain at least 14 serovars^{10,24}. *Ureaplasma* spp. are commensals of the female genital tract and have an average colonization rate of 40-80%^{25,26}. UP is more frequently isolated from the female lower genital tract than UU and serovar 3 is the most common clinical isolate¹⁰. Despite the clear association between *Ureaplasma* spp. and chorioamnionitis^{10,27,28}, its causative role in the pathophysiology of chorioamnionitis, intrauterine infection and FIRS is debated, since the inflammatory response to *Ureaplasma* spp. is variable and many women do not experience adverse pregnancy outcomes despite *Ureaplasma* colonization²⁵. *Ureaplasma* is known for its capacities to avoid immune detection by the host and can cause chronic asymptomatic *in utero* infections¹⁰. In addition, chorioamnionitis is often polymicrobial^{10,29}, making it difficult to pinpoint *Ureaplasma* as the responsible microbe¹⁰. Nevertheless, several findings support a role for *Ureaplasma* spp. in

the pathophysiology of chorioamnionitis and its sequelae. *Ureaplasma* spp. have been shown to induce histological chorioamnionitis also in absence of other microorganisms^{10,30} and may provoke more severe IA infections than other microorganisms³¹. In a cohort study, *Ureaplasma* spp. respiratory tract colonization was associated with histological chorioamnionitis, fetal vasculitis and increased concentrations of IL6 and IL1 β in cord blood³².

Neonatal consequences of chorioamnionitis, intra-uterine inflammation and FIRS

Chorioamnionitis and FIRS are both associated with a higher incidence of adverse neonatal outcomes^{14,15,33-35}, most notably neonatal death³³. Specific postnatal diseases that are associated with (clinical) chorioamnionitis and FIRS include (early-onset) sepsis^{33,34}, respiratory distress syndrome³³, bronchopulmonary dysplasia^{33,36}, intraventricular hemorrhage^{33,34,37}, periventricular leukomalacia³³, retinopathy of prematurity³⁸ and necrotizing enterocolitis (NEC)^{34,39}. Part of this association can be causally explained by the role of chorioamnionitis and FIRS in the induction of premature birth^{33,36,38}. However, fetal plasma IL6 levels are predictive for severe neonatal morbidity, regardless of, amongst others, gestational age and cause of preterm delivery⁴⁰. FIRS is believed to affect multiple fetal organs *in utero* and during the subsequent neonatal period, thereby increasing the risk of postnatal disease^{14,15,35,41} (**Figure 1.1**).

In addition to the general association of chorioamnionitis and FIRS with adverse fetal outcomes, colonization and infection with *Ureaplasma* spp. have been linked with detrimental neonatal effects. *Ureaplasma* colonization of the respiratory tract has been associated with the development of bronchopulmonary dysplasia⁴² and *Ureaplasma* spp. can cause neonatal sepsis and meningitis⁴³. Moreover, colonization of preterm infants (<33 weeks GA) with *Ureaplasma* spp. has been reported to increase NEC risk 2-fold to 3-fold^{32,44}. A role for *Ureaplasma* spp. in the pathophysiology of perinatal diseases is also supported by evidence from experimental studies. Studies in a fetal ovine chorioamnionitis models have demonstrated harmful effects of IA exposure to UP serovar 3, as acute intrauterine exposure induced gut inflammation, intestinal epithelial damage, gut barrier loss and disturbed enterocyte proliferation, differentiation and maturation⁴⁵ and chronic intrauterine exposure induced detrimental cerebral changes, both of which may predispose to postnatal disease^{45,46}. Effects of UP on the fetal intestine were largely dependent on IL1 signaling⁴⁵, which suggests that *Ureaplasma* spp.-induced intestinal inflammation as well as subsequent intestinal damage and disturbance of normal gut development at least in part explain the epidemiological association between *Ureaplasma* colonization and NEC.

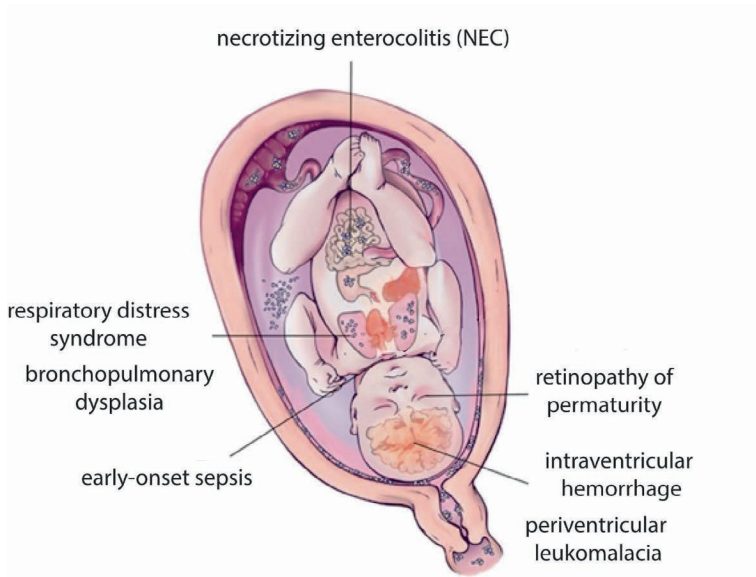


Figure 1.1 Neonatal consequences of (clinical) chorioamnionitis and FIRS.
Adapted from Gantert et al. *J Perinatol.* 2010;30 Suppl: S21-30.

Treatment options for chorioamnionitis and intra-uterine infection or inflammation

Currently, the treatment of chorioamnionitis and its sequelae, clinically referred to as intrauterine inflammation, intrauterine infection or both (Triple I), focuses on alleviating symptoms and risk factors, rather than addressing the cause of the disease¹¹. Generally, in women with confirmed or suspected IA infection, labor is induced and intra-partum antibiotic therapy is initiated^{47,48}. Induction of labor is often regarded a necessity, as intrauterine bacteria may form biofilms that are difficult to treat with antibiotics and an intrauterine cytokine storm resulting from intrauterine infection is largely irreversible⁶. In addition to the intra-partum maternal treatment, neonates are often treated with antibiotics while awaiting the results of additional laboratory diagnostics, such as C reactive protein and blood culture^{48,49}. The decision to start neonatal antibiotic therapy is based on a combination of maternal risk factors (e.g., maternal fever, prolonged rupture of membranes, and maternal group B streptococcus colonization status) as well as the clinical status of the neonate (e.g., clinical characteristics such as respiratory distress, neonatal fever, and feeding problems)^{48,49}.

Unfortunately, to date no (prenatal) treatment strategies are available to address fetal systemic inflammation and tissue inflammation resulting from chorioamnionitis, such as the fetal gut inflammation, that likely predisposes to postnatal development of NEC.

Necrotizing enterocolitis: a devastating disease that still is incompletely understood

NEC is a gastrointestinal emergency that primarily affects premature neonates and is characterized by severe intestinal inflammation and—in later stages—intestinal necrosis⁵⁰. Although NEC can affect the gastrointestinal tract from stomach to distal colon, it is most commonly found in terminal ileum and ascending colon⁵¹. NEC affects around 7% of infants at the neonatal intensive care unit (NICU) and its incidence increases with decreasing gestational age and birth weight^{50,52}. Despite advancing medical care, NEC incidence has not decreased over the years, which is partly caused by increased survival of extreme premature neonates⁵²⁻⁵⁴. NEC is responsible for 10% of NICU deaths and thereby forms a major cause of death in premature neonates⁵⁵. Mortality in NEC patients is inversely correlated with gestational age and birth weight. It generally ranges from 15 to 30%^{50,56}, but can be as high as 50% in infants requiring surgical intervention^{57,58}. Besides its considerable mortality, NEC is a risk factor for the development of long-term morbidities, such as short bowel syndrome^{58,59}, intestinal failure⁵⁸⁻⁶⁰, intestinal failure associated liver disease^{61,62}, growth retardation⁶³⁻⁶⁵, and neurodevelopmental delays^{50,66}. Although not extensively studied, surgical NEC is reported to be associated with long-term reduction of quality of life⁶⁷. Additionally, NEC poses a significant economic burden both on society and the parents and/or patient⁶⁸. Direct surplus costs of NEC, including prolonged hospital stay, have been estimated to range from \$70,000 for medical NEC up to \$180,000 for surgical NEC^{69,70}. In addition, long-term care for NEC survivors, especially when NEC-related morbidities are present, further increases costs^{68,71}.

NEC pathophysiology is multifactorial and, despite many decades of research, remains incompletely understood⁷² (**Figure 1.2**). Prematurity is a major risk factor, because it is associated with hampered intestinal barrier function, vascular dysfunction, disturbed digestion and absorption capacities, immature intestinal motility, and immaturity of the (intestinal) immune defense⁵⁰. In addition, microbial dysbiosis is an important factor contributing to NEC pathophysiology⁷³. Several genetic polymorphisms that impact such processes as immune defense, regulation of oxidative stress, and regulation of apoptosis and cellular repair increase the risk of NEC development⁷⁴. Last, enteral feeding is a pivotal factor modulating NEC pathogenesis. Over 90% of infants that develop NEC have been enterally fed⁵⁰ and timing of NEC is closely related to start of enteral feeding⁷⁵. On the other hand, the risk of NEC increases with delay of enteral feeding⁷⁶, and human milk feeding is highly protective against NEC development⁷⁷.

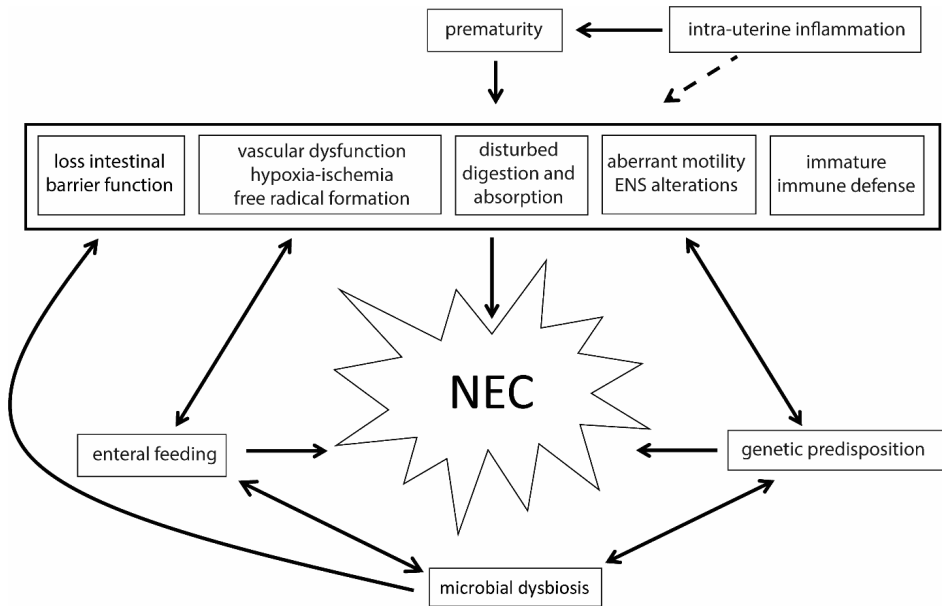


Figure 1.2 Pathophysiology of necrotizing enterocolitis (NEC).
Adapted from Lin et al. Lancet. 2006;368(9543):1271-83.

Of note, since many diseases of the premature neonate, including NEC⁷⁸, have clear prenatal risk factors that influence outcome beyond the induction of preterm birth, the pathophysiological onset of these diseases probably lies already *in utero* in at least a subset of infants. In a broader context, this concept of fetal and early postnatal life shaping both health and disease for later postnatal life is referred to as Developmental Origins of Health and Disease (DOHaD)⁷⁹. The postulated role of fetal involvement in NEC onset suggests that the window of therapeutic opportunity starts prenatally and that intervening *in utero* is a promising strategy to prevent NEC and improve neonatal outcomes.

Diagnosis and treatment of necrotizing enterocolitis

NEC diagnosis is based on several general clinical symptoms such as increase of apneas, bradycardia and temperature instability as well as gastrointestinal symptoms including abdominal distention, feeding intolerance, villous vomiting and rectal bleeding or bloody stools in combination with radiographic findings such as pneumatosis intestinalis, pneumoperitoneum and portal venous gas⁸⁰. Depending on clinical and radiographic severity, NEC can be staged with the modified Bell's criteria as suspected NEC (Bell's stage I), definite NEC (Bell's stage II) or severe NEC (Bell's stage III)⁸¹. Nevertheless, especially signs and symptoms of early or less severe Bell's stage I NEC are non-specific and difficult to diagnose^{72,82}. Moreover, early diagnosis of NEC is challenging as it often rapidly progresses

to a fulminant disease and can cause septic shock, multi-organ failure and even death within a few hours to days⁷².

Treatment of NEC depends on its severity. It normally consists of withholding enteral feeding, gastric decompression by placement of a gastric tube, and intravenous administration of broad-spectrum antibiotics⁸⁰. Further, additional cardiovascular neonatal support by mechanical ventilation and inotropic medication may be necessary⁸⁰. Surgical intervention, in which necrotic parts of the bowel are removed, is required in up to 50% of patients⁸⁰. Despite being a long-lasting topic of research, NEC treatment remains largely symptomatic; due to the fulminant nature of NEC and its complex and multifactorial pathophysiology, it is difficult to majorly improve treatment strategies⁷². Consequently, current NEC research is mainly aimed at developing new preventative approaches⁷².

The enteric nervous system: the brain of the gut

The enteric nervous system (ENS), often considered 'the brain of the gut', is the collection of neurons and supporting cells in the gastrointestinal tract⁸³. The ENS contains somewhere between 200-600 million neurons, most of which are present in small ganglia in either the myenteric or the submucosal plexus⁸⁴ (**Figure 1.3**). The myenteric plexus is mainly involved in regulating intestinal motor function and is positioned between the circular and longitudinal muscle layers of the entire gastrointestinal tract⁸³. The submucosal plexus is primarily involved in regulating mucosal secretion and absorption as well as vascular tone and lies between the muscularis mucosa and the circular muscle layer in small intestine and colon^{83,84}. The myenteric and the submucosal ganglia are interconnected by nerve fiber bundles⁸⁵. Besides the muscles in the gut wall, ENS nerve fiber bundles innervate blood vessels, mucosa, entero-endocrine cells and gut associated lymphoid tissue⁸⁵. The ENS of the small and large intestine can function independently of the central nervous system (CNS) and contains many complete reflex circuits⁸⁴. Nevertheless, the ENS is connected to the CNS via the vagal nerve and pelvic nerves, both containing parasympathetic fibers and sympathetic pathways⁸⁴, and, importantly, information flow between the two is bidirectional^{84,86}.

Several subtypes of neurons, which can roughly be divided into motor neurons, sensory neurons and interneurons, are involved in ENS signaling and these neurons use various neurotransmitters^{84,87}. Excitatory motor neurons that project towards circular and longitudinal muscles most often contain acetylcholine, which is produced by choline acetyltransferase (CHAT), whereas inhibitory motor neurons use, amongst others, NO as neurotransmitter produced by neuronal nitric oxide synthase (nNOS)⁸⁷. Efferent motor neurons that project to the mucosa to regulate mucosal secretions and the tonus of blood vessels contain neurotransmitters such as vasoactive intestinal peptide (VIP) (non-cholinergic neurons) or acetylcysteine (cholinergic neurons)^{84,87}. Sensory neurons (intrinsic and extrinsic primary afferent neurons) act as chemo- and mechano-receptors, thereby transferring signals of the physical and chemical environment of the gut, such as mucosal distortion, muscle movements, and chemical content of the intestinal lumen⁸⁸. As such, they are the first part of many intrinsic feedback loops of the ENS⁸⁸. Sensory neuron axons are localized just below the intestinal epithelium in the lamina propria and lie in close proximity

of other neurons and ganglia⁸⁸. Interneurons, which interconnect different types of neurons in the ENS, can contain a broad range of neurotransmitters such as acetylcholine, somatostatin, NO and serotonin⁸⁴. Last, sympathetic neurons that modulate the ENS are largely noradrenergic⁸⁵, whereas parasympathetic neurons are cholinergic⁸⁹.

Besides neurons, enteric glial cells are an important part of the ENS^{90,91}. They surround neuronal cell bodies and interact with neuronal axons and majorly outnumber the amount of neurons in the ENS⁹¹. Enteric glial cells are considered the intestinal counterpart of astrocytes in the CNS⁹⁰. Although much is still unknown about the function of enteric glial cells *in vivo*, it is clear that enteric glial cells are important for the homeostasis and structural integrity of enteric neurons, modulate ENS signaling, and are involved in the regulation of gut barrier function^{91,92}. Moreover, these cells are crucial in the ENS response to injury and inflammation, where they become activated, proliferate, and stimulate neurogenesis and promote restitution of barrier function^{91,92}.

Importantly, the enteric nervous system, the intestinal epithelium, the immune system, and the intestinal microbiome are in near proximity of each other, and their function is closely connected^{93,94}. For instance, neuropeptides produced by the ENS can alter the function of intestinal epithelial cells and several immune cells such as lymphocytes, macrophages, and mast cells⁹³, and neuropeptides produced by immune cells can regulate ENS signaling⁹³. Moreover, microbiota modulate ENS development and function directly and indirectly via, amongst others, toll like receptor (TLR) signaling and hormone production by entero-endocrine cells^{95,96}.

The enteric nervous system develops from cells that migrate from then neural crest towards the foregut, midgut, and hindgut during embryonic development^{97,98}. This migration goes from proximal to distal and is completed around week 7-8 of human GA, after which additional migration, proliferation, and differentiation of ENS cells takes place^{97,98}. This process is influenced by a plethora of transcription factors, neurotrophic factors, such as glial cell derived neurotrophic factor (GDNF), and extracellular matrix components⁹⁹. Interestingly, further ENS development is considered to be 'outside-in', as myenteric plexus development precedes that of the submucosal plexus by around 3 weeks⁹⁸. By week 14, all ENS components, including myenteric and submucosal plexus, are assembled⁹⁹. Following structural ENS constitution, which largely takes places in the first trimester, the ENS further matures during the second and third trimester of pregnancy, by, amongst others, neurite outgrowth and the development of densely interconnected neuronal networks, and step by step gains its function¹⁰⁰⁻¹⁰³. Moreover, ENS development continues postnatally, when its development is further shaped by the immune system, enteral feeding, and microbial colonization^{96,103,104}.

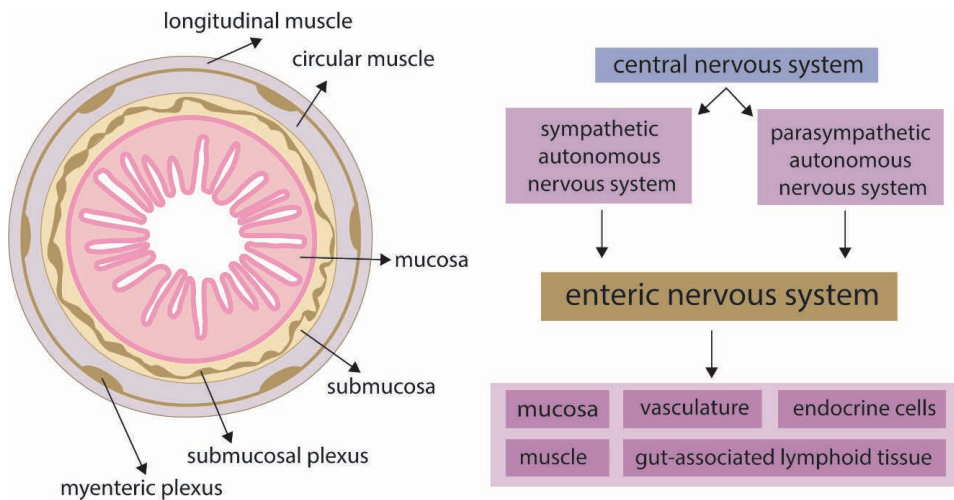


Figure 1.3 Schematic overview of the ENS.

Necrotizing enterocolitis and the enteric nervous system

Immature intestinal motility is one of the postulated risk factors for NEC development^{50,105}, as it can contribute to impaired microbial clearing from the intestinal lumen and subsequent microbial dysbiosis¹⁰⁵. Preterm infants have immature small intestinal motor patterns compared to term infants¹⁰⁶⁻¹⁰⁸, but their motility gradually matures under influence of enteral nutrition^{105,107,109,110}. Interestingly, neonates that suffered from perinatal asphyxia, which increases the risk of NEC development¹¹¹, also have poor intestinal motility compared to healthy controls¹¹². Structural abnormalities of the ENS have been observed in intestinal biopsies of infants with NEC, characterized by loss of neurons and glial cells in the myenteric and the submucosal plexus¹¹³⁻¹¹⁷. Further, reduced levels of the neurotransmitter VIP¹¹³ as well as neurotransmitter synthesizing enzymes nNOS^{113,115} and CHAT¹¹⁵ were observed in intestinal tissue of patients with NEC compared to controls.

Currently, it remains incompletely understood whether the ENS alterations associated with NEC are involved in NEC pathophysiology, or only reflect intestinal damage caused by NEC. However, evidence is emerging that favors a role for ENS alterations and dysmotility in the (downstream) pathogenesis of NEC. Ablation of enteric glial cells in transgenic mice induces a NEC-like intestinal phenotype^{90,117,118}. In pig and murine NEC models, alterations in gut transit time were observed prior to radiological signs of NEC¹¹⁹, intestinal inflammation¹¹⁷ and histological NEC¹¹⁷ appeared. Moreover, in a mouse NEC model, pharmacological restoration of gut motility reduced NEC severity¹¹⁷. Last, neural stem cell transplantation reduced ENS alterations, improved intestinal motility, and concomitantly reduced intestinal damage and mortality in a rat NEC model¹¹⁵. Nevertheless, additional studies are needed to disclose the precise role of the ENS in the pathophysiology of NEC.

Intestinal barrier function: mucus and more

The intestinal barrier separates the intestinal lumen from the internal environment¹²⁰. A healthy intestinal barrier allows absorption of nutrients and fluids, while preventing noxious substances such as bacteria and (bacteria-derived) toxins from reaching the tissue underneath the intestinal epithelial layer¹²⁰. The intestinal barrier is highly dynamic and consists of several interconnected parts^{120,121}. The first part of the barrier is formed by commensal gut bacteria that prevent colonization by pathogenic bacteria¹²¹. In addition, commensal bacteria contribute to maintenance and repair of other parts of the intestinal barrier¹²¹. Second, the intestinal mucus layer and antimicrobial peptides and secretory IgA herein are of pivotal importance¹²¹. Antimicrobial peptides, such as defensins and lysozyme, are produced by Paneth cells and—to a lesser extent—by other epithelial cell types, such as enterocytes, and contribute to barrier function by directly killing microbes and modulating the host immune response^{122,123}. Secretory IgA is produced by plasma cells and promotes the clearance of pathogenic microbes and their antigens through blocking of epithelial receptors and mucus entrapment^{124,125}. Last, intestinal epithelial cells are tightly interconnected by an apical junctional complex of adherens junctions, tight junctions, and desmosomes¹²⁶, thereby preventing paracellular transfer of bacteria and their toxins.

The mucus layer forms a passive barrier that limits the number of bacteria reaching the intestinal epithelium in the small intestine^{120,121}. The small-intestinal mucus layer is present between the crypts and also covers the villus surface¹²⁷. Mucus consists of water and several proteins, of which (MUC2) is the most prominent one¹²⁸. MUC2 polymers form a net-like structure that, in the presence of water, forms a gel-like layer that can be moved through the small intestine by peristalsis¹²⁷. MUC2 and other mucus constituents are produced by Goblet cells, which specialize in the formation and secretion of mucus¹²⁸. Goblet cells arise from transit-amplifying cells following differentiation that is, amongst others, controlled by the transcription factor SAM Pointed Domain Containing ETS Transcription Factor (SPDEF)¹²⁹.

Multiple organelles are involved in the synthesis of MUC2 in the Goblet cell¹³⁰. Following mRNA translation, the MUC2 protein is transported to the endoplasmic reticulum (ER), where dimerization transpires by the formation of disulfide bonds at the C-terminal of the protein¹³⁰. Thereafter, MUC2 dimers are transported to the Golgi apparatus, where O-glycosylation occurs^{128,130}. Following further packaging steps in the trans Golgi network, mucin net-like sheet can be secreted by the Goblet cell^{128,130}. Small intestinal Goblet cells secrete their mucus upon stimulation, for instance by endocytosis of luminal material or in response to acetylcholine¹²⁸.

Necrotizing enterocolitis and the intestinal mucus barrier

Immaturity of the intestinal barrier, including the mucus barrier, is an important risk factor for NEC development⁵⁰. Preterm infants were observed to have a reduced stool mucus glycoprotein content compared to term controls, suggesting that epithelial mucin production matures during gestation¹³¹. Moreover, the intestinal barrier further impaired during NEC, which augments the disease process and contributes to a vicious cycle of inflammation and intestinal damage.³²⁻¹³⁴. Patients with NEC have lower numbers of mucin-

containing intestinal Goblet cells and Paneth cells compared to controls^{135,136}, and a decrease in the number of Goblet cells is also observed in experimental NEC models¹³⁷⁻¹³⁹. Mice with aberrant MUC2 were observed to have an increased NEC incidence and increased NEC severity upon exposure to a protocol to induce experimental NEC¹³⁹. Additionally, exposure to NEC stressors in a rat NEC model modified mucus permeability and altered mucus structure¹⁴⁰.

Promising preventative approach: breast milk and breast milk components

Feeding breast milk to infants has long been recognized as an effective strategy to prevent NEC⁷⁷, ever since Lucas et al. reported that NEC incidence is reduced by 10-fold when human milk is used as the exclusive enteral feeding and by 3 to 5-fold when combined with feeding of infant formula⁷⁷. The effects of human milk on NEC incidence are dose-dependent, and even adding little amounts of human milk to infant formula was shown to reduce NEC risk¹⁴¹. In addition, breast milk may protect preterm neonates against late-onset sepsis¹⁴¹ and bronchopulmonary dysplasia¹⁴², and is further regarded as supportive for neurodevelopment^{143,144}. Therefore, breast milk is currently the first choice of enteral nutrition provided at the NICU^{145,146}. The protective role of breast milk can be explained by the large amount of bioactive components present in breast milk that, together, act on a broad range of disease mechanisms involved in NEC pathogenesis, such as improvement of barrier function and reduction of intestinal inflammation¹⁴⁷⁻¹⁴⁹. Examples of these bioactive components include epidermal growth factor (EGF), heparin-binding EGF-like growth factor (HB-EGF), human milk oligosaccharides (HMO), lactoferrin, alkaline phosphatase and secretory IgA (sIgA), all of which, as single interventions, have been extensively studied in the context of NEC^{148,149}. From this versatile list of important nutritional factors, we will—in this thesis—primary focus on plant sterols, whey proteins, and whey peptides. Although these nutritional components to date have been less frequently studied in the perinatal context, several aspects make them interesting candidates for preventing perinatal gut inflammation. Plant sterols were shown to have anti-inflammatory effects in case of inflammatory bowel disease^{150,151}. Moreover, in a pilot study with an ovine LPS-induced chorioamnionitis model, intra-amniotic plant sterol administration prevented chorioamnionitis induced fetal gut inflammation and mucosal injury¹⁵¹, indicating that plant sterols potentially are a promising intervention in the perinatal context. Whey proteins and peptides have been implicated in promoting gut health through, amongst others, anti-inflammatory, antioxidant, and barrier protective effects¹⁵²⁻¹⁵⁴. Of note, since breast milk contains such a plethora of bioactive compounds, it is highly likely that the best biological effect can be achieved by combining several factors rather than studying single interventions.

Unfortunately, many mothers do not (immediately) yield enough breast milk, partly because initiation of breastfeeding is more difficult after preterm labor¹⁵⁵ and mothers' own milk feeding is regularly discontinued due to various reasons^{156,157}. In addition, although rare, mothers' own milk feeding is sometimes contraindicated, for instance due to maternal medication use or maternal infection¹⁵⁸. Pasteurized donor milk, often donated to breast

milk banks by mothers who have been lactating for a longer period of time, is increasingly being used as alternative to formula feeding in premature infants for whom insufficient or no mothers' own milk is available¹⁵⁹. Preliminary evidence suggests the use of donor milk also reduces NEC risk^{160,161}. Nevertheless, part of the biologically active substances in breast milk are lost during pasteurization and freezing of donor breast milk¹⁶². In addition, the composition of donor milk might not be optimal for the NICU population as breast milk composition is, amongst others, determined by stage of lactation and gestational age of the child^{163,164}, and some safety concerns have been raised regarding the risk of infection related to the use of donor milk¹⁶⁵.

Thus, although breastmilk is the optimal nutrition for the preterm infant, mothers' own milk is not always available and donor milk is not a full-fledged replacement. The development of nutritional interventions containing (combinations of) bioactive human breast milk components holds great promise to bridge this gap and provide novel preventative strategies to reduce the incidence and severity of NEC.

Translational animal models: of mice and sheep

Animal models are of great value in the research of perinatal diseases. In experimental animal models, different microbial or disease-inducing triggers can be administered at a specific moment during gestation or early postnatal life. In addition, outcomes can be studied at a defined time point after exposure. By combining different lengths of exposure to microbial triggers or a disease-inducing protocol, changes during chorioamnionitis or NEC can be studied over time, which aids in gaining insight into the biological processes underlying the observed changes. Moreover, in animal studies, novel treatment strategies can be tested to ensure effectivity and safety before, eventually, these interventions can be translated to vulnerable neonates.

Various species have been used in the modeling of chorioamnionitis, such as mice¹⁶⁶, rats¹⁶⁷, guinea pigs¹⁶⁸, rabbits¹⁶⁹, pigs¹⁷⁰, and rhesus macaques¹⁷¹. All these models have their specific pros and cons, and the choice of a model depends on several aspects¹⁷². Generally, large animal models, such as pig, sheep and macaque models, are of great value because they are closer to human physiology and allow complex procedures such as intra-uterine instrumentation¹⁷³. Although non-human primates come closest to humans, using such models is—for ethical reasons—only allowed by Dutch and European law under strictly defined circumstances. Fortunately, sheep, which have been extensively used to model chorioamnionitis¹⁷⁴⁻¹⁷⁶, form a good alternative for several reasons. Their organ development, including lung, brain, and intestinal development, closely mimics that of human fetuses¹⁷⁴. Intestinal villus formation is completed at an early gestational age in sheep and humans, which is not the case for rodents. Additionally, whereas intestinal crypt formation is completed well before birth in sheep and humans, it only takes place postnatally in rodents¹⁷⁴. Perinatal intestinal development in (premature) sheep is well characterized¹⁷⁷⁻¹⁸⁰. Last, the relatively long pregnancy duration of ~150 days in sheep allows for longer study periods in which for instance acute and chronic intra-amniotic inflammation can be compared and the effects of inflammation or interventions during different developmental phases can be investigated¹⁷⁴. Taken together, this makes the sheep

chorioamnionitis model a very relevant one to study the effects of chorioamnionitis and nutritional interventions on the fetal gut with.

Like chorioamnionitis models, NEC models have been developed in multiple species, including mice^{181,182}, rats¹⁸³, rabbits¹⁸⁴, quails¹⁸⁵, pigs¹⁸⁶ and baboons¹⁸⁷. Rodent models are most frequently used in NEC research as they are suitable for the development of transgenic models¹⁷³. In addition, rodent studies are less expensive, easier to perform, and thereby less time- and labor-consuming than large-animal studies¹⁷³. Although it is notably difficult to include all aspects of the complex NEC pathophysiology in an animal model, rodent NEC models reflect the histopathological damage and cytokine profile of clinical NEC¹⁸⁸. Moreover, experimental NEC induction in these models frequently covers important pathophysiological mechanisms of NEC, such as hypoxia, exposure to LPS, and formula feeding¹⁸⁸. Collectively, NEC models, such as the murine NEC model used in this thesis¹⁸¹, form a suitable model for in depth analysis of NEC pathophysiology.

Human intestinal organoids as novel in vitro screening model

Organoids, also called mini-organs, are three-dimensional (3D) *in vitro* cell cultures that self-organize, differentiate into functional cell types, and recapitulate the structure and function of their organ *in vivo*¹⁸⁹. Organoid technology has emerged over the last few decades and is currently extensively used to study human organ development and diseases¹⁸⁹. Organoids can be formed out of embryonic stem cells (ESCs), induced pluripotent stem cells (iPSCs), or from fetal, neonatal, or adult stem cells from primary tissue (ASCs)¹⁹⁰. Whereas the formation of organoids derived from ESCs or iPSCs is a difficult, time-consuming, and costly process, generation of organoids from ASCs is much less complicated¹⁹¹.

Human intestinal organoids formed out of ASCs (here referred to as HIOs) took flight in 2009 with pioneer work by Sato et al. who showed the long-term culture of small-intestinal organoids from adult intestinal epithelial stem cells that had been isolated from intestinal crypts^{189,192}. In this model, crypts are isolated from human intestinal tissue and seeded in a basement membrane matrix, in which they quickly form 3D HIOs¹⁹² (**Figure 1.4**). The HIOs are cultured in a medium that contains many factors that mimic the natural stem-cell niche environment and promote intestinal epithelial proliferation (e.g., Wtn3a, Rspodin1 and epidermal growth factor [EGF])¹⁹². Whereas HIOs self-differentiate to some extent, further differentiation of the organoid epithelial cells can be achieved by manipulating the composition of the HIO's culture medium^{193,194}. HIOs derived from small amounts of tissue can be expanded and propagated for a long time, while remaining genetically stable¹⁹⁰, which makes them suitable for large-scale experiments and medium-to-high-throughput screening^{195,196}. Moreover, HIOs enable studies with human material that are difficult or even impossible with human subjects¹⁹¹ and can contribute to the reduction of animal experiments¹⁹⁷.

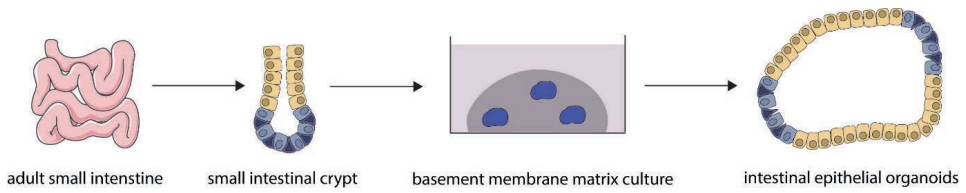


Figure 1.4 Culture of human intestinal organoids from human intestinal tissue.

Importantly, HIOs only contain the epithelial layer of the intestine. This allows for in-depth study of the response of the intestinal epithelial layer to various stimuli, but also means that, in order to study interaction of the intestinal epithelial layer with other relevant factors such as the immune system, the ENS, vasculature, and the intestinal microbiome, the model needs to be extended¹⁹⁸. In addition, since proteins in the basement membrane matrix determine HIO's polarity, the apical membrane of the intestinal epithelial cells in a 3D HIO is generally enclosed in the HIO lumen¹⁹⁹. In circumstances in which apical availability of the intestinal epithelial cells is important, such as studies with nutritional interventions, this is a disadvantage. However, this can be overcome by several solutions, such as micro-injection of the organoids²⁰⁰, organoid culture in absence of the extracellular matrix proteins¹⁹⁹, and two-dimensional (2D) monolayer culture of HIOs^{193,201} (**Figure 1.5**).

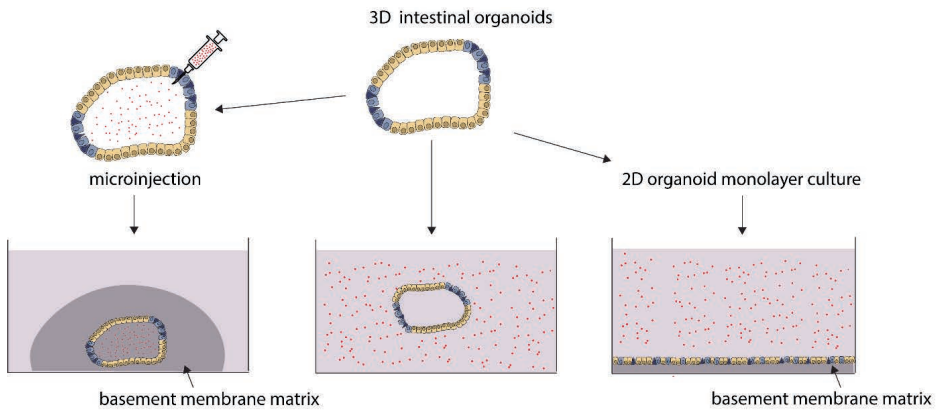


Figure 1.5 Strategies to improve apical accessibility of the HIOs.

HIOs have already been used to model a broad range of gastrointestinal diseases, such as inflammatory bowel disease²⁰², ischemia-reperfusion injury²⁰³, celiac disease²⁰⁴, infections (both viral and bacterial)²⁰⁵⁻²⁰⁷, and colorectal cancer²⁰⁸. In addition, some studies have used HIOs from neonatal or fetal tissue to model NEC through basolateral administration of lipopolysaccharides (LPS) or commensal bacteria²⁰⁹⁻²¹¹. Besides, HIOs have been used in

studies regarding nutrient uptake and metabolism^{212,213}. Altogether, this makes human intestinal organoids a promising model for screening the effects of (combinations of) nutritional interventions in a broad set of gastrointestinal diseases.

Aims and outline of this thesis

Despite many years of research into single-component postnatal feeding interventions, NEC occurrence has not been majorly reduced yet, indicating alternative research strategies are desired. This thesis aims to provide a framework for the improvement of preventative enteral feeding measures for NEC, by applying novel strategies that specifically acknowledge the multifactorial pathophysiology of NEC and its postulated prenatal onset.

This is addressed by:

- 1) providing insight into the current state of evidence on the effectiveness of enteral feeding interventions and the pathophysiological mechanisms these interventions address, as well as on ways to improve the research of preventative enteral feeding strategies for NEC;
- 2) increasing insight into NEC pathogenesis by exploring the effects of chorioamnionitis, which is one of the most important (prenatal) risk factors for NEC development, on the ENS and mucus barrier of the fetal gut, and by exploring the effects of NEC on the ENS in a murine NEC model;
- 3) investigating the effects of an *in utero* enteral feeding intervention on the fetal gut during chorioamnionitis;
- 4) developing a novel human intestinal organoid model that enables screening of (combinations of) nutritional interventions in the context of hypoxia-induced intestinal inflammation and investigating the effects of (hydrolyzed) whey in this model.

In **chapter 2**, we systematically reviewed the current evidence on the prevention of NEC via enteral feeding interventions. Data from experimental NEC animal models and human trials was reviewed. Outcome measures were incidence and severity of NEC as well as the effect on different pathophysiological mechanisms of NEC. In addition, ways to improve research of enteral feeding interventions in NEC were identified.

In **chapter 3 and 4**, we investigated the effects of chorioamnionitis on the fetal ENS, in order to gain more insight into the pathophysiological mechanisms of NEC. In **chapter 3**, we studied the longitudinal effects of IA LPS exposure on the fetal ENS. In **chapter 4**, the effects on the fetal ENS of acute IA exposure to LPS and chronic exposure to UP were compared. In addition, combined exposure to acute LPS and chronic UP was studied to investigate the effects of repetitive microbial exposure on the fetal ENS. In **chapter 5**, we evaluated ENS alterations in a validated murine model of NEC to gain insight into ENS changes during postnatal development of NEC.

In **chapter 6**, we examined alterations of goblet cells and mechanisms underlying these alterations over time during IA LPS-induced chorioamnionitis. In **chapter 7**, the effects of IA UP exposure on the intestinal goblet cells and the functional consequences for the mucus layer were investigated in detail. Moreover, goblet cell characteristics following

chorioamnionitis in this pre-clinical model were compared with findings in clinical NEC biopsies and matched controls.

In **chapter 8**, we investigated whether an early preventative enteral feeding intervention with plant sterols *in utero* improved fetal gut outcome following UP-induced chorioamnionitis. In **chapter 9**, we extended a validated HIO model to enable screening of enteral nutritional interventions during health and during a hypoxia-mediated inflammatory disease state. In addition, we tested the effects of different whey protein fractions as enteral nutritional intervention in this model.

In **chapter 10** the key findings of this thesis are summarized and discussed in the context of the current literature, as well as their clinical implications and significance for future research. Last, in **chapter 11**, the scientific and social impact of this dissertation is examined.

References

1. Harrison MS, Goldenberg RL. Global burden of prematurity. *Semin Fetal Neonatal Med.* 2016;21(2):74-9.
2. Goldenberg RL, Culhane JF, Iams JD, Romero R. Epidemiology and causes of preterm birth. *Lancet.* 2008;371(9606):75-84.
3. Frey HA, Klebanoff MA. The epidemiology, etiology, and costs of preterm birth. *Semin Fetal Neonatal Med.* 2016;21(2):68-73.
4. Cheah IGS. Economic assessment of neonatal intensive care. *Translational pediatrics.* 2019;8(3):246-56.
5. Goldenberg RL, Hauth JC, Andrews WW. Intrauterine infection and preterm delivery. *N Engl J Med.* 2000;342(20):1500-7.
6. Kim CJ, Romero R, Chaemsaithong P, Chaiyasit N, Yoon BH, Kim YM. Acute chorioamnionitis and funisitis: definition, pathologic features, and clinical significance. *Am J Obstet Gynecol.* 2015;213(4 Suppl):S29-52.
7. Cappelletti M, Presicce P, Kallapur SG. Immunobiology of Acute Chorioamnionitis. *Front Immunol.* 2020;11:649.
8. Tita ATN, Andrews WW. Diagnosis and management of clinical chorioamnionitis. *Clin Perinatol.* 2010;37(2):339-54.
9. Goldstein JA, Gallagher K, Beck C, Kumar R, Gernand AD. Maternal-Fetal Inflammation in the Placenta and the Developmental Origins of Health and Disease. *Front Immunol.* 2020;11:531543.
10. Sweeney EL, Dando SJ, Kallapur SG, Knox CL. The Human *Ureaplasma* Species as Causative Agents of Chorioamnionitis. *Clin Microbiol Rev.* 2016;30(1):349-79.
11. Peng CC, Chang JH, Lin HY, Cheng PJ, Su BH. Intrauterine inflammation, infection, or both (Triple I): A new concept for chorioamnionitis. *Pediatr Neonatol.* 2018;59(3):231-7.
12. Maki Y, Furukawa S, Nakayama T, Oohashi M, Shiiba N, Furuta K, et al. Clinical chorioamnionitis criteria are not sufficient for predicting intra-amniotic infection. *J Matern Fetal Neonatal Med.* 2020:1-6.
13. Cohen-Cline HN, Kahn TR, Hutter CM. A population-based study of the risk of repeat clinical chorioamnionitis in Washington State, 1989-2008. *Am J Obstet Gynecol.* 2012;207(6):473.e1-7.
14. Gotsch F, Romero R, Kusanovic JP, Mazaki-Tovi S, Pineles BL, Erez O, et al. The fetal inflammatory response syndrome. *Clin Obstet Gynecol.* 2007;50(3):652-83.
15. Jung E, Romero R, Yeo L, Diaz-Primeria R, Marin-Concha J, Para R, et al. The fetal inflammatory response syndrome: the origins of a concept, pathophysiology, diagnosis, and obstetrical implications. *Semin Fetal Neonatal Med.* 2020;25(4):101146.
16. Goldenberg RL, Culhane JF, Johnson DC. Maternal infection and adverse fetal and neonatal outcomes. *Clin Perinatol.* 2005;32(3):523-59.
17. Yoon BH, Romero R, Moon JB, Shim SS, Kim M, Kim G, et al. Clinical significance of intra-amniotic inflammation in patients with preterm labor and intact membranes. *Am J Obstet Gynecol.* 2001;185(5):1130-6.
18. Lahra MM, Beeby PJ, Jeffery HE. Intrauterine inflammation, neonatal sepsis, and chronic lung disease: a 13-year hospital cohort study. *Pediatrics.* 2009;123(5):1314-9.
19. Iwatani S, Kobayashi T, Matsui S, Hirata A, Yamamoto M, Yoshida M, et al. Gestational Age Dependency of Umbilical Cord Serum IL-6 Levels for Detecting Fetal Inflammation. *Am J Perinatol.* 2020.
20. Romero R, Soto E, Berry SM, Hassan SS, Kusanovic JP, Yoon BH, et al. Blood pH and gases in fetuses in preterm labor with and without systemic inflammatory response syndrome. *J Matern Fetal Neona.* 2012;25(7):1160-70.
21. Romero R, Savasan ZA, Chaiworapongsa T, Berry SM, Kusanovic JP, Hassan SS, et al. Hematologic profile of the fetus with systemic inflammatory response syndrome. *J Perinat Med.* 2011;40(1):19-32.
22. Gomez R, Ghezzi F, Römern R, Yoon BH, Mazor M, Berry SM. Two thirds of human fetuses with microbial invasion of the amniotic cavity have a detectable systemic cytokine response before birth. *Acta Diabetol Lat.* 1997;176(1 part II):S14.
23. DiGiulio DB, Romero R, Amogan HP, Kusanovic JP, Bik EM, Gotsch F, et al. Microbial prevalence, diversity and abundance in amniotic fluid during preterm labor: a molecular and culture-based investigation. *PLoS One.* 2008;3(8):e3056.

24. Robertson JA, Stemke GW, Davis JW, Harasawa R, Thirkell D, Kong F, et al. Proposal of *Ureaplasma parvum* sp. nov. and emended description of *Ureaplasma urealyticum* (Shepard et al. 1974) Robertson et al. 2001. *Int J Syst Evol Microbiol*. 2002;52(Pt 2):587-97.
25. Cassell GH, Waites KB, Watson HL, Crouse DT, Harasawa R. *Ureaplasma urealyticum* intrauterine infection: role in prematurity and disease in newborns. *Clin Microbiol Rev*. 1993;6(1):69-87.
26. Larsen B, Hwang J. *Mycoplasma, Ureaplasma, and adverse pregnancy outcomes: a fresh look*. *Infect Dis Obstet Gynecol*. 2010.
27. Sprong KE, Mabenge M, Wright CA, Govender S. *Ureaplasma* species and preterm birth: current perspectives. *Crit Rev Microbiol*. 2020:1-13.
28. Kikhney J, von Schöning D, Steding I, Schulze J, Petrich A, Hiergeist A, et al. Is *Ureaplasma* spp. the leading causative agent of acute chorioamnionitis in women with preterm birth? *Clin Microbiol Infect*. 2017;23(2):119.e1-e7.
29. Romero R, Schaudinn C, Kusanovic JP, Gorur A, Gotsch F, Webster P, et al. Detection of a microbial biofilm in intraamniotic infection. *Am J Obstet Gynecol*. 2008;198(1):135.e1-5.
30. Sweeney EL, Kallapur SG, Gisslen T, Lambers DS, Choungnet CA, Stephenson SA, et al. Placental Infection With *Ureaplasma* species Is Associated With Histologic Chorioamnionitis and Adverse Outcomes in Moderately Preterm and Late-Preterm Infants. *J Infect Dis*. 2016;213(8):1340-7.
31. Oh KJ, Lee KA, Sohn YK, Park CW, Hong JS, Romero R, et al. Intraamniotic infection with genital mycoplasmas exhibits a more intense inflammatory response than intraamniotic infection with other microorganisms in patients with preterm premature rupture of membranes. *Am J Obstet Gynecol*. 2010;203(3):211 e1-8.
32. Okogbule-Wonodi AC, Gross GW, Sun CC, Agthe AG, Xiao L, Waites KB, et al. Necrotizing enterocolitis is associated with *ureaplasma* colonization in preterm infants. *Pediatr Res*. 2011;69(5 Pt 1):442-7.
33. Tang Q, Zhang L, Li H, Shao Y. The fetal inflammation response syndrome and adverse neonatal outcomes: a meta-analysis. *J Matern Fetal Neonatal Med*. 2019:1-13.
34. Venkatesh KK, Jackson W, Hughes BL, Laughon MM, Thorp JM, Stamilio DM. Association of chorioamnionitis and its duration with neonatal morbidity and mortality. *J Perinatol*. 2019.
35. Gantert M, Been JV, Gavilanes AW, Garnier Y, Zimmermann LJ, Kramer BW. Chorioamnionitis: a multiorgan disease of the fetus? *J Perinatol*. 2010;30 Suppl:S21-30.
36. Villamor-Martinez E, Álvarez-Fuente M, Ghazi AMT, Degraeuwe P, Zimmermann LJ, Kramer BW, et al. Association of Chorioamnionitis With Bronchopulmonary Dysplasia Among Preterm Infants: A Systematic Review, Meta-analysis, and Metaregression. *JAMA Network Open*. 2019;2(11):e1914611.
37. Villamor-Martinez E, Fumagalli M, Mohammed Rahim O, Passera S, Cavallaro G, Degraeuwe P, et al. Chorioamnionitis Is a Risk Factor for Intraventricular Hemorrhage in Preterm Infants: A Systematic Review and Meta-Analysis. *Front Physiol*. 2018;9:1253.
38. Villamor-Martinez E, Cavallaro G, Raffaelli G, Mohammed Rahim OMM, Gulden S, Ghazi AMT, et al. Chorioamnionitis as a risk factor for retinopathy of prematurity: An updated systematic review and meta-analysis. *PLoS One*. 2018;13(10):e0205838.
39. Been JV, Lievens S, Zimmermann LJ, Kramer BW, Wolfs TG. Chorioamnionitis as a risk factor for necrotizing enterocolitis: a systematic review and meta-analysis. *J Pediatr*. 2013;162(2):236-42 e2.
40. Gomez R, Romero R, Ghezzi F, Yoon BH, Mazor M, Berry SM. The fetal inflammatory response syndrome. *Am J Obstet Gynecol*. 1998;179(1):194-202.
41. Bersani I, Thomas W, Speer CP. Chorioamnionitis--the good or the evil for neonatal outcome? *J Matern Fetal Neonatal Med*. 2012;25 Suppl 1:12-6.
42. Schelonka RL, Katz B, Waites KB, Benjamin DK, Jr. Critical appraisal of the role of *Ureaplasma* in the development of bronchopulmonary dysplasia with metaanalytic techniques. *Pediatr Infect Dis J*. 2005;24(12):1033-9.
43. Stol K, Jans J, Ott de Bruin L, Unger W, van Rossum A. Perinatal Infections With *Ureaplasma*. *Pediatr Infect Dis J*. 2021;40(5s):S26-s30.
44. Viscardi RM. *Ureaplasma* species: role in neonatal morbidities and outcomes. *Arch Dis Child Fetal Neonatal Ed*. 2014;99(1):F87-92.
45. Wolfs TG, Kallapur SG, Knox CL, Thuijls G, Nitsos I, Polglase GR, et al. Antenatal *ureaplasma* infection impairs development of the fetal ovine gut in an IL-1-dependent manner. *Mucosal Immunol*. 2013;6(3):547-56.

46. Gussenhoven R, Ophelders DRMG, Kemp MW, Payne MS, Spiller OB, Beeton ML, et al. The Paradoxical Effects of Chronic Intra-Amniotic Ureaplasma parvum Exposure on Ovine Fetal Brain Development. *Dev Neurosci*. 2017;39(6):472-86.
47. Committee Opinion No. 712: Intrapartum Management of Intraamniotic Infection. *Obstet Gynecol*. 2017;130(2):e95-e101.
48. Neonatal Institute for Health and Care Excellence (2015) Preterm labour and birth (NICE guideline 25).
49. Nederlandse Vereniging voor Obstetrie en Gynaecologie Preventie en behandeling van early-onset neonatale infecties. 2017.
50. Lin PW, Stoll BJ. Necrotising enterocolitis. *Lancet*. 2006;368(9543):1271-83.
51. Sharma R, Hudak ML. A clinical perspective of necrotizing enterocolitis: past, present, and future. *Clin Perinatol*. 2013;40(1):27-51.
52. Alsaied A, Islam N, Thalib L. Global incidence of Necrotizing Enterocolitis: a systematic review and Meta-analysis. *BMC Pediatr*. 2020;20(1):344.
53. Han SM, Hong CR, Knell J, Edwards EM, Morrow KA, Soll RF, et al. Trends in incidence and outcomes of necrotizing enterocolitis over the last 12 years: A multicenter cohort analysis. *J Pediatr Surg*. 2020;55(6):998-1001.
54. Heida FH, Stolwijk L, Loos MH, van den Ende SJ, Onland W, van den Dungen FA, et al. Increased incidence of necrotizing enterocolitis in the Netherlands after implementation of the new Dutch guideline for active treatment in extremely preterm infants: Results from three academic referral centers. *J Pediatr Surg*. 2017;52(2):273-6.
55. Jacob J, Kamitsuka M, Clark RH, Kelleher AS, Spitzer AR. Etiologies of NICU deaths. *Pediatrics*. 2015;135(1):e59-65.
56. Fitzgibbons SC, Ching Y, Yu D, Carpenter J, Kenny M, Weldon C, et al. Mortality of necrotizing enterocolitis expressed by birth weight categories. *J Pediatr Surg*. 2009;44(6):1072-5; discussion 5-6.
57. Blakely ML, Lally KP, McDonald S, Brown RL, Barnhart DC, Ricketts RR, et al. Postoperative outcomes of extremely low birth-weight infants with necrotizing enterocolitis or isolated intestinal perforation: a prospective cohort study by the NICHD Neonatal Research Network. *Ann Surg*. 2005;241(6):984-9; discussion 9-94.
58. Murthy K, Yanowitz TD, DiGeronimo R, Dykes FD, Zaniletti I, Sharma J, et al. Short-term outcomes for preterm infants with surgical necrotizing enterocolitis. *J Perinatol*. 2014;34(10):736-40.
59. Amin SC, Pappas C, Iyengar H, Maheshwari A. Short bowel syndrome in the NICU. *Clin Perinatol*. 2013;40(1):53-68.
60. Duggan CP, Jaksic T. Pediatric Intestinal Failure. *N Engl J Med*. 2017;377(7):666-75.
61. Zeng S, Li X, Deng C, Li L, Guo C. Evaluation of parenteral nutrition-associated liver disease in surgical infants for necrotizing enterocolitis. *Medicine*. 2020;99(2):e18539-e.
62. Tillman EM, Norman JL, Huang EY, Lazar LF, Crill CM. Evaluation of parenteral nutrition-associated liver disease in infants with necrotizing enterocolitis before and after the implementation of feeding guidelines. *Nutr Clin Pract*. 2014;29(2):234-7.
63. Hong CR, Fullerton BS, Mercier CE, Morrow KA, Edwards EM, Ferrelli KR, et al. Growth morbidity in extremely low birth weight survivors of necrotizing enterocolitis at discharge and two-year follow-up. *J Pediatr Surg*. 2018;53(6):1197-202.
64. McNelis K, Goddard G, Jenkins T, Poindexter A, Wessel J, Helmrath M, et al. Delay in achieving enteral autonomy and growth outcomes in very low birth weight infants with surgical necrotizing enterocolitis. *J Perinatol*. 2021;41(1):150-6.
65. Zozaya C, Shah J, Pierro A, Zani A, Synnes A, Lee S, et al. Neurodevelopmental and growth outcomes of extremely preterm infants with necrotizing enterocolitis or spontaneous intestinal perforation. *J Pediatr Surg*. 2021;56(2):309-16.
66. Schulzke SM, Deshpande GC, Patole SK. Neurodevelopmental outcomes of very low-birth-weight infants with necrotizing enterocolitis: a systematic review of observational studies. *Arch Pediatr Adolesc Med*. 2007;161(6):583-90.
67. Amin R, Knezevich M, Lingongo M, Szabo A, Yin Z, Oldham KT, et al. Long-term Quality of Life in Neonatal Surgical Disease. *Ann Surg*. 2018;268(3):497-505.
68. Mowitz ME, Dukhovny D, Zupancic JAF. The cost of necrotizing enterocolitis in premature infants. *Semin Fetal Neonatal Med*. 2018;23(6):416-9.

69. Bisquera JA, Cooper TR, Berseth CL. Impact of necrotizing enterocolitis on length of stay and hospital charges in very low birth weight infants. *Pediatrics*. 2002;109(3):423-8.
70. Ganapathy V, Hay JW, Kim JH. Costs of necrotizing enterocolitis and cost-effectiveness of exclusively human milk-based products in feeding extremely premature infants. *Breastfeed Med*. 2012;7(1):29-37.
71. Ganapathy V, Hay JW, Kim JH, Lee ML, Rechtman DJ. Long term healthcare costs of infants who survived neonatal necrotizing enterocolitis: a retrospective longitudinal study among infants enrolled in Texas Medicaid. *BMC Pediatr*. 2013;13:127.
72. Neu J, Walker WA. Necrotizing enterocolitis. *N Engl J Med*. 2011;364(3):255-64.
73. Pammi M, Cope J, Tarr PI, Warner BB, Morrow AL, Mai V, et al. Intestinal dysbiosis in preterm infants preceding necrotizing enterocolitis: a systematic review and meta-analysis. *Microbiome*. 2017;5(1):31.
74. Cuna A, Sampath V. Genetic alterations in necrotizing enterocolitis. *Semin Perinatol*. 2017;41(1):61-9.
75. Vaks Y, Birnie KL, Carmichael SL, Hernandez-Boussard T, Benitz WE. Temporal Relationship of Onset of Necrotizing Enterocolitis and Introduction of Enteric Feedings and Powdered Milk Fortifier. *Am J Perinatol*. 2018;35(7):616-23.
76. Kirtsman M, Yoon EW, Ojah C, Cieslak Z, Lee SK, Shah PS. Nil-per-os days and necrotizing enterocolitis in extremely preterm infants. *Am J Perinatol*. 2015;32(8):785-94.
77. Lucas A, Cole TJ. Breast milk and neonatal necrotising enterocolitis. *Lancet*. 1990;336(8730):1519-23.
78. Watson SN, McElroy SJ. Potential Prenatal Origins of Necrotizing Enterocolitis. *Gastroenterol Clin North Am*. 2021;50(2):431-44.
79. Hanson MA, Gluckman PD. Early developmental conditioning of later health and disease: physiology or pathophysiology? *Physiol Rev*. 2014;94(4):1027-76.
80. Rich BS, Dolgin SE. Necrotizing Enterocolitis. *Pediatr Rev*. 2017;38(12):552-9.
81. Walsh MC, Kliegman RM. Necrotizing enterocolitis: treatment based on staging criteria. *Pediatr Clin North Am*. 1986;33(1):179-201.
82. Gordon P, Christensen R, Weitkamp JH, Maheshwari A. Mapping the New World of Necrotizing Enterocolitis (NEC): Review and Opinion. *The e-journal of neonatology research*. 2012;2(4):145-72.
83. Goyal RK, Hirano I. The enteric nervous system. *N Engl J Med*. 1996;334(17):1106-15.
84. Furness JB, Callaghan BP, Rivera LR, Cho HJ. The enteric nervous system and gastrointestinal innervation: integrated local and central control. *Adv Exp Med Biol*. 2014;817:39-71.
85. Furness JB. The enteric nervous system and neurogastroenterology. *Nat Rev Gastroenterol Hepatol*. 2012;9(5):286-94.
86. Yoo BB, Mazmanian SK. The Enteric Network: Interactions between the Immune and Nervous Systems of the Gut. *Immunity*. 2017;46(6):910-26.
87. Furness JB. Types of neurons in the enteric nervous system. *J Auton Nerv Syst*. 2000;81(1-3):87-96.
88. Furness JB, Jones C, Nurgali K, Clerc N. Intrinsic primary afferent neurons and nerve circuits within the intestine. *Prog Neurobiol*. 2004;72(2):143-64.
89. Browning KN, Travaglini RA. Central nervous system control of gastrointestinal motility and secretion and modulation of gastrointestinal functions. *Compr Physiol*. 2014;4(4):1339-68.
90. Bush TG. Enteric glial cells. An upstream target for induction of necrotizing enterocolitis and Crohn's disease? *Bioessays*. 2002;24(2):130-40.
91. Rühl A, Nasser Y, Sharkey KA. Enteric glia. *Neurogastroenterol Motil*. 2004;16 Suppl 1:44-9.
92. Gulbransen BD, Sharkey KA. Novel functional roles for enteric glia in the gastrointestinal tract. *Nat Rev Gastroenterol Hepatol*. 2012;9(11):625-32.
93. Genton L, Kudsk KA. Interactions between the enteric nervous system and the immune system: role of neuropeptides and nutrition. *Am J Surg*. 2003;186(3):253-8.
94. Saldana-Morales FB, Kim DV, Tsai M-T, Diehl GE. Healthy Intestinal Function Relies on Coordinated Enteric Nervous System, Immune System, and Epithelium Responses. *Gut microbes*. 2021;13(1):1-14.
95. Heiss CN, Olofsson LE. The role of the gut microbiota in development, function and disorders of the central nervous system and the enteric nervous system. *J Neuroendocrinol*. 2019;31(5):e12684.
96. Joly A, Leulier F, De Vadder F. Microbial Modulation of the Development and Physiology of the Enteric Nervous System. *Trends Microbiol*. 2020.
97. Nagy N, Goldstein AM. Enteric nervous system development: A crest cell's journey from neural tube to colon. *Semin Cell Dev Biol*. 2017;66:94-106.
98. Rao M, Gershon MD. Enteric nervous system development: what could possibly go wrong? *Nat Rev Neurosci*. 2018;19(9):552-65.

99. Wallace AS, Burns AJ. Development of the enteric nervous system, smooth muscle and interstitial cells of Cajal in the human gastrointestinal tract. *Cell Tissue Res.* 2005;319(3):367-82.
100. Burns AJ, Roberts RR, Bornstein JC, Young HM. Development of the enteric nervous system and its role in intestinal motility during fetal and early postnatal stages. *Semin Pediatr Surg.* 2009;18(4):196-205.
101. Fekete E, Resch BA, Benedeczky I. Histochemical and ultrastructural features of the developing enteric nervous system of the human foetal small intestine. *Histol Histopathol.* 1995;10(1):127-34.
102. Fekete E, Bagyánszki M, Resch BA. Prenatal development of the myenteric plexus in the human fetal small intestine. *Acta Biol Szeged [Internet].* 2000;44(1-4):3-19.
103. Hao MM, Foong JP, Bornstein JC, Li ZL, Vanden Berghe P, Boesmans W. Enteric nervous system assembly: Functional integration within the developing gut. *Dev Biol.* 2016;417(2):168-81.
104. Fichter M, Klotz M, Hirschberg DL, Waldura B, Schofer O, Ehnert S, et al. Breast milk contains relevant neurotrophic factors and cytokines for enteric nervous system development. *Mol Nutr Food Res.* 2011;55(10):1592-6.
105. Berseth CL. Gut motility and the pathogenesis of necrotizing enterocolitis. *Clin Perinatol.* 1994;21(2):263-70.
106. Ittmann PI, Amarnath R, Berseth CL. Maturation of antroduodenal motor activity in preterm and term infants. *Dig Dis Sci.* 1992;37(1):14-9.
107. al Tawil Y, Berseth CL. Gestational and postnatal maturation of duodenal motor responses to intragastric feeding. *J Pediatr.* 1996;129(3):374-81.
108. Berseth CL. Gestational evolution of small intestine motility in preterm and term infants. *J Pediatr.* 1989;115(4):646-51.
109. Berseth CL, Nordyke C. Enteral nutrients promote postnatal maturation of intestinal motor activity in preterm infants. *Am J Physiol.* 1993;264(6 Pt 1):G1046-51.
110. Berseth CL. Effect of early feeding on maturation of the preterm infant's small intestine. *J Pediatr.* 1992;120(6):947-53.
111. Gregory KE. Clinical predictors of necrotizing enterocolitis in premature infants. *Nurs Res.* 2008;57(4):260-70.
112. Berseth CL, McCoy HH. Birth asphyxia alters neonatal intestinal motility in term neonates. *Pediatrics.* 1992;90(5):669-73.
113. Sigge W, Wedel T, Kuhnel W, Krammer HJ. Morphologic alterations of the enteric nervous system and deficiency of non-adrenergic non-cholinergic inhibitory innervation in neonatal necrotizing enterocolitis. *Eur J Pediatr Surg.* 1998;8(2):87-94.
114. Wedel T, Krammer HJ, Kuhnel W, Sigge W. Alterations of the enteric nervous system in neonatal necrotizing enterocolitis revealed by whole-mount immunohistochemistry. *Pediatr Pathol Lab Med.* 1998;18(1):57-70.
115. Zhou Y, Yang J, Watkins DJ, Boomer LA, Matthews MA, Su Y, et al. Enteric nervous system abnormalities are present in human necrotizing enterocolitis: potential neurotransplantation therapy. *Stem Cell Res Ther.* 2013;4(6):157-.
116. Fagbemi AO, Torrente F, Puleston J, Lakhoo K, James S, Murch SH. Enteric neural disruption in necrotizing enterocolitis occurs in association with myenteric glial cell CCL20 expression. *J Pediatr Gastroenterol Nutr.* 2013;57(6):788-93.
117. Kovler ML, Gonzalez Salazar AJ, Fulton WB, Lu P, Yamaguchi Y, Zhou Q, et al. Toll-like receptor 4-mediated enteric glia loss is critical for the development of necrotizing enterocolitis. *Sci Transl Med.* 2021;13(612):eabg3459.
118. Bush TG, Savidge TC, Freeman TC, Cox HJ, Campbell EA, Mucke L, et al. Fulminant jejuno-ileitis following ablation of enteric glia in adult transgenic mice. *Cell.* 1998;93(2):189-201.
119. Chen W, Sun J, Kappel SS, Gormsen M, Sangild PT, Aunsholt L. Gut transit time, using radiological contrast imaging, to predict early signs of necrotizing enterocolitis. *Pediatr Res.* 2020.
120. Schoultz I, Keita Å V. The Intestinal Barrier and Current Techniques for the Assessment of Gut Permeability. *Cells.* 2020;9(8).
121. Thoo L, Noti M, Krebs P. Keep calm: the intestinal barrier at the interface of peace and war. *Cell Death Dis.* 2019;10(11):849.
122. Muniz L, Knosp C, Yeretsian G. Intestinal antimicrobial peptides during homeostasis, infection, and disease. *Front Immunol.* 2012;3(310).
123. Zhang L-j, Gallo RL. Antimicrobial peptides. *Curr Biol.* 2016;26(1):R14-R9.

124. Pabst O, Slack E. IgA and the intestinal microbiota: the importance of being specific. *Mucosal Immunol.* 2020;13(1):12-21.
125. Mantis NJ, Rol N, Corthésy B. Secretory IgA's complex roles in immunity and mucosal homeostasis in the gut. *Mucosal Immunol.* 2011;4(6):603-11.
126. Sánchez de Medina F, Romero-Calvo I, Mascaraque C, Martínez-Augustin O. Intestinal Inflammation and Mucosal Barrier Function. *Inflamm Bowel Dis.* 2014;20(12):2394-404.
127. Johansson ME, Sjövall H, Hansson GC. The gastrointestinal mucus system in health and disease. *Nat Rev Gastroenterol Hepatol.* 2013;10(6):352-61.
128. Birchenough GMH, Johansson MEV, Gustafsson JK, Bergström JH, Hansson GC. New developments in goblet cell mucus secretion and function. *Mucosal Immunol.* 2015;8(4):712-9.
129. Gregorieff A, Stange DE, Kujala P, Begthel H, van den Born M, Korving J, et al. The ets-domain transcription factor Spdef promotes maturation of goblet and paneth cells in the intestinal epithelium. *Gastroenterology.* 2009;137(4):1333-45.e1-3.
130. Pelaseyed T, Bergström JH, Gustafsson JK, Ermund A, Birchenough GM, Schütte A, et al. The mucus and mucins of the goblet cells and enterocytes provide the first defense line of the gastrointestinal tract and interact with the immune system. *Immunol Rev.* 2014;260(1):8-20.
131. Ryley HC, Rennie D, Bradley DM. The composition of a mucus glycoprotein from meconium of cystic fibrosis, healthy pre-term and full-term neonates. *Clin Chim Acta.* 1983;135(1):49-56.
132. Moore SA, Nighot P, Reyes C, Rawat M, McKee J, Lemon D, et al. Intestinal barrier dysfunction in human necrotizing enterocolitis. *J Pediatr Surg.* 2016;51(12):1907-13.
133. Anand RJ, Leaphart CL, Mollen KP, Hackam DJ. The role of the intestinal barrier in the pathogenesis of necrotizing enterocolitis. *Shock.* 2007;27(2):124-33.
134. Halpern MD, Denning PW. The role of intestinal epithelial barrier function in the development of NEC. *Tissue barriers.* 2015;3(1-2):e1000707.
135. McElroy SJ, Prince LS, Weitkamp JH, Reese J, Slaughter JC, Polk DB. Tumor necrosis factor receptor 1-dependent depletion of mucus in immature small intestine: a potential role in neonatal necrotizing enterocolitis. *Am J Physiol Gastrointest Liver Physiol.* 2011;301(4):G656-66.
136. Schaart MW, de Bruijn AC, Bouwman DM, de Krijger RR, van Goudoever JB, Tibboel D, et al. Epithelial functions of the residual bowel after surgery for necrotising enterocolitis in human infants. *J Pediatr Gastroenterol Nutr.* 2009;49(1):31-41.
137. Clark JA, Doelle SM, Halpern MD, Saunders TA, Holubec H, Dvorak K, et al. Intestinal barrier failure during experimental necrotizing enterocolitis: protective effect of EGF treatment. *Am J Physiol Gastrointest Liver Physiol.* 2006;291(5):G938-49.
138. Li B, Hock A, Wu RY, Minich A, Botts SR, Lee C, et al. Bovine milk-derived exosomes enhance goblet cell activity and prevent the development of experimental necrotizing enterocolitis. *PLoS One.* 2019;14(1):e0211431.
139. Martin NA, Mount Patrick SK, Estrada TE, Frisk HA, Rogan DT, Dvorak B, et al. Active transport of bile acids decreases mucin 2 in neonatal ileum: implications for development of necrotizing enterocolitis. *PLoS One.* 2011;6(12):e27191.
140. Lock JY, Carlson TL, Yu Y, Lu J, Claud EC, Carrier RL. Impact of Developmental Age, Necrotizing Enterocolitis Associated Stress, and Oral Therapeutic Intervention on Mucus Barrier Properties. *Sci Rep.* 2020;10(1):6692.
141. Miller J, Tonkin E, Damarell RA, McPhee AJ, Sukanuma M, Sukanuma H, et al. A Systematic Review and Meta-Analysis of Human Milk Feeding and Morbidity in Very Low Birth Weight Infants. *Nutrients.* 2018;10(6):707.
142. Villamor-Martínez E, Pierro M, Cavallaro G, Mosca F, Villamor E. Mother's Own Milk and Bronchopulmonary Dysplasia: A Systematic Review and Meta-Analysis. *Frontiers in pediatrics.* 2019;7:224-.
143. Ottolini KM, Andescavage N, Kapse K, Jacobs M, Limperopoulos C. Improved brain growth and microstructural development in breast milk-fed very low birth weight premature infants. *Acta Paediatr.* 2020;109(8):1580-7.
144. Blesa M, Sullivan G, Anblagan D, Telford EJ, Quigley AJ, Sparrow SA, et al. Early breast milk exposure modifies brain connectivity in preterm infants. *Neuroimage.* 2019;184:431-9.

145. Fallon EM, Nehra D, Potemkin AK, Gura KM, Simpser E, Compher C, et al. A.S.P.E.N. clinical guidelines: nutrition support of neonatal patients at risk for necrotizing enterocolitis. *JPEN J Parenter Enteral Nutr.* 2012;36(5):506-23.
146. EFCNI, Embleton ND, Koletzko B et al., European Standards of Care for Newborn Health: Establishment of enteral feeding in preterm infants. 2018.
147. Thai JD, Gregory KE. Bioactive Factors in Human Breast Milk Attenuate Intestinal Inflammation during Early Life. *Nutrients.* 2020;12(2).
148. Andreas NJ, Kampmann B, Mehring Le-Doare K. Human breast milk: A review on its composition and bioactivity. *Early Hum Dev.* 2015;91(11):629-35.
149. Chatterton DE, Nguyen DN, Bering SB, Sangild PT. Anti-inflammatory mechanisms of bioactive milk proteins in the intestine of newborns. *Int J Biochem Cell Biol.* 2013;45(8):1730-47.
150. te Velde AA, Brull F, Heinsbroek SE, Meijer SL, Lutjohann D, Vreugdenhil A, et al. Effects of Dietary Plant Sterols and Stanol Esters with Low- and High-Fat Diets in Chronic and Acute Models for Experimental Colitis. *Nutrients.* 2015;7(10):8518-31.
151. Plat J, Baumgartner S, Vanmierlo T, Lütjohann D, Calkins KL, Burrin DG, et al. Plant-based sterols and stanols in health & disease: "Consequences of human development in a plant-based environment?". *Prog Lipid Res.* 2019;74:87-102.
152. Sprong RC, Schonewille AJ, van der Meer R. Dietary cheese whey protein protects rats against mild dextran sulfate sodium-induced colitis: role of mucin and microbiota. *J Dairy Sci.* 2010;93(4):1364-71.
153. Schaafsma G. Health issues of Whey Proteins: 3. Gut Health Promotion. *Current Topics in Nutraceutical Research.* 2007;5(1):29-34.
154. Hering NA, Andres S, Fromm A, van Tol EA, Amasheh M, Mankertz J, et al. Transforming growth factor- β , a whey protein component, strengthens the intestinal barrier by upregulating claudin-4 in HT-29/B6 cells. *J Nutr.* 2011;141(5):783-9.
155. Cregan MD, De Mello TR, Kershaw D, McDougall K, Hartmann PE. Initiation of lactation in women after preterm delivery. *Acta Obstet Gynecol Scand.* 2002;81(9):870-7.
156. Wilson E, Edstedt Bonamy A-K, Bonet M, Toome L, Rodrigues C, Howell EA, et al. Room for improvement in breast milk feeding after very preterm birth in Europe: Results from the EPICE cohort. *Matern Child Nutr.* 2018;14(1):e12485.
157. Heller N, Rüdiger M, Hoffmeister V, Mense L. Mother's Own Milk Feeding in Preterm Newborns Admitted to the Neonatal Intensive Care Unit or Special-Care Nursery: Obstacles, Interventions, Risk Calculation. *Int J Environ Res Public Health.* 2021;18(8).
158. Breastfeeding and the use of human milk. *Pediatrics.* 2012;129(3):e827-41.
159. Haiden N, Ziegler EE. Human Milk Banking. *Ann Nutr Metab.* 2016;69 Suppl 2:8-15.
160. Quigley M, Embleton ND, McGuire W. Formula versus donor breast milk for feeding preterm or low birth weight infants. *The Cochrane database of systematic reviews.* 2019;7(7):Cd002971.
161. Cohen M, Steffen E, Axelrod R, Patel SN, Toczylowski K, Perdon C, et al. Availability of Donor Human Milk Decreases the Incidence of Necrotizing Enterocolitis in VLBW Infants. *Adv Neonatal Care.* 2020.
162. Colaizzi TT. Effects of milk banking procedures on nutritional and bioactive components of donor human milk. *Semin Perinatol.* 2021:151382.
163. Sánchez Luna M, Martin SC, Gómez-de-Orgaz CS. Human milk bank and personalized nutrition in the NICU: a narrative review. *Eur J Pediatr.* 2021;180(5):1327-33.
164. Valentine CJ, Morrow G, Reisinger A, Dingess KA, Morrow AL, Rogers LK. Lactational Stage of Pasteurized Human Donor Milk Contributes to Nutrient Limitations for Infants. *Nutrients.* 2017;9(3).
165. Cormontagne D, Rigourd V, Vidic J, Rizzotto F, Bille E, Ramarao N. *Bacillus cereus* Induces Severe Infections in Preterm Neonates: Implication at the Hospital and Human Milk Bank Level. *Toxins (Basel).* 2021;13(2).
166. Juber BA, Elgin TG, Fricke EM, Gong H, Reese J, McElroy SJ. A Murine Model of Fetal Exposure to Maternal Inflammation to Study the Effects of Acute Chorioamnionitis on Newborn Intestinal Development. *Journal of visualized experiments : JoVE.* 2020(160).
167. Maxwell JR, Yellowhair TR, Davies S, Rogers DA, McCarron KL, Savage DD, et al. Prenatal Alcohol Exposure and Chorioamnionitis Results in Microstructural Brain Injury in a Preclinical Investigation. *Ann Pediatr Res.* 2020;4(1).

168. Wang B, Navath RS, Menjoge AR, Balakrishnan B, Bellair R, Dai H, et al. Inhibition of bacterial growth and intramniotic infection in a guinea pig model of chorioamnionitis using PAMAM dendrimers. *Int J Pharm.* 2010;395(1-2):298-308.
169. Shi Z, Vasquez-Vivar J, Luo K, Yan Y, Northington F, Mehrmohammadi M, et al. Ascending Lipopolysaccharide-Induced Intrauterine Inflammation in Near-Term Rabbits Leading to Newborn Neurobehavioral Deficits. *Dev Neurosci.* 2018;40(5-6):534-46.
170. Nguyen DN, Thymann T, Goericke-Pesch SK, Ren S, Wei W, Skovgaard K, et al. Prenatal Intra-Amniotic Endotoxin Induces Fetal Gut and Lung Immune Responses and Postnatal Systemic Inflammation in Preterm Pigs. *Am J Pathol.* 2018;188(11):2629-43.
171. Rueda CM, Presicce P, Jackson CM, Miller LA, Kallapur SG, Jobe AH, et al. Lipopolysaccharide-Induced Chorioamnionitis Promotes IL-1-Dependent Inflammatory FOXP3+ CD4+ T Cells in the Fetal Rhesus Macaque. *J Immunol.* 2016;196(9):3706-15.
172. Lu P, Sodhi CP, Jia H, Shaffiey S, Good M, Branca MF, et al. Animal models of gastrointestinal and liver diseases. Animal models of necrotizing enterocolitis: pathophysiology, translational relevance, and challenges. *Am J Physiol Gastrointest Liver Physiol.* 2014;306(11):G917-28.
173. Ziegler A, Gonzalez L, Bliklager A. Large Animal Models: The Key to Translational Discovery in Digestive Disease Research. *Cell Mol Gastroenterol Hepatol.* 2016;2(6):716-24.
174. Wolfs TG, Jellema RK, Turrisi G, Becucci E, Buonocore G, Kramer BW. Inflammation-induced immune suppression of the fetus: a potential link between chorioamnionitis and postnatal early onset sepsis. *J Matern Fetal Neonatal Med.* 2012;25 Suppl 1:8-11.
175. Paton MCB, McDonald CA, Allison BJ, Fahey MC, Jenkin G, Miller SL. Perinatal Brain Injury As a Consequence of Preterm Birth and Intrauterine Inflammation: Designing Targeted Stem Cell Therapies. *Front Neurosci.* 2017;11:200.
176. Cheah FC, Pillow JJ, Kramer BW, Polglase GR, Nitsos I, Newnham JP, et al. Airway inflammatory cell responses to intra-amniotic lipopolysaccharide in a sheep model of chorioamnionitis. *Am J Physiol Lung Cell Mol Physiol.* 2009;296(3):L384-93.
177. Trahair J, Robinson P. The development of the ovine small intestine. *Anat Rec.* 1986;214(3):294-303.
178. Trahair JF, Robinson PM. An integrated model for intestinal development in the fetal sheep. *Reprod Nutr Dev.* 1987;27(4):849-57.
179. Flores TJ, Nguyen VB, Widdop RE, Sutherland MR, Polglase GR, Abud HE, et al. Morphology and Function of the Lamb Ileum following Preterm Birth. *Frontiers in pediatrics.* 2018;6:8.
180. Trahair JF, Robinson PM. Perinatal development of the small intestine of the sheep. *Reprod Nutr Dev.* 1986;26(6):1255-63.
181. Tian R, Liu SX, Williams C, Soltau TD, Dimmitt R, Zheng X, et al. Characterization of a necrotizing enterocolitis model in newborn mice. *Int J Clin Exp Med.* 2010;3(4):293-302.
182. Mihi B, Lanik WE, Gong Q, Good M. A Mouse Model of Necrotizing Enterocolitis. *Methods Mol Biol.* 2021;2321:101-10.
183. Zani A, Cordischi L, Cananzi M, De Coppi P, Smith VV, Eaton S, et al. Assessment of a neonatal rat model of necrotizing enterocolitis. *Eur J Pediatr Surg.* 2008;18(6):423-6.
184. Erdener D, Bakirtas F, Alkanat M, Mutaf I, Habif S, Bayindir O. Pentoxifylline does not prevent hypoxia/reoxygenation-induced necrotizing enterocolitis. An experimental study. *Biol Neonate.* 2004;86(1):29-33.
185. Waligora-Dupriet AJ, Dugay A, Auzeil N, Nicolis I, Rabot S, Huerre MR, et al. Short-chain fatty acids and polyamines in the pathogenesis of necrotizing enterocolitis: Kinetics aspects in gnotobiotic quails. *Anaerobe.* 2009;15(4):138-44.
186. Burrin D, Sangild PT, Stoll B, Thymann T, Buddington R, Marini J, et al. Translational Advances in Pediatric Nutrition and Gastroenterology: New Insights from Pig Models. *Annu Rev Anim Biosci.* 2020;8:321-54.
187. Namachivayam K, Blanco CL, MohanKumar K, Jagadeeswaran R, Vasquez M, McGill-Vargas L, et al. Smad7 inhibits autocrine expression of TGF- β 2 in intestinal epithelial cells in baboon necrotizing enterocolitis. *Am J Physiol Gastrointest Liver Physiol.* 2013;304(2):G167-80.
188. Sodhi C, Richardson W, Gribar S, Hackam DJ. The development of animal models for the study of necrotizing enterocolitis. *Dis Model Mech.* 2008;1(2-3):94-8.
189. Corrò C, Novellasdemunt L, Li VSW. A brief history of organoids. *Am J Physiol Cell Physiol.* 2020;319(1):C151-C65.

190. Fatehullah A, Tan SH, Barker N. Organoids as an in vitro model of human development and disease. *Nat Cell Biol.* 2016;18(3):246-54.
191. Kim J, Koo B-K, Knoblich JA. Human organoids: model systems for human biology and medicine. *Nat Rev Mol Cell Biol.* 2020;21(10):571-84.
192. Sato T, Vries RG, Snippert HJ, van de Wetering M, Barker N, Stange DE, et al. Single Lgr5 stem cells build crypt-villus structures in vitro without a mesenchymal niche. *Nature.* 2009;459(7244):262-5.
193. VanDussen KL, Marinsshaw JM, Shaikh N, Miyoshi H, Moon C, Tarr PI, et al. Development of an enhanced human gastrointestinal epithelial culture system to facilitate patient-based assays. *Gut.* 2015;64(6): 911-20.
194. Kozuka K, He Y, Koo-McCoy S, Kumaraswamy P, Nie B, Shaw K, et al. Development and Characterization of a Human and Mouse Intestinal Epithelial Cell Monolayer Platform. *Stem Cell Reports.* 2017;9(6): 1976-90.
195. Putker M, Millen R, Overmeer R, Driehuis E, Zandvliet M, Clevers H, et al. Medium-Throughput Drug- and Radiotherapy Screening Assay using Patient-Derived Organoids. *Journal of visualized experiments : JoVE.* 2021(170).
196. Brandenburg N, Hoehnel S, Kuttler F, Homicsko K, Ceroni C, Ringel T, et al. High-throughput automated organoid culture via stem-cell aggregation in microcavity arrays. *Nat Biomed Eng.* 2020;4(9):863-74.
197. Bédard P, Gauvin S, Ferland K, Caneparo C, Pellerin É, Chabaud S, et al. Innovative Human Three-Dimensional Tissue-Engineered Models as an Alternative to Animal Testing. *Bioengineering (Basel).* 2020;7(3):115.
198. Dedhia PH, Bertaux-Skeirik N, Zavros Y, Spence JR. Organoid Models of Human Gastrointestinal Development and Disease. *Gastroenterology.* 2016;150(5):1098-112.
199. Co JY, Margalef-Català M, Li X, Mah AT, Kuo CJ, Monack DM, et al. Controlling Epithelial Polarity: A Human Enteroid Model for Host-Pathogen Interactions. *Cell reports.* 2019;26(9):2509-20.e4.
200. Williamson IA, Arnold JW, Samsa LA, Gaynor L, DiSalvo M, Cocchiari JL, et al. A High-Throughput Organoid Microinjection Platform to Study Gastrointestinal Microbiota and Luminal Physiology. *Cell Mol Gastroenterol Hepatol.* 2018;6(3):301-19.
201. Liu Y, Chen YG. 2D- and 3D-Based Intestinal Stem Cell Cultures for Personalized Medicine. *Cells.* 2018;7(12).
202. Dotti I, Salas A. Potential Use of Human Stem Cell-Derived Intestinal Organoids to Study Inflammatory Bowel Diseases. *Inflamm Bowel Dis.* 2018.
203. Kip AM, Soons Z, Mohren R, Duivenvoorden AAM, Röth AAJ, Cillero-Pastor B, et al. Proteomics analysis of human intestinal organoids during hypoxia and reoxygenation as a model to study ischemia-reperfusion injury. *Cell Death Dis.* 2021;12(1):95.
204. Freire R, Ingano L, Serena G, Cetinbas M, Anselmo A, Sapone A, et al. Human gut derived-organoids provide model to study gluten response and effects of microbiota-derived molecules in celiac disease. *Sci Rep.* 2019;9(1):7029.
205. Ettayebi K, Crawford SE, Murakami K, Broughman JR, Karandikar U, Tenge VR, et al. Replication of human noroviruses in stem cell-derived human enteroids. *Science.* 2016;353(6306):1387-93.
206. Saxena K, Blutt SE, Ettayebi K, Zeng X-L, Broughman JR, Crawford SE, et al. Human Intestinal Enteroids: a New Model To Study Human Rotavirus Infection, Host Restriction, and Pathophysiology. *J Virol.* 2016;90(1):43.
207. Huang J, Zhou C, Zhou G, Li H, Ye K. Effect of *Listeria monocytogenes* on intestinal stem cells in the co-culture model of small intestinal organoids. *Microb Pathog.* 2021:104776.
208. Drost J, van Jaarsveld RH, Ponsioen B, Zimmerlin C, van Boxtel R, Buijs A, et al. Sequential cancer mutations in cultured human intestinal stem cells. *Nature.* 2015;521(7550):43-7.
209. Ares GJ, Buonpane C, Yuan C, Wood D, Hunter CJ. A Novel Human Epithelial Enteroid Model of Necrotizing Enterocolitis. *Journal of visualized experiments : JoVE.* 2019(146).
210. Buonpane C, Ares G, Yuan C, Schlegel C, Liebe H, Hunter CJ. Experimental Modeling of Necrotizing Enterocolitis in Human Infant Intestinal Enteroids. *J Invest Surg.* 2020:1-8.
211. Senger S, Ingano L, Freire R, Anselmo A, Zhu W, Sadreyev R, et al. Human Fetal-Derived Enterospheres Provide Insights on Intestinal Development and a Novel Model to Study Necrotizing Enterocolitis (NEC). *Cell Mol Gastroenterol Hepatol.* 2018;5(4):549-68.
212. Zietek T, Rath E, Haller D, Daniel H. Intestinal organoids for assessing nutrient transport, sensing and incretin secretion. *Sci Rep.* 2015;5:16831.

213. Zietek T, Giesbertz P, Ewers M, Reichart F, Weinmüller M, Urbauer E, et al. Organoids to Study Intestinal Nutrient Transport, Drug Uptake and Metabolism – Update to the Human Model and Expansion of Applications. *Front Bioeng Biotechnol.* 2020;8(1065).

Part I

**Enteral nutritional interventions and NEC:
the current state of evidence**

Chapter 2

Enteral feeding interventions in the prevention of necrotizing enterocolitis: a systematic review of experimental and clinical studies

I.H. de Lange, C. van Gorp, L.D. Eeftinck Schattenkerk, W.G. van Gemert,
J.P.M. Derikx, and T.G.A.M. Wolfs

Nutrients. 2021;13(5):1726

Abstract

Necrotizing enterocolitis (NEC), which is characterized by severe intestinal inflammation and in advanced stages necrosis, is a gastrointestinal emergency in the neonate with high mortality and morbidity. Despite advancing medical care, effective prevention strategies remain sparse. Factors contributing to the complex pathogenesis of NEC include immaturity of the intestinal immune defense, barrier function, motility and local circulatory regulation and abnormal microbial colonization. Interestingly, enteral feeding is regarded as an important modifiable factor influencing NEC pathogenesis. Moreover, breast milk, which forms the currently most effective prevention strategy, contains many bioactive components that are known to support neonatal immune development and promote healthy gut colonization. This systematic review describes the effect of different enteral feeding interventions on the prevention of NEC incidence and severity and the effect on pathophysiological mechanisms of NEC, in both experimental NEC models and clinical NEC. Besides, pathophysiological mechanisms involved in human NEC development are briefly described to give context for the findings of altered pathophysiological mechanisms of NEC by enteral feeding interventions.

Introduction

Necrotizing enterocolitis (NEC) is a multifactorial disease, characterized by severe intestinal inflammation and, in advancing disease, gut necrosis, that mainly affects premature neonates¹. Around 5 to 10% of very low birth weight (VLBW) infants develop NEC, with the highest incidence among neonates with an extremely low birth weight (ELBW)². Despite advancing medical care, NEC incidence has not substantially decreased over time, mainly due to increased early survival of neonates³⁻⁵. NEC mortality is inversely correlated with birth weight and generally ranges from 15% to 30%^{2,6}. However, case fatality can increase up to 50% for ELBW infants treated surgically^{6,7}. Being responsible for 10% of NICU deaths, NEC represents an important cause of death in this setting⁸. Moreover, infants that do recover from NEC suffer from several long-term morbidities such as growth retardation⁹, short bowel syndrome¹⁰, intestinal failure¹¹, intestinal failure-associated liver disease and neurodevelopmental delays¹². Although the precise healthcare costs of NEC are difficult to estimate¹³, the costs undoubtedly exceed those of matched controls, with estimates of around \$70,000 extra hospital costs for medical NEC and around \$180,000 for surgical NEC¹⁴. Moreover, life-long care for patients with morbidities following NEC will impose an even higher financial burden on both society and the individual patient¹⁵. NEC thus forms an important health issue that has high impact on the patient and its parents and also leads to a significant economic burden.

Due to its complex pathophysiology and fulminant nature, NEC treatment remains, despite advancing medical care, largely symptomatic¹. Moreover, effective prevention strategies are sparse¹. Factors contributing to the excessive intestinal inflammation in NEC include immaturity of the intestinal immune defense, barrier function, motility and local circulatory regulation and abnormal microbial colonization^{1,6}. Interestingly, NEC almost exclusively develops in infants that have been enterally fed and the NEC risk increases with delay of enteral feeding, indicating enteral feeding is an important target to modify NEC pathogenesis¹⁶⁻¹⁸. Breast milk contains many bioactive components that are known to shape neonatal (intestinal) immune development¹⁹ and promote healthy gut colonization²⁰, thereby preventing intestinal inflammation¹⁹. Consequently, although not completely effective, breast milk is highly protective against NEC development and is currently considered the most effective preventive strategy^{21,22}. Accordingly, several enteral feeding interventions that use donor breast milk or feeding components derived from breast milk have been studied over the past years as potential strategies for prevention of NEC^{1,23}. This systematic review aims to describe the effect of different enteral feeding interventions on the prevention of NEC incidence and severity and the effect on pathophysiological mechanisms of NEC (intestinal inflammation, systemic inflammation, intestinal barrier function, vascular dysfunction/hypoxia-ischemia/free radical formation, intestinal epithelial cell death/altered proliferation, microbial dysbiosis, disturbed digestion and absorption and enteric nervous system alterations), in both experimental NEC models and clinical NEC. Besides, pathophysiological mechanisms involved in human NEC development are briefly described to contextualize the findings of altered pathophysiological mechanisms of NEC by enteral feeding interventions.

Materials and methods

Search strategy

To identify all relevant publications, the electronic databases PubMed, Embase and the Cochrane library were searched to select records published from inception until December 2020 that studied the effect of enteral feeding interventions in the prevention of NEC incidence and severity or pathophysiological mechanisms of NEC. An overview of the performed searches can be found in **Supplementary Tables S2.1–S2.3**. Both single and hierarchical search terms (e.g., MESH) were used. General search terms for nutritional interventions as well as terms for specific nutritional interventions often used in the context of NEC (expert opinion) (alkaline phosphatase (ALPI), epidermal growth factor (EGF)/heparin-binding EGF-like growth factor (HB-EGF), erythropoietin (EPO), exosomes, gangliosides, glutamine, immunoglobulins, insulin like growth factor (IGF), milk fat globule membrane, oligosaccharides, osteopontin, platelet-activating factor acetylhydrolase (PAF-AH), polyunsaturated fatty acids (PUFA), transforming growth factor β (TGF β), vitamin A and vitamin D) were incorporated in the search. For the search in the Cochrane library, results were filtered as to only retrieve Cochrane reviews. Last, references of included studies were cross-checked for additional studies that did not emerge in the original search. No restrictions were applied on study design or language. Results from the different searches were combined and after automatic removal of duplicates, the remaining records were screened for eligibility. No review protocol was published.

Selection criteria

We included experimental animal studies (any experimental NEC model), RCTs and meta-analysis that reported on the effect of enteral feeding interventions on the prevention of NEC (incidence, severity (histological or clinical), NEC related mortality) or the prevention of pathophysiological mechanisms of NEC (intestinal inflammation, systemic inflammation, intestinal barrier function, vascular dysfunction/hypoxia-ischemia/free radical formation, intestinal epithelial cell death/altered proliferation, microbial dysbiosis, disturbed digestion and absorption and enteric nervous system alterations). Studies that did not relate to enteral feeding interventions as preventative treatment for NEC were excluded. Experimental studies with an enteral feeding intervention that started simultaneously with a NEC-inducing protocol were regarded as preventive. Studies that investigated intraperitoneal or intravenous administration were excluded (no enteral intervention). Regarding clinical studies, meta-analyses were included whenever possible. Meta-analyses of which a more recent or relevant (e.g., more studies included on NEC outcome) version was available, either by the same authors or different authors on the same subject, were excluded. RCTs were only included if: (1) a meta-analysis was not available or (2) the RCT was not included in a meta-analysis and was relatively large (N \geq 50% of infants included in the meta-analysis) or (3) the RCT reported the effect of enteral feeding interventions on one of the pathophysiological mechanisms of NEC. RCTs that were excluded because of their low sample size relative to an earlier published meta-analysis are displayed in **Supplementary Table S2.4**^{24–27}. Exclusion of these RCTs did not influence the findings and conclusions of this

systematic review. No narrative reviews, in vitro studies, research protocols, comments on original articles, guidelines or conference abstracts were included.

Selection process

Rayyan, online software enabling blind screening for reviewers²⁸, was used by to independent authors (I.H.d.L., C.v.G.) for article selection. Disagreements were solved by discussion. A third author was consulted in case consensus was not reached (T.G.A.M.W). In the first round, articles were screened based on title and abstract. In the second round, articles were full text screened.

Data extraction

Data was extracted by one author (I.H.d.L.) from the included publications and corresponding supplementary files. When in doubt, inclusion of data was discussed with a second author (C.v.G.). All data related to the outcomes of interest (NEC incidence/severity/mortality and the pathophysiological hallmarks of NEC) were included. Data were first clustered based on type of study (experimental animal study or human trial), a second clustering was applied based on outcome reported and the last clustering was based on type of enteral feeding intervention (fat-based, carbohydrate / sugar-based, protein / amino acid-based, hormone / growth factor / vitamin-based, probiotic interventions and other interventions) (**Figure 2.1**). Additional parameters extracted were author, year of publication, experimental NEC model used (experimental animal studies), type of study (human studies), sample size, in- and exclusion criteria (human studies), intervention and control, sample size/power calculation and (primary and secondary) outcomes studied. For experimental animal studies, data are reported for the enteral feeding intervention group(s) compared to an untreated NEC protocol exposed group. For human studies, data are reported for the enteral feeding interventions treated group compared to an untreated (placebo) group.

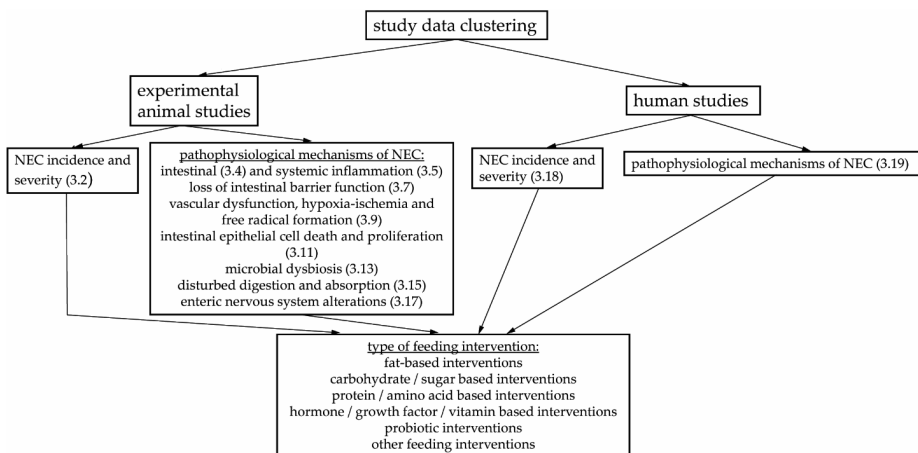


Figure 2.1 Overview of clustering of extracted data. The number in parentheses refers to the result section the data is incorporated in.

Risk of bias assessment

The methodological quality and risk of bias of the different included studies were assessed with the use of the SYRCLE's risk of bias tool²⁹ (experimental animal studies), the Jadad scoring system³⁰ (RCTs) and the AMSTAR measurement tool (meta-analyses)³¹. The assessment was performed by two independent authors (I.H.d.L and L.D.E.S.). Disagreements were resolved by discussion.

Certainty of evidence assessment

Certainty of evidence of the effect of enteral feeding interventions tested in clinical studies (RCTs and meta-analyses) on NEC incidence or mortality was assessed with the GRADE approach³². These interventions were scored for limitations in study design or execution (risk of bias), inconsistency of results, indirectness of evidence, imprecision and the risk of publication bias by two independent authors (I.H.d.L. and C.v.G.). Disagreements were resolved by discussion. The scores on individual assessment points were combined in an overall estimation of certainty of evidence. Certainty of evidence is reported as “high” (we are very confident that the true effect lies close to that of the estimate of the effect), “moderate” (we are moderately confident in the effect estimate: the true effect is likely to be close to the estimate of the effect, but there is a possibility that it is substantially different), “low” (our confidence in the effect estimate is limited: the true effect may be substantially different from the estimate of the effect) or “very low” (we have very little confidence in the effect estimate: the true effect is likely to be substantially different from the estimate of effect)³². Certainty of evidence was not scored for animal studies. Although a GRADE scoring system for animal studies has been suggested³³, implementation of this methodology is still in its infancy and many aspects needed to adequately assess certainty of evidence from animal studies, such as 95% confidence intervals (CI) and power calculations, are seldomly reported.

Results

Study characteristics

We identified a total number of 5883 records. After automatic removal of duplicates (1327 records), the remaining records (4573 records) were screened for eligibility (**Figure 2.2**). Of these articles, 4257 records were excluded in the first round. All of the remaining 316 articles could be retrieved. In the second round full-text screening, another 177 articles were excluded. An overview of the study characteristics of the included studies can be found in **Supplementary Table S2.5** (included experimental animal studies), **Supplementary Table S2.6** (included clinical trials), and **Supplementary Table S2.7** (included systematic reviews and meta-analyses). Whereas the risk of bias for the included animal studies (**Supplementary Table S2.8**) was in general unclear due to poor reporting of methodological details in these articles, the risk of bias for included RCTs (**Supplementary Table S2.9**) and meta-analyses (**Supplementary Table S2.10**) was predominantly low.

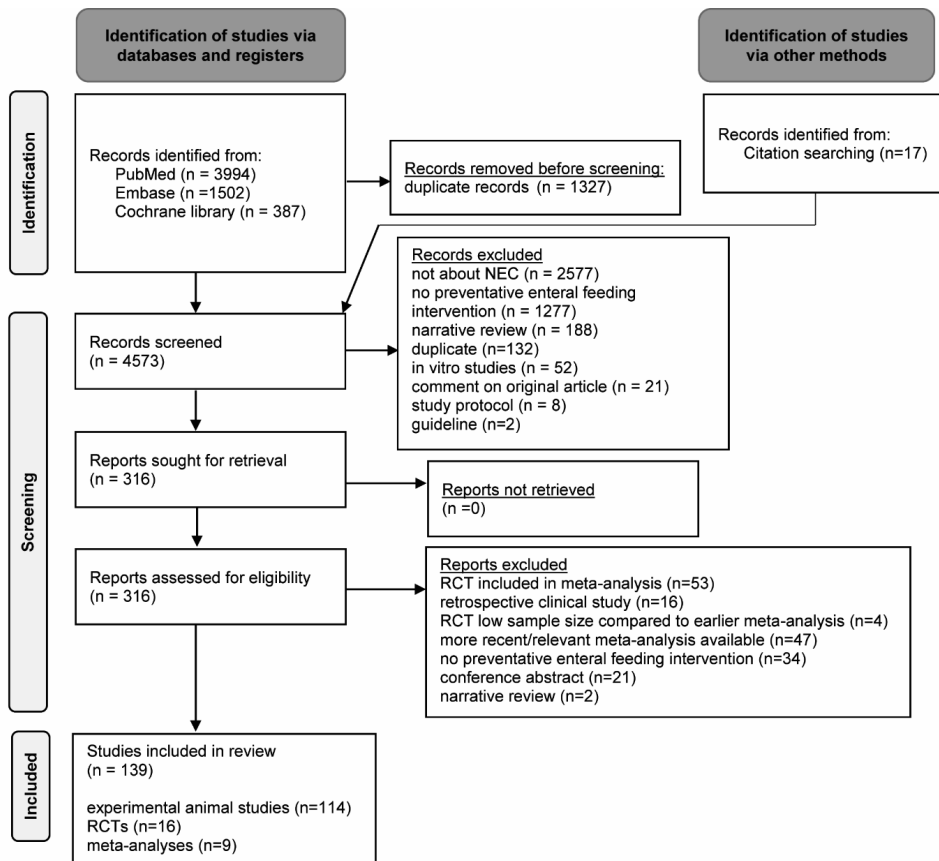


Figure 2.2 Flowchart of the article selection. Adapted from the PRISMA 2020 statement. Page MJ, McKenzie JE, Bossuyt PM, Boutron I, Hoffmann TC, Mulrow CD, Shamseer L, Tetzlaff JM, Akl EA, Brennan SE, et al. The PRISMA 2020 statement: An updated guideline for reporting systematic reviews. *BMJ* 2021, 372, n71.³⁴

Enteral feeding interventions affecting NEC incidence and severity in animal studies

Evidence of successful NEC prevention through enteral nutritional interventions in experimental animal models of NEC is abundantly present. In these models, many enteral nutritional interventions have been shown to reduce NEC incidence (**Table 2.1**), NEC severity (**Table 2.2**), clinical disease score or signs/symptoms (**Table 2.3**) and to improve survival (**Table 2.4**). Studies that did not report statistically significant preventative effects of enteral feeding interventions on NEC incidence, histological injury scores, clinical disease score or signs and symptoms or survival are summarized in **Table 2.5**. Importantly, supplementation of bovine lactoferrin increased the NEC severity score and elevated

intestinal apoptosis and inflammation in a preterm pig NEC model^{35,36}, demonstrating that postulated beneficial enteral feeding interventions can also be harmful. This harmful effect may be caused by activation of the nuclear factor kappa-light-chain-enhancer of activated B cells (NFκβ) pathway and stimulation of interleukin 8 (IL8) release by enterocytes by a high dose of lactoferrin³⁵. In addition, supplementation of formula with HB-EGF in a rat NEC model induced a dose dependent reduction of NEC incidence, with a therapeutic effect of moderate HB-EGF dosages that was not observed with either a low or a high HB-EGF dose³⁷. This example highlights the importance of understanding the dose dependent working mechanisms of protective breast milk components. Some studies already provide mechanistic insight in the potential working mechanisms involved. For instance, the preventive effect of HMO was abolished in the presence of an inhibitor of the endoplasmic reticulum (ER) stress chaperone protein disulfide isomerase (PDI), suggesting PDI function is necessary for enteral HMO induced reduction of NEC incidence³⁸. The protective effects of *Lactobacillus rhamnosus* on NEC severity score are toll like receptor 9 (TLR9) signaling dependent, as protective effects disappeared in TLR9 knock-down animals³⁹. In addition, the protective effects of enteral administration of amniotic fluid in a mouse NEC model were demonstrated to be largely dependent on EGFR signaling, as the preventative effects mostly disappeared in the presence of the EGFR inhibitor cetuximab and with the use of amniotic fluid that was depleted of EGF⁴⁰. Besides the supplemented substance and dose, timing and duration of the intervention are important. Addition of HB-EGF to all feeds, four feeds or two feeds per day reduced NEC incidence in a rat NEC model, while this was not the case when HB-EGF was only added to one feed per day⁴¹. In contrast to enteral HMO administration that was started within 24 h after birth and was continued during the duration of the study, enteral HMO administration that was started after the first 24 h or only given in the first 24 h did not result in improved histological NEC scores in a rat NEC model⁴². Similarly, enteral administration of HB-EGF successfully reduced NEC incidence when administration started within 12 h after birth, but not when supplementation was only initiated at or after 24 h⁴¹. Another interesting finding is that maternal feeding of a diet enriched with docosahexaenoic acid (DHA) or eicosapentaenoic acid (EPA) during pregnancy reduced NEC incidence in the offspring in a mouse NEC model⁴³, indicating that the fetus can already be targeted prenatally with a nutritional intervention to prevent NEC.

Table 2.1 Enteral feeding interventions reducing NEC incidence in experimental animal models of NEC.

Fat-based interventions	AA and DHA ⁴⁴ Egg phospholipids ⁴⁴ PUFA ⁴⁵ BCFA ⁴⁶ Pomegranate seed oil ⁴⁷ MFGM ⁴⁸ DHA or EPA maternal intervention during pregnancy ⁴³
Carbohydrate/sugar-based Interventions	HMO ⁴⁹ GD3 ⁵⁰
Protein/amino acid-based interventions	Lactadherin ⁵¹ rPAF-AH ⁵²
Hormone/growth factor/vitamin-based interventions	EGF ^{37,41,53-56} HB-EGF ^{37,41,57-62} HGF ⁶³ TGF- β 1 ⁶⁴ IGF1 ⁶⁵ EPO ⁶⁶
Probiotic interventions	<i>Lactobacillus reuteri</i> DSM 17938 ⁶⁷⁻⁷⁰ <i>Lactobacillus reuteri</i> ATCC PTA 4659 ⁶⁸ <i>Lactobacillus reuteri</i> biofilm on unloaded microspheres ^{71,72} <i>Lactobacillus reuteri</i> biofilm on MRS loaded microspheres ⁷¹ <i>Lactobacillus reuteri</i> biofilm on sucrose loaded microspheres ⁷² <i>Lactobacillus reuteri</i> biofilm on maltose loaded microspheres ⁷² <i>Bifidobacterium bifidum</i> OLB6378 ^{73,74} <i>Bifidobacterium infantis</i> ⁷⁵ <i>Bifidobacterium adolescentis</i> ⁷⁶ probiotic mixture (<i>Bifidobacterium animalis</i> DSM15954, <i>Lactobacillus acidophilus</i> DSM13241, <i>Lactobacillus casei</i> ATCC55544, <i>Lactobacillus pentosus</i> DSM14025 and <i>Lactobacillus plantarum</i> DSM13367) ⁷⁷
Other interventions	Amniotic fluid ⁶³ Human breast milk extracellular vesicles ⁷⁸ Berberine ⁷⁹ Surfactant protein a ⁸⁰ Human β -defensin-3 ⁸¹

AA, arachidonic acid; DHA, docosahexaenoic acid; PUFA, polyunsaturated fatty acids; BCFA, branched chain fatty acids; MFGM, milk fat globule membrane; EPA, eicosapentaenoic acid; HMO, human milk oligosaccharides; GD3, ganglioside D3; rPAF-AH, recombinant platelet-activating factor acetylhydrolase; EGF, epidermal growth factor; HB-EGF, hemoglobin-binding EGF-like growth factor; HGF, hepatocyte growth factor; TGF- β 1, transforming growth factor β 1, IGF1, insulin-like growth factor 1.

Table 2.2 Enteral feeding interventions improving histological injury scores in experimental animal models of NEC.

Fat-based interventions	Fish oil (rich in n-3 PUFA) ^{82,83} MPL ⁸⁴ MFGM ⁴⁸ Very low fat diet ⁸⁵ Reduced long chain triacylglycerol diet (considered pre-digested) ⁸⁵ Pomegranate seed oil ⁴⁷
Carbohydrate/sugar-based interventions	HMO ^{38,42,49,86-90} Neutral HMO (no sialic acids) ⁴² -2 HMO (two sialic acids) ⁴² DSLNT (HMO) ⁴² DSLNT (synthetic disialyl glycan) ^{89,90} DS'LNnT (synthetic disialyl glycan) ^{89,90} 2'-FL ^{87,91,92} 6'-SL ⁹² 2'-FL and 6'-SL ^{42,92} Sialylated HMO ⁹³ Sialylated GOS ⁸⁷ GD3 ⁵⁰ Hyaluronan 35 kD ⁹⁴
Protein/amino acid-based interventions	L-Glutamine/glutamine ^{84,95-97} Arginine ^{98,99} L-Carnitine ⁹⁹ N-Acetylcysteine ⁸⁵ Lactadherin ⁵¹ OPN ¹⁰⁰ Lactoferrin ¹⁰¹ IAP ^{102,103}
Hormone/growth factor/vitamin-based interventions	EGF ^{53,54,56} Recombinant EGF from soybean extract ¹⁰⁴ HB-EGF ^{41,58-60,62,105,106} HGF ⁶³ relaxin ¹⁰⁷ TGF- β 1 ⁶⁴ TGF- β 2 ¹⁰⁸ ATRA ^{109,110} Vitamin A ¹¹¹ Vitamin D ¹¹²
Probiotic interventions	<i>Bacteroides fragilis</i> ZY-312 ¹¹³ <i>Lactobacillus reuteri</i> DSM 17938 ^{68,69} <i>Lactobacillus reuteri</i> ATCC PTA 4659 ⁶⁸ <i>Lactobacillus reuteri</i> biofilm on unloaded microspheres ^{71,72} <i>Lactobacillus reuteri</i> biofilm on MRS loaded microspheres ⁷¹ <i>Lactobacillus reuteri</i> biofilm on sucrose loaded microspheres ⁷² <i>Lactobacillus reuteri</i> biofilm on maltose loaded microspheres ⁷² <i>Bifidobacterium microcapsules</i> ¹¹⁴ <i>Bifidobacterium mixture</i> ¹¹⁵ <i>Bifidobacterium adolescentis</i> ⁷⁶ <i>Bifidobacterium infantis</i> ¹¹⁶ <i>Bifidobacterium bifidum</i> OLB6378 ⁷⁴ <i>Bifidobacterium breve</i> M-16V ¹¹⁷

Table 2.2 (continued)

	<i>Lactobacillus rhamnosus</i> HN001 (live) ³⁹ <i>Lactobacillus rhamnosus</i> HN001 (dead) ³⁹ <i>Lactobacillus rhamnosus</i> isolated DNA ³⁹ Probiotic mixture (<i>Bifidobacterium animalis</i> DSM15954, <i>Lactobacillus acidophilus</i> DSM13241, <i>Lactobacillus casei</i> ATCC55544, <i>Lactobacillus pentosus</i> DSM14025 and <i>Lactobacillus</i> <i>plantarum</i> DSM13367) ⁷⁷ CpG-DNA ³⁹ Bovine milk exosomes ¹¹⁸ Native human breast milk exosomes ^{78,119} Pasteurized human breast milk exosomes ¹¹⁹ Preterm human breast milk exosomes ¹²⁰ Ginger ¹²¹ Fennel seed extracts ¹²² Amniotic fluid ^{40,63,123} Curcumin ¹²⁴ Sesamol ¹²⁵ Astragaloside iv ¹²⁶ Resveratrol ¹²⁷ Berberine ⁷⁹ Surfactant protein a ⁸⁰ Human β -defensin-3 ⁸¹
--	---

PUFA, polyunsaturated fatty acids; MPL milk polar lipids; MFGM, milk fat globule membrane; HMO, human milk oligosaccharides; DSLNT, disialyllacto-N-tetraose; 2'-FL, 2'-fucosyllactose; 6'-SL, 6'-sialyllactose; GOS: galacto-oligosaccharides; GD3, ganglioside D3; OPN, osteopontin; EGF, epidermal growth factor; HB-EGF, hemoglobin-binding EGF-like growth factor; HGF, hepatocyte growth factor; TGF- β 1, transforming growth factor β 1; TGF- β 2, transforming growth factor β 2; ATRA, all-*trans* retinoic acid.

Table 2.3 Enteral feeding interventions reducing clinical disease score or signs and symptoms in experimental animal models of NEC.

Fat-based interventions	DHA and EPA ⁸³ MFGM ⁴⁸ Very low fat diet ⁸⁵ Reduced long chain triacylglycerol diet (considered pre-digested) ⁸⁵ MPL ⁸⁴
carbohydrate/sugar based interventions	2'-FL ^{91,92} 6'-SL ⁹² 2'-FL and 6'-SL ⁹² FOS ¹²⁸ GD3 ⁵⁰
Protein/amino acid based interventions	Lactadherin ⁵¹ CGMP ¹²⁹ OPN ¹²⁹
Hormone/growth factor/vitamin based interventions	EGF ⁵⁴ HB-EGF ⁵⁸ IGF1 ⁶⁵ Vitamin D ¹¹² Relaxin ¹⁰⁷

Table 2.3 (continued)

Probiotic interventions	<i>Lactobacillus reuteri</i> DSM17938 ⁷⁰ <i>Bifidobacterium infantis-longum</i> strain CUETM 89-215 ¹³⁰ <i>Bifidobacterium adolescentis</i> ⁷⁶ <i>Bacteroides fragilis</i> ZY-312 ¹¹³ <i>Lactobacillus rhamnosus</i> HN001 (live) ³⁹ <i>Lactobacillus rhamnosus</i> HN001 (dead) ³⁹ <i>Lactobacillus rhamnosus</i> isolated DNA ³⁹
Other interventions	Ginger ¹²¹ Fennel seed extracts ¹²² Amniotic fluid ¹²³ Sesamol ¹²⁵ Human β -defensin-3 ⁸¹

DHA, docosahexaenoic acid; EPA, eicosapentaenoic acid; MFGM, milk fat globule membrane; MPL milk polar lipids; 2'-FL, 2'-fucosyllactose; 6'-SL, 6'-sialyllactose; GD3, ganglioside D3; CGMP, caseinoglycomacropeptide; OPN, osteopontin; EGF, epidermal growth factor; HB-EGF, hemoglobin-binding EGF-like growth factor; IGF1, insulin-like growth factor 1.

Table 2.4 Enteral feeding interventions improving survival in experimental animal models of NEC.

Fat-based interventions	PUFA ⁴⁵ MFGM ⁴⁸
Carbohydrate/sugar-based interventions	HMO ^{42,49,88} Hyaluronan 35 kD ⁹⁴
Protein/amino acid-based interventions	Lactadherin ⁵¹ Lysozyme ¹³¹ rPAF-AH ⁵²
Hormone/growth factor/vitamin-based interventions	HB-EGF ^{41,58,59,62,105}
Probiotic interventions	<i>Bacteroides fragilis</i> ZY-312 ¹¹³ <i>Lactobacillus reuteri</i> DSM 17938 ^{68,69,132} <i>Lactobacillus reuteri</i> ATCC PTA 4659 ⁶⁸ <i>Lactobacillus reuteri</i> biofilm on sucrose loaded microspheres ⁷² <i>Lactobacillus reuteri</i> biofilm on maltose loaded microspheres ⁷² <i>Bifidobacterium adolescentis</i> ⁷⁶ <i>Bifidobacterium infantis</i> ⁷⁵ <i>Bifidobacterium breve</i> M-16V ¹¹⁷
Other interventions	Surfactant protein A ⁸⁰ Human β -defensin-3 ⁸¹

PUFA, polyunsaturated fatty acids; MFGM, milk fat globule membrane; HMO, human milk oligosaccharides; rPAF-AH, recombinant platelet-activating factor acetylhydrolase; HB-EGF, hemoglobin-binding EGF-like growth factor.

Table 2.5 Overview of studies that did not report statistically significant preventative effects of enteral feeding interventions on NEC incidence, histological injury scores, clinical disease scores or signs and symptoms or survival in experimental animal models of NEC.

NEC Incidence	
Carbohydrate/sugar-based interventions	2'-FL ¹³³ Gangliosides ¹⁰⁰ SL ¹⁰⁰ Lactose ⁹² Mixture of 4 HMO ¹³⁴ Mixture of 25 HMO ¹³⁴ IFOS ⁴⁹
Protein/amino acid-based interventions	OPN ^{100,129} CGMP ¹²⁹ Bovine lactoferrin ^{35,36}
Probiotic interventions	<i>Lactobacillus reuteri</i> DSM 20016 ^{71,72}
Other interventions	amniotic fluid ¹²³
NEC histological injury scores	
Fat-based interventions	
Carbohydrate/sugar-based interventions	2'-FL ¹³³ GOS ^{42,89} Lactose ³⁸ 0 HMO (no sialic acids) ⁴² -1 HMO (one sialic acid) ⁴² -3 HMO (three sialic acids) ⁴² -4 HMO (four sialic acids) ⁴² Mixture of 4 HMO ¹³⁴ Mixture of 25 HMO ¹³⁴ 3'''-sLNnT ⁸⁹ GD3 ⁸⁹ DSLac ⁸⁹ Neu5GC-DS'LNT ⁹⁰ DS'LNT ⁹⁰ DSTa ⁹⁰ DSGalB ⁹⁰ Gangliosides ¹⁰⁰ SL ¹⁰⁰
Protein/amino acid-based interventions	Bovine lactoferrin ^{35,36} (even higher score for ³⁶) OPN ¹²⁹ CGMP ¹²⁹
Probiotic interventions	<i>Lactobacillus reuteri</i> DSM 20016 ⁷¹
NEC clinical disease score or signs and symptoms	
Fat-based interventions	BCFA ⁴⁶
carbohydrate/sugar based interventions	Lactose ⁹² HMO ^{38,42} Mixture of four HMO ¹³⁴ Mixture of 25 HMO ¹³⁴ 2'-FL ¹³³ GOS/FOS ^{135,136} GOS ⁴²
Protein/amino acid-based interventions	Glutamine ⁹⁶ OPN ¹²⁹ CGMP ¹²⁹
Probiotic interventions	<i>Saccharomyces Boulardii</i> ^{135,136}
Other interventions	Resveratrol ¹²⁷

Table 2.5 (continued)

NEC survival	
Fat-based interventions	Pomegranate seed oil ⁴⁷ DHA ¹³¹ DHA or EPA maternal intervention during pregnancy ⁴³
Carbohydrate/sugar-based Interventions	GOS/FOS ¹³⁵ GOS ⁴² IFOS ⁴⁹
Hormone/growth factor/vitamin-based interventions	EGF ^{104,137}
Probiotic interventions	<i>Saccharomyces boulardii</i> ¹³⁵ <i>Lactobacillus reuteri</i> DSM 20016 ⁷² <i>Lactobacillus reuteri</i> biofilm on unloaded microspheres ⁷²

DHA, docosahexaenoic acid; EPA, eicosapentaenoic acid; BCFA, branched chain fatty acids; HMO, human milk oligosaccharides; 2'-FL, 2'-fucosyllactose; SL, sialic acids; GOS, galacto-oligosaccharides; FOS, fructo-oligosaccharides; IFOS, infant formula oligosaccharides; GD3, ganglioside D3; EGF, epidermal growth factor; DSLac, disialyllactose; DSTa, disialyl T-antigen tetraose; 3'''-sLNnt, 3'''-sialyllacto-N-neotetraose; DSGalB, disialyl galactobiose; DS'LNnt, a2-6-linked disialyllacto-N-neotetraose; DS'LNT, a2-6-linked disialyllacto-N-tetraose; CGMP: caseinoglycomacropeptide; OPN: osteopontin.

NEC pathophysiology: intestinal and systemic inflammation

Both intestinal and systemic inflammation are essential hallmarks of NEC pathophysiology. Acute NEC is characterized by increased intestinal expression of various cytokines, such as interleukin 1 α (IL1 α)¹³⁸, IL1 β ¹³⁹, TNF α ¹³⁹, IL6¹⁴⁰ and IL10¹⁴⁰, whereas TGF- β tissue expression is decreased¹⁰⁸. Intestinal cytokine levels normalize after recovery from NEC¹³⁹. NEC is characterized by an increased number of polymorphonuclear leukocytes¹⁴¹, neutrophil extracellular trap activation and release¹⁴², and an increased number of macrophages in the intestine¹⁴¹. In addition, mRNA levels of C-X-C motif chemokine 5 (CXCL5), a chemokine stimulating influx of neutrophils were elevated in intestinal samples from infants with NEC compared to controls¹⁴¹. Moreover, a reduced proportion of functional regulatory T cells (Treg) in the intestine of NEC patients was observed compared to age-matched controls that was accompanied by a pro-inflammatory cytokine expression profile characteristic of inhibited Treg development¹⁴³. As the proportion of Treg was restored after NEC recovery, it is likely that the strong inflammatory response during NEC temporarily inhibits Treg development¹⁴³. In addition, an increased frequency of a subset of Treg, namely C-C motif chemokine receptor 9 (CCR9)-positive interleukin 17 (IL-17) producing Treg with strongly impaired immunosuppressive capacities, was found in peripheral blood during NEC and the conversion of CCR9+ Treg into this IL-17 producing subset was promoted by IL-6¹⁴⁴. Interestingly, in mice, treatment with anti-interleukin 6 receptor antibodies ameliorated NEC mortality, severity and morbidity and restored the balance between Treg and Th17 producing cells in peripheral blood, indicating a role for both cell types in the pathogenesis of NEC¹⁴⁴. Altered expression and/or signaling of pattern recognition receptors (PRRs) is clearly involved in the pathogenesis of NEC¹⁴⁵. Firstly, the role of toll like receptor 4 (TLR4) and some other TLRs, have been studied intensively in NEC pathogenesis¹⁴⁶. In small intestinal specimen from infants with NEC, an increased mRNA expression^{147,148} and increased protein levels^{148,149} of TLR4 were found. Protein levels of TLR9 were reduced in the

intestine of infants with NEC¹⁴⁹. TLR4 knockout mice¹⁴⁷ as well as mice with a non-functioning mutation in TLR4¹⁴⁸ are protected against experimental NEC. Reduced intestinal mRNA levels of negative regulators of TLR4 signaling (single IL1 receptor-related protein (SIGIRR), Toll-interacting protein (TOLLIP) and A20) have been observed in NEC¹⁵⁰ and mutations causing a loss of function of SIGIRR are associated with NEC¹⁵¹. However, a prospective multicenter cohort study failed to show an association between genetic variants of TLR4, toll like receptor 2 (TLR2), toll like receptor 5 (TLR5), TLR9 or IL1 receptor-associated kinase 1 (IRAK1) and NEC¹⁵². Moreover, we previously reported that Myeloid Differentiation factor 2 (MD-2) could not be detected in the intestine or immune cells of infants with NEC, suggesting impaired LPS signaling¹⁵³. This was confirmed by another study observing reduced protein levels of MD-2 and also TLR4 in the intestine of two NEC patients compared to control tissue from stoma closure of these two patients¹⁵⁴. Last, nucleotide-binding oligomerisation domain (NOD)-like receptors are likely to be involved in NEC pathogenesis¹⁴⁵. Mutations in the NOD2 gene, leading to loss of function, have been associated with an increased risk of severe NEC requiring surgery^{151,155}.

In addition to intestinal inflammation, infants with NEC have higher blood levels of pro-inflammatory mediators PAF¹⁵⁶, tumor necrosis factor α (TNF α), interleukin 6 (IL6)^{157,158} and IL8^{157,158} and the anti-inflammatory cytokine interleukin 10 (IL10)¹⁵⁸. Moreover, blood levels of IL6¹⁵⁸, IL8^{158,159} and interleukin 1 β (IL1 β)¹⁵⁹ as well as interleukin 1 receptor antagonist (IL1ra)¹⁵⁹ and IL10¹⁵⁹ are higher in severe NEC compared to mild or moderate NEC¹⁵⁹. Higher blood levels of interleukin 2 (IL2) and TGF- β are associated with a decreased NEC risk¹⁵⁷.

Enteral feeding and intestinal inflammation in animal models of NEC

Intestinal inflammation is, in preclinical studies, the most extensively studied pathophysiological mechanism of NEC and many enteral feeding interventions reduce intestinal inflammation in animal models of NEC (**Table 2.6**).

Fat-based feeding interventions

Fat-based feeding interventions, such as polyunsaturated fatty acids (PUFA, including DHA, EPA, arachidonic acid (AA) and egg phospholipids), branched chain fatty acids (BCFA), bovine milk fat globule membrane (MFGM) and milk polar lipids (MPL), are extensively studied in relation to intestinal inflammation.

Supplementation of enteral feeding with fish oil, rich in n-3 PUFA such as DHA and EPA, prevents an increase in intestinal PAF and leukotriene B4 in a mouse NEC model⁸² and partially prevents a rise in intestinal IL6 and TNF α protein expression in a rat NEC model⁸³. Enrichment of formula feeding with DHA and arachidonic acid (AA) in a rat NEC model reduced intestinal mRNA levels of the PAF synthesizing enzyme phospholipase A2-II (PLA2) and of the PAF receptor (PAFR)⁴⁵. Supplementation of egg phospholipids, AA and DHA or DHA alone lowers intestinal PAFR gene expression⁴⁴. Enteral supplementation with egg phospholipids decreased gut TLR4 and ileal TLR2 mRNA expression in rats⁴⁴. Finally, AA and DHA, but not DHA alone, lowered intestinal TLR4 mRNA expression, suggesting AA is the responsible agent for the found effects⁴⁴. Interestingly, a maternal feeding intervention in rats with a DHA or EPA enriched diet during pregnancy resulted in increased levels of both

DHA and EPA in the fetal intestine and reduced small intestinal mRNA expression of NFκB inhibitor α (IκBα), NFκB inhibitor β (IκBβ) and peroxisome proliferator-activated receptor γ (PPARγ) in the offspring⁴³, demonstrating that postnatal gut inflammation can already be targeted prenatally. Addition of BCFA to rat formula feeding increases intestinal IL10 mRNA levels more than threefold and also enhances IL10 protein levels⁴⁶. A very low fat or reduced long chain triacylglycerol diet (considered pre-digested as its digestion is not dependent on intestinal lipases) reduces intestinal mRNA expression of IL1β and TNFα⁸⁵. Enteral supplementation of bovine MFGM reduces ileal mRNA expression of IL1β, TNFα and IL6, as well as protein expression of TLR4⁴⁸, whereas TLR9 signaling remained unaffected⁴⁸. Enteral treatment with MPL, which are abundantly present in MFGM, increased intestinal IL10 protein expression, while decreasing intestinal TNFα, IL6 and IL8 protein expression and TLR4 immunoreactivity⁸⁴. In addition, MPL inhibited NEC induced intestinal p65 and p50 expression⁸⁴. Pomegranate seed oil, rich in unsaturated fatty acids such as conjugated linolenic acids and oleic acid, blocks an increase in ileal gene expression of IL6, IL8, IL12, interleukin 23 (IL23) and TNFα in neonatal rats during NEC⁴⁷. Taken together, numerous fat-based feeding interventions possess immune modulatory activities, making them promising candidates for NEC prevention in a clinical setting.

Carbohydrate or sugar-based feeding interventions

Secondly, interventions using carbohydrate/sugar based dietary interventions have been shown to be successful in reducing intestinal inflammation, either by downregulating pro-inflammatory cytokines or by upregulating anti-inflammatory mediators. In a murine NEC model, addition of the neutral HMO 2'-fucosyllactose (2'-FL) to formula feeding reduced intestinal gene expression of IL6, IL1β and TLR4⁹¹. Enteral administration of the HMO 2'-FL, 6'-sialyllactose (6'-SL) or a combination of both reduced intestinal mRNA levels of TNFα (murine and pig model), IL1β (pig model) and TLR4 (murine and pig model), while this effect was not observed with enteral administration of lactose⁹². In other studies, addition of HMO to formula feeding reduced ileal mRNA levels of IL6⁴⁹, IL8⁴⁹, IL1β⁴⁹ and TLR4⁴⁹ and ileal protein levels of IL6⁴⁹ and IL8^{49,88}. In addition, HMO reduced intestinal protein levels of phosphorylated NFκβ, phosphorylated IκBα and TLR4⁴⁹. In a preterm pig model of NEC, enteral administration of a mixture of four HMO increased small intestinal mRNA expression of IL10, IL12, TGF-β and TLR4, whereas other cytokines and TLR such as IL8, IFNγ, TNFα and TLR2 were not affected¹³⁴. Enteral administration of sialylated HMO (containing 6'-SL, 3'-SL and DSLNT) reduced ileal mast cell counts and dipeptidylpeptidase I (DPPI) activity and concomitantly reduced ileal protein levels of IL6 and TNFα⁹³. Enteral administration of GOS/FOS decreased terminal ileum IL1β and TNFα protein levels and the mRNA expression of several pro-inflammatory cytokines including IL6, IL1β and TNFα in a rat NEC model¹³⁶. NEC protocol exposed rats that are orally treated with ganglioside D3 (GD3) had lower ileal protein levels of TNFα, IL6, C-C motif chemokine ligand 5 (CCL5) and L-selectin, combined with higher protein levels of anti-inflammatory mediators TIMP metalloproteinase inhibitor 1 (TIMP1), IL1ra and IL10 than animals that were not treated with GD3⁵⁰. Furthermore, in the same rat model, protein expression of the Treg marker forkhead box P3 (FoxP3) was upregulated by the GD3 treatment and more ileal Foxp3+ cells were observed in the GD3 supplemented group⁵⁰.

Protein or amino acid-based feeding interventions

Various interventions using proteins or amino acids, such as IAP, lactoferrin, N-acetylcysteine, arginine and glutamine, have been used as nutritional interventions to reduce intestinal inflammation.

In a study using a neonatal rat NEC model, enteral administration of IAP preserved endogenous ileal IAP mRNA expression and dose dependently decreased ileal TNF α mRNA expression¹⁶⁰. In preterm pigs, enteral bovine lactoferrin administration reduced proximal intestinal IL1 β , but not IL8, protein levels³⁵. Terminal ileum mRNA expression levels of IL6 and TNF α were reduced by enteral feeding supplemented with lactoferrin in a murine NEC model¹⁰¹. Oral administration of N-acetylcysteine reduced intestinal mRNA levels of IL1 β and TNF α ⁸⁵. Arginine supplementation reduced ileal IL6 and TNF α mRNA levels⁹⁸. Glutamine supplementation decreased intestinal protein concentrations of TNF α ^{84,95}, IL6 and IL8 and decreased TLR4, p65 and p50 immunoreactivity⁸⁴, while increasing intestinal IL-10 protein concentrations⁸⁴. In addition, upon enteral glutamine supplementation, mRNA and protein expression of TLR2 and TLR4 were lowered in ileum and colon, but not jejunum, of NEC protocol exposed rats⁹⁷.

Hormone, growth factor or vitamin-based feeding interventions

Growth factors and hormones form another group of nutritional interventions with promising results regarding the reduction of intestinal inflammation in experimental models of NEC. In a NEC rat model, enteral administration of EGF decreased intestinal mRNA expression of interleukin 18 (IL18), while increasing mRNA expression of IL10 and the IL10 transcription factor specificity protein 1 (Sp1)⁵³. Recombinant EGF from soybean extract reduced intestinal mRNA levels of cyclooxygenase 2 (COX-2) upon orogastric administration in a rat NEC model¹⁰⁴. Gastric gavage of HB-EGF in a murine NEC model reduced the number of pro-inflammatory M1 and increased the number of immune modulatory M2 macrophages in the intestine⁵⁷. Oral administration of TGF- β 1 in a neonatal rat NEC model increased SMAD family member 2 (Smad2) activation/phosphorylation, reduced the number of phosphorylated NF κ B positive intestinal epithelial cells and prevented a NEC induced decrease of the NF κ B regulator I κ B α ⁶⁴. Oral administration of IGF1 in a rat NEC model reduced intestinal TLR4 and NF κ B mRNA expression and IL6 protein expression⁶⁵.

Vitamins such as vitamin A are often studied as nutritional interventions in the context of NEC. Intra-gastric vitamin A supplementation significantly lowered intestinal IL6 and TNF α levels, both on protein and mRNA level, compared to NEC only animals¹¹¹. Enteral treatment with all-trans retinoic acid (ATRA), a vitamin A metabolite, reduced ileal mRNA expression of IL6 and IL17 in a murine NEC model¹¹⁰. In addition, an increase of Treg (Foxp3+CD4+ T cells) and a decrease of CD4+Th17 cells upon enteral ATRA treatment was observed with fluorescence-activated cell sorting of lamina propria CD4+ T cells¹¹⁰. In another murine NEC study, enteral ATRA decreased the ileal mRNA expression of pro-inflammatory cytokines IL1 β and IL6¹⁰⁹. Moreover, ATRA supplementation prevented NEC induced loss of Treg (preserved Foxp3 mRNA expression) and induction of Th17 cells (reduced IL17 mRNA expression) in CD4+ T cells isolated from the intestinal lamina propria¹⁰⁹. In a mouse model

of NEC, vitamin D decreased intestinal protein and mRNA expression of IL6, IL1 β and TNF α ¹¹².

Probiotic feeding interventions

Probiotics are also a widely studied group of nutritional interventions. In a mice NEC model, reduction of terminal ileum IL1 β ^{69,70} and TNF α ⁷⁰ mRNA and protein levels upon oral administration of *Lactobacillus reuteri* DSM 17938 was found. In a rat NEC model, both *Lactobacillus reuteri* DSM 17938 and *Lactobacillus reuteri* ATCC PTA 4659 reduced intestinal mRNA expression of TLR1, TLR4, IL6, TNF α and NF κ B and protein expression of TNF α , IL1 β , TLR4 and phosphorylated I κ B, while increasing the mRNA expression of IL10⁶⁸. Moreover, *Lactobacillus reuteri* DSM 17938 inhibited mRNA expression of the TLR interaction proteins mitogen-activated protein kinase 8 interaction protein 3 and increased NF κ B inhibitor- β , while *Lactobacillus reuteri* ATCC PTA 4659 inhibited myelin and lymphocyte protein mRNA expression (also TLR interaction protein)⁶⁸. Supplementing formula with *Lactobacillus reuteri* DSM 17938 reduced the percentage of activated effector CD4+ T cells in the intestine, increased the proportion of CD4+ Foxp3+ Treg and tolerogenic dendritic cells in the gut and reduced intestinal protein levels of the pro-inflammatory cytokines IL1 β and IFN γ ⁶⁷. All these effects were TLR2 dependent, as they did not occur in TLR2 -/- mice⁶⁷. In another study, *Lactobacillus reuteri* DSM 17938 increased the percentage of Foxp3+ CD4+ Treg cells and Foxp3+ CD4+ CD8+ Treg cells in the terminal ileum of rats, while decreasing the percentage of Foxp3+ CD4+ CD8+ Treg cells in the mesenteric lymph nodes, indicating migration of Tregs from the lymph nodes to the intestine following treatment with this probiotic agent¹³². In a murine NEC model, *Lactobacillus reuteri* DSM 17938 normalized the frequency of CD4+ Foxp3+ Treg cells in both ileum and mesenteric lymph nodes⁶⁹. As most of these Treg in ileum as well as in the mesenteric lymph nodes were Helios positive, the cells are likely to be of thymic origin⁶⁹. In addition, enteral treatment with *Lactobacillus reuteri* DSM 17938 reduced the increase of activated effector/memory T cells (CD44+CD45RBlo) and transitional effector T cells (CD44+CD45Rbhi) in the ileum during NEC⁶⁹. Interestingly, enteral administration of *Lactobacillus reuteri* biofilms on sucrose or maltose loaded microspheres, but not administration of unbound *Lactobacillus reuteri*, reduced small intestinal mRNA levels of IL6, IL1 β , C-C motif chemokine ligand 2 (CCL2), C-X-C motif chemokine 1 (CXCL1) and IL10 in a rat NEC model⁷². Enteral *Lactobacillus rhamnosus* GG, both in a low and higher dosage, reduced TLR4 expression (mRNA) and increased SIGIRR (mRNA, protein) and A20 (mRNA) levels¹⁶¹. In addition, mediators of the TLR4 signaling pathway phosphorylated IKK β and phosphorylated p65 were reduced on protein level concomitant with a reduced intestinal inflammation on mRNA level (Intercellular Adhesion Molecule 1 (ICAM-1), IL8, IL1 β) and protein level (ICAM-1, IL1 β)¹⁶¹. The strain *Bifidobacterium bifidum* OLB6378 normalized ileum IL6 levels in NEC rats⁷³. Orogastric administration of *Bifidobacterium infantis* reduced mRNA expression of the PAF synthesizing enzyme phospholipase-A2 II (PLA2 II)⁷⁵. Intra-gastric administration of Bifidobacterium microcapsules in a rat NEC model reduced ileal protein expression of TLR4, TLR2 and NF κ B p65¹¹⁴. Enrichment of formula feeding with *Bifidobacterium adolescentis* decreased ileal mRNA expression of TLR4, while increasing the mRNA expression of the negative regulators of TLR signaling TOLLIP and SIGIRR⁷⁶. In addition, enteral administration of *Bacteroides*

fragilis strain ZY-312 decreased intestinal IL1 β protein expression in a rat NEC model¹¹³. Enteral administration of *Bifidobacterium breve* M-16V reduced ileal mRNA levels of TLR4, IL1 β , IL6, TNF α and IL10 and increased the mRNA levels of TLR2 in a rat NEC model¹¹⁷. In addition, ileal protein levels of macrophage inflammatory protein 1 α (MIP1 α) and IL1 β were increased by this intervention¹¹⁷. In a rat NEC model, enteral administration of *Saccharomyces boulardii* reduced terminal ileum protein concentrations of IL1 β , IL6 and TNF α and the mRNA expression of several pro-inflammatory cytokines including IFN β and TNF α ¹³⁶. Last, oral supplementation of the TLR9 ligand GpG-DNA, reduced terminal ileum IL6 mRNA expression in a murine NEC model³⁹. In accordance with the extensive evidence on the immunomodulatory effect of probiotics in animal models of NEC, probiotics are currently the most promising enteral feeding intervention for the prevention of NEC in clinical practice.

Table 2.6 Effect of enteral feeding interventions that reduce intestinal inflammation in experimental animal models of NEC.

Enteral Feeding Intervention	Effect on Intestinal Inflammation (Compared to NEC Protocol Exposure without Feeding Intervention)
Fat-based interventions	
Fish oil (n-3 PUFA)	Intestinal PAF (protein) ↓ ⁸² Intestinal leukotriene B4 (protein) ↓ ⁸² Intestinal IL6 (protein) ↓ ⁸³ Intestinal TNFα (protein) ↓ ⁸³
AA + DHA	Duodenal, jejunal and ileal TLR 4 (mRNA) ↓ ⁴⁴ Intestinal TLR2 (mRNA) = ⁴⁴ Intestinal PLA2-II (mRNA) ↓ ⁴⁵ Intestinal PLA2-II (mRNA) = ⁴⁴ Ileal, colonic and intestinal PAFR (mRNA) ↓ ^{44,45}
DHA	Intestinal TLR4 (mRNA) = ⁴⁴ Intestinal TLR2 (mRNA) = ⁴⁴ Intestinal PLA2-II (mRNA) = ⁴⁴ Ileum and colon PAFR (mRNA) ↓ ⁴⁴
DHA (maternal intervention)	Ileal DHA ↑ ⁴³ Ileal EPA ↑ ⁴³ Small intestinal ikbα (mRNA) ↓ ⁴³ Small intestinal ikBβ (mRNA) ↓ ⁴³ Small intestinal PPARγ (mRNA) ↓ ⁴³
EPA (maternal intervention)	Ileal DHA ↑ ⁴³ Ileal EPA ↑ ⁴³ Small intestinal ikBα (mRNA) ↓ ⁴³ Small intestinal ikBβ (mRNA) ↓ ⁴³ Small intestinal PPARγ (mRNA) ↓ ⁴³
Egg phospholipids	Intestinal TLR 4 (mRNA) ↓ ⁴⁴ Ileal TLR2 (mRNA) ↓ ⁴⁴ Intestinal PLA2 (mRNA) = ⁴⁴ Ileal and colonic PAFR (mRNA) ↓ ⁴⁴
BCFA	Ileal IL10 (mRNA) ↑ ⁴⁶ Ileal IL10 (protein) ↑ ⁴⁶
Pomegranate seed oil	Ileal IL6 (mRNA) ↓ ⁴⁷ Ileal IL8 (mRNA) ↓ ⁴⁷ Ileal IL12 (mRNA) ↓ ⁴⁷ Ileal IL23 (mRNA) ↓ ⁴⁷ Ileal TNFα (mRNA) ↓ ⁴⁷
Pre-digested fat (less long chain triacylglycerol, not dependent on intestinal lipases)	Intestinal IL1β (mRNA) ↓ ⁸⁵ Intestinal TNFα (mRNA) ↓ ⁸⁵
Very low-fat diet	Intestinal IL1β (mRNA) ↓ ⁸⁵ Intestinal TNFα (mRNA) ↓ ⁸⁵
MFGM	Ileal IL6 (mRNA) ↓ ⁴⁸ Ileal IL1β (mRNA) ↓ ⁴⁸ Ileal TNFα (mRNA) ↓ ⁴⁸ Ileal TLR4 (protein) ↓ ⁴⁸

Table 2.6 (continued)

MPL	Intestinal IL10 (protein) ↑ ⁸⁴ Intestinal TNFα (protein) ↓ ⁸⁴ Intestinal IL6 (protein) ↓ ⁸⁴ Intestinal IL8 (protein) ↓ ⁸⁴ Intestinal TLR4 (protein) ↓ ⁸⁴ Intestinal p65 (protein) ↓ ⁸⁴ Intestinal p50 (protein) ↓ ⁸⁴
Carbohydrate/sugar-based interventions	
HMO	Ileal IL6 (mRNA) ↓ ⁴⁹ Ileal IL8 (mRNA) ↓ ⁴⁹ Ileal IL1β (mRNA) ↓ ⁴⁹ Ileal TLR4 (mRNA) ↓ ⁴⁹ Ileal IL6 (protein) ↓ ⁴⁹ Ileal IL8 (protein) ↓ ^{49,88} Ileal phosphorylated NFκβ (protein) ↓ ⁴⁹ Ileal phosphorylated IκBα (protein) ↓ ⁴⁹ Ileal TLR4 (protein) ↓ ⁴⁹
Mixture of four HMO	Small intestinal IL10 (mRNA) ↑ ¹³⁴ Small intestinal IL12 (mRNA) ↑ ¹³⁴ Small intestinal TGF-β (mRNA) ↑ ¹³⁴ Small intestinal TLR4 (mRNA) ↑ ¹³⁴ Small intestinal IL8 (mRNA) = ¹³⁴ Small intestinal IFNγ (mRNA) = ¹³⁴ Small intestinal TNFα (mRNA) = ¹³⁴ Small intestinal TLR2 (mRNA) = ¹³⁴
2'-FL	Intestinal IL6 (mRNA) ↓ ⁹¹ (Small) intestinal IL1β (mRNA) ↓ ^{91,92} Small intestinal TNFα (mRNA) ↓ ⁹² (Small) intestinal TLR4 (mRNA) ↓ ^{91,92}
6'-SL	Small intestinal IL1β (mRNA) ↓ ⁹² Small intestinal TNFα (mRNA) ↓ ⁹² Small intestinal TLR4 (mRNA) ↓ ⁹²
2'-FL + 6'-SL	Small intestinal IL1β (mRNA) ↓ ⁹² Small intestinal TNFα (mRNA) ↓ ⁹² Small intestinal TLR4 (mRNA) ↓ ⁹²
Sialylated HMO	Ileal mast cell counts ↓ ⁹³ Ileal DPPi activity ↓ ⁹³ Ileal IL6 (protein) ↓ ⁹³ Ileal TNFα (protein) ↓ ⁹³
GOS/FOS	Terminal ileum IL1β (protein) ↓ ¹³⁶ Terminal ileum TNFα (protein) ↓ ¹³⁶ Terminal ileum IL1β (mRNA) ↓ ¹³⁶ Terminal ileum TNFα (mRNA) ↓ ¹³⁶ Terminal ileum IL6 (mRNA) ↓ ¹³⁶
GD3	Ileal TNFα (protein) ↓ ⁵⁰ Ileal IL6 (protein) ↓ ⁵⁰ Ileal CCL5 (protein) ↓ ⁵⁰ Ileal L-selectin (protein) ↓ ⁵⁰ Ileal TIMP1 (protein) ↑ ⁵⁰ Ileal IL1ra (protein) ↑ ⁵⁰ Ileal IL10 (protein) ↑ ⁵⁰ Ileal Foxp3 (protein) ↑ ⁵⁰ Ileal Foxp3 cellcount ↑ ⁵⁰

Table 2.6 (continued)

Enteral Feeding Intervention	Effect on Intestinal Inflammation (Compared to NEC Protocol Exposure without Feeding Intervention)
Protein/amino acid-based interventions	
IAP	Ileal endogenous IAP (mRNA) ↑ ¹⁶⁰ Ileal TNFα (mRNA) ↓ ¹⁶⁰
L-Glutamine/glutamine	Intestinal TNFα (protein) ↓ ⁹⁵ Intestinal IL10 (protein) ↑ ⁸⁴ Intestinal TNFα (protein) ↓ ⁸⁴ Intestinal IL6 (protein) ↓ ⁸⁴ Intestinal IL8 (protein) ↓ ⁸⁴ Intestinal TLR4 (protein) ↓ ⁸⁴ Intestinal p65 (protein) ↓ ⁸⁴ Intestinal p50 (protein) ↓ ⁸⁴ Jejununal, ileal and colonic TLR4 (protein) ↓ ⁹⁷ Jejununal, ileal and colonic TLR4 (mRNA) ↓ ⁹⁷ Jejununal, ileal and colonic TLR2 (protein) ↓ ⁹⁷ Jejununal, ileal and colonic TLR2 (mRNA) ↓ ⁹⁷
Arginine	Ileal IL6 (mRNA) ↓ ⁹⁸ Ileal TNFα (mRNA) ↓ ⁹⁸
N-Acetylcysteine	Intestinal IL1β (mRNA) ↓ ⁸⁵ Intestinal TNFα (mRNA) ↓ ⁸⁵
Lactoferrin	Ileal IL6 (mRNA) ↓ ¹⁰¹ Ileal TNFα (mRNA) ↓ ¹⁰¹
Bovine lactoferrin	Proximal small intestinal IL1β (protein) ↓ ³⁵
Hormone/growth factor/vitamin based interventions	
EGF	Ileal IL18 (mRNA) ↓ ⁵³ Ileal IL10 (mRNA) ↑ ⁵³ Ileal Sp1 (mRNA) ↑ ⁵³
Recombinant EGF from soybean extract	Ileal COX2 (mRNA) ↓ ¹⁰⁴
HB-EGF	Intestinal M1 macrophages cellcount (CD86) ↓ ⁵⁷ Intestinal % M1 macrophages/total macrophages (CD86/CD68) ↓ ⁵⁷ Intestinal M2 macrophages cellcount (CD206) ↑ ⁵⁷ Intestinal % M1 macrophages/total macrophages (CD206/CD68) ↑ ⁵⁷
TGF-β1	Ileal Smad2 activation/phosphorylation ↑ ⁶⁴ Ileal phosphorylated NFκβ positive intestinal epithelial cells ↓ ⁶⁴ Ileal IκBα (protein) ↑ ⁶⁴
IGF1	Ileal TLR4 (mRNA) ↓ ⁶⁵ Ileal NFκβ (mRNA) ↓ ⁶⁵ Ileal IL6 (protein) ↓ ⁶⁵
Vitamin A	Intestinal IL6 (protein) ↓ ¹¹¹ Intestinal TNFα (protein) ↓ ¹¹¹
ATRA	Foxp3 (mRNA) in CD4+ T cells from lamina propria ↑ ¹⁰⁹ IL17 (mRNA) in CD4+ T cells from lamina propria ↓ ¹⁰⁹ FoxP3+ CD4+ T cells from lamina propria (FACs) ↑ ¹¹⁰ CD4+ Th17 cells from lamina propria (FACs) ↓ ¹¹⁰ Ileal IL1β (mRNA) ↓ ¹⁰⁹ Ileal IL6 (mRNA) ↓ ^{109,110} Ileal IL17 (mRNA) ↓ ¹¹⁰

Table 2.6 (continued)

Vitamin D	Intestinal IL6 (mRNA) ↓ ¹¹² Intestinal IL1β (mRNA) ↓ ¹¹² Intestinal TNFα (mRNA) ↓ ¹¹² Intestinal IL6 (protein) ↓ ¹¹² Intestinal IL1β (protein) ↓ ¹¹² Intestinal TNFα (protein) ↓ ¹¹²
Probiotic interventions	
<i>Lactobacillus reuteri</i> DSM 17938	Intestinal % CD4+ Foxp3+ Treg ↑ ^{67,69,132} Mesenteric lymph nodes % CD4+ Foxp3+ Treg ↑ ⁶⁹ Terminal ileum % Foxp3+ CD4+CD8+ Treg cells ↑ ¹³² Mesenteric lymph nodes % Foxp3+ CD4+CD8+ Treg cells ↓ ¹³² Intestinal % tolerogenic DC ↑ ⁶⁷ Intestinal % activated CD4+ Teff ↓ ⁶⁷ Intestinal % activated effector/memory T cells (CD44+CD45RBlo) ↓ ⁶⁹ Intestinal % transitional effector T cells (CD44+CD45RBhi) ↓ ⁶⁹ Ileal IL10 (mRNA) ↑ ⁶⁸ Ileal IL6 (mRNA) ↓ ⁶⁸ Ileal TNFα (mRNA) ↓ ^{68,70} Ileal TLR4 (mRNA) ↓ ⁶⁸ Ileal TLR1 (mRNA) ↓ ⁶⁸ Ileal NFκβ (mRNA) ↓ ⁶⁸ Ileal IL1β (mRNA) ↓ ^{69,70} Ileal IL1β (protein) ↓ ⁶⁷⁻⁷⁰ Ileal IFNγ (protein) ↓ ⁶⁷ Ileal TNFα (protein) ↓ ^{68,70} Ileal TLR4 (protein) ↑ ⁶⁸ Ileal phosphorylated Iκβ (protein) ↑ ⁶⁸ Ileal mitogen-activated protein kinase 8 interaction protein 3 (mRNA) ↓ ⁶⁸ Ileal NFκβ inhibitor-β (mRNA) ↑ ⁶⁸
<i>Lactobacillus reuteri</i> ATCC PTA 4659	Ileal IL6 (mRNA) ↓ ⁶⁸ Ileal TNFα (mRNA) ↓ ⁶⁸ Ileal TLR4 (mRNA) ↓ ⁶⁸ Ileal TLR1 (mRNA) ↓ ⁶⁸ Ileal NFκβ (mRNA) ↓ ⁶⁸ Ileal TNFα (protein) ↓ ⁶⁸ Ileal IL1β (protein) ↓ ⁶⁸ Ileal TLR4 (protein) ↑ ⁶⁸ Ileal phosphorylated Iκβ (protein) ↑ ⁶⁸ Ileal IL10 (mRNA) ↑ ⁶⁸ Ileal myelin and lymphocyte protein (mRNA) ↓ ⁶⁸
<i>Lactobacillus rhamnosus</i> GG	Ileal TLR4 (mRNA) ↓ ¹⁶¹ Ileal SIGIRR (mRNA) ↑ ¹⁶¹ Ileal SIGIRR (protein) ↑ ¹⁶¹ Ileal A20 (mRNA) ↑ ¹⁶¹ Ileal p-IKKβ (protein) ↓ ¹⁶¹ Ileal p-p65 (protein) ↓ ¹⁶¹ Ileal ICAM-1 (protein) ↓ ¹⁶¹ Ileal ICAM-1 (mRNA) ↓ ¹⁶¹ Ileal IL1β (protein) ↓ ¹⁶¹ Ileal IL1β (mRNA) ↓ ¹⁶¹ Ileal IL8 (mRNA) ↓ ¹⁶¹

Table 2.6 (continued)

Enteral Feeding Intervention	Effect on Intestinal Inflammation (Compared to NEC Protocol Exposure without Feeding Intervention)
<i>Lactobacillus reuteri</i> DSM 20016	Small intestinal IL6 (mRNA) = ⁷² small intestinal IL1 β (mRNA) = ⁷² Small intestinal CCL2 (mRNA) = ⁷² Small intestinal CXCL1 (mRNA) = ⁷² Small intestinal IL10 (mRNA) = ⁷²
<i>Lactobacillus reuteri</i> biofilm on sucrose loaded microspheres	Small intestinal IL6 (mRNA) ↓ ⁷² small intestinal IL1 β (mRNA) ↓ ⁷² Small intestinal CCL2 (mRNA) ↓ ⁷² Small intestinal CXCL1 (mRNA) ↓ ⁷² Small intestinal IL10 (mRNA) ↓ ⁷²
<i>Bifidobacterium bifidum</i> OLB6378	Ileal IL6 (mRNA) ↓ ⁷³
<i>Bifidobacterium infantis</i>	Intestinal PLA2 II (mRNA) ↑ ⁷⁵
<i>Bifidobacterium microcapsules</i>	Ileal TLR4 (protein) ↓ ¹¹⁴ Ileal TLR2 (protein) ↓ ¹¹⁴ Ileal NF κ B p65 (protein) ↓ ¹¹⁴
<i>Bifidobacterium adolescentis</i>	Ileal TLR4 (mRNA) ↓ ⁷⁶ Ileal TOLLIP (mRNA) ↑ ⁷⁶ Ileal SIGIRR (mRNA) ↑ ⁷⁶
<i>Bifidobacterium breve</i> M-16V	Ileal TLR4 (mRNA) ↓ ¹¹⁷ Ileal IL1 β (mRNA) ↓ ¹¹⁷ Ileal IL6 (mRNA) ↓ ¹¹⁷ Ileal TNF α (mRNA) ↓ ¹¹⁷ Ileal IL10 (mRNA) ↓ ¹¹⁷ Ileal TLR2 (mRNA) ↑ ¹¹⁷ Ileal MIP1 α (protein) ↓ ¹¹⁷ Ileal IL1 β (protein) ↓ ¹¹⁷
<i>Bacteroides fragilis</i> ZY-312	Intestinal IL1 β (protein) ↓ ¹¹³
<i>Saccharomyces Boulardii</i>	Terminal ileum IL1 β (protein) ↓ ¹³⁶ Terminal ileum IL6 (protein) ↓ ¹³⁶ Terminal ileum TNF α (protein) ↓ ¹³⁶ Terminal ileum IFN β (mRNA) ↓ ¹³⁶ Terminal ileum TNF α (mRNA) ↓ ¹³⁶
CpG-DNA	Ileal IL6 (mRNA) ↓ ³⁹
Other interventions	
Ginger	Intestinal IL1 β (protein) ↓ ¹²¹ Intestinal IL6 (protein) ↓ ¹²¹ Intestinal TNF α (protein) ↓ ¹²¹ Intestinal MPO (protein) ↓ ¹²¹
Fennel seed extracts	Intestinal IL6 (protein) ↓ ¹²² Intestinal TNF α (protein) ↓ ¹²² Intestinal MPO (protein) ↓ ¹²²
Bovine milk exosomes	Distal ileal MPO (protein) ↓ ¹¹⁸
Human milk exosomes	Ileal IL6 (mRNA) ↓ ¹¹⁹ Ileal MPO (protein) ↓ ¹¹⁹

Table 2.6 (continued)

Amniotic fluid	Ileal CXCL2 (mRNA) ↓ ⁶³
	Ileal CXCL5 (mRNA) ↓ ⁶³
	Ileal CCL2 (mRNA) ↓ ⁶³
	Ileal CCL5 (mRNA) ↓ ⁶³
	Ileal IFN γ (mRNA) ↓ ⁶³
	Distal small intestinal IFN γ (mRNA) ↓ ¹²³
	Distal small intestinal IL1 α (mRNA) ↓ ¹²³
	Distal small intestinal TNF α (mRNA) ↓ ¹²³
	Middle small intestinal IL1 α (mRNA) ↓ ¹²³
	Middle small intestinal TNF α (mRNA) ↓ ¹²³
	Middle small intestinal IL6 (mRNA) ↓ ¹²³
	Middle small intestinal IL8 (mRNA) ↓ ¹²³
	Curcumin
Intestinal IL6 (protein) ↓ ¹²⁴	
Intestinal IL18 (protein) ↓ ¹²⁴	
Intestinal TNF α (protein) ↓ ¹²⁴	
Intestinal TLR4 (protein) ↓ ¹²⁴	
Intestinal SIRT1 (protein) ↑ ¹²⁴	
Intestinal NRF2 (protein) ↑ ¹²⁴	
Intestinal TLR4 (mRNA) ↓ ¹²⁴	
Intestinal SIRT1 (mRNA) ↑ ¹²⁴	
Intestinal NRF2 (mRNA) ↑ ¹²⁴	
Surfactant protein A	Ileal IL1 β (protein) ↓ ⁸⁰
	Ileal TNF α (protein) ↓ ⁸⁰
	Ileal IFN γ (protein) ↓ ⁸⁰
	Ileal TLR4 (protein) ↓ ⁸⁰
Human β -defensin-3	Ileal TNF α (mRNA) ↓ ⁸¹
	Ileal IL6 (mRNA) ↓ ⁸¹
	Ileal IL10 (mRNA) ↓ ⁸¹
Berberine	Ileal TLR4 (protein) ↓ ⁷⁹
	Ileal IL6 (protein) ↓ ⁷⁹
	Ileal IL10 (protein) ↓ ⁷⁹
	Ileal TLR4 (mRNA) ↓ ⁷⁹
	Ileal NF κ B (mRNA) ↓ ⁷⁹
Astragaloside IV	Ileal TNF α (mRNA) ↓ ⁷⁹
	Distal ileal TNF α (mRNA) ↓ ¹²⁶
	Distal ileal IL1 β (mRNA) ↓ ¹²⁶
	Distal ileal IL6 (mRNA) ↓ ¹²⁶
	Distal ileal NF κ B p65 (mRNA) ↓ ¹²⁶
	Distal ileal MPO (protein) ↓ ¹²⁶
	Distal ileal p-NF κ B p65/ NF κ B p65 (protein) ↓ ¹²⁶
	Distal ileal p-I κ B α / I κ B α (protein) ↓ ¹²⁶
	Distal ileal p-I κ B α (protein) ↓ ¹²⁶
	Distal ileal p-NF κ B p65 (protein) ↓ ¹²⁶
Distal ileal NF κ B p65 (protein) ↓ ¹²⁶	
Distal ileal I κ B α (protein) ↑ ¹²⁶	

↑ depicts an increase, ↓ depicts a decrease; PUFA, polyunsaturated fatty acids; AA, arachidonic acid; DHA, docosahexaenoic acid; EPA, eicosapentaenoic acid; BCFA, branched chain fatty acids; MFGM, milk fat globule membrane; MPL, milk polar lipids; HMO, human milk oligosaccharides; 2'-FL, 2'-fucosyllactose; 6'-SL, 6'-sialyllactose; GOS, galacto-oligosaccharides; FOS, fructo-oligosaccharides; GD3, ganglioside D3; IAP, intestinal alkaline phosphatase; EGF, epidermal growth factor; HB-EGF, hemoglobin-binding EGF-like growth factor; HGF, hepatocyte growth factor; TGF- β 1, transforming growth factor β 1; IGF1, insulin-like growth factor 1; ATRA, all-*trans*-retinoic acid.

Other enteral feeding interventions

Finally, several other food components have been linked to immune modulatory effects within the context of NEC. Ginger intake by rats with NEC reduces intestinal protein concentrations of IL1 β , IL6, TNF α and myeloperoxidase (MPO)¹²¹. Enteral administration of fennel seed extracts reduces intestinal protein concentrations of MPO, TNF α and IL6¹²². Bovine milk exosomes administered through gavage normalized terminal ileum protein expression of MPO in NEC mice¹¹⁸. Both native and pasteurized exosomes from human breast milk were able to reduce distal ileum IL6 mRNA levels and MPO activity (MPO protein levels) in a mouse NEC model¹¹⁹. Addition of rat amniotic fluid to formula feeding reduced ileal mRNA expression of the chemokines C-X-C motif chemokine 2 (CXCL2), CXCL5, CCL2, CCL5 and the pro-inflammatory cytokine IFN γ in rats that developed NEC⁶³. In a preterm pig NEC model, enteral treatment with amniotic fluid reduced the distal small intestinal mRNA expression of IFN γ , IL1 α and TNF α and middle small intestinal mRNA expression of IL1 α , TNF α , IL6 and IL8 compared to formula fed pigs that developed NEC¹²³. Oral administration of curcumin dose dependently reduced intestinal protein levels of IL1 β , IL6, IL1, TNF α and protein and mRNA levels of TLR4 while increasing protein and mRNA levels of SIRT1 and nuclear factor erythroid 2-related factor 2 (NRF2)¹²⁴. In a rat NEC model, addition of surfactant protein A to formula feeding reduced ileal IL1 β , TNF α and TLR4 protein levels, but did not affect ileal IFN γ concentrations⁸⁰. Administration of human β -defensin-3 in a rat NEC model reduced ileal mRNA expression of TNF α , IL6 and IL10⁸¹. Enteral berberine reduced ileal protein concentrations of TLR4, IL6 and IL10 and reduced mRNA levels of TLR4, NF κ β and TNF α ⁷⁹. Finally, enteral administration of astragaloside IV, a flavonoid from the plant *Astragalus membranaceus* dose dependently decreased mRNA levels of TNF α , IL6, IL1 β and NF κ β p65, decreased MPO protein levels and decreased the phosphorylation rate of NF κ β p65 and that of I κ B α in the distal ileum of NEC protocol exposed rats¹²⁶.

Table 2.7 Effect of enteral feeding interventions that reduce systemic inflammation in experimental animal models of NEC.

Enteral Feeding Intervention	Effect on Systemic Inflammation (Compared to NEC Protocol Exposure without Feeding Intervention)
Carbohydrate/sugar-based interventions	
HMO	Serum IL8 (protein) ↓ ^{49,88}
Hyaluronan 35 kD	Plasma TNFα (protein) ↓ ⁹⁴ Serum CXCL1 (protein) ↓ ⁹⁴ Serum IL12p70 (protein) ↓ ⁹⁴ Serum IL6 (protein) ↓ ⁹⁴ Serum IFNγ (protein) ↓ ⁹⁴
Protein/amino acid-based interventions	
IAP	Serum TNFα (protein) ↓ (dose dependent) ¹⁶² Serum IL1β (protein) ↓ (dose dependent) ¹⁶² Serum IL6 (protein) ↓ (dose dependent) ¹⁶²
Hormone/growth factor/vitamin-based interventions	
TGF-β	Serum IL6 (protein) ↓ ⁶⁴ Serum IFNγ (protein) ↓ ⁶⁴
Probiotic interventions	
<i>Bacteroides fragilis</i> ZY-312	Serum TNFα (protein) ↓ ¹¹³ Serum IFNγ (protein) ↓ ¹¹³ Serum IL10 (protein) ↑ ¹¹³
Other interventions	
Berberine	Serum IL6 (protein) ↓ ⁷⁹ serum IL10 (protein) ↓ ⁷⁹
Human β-defensin-3	Serum TNFα (protein) ↓ ⁸¹
Astragaloside IV	Serum TNFα (protein) ↓ ¹²⁶ Serum IL6 (protein) ↓ ¹²⁶ serum IL1β (protein) ↓ ¹²⁶

↑ depicts an increase, ↓ depicts a decrease; HMO, human milk oligosaccharides; IAP, intestinal alkaline phosphatase; TGF-β, transforming growth factor β.

NEC pathophysiology: loss of intestinal barrier function

The intestinal barrier consists of several parts that together protect the host against luminal microbiota and their toxins, while preserving the capacity to absorb nutrients¹⁶³. It is formed by a biofilm of commensal bacteria, a mucus barrier, antimicrobial peptides (AMPs) secreted by enterocytes and Paneth cells, secretory IgA released by plasma cells and intestinal epithelial cells that are interconnected by an apical junction complex containing adherens junctions, desmosomes and tight junctions (TJ)¹⁶³. TJ regulate paracellular permeability and consist amongst others of claudins, occludin, junctional adhesion molecules (JAM) and zonulae occludens (ZO) proteins¹⁶³. Importantly, regulation of paracellular permeability by TJ proteins is a complex process, in which some proteins reduce permeability (such as occludin) while others promote permeability (such as claudin-2)^{164,165}. In premature infants, several components of the intestinal barrier are still immature

predisposing them to NEC development^{6,166}. During NEC, these components are further impaired, resulting in a defective barrier function. The mucus barrier is affected during NEC; in severely damaged regions of human NEC biopsies fewer goblet cells are present^{167,168}, whereas in mildly injured regions similar or even increased numbers of goblet cells are observed¹⁶⁷. In addition, reduced numbers of Paneth cells have been described in human NEC^{167,168} and increased mRNA expression of defensin A5 and A6, an unaffected protein expression of defensin A5¹⁶⁹ and decreased protein expression of defensin A6¹⁷⁰. In fecal samples, the percentage of intestinal bacteria bound by IgA negatively correlates with NEC development¹⁷¹. In biopsies from infants with NEC, transepithelial electrical resistance was lower and flux of mannitol was higher, indicating increased intestinal permeability compared to controls¹⁷². Reported alterations of apical junction complex proteins in human NEC specimen include a reduced mRNA expression of occludin^{172,173}, claudin-4¹⁷³, vinculin¹⁷³ and ZO-1¹⁷³, reduced immunoreactivity of occludin and ZO-1 in jejunum and ileum¹⁷³, increased immunoreactivity for claudin-2 in both colon and small intestine¹¹⁶ and an increased protein expression and internalization of claudin-2¹⁷⁴. Of note, one study did not find differences in expression or distribution of occludin and ZO-1¹¹⁶.

Enteral feeding and loss of intestinal barrier function in animal models of NEC

Many enteral feeding interventions have been studied in the context of NEC induced intestinal barrier loss (**Table 2.8**). Often, both structural (such as TJ expression and goblet cell counts) and functional read-outs were studied.

Fat-based feeding interventions

PUFA is the only fat-based feeding intervention that has been studied in relation to intestinal barrier function in NEC. Enteral treatment with PUFA (AA and DHA) reduced endotoxemia, as a read-out for barrier function loss, after 48 h in a rat NEC model, an effect that was interestingly abolished by additional supplementation with nucleotides⁴⁵. Enteral supplementation of DHA in a rat NEC model resulted in a less permeable mucus barrier, reflected by reduced effective diffusivity of amine and carboxyl modified particles, less linear movements of *Escherichia coli* through intestinal mucus and reduced *Escherichia coli* movement speed through intestinal mucus¹³¹. Mucus contained less sialic acid upon DHA administration, but mucus structure, analysed with confocal imaging and scanning electron microscopy (SEM), was hardly altered by DHA administration¹³¹.

Carbohydrate or sugar-based feeding interventions

Secondly, carbohydrate or sugar-based dietary interventions have been studied. In mice, hyaluronan 35 kD in both a low (15 mg/kg) and high (30 mg/kg) dose prevented NEC induced increase in gut permeability, measured with oral administration of fluorescein isothiocyanate (FITC)-labelled dextran 4 kD and in the higher dose also reduced bacteraemia⁹⁴. In addition, hyaluronan 35 kD treatment increased the expression of the TJ proteins occludin, claudin-2, -3 and -4 and ZO-1 both in control and NEC protocol treated animals and the localization of occludin and claudin-3 were normalized in these animals⁹⁴. NEC induced increase in paracellular translocation of FITC-labelled dextran was reduced by

enteral HMO administration in a murine NEC model³⁸. In addition, HMO administration normalizes the number of goblet cells in the intestinal villi (mucin 2 (Muc2) positive cells) that is decreased by NEC protocol exposure^{38,86} and tended to increase the mRNA expression of Muc2 and trefoil factor 3 (TFF3) in NEC protocol exposed mice³⁸. Interestingly, the effect of enteral HMO treatment on goblet cell numbers was abolished in the presence of an inhibitor of the ER chaperone protein PDI, suggesting a mechanism behind the protective effects of HMO administration could be induction of the unfolded protein response (UPR)³⁸. In a preterm pig model of NEC, enrichment of formula feeding with a mixture of four HMO did not prevent small intestinal adhesion and tissue invasion of bacteria measured with fluorescence in situ hybridization staining and did not change small intestinal mRNA expression of mucin 1 (Muc1) and Muc2¹³⁴.

Protein or amino acid-based feeding interventions

Lactoferrin, lysozyme, IAP and lactadherin are the protein/amino acid-based enteral feeding interventions that have been studied in relation to barrier function in experimental models of NEC. In a preterm pig NEC model, enteral bovine lactoferrin administration was associated with increased intestinal permeability, as demonstrated by an increased lactulose mannitol ratio following a dual sugar absorption test³⁵. Enteral supplementation of lysozyme in a rat NEC model resulted in a less permeable mucus barrier, as reflected by reduced effective diffusivity of amine and carboxyl modified particles, less linear movements of *E. coli* through intestinal mucus and reduced *E. coli* movement speed through intestinal mucus¹³¹. In addition, lysozyme supplementation lowered the amount of sialic acid in the intestinal mucus and was associated with an altered mucus structure analysed with confocal imaging and SEM¹³¹. Ex-vivo measurement of ileal barrier function with FITC-labelled dextran 10 kD showed enteral IAP, both in low and a high dose, prevented an increased intestinal permeability in a rat NEC model¹⁰³. Furthermore, protein expression of claudin-1 decreased and protein expression of claudin-3 increased with IAP administration, while occludin and ZO-1 or the mRNA expression of these proteins remained unaltered¹⁰³. Another study using enteral IAP reported reduced plasma endotoxemia at higher, but not at a low dose¹⁶⁰. Lactadherin supplementation in a rat NEC model reduced leakage of FITC-labelled dextran from the intestinal lumen into the blood⁵¹. Furthermore, enteral lactadherin administration reduced NEC induced disruption of cell junctions, improved anchoring of TJ complexes and reduces the space between adjacent cells, as was observed with transmission electron microscopy⁵¹. Enteral lactadherin prevented NEC induced increase of mRNA levels for claudin-3 and Junctional Adhesion Molecule A (JAM-A) and the protein levels of claudin-3, JAM-A and E-cadherin⁵¹. In addition, its administration changed localization of claudin-3 towards the cell membranes and along the crypt-villus junction, which was also seen in the dam fed control group⁵¹. Localization of occludin was also normalized by lactadherin treatment, as in the control group it was predominantly expressed at the cell membranes along the villus. E-cadherin localization of E-cadherin was also changed by lactadherin treatment⁵¹. No differences in JAM-A localization were found in NEC or lactadherin supplementation compared to controls⁵¹.

Hormone, growth factor or vitamin-based feeding interventions

Various hormone and growth factor-based enteral feeding interventions have been shown to improve intestinal barrier function in experimental models of NEC. Rat EGF reduced paracellular intestinal permeability, measured with blood levels and kidney levels of [³H]lactulose after oral administration¹³⁷. Transcellular permeability was not affected by the NEC protocol or EGF treatment¹³⁷. In addition, ileal mRNA and protein levels of occludin and claudin-3 and jejunum mRNA and protein levels of claudin-3 were reduced by EGF treatment to dam fed control levels and occludin and claudin-3 in the ileum were redistributed towards the apical and basolateral membranes along the crypt-villus axis contributing to a functional TJ barrier¹³⁷. JAM-A and ZO-1 were more markedly/sharply expressed on immunofluorescence pictures following oral recombinant EGF from soybean administration, probably indicating better incorporation in TJ complexes of these proteins¹⁰⁴. Enteral EGF treatment of NEC protocol exposed mice also significantly increased the number of goblet cells (Muc2) in the ileum and thickened the villus mucus layer compared to both NEC protocol exposed and control mice¹³⁷. In addition, ileal mRNA level of Muc2 was increased by EGF treatment in rat and mouse models of NEC^{37,137}. Importantly, an increased mRNA expression of mouse atonal homolog 1 (Math1), a transcription factor that is important for secretory cell lineage differentiation, was found in both ileum and jejunum upon EGF treatment, suggesting enteral EGF promotes goblet cell maturation and differentiation¹³⁷. Finally, SEM of ileal goblet cells showed normalization of the goblet cell phenotype that was disturbed in NEC animals by EGF treatment, with mucin droplets on the outer cell surface¹³⁷. In both rat^{58,62,105} and mouse^{61,175} NEC models, in which intestinal permeability was measured by administration of oral 73 kD FITC-labelled dextran, intestinal permeability was considerably reduced by HB-EGF treatment, both at 48 h^{61,62,105}, 72 h^{62,105} and 96 h¹⁷⁵ after birth. Enteral HB-EGF administration significantly increased ileal mRNA levels of Muc2 compared to both NEC protocol exposed and dam fed animals³⁷. Another study reported enteral administration of HB-EGF prevented a loss of goblet cells (alcian blue/periodic acid–Schiff (AB-PAS)) in the jejunum of NEC protocol stressed rats¹⁷⁶. In addition, bacterial adherence to intestinal villi in experimental NEC was prevented by HB-EGF addition to formula feeding in a rat NEC model⁵⁹. The effects of enteral administration of erythropoietin (EPO) on intestinal barrier function in NEC were assessed in a rat NEC model⁶⁶. Paracellular intestinal permeability, measured with a FITC-labelled dextran 10 kD assay, was almost completely reduced to control levels by enteral EPO administration⁶⁶. In addition, EPO administration prevented loss of ZO-1 in the TJ of histological normal ileal villi from NEC exposed animals. EPO treatment, however, did not alter claudin-1, claudin-3, E-cadherin or β -catenin protein levels in experimental NEC. It was shown the effects of EPO on the intestinal barrier function may be PI3k/Akt signaling pathway related⁶⁶. Interestingly, in the same study, enteral administration of TGF- β failed to protect the intestinal barrier function and did not activate Akt⁶⁶. Administration of IGF1 prevented a decrease in Muc2 protein levels at 24 h in NEC protocol exposed rats and induced an increase in Muc2 protein level at 72 h compared to control and NEC protocol exposed animals⁶⁵. In addition, IGF1 prevented a NEC protocol decrease in secretory IgA levels at 72 h, but not at 24 h and 48 h⁶⁵.

In contrast to hormones and growth factors, evidence for vitamin driven effects on the intestinal barrier is scarce; Enteral vitamin A administration increased the intestinal protein expression of the TJ proteins claudin-1, occludin and ZO-1 in a murine NEC model¹¹¹.

Probiotic feeding interventions

Many probiotic feeding interventions can improve intestinal barrier functions in the context of NEC. Administration of a *Bifidobacterium* mixture in a rat NEC model increased ileal protein and mRNA expression of β defensin 2¹¹⁵. Daily orogastric administration of *Bifidobacterium infantis* reduced endotoxemia by 10-fold at 48 h in a rat NEC model. In contrast, no differences were seen when the intestinal barrier function was assessed with an oral FITC-labelled dextran assay at 8 h, 24 h or 48 h⁷⁵. The authors suggested that *Bifidobacterium infantis* may protect TJ, thereby preventing bacterial transfer, whereas mucosal barrier loss leading to FITC-labelled dextran leakage could be dependent on other mechanisms such as apoptosis that were not inhibited by *Bifidobacterium infantis*⁷⁵. In a murine NEC model, enteral administration of *Bifidobacterium infantis* prior to NEC induction partially prevented internalisation of claudin-4 into the enterocyte cytoplasm and preserved claudin-4 protein expression, occludin presence at the TJ complex and co-fractionation of claudins-2 and -4 and the membrane lipid-raft protein caveolin 1. Moreover, in this study, *Bifidobacterium infantis* administration reduced intestinal permeability as measured with an oral FITC-dextran assay¹¹⁶. *Bifidobacterium bifidum* prevented a NEC induced increase in the TJ proteins occludin and claudin-3 and normalized the cellular distribution and localization of these proteins, suggesting enhanced development and formation of functional TJ in a rat model⁷³. In addition, although protein levels did not change, cellular distribution and localization of adherence junctions α -catenin, β -catenin and E-cadherin were partially normalized towards the situation in dam fed animals⁷³. In the same study, enteral administration of *Bifidobacterium bifidum* further reduced the ileal Muc2 mRNA expression in NEC exposed animals and did not prevent NEC induced reduction of Muc2-positive cells⁷³. On the other hand, *Bifidobacterium bifidum* treatment partially prevented NEC induced increase of mucin 3 (Muc3) mRNA expression. TFF3 was not affected by either NEC or *Bifidobacterium bifidum* treatment on mRNA level, but on protein level NEC protocol exposed animals showed an increase in TFF3-positive cells that was completely prevented by *Bifidobacterium bifidum*⁷³. Ileal mRNA expression of ZO-1, claudin-1 and occluding were reduced (normalization towards breast fed controls) by enteral administration of *Bifidobacterium breve* M-16V in a rat NEC model¹¹⁷. Pre-treatment with *Bacteroides fragilis* strain ZY-312 before *Cronobacter sakazkii* induced NEC improves the intestinal barrier function (FITC-labelled dextran 4 kD assay) and increases the ZO-1 expression compared to NEC protocol exposed rats that were not pre-treated¹¹³. In addition, intestinal protein levels of IgA were increased following *Bacteroides fragilis* pre-treatment compared to NEC protocol exposed animals¹¹³. Enteral administration of *Lactobacillus reuteri* biofilms on unloaded⁷¹, MRS loaded microspheres⁷¹, sucrose loaded microspheres⁷² and maltose loaded microspheres⁷², but not administration of unbound *Lactobacillus reuteri*^{71,72}, improved intestinal barrier function measured by a functional orogastric FITC-dextran assay in a rat NEC model. Finally, *Lactobacillus rhamnosus* GG reduced NEC-protocol induced mucosal infiltration of bacteria following enteral administration¹⁶¹.

Other enteral feeding interventions

Oral supplementation of bovine milk exosomes prevented NEC induced decrease of goblet cells (AB-PAS, Muc2) in mice¹¹⁸. The number of cells positive for GRP94, an ER chaperone protein that has a crucial role in goblet cell maintenance and a co-receptor for Wnt signaling was reduced in mice exposed to a NEC protocol, however, this was largely prevented by bovine milk exosome administration¹¹⁸. In addition, human breast milk exosomes partially prevented NEC induced reduction of goblet cells (Muc2) and Muc2 mRNA expression upon enteral administration in a mouse NEC model¹¹⁹. Enteral administration of berberine increased ileal protein levels of Muc2 and secretory IgA⁷⁹. Finally, enteral human β -defensin-3 preserved ZO-1 protein expression that was lost by exposure to the NEC inducing protocol in a rat NEC model⁸¹.

Table 2.8 Effect of enteral feeding interventions that improve intestinal barrier function in experimental animal models of NEC.

Enteral Feeding Intervention	Effect on Intestinal Barrier Function (Compared to NEC Protocol Exposure without Feeding Intervention)
Fat-based interventions	
PUFA	Endotoxemia (plasma) ↓ ⁴⁵
DHA	Ileal effective diffusivity amine modified particles ↓ ¹³¹ Ileal effective diffusivity carboxyl modified particles ↓ ¹³¹ Ileal linear movements <i>E. coli</i> through intestinal mucus ↓ ¹³¹ Ileal movement speed <i>E. coli</i> through intestinal mucus ↓ ¹³¹ Ileal sialic acid content mucus ↓ ¹³¹ Ileal mucus structure (confocal imaging/SEM) = ¹³¹
Carbohydrate/sugar-based interventions	
Hyaluronan 35 kD	Intestinal permeability (functional orogastric FITC-dextran assay) ↓ ⁹⁴ Small intestinal occludin (protein) ↑ ⁹⁴ Small intestinal claudin-4 (protein) ↑ ⁹⁴ Small intestinal claudin-3 (protein) ↑ ⁹⁴ Small intestinal claudin-2 (protein) ↑ ⁹⁴ Small intestinal ZO-1 (protein) ↑ ⁹⁴ Small intestinal occludin localization ⁹⁴ Small intestinal claudin-3 localization ⁹⁴
HMO	Intestinal permeability (functional orogastric FITC-dextran assay) ↓ ³⁸ Ileal number Muc2-positive cells ↑ ^{38,86} Ileal Muc2 (mRNA) ↑ (trend) ³⁸ Ileal TFF3 (mRNA) ↑ (trend) ³⁸
Mixture of four HMOs	Small intestinal bacterial adhesion and tissue invasion = ¹³⁴ Small intestinal Muc1 (mRNA) = ¹³⁴ Small intestinal Muc2 (mRNA) = ¹³⁴

Table 2.8 (continued)

Protein/amino acid-based interventions	
IAP	Ileal intestinal permeability (ex-vivo FITC-dextran assay) ↓ ¹⁰³ Ileal claudin-1 (protein) ↓ ¹⁰³ Ileal claudin-3 (protein) ↑ ¹⁰³ Ileal occludin (protein) = ¹⁰³ Ileal ZO-1 (protein) = ¹⁰³ Ileal claudin-1 (mRNA) = ¹⁰³ Ileal claudin-3 (mRNA) = ¹⁰³ Ileal occludin (mRNA) = ¹⁰³ Ileal ZO-1 (mRNA) = ¹⁰³ Endotoxemia (plasma) ↓ ¹⁶⁰
Bovine lactoferrin	Lactulose/mannitol recovery ratio in urine ↑ (only in animals with NEC) ³⁵
Lysozyme	Ileal effective diffusivity amine modified particles ↓ ¹³¹ Ileal effective diffusivity carboxyl modified particles ↓ ¹³¹ Ileal linear movements e coli through intestinal mucus ↓ ¹³¹ Ileal movement speed e coli through intestinal mucus ↓ ¹³¹ Ileal sialic acid content mucus ↓ ¹³¹
Lactadherin	Ileal mucus structure (confocal imaging/SEM) changed ¹³¹ Intestinal permeability (ex-vivo FITC-dextran assay) ↓ ⁵¹ Ileal organization of cell junctions, anchoring of the TJ complexes and space between adjacent Cells improved (transmission electron microscopy) ⁵¹ Ileal claudin-3 (mRNA) ↓ ⁵¹ Ileal JAM-A (mRNA) ↓ ⁵¹ Ileal claudin-3 (protein) ↓ ⁵¹ Ileal JAM-A (protein) ↓ ⁵¹ Ileal E-cadherin (protein) ↓ ⁵¹ Ileal claudin-3 distribution towards cell membranes along crypt-villus junction (normalization) ⁵¹ Ileal occludin distribution towards cell membranes along villus (normalization) ⁵¹ Ileal E-cadherin distribution towards cell membranes of villus and basolateral region of crypt cells ⁵¹ Ileal JAM-A distribution = ⁵¹
Hormone/growth factor/vitamin- based interventions	
EGF	Paracellular intestinal permeability (functional orogastric [³ H]lactulose assay) ↓ ¹³⁷ Transcellular intestinal permeability (functional orogastric [³ H]rhamnose assay) = ¹³⁷ Ileal occludin (mRNA) ↓ ¹³⁷ Jejunal and ileal claudin-3 (mRNA) ↓ ¹³⁷ Ileal occludin (protein) ↓ ¹³⁷ Jejunal and ileal claudin-3 (protein) ↓ ¹³⁷ Ileal occludin distribution towards apical and basolateral membrane of crypt-villus axis ¹³⁷ Ileal claudin-3 distribution towards apical and basolateral membrane of crypt-villus axis ¹³⁷ Ileal number of goblet cells (Muc2 protein) ↑ ¹³⁷ Ileal mucus layer on top villi tips ↑ ¹³⁷ Ileal Muc2 (mRNA) ↑ ¹³⁷ Jejunal and ileal Math1 (mRNA) ↑ ¹³⁷ Ileal goblet cell phenotype normalized (scanning electron microscopy) ¹³⁷

Table 2.8 (continued)

Enteral Feeding Intervention	Effect on Intestinal Barrier Function (Compared to NEC Protocol Exposure without Feeding Intervention)
Recombinant EGF from soybean extract HB-EGF	Ileal ZO-1 more sharply expressed, better incorporation in TJ (IF) ¹⁰⁴ Ileal JAM-A more sharply expressed, better incorporation in TJ (IF) ¹⁰⁴ Intestinal permeability (functional orogastric FITC-dextran assay) ↓ ^{58,61,105,175} Ileal Muc2 (mRNA) ↑ ³⁷ Jejunal goblet cell number (AB/PAS) ↑ ¹⁷⁶ Ileal bacterial adherence to intestinal villi ↓ (scanning electron microscope) ⁵⁹
IGF1	Ileal secretory IgA (protein) ↑ ⁶⁵ Ileal Muc2 (protein) ↑ ⁶⁵
EPO	Intestinal permeability (functional orogastric FITC-dextran assay) ↓ ⁶⁶ Intestinal ZO-1 loss from TJ intact villi (protein) ↓ ⁶⁶ Intestinal claudin-1 (protein) = ⁶⁶ Intestinal claudin-3 (protein) = ⁶⁶ Intestinal E-cadherin (protein) = ⁶⁶ Intestinal β-catenin (protein) = ⁶⁶ Intestinal p-Akt (protein) ↑ ⁶⁶
Vitamin A	Intestinal claudin-1 (protein) ↑ ¹¹¹ Intestinal occludin (protein) ↑ ¹¹¹ Intestinal ZO-1 (protein) ↑ ¹¹¹
Probiotic interventions	
<i>Bifidobacterium</i> mixture	Ileal β defensin (protein) ↑ ¹¹⁵ Ileal β defensin (mRNA) ↑ ¹¹⁵
<i>Bifidobacterium infantis</i>	Endotoxemia (plasma) ↓ ⁷⁵ Intestinal permeability (functional orogastric FITC-dextran assay) ↓ ¹¹⁶ Small intestinal internalization of claudin-4 in enterocyte cytoplasm (protein) ↓ ¹¹⁶ Small intestinal claudin-4 expression in TJ complex (protein) ↑ ¹¹⁶ Small intestinal occludin expression in TJ complex (protein) ↑ ¹¹⁶ Small intestinal co-fractioning of claudins-2 and -4 and caveolin 1 (protein) ↑ ¹¹⁶ intestinal permeability (functional orogastric FITC-dextran assay) ↓ ¹¹⁶
<i>Bifidobacterium bifidum</i> OLB6378	Ileal occludin (protein) ↓ ⁷³ Ileal claudin-3 (protein) ↓ ⁷³ Ileal occludin distribution towards crypts (normalization) ⁷³ Ileal claudin-3 distribution towards crypts and cell membrane (normalization) ⁷³ Ileal α-catenin (protein) = ⁷³ Ileal β-catenin (protein) = ⁷³ Ileal e-cadherin (protein) = ⁷³ Ileal α-catenin distribution towards complete villus length and cell membrane (normalization) ⁷³ Ileal β-catenin distribution towards complete villus length except for villi tips and cell membrane (normalization) ⁷³ Ileal e-cadherin distribution towards crypts and cell membrane (normalization) ⁷³ Ileal muc2 (mRNA) ↓ ⁷³ Ileal Muc3 (mRNA) ↓ ⁷³ Ileal TFF3 (mRNA) = ⁷³ Ileal number of goblet cells (Muc2 protein) = ⁷³ Ileal number of TFF3 positive cells (TFF3 protein) ↓ ⁷³

Table 2.8 (continued)

<i>Bifidobacterium breve</i> M-16V	Ileal ZO-1 (mRNA) ↓ ¹¹⁷ Ileal claudin-1 (mRNA) ↓ ¹¹⁷ Ileal occludin (mRNA) ↓ ¹¹⁷
<i>Bacteroides fragilis</i> strain ZY-312	Intestinal permeability (functional orogastric FITC-dextran assay) ↓ ¹¹³ Intestinal ZO-1 (protein) ↑ ¹¹³ Intestinal secretory IgA (protein) ↑ ¹¹³
<i>Lactobacillus reuteri</i> DSM 20016	Intestinal permeability (functional orogastric FITC-dextran assay) = ^{71,72}
<i>Lactobacillus reuteri</i> biofilm on unloaded microspheres	Intestinal permeability (functional orogastric FITC-dextran assay) ↓ ⁷¹
<i>Lactobacillus reuteri</i> biofilm on MRS loaded microspheres	Intestinal permeability (functional orogastric FITC-dextran assay) ↓ ⁷¹
<i>Lactobacillus reuteri</i> biofilm on sucrose loaded microspheres	Intestinal permeability (functional orogastric FITC-dextran assay) ↓ ⁷²
<i>Lactobacillus reuteri</i> biofilm on maltose loaded microspheres	Intestinal permeability (functional orogastric FITC-dextran assay) ↓ ⁷²
<i>Lactobacillus rhamnosus</i> GG	Colonic mucosal infiltration of bacteria (EUB338 staining) ↓ ¹⁶¹
Other interventions	
Bovine milk exosomes	Distal ileal number of goblet cells (Muc2 protein) ↑ ¹¹⁸ Distal ileal number of goblet cells (AB-PAS) ↑ ¹¹⁸ Distal ileal number of GRP93 positive cells (protein) ↑ ¹¹⁸
Human breast milk exosomes	Distal ileal number of goblet cells (Muc2 protein) ↑ ¹¹⁹ Distal ileal Muc2 (mRNA) ↑ ¹¹⁹
Berberine	Distal ileal Muc2 (protein) ↑ ⁷⁹ Distal ileal secretory IgA (protein) ↑ ⁷⁹
Human β-defensin-3	Terminal ileal ZO-1 (protein) ↑ ⁸¹

↑ depicts an increase, ↓ depicts a decrease; PUFA, polyunsaturated fatty acids; DHA, docosahexaenoic acid; HMO, human milk oligosaccharides; IAP, intestinal alkaline phosphatase; EGF, epidermal growth factor; HB-EGF, hemoglobin-binding EGF-like growth factor; EPO, erythropoietin.

NEC pathophysiology: vascular dysfunction, hypoxia-ischemia and free radical formation

Intestinal microvasculature alterations, hypoxia, ischemia and oxidative stress (increased reactive oxygen and nitrogen species (together called ROS)) are important factors contributing to NEC pathogenesis. In physiological conditions, intestinal vasodilatation counterbalances effects of vasoconstriction, thereby facilitating appropriate intestinal blood supply¹⁷⁷. During NEC, the balance between vasodilatation and vasoconstriction is disturbed, leading to hypoxia, ischemia and ROS formation. In premature neonates, increased vascular resistance in the superior mesenteric artery (measured with Doppler flow velocimetry) was associated with an increased risk of developing NEC¹⁷⁸. An important intestinal vasodilator that has been studied intensively in the context of NEC is NO. NO is synthesized from arginine by NOS. NOS has three isoforms of which inducible NOS (iNOS) and endothelial NOS (eNOS) are of importance for NEC pathogenesis. eNOS is naturally expressed in the

intestinal vasculature and provides background levels of NO¹⁷⁷. In tissue from infants with NEC it was found that although eNOS protein expression was not reduced during NEC, eNOS function was hampered¹⁷⁹. In contrast to the protective effects of low levels of NO derived from eNOS, excessive NO production by iNOS seems to contribute to NEC pathogenesis^{177,180}. iNOS has been observed to be upregulated in the enterocytes of infants with NEC¹⁸¹. NO or reactive species derived from NO have been implied to suppress intestinal oxygen consumption¹⁸² and inhibit enterocyte proliferation and migration^{177,180}. Moreover, they increase gut barrier permeability by affecting TJ and gap junctions or inducing enterocyte apoptosis and necrosis^{177,180,183}. In addition to changes in vasodilators, higher concentrations of the potent vasoconstrictor endothelin-1 (ET-1) and vasoconstriction are found in diseased parts of the intestine resected from NEC patients when compared with relatively healthy parts of the same resected gut¹⁸⁴. Of importance, several inflammatory mediators, have been shown to influence vascular tone via vasoconstrictors and vasodilators; for instance, PAF increases ET-1 mediated vasoconstriction and thereby contributes to impaired blood flow in NEC¹⁷⁷.

Enteral feeding and vascular dysfunction, hypoxia-ischemia and free radical formation in animal models of NEC

Several studies have described the effect of enteral feeding interventions on either ROS, iNOS expression, antioxidant capacity or intestinal vasculature in animal models of NEC (Table 2.9).

Fat-based feeding interventions

Fat-based dietary interventions may reduce oxidative stress in the context of NEC. iNOS mRNA expression was not altered by enteral administration of PUFA with or without nucleotides⁴⁵. However, pre-digested or very low-fat formula feeding reduced intestinal lipid accumulation and accumulation of ROS in the distal ileum of NEC-protocol exposed mice⁸⁵. In addition, both diets reduced intestinal malonaldehyde (MDA) protein levels, indicating reduced lipid oxidation⁸⁵. Enteral administration of MFGM in a rat NEC model lowered ileum iNOS mRNA expression and MDA protein levels and prevented a NEC induced decrease of antioxidant enzyme superoxide dismutase (SOD) protein levels⁴⁸.

Carbohydrate or sugar-based feeding interventions

HMO have been shown to positively influence blood flow and reduce oxidative stress in experimental NEC. Enteral administration of the HMO 2'-FL increased mesenteric blood flow as measured with mesenteric micro-angiography to the levels of breast-fed mice in a murine NEC model⁹¹. This effect was mediated through preserved eNOS expression and function⁹¹ and reduced intestinal iNOS mRNA expression⁹¹. In both a murine and pig model of NEC, 2'-FL, 6'-SL and a combination of 2'-FL and 6'-SL reduced intestinal 3'-nitrotyrosine levels, a marker for nitrogen free radical species, indicating reduced oxidative stress⁹². GOS/FOS administration increased terminal ileum mRNA expression of the anti-oxidant enzymes SOD-1¹³⁵, SOD-3¹³⁶, glutathione peroxidase (GSH-Px)-1¹³⁵, GSH-Px-7¹³⁵ and catalase (CAT)¹³⁵ in a rat NEC model.

Protein or amino acid-based feeding interventions

Mainly amino acid-based feeding interventions have been shown to influence oxidative stress. Enteral supplementation of both L-carnitine and L-arginine normalized the level of thiobarbituric acid reactive substances, suggesting reduced lipid peroxidation and/or increased antioxidant activity in a murine NEC model⁹⁹. However, antioxidant enzymes tissue SOD and CAT activity was not altered by either L-carnitine or L-arginine supplementation⁹⁹. Although L-arginine supplementation also increased nitrate levels (stable metabolite of NO), this was not statistically significant compared to untreated NEC protocol exposed animals⁹⁹. Intestinal hypoxia, as evaluated by pimonidazole staining, was reduced by enteral supplementation of arginine in a murine NEC model⁹⁸. This effect was probably mediated by improved blood flow following increased vasodilatation, as arginine supplementation to formula increased postprandial arterial diameter in the intestinal microcirculation⁹⁸. Addition of N-acetylcysteine to standard formula reduced both ROS levels and lipid peroxidation (MDA) in the terminal ileum of NEC-protocol exposed mice⁸⁵. Glutamine administration did not reduce terminal ileum nitric oxide production in a rat NEC model⁹⁶. Enteral IAP administration inhibits ileal iNOS mRNA expression, both in high and lower dosages, in a rat NEC model¹⁶⁰. In addition, enteral IAP dose dependently decreased ileal levels of nitrogen free radical species¹⁶⁰.

Hormone or growth factor-based feeding interventions

Soybean-derived recombinant human EGF reduced ileal iNOS mRNA levels upon enteral supplementation in a rat NEC model¹⁰⁴. An elegant study by Yu et al. in a rat NEC model observed that enteral HB-EGF administration preserved villus microvascular blood flow, prevented NEC induced changes in intestinal villus microvascular structure and significantly increased submucosal intestinal blood flow¹⁰⁶. In addition, oral administration of the hormone relaxin increases ileal blood flow measured by laser Doppler flowmetry in a rat NEC model¹⁰⁷. In a mouse NEC model, enteral vitamin D administration decreased MDA protein expression (reduced lipid oxidation) and increased GSH-Px protein expression¹¹².

Probiotic feeding interventions

Several probiotic interventions effectively reduce oxidative stress in experimental NEC. *Lactobacillus rhamnosus* supplementation (both alive and dead) as well as supplementation of *Lactobacillus rhamnosus* isolated microbial DNA reduced terminal ileum mRNA expression of iNOS in a murine NEC model and in a premature piglet NEC model³⁹. This effect is likely mediated through TLR9 signaling, as it was not observed in TLR9 knock-down animals³⁹. Also oral administration of CpG-DNA, a ligand of TLR9 signaling, reduced terminal ileum iNOS mRNA levels in mice³⁹. *Bacteroides fragilis* strain ZY-312 prevents *Cronobacter sakazakii* induced iNOS induction in a rat NEC model¹¹³. *Lactobacillus reuteri* DSM17938 administration increased SOD activity, SOD inhibition rate and glutathione (GSH) protein levels while decreasing glutathione disulphide (GSSG) protein levels, MDA protein levels and the GSSG/GSH ratio, suggesting improved antioxidant capacity and reduced oxidative stress⁷⁰. In a rat NEC model, enteral administration of *Saccharomyces boulardii* increased

the mRNA expression of SOD-1¹³⁵, SOD-3¹³⁶, GSH-Px-1¹³⁵, GSH-Px-3¹³⁵, GSH-Px-4¹³⁵, GSH-Px-7¹³⁵ and CAT¹³⁵ in the terminal ileum.

Other enteral feeding interventions

Oral treatment with ginger increased intestinal protein levels of the antioxidant enzymes SOD and GSH-Px and reduced protein levels of the oxidative stress markers MDA and xanthine oxidase (XO)¹²¹. Intestinal MDA protein levels were also significantly reduced by oral sesamol treatment, concomitant with increased SOD protein levels¹²⁵. In addition, levels of the GSH-Px were increased, without reaching statistical significance¹²⁵. Enteral treatment with fennel seed extracts in a rat model of NEC decreased the intestinal total oxidant status, the oxidative stress index, the amount of advanced oxidation protein products and the concentration of lipid hydroperoxide and 8-hydroxydeoxyguanosine (oxidized guanine, 8-OHdG), while increasing the total antioxidant status, indicating reduced oxidative stress¹²². Addition of rat amniotic fluid to formula feeding reduced intestinal mRNA levels of iNOS in a rat NEC model⁶³. Enteral administration of amniotic fluid also reduced distal small intestinal iNOS mRNA levels in a preterm pig model of NEC¹²³ and terminal ileum iNOS protein and mRNA expression in a mouse model of NEC⁴⁰. Interestingly, these effects may be EGFR signaling mediated, as the effects on iNOS expression were largely lost with co-administration of the EGFR inhibitor cetuximab or with amniotic fluid depleted of EGF⁴⁰. Berberine administration reduced ileal iNOS mRNA expression in a rat NEC model⁷⁹. In addition, in a rat NEC model, oral administration of the flavonoid astragaloside IV dose dependently increased distal ileum protein concentrations of GSH and SOD, while decreasing protein levels of MDA, indicating reduction of oxidative stress by astragaloside IV¹²⁶. Finally, enteral supplementation with resveratrol, a polyphenol produced by plants, prevented a NEC induced increase in ileal iNOS protein expression in a rat NEC model¹²⁷.

Table 2.9 Effect of enteral feeding interventions that reduce vascular dysfunction, hypoxia and free radical formation in experimental animal models of NEC.

Enteral Feeding Intervention	Effect on Vascular Dysfunction, Hypoxia and Free Radical Formation (Compared to NEC Protocol Exposure without Feeding Intervention)
Fat-based interventions	
PUFA	Intestinal iNOS (mRNA) = ⁴⁵
Pre-digested fat (less long chain triacylglycerol, not dependent on intestinal lipases)	Ileal ROS accumulation ↓ (DHE staining) ⁸⁵ Ileal MDA (protein) ↓ ⁸⁵
Very low-fat diet	Ileal ROS accumulation ↓ (DHE staining) ⁸⁵ Ileal MDA (protein) ↓ ⁸⁵
MFGM	Ileal iNOS (mRNA) ↓ ⁴⁸ Intestinal MDA (protein) ↓ ⁴⁸ Intestinal SOD (protein) ↑ ⁴⁸
Carbohydrate/sugar-based interventions	
2'-FL	Mesenteric blood flow ↑ (mesenteric micro-angiography) (eNOS dependent) ⁹¹ Intestinal iNOS (mRNA) ↓ ⁹¹ Small intestinal free nitrogen species, 3-nitrotyrosine (protein) ↓ ⁹²
6'-SL	Small intestinal free nitrogen species, 3-nitrotyrosine (protein) ↓ ⁹²
2'-FL + 6'-SL	Small intestinal free nitrogen species, 3-nitrotyrosine (protein) ↓ ⁹²

Table 2.9 (continued)

GOS/FOS	Terminal ileum SOD-1 (mRNA) ↑ ¹³⁵ Terminal ileum SOD-3 (mRNA) ↑ ¹³⁶ Terminal ileum GSH-Px-1 ↑ ¹³⁵ Terminal ileum GSH-Px-7 ↑ ¹³⁵ Terminal ileum CAT ↑ ¹³⁵
Protein/amino acid-based interventions	
L-Arginine	Intestinal thiobarbituric acid reactive substances ↓ ⁹⁹ Intestinal SOD (protein) = ⁹⁹ Intestinal CAT (protein) = ⁹⁹ Intestinal nitrate (stable metabolite of NO) ↑ (NS) ⁹⁹ Intestinal hypoxia ↓ (pimnidazole) ⁹⁸ Postprandial arterial diameter intestinal microcirculation ↑ ⁹⁸
L-Carnitine	Intestinal thiobarbituric acid reactive substances ↓ ⁹⁹ Intestinal SOD (protein) = ⁹⁹ Intestinal CAT (protein) = ⁹⁹
Glutamine IAP	Terminal ileal NO production = ⁹⁶ Ileal iNOS (MMA) ↓ ¹⁶⁰
N-Acetylcysteine	Ileal free nitrogen species, 3-nitrotyrosine (protein) ↓ ¹⁶⁰ Ileal ROS accumulation ↓ (DHE staining) ⁸⁵ Ileal MDA (protein) ↓ ⁸⁵
Hormone/growth factor / Vitamin-based interventions	
Recombinant EGF from soybean extract	ileal iNOS (mRNA) ↓ ¹⁰⁴
HB-EGF	Villus microvascular blood flow ↑ (angiography) ¹⁰⁶ Villus microvascular structure preserved (angiography, scanning electron microscopy) ¹⁰⁶ Submucosal intestinal blood flow ↑ (angiography) ¹⁰⁶
Relaxin	Ileal blood flow ↑ (laser Doppler flowmetry) ¹⁰⁷
Vitamin D	Intestinal MDA (protein) ↓ ¹¹² Intestinal GSH-Px (protein) ↑ ¹¹²
Probiotic interventions	
<i>Bacteroides fragilis</i> strain ZY-312	Intestinal iNOS (protein) ↓ ¹¹³
<i>Lactobacillus rhamnosus</i> HN001 (alive)	Terminal ileal iNOS (mRNA) ↓ (TLR9 dependent) ³⁹
<i>Lactobacillus rhamnosus</i> HN001 (dead, UV-radiated)	Terminal ileal iNOS (mRNA) ↓ ³⁹
<i>Lactobacillus rhamnosus</i> HN001 isolated microbial DNA	Terminal ileal iNOS (mRNA) ↓ ³⁹
CpG-DNA	Terminal ileal iNOS (mRNA) ↓ ³⁹
<i>Lactobacillus reuteri</i> DSM 17938	Terminal ileal SOD activity (U/mg protein) ↑ ⁷⁰ Terminal ileal SOD inhibition rate (%) ↑ ⁷⁰ Terminal ileal GSSG concentration (protein) ↓ ⁷⁰ Terminal ileal GSH concentration (protein) ↑ ⁷⁰ Terminal ileal GSSG/GSH ratio (protein) ↓ ⁷⁰ Terminal ileal MDA concentration (protein) ↓ ⁷⁰

Table 2.9 (continued)

Enteral Feeding Intervention	Effect on Vascular Dysfunction, Hypoxia and Free Radical Formation (Compared to NEC Protocol Exposure without Feeding Intervention)
<i>Saccharomyces Boulardii</i>	Terminal ileal SOD-1 (mRNA) ↑ ¹³⁵ Terminal ileal SOD-3 (mRNA) ↑ ¹³⁶ Terminal ileal GSH-Px-1 ↑ ¹³⁵ Terminal ileal GSH-Px-3 ↑ ¹³⁵ Terminal ileal GSH-Px-4 ↑ ¹³⁵ Terminal ileal GSH-Px-7 ↑ ¹³⁵ Terminal ileal CAT ↑ ¹³⁵
Other interventions	
Ginger	Intestinal SOD (protein) ↑ ¹²¹ Intestinal GSH-Px (protein) ↑ ¹²¹ Intestinal MDA (protein) ↓ ¹²¹ Intestinal XO (protein) ↓ ¹²¹
Sesamol	Intestinal SOD (protein) ↑ ¹²⁵ Intestinal GSH-Px (protein) ↑ (NS) ¹²⁵ Intestinal MDA (protein) ↓ ¹²⁵
Fennel seed extracts	Intestinal total oxidant status (μmol H ₂ O ₂ equivalent/g protein) ↓ ¹²² Intestinal oxidative stress index (total oxidant status/total antioxidant status) ↓ ¹²² intestinal advanced oxidation protein products (ng/mg protein) ↓ ¹²² intestinal lipid hydroperoxide (nmol/L) ↓ ¹²² intestinal 8-hydroxydeoxyguanosine (8-OHdG, ng/mL) ↓ ¹²² intestinal total antioxidant status (mmol Trolox equivalent/g protein) ↑ ¹²²
Amniotic fluid	intestinal iNOS (mRNA) ↓ ⁶³ distal small intestinal/terminal ileum iNOS (mRNA) ↓ ^{40,123} terminal ileum iNOS (protein) ↓ ⁴⁰
Berberine	ileal iNOS (mRNA) ↓ ⁷⁹
Astragaloside IV	distal ileum GSH (protein) ↑ ¹²⁶ distal ileum SOD (protein) ↑ ¹²⁶ distal ileum MDA (protein) ↓ ¹²⁶
Resveratrol	ileum iNOS (protein) ↓ ¹²⁷

↑ depicts an increase, ↓ depicts a decrease; PUFA, polyunsaturated fatty acids; MFGM, milk fat globule membrane; 2'-FL, 2'-fucosyllactose; 6'-SL, 6'-sialyllactose; GOS: galacto-oligosaccharides; FOS, fructo-oligosaccharides; IAP, intestinal alkaline phosphatase; EGF, epidermal growth factor; HB-EGF, hemoglobin-binding EGF-like growth factor.

NEC pathophysiology: intestinal epithelial cell death and proliferation

Several forms of cell death can be distinguished in the intestinal epithelium including apoptosis, necrosis and necroptosis¹⁸⁵ and all of these mechanisms have been described in NEC pathophysiology^{181,186}. Whereas necrosis is uncontrolled and comes with collateral damage, both apoptosis and necroptosis are tightly regulated by several cellular pathways¹⁸⁵. Increased apoptosis is detected in the intestinal epithelium of NEC patients; increased terminal deoxynucleotidyl transferase dUTP nick end labelling (TUNEL) staining was observed in villus enterocytes in NEC biopsies¹⁸¹ and mRNA and protein expression of caspase 3 and Bax were found to be increased in ileum of patients with NEC compared to controls¹⁸⁷. In addition, the mRNA expression of the anti-apoptotic Bcl2 was decreased¹⁸⁷. NEC is also associated with intestinal upregulated mRNA expression of the three major necroptosis pathway genes and mRNA expression of these genes positively correlates with

disease severity¹⁸⁶. Also on protein level increased necroptosis is detected in specimen from infants with NEC¹⁸⁶. In experimental NEC (murine model), both pharmacological and genetic inhibition of necroptosis decreased intestinal epithelial cell death and mucosal inflammation, suggesting a role for necroptosis in NEC pathogenesis¹⁸⁶. Last, autophagy, is observed at higher levels in NEC tissue compared to control tissue^{55,188}. Autophagy is the transfer of cytoplasmic components, organelles or infectious agents to lysosomes for degradation¹⁸⁹. Although this is in principle a cell survival mechanism, it ultimately lead to cell death¹⁸⁹. Another mechanism that may contribute to cell death in NEC is intestinal endoplasmic reticulum (ER) stress. In tissue of a subset of patients with acute NEC splicing of the ER stress related protein X-box binding protein 1 (XBP1) was detected with concomitant increased mRNA and protein expression of ER stress markers binding immunoglobulin protein (BiP) and C/EBP homologous protein (CHOP), suggesting increased ER stress¹⁹⁰. Importantly, ER stress correlated with increased morphological damage and intestinal inflammation and worse surgical outcome¹⁹⁰. Finally, increased mRNA expression of spliced XBP1 is reported in combination with increased BiP protein expression and increased apoptosis in the crypts in NEC patients compared to controls¹⁹¹.

Besides cell death, intestinal epithelial proliferation is changed during NEC. In gut samples from infants with NEC, reduced proliferation was observed in intestinal crypts¹⁸⁶. In contrast, a study by Schaart et al. found increased proliferation in both severely and mildly damaged small intestine and colon of infants with NEC¹⁶⁷, indicating that NEC severity might be an important determinant herein. Vieten et al. reported loss of villus length in the small bowel of NEC patients, concomitant with an increased crypt depth suggesting hyperplasia and increased numbers of proliferating cells in the remaining viable crypts in both small intestine and colon. This suggests a compensatory proliferative response is triggered in NEC, that is insufficient to compensate the rapid mucosal damage in NEC¹⁹². Finally, loss of leucine-rich repeat-containing G-protein coupled receptor 5 (LGR5) positive stem cells was observed in human intestine resected from NEC patients compared to intestine resected from an aged-matched control infant with ileal atresia¹⁷⁶.

Enteral feeding and intestinal epithelial cell death and proliferation in animal models of NEC

An overview of enteral feeding interventions with cell death or proliferation as read-out is presented in **Table 2.10**.

Fat-based feeding interventions

Both PUFA and MPL were studied in relation to cell death in experimental NEC. Pre-treatment of rats with fish oil (rich in the PUFA DHA and EPA) reduced intestinal protein levels of BiP and the pro-apoptotic protein caspase 12, indicating reduced intestinal ER stress and potential protection against apoptosis⁸³. However, in another study, enteral supplementation of PUFA did not reduce the level of intestinal epithelial apoptosis in experimental NEC⁴⁵. In contrast, enteral administration of MPL, which are abundantly present in MFGM, did dose dependently decrease intestinal epithelial cell apoptosis indicated by decreased expression of the pro-apoptotic protein Bax, increased expression of

the anti-apoptotic protein Bcl-2 and inhibited caspase activity (expression of caspase 9 and caspase 3 and TUNEL)⁸⁴. Formula feeding supplemented with pomegranate seed oil normalized mean ileal villus length of NEC protocol exposed rats and increased ileal epithelial cell proliferation⁴⁷.

Carbohydrate or sugar based feeding interventions

HMO have been shown to promote intestinal proliferation and reduce apoptosis in the context of NEC. In a mouse NEC model, orogastric administration of HMO restored the amount of cells positive for the proliferation marker Ki67 in the ileum^{49,86,88}, whereas this effect was not seen with supplementation with infant formula oligosaccharides⁴⁹. In addition, loss of Sox9-positive stem cells was prevented by HMO treatment, but not by infant formula oligosaccharides⁴⁹. In a preterm pig model of NEC, treatment with a mixture of four HMO did not change small intestinal mRNA expression of proliferating cell nuclear antigen (PCNA)¹³⁴. Enteral administration of HMO reduced apoptosis (TUNEL)⁸⁶ and decreased ileal cleaved caspase-3 and hypoxia-inducible factor 1 α (HIF1 α) protein levels⁸⁸ in a murine NEC model. Both in a pig and murine NEC model, enteral administration of 2'-FL, 6'-SL and a combination of the two reduced intestinal epithelial apoptosis⁹².

Protein or amino acid-based feeding interventions

Enteral administration of glutamine in a mouse model of NEC decreases intestinal epithelial cell apoptosis (TUNEL assay) and decreases expression of pro-apoptotic proteins Bax, caspase 9 and caspase 3 while increasing Bcl-2 protein expression (anti-apoptotic)⁸⁴. In addition, enteral glutamine lowered caspase 3 protein expression in jejunum, ileum and colon in a rat model of NEC⁹⁷. The potential harmful effects of nutritional interventions are demonstrated by a study of high-dose (10 g/L) lactoferrin supplementation in a preterm pig model of NEC. In this study, lactoferrin supplementation decreased villus length/crypt depth ratio, suggesting decreased proliferation or increased cell death in the intestinal epithelium³⁶. In addition, the Bax/Bcl-2 ratio and HIF1 α protein levels were elevated by supplementation of formula with lactoferrin, whereas protein levels of pro-caspase 3 and cleaved caspase 3 were not affected³⁶. These detrimental effects are likely caused by the high dose of the lactoferrin used, as in in vitro experiments with cultured intestinal epithelial cells a high dose, but not lower doses, of bovine lactoferrin upregulated the expression of pro-apoptotic proteins and HIF1 α signaling pathway proteins and downregulated that of anti-apoptotic proteins and proteins related to cell proliferation³⁶. In another study using a mouse model of NEC, enteral recombinant lactoferrin administration (6 g/L) prevented a NEC protocol induced decrease in Ki67 immunoreactivity, preserved beta-catenin immunoreactivity and restored LGR5 mRNA levels in the distal ileum¹⁰¹. Together, these studies demonstrate that the dose of the nutritional intervention studied is important and should be taken into account when designing a clinical trial.

Hormone, growth factor or vitamin-based feeding interventions

Effects of hormones and growth factors on intestinal epithelial proliferation and cell death have been studied extensively. Enteral EGF increased intestinal villus length through

hyperplasia, but had no effect on intestinal epithelial proliferation as measured by PCNA immunoreactivity in experimental NEC¹⁹³. In addition, EGF decreased levels of Bax¹⁹³, increased levels of Bcl-2¹⁹³ and decreased the Bax-to-Bcl-2 ratio both on mRNA¹⁹³ and protein level^{37,193}. In line, EGF markedly decreased cleaved caspase 3 immunoreactivity at the villus tips¹⁹³. Ileal protein levels of Beclin 1 and LC3II, both important autophagy regulators, as well as the ratio between LC3II and LC3I were decreased by EGF treatment in NEC protocol exposed rats, indicating reduced autophagy⁵⁵. This finding was supported by an increase of the autophagy substrate p62 by orogastric EGF administration⁵⁵. Moreover, whereas typical signs of autophagy such as autophagosomes, autophagolysosomes and vacuoles were present in only NEC protocol exposed animals, these structural abnormalities were virtually absent in NEC protocol exposed animals that were treated with enteral EGF⁵⁵. Enteral HB-EGF decreased intestinal TUNEL score and cleaved caspase 3 score in a rat NEC model, indicating enteral HB-EGF treatment reduces intestinal epithelial apoptosis⁶⁰. However, in another study the Bax-to-Bcl-2 protein ratio was unaltered³⁷. Enteral HB-EGF improved bromodeoxyuridine (BrdU)-positive cell migration along the crypt-villus axis^{59,61} and increased intestinal epithelial proliferation (number of BrdU-positive cells) in experimental NEC⁵⁹. In addition, in a mouse NEC model, enteral HB-EGF increased the small intestinal mRNA levels of integrin subunits $\alpha 5$ and $\beta 1$ (but not integrin subunits $\alpha 1$, $\alpha 2$, $\alpha 3$ or $\alpha 6$) and the protein concentrations of integrin subunits $\alpha 5$ and $\beta 1$ that were reduced by the NEC inducing protocol⁶¹. Orogastic HB-EGF administration increased proliferation of crypt epithelial cells that was reduced by NEC protocol exposure and prevents reduction of the number of enterocytes per villus in the jejunum of rats subjected to an experimental NEC model¹⁷⁶. In addition, the number of LGR5+/prominin-1+ stem cells was significantly increased by HB-EGF administration in NEC protocol exposed rats¹⁷⁶.

In the small intestine of NEC protocol exposed animals without intestinal necrosis, Beclin 1 and LC3 immunoreactivity and Beclin 1 and LC3II protein levels were decreased and p62 immunoreactivity and protein levels were increased in EPO treated animals compared to non-EPO treated animals¹⁹⁴. In addition, cleaved caspase 3 immunoreactivity was reduced and Bcl-2 protein levels were increased by orogastric EPO exposure¹⁹⁴. In vitro evidence from an IEC-6 cell line suggests the found effects on autophagy and apoptosis are mediated through Akt/mTOR and MAPK/ERK signaling pathways respectively¹⁹⁴.

Evidence on the effect of vitamins on intestinal cell death and proliferation are sparse. One study investigating the effects of enteral ATRA administration found decreased levels of apoptosis in the terminal ileum intestinal crypts and preserved proliferative capacity of crypt intestinal epithelial cells in NEC protocol exposed mice¹⁰⁹. In addition, vitamin D was shown to reduce cleaved caspase 3 protein expression, whereas Bcl-2 and Ki67 protein expression were increased, suggesting reduced apoptosis and increased proliferation¹¹².

Probiotic feeding interventions

The only probiotic feeding interventions studied in relation to intestinal cell death are *Bacteroides fragilis*, *Lactobacillus rhamnosus*, *Bifidobacterium bifidum* and *Bifidobacterium breve*. Pre-treatment with *Bacteroides fragilis* strain ZY-312 lowered intestinal protein levels of caspase 3 and Bax and increased protein levels of Bcl-2 in a *Cronobacter sakazakii*-induced rat NEC model, indicating *Bacteroides fragilis* modulates apoptosis upon enteral

administration¹¹³. In addition, treatment with *Bacteroides fragilis* reduced NEC-protocol induced inflammasome expression and pyroptosis, as demonstrated by reduced protein levels of NLRP3 inflammasome proteins (caspase-1, ASC and NLRP3), IL1 β and gasdermin-D¹¹³. *Lactobacillus rhamnosus* GG administration partially prevents intestinal apoptosis in a mouse NEC model¹⁶¹. *Bifidobacterium bifidum* administration in a rat NEC model decreased ileal protein levels of Bax, increased protein levels of Bcl-w, reduced the Bax/Bcl-2 ratio and decreased the number of apoptotic cells (CC3-positive cells)⁷⁴. This effect seems to be COX-2 mediated as ileal COX-2 immunoreactivity and prostaglandin E2 concentrations were upregulated by *Bifidobacterium bifidum* treatment and simultaneous administration of a COX-2 inhibitor abolished the observed reduction of apoptosis⁷⁴. Last, supplementation of formula feeding with *Bifidobacterium breve* M-16V in a rat NEC model reduced the ileal mRNA expression of caspase 3¹¹⁷.

Other enteral feeding interventions

A broad range of other enteral feeding interventions has been shown to reduce intestinal cell death and promote proliferation in experimental models of NEC. Administration of amniotic fluid in a mouse NEC model restored terminal ileum epithelial proliferation (PCNA immunoreactivity) in a largely EGFR dependent manner⁴⁰. Enteral ginger treatment in NEC protocol exposed rats decreased TUNEL-positive, caspase 3-positive and caspase 8-positive cell numbers and decreased caspase 3 protein levels, indicated reduced apoptosis¹²¹. Administration of fennel seed extracts decreased the amount of caspase 3-, caspase 8- and caspase 9-positive cells in the terminal ileum and decreased intestinal caspase 3 protein levels¹²². Supplementation of formula feeding with preterm human milk exosomes prevented NEC-protocol induced reduction in enterocyte proliferation in a rat NEC model¹²⁰. The number of Bcl-2- and caspase 3-positive cells were significantly decreased in the intestine of NEC protocol exposed rats that were orally treated with sesamol compared to non-treated rats¹²⁵. Enteral administration of curcumin in a rat NEC model decreased intestinal protein and mRNA expression of caspase 1 and NLRP3 in a SIRT1 mediated fashion, suggesting curcumin reduces pyroptosis¹²⁴.

Table 2.10 Effect of enteral feeding interventions that decrease intestinal epithelial cell death and increase proliferation in experimental animal models of NEC.

Enteral Feeding Intervention	Effect on Intestinal Epithelial Cell Death and Proliferation (Compared to NEC Protocol Exposure without Feeding Intervention)
Fat-based interventions	
Fish oil (rich in n-3 PUFA)	Small intestinal BiP (protein) ↓ ⁸³ Small intestinal caspase 12 (protein) ↓ ⁸³
PUFA	Intestinal apoptosis (TUNEL) = ⁴⁵
MPL	Small intestinal apoptosis (TUNEL) ↓ ⁸⁴ Small intestinal Bax (protein) ↓ ⁸⁴ Small intestinal Bcl-2 (protein) ↑ ⁸⁴ Small intestinal caspase 9 (protein) ↓ ⁸⁴ Small intestinal caspase 3 protein) ↓ ⁸⁴
Pomegranate seed oil	Mean ileal villus length ↑ ⁴⁷ Ileal epithelial cell proliferation (PCNA) ↑ ⁴⁷

Table 2.10 (continued)

Carbohydrate/sugar-based interventions	
HMO	(Terminal) ileal Ki67-positive cells ↑ ^{49,86,88} Ileal Sox9-positive cells ↑ ⁴⁹ Terminal ileal TUNEL (protein) ↓ ⁸⁶ Ileal cleaved caspase 3 (protein) ↓ ⁸⁸ Ileal HIF1α (protein) ↓ ⁸⁸
Mixture of four HMOs	Small intestinal PCNA (mRNA) = ¹³⁴
2'-FL	Small intestinal apoptosis (TUNEL) ↓ ⁹²
6'-SL	Small intestinal apoptosis (TUNEL) ↓ ⁹²
2'-FL + 6'-SL	Small intestinal apoptosis (TUNEL) ↓ ⁹²
Protein/amino acid-based interventions	
Lactoferrin	Proximal intestinal villus length/crypt depth ratio ↓ ³⁶ Middle intestinal Bax-to-Bcl-2 ratio (protein) ↑ ³⁶ Middle intestinal HIF-1α (protein) ↑ ³⁶ Middle intestinal pro-caspase 3 (protein) = ³⁶ Middle intestinal CC3 (protein) = ³⁶ Distal ileal Ki67 (protein) ↑ ¹⁰¹ Distal ileal β-catenin (protein) ↑ ¹⁰¹ Distal ileal LGR5 (mRNA) ↑ ¹⁰¹
L-Glutamine/glutamine	Small intestinal apoptosis (TUNEL) ↓ ⁸⁴ Small intestinal Bax (protein) ↓ ⁸⁴ Small intestinal Bcl-2 (protein) ↑ ⁸⁴ Small intestinal caspase 9 (protein) ↓ ⁸⁴ Small intestinal caspase 3 (protein) ↓ ⁸⁴ Jejunum, ileum and colon caspase 3 (protein) ↓ ⁹⁷
Hormone/growth factor/vitamin-based interventions	
EGF	Ileal villus length ↑ ¹⁹³ Ileal epithelial proliferation (PCNA) = ¹⁹³ Ileal Bax (mRNA) ↓ ¹⁹³ Ileal Bax (protein) ↓ ¹⁹³ Ileal Bcl-2 (mRNA) ↑ ¹⁹³ Ileal Bcl-2 (protein) ↑ ¹⁹³ Ileal Bax-to-Bcl-2 ratio (mRNA) ↓ ¹⁹³ Ileal CC3 villus tips (protein) ↓ ¹⁹³ Ileal Bax-to-Bcl-2 ratio (protein) ↓ ^{37,193} Ileal Beclin 1 (protein) ↓ ⁵⁵ Ileal LC3II (protein) ↓ ⁵⁵ Ileal LC3II/LCRI ratio (protein) ↓ ⁵⁵ Ileal p62 (protein) ↑ ⁵⁵ Ileal autophagy signs (autophagosomes, autophagolysosomes, vacuoles) (transmission electron microscopy) ↓ ⁵⁵

Table 2.10 (continued)

Enteral Feeding Intervention	Effect on Intestinal Epithelial Cell Death and Proliferation (Compared to NEC Protocol Exposure without Feeding Intervention)
HB-EGF	Intestinal TUNEL score (protein) ↓ ⁶⁰ Intestinal CC3 score (protein) ↓ ⁶⁰ Ileal cell migration (BrdU-positive cells) ↑ ^{59,61} Small intestinal integrin subunit α5 (mRNA) ↑ ⁶¹ Small intestinal integrin subunit β1 (mRNA) ↑ ⁶¹ Small intestinal integrin subunit α1 (mRNA) = ⁶¹ Small intestinal integrin subunit α2 (mRNA) = ⁶¹ Small intestinal integrin subunit α3 (mRNA) = ⁶¹ Small intestinal integrin subunit α6 (mRNA) = ⁶¹ Small intestinal integrin subunit α5 (protein) ↑ ⁶¹ Small intestinal integrin subunit β1 (protein) ↑ ⁶¹ Ileal epithelial cell proliferation (number of BrdU-positive cells) ↑ ⁵⁹ Ileal Bax-to-Bcl-2 ratio (protein) = ³⁷ Jejunal crypt epithelial cell proliferation (PCNA) ↑ ¹⁷⁶ Jejunal number of enterocytes per villus ↑ ¹⁷⁶ Jejunal number of LGR5+/prominin-1+ stem cells ↑ ¹⁷⁶
EPO	Ileal Beclin 1 immunoreactivity ↓ ¹⁹⁴ Ileal LC3 immunoreactivity ↓ ¹⁹⁴ Small intestinal Beclin 1 (protein) ↓ ¹⁹⁴ Small intestinal LC3II (protein) ↓ ¹⁹⁴ Ileal p62 immunoreactivity ↑ ¹⁹⁴ Small intestinal p62 (protein) ↑ ¹⁹⁴ Ileal CC3 immunoreactivity ↓ ¹⁹⁴ Small intestinal Bcl-2 (protein) ↑ ¹⁹⁴
ATRA	Terminal ileal apoptosis intestinal crypts (TUNEL) ↓ ¹⁰⁹ Terminal ileal proliferation crypt intestinal epithelial cells (Ki67, BrdU) ↑ ¹⁰⁹
Vitamin D	Intestinal cleaved caspase 3 (protein) ↓ ¹¹² Intestinal Bcl-2 (protein) ↑ ¹¹² Intestinal Ki67 (protein) ↑ ¹¹²
Probiotic interventions	
<i>Bacteroides fragilis</i> strain ZY-312	Intestinal CC3 (protein) ↓ ¹¹³ Intestinal Bax (protein) ↓ ¹¹³ Intestinal Bcl-2 (protein) ↓ ¹¹³ Intestinal caspase 1 (protein) ↓ ¹¹³ Intestinal ASC (protein) ↓ ¹¹³ Intestinal NLRP3 (protein) ↓ ¹¹³ Intestinal IL1β (protein) ↓ ¹¹³ Intestinal gasdermin-D (protein) ↓ ¹¹³
<i>Lactobacillus rhamnosus</i> GG	Ileal CC3 (protein) ↓ ¹⁶¹ Ileal apoptotic index (TUNEL) ↓ ¹⁶¹
<i>Bifidobacterium bifidum</i> OLB6378	Ileal Bax (protein) ↓ ⁷⁴ Ileal Bcl-w (protein) ↑ ⁷⁴ Ileal Bax/Bcl-w ratio ↓ ⁷⁴ Ileal CC3-positive cell number ↓ ⁷⁴
<i>Bifidobacterium breve</i> M-16V	Ileal caspase 3 (mRNA) ↓ ¹¹⁷

Table 2.10 (continued)

Other interventions	
Amniotic fluid	Terminal ileal PCNA immunoreactivity ↑ ⁴⁰
Ginger	Intestinal TUNEL-positive cell number ↓ ¹²¹ Intestinal C3-positive cell number ↓ ¹²¹ Intestinal C8-positive cell number ↓ ¹²¹ Intestinal caspase 3 (protein) ↓ ¹²¹
Fennel seed extracts	Terminal ileal C3-positive cells number ↓ ¹²² Terminal ileal C8-positive cells number ↓ ¹²² Terminal ileal C9-positive cells number ↓ ¹²² Intestinal C3 concentration (protein) ↓ ¹²²
Preterm human breast milk exosomes	Intestinal enterocyte proliferation (BrdU) ↑ ¹²⁰
Sesamol	Intestinal Bcl-2-positive cell number ↓ ¹²⁵ Intestinal caspase-3 positive cell number ↓ ¹²⁵
Curcumin	Intestinal caspase 1 (protein) ↓ ¹²⁴ Intestinal NLRP3 (protein) ↓ ¹²⁴ Intestinal caspase 1 (mRNA) ↓ ¹²⁴ Intestinal NLRP3 (mRNA) ↓ ¹²⁴

↑ depicts an increase, ↓ depicts a decrease; PUFA, polyunsaturated fatty acids; MPL, milk polar lipids; HMO, human milk oligosaccharides; EGF, epidermal growth factor; HB-EGF, hemoglobin-binding EGF-like growth factor; EPO, erythropoietin; ATRA, all-*trans* retinoic acid.

NEC pathophysiology: microbial dysbiosis

Inappropriate microbial colonization or dysbiosis is considered to be an important factor contributing to NEC pathogenesis¹, although reports on the precise microbial colonization patterns or strains involved are conflicting¹⁹⁵. A predominance of gram-negative bacteria from the phylum *Proteobacteria*, the class *Gammaproteobacteria* and the families *Enterobacteriaceae*, *Vibrionaceae* and *Pseudomonadaceae* are most strongly linked with NEC development¹⁹⁵. Importantly, in a meta-analysis by Pammi et al. an increased relative abundance of the phylum *Proteobacteria* and a decrease of the phyla *Firmicutes* and *Bacteroides* were found prior to NEC onset¹⁹⁶. In addition, a higher bacterial replication rate of all bacteria and especially *Enterobacteriaceae* has been linked to subsequent NEC development¹⁹⁷. Although the intrauterine environment is not sterile¹⁹⁸, the major microbial colonization undoubtedly takes place in the first hours to days after birth and is influenced by various factors such as enteral feeding, gestational age, mode of delivery and antibiotic use^{199,200}. The underdeveloped gut barrier of preterm born infants makes them vulnerable to the effects of a disturbed microbial colonization¹⁹⁵. Mechanisms through which microbial dysbiosis can contribute to NEC pathogenesis include excessive TLR4 stimulation by endotoxin, disturbance of a balanced luminal short chain fatty acid (SCFA) content and changes in intestinal motility²⁰¹.

Enteral feeding and microbial dysbiosis in animal models of NEC

Unfortunately, not many enteral feeding intervention studies have taken microbial changes into account (Table 2.11).

Fat-based feeding interventions

BCFA form a fat-based enteral feeding intervention known to influence microbial composition. Enteral treatment with BCFA increased the abundance of *Bacillaceae* and *Pseudomonadaceae* on family level and increased the relative abundance of *Bacillus subtilis* at species level in cecal samples of NEC protocol exposed rats to levels comparable to dam fed control animals⁴⁶. In addition, relative abundance of *Bacillus subtilis* was higher in healthy than in diseased animals⁴⁶. Finally, BCFA administration increased the relative abundance of the species *Pseudomonas aeruginosa* to levels even higher than in dam fed animals⁴⁶. As *Bacillus subtilis* is used as a probiotic, the BCFA induced increase in the relative abundance of this species is considered beneficial, for *Pseudomonas aeruginosa* this is unclear⁴⁶.

Carbohydrate or sugar-based feeding interventions

As HMO are considered to be important prebiotics, it is not surprising these components have been studied in relation to intestinal microbial composition. Good et al. studied the effects of enteral treatment with the HMO 2'-FL in a murine NEC model on the abundance of several microbial taxa in faecal content by 16S ribosomal RNA amplicon sequence analysis. They observed in NEC mice an increased abundance of *Enterobacteriaceae* and decreased abundance of *Lactobacillaceae* following HMO treatment⁹¹. However, the β -diversity was also reduced, indicating a more homogenous intestinal microbiome upon enteral HMO treatment⁹¹. In a pig NEC model, enteral administration of 2'-FL did not reduce cecal microbial colonization density and did not change microbial α -diversity in cecal tissue and cecal content, however, the proportion of genus *Enterococcus* in cecal content was increased by administration of 2'-FL¹³³. Also in a pig NEC model, administration of a mixture of >25 HMO components did not change the colonic relative abundance of different genera²⁰². Administration of a mixture of four HMO did not change colonic microbial diversity (number of bacterial operational taxonomic units (OUT) per sample)¹³⁴ or the relative abundance of different genera²⁰² in a preterm pig model of NEC. Within the total microbial community, no differences were observed in clustering, however, on the individual level HMO treated animals had a lower number of the genus *Fusobacterium* and this number was, although not statistically significantly, related to NEC development¹³⁴.

Protein or amino acid-based feeding interventions

In a preterm pig model of NEC, enriching formula feeding with caseino-glycomacropeptide (CGMP) or osteopontin (OPN) did not influence colon microbiota composition (similar α diversity and no significant changes in abundance of genera)¹²⁹.

Hormone, growth factor or vitamin-based feeding interventions

Enteral vitamin A treatment in a murine NEC model had a strong influence on the microbial composition of intestinal tract content, accounting for 67.8% and 66.1% for the total variations observed on phylum and genus level, respectively¹¹¹. Vitamin A treatment specifically decreased the abundance of the phylum *Proteobacteria* and the genera *Escherichia-Shigella*, *Lactobacillus*, *Acinetobacter* and *Gemella* and increased the phylum

Bacteroidetes and the genera *Romboutsia*, *Bacteroides* and *Parabacteroides*¹¹¹ compared to control animals. The proportion of the phylum *Firmicutes* was not affected by vitamin A administration¹¹¹.

Probiotic feeding interventions

In a quail NEC model, oral inoculation with *Bifidobacterium infantis-longum* decreased cecal bacterial counts of *Clostridium perfringens*, without altering counts of *Clostridium difficile*¹³⁰. Administration of *Bacteroides fragilis* strain ZY-312 in a rat NEC model partially rescued the number of OTU in fecal samples, partially prevented a NEC induced reduction of the abundance of phylum *Bacteroidetes* and decreased the relative abundance of the phylum *Proteobacteria*¹¹³. In a rat NEC model, administration of *Lactobacillus reuteri* biofilms on maltose loaded microspheres shifted the fecal microbiome of NEC stressed rat pups more towards that of breastfed control pups than unbound *Lactobacillus reuteri* (16S rRNA sequencing analysis)⁷². On taxa level, *Lactobacillus* spp. abundance, which was negatively correlated to histological NEC severity, increased after *Lactobacillus reuteri* administration (both unbound and biofilm associated) and was more effectively maintained by administration of *Lactobacillus reuteri* as a biofilm on maltose loaded microspheres than by unbound *Lactobacillus reuteri*⁷². *Lactobacillus reuteri* bound to maltose loaded biospheres and unbound *Lactobacillus reuteri* effectively reduced the relative abundance of the potentially pathogenic *Enterobacter* spp⁷². Finally, enteral administration of a mixture of probiotics (containing *Bifidobacterium animalis* and several *Lactobacillus species*) changed the general colonization pattern in distal ileum and colon (T-RFLP analysis), with a decrease in colonization density of *Clostridium perfringens*, and altered the relative proportion of several culturable bacteria⁷⁷. It decreased the abundance of *Clostridia* (distal small intestinal homogenate and colon content) and *Enterococci* (stomach content and distal small intestinal homogenate) and increased the abundance of lactic acid bacteria (stomach content and colon content), *Lactobacilli* (stomach content and distal small intestinal homogenate) and total anaerobes (colon content)⁷⁷.

Other enteral feeding interventions

Enteral administration of amniotic fluid reduces distal small intestinal bacterial colonization in a pig model of NEC. In addition, colonic bacterial composition was changed towards controls by enteral administration of amniotic fluid¹²³.

Table 2.11 Effect of enteral feeding interventions that affect microbial dysbiosis in experimental animal models of NEC.

Enteral Feeding Intervention	Effect on Microbial Dysbiosis (Compared to NEC Protocol Exposure without Feeding Intervention)
Fat-based interventions	
BCFA	Cecal <i>Bacillaceae</i> (family) abundance ↑ ⁴⁶
	Cecal <i>Pseudomonadaceae</i> (family) abundance ↑ ⁴⁶
	Cecal <i>Bacillus subtilis</i> (species) abundance ↑ ⁴⁶
	Cecal <i>Pseudomonas aeruginosa</i> (species) abundance ↑ ⁴⁶

Table 2.11 (continued)

Enteral Feeding Intervention	Effect on Microbial Dysbiosis (Compared to NEC Protocol Exposure without Feeding Intervention)
Carbohydrate/sugar-based interventions	
2'-FL	Fecal <i>Enterobacteriaceae</i> (family) abundance = ⁹¹ Fecal <i>Lactobacillaceae</i> (family) abundance = ⁹¹ Fecal microbiota β -diversity \downarrow ⁹¹ Cecal microbial colonization density (FISH) = ¹³³ α -Diversity cecal tissue = ¹³³ α -Diversity cecal content = ¹³³ Proportion <i>Enterococcus</i> (genus) in cecal content \uparrow ¹³³
Mixture of four HMOs	Colonic microbial diversity (number of OTU per sample) = ¹³⁴ Colonic microbial clustering = ¹³⁴ Colonic relative abundance genera OTU = ²⁰² Colonic number of <i>Fusobacterium</i> (genus) on individual level \downarrow ¹³⁴
Mixture of >25 HMO components	Colonic relative abundance genera OTU = ²⁰²
Protein/amino acid-based interventions	
OPN	Colonic microbial α diversity = ¹²⁹ Colonic microbial abundance of genera = ¹²⁹
CGMP	Colonic microbial α diversity = ¹²⁹ Colonic microbial abundance of genera = ¹²⁹
Vitamin-based interventions	
Vitamin A	Fecal Proteobacteria (phylum) abundance \downarrow ¹¹¹ Fecal Escherichia-Shigella (genus) abundance \downarrow ¹¹¹ Fecal Lactobacillus (genus) abundance \downarrow ¹¹¹ Fecal Acinetobacter (genus) abundance \downarrow ¹¹¹ Fecal Gemella (genus) abundance \downarrow ¹¹¹ Fecal Bacteroidetes (phylum) abundance \uparrow ¹¹¹ Fecal Bacteroides (genus) abundance \uparrow ¹¹¹ Fecal Romboutsia (genus) abundance \uparrow ¹¹¹ Fecal Parabacteroides (genus) abundance \uparrow ¹¹¹
Probiotic interventions	
Bifidobacterium infantis-longum strain CUETM 89-215	Cecal Clostridium perfringens (species) count \downarrow ¹³⁰ Cecal Clostridium difficile (species) count \downarrow ¹³⁰
Bacteroides fragilis strain ZY-312	Fecal number of OTU \uparrow ¹¹³ Fecal relative abundance Bacteroidetes (phylum) \uparrow ¹¹³ Fecal relative abundance Proteobacteria (phylum) \downarrow ¹¹³
Lactobacillus reuteri DSM 20016	Fecal Lactobacillus (genus) abundance \uparrow ⁷² Fecal Enterobacter (genus) abundance \downarrow ⁷²
Lactobacillus reuteri biofilm on maltose loaded microspheres	Shift of fecal microbiome towards breastfed controls (16S sRNA sequencing) ⁷² Fecal Lactobacillus (genus) abundance \uparrow ⁷² Fecal Enterobacter (genus) abundance \downarrow ⁷²

Table 2.11 (continued)

Probiotic mixture (<i>Bifidobacterium animalis</i> DSM15954, <i>Lactobacillus</i> <i>acidophilus</i> DSM13241, <i>Lactobacillus casei</i> ATCC55544, <i>Lactobacillus pentosus</i> DSM14025 and <i>Lactobacillus</i> <i>plantarum</i> DSM13367)	Distal small intestinal general colonization pattern (T-RFLP analysis) changed ⁷⁷ Colonic general colonization pattern (T-RFLP analysis) changed ⁷⁷ Distal small intestinal colonization density of <i>Clostridium perfringens</i> ↓ ⁷⁷ Distal small intestinal homogenate relative proportion <i>Clostridium</i> (genus) ↓ ⁷⁷ Colonic content relative proportion <i>Clostridium</i> (genus) ↓ ⁷⁷ Distal small intestinal homogenate relative proportion <i>Enterococcus</i> (genus) ↓ ⁷⁷ Stomach content relative proportion <i>Enterococcus</i> (genus) ↓ ⁷⁷ Colon content relative proportion lactic acid bacteria ↑ ⁷⁷ Stomach content relative proportion lactic acid bacteria ↑ ⁷⁷ Distal small intestinal homogenate relative proportion <i>Lactobacillus</i> (genus) ↑ ⁷⁷ Stomach content relative proportion <i>Lactobacillus</i> (genus) ↑ ⁷⁷ Colon content relative proportion total anaerobes ↑ ⁷⁷
Other interventions	
Amniotic fluid	Distal small intestinal bacterial colonization (general eubacterial probe) ↓ ¹²³ Colonic bacterial colonization normalized (PCA of T-RFLP analysis) ¹²³

↑ depicts an increase, ↓ depicts a decrease; BCFA, branched chain fatty acids; 2'-FL, 2'-fucosyllactose; HMO, human milk oligosaccharides; OPN, osteopontin; CGMP, caseinoglycomacropeptide.

NEC pathophysiology: disturbed digestion and absorption

Another factor that may contribute to NEC pathogenesis is carbohydrate maldigestion and malabsorption. Lactases and other disaccharidases are present at lower levels in premature infants than in term born infants, indicating that carbohydrate digestion in premature children is hampered²⁰³. In addition, there are some indications this may be further disturbed in infants that develop NEC. Book et al. found that infants with NEC have higher levels of fecal reducing substances, indicative of lactose malabsorption, than infants without gastrointestinal disease and higher levels were often detected before onset of clinical symptoms²⁰⁴. In tissue specimens from infants with NEC, no or only weak GLUT5, GLUT2 and lactase protein expression was observed, while these proteins were present in control tissue, whereas sucrose-isomaltase protein expression was preserved¹⁶⁷. If carbohydrates such as lactose are not sufficiently digested and absorbed, they will reach the colon where they are subject to fermentation by colonic microbiota and lead to increased levels of fermentation products such as gasses (H₂, CH₄, CO₂), SCFA and lactate²⁰⁵. These fermentation products could contribute to intestinal damage through local acidosis, stimulation of bacterial growth and potentially through induction of inflammation²⁰⁶. In line, a NEC study in preterm pigs showed that feeding with a maltodextrin-based formula that was malabsorbed, was associated with increased NEC incidence and severity, altered microbial and SCFA profiles compared to preterm pigs treated with a lactose-based formula that is easier to absorb²⁰⁷. Maldigestion and malabsorption can also result from NEC due to enterocyte loss or brush border destruction.

Enteral feeding and disturbed digestion and absorption in animal models of NEC

The influence of enteral nutritional interventions has been studied exclusively in pig models of NEC (**Table 2.12**). Importantly, in pigs and other large animals, changes in digestive

enzyme activity and absorption in response to enteral nutrition seem to largely parallel that of human neonates^{208,209}, making large animal models particularly suitable for changes in digestion and absorption in the context of NEC.

Carbohydrate or sugar-based feeding interventions

Currently, the only carbohydrate or sugar-based feeding intervention that has been shown to modestly influence digestion and absorption in experimental NEC are HMO. Enriching formula with a mixture of four HMO in a pig NEC model did not result in altered galactose or lactose absorption or brush border enzyme activities in the small intestine and did not change intestinal mRNA expression of sucrase, lactase, IAP and sodium/glucose transporter 1 (SGLT1) either¹³⁴. However, colonic butyric acid concentrations slightly decreased after HMO administration¹³⁴. A mixture of more than 25 HMO also did not change galactose and lactose absorption, but increased enzyme activity levels of lactase, aminopeptidase A, aminopeptidase N and dipeptidyl peptidase IV (DPPIV) in the distal small intestine compared to controls¹³⁴. Feeding of preterm pigs with formula enriched by gangliosides or sialic acids (SL) did not rescue intestinal enzyme activity or intestinal hexose absorption in an experimental NEC model¹⁰⁰. Finally, in a pig NEC model, enteral administration of 2'-FL did not improve galactose absorption or change the activity of several brush border enzymes¹³³.

Protein or amino acid-based feeding interventions

OPN, lactoferrin and CGMP were studied in relation to digestion and absorption in preterm pig models of NEC. No effects were seen of OPN enriched formula diet on digestive enzyme activity and intestinal hexose absorption^{100,129}. A formula diet enriched with bovine lactoferrin neither changed intestinal absorption as measured by an oral bolus of galactose and lactose, nor changed brush border membrane enzyme activities in proximal, middle or distal small intestine³⁵. In another pig NEC study, lactase activity in the middle part of the small intestine was increased by enteral supplementation of CGMP, while no effect was observed in the proximal or distal small intestine¹²⁹. Plasma galactose levels upon an enteral bolus of galactose, suitable as a marker for hexose absorption, were increased in enteral CGMP supplementation, but this difference did not reach statistical significance¹²⁹.

Probiotic feeding interventions

In a pig NEC model, enteral administration of a probiotic mixture containing *Bifidobacterium animalis* and several *Lactobacillus* strains increased distal intestinal enzyme activity of the brush border enzymes aminopeptidase A and aminopeptidase N without changing lactase and maltase enzyme activity⁷⁷.

Other enteral feeding interventions

Enteral feeding with formula supplemented with amniotic fluid increased maltase activity in the proximal and middle small intestine and increased galactose absorption compared to feeding with unsupplemented formula in a pig NEC model¹²³.

Table 2.12 Effect of enteral feeding interventions that affect digestion and absorption in experimental animal models of NEC.

Enteral Feeding Intervention	Effect on Digestion and Absorption (Compared to NEC Protocol Exposure without Feeding Intervention)
Carbohydrate/sugar-based interventions	
Gangliosides	Intestinal enzyme activity small intestine = ¹⁰⁰ Intestinal hexose absorption (galactose lactose absorption test) = ¹⁰⁰
SL	Intestinal enzyme activity small intestine = ¹⁰⁰ Intestinal hexose absorption (galactose lactose absorption test) = ¹⁰⁰
HMO mixture of four components	Intestinal hexose absorption (galactose lactose absorption test) = ¹³⁴ Intestinal enzyme activity small intestine = ¹³⁴ Colonic butyric acid (protein) ↑ ¹³⁴ Small intestinal sucrase (mRNA) = ¹³⁴ Small intestinal lactase (mRNA) = ¹³⁴ Small intestinal alkaline phosphatase (mRNA) = ¹³⁴ small intestinal SGLT1 (mRNA) = ¹³⁴
HMO mixture >25 components	Intestinal hexose absorption (galactose lactose absorption test) = ¹³⁴ Distal small intestinal lactase enzyme activity ↑ ¹³⁴ Distal small intestinal aminopeptidase A enzyme activity ↑ ¹³⁴ Distal small intestinal aminopeptidase N enzyme activity ↑ ¹³⁴ Distal small intestinal dipeptidyl peptidase IV enzyme activity ↑ ¹³⁴
2'-FL	Galactose absorptive capacity = (galactose mannitol absorption test) ¹³³ Proximal/middle/distal small intestinal enzyme activity (sucrose, maltase, lactase, ApN, ApA, DPPIV) = ¹³³ Colon small intestinal enzyme activity (sucrose, maltase, lactase, ApN, ApA, DPPIV) = ¹³³
Protein/amino acid-based interventions	
OPN	Intestinal enzyme activity small intestine = ^{100,129} Intestinal hexose absorption (galactose lactose absorption test) = ^{100,129}
bovine lactoferrin	Small intestine enzyme activity = ³⁵ Intestinal hexose absorption (galactose lactose absorption test) = ³⁵
CGMP	Middle small intestinal lactase enzyme activity ↑ ¹²⁹ Proximal small intestinal lactase enzyme activity = ¹²⁹ Distal small intestinal lactase enzyme activity = ¹²⁹ Intestinal hexose absorption (galactose lactose absorption test) = ¹²⁹
Probiotic interventions	
Probiotic mixture (<i>Bifidobacterium animalis</i> DSM15954, <i>Lactobacillus</i> <i>acidophilus</i> DSM13241, <i>Lactobacillus casei</i> ATCC55544, <i>Lactobacillus pentosus</i> DSM14025 and <i>Lactobacillus</i> <i>plantarum</i> DSM13367)	Distal small intestinal lactase enzyme activity = ⁷⁷ Distal small intestinal maltase enzyme activity = ⁷⁷ Distal small intestinal ApA enzyme activity ↑ ⁷⁷ Distal small intestinal ApN enzyme activity ↑ ⁷⁷
Other interventions	
Amniotic fluid	Proximal small intestine maltase enzyme activity ↑ ¹²³ Middle small intestinal maltase enzyme activity ↑ ¹²³

↑ depicts an increase, ↓ depicts a decrease; SL, sialic acids; HMO, human milk oligosaccharides; 2'-FL, 2'-fucosyllactose; OPN, osteopontin; CGMP, caseinoglycomacropeptide.

NEC pathophysiology: enteric nervous system alterations

The enteric nervous system (ENS) is a large and complex division of the peripheral nerve system that resides in the gut²¹⁰. It can morphologically be divided in the myenteric and submucosal plexus²¹⁰. The ENS is involved in a variety of functions including gut motility, endocrine and exocrine secretions, microcirculation, regulation of immunity and gut barrier integrity^{211–213}. Several studies have described alterations of the ENS in NEC. In intestinal segments of infants with NEC, morphological changes were observed in myenteric plexus, internal and external submucosal plexus concomitant with a loss of neurons and glial cells^{214,215}. In addition, vasoactive intestinal peptide and NOS immunoreactivity was lost in the submucosal plexus of NEC patients²¹⁵. A more recent study compared the myenteric plexus in tissue specimens from infants with NEC during acute disease and at the moment of stoma closure with gestational age matched control tissue²¹⁶. Acute NEC was characterized by reduction of neuron and glial cell numbers per ganglion and a reduced number of nNOS expressing neurons²¹⁶. Moreover, mRNA expression of nNOS and choline acetyltransferase (ChAT), two important regulators of intestinal motility, was reduced in acute NEC and increased CC3 immunoreactivity was present in both submucosal and myenteric plexus of acute NEC patients compared to control patients²¹⁶. Although the total number of neurons per ganglion was recovered at the moment of stoma closure, this was not the case for the number of glial cells, the number of nNOS expressing neurons and nNOS mRNA expression²¹⁶. Finally, Fagbemi et al. reports that ENS alterations in intestinal samples from infants with NEC are heterogeneous²¹⁷. Whereas some infants had a disturbed architecture of the myenteric plexus with loss of mucosal and submucosal innervation and reduced expression of the glial cell marker glial fibrillary acidic protein (GFAP), no abnormalities were observed in samples from other affected children²¹⁷. Although it is still unclear whether ENS alterations in NEC merely result from NEC or are involved in its pathophysiology, several findings support the latter scenario. First, ablation of glial cells is a plausible upstream target of NEC pathophysiology²¹⁸. Second, in a rat model of NEC, neural stem cell transplantation reduced ENS alterations and was associated with improved intestinal motility and survival²¹⁶. Third, in a preterm pig NEC model, region dependent changes in gut transit time were observed before radiological signs of NEC appeared, suggesting dysmotility may precede NEC development²¹⁹. Enteroendocrine cells are chemo-sensing intestinal epithelial cells that play a key role in gastrointestinal secretion, motility and metabolism and signal amongst others through the ENS²²⁰. They are involved in the regulation of mucosal immunology and may be involved in NEC pathophysiology²²¹, although, in surgical NEC specimen, the number of enteroendocrine cells was not altered compared to controls¹⁶⁸.

Enteral feeding and enteric nervous system alterations in animal models of NEC

To date, only enteral feeding interventions with HB-EGF have been studied in relation to the ENS and enteroendocrine cells during NEC (**Table 2.13**). Enteral HB-EGF improved intestinal motility measured with a dye migration assay in a rat NEC model, although a reduction of total neuron counts in the ENS of NEC protocol exposed rats was not prevented by HB-EGF treatment¹⁷⁵. In another study that used a rat NEC model, HB-EGF administration preserved the neuronal and glial cell integrity and nNOS expression and prevented neuronal

degeneration and apoptosis during NEC²²². Lastly, enteral administration of HB-EGF partially prevented NEC induced reduction of enteroendocrine cells in a rat model of NEC¹⁷⁶.

Table 2.13 Effect of enteral feeding interventions that affect the enteric nervous system in experimental animal models of NEC.

Enteral Feeding Intervention	Effect on Enteric Nervous System (Compared to NEC Protocol Exposure without Feeding Intervention)
Hormone/growth factor/vitamin-based interventions	
HB-EGF	Intestinal motility (dye migration assay) ↑ ¹⁷⁵ Intestinal neuronal integrity Hu/D (protein) ↑ ²²² Intestinal total neuronal count Hu/D = ¹⁷⁵ Intestinal glial cell integrity GFAP (protein) ↑ ²²² Intestinal nNOS expression (protein) ↑ ²²² Intestinal neuronal apoptosis HuC/D TUNEL (protein) ↑ ²²² Intestinal neuronal degeneration HuC/D Fluor Jade C (protein) ↑ ²²² Jejunal entero-endocrine cells Chromogranin A (protein) ↑ ¹⁷⁶

↑ depicts an increase, ↓ depicts a decrease; HB-EGF, hemoglobin-binding EGF-like growth factor.

Enteral feeding interventions affecting NEC incidence and severity in human studies

Many clinical trials have evaluated the effect of enteral nutritional interventions on NEC incidence or NEC related mortality (**Table 2.14**). Unfortunately, many interventions that are successful in animal models of NEC fail to show an effect in the clinical situation. Moreover, the certainty of evidence is often moderate to low and almost all studies are underpowered, which is likely to be, at least in part, responsible for the lack of successful enteral feeding interventions in clinical trials. **Supplementary Table S2.11** provides a detailed overview of the GRADE scoring of the evidence from clinical trials, the results are summarized in **Table 2.14**.

Fat-based feeding interventions

In a meta-analysis including 11 randomized controlled trials (RCTs) with $N=1753$ neonates, supplementation of n-3 long chain PUFA did not result in a reduced NEC incidence²²³. The effect of n-3 long chain PUFA supplementation was more favourable in preterm infants ≤ 32 weeks, but did not reach statistical significance²²³. In a more recent large RCT, enteral supplementation with an emulsion rich in DHA also did not result in a reduced NEC incidence²²⁴. Certainty of evidence is low.

Carbohydrate or sugar-based feeding interventions

In a meta-analysis, enteral administration of prebiotics (short-chain galacto-oligosaccharides (SC-GOS), long-chain fructo-oligosaccharides (LC-FOS), pectin-derived acidic oligosaccharides (pAOS), oligosaccharides, fructans, inulin or oligofructose) did not alter NEC incidence (RR 0.79 (95% CI 0.44–1.44))²²⁵ (low certainty of evidence).

Protein or amino acid-based feeding interventions

A recent meta-analysis including seven RCTs reported no difference in stage II or III NEC with enteral lactoferrin supplementation²²⁶, however, with only a low grade of certainty (GRADE approach). A meta-analysis studying the effect of enteral and parenteral arginine administration on NEC incidence (3 RCTs included, two out of three RCTs exclusively studied enteral administration) observed a lower risk of NEC development with arginine treatment (relative risk (RR) 0.38, 95% CI 0.23–0.64, number needed to treat (NNT) 6) and a statistically significant reduction of death due to NEC (RR 0.18, 95% CI 0.03–1.00, NNT 20)²²⁷, with a moderate/low certainty of evidence (GRADE approach). Enteral glutamine supplementation did not reduce NEC incidence in a meta-analysis²²⁸; certainty evidence was low (GRADE approach). Oral administration of IgG or a combination of IgG and IgA did not result in a reduced incidence of NEC (RR 0.84, 95% CI 0.57–1.25), need for NEC related surgery (RR 0.21, 95% CI 0.02–1.75) or death from NEC (RR 1.10, 95% CI 0.47–2.59) in a meta-analysis²²⁹, with low to very low certainty of evidence (GRADE approach).

Hormone, growth factor or vitamin-based feeding interventions

The effects of EPO were studied in a meta-analysis, in which no effect was found on NEC incidence (RR 0.62 (95% CI 0.15–2.59)²³⁰. Also in two more recent small RCTs, no effect was found of enteral EPO administration on NEC incidence^{231,232}. A small RCT studying the effects of enteral granulocyte colony-stimulating factor (G-CSF) also did not find a reduced NEC incidence²³³. Another RCT did not find a reduction of NEC incidence with enteral supplementation of artificial amniotic fluid (rich in G-CSF) or artificial amniotic fluid and recombinant human EPO²³¹. Lastly, two small RCTs studied the effects of oral supplementation of vitamin A with NEC incidence as a secondary outcome, but did not find differences ((RR 1.14, 95% CI 0.66–1.66)²³⁴ and (RR 0.69, 95% CI 0.27–1.76)²³⁵ respectively). For all these interventions, certainty of evidence was low or very low (GRADE approach).

Probiotic feeding interventions

Probiotic enteral feeding interventions are increasingly used in the neonatal intensive care unit²³⁶ and are the most studied group of enteral nutritional interventions for the reduction of NEC incidence²³⁷. In a recent systematic review and network meta-analysis including 56 RCTs (with in total $N=12,738$ infants) reporting on severe NEC (stage II or higher), combinations of *Lactobacillus* spp. And *Bifidobacterium* spp. Or *Bifidobacterium animalis* subsp. *Lactis* were the most effective probiotic interventions²³⁸. Certainty of evidence was estimated to be moderate (GRADE approach). In addition, interventions using *Lactobacillus reuteri* or *Lactobacillus rhamnosus* were effective against severe NEC, although the effect size was lower than the aforementioned probiotic interventions²³⁸ (moderate/low certainty of evidence). Interventions using a combination of *Lactobacillus* spp., *Bifidobacterium* spp. and *Enterococcus* or a combination of *Bacillus* spp. and *Enterococcus* spp. reduced NEC incidence with the biggest effect size, however, with only low grade of certainty (GRADE approach)²³⁸. Another network meta-analysis observed statistically significant reduction of NEC incidence with probiotic interventions using *Bifidobacterium lactis* Bb-12 or B-94, *Lactobacillus reuteri* ATCC55730 or DSM17938, *Lactobacillus rhamnosus* GG, the

combination of *Bifidobacterium bifidum*, *Bifidobacterium infantis*, *Bifidobacterium longum* and *Lactobacillus acidophilus*, the combination of *Bifidobacterium infantis* Bb-02, *Bifidobacterium lactis* Bb-12 and *Streptococcus thermophilus* TH-4 and the combination of *Bifidobacterium longum* 35624 and *Lactobacillus rhamnosus* GG²³⁹. Certainty of evidence was estimated to be moderate to low (GRADE approach). In line with the evidence from this latter network meta-analysis, the European Society for Pediatric Gastroenterology Hepatology and Nutrition (ESPGHAN) committee on nutrition and the ESPGHAN working group for probiotics and prebiotics at present conditionally recommend to provide either *Lactobacillus rhamnosus* GG ATCC53103 or the combination of *Bifidobacterium infantis* Bb-02, *Bifidobacterium lactis* Bb-12, and *Streptococcus thermophilus* TH-4 as a preventive treatment to reduce NEC incidence²⁴⁰.

Other feeding interventions

In a relatively small multi-center RCT, enteral administration of carotenoids did not alter NEC incidence (OR 0.34 (95% CI 0.07–1.66)²⁴¹. A mixture of probiotics, prebiotics and lactoferrin did reduce the overall NEC incidence and the incidence of NEC stage ≥ 2 in a small RCT ((RR 0.16 (95% CI 0.03–0.77) and RR 0.56 (95% CI 0.47–0.67) respectively)²⁴². For both interventions, certainty of evidence was scored as low.

Enteral feeding interventions affecting pathophysiological mechanisms of NEC in human studies

Evidence from human studies on enteral feeding interventions that positively influence potential pathophysiological mechanisms behind NEC are sparse as it is difficult to study these outcome measures in (preterm) infants (**Table 2.15**). Nevertheless, overlap between mechanisms found in animal studies and effects observed in humans indicate evidence from animal studies likely provide insights valuable to the human NEC situation.

Carbohydrate or sugar based feeding interventions

In a small RCT with 10 prebiotic supplemented and 13 only formula fed infants, 30 days of prebiotic supplementation of formula feeding with a mixture of SC-GOS and LC-FOS increased the percentage of gastric slow wave propagation measured with electrogastrography and decreased the gastric half emptying times inducing a gastrointestinal motility pattern comparable to breastmilk fed infants²⁴³. In another small RCT, enrichment of formula feeding with GOS and FOS decreased intestinal transit time (assessed by gastrointestinal passage of carmine red)²⁴⁴. In addition, stool viscosity was increased and stool pH was reduced, suggesting increased SCFA production by colonic fermentation upon GOS and FOS administration²⁴⁴. Enteral supplementation of SC-GOS, LC-FOS and acidic oligosaccharides (AOS) to preterm infants did not change fecal IL8 or calprotectin concentrations over time in a RCT²⁴⁵.

Table 2.14 Enteral feeding interventions reducing NEC incidence or mortality in human studies.

Intervention	Enteral Feeding Intervention Study, N	Effect on NEC Incidence		Anticipated Absolute Effects Risk with No Enteral Feeding Intervention (95% CI)	Certainty of Evidence (GRADE)
		Observed Relative Effect	Risk with No Enteral Feeding Intervention		
Fat-Based Interventions					
n-3 PUFA	Meta-analysis, 11 RCTs, N=1753 neonates	RR 1.17 (95% CI 0.77–1.79) (incidence all neonates) [223]	28 per 1000	5 more per 1000 more (from 6 less per 1000 to 50 more per 1000)	Low ⊕⊕⊖⊖ (risk of bias, imprecision)
		RR 0.50 (95% CI 0.23–1.10) (incidence neonates <32 weeks) [223]	58 per 1000	29 less per 1000 (from 45 less per 1000 to 6 more per 1000)	Low ⊕⊕⊖⊖ (risk of bias, imprecision)
DHA	RCT, N = 1205 neonates	RR 1.16 (95% CI 0.79–1.69) (incidence) [224]	71 per 1000	11 more per 1000 (from 15 less per 1000 to 49 more per 1000)	Low ⊕⊕⊖⊖ (imprecision)
Carbohydrate or sugar-based interventions					
Prebiotics	Meta-analysis, 6 RCTs, N=737 neonates	RR 0.79 (95% CI 0.44–1.44) (incidence) [225]	112 per 1000	24 less per 1000 (from 63 less per 1000 to 49 more per 1000)	Low ⊕⊕⊖⊖ (inconsistency, imprecision)
Protein or amino acid-based interventions					
Lactoferrin	Meta-analysis, 7 RCTs, N = 4874 neonates	RR 0.90 (95% CI 0.69–1.17) (incidence stage II or III NEC) [226]	47 per 1000	5 per 1000 less (from 15 per 1000 less to 8 per 1000 more)	Low ⊕⊕⊖⊖ (risk of bias, imprecision)
Arginine	Meta-analysis, 3 RCTs, N = 285 neonates	RR 0.38 (95% CI 0.23–0.64) (incidence) [227]	303 per 1000	188 per 1000 less (from 233 less per 1000 to 109 less per 1000)	Moderate ⊕⊕⊖⊖ (imprecision)
		RR 0.18 (95% CI 0.03–1.00) (death due to NEC) [227]	55 per 1000	45 less per 1000 (from 53 less per 1000 to 0 less per 1000)	Low ⊕⊕⊖⊖ (imprecision)

Table 2.14 (continued)

Intervention	Study, N	Observed Relative Effect	Anticipated Absolute Effects		Certainty of Evidence (GRADE)
			Risk with No Enteral Feeding Intervention	Risk with Enteral Feeding Intervention (95% CI)	
Glutamine	Meta-analysis, 7 RCTs, N=1172 neonates	RR 0.73 (95% CI 0.49–1.08) (incidence) [228]	90 per 1000	24 less per 1000 (from 46 less per 1000 to 8 more per 1000)	Low ⊕⊕⊕⊕ (imprecision, publication bias)
IgG or IgG + IgA	meta-analysis, 3 clinical trials, N=2095 neonates	RR 0.84 (95% CI 0.57–1.25) (incidence) [229]	55 per 1000	9 less per 1000 (from 24 less per 1000 to 14 more per 1000)	Low ⊕⊕⊕⊕ (risk of bias)
		RR 0.21 (95% CI 0.02–1.75) (NEC related surgery) [229]	25 per 1000	20 less per 1000 (from 25 less per 1000 to 19 more per 1000)	Very low ⊕⊕⊕⊕ (risk of bias, imprecision)
		RR 1.10 (95% CI 0.47–2.59) (death due to NEC) [229]	10 per 1000	1 per 1000 more (from 5 less per 1000 to 16 more per 1000)	Very low ⊕⊕⊕⊕ (risk of bias, imprecision)
Hormone/growth factor/vitamin-based interventions					
EPO	Meta-analysis, 2 RCTs, N=110 neonates	RR 0.62 (95% CI 0.15–2.59) (incidence stage II or III NEC) (NS) [230]	61 per 1000	24 less per 1000 (from 52 less per 1000 to 97 more per 1000)	Very low ⊕⊕⊕⊕ (inconsistency imprecision)
	RCT, N=120 neonates	2.8 pp increase (11.1% control group, 13.9% EPO group) (NS) (incidence) [232]	111 per 1000	28 less per 1000 (no CI reported)	Very low ⊕⊕⊕⊕ (risk of bias, inconsistency imprecision)
	RCT, N=100 neonates	2 pp reduction (8% control group, 6% EPO group) (NS) (incidence) [231]	80 per 1000	20 less per 1000 (no CI reported)	(risk of bias, inconsistency imprecision)
EPO + G-CSF	RCT, N=50 neonates	10 pp reduction ((10% control group, 0% EPO group) (NS) (incidence) [233])	100 per 1000	100 per 1000 less (no CI reported)	Low ⊕⊕⊕⊕ (imprecision)
G-CSF	RCT, N=50 neonates	10 pp reduction (10% control group, 0% EPO group) (NS) (incidence) [233]	100 per 1000	100 per 1000 less (no CI reported)	Low ⊕⊕⊕⊕ (imprecision)
G-CSF (in artificial amniotic fluid)	RCT, N=100 neonates	2 pp reduction (8% control group, 6% EPO group) (NS) (incidence) [231]	80 per 1000	20 per 1000 less (no CI reported)	Very low ⊕⊕⊕⊕ (risk of bias, imprecision)

Table 2.14 (continued)

Intervention	Enteral Feeding Intervention Study, N	Effect on NEC Incidence		Anticipated Absolute Effects		Certainty of Evidence (GRADE)
		Observed Relative Effect	Risk with No Enteral Feeding Intervention	Risk with Enteral Feeding Intervention	Risk with Enteral Feeding Intervention (95% CI)	
G-CSF (in artificial amniotic fluid)	RCT, N=100 neonates	2 pp reduction (8% control group, 6% EPO group) (NS) (incidence) [231]	80 per 1000	20 per 1000 less (no CI reported)	Very low (risk of bias, imprecision) $\oplus\ominus\ominus\ominus$	
Vitamin A	RCT, N=154 neonates	RR 1.14 (95% CI 0.66–1.66) (incidence) [234]	91 per 1000	13 per 1000 more (from 31 per 1000 less to 60 per 1000 more)	Low (risk of bias, imprecision) $\oplus\ominus\ominus\ominus$	
	RCT, N=262 neonates	RR 0.69 (95% CI 0.27–1.76) (incidence) [235]	77 per 1000	24 per 1000 less (from 56 per 1000 less to 59 per 1000 more)	(risk of bias, imprecision) $\oplus\ominus\ominus\ominus$	
Probiotic interventions						
Probiotics	(network) meta-analysis, 56 RCTs, N=12,738 neonates					
<i>Lactobacillus</i> spp. and <i>Bifidobacterium</i> spp.	11 RCTs, N=1878 neonates	OR 0.35 (95% CI 0.20–0.59) (incidence stage II or III) NEC [238]	63 per 1000	41 per 1000 less (from 51 per 1000 less to 26 per 1000 less)	Moderate (indirectness) $\oplus\oplus\ominus\ominus$	
<i>Bifidobacterium animalis</i> subsp. <i>Lactis</i>	5 RCTs, 628 neonates	OR 0.31 (95% CI 0.13–0.74) (incidence stage II or III) NEC [238]	94 per 1000	44 per 1000 less (from 56 per 1000 less to 16 per 1000 less)	Moderate (imprecision) $\oplus\oplus\ominus\ominus$	
<i>Lactobacillus reuteri</i>	5 RCTs, N=1388 neonates	OR 0.55 (95% CI 0.34–0.91) (incidence stage II or III) NEC [238]	71 per 1000	28 per 1000 less (from 42 per 1000 less to 5 per 1000 less)	Low (imprecision, indirectness) $\oplus\oplus\ominus\ominus$	
<i>Lactobacillus rhamnosus</i>	5 RCTs, N=839 neonates	OR 0.44 (95% CI 0.21–0.90) (incidence stage II or III) NEC [238]	60 per 1000	35 per 1000 less (from 50 per 1000 less to 5 per 1000 less)	Moderate (imprecision) $\oplus\oplus\ominus\ominus$	

Table 2.14 (continued)

Intervention	Study, N	Observed Relative Effect	Anticipated Absolute Effects		Certainty of Evidence (GRADE)
			Risk with No Enteral Feeding Intervention	Risk with Enteral Feeding Intervention (95% CI)	
Combination of <i>Lactobacillus</i> spp., <i>Bifidobacterium</i> spp. and <i>Enterococcus</i> spp. 7 RCTs, N=1950 neonates		OR 0.28 (95% CI 0.16–0.49) (incidence stage II or III NEC) [238]	63 per 1000	46 per 1000 less (from 54 per 1000 less to 32 per 1000 less)	Low ⊕⊕⊖⊖ (risk of bias)
Combination of <i>Bacillus</i> spp. and <i>Enterococcus</i> spp. 1 RCT, N=355 neonates Network meta-analysis		OR 0.23 (95% CI 0.08–0.63) (incidence stage II or III NEC) [238]	110 per 1000	49 per 1000 less (from 59 per 1000 less to 23 per 1000 less)	Moderate ⊕⊕⊕⊖ (imprecision)
43 RCTs, N=10,651 neonates <i>Bifidobacterium lactis</i> Bb-12 or B-94		RR 0.25 (95% CI 0.10–0.56) (incidence) [239]	100 per 10000	75 per 1000 less (from 90 per 1000 less to 44 per 1000 less)	Moderate ⊕⊕⊕⊖ (imprecision)
5 RCTs, N=828 neonates <i>Lactobacillus reuteri</i> ATCC5730 or DSM17938		RR 0.43 (95% CI 0.16–0.98) (incidence) [239]	92 per 1000	52 per 1000 less (from 77 per 1000 less to 2 per 1000 less)	Low ⊕⊕⊖⊖ (imprecision, indirectness)
4 RCTs, N=1459 neonates <i>Lactobacillus rhamnosus</i> GG		RR 0.24 (95% CI 0.064–0.67) (incidence) [239]	24 per 1000	18 per 1000 less (from 22 per 1000 less to 8 per 1000 less)	Low ⊕⊕⊖⊖ (imprecision, indirectness)
6 RCTs, N=1507 neonates Combination of <i>Bifidobacterium bifidum</i> , <i>Bifidobacterium infantis</i> , <i>Bifidobacterium longum</i> and <i>Lactobacillus acidophilus</i>		RR 0.25 (95% CI 0.051–0.89) (incidence) [239]	129 per 1000	97 per 1000 less (from 122 per 1000 less to 14 per 1000 less)	Low ⊕⊕⊖⊖ (imprecision)
2 RCTs, N=247 neonates					

Table 2.14 (continued)

Intervention	Enteral Feeding Intervention Study, N	Effect on NEC Incidence		Risk with No Enteral Feeding Intervention	Risk with Enteral Feeding Intervention (95% CI)	Certainty of Evidence (GRADE)
		Observed Relative Effect	Anticipated Absolute Effects			
	Combination of <i>Bifidobacterium infantis</i> Bb-02, <i>Bifidobacterium lactis</i> Bb-12 and <i>Streptococcus thermophilus</i> TH-4	RR 0.29 (95% CI 0.073–0.78) (incidence) [239]	54 per 1000	38 per 1000 less (from 50 per 1000 less to 12 per 1000 less)	Low ⊕⊕⊕⊖ (inconsistency, imprecision)	
						2 RCTs, N=1244 neonates
	<i>Bifidobacterium longum</i> 35624 and <i>Lactobacillus rhamnosus</i> GG	RR 0.18 (95% CI 0.020–0.89) (incidence) [239]	42 per 1000	34 per 1000 less (from 41 per 1000 less to 5 per 1000 less)	Low ⊕⊕⊕⊖ (imprecision)	
						2 RCTs, N=285 neonates
Other interventions						
Carotenoids	RCT, N=229 neonates	OR 0.34 (95% CI 0.07–1.66) (incidence stage II or III NEC) [241]	52 per 1000	34 per 1000 less (from 48 per 1000 less to 60 per 1000 more)	Low ⊕⊕⊕⊖ (imprecision)	
Mixture of probiotics, prebiotics and lactoferrin	RCT, N=208 neonates	RR 0.16 (95% CI 0.03–0.77) (incidence) [242]	106 per 1000	89 per 1000 less (from 103 per 1000 less to 24 per 1000 less)	Low ⊕⊕⊕⊖ (imprecision)	
		RR 0.56 (95% CI 0.47–0.67) (incidence stage II or III NEC) [242]	38 per 1000	17 per 1000 less (from 20 per 1000 less to 13 per 1000 less)	Low ⊕⊕⊕⊖ (imprecision)	

⊕⊕⊕⊕ depicts high certainty of evidence, ⊕⊕⊕⊖ depicts moderate certainty of evidence, ⊕⊕⊕⊖ depicts low certainty of evidence, ⊕⊕⊕⊖ depicts very low certainty of evidence; PUFA, polyunsaturated fatty acids; DHA, docosahexaenoic acid; SC-GOS, short chain galacto-oligosaccharides; LC-FOS, long chain fructo-oligosaccharides; EPO, erythropoietin; G-CSF, granulocyte colony-stimulating factor; OR, odds ratio; RR, relative risk; CI, confidence interval.

Table 2.15 Effect of enteral feeding interventions that affect pathophysiological mechanisms of NEC in human studies.

Enteral Feeding Intervention	Effect on Pathophysiological Mechanism (Compared to Placebo/No Intervention)
Carbohydrate or sugar-based interventions	
(SC) GOS + (LC) FOS	% Gastric slow wave propagation (electrogastrography) ↑ ²⁴³ Gastric half emptying time (echography) ↓ ²⁴³ Intestinal transit time (passage carmine red) ↑ ²⁴⁴ Stool pH ↓ ²⁴⁴ Stool viscosity ↑ ²⁴⁴
SC GOS + LC FOS + AOS	Fecal IL8 = ²⁴⁵ Fecal calprotectin = ²⁴⁵
Protein or amino acid-based interventions	
Lactoferrin	Whole blood CD4+ CD25 ^{high} Foxp3+ Treg cell number ↑ ²⁴⁶
L-Glutamine	Lactulose recovery in urine day 7 ↓ ²⁴⁷ Lactulose recovery in urine day 30 ↓ ²⁴⁷ Lactulose/mannitol recovery ratio in urine day 7 ↓ ²⁴⁷ Lactulose/mannitol recovery ratio in urine day 30 ↓ ²⁴⁷
Probiotic interventions	
<i>Lactobacillus reuteri</i>	% Gastric slow wave propagation (electrogastrography) ↑ ²⁴³ Gastric half emptying time (echography) ↓ ²⁴³
<i>Bifidobacterium lactis</i>	Lactulose/mannitol recovery ratio in urine day 30 ↓ ²⁴⁸
Other interventions	
Mixture of probiotics, prebiotics and lactoferrin	Serum IL5 (protein) at 0, 14 and 28 days = ²⁴⁹ Serum IL10 (protein) at 0, 14 and 28 days (protein) = ²⁴⁹ Serum IL17 (protein) at 0, 14 and 28 days = ²⁴⁹ Serum IFN γ (protein) 0, 14 days = ²⁴⁹ Serum IFN γ (protein) 28 days ↑ ²⁴⁹

↑ depicts an increase, ↓ depicts a decrease; SC-GOS, short chain galacto-oligosaccharides; LC-FOS, long chain fructo-oligosaccharides.

Protein or amino acid-based feeding interventions

In a randomized controlled trial, infants orally treated with lactoferrin had a bigger increase in CD4+ CD25^{high} Foxp3+ Treg cells at discharge compared to controls²⁴⁶. In a double-blinded placebo-controlled trial, the effect of enteral administration of L-glutamine on intestinal barrier function was assessed with a dual sugar (mannitol, lactulose) absorption test. Both the urine recovery of lactulose and the ratio between urine recovery of lactulose and mannitol was lower after 7 and 30 days in infants treated with L-glutamine compared to placebo treated infants, demonstrating that L-glutamine positively influenced gut barrier function²⁴⁷.

Probiotic feeding interventions

Thirty days of prebiotic supplementation of formula feeding with a *Lactobacillus reuteri* normalized gastrointestinal motility by increasing the percentage of gastric slow wave

propagation measured and decreasing the gastric half emptying in a small RCT with preterm infants²⁴³. In addition, in a small RCT, enteral administration of a formula with added *Bifidobacter lactis* improved intestinal barrier function (decreased lactulose mannitol ratio in urine) at 30 days postnatally²⁴⁸.

Other feeding interventions

Enteral administration of a mixture of probiotics, prebiotics and lactoferrin slightly increased systemic IFN γ protein levels at 28 days of life, but did not affect several other cytokines (IL5, IL10 and IL17) in a RCT in premature infants²⁴⁹.

Interaction between feeding components and NEC

Despite the complex and rich composition of breastmilk and the concomitant presence of many bioactive factors^{19,250} that are considered a major factor in the prevention of NEC, remarkably few studies have investigated the interaction or potential synergistic effect between two or more of these bioactive substances. In a quail NEC model, addition of FOS to the feeding enhanced the reduction of cecal *Clostridium perfringens* counts by *Bifidobacteria*, an effect that was not observed by FOS administration in absence of *Bifidobacteria*^{128,130}. In a recent meta-analysis, enteral supplementation of lactoferrin did not reduce the incidence of NEC (RR 0.90, 95% CI 0.69–1.17), whereas concomitant administration of lactoferrin and probiotics did result in a statistically significant reduction of NEC incidence (RR 0.04, 95% CI 0.00–0.62); however, these results need to be interpreted with caution due to (very) low certainty of evidence^{226,251}. Dvorak et al. investigated potential synergistic effects of EGF and HB-EGF in a rat model of NEC, but did not find additional protective effects against NEC³⁷. Similarly, D'Souza et al. did not find benefits of combining enteral administration of the probiotic *Saccharomyces Boulardii* and GOS/FOS¹³⁵. That combined enteral administration of nutritional components can also reduce the therapeutic effect was observed in a rat NEC model, where nucleotide administration abolished the PUFA induced reduction of mortality, gut necrosis, endotoxemia and intestinal PLA₂ and PAFR mRNA expression⁴⁵.

Enteral feeding strategies and NEC: feeding regimens, fortifiers and more

Besides the content of enteral nutrition, various other aspects of enteral feeding are likely to be related to the risk of NEC development and should be taken into account when designing trials studying enteral nutritional interventions for the prevention of NEC. Although evidence is not conclusive, factors that could be of relevance, especially for high risk populations such as ELBW infants, include the dose, duration and timing of trophic feeding/minimal enteral nutrition, the use of human milk-derived fortifiers, feed osmolality and standardized feeding regimens^{252,253}.

Discussion

Experiments in animal models of NEC provide a large amount of evidence of the beneficial effect of enteral nutritional interventions for preventing NEC incidence, severity, signs and

symptoms, and mortality, as well as for ameliorating several pathophysiological processes related to NEC development including intestinal inflammation and intestinal barrier loss. A broad range of nutritional substances has been reported to be effective in several complementary experimental models, e.g., in different species and with different ways of inducing NEC. Especially HMO and growth factor-based interventions such as HB-EGF and EGF are promising as they have been shown to be effective in many experimental studies in which they target a broad range of pathophysiological mechanisms. Although some studies provide excellent insight in the underlying working mechanisms, addressing this for a broader range of interventions could be of great benefit to predict potential synergistic action between different substances of interest. This should therefore be subject of further research.

Despite the large amount of evidence from animal models, remarkably few enteral feeding interventions (e.g., arginine and probiotics) have been shown to be effective in meta-analyses of clinical trials. To date, only probiotics have reduced NEC incidence in adequately powered clinical studies and these interventions thereby form a promising preventive therapy, although even for these interventions certainty of evidence is at best moderate. Hence, the translation from preclinical findings in animal models to clinical practice remains challenging. Several underlying problems may be responsible for this arduous translation.

First, animal experiment related factors are in play. The current evidence from animal studies needs to be interpreted with caution, primarily due to the difficulty to adequately assess risk of bias in most animal studies and to determine certainty of evidence. Dissemination bias is likely present in animal studies of NEC, as researchers estimate that, in general, only around 50–60% of conducted animal studies^{254,255} and data of only 26% of animals used are published²⁵⁵. Importantly, one of the main reasons for not publishing a study appears to be non-statistically significant results²⁵⁴. Moreover, other sources of bias may be present in experimental animal studies and are difficult to detect as many methodological aspects of the studies that are important for assessment of bias are poorly reported, both in studies incorporated in this systematic review and animal experiments in general²⁵⁶. Additionally, adequately assessing certainty of evidence from animal studies³³ is currently hampered, since amongst others confidence intervals and power calculations are often not reported. Due to (dissemination) bias, reports in literature of successful enteral feeding interventions in animal models may not reflect the true biological potential of the tested substance. Thus, based on the current evidence, it difficult to establish which preclinically studied interventions are most promising (considered safe, clinically relevant effect size, moderate to high certainty of evidence) and, hence, should be pursued in clinical trials. Besides, a smooth transition from animal research to clinical practice is hampered by the fact that experimental NEC modeling is still suboptimal. Notwithstanding the fact that many disease characteristics and a number of pathophysiological mechanisms involved in NEC are included in the current animal models of NEC, it is likely at least part of its complex pathophysiology is not adequately covered by the current models²⁵⁷. In addition, animal models are inherently limited due to the difficulty of using animals that are preterm and have bacterial colonization of the gut comparable to the human situation and differences between human and animal physiology^{257–260}.

Second, factors related to the conduct of clinical trials are involved. Many clinical trials are not designed with NEC incidence as primary outcome and are underpowered to convincingly prove a clinically significant beneficial effect. As Xiong et al. have nicely ascertained, the number of neonates required to prove a 20% relative risk reduction with 80% power assuming a 5% incidence of NEC is over 10,000²³⁷. Including this amount of neonates in a study requires multi-center and international collaboration, which is logistically challenging and expensive. Moreover, NEC is not clearly defined and NEC diagnoses likely consist of a mixture of 'classical' NEC and closely related pathologies such as transfusion-related NEC, ischemic intestinal necrosis, spontaneous intestinal perforation and food protein intolerance enterocolitis syndrome^{261,262}. It is likely that NEC(-like) diseases require a different treatment and that poorer effects of treatment will be found in clinical trials in which all these disease entities are pooled as one group.

Third, it is challenging to determine the optimal therapeutic regimen (dose, frequency, timing). Even though dose is of clear importance for the therapeutic effect^{36,101}, most animal studies only test a single dose and frequency of administration and it is therefore unclear how the dose and administration regimen used in animal studies should be translated to the human neonate. Of note, the optimal dose for the human neonate may be very well dependent on individual baseline levels, e.g., an infant with baseline deficit of a specific nutritional component may benefit from a higher dosage than an infant with baseline values within the normal range. Furthermore, timing of the feeding intervention often differs between animal studies and clinical trials. Due to the rapid nature of NEC progression following its onset, the value of nutritional interventions lies in prevention of NEC rather than treatment of ongoing NEC and as such, enteral feeding interventions are used as prevention in clinical trials. However, in animal models, enteral feeding interventions are almost always started in parallel to a NEC inducing protocol, and can therefore probably not be (fully) regarded as preventive. Studies looking at interventions at an earlier moment, such as in utero nutritional interventions, are in this context valuable⁴³.

Last, surprisingly few animal studies have looked at enteral feeding interventions with a combination of several bioactive substances, although this is, in light of the complex composition of breastmilk and the multifactorial nature of NEC pathogenesis, likely to be of pivotal importance.

Considering the abovementioned factors that hinder development of successful clinically applicable enteral nutritional interventions to reduce NEC incidence, several aspects should be improved. Future clinical trials investigating the potential of enteral feeding interventions to reduce NEC incidence should be adequately powered to at least be able to fairly estimate effect size and preferably reach statistical significance. In addition, clinical researchers should strive for the use of a clearer definition of NEC, ideally after international consensus regarding this definition in the field of NEC research. To this end, international collaboration between (pre)clinical NEC researchers and clinicians is essential.

Preclinical studies remain important to further understand NEC pathophysiology and optimize the current experimental models of NEC. In addition, the development of new human tissue based experimental models such as intestinal organoids, NEC-in-a-dish and gut-on-a-chip models is of importance^{260,263,264}. In future preclinical experiments issues such as timing of intervention and dose/treatment regimen should be taken into account.

Negative findings should be published, which could be stimulated by voluntary or mandatory registration of conducted (animal) studies as is more and more common practice in the clinical research field²⁵⁵. Moreover, the reporting quality of methodological aspects in experimental studies should be significantly improved to enable fair assessment of risk of bias and certainty of evidence. Finally, studying combinations of the most promising single substances based on findings in single component supplementation studies and on biological working mechanisms is likely to be of pivotal importance for finding effective enteral nutritional interventions that reduce clinical NEC incidence.

References

1. Neu J, Walker WA. Necrotizing enterocolitis. *New Engl. J. Med.* 2011;364:255–264.
2. Fitzgibbons SC, Ching Y, Yu D, Carpenter J, Kenny M, Weldon C, Lillehei C, Valim C, Horbar JD, Jaksic T. Mortality of necrotizing enterocolitis expressed by birth weight categories. *J. Pediatr. Surg.* 2009;44:1072–1075.
3. Alsaied A, Islam N, Thalib L. Global incidence of Necrotizing Enterocolitis: A systematic review and Meta-analysis. *Bmc Pediatr.* 2020;20:344.
4. Han SM, Hong CR, Knell J, Edwards EM, Morrow KA, Soll RF, Modi BP, Horbar JD, Jaksic T. Trends in incidence and outcomes of necrotizing enterocolitis over the last 12 years: A multicenter cohort analysis. *J. Pediatr. Surg.* 2020;55:998–1001.
5. Heida FH, Stolwijk L, Loos MH, van den Ende SJ, Onland W, van den Dungen FA, Kooi EM, Bos AF, Hulscher JB, Bakx R. Increased incidence of necrotizing enterocolitis in the Netherlands after implementation of the new Dutch guideline for active treatment in extremely preterm infants: Results from three academic referral centers. *J. Pediatr. Surg.* 2017;52:273–276.
6. Lin PW, Stoll BJ. Necrotizing enterocolitis. *Lancet* 2006;368:1271–1283.
7. Blakely ML, Lally KP, McDonald S, Brown RL, Barnhart DC, Ricketts RR, Thompson WR, Scherer LR, Klein MD, Letton RW, et al. Postoperative outcomes of extremely low birth-weight infants with necrotizing enterocolitis or isolated intestinal perforation: A prospective cohort study by the NICHD Neonatal Research Network. *Ann. Surg.* 2005;241:984–989.
8. Jacob J, Kamitsuka M, Clark RH, Kelleher AS, Spitzer AR. Etiologies of NICU deaths. *Pediatrics* 2015; 135:e59–e65.
9. Hong CR, Fullerton BS, Mercier CE, Morrow KA, Edwards EM, Ferrelli KR, Soll RF, Modi BP, Horbar JD, Jaksic T. Growth morbidity in extremely low birth weight survivors of necrotizing enterocolitis at discharge and two-year follow-up. *J. Pediatr. Surg.* 2018;53:1197–1202.
10. Mutanen A, Wales PW. Etiology and prognosis of pediatric short bowel syndrome. *Semin. Pediatr. Surg.* 2018;27:209–217.
11. Duggan CP, Jaksic T. Pediatric Intestinal Failure. *N. Engl. J. Med.* 2017;377:666–675.
12. Schulzke SM, Deshpande GC, Patole SK. Neurodevelopmental outcomes of very low-birth-weight infants with necrotizing enterocolitis: A systematic review of observational studies. *Arch. Pediatr. Adolesc. Med.* 2007;161:583–590.
13. Mowitz ME, Dukhovny D, Zupancic JAF. The cost of necrotizing enterocolitis in premature infants. *Semin. Fetal Neonatal Med.* 2018;23:416–419.
14. Bisquera JA, Cooper TR, Berseth CL. Impact of necrotizing enterocolitis on length of stay and hospital charges in very low birth weight infants. *Pediatrics* 2002;109:423–428.
15. Ganapathy V, Hay JW, Kim JH, Lee ML, Rechtman DJ. Long term healthcare costs of infants who survived neonatal necrotizing enterocolitis: A retrospective longitudinal study among infants enrolled in Texas Medicaid. *Bmc Pediatr.* 2013;13:127.
16. Christian VJ, Polzin E, Welak S. Nutrition Management of Necrotizing Enterocolitis. *Nutr. Clin. Pr.* 2018;33:476–482.
17. Vaks Y, Birnie KL, Carmichael SL, Hernandez-Boussard T, Benitz WE. Temporal Relationship of Onset of Necrotizing Enterocolitis and Introduction of Enteric Feedings and Powdered Milk Fortifier. *Am. J. Perinatol.* 2018;35:616–623.
18. Kirtsman M, Yoon EW, Ojah C, Cieslak Z, Lee SK, Shah PS. Nil-per-os days and necrotizing enterocolitis in extremely preterm infants. *Am. J. Perinatol.* 2015;32:785–794.
19. Thai JD, Gregory KE. Bioactive Factors in Human Breast Milk Attenuate Intestinal Inflammation during Early Life. *Nutrients* 2020;12(2):581.
20. Gopalakrishna KP, Hand TW. Influence of Maternal Milk on the Neonatal Intestinal Microbiome. *Nutrients* 2020;12(3):823.
21. Lucas A, Cole TJ. Breast milk and neonatal necrotizing enterocolitis. *Lancet* 1990;336:1519–1523.
22. Altobelli E, Angeletti PM, Verrotti A, Petrocelli R. The Impact of Human Milk on Necrotizing Enterocolitis: A Systematic Review and Meta-Analysis. *Nutrients* 2020;12(5):1322.

23. Quigley M, Embleton ND, McGuire W. Formula versus donor breast milk for feeding preterm or low birth weight infants. *Cochrane Database Syst. Rev.* 2019;7:Cd002971.
24. Tarnow-Mordi WO, Abdel-Latif ME, Martin A, Pammi M, Robledo K, Manzoni P, Osborn D, Lui K, Keech A, Hague W, et al. The effect of lactoferrin supplementation on death or major morbidity in very low birthweight infants (LIFT): A multicentre, double-blind, randomised controlled trial. *Lancet. Child Adolesc. Health* 2020;4:444–454.
25. Cui X, Shi Y, Gao S, Xue X, Fu J. Effects of *Lactobacillus reuteri* DSM 17938 in preterm infants: A double-blinded randomized controlled study. *Ital. J. Pediatr.* 2019;45:140.
26. Maamouri G, Zegheibzadeh F, Khatam F, Boskabadi H. The Impact of Oral Glutamine Supplementation on Prevention of Nosocomial Infections in Preterm Infants. *Iran. J. Neonatol. Ijn* 2016;7:19–24.
27. Gómez-Rodríguez G, Amador-Licona N, Daza-Benítez L, Barbosa-Sabanero G, Carballo-Magdaleno D, Aguilar-Padilla R, González-Ramírez E. Single strain versus multispecies probiotic on necrotizing enterocolitis and faecal IgA levels in very low birth weight preterm neonates: A randomized clinical trial. *Pediatr. Neonatol.* 2019;60:564–569.
28. Ouzzani M, Hammady H, Fedorowicz Z, Elmagarmid A. Rayyan-a web and mobile app for systematic reviews. *Syst. Rev.* 2016;5:210.
29. Hooijmans CR, Rovers MM, de Vries, R.B, Leenaars, M, Ritskes-Hoitinga, M, Langendam, M.W. SYRCLE's risk of bias tool for animal studies. *BMC Med. Res. Methodol.* 2014;14:43.
30. Jadad AR, Moore RA, Carroll D, Jenkinson C, Reynolds DJ, Gavaghan DJ, McQua, HJ. Assessing the quality of reports of randomized clinical trials: Is blinding necessary? *Control. Clin. Trials* 1996;17: 1–12.
31. Shea BJ, Grimshaw JM, Wells GA, Boers M, Andersson N, Hamel C, Porter AC, Tugwell P, Moher D, Bouter LM. Development of AMSTAR: A measurement tool to assess the methodological quality of systematic reviews. *BMC Med. Res. Methodol.* 2007;7:10.
32. Schünemann H, Brożek J, Guyatt G, Oxman A. *GRADE Handbook for Grading Quality of Evidence and Strength of Recommendations*. Updated October 2013; The GRADE Working Group, Hamilton, Canada: 2013.
33. Wei D, Tang K, Wang Q, Estill J, Yao L, Wang X, Chen Y, Yang K. The use of GRADE approach in systematic reviews of animal studies. *J. Evid. Based Med.* 2016;9:98–104.
34. Page MJ, McKenzie JE, Bossuyt PM, Boutron I, Hoffmann TC, Mulrow CD, Shamseer L, Tetzlaff JM, Akl EA, Brennan SE, et al. The PRISMA 2020 statement: An updated guideline for reporting systematic reviews. *BMJ* 2021;372:n71.
35. Nguyen DN, Li Y, Sangild PT, Bering SB, Chatterton DE. Effects of bovine lactoferrin on the immature porcine intestine. *Br. J. Nutr.* 2014;111:321–331.
36. Nguyen DN, Jiang P, Stensballe A, Bendixen E, Sangild PT, Chatterton DE. Bovine lactoferrin regulates cell survival, apoptosis and inflammation in intestinal epithelial cells and preterm pig intestine. *J. Proteom.* 2016;139:95–102.
37. Dvorak B, Khailova L, Clark JA, Hosseini DM, Arganbright KM, Reynolds CA, Halpern MD. Comparison of epidermal growth factor and heparin-binding epidermal growth factor-like growth factor for prevention of experimental necrotizing enterocolitis. *J. Pediatr. Gastroenterol. Nutr.* 2008;47:11–18.
38. Wu RY, Li B, Koike Y, Maattanen P, Miyake H, Cadete M, Johnson-Henry KC, Botts SR, Lee C, Abrahamsson TR, et al. Human Milk Oligosaccharides Increase Mucin Expression in Experimental Necrotizing Enterocolitis. *Mol. Nutr. Food Res.* 2019;63:e1800658.
39. Good M, Sodhi CP, Ozolek JA, Buck RH, Goehring KC, Thomas DL, Vikram A, Bibby K, Morowitz MJ, Firek B, et al. *Lactobacillus rhamnosus* HN001 decreases the severity of necrotizing enterocolitis in neonatal mice and preterm piglets: Evidence in mice for a role of TLR9. *Am. J. Physiol. Gastrointest. Liver Physiol.* 2014;306:G1021–G1032.
40. Good M, Siggers RH, Sodhi CP, Afrazi A, Alkhudari F, Egan CE, Neal MD, Yazji I, Jia H, Lin J, et al. Amniotic fluid inhibits Toll-like receptor 4 signaling in the fetal and neonatal intestinal epithelium. *Proc. Natl. Acad. Sci. USA* 2012;109:11330–11335.
41. Radulescu A, Zorko NA, Yu X, Besner GE. Preclinical neonatal rat studies of heparin-binding EGF-like growth factor in protection of the intestines from necrotizing enterocolitis. *Pediatr. Res.* 2009; 65: 437-442.

42. Jantscher-Krenn E, Zhrebtsov M, Nissan C, Goth K, Guner YS, Naidu N, Choudhury B, Grishin AV, Ford HR, Bode L. The human milk oligosaccharide disialyllacto-N-tetraose prevents necrotizing enterocolitis in neonatal rats. *Gut* 2012;61:1417–1425.
43. Ohtsuka Y, Okada K, Yamakawa Y, Ikuse T, Baba Y, Inage E, Fujii T, Izumi H, Oshida K, Nagata S, et al. omega-3 fatty acids attenuate mucosal inflammation in premature rat pups. *J. Pediatr. Surg.* 2011;46:489–495.
44. Lu J, Jilling T, Li D, Caplan MS. Polyunsaturated fatty acid supplementation alters proinflammatory gene expression and reduces the incidence of necrotizing enterocolitis in a neonatal rat model. *Pediatr. Res.* 2007;61:427–432.
45. Caplan MS, Russell T, Xiao Y, Amer M, Kaup S, Jilling T. Effect of polyunsaturated fatty acid (PUFA) supplementation on intestinal inflammation and necrotizing enterocolitis (NEC) in a neonatal rat model. *Pediatr. Res.* 2001;49:647–652.
46. Ran-Ressler RR, Khailova L, Arganbright KM, Adkins-Rieck CK, Jouni ZE, Koren O, Ley RE, Brenna JT, Dvorak B. Branched chain fatty acids reduce the incidence of necrotizing enterocolitis and alter gastrointestinal microbial ecology in a neonatal rat model. *PLoS One* 2011;6:e29032.
47. Coursodon-Boydiddle CF, Snarrenberg CL, Adkins-Rieck CK, Bassaganya-Riera J, Hontecillas R, Lawrence P, Brenna JT, Jouni ZE, Dvorak B. Pomegranate seed oil reduces intestinal damage in a rat model of necrotizing enterocolitis. *Am. J. Physiol. Gastrointest. Liver Physiol.* 2012;303:G744–751.
48. Zhang D, Wen J, Zhou J, Cai W, Qian L. Milk Fat Globule Membrane Ameliorates Necrotizing Enterocolitis in Neonatal Rats and Suppresses Lipopolysaccharide-Induced Inflammatory Response in IEC-6 Enterocytes. *J. Parenter. Enter. Nutr.* 2019;43(7):863–873.
49. Wang C, Zhang M, Guo H, Yan J, Liu F, Chen J, Li Y, Ren F. Human Milk Oligosaccharides Protect Against Necrotizing Enterocolitis by Inhibiting Intestinal Damage Via Increasing the Proliferation of Crypt Cells. *Mol. Nutr. Food Res.* 2019;63(18):e1900262.
50. Xu J, Anderson V, Schwarz SM. Dietary GD3 ganglioside reduces the incidence and severity of necrotizing enterocolitis by sustaining regulatory immune responses. *J. Pediatr. Gastroenterol. Nutr.* 2013;57:550–556.
51. Shen H, Lei Y, He X, Liu D, He Z. Role of lactadherin in intestinal barrier integrity in experimental neonatal necrotizing enterocolitis. *J. Cell. Biochem.* 2019;120(12):19509–19517.
52. Caplan MS, Lickerman M, Adler L, Dietsch GN, Yu A. The role of recombinant platelet-activating factor acetylhydrolase in a neonatal rat model of necrotizing enterocolitis. *Pediatr. Res.* 1997;42: 779–783.
53. Halpern MD, Dominguez JA, Dvorakova K, Holubec H, Williams CS, Meza YG, Ruth MC, Dvorak B. Ileal cytokine dysregulation in experimental necrotizing enterocolitis is reduced by epidermal growth factor. *J. Pediatr. Gastroenterol. Nutr.* 2003;36:126–133.
54. Dvorak B, Halpern MD, Holubec H, Williams CS, McWilliam DL, Dominguez JA, Stepankova R, Payne CM, McCuskey RS. Epidermal growth factor reduces the development of necrotizing enterocolitis in a neonatal rat model. *Am. J. Physiol. Gastrointest. Liver Physiol.* 2002;282:G156–G164.
55. Maynard AA, Dvorak K, Khailova L, Dobrenen H, Arganbright KM, Halpern MD, Kurundkar AR, Maheshwari A, Dvorak B. Epidermal growth factor reduces autophagy in intestinal epithelium and in the rat model of necrotizing enterocolitis. *Am. J. Physiol. Gastrointest. Liver Physiol.* 2010;299: G614–G622.
56. Khailova L, Dvorak K, Arganbright KM, Williams CS, Halpern MD, Dvorak B. Changes in hepatic cell junctions structure during experimental necrotizing enterocolitis: Effect of EGF treatment. *Pediatr. Res.* 2009;66:140–144.
57. Wei J, Besner GE. M1 to M2 macrophage polarization in heparin-binding epidermal growth factor-like growth factor therapy for necrotizing enterocolitis. *J. Surg. Res.* 2015;197:126–138.
58. Yang J, Watkins D, Chen CL, Bhushan B, Zhou Y, Besner GE. Heparin-binding epidermal growth factor-like growth factor and mesenchymal stem cells act synergistically to prevent experimental necrotizing enterocolitis. *J. Am. Coll. Surg.* 2012;215:534–545.
59. Feng J, Besner GE. Heparin-binding epidermal growth factor-like growth factor promotes enterocyte migration and proliferation in neonatal rats with necrotizing enterocolitis. *J. Pediatr. Surg.* 2007;42: 214–220.

60. Feng J, El-Assal ON, Besner GE. Heparin-binding epidermal growth factor-like growth factor reduces intestinal apoptosis in neonatal rats with necrotizing enterocolitis. *J. Pediatr. Surg.* 2006; 41:742–747; discussion 742–747.
61. Su Y, Yang J, Besner GE. HB-EGF promotes intestinal restitution by affecting integrin-extracellular matrix interactions and intercellular adhesions. *Growth Factors* 2013;31:39–55.
62. Feng J, El-Assal ON, Besner GE. Heparin-binding EGF-like growth factor (HB-EGF) and necrotizing enterocolitis. *Semin. Pediatr. Surg.* 2005;14:167–174.
63. Jain SK, Baggerman EW, Mohankumar K, Namachivayam K, Jagadeeswaran R, Reyes VE, Maheshwari A. Amniotic fluid-borne hepatocyte growth factor protects rat pups against experimental necrotizing enterocolitis. *Am. J. Physiol. Gastrointest. Liver Physiol.* 2014;306:G361–G369.
64. Shiou SR, Yu Y, Guo Y, Westerhoff M, Lu L, Petrof EO, Sun J, Claud EC. Oral administration of transforming growth factor-beta1 (TGF-beta1) protects the immature gut from injury via Smad protein-dependent suppression of epithelial nuclear factor kappaB (NF-kappaB) signaling and proinflammatory cytokine production. *J. Biol. Chem.* 2013;288:34757–34766.
65. Tian F, Liu GR, Li N, Yuan G. Insulin-like growth factor I reduces the occurrence of necrotizing enterocolitis by reducing inflammatory response and protecting intestinal mucosal barrier in neonatal rats model. *Eur. Rev. Med. Pharm. Sci.* 2017; 21:4711–4719.
66. Shiou SR, Yu Y, Chen S, Ciancio MJ, Petrof EO, Sun J, Claud EC. Erythropoietin protects intestinal epithelial barrier function and lowers the incidence of experimental neonatal necrotizing enterocolitis. *J. Biol. Chem.* 2011;286:12123–12132.
67. Hoang TK, He B, Wang T, Tran DQ, Rhoads JM, Liu Y. Protective effect of *Lactobacillus reuteri* DSM 17938 against experimental necrotizing enterocolitis is mediated by Toll-like receptor 2. *Am. J. Physiol. Gastrointest. Liver Physiol.* 2018;315:G231–G240.
68. Liu Y, Fatheree NY, Mangalat N, Rhoads JM. *Lactobacillus reuteri* strains reduce incidence and severity of experimental necrotizing enterocolitis via modulation of TLR4 and NF-kappaB signaling in the intestine. *Am. J. Physiol. Gastrointest. Liver Physiol.* 2012;302:G608–G617.
69. Liu Y, Tran DQ, Fatheree NY, Marc Rhoads J. *Lactobacillus reuteri* DSM 17938 differentially modulates effector memory T cells and Foxp3+ regulatory T cells in a mouse model of necrotizing enterocolitis. *Am. J. Physiol. Gastrointest. Liver Physiol.* 2014;307:G177–G186.
70. Tang J, Guo C, Gong F. Protective effect of *Lactobacillus reuteri* against oxidative stress in neonatal mice with necrotizing enterocolitis. *Nan Fang Yi Ke Da Xue Xue Bao* 2019;39:1221–1226.
71. Olson JK, Rager TM, Navarro JB, Mashburn-Warren L, Goodman SD, Besner GE. Harvesting the benefits of biofilms: A novel probiotic delivery system for the prevention of necrotizing enterocolitis. *J. Pediatr. Surg.* 2016;51:936–941.
72. Olson JK, Navarro JB, Allen JM, McCulloh CJ, Mashburn-Warren L, Wang Y, Varaljay VA, Bailey MT, Goodman SD, Besner GE. An enhanced *Lactobacillus reuteri* biofilm formulation that increases protection against experimental necrotizing enterocolitis. *Am. J. Physiol. Gastrointest. Liver Physiol.* 2018;315:G408–G419.
73. Khailova L, Dvorak K, Arganbright KM, Halpern MD, Kinouchi T, Yajima M, Dvorak B. *Bifidobacterium bifidum* improves intestinal integrity in a rat model of necrotizing enterocolitis. *Am. J. Physiol. Gastrointest. Liver Physiol.* 2009;297:G940–G949.
74. Khailova L, Mount Patrick SK, Arganbright KM, Halpern MD, Kinouchi T, Dvorak B. *Bifidobacterium bifidum* reduces apoptosis in the intestinal epithelium in necrotizing enterocolitis. *Am. J. Physiol. Gastrointest. Liver Physiol.* 2010;299:G1118–G1127.
75. Caplan MS, Miller-Catchpole R, Kaup S, Russell, T, Lickerman M, Amer M, Xiao Y, Thomson R, Jr. *Bifidobacterial* supplementation reduces the incidence of necrotizing enterocolitis in a neonatal rat model. *Gastroenterology* 1999;117:577–583.
76. Wu W, Wang Y, Zou J, Long F, Yan H, Zeng L, Chen Y. *Bifidobacterium adolescentis* protects against necrotizing enterocolitis and upregulates TOLLIP and SIGIRR in premature neonatal rats. *Bmc Pediatr.* 2017;17:1.
77. Siggers RH, Siggers J, Boye M, Thymann T, Mølbak L, Leser T, Jensen BB, Sangild PT. Early administration of probiotics alters bacterial colonization and limits diet-induced gut dysfunction and severity of necrotizing enterocolitis in preterm pigs. *J. Nutr.* 2008;138:1437–1444.

78. Pisano C, Galley J, Elbahrawy M, Wang Y, Farrell A, Brigstock D, Besner GE. Human Breast Milk-Derived Extracellular Vesicles in the Protection Against Experimental Necrotizing Enterocolitis. *J. Pediatr. Surg.* 2020;55:54–58.
79. Jing Y, Peng F, Shan Y, Jiang J. Berberine reduces the occurrence of neonatal necrotizing enterocolitis by reducing the inflammatory response. *Exp. Med.* 2018;16:5280–5285.
80. Quintanilla HD, Liu Y, Fatheree NY, Atkins CL, Hashmi SS, Floros J, McCormack FX, Rhoads JM, Alcorn JL. Oral administration of surfactant protein-a reduces pathology in an experimental model of necrotizing enterocolitis. *J. Pediatr. Gastroenterol. Nutr.* 2015;60:613–620.
81. Sheng Q, Lv Z, Cai W, Song H, Qian L, Mu H, Shi J, Wang X. Human β -defensin-3 promotes intestinal epithelial cell migration and reduces the development of necrotizing enterocolitis in a neonatal rat model. *Pediatr. Res.* 2014;76:269–279.
82. Akisu M, Baka M, Coker I, Kultursay N, Huseyinov A. Effect of dietary n-3 fatty acids on hypoxia-induced necrotizing enterocolitis in young mice. n-3 fatty acids alter platelet-activating factor and leukotriene B4 production in the intestine. *Biol. Neonate* 1998;74:31–38.
83. Zhu X, Cui N, Yu L, Cheng P, Cui M, Zhu X, Wang J. Potential role of endoplasmic reticulum stress is involved in the protection of fish oil on neonatal rats with necrotizing enterocolitis. *Sci. Rep.* 2020;10:6448.
84. Yang Y, Zhang T, Zhou G, Jiang X, Tao M, Zhang J, Zeng X, Wu Z, Pan D, Guo Y. Prevention of Necrotizing Enterocolitis through Milk Polar Lipids Reducing Intestinal Epithelial Apoptosis. *J. Agric. Food Chem.* 2020;68(26):7014-7023.
85. Sodhi CP, Fulton WB, Good M, Vurma M, Das T, Lai CS, Jia H, Yamaguchi Y, Lu P, Prindle T, et al. Fat composition in infant formula contributes to the severity of necrotising enterocolitis. *Br. J. Nutr.* 2018;120:665–680.
86. Li B, Pierro A. Human milk oligosaccharides protect against necrotizing enterocolitis by activating intestinal cell differentiation. *Mol. Nutr. Food Res.* 2020:e2000519.
87. Autran CA, Schoterman MH, Jantscher-Krenn E, Kamerling JP, Bode L. Sialylated galactooligosaccharides and 2'-fucosyllactose reduce necrotising enterocolitis in neonatal rats. *Br. J. Nutr.* 2016;116:294–299.
88. Wang C, Zhang M, Guo H, Yan J, Chen L, Teng W, Ren F, Li Y, Wang X, Luo J, et al. Human Milk Oligosaccharides Activate Epidermal Growth Factor Receptor and Protect Against Hypoxia-Induced Injuries in the Mouse Intestinal Epithelium and Caco2 Cells. *J. Nutr.* 2020;150:756–762.
89. Yu H, Lau K, Thon V, Autran CA, Jantscher-Krenn E, Xue M, Li Y, Sugiarto G, Qu J, Mu S, et al. Synthetic disialyl hexasaccharides protect neonatal rats from necrotizing enterocolitis. *Angew. Chem. Int. Ed. Engl.* 2014;53:6687–6691.
90. Yu H, Yan X, Autran CA, Li Y, Etzold S, Latasiewicz J, Robertson BM, Li J, Bode L, Chen X. Enzymatic and Chemoenzymatic Syntheses of Disialyl Glycans and Their Necrotizing Enterocolitis Preventing Effects. *J. Org. Chem.* 2017;82:13152–13160.
91. Good M, Sodhi CP, Yamaguchi Y, Jia H, Lu P, Fulton WB, Martin LY, Prindle T, Nino DF, Zhou Q, et al. The human milk oligosaccharide 2'-fucosyllactose attenuates the severity of experimental necrotising enterocolitis by enhancing mesenteric perfusion in the neonatal intestine. *Br. J. Nutr.* 2016;116:1175–1187.
92. Sodhi CP, Wipf P, Yamaguchi Y, Fulton WB, Kovler M, Nino DF, Zhou Q, Banfield E, Werts AD, Ladd MR, et al. The human milk oligosaccharides 2'-fucosyllactose and 6'-sialyllactose protect against the development of necrotizing enterocolitis by inhibiting toll-like receptor 4 signaling. *Pediatr. Res.* 2021;89(1):91-101.
93. He-Yang J, Zhang W, Liu J, Xue P, Zhou X. Human breast milk oligosaccharides attenuate necrotizing enterocolitis in rats by suppressing mast cell accumulation, DPPI activity and TLR4 expression in ileum tissue, and regulating mitochondrial damage of Caco-2 cells. *Int. Immunopharmacol.* 2020;88:106881.
94. Gunasekaran A, Eckert J, Burge K, Zheng W, Yu Z, Kessler S, de la Motte C, Chaaban H. Hyaluronan 35 kDa enhances epithelial barrier function and protects against the development of murine necrotizing enterocolitis. *Pediatr. Res.* 2020;87(7):1177-1184.

95. Akisu M, Baka M, Huseyinov A, Kultursay N. The role of dietary supplementation with L-glutamine in inflammatory mediator release and intestinal injury in hypoxia/reoxygenation-induced experimental necrotizing enterocolitis. *Ann. Nutr. Metab.* 2003;47:262–266.
96. Dilsiz A, Ciftci I, Aktan TM, Gurbilek M, Karagozlu E. Enteral glutamine supplementation and dexamethasone attenuate the local intestinal damage in rats with experimental necrotizing enterocolitis. *Pediatr. Surg. Int.* 2003;19:578–582
97. Zhou W, Li W, Zheng XH, Rong X, Huang LG. Glutamine downregulates TLR-2 and TLR-4 expression and protects intestinal tract in preterm neonatal rats with necrotizing enterocolitis. *J. Pediatr. Surg.* 2014;49:1057–1063.
98. Chen Y, Koike Y, Chi L, Ahmed A, Miyake H, Li B, Lee C, Delgado-Olguin P, Pierro A. Formula feeding and immature gut microcirculation promote intestinal hypoxia, leading to necrotizing enterocolitis. *Dis. Model. Mech.* 2019;12(12):dmm040998.
99. Akisu M, Ozmen D, Baka M, Habif S, Yalaz M, Arslanoglu S, Kultursay N, Bayindir O. Protective effect of dietary supplementation with L-arginine and L-carnitine on hypoxia/reoxygenation-induced necrotizing enterocolitis in young mice. *Biol. Neonate* 2002;81:260–265.
100. Moller HK, Thymann T, Fink LN, Frokiaer H, Kvistgaard AS, Sangild PT. Bovine colostrum is superior to enriched formulas in stimulating intestinal function and necrotizing enterocolitis resistance in preterm pigs. *Br. J. Nutr.* 2011;105:44–53.
101. Liu J, Zhu HT, Li B, Robinson SC, Lee C, O’Connell JS, Bindi E, Zheng S, Sherman PM, Pierro A. Lactoferrin Reduces Necrotizing Enterocolitis Severity by Upregulating Intestinal Epithelial Proliferation. *Eur. J. Pediatr. Surg.* 2020;30(1):90-95.
102. Whitehouse JS, Riggle KM, Purpi DP, Mayer AN, Pritchard KA, Jr, Oldham KT, Gourlay DM. The protective role of intestinal alkaline phosphatase in necrotizing enterocolitis. *J. Surg. Res.* 2010;163:79–85.
103. Rentea RM, Liedel JL, Welak SR, Cassidy LD, Mayer AN, Pritchard KA, Jr, Oldham KT, Gourlay DM. Intestinal alkaline phosphatase administration in newborns is protective of gut barrier function in a neonatal necrotizing enterocolitis rat model. *J. Pediatr. Surg.* 2012;47:1135–1142.
104. Isani M, Illingworth L, Herman E, Schmidt M, Barron L, Bowling J, Elizee M, Bai I, Gayer C, Grishin A, et al. Soybean-derived recombinant human epidermal growth factor protects against experimental necrotizing enterocolitis. *J. Pediatr. Surg.* 2018;53:1203–1207.
105. Feng J, El-Assal ON, Besner GE. Heparin-binding epidermal growth factor-like growth factor decreases the incidence of necrotizing enterocolitis in neonatal rats. *J. Pediatr. Surg.* 2006;41:144–149; discussion 144-149.
106. Yu X, Radulescu A, Zorko N, Besner GE. Heparin-binding EGF-like growth factor increases intestinal microvascular blood flow in necrotizing enterocolitis. *Gastroenterology* 2009;137:221–230.
107. Matheson PJ, Walker SK, Maki AC, Shaheen SP, Neal Garrison R, Downard CD. Oral relaxin maintains intestinal blood flow in a rat model of NEC. *J. Pediatr. Surg.* 2014;49:961–964; discussion 964–965.
108. Maheshwari A, Kelly DR, Nicola T, Ambalavanan N, Jain SK, Murphy-Ullrich J, Athar M, Shimamura M, Bhandari V, Aprahamian C, et al. TGF-beta2 suppresses macrophage cytokine production and mucosal inflammatory responses in the developing intestine. *Gastroenterology* 2011;140:242–253.
109. Nino DF, Sodhi CP, Egan CE, Zhou Q, Lin J, Lu P, Yamaguchi Y, Jia H, Martin LY, Good M, et al. Retinoic Acid Improves Incidence and Severity of Necrotizing Enterocolitis by Lymphocyte Balance Restitution and Repopulation of LGR5+ Intestinal Stem Cells. *Shock* 2017;47:22–32.
110. Egan CE, Sodhi CP, Good M, Lin J, Jia H, Yamaguchi Y, Lu P, Ma C, Branca MF, Weyandt S, et al. Toll-like receptor 4-mediated lymphocyte influx induces neonatal necrotizing enterocolitis. *J. Clin. Investig.* 2016;126:495–508.
111. Xiao S, Li Q, Hu K, He Y, Ai Q, Hu L, Yu J. Vitamin A and Retinoic Acid Exhibit Protective Effects on Necrotizing Enterocolitis by Regulating Intestinal Flora and Enhancing the Intestinal Epithelial Barrier. *Arch. Med. Res.* 2018;49:1–9.
112. Lyu C, Jiang S, Kong M, Chen X, Zhang L. Vitamin D protects against necrotizing enterocolitis in newborn mice by activating the ERK signalling pathway. *Mol Med Rep* 2020;22:2107–2114.
113. Fan H, Chen Z, Lin R, Liu Y, Wu X, Puthiyakunnon S, Wang Y, Zhu B, Zhang Q, Bai Y, et al. *Bacteroides fragilis* Strain ZY-312 Defense against *Cronobacter sakazakii*-Induced Necrotizing Enterocolitis In Vitro and in a Neonatal Rat Model. *mSystems* 2019;4(4):e00305-19.

114. Zhou W, Lv H, Li M.X, Su H, Huang LG, Li J, Yuan WM. Protective effects of bifidobacteria on intestines in newborn rats with necrotizing enterocolitis and its regulation on TLR2 and TLR4. *Genet. Mol. Res.* 2015;14:11505–11514.
115. Lu WC, Zheng X, Liu JF, Wu WC, Chen XY, Wei HB, Li CL, Lin MJ. Effect of Bifidobacterium on the expression of β -defensin-2 in intestinal tissue of neonatal rats with necrotizing enterocolitis. *Zhongguo Dang Dai Er Ke Za Zhi* 2018;20:224–229.
116. Bergmann KR, Liu SX, Tian R, Kushnir A, Turner JR, Li HL, Chou PM, Weber CR, De Plaen IG. Bifidobacteria stabilize claudins at tight junctions and prevent intestinal barrier dysfunction in mouse necrotizing enterocolitis. *Am. J. Pathol.* 2013;182:1595–1606.
117. Satoh T, Izumi H, Iwabuchi N, Odamaki T, Namba K, Abe F, Xiao JZ. Bifidobacterium breve prevents necrotising enterocolitis by suppressing inflammatory responses in a preterm rat model. *Benef. Microbes* 2016;7:75–82.
118. Li B, Hock A, Wu RY, Minich A, Botts SR, Lee C, Antounians L, Miyake H, Koike Y, Chen Y, et al. Bovine milk-derived exosomes enhance goblet cell activity and prevent the development of experimental necrotizing enterocolitis. *PLoS One* 2019;14:e0211431.
119. Miyake H, Lee C, Chusilp S, Bhalla M, Li B, Pitino M, Seo S, O'Connor DL, Pierro A. Human breast milk exosomes attenuate intestinal damage. *Pediatr. Surg. Int.* 2020;36(2):155-163.
120. Wang X, Yan X, Zhang L, Cai J, Zhou Y, Liu H, Hu Y, Chen W, Xu S, Liu P, et al. Identification and Peptidomic Profiling of Exosomes in Preterm Human Milk: Insights Into Necrotizing Enterocolitis Prevention. *Mol. Nutr. Food Res.* 2019:e1801247,.
121. Cakir U, Tayman C, Serkant U, Yakut HI, Cakir E, Ates U, Koyuncu I, Karaogul E. Ginger (*Zingiber officinale* Roscoe) for the treatment and prevention of necrotizing enterocolitis. *J. Ethnopharmacol.* 2018;225:297–308,.
122. Yakut HI, Koyuncu E, Cakir U, Tayman C, Koyuncu İ, Taskin Turkmenoglu T, Cakir E, Ozyazici A, Aydogan S, Zenciroglu A. Preventative and therapeutic effects of fennel (*Foeniculum vulgare*) seed extracts against necrotizing enterocolitis. *J. Food Biochem.* 2020:e13284.
123. Siggers J, Ostergaard MV, Siggers RH, Skovgaard K, Mølbak L, Thymann T, Schmidt M, Møller HK, Purup S, Fink LN, et al. Postnatal amniotic fluid intake reduces gut inflammatory responses and necrotizing enterocolitis in preterm neonates. *Am. J. Physiol. Gastrointest. Liver Physiol.* 2013;304: G864–G875.
124. Yin Y, Wu X, Peng B, Zou H, Li S, Wang J, Cao J. Curcumin improves necrotising microscopic colitis and cell pyroptosis by activating SIRT1/NRF2 and inhibiting the TLR4 signalling pathway in newborn rats. *Innate Immun.* 2020;26(7):609-617.
125. Cigsar EB, Ali Karadag C, Tanik C, Fatih Aydin A, Ihsan Dokucu A. The protective effects of sesamol in a neonatal rat model of necrotizing enterocolitis. *J. Matern. Fetal Neonatal Med.* 2018;1–6:
126. Cai Z, Liu J, Bian H, Cai J. Astragaloside IV ameliorates necrotizing enterocolitis by attenuating oxidative stress and suppressing inflammation via the vitamin D3-upregulated protein 1/NF- κ B signaling pathway. *Exp. Med.* 2016;12:2702–2708.
127. Ergün O, Ergün G, Oktem G, Selvi N, Doğan H, Tunçyürek M, Saydam G, Erdener A. Enteral resveratrol supplementation attenuates intestinal epithelial inducible nitric oxide synthase activity and mucosal damage in experimental necrotizing enterocolitis. *J. Pediatr. Surg.* 2007;42: 1687–1694.
128. Catala I, Butel M.J, Bensaada M, Popot F, Tessedre AC, Rimbault A, Szyliet O. Oligofructose contributes to the protective role of bifidobacteria in experimental necrotising enterocolitis in quails. *J. Med. Microbiol.* 1999;48:89–94.
129. Ren S, Hui Y, Goericke-Pesch S, Pankratova S, Kot W, Pan X, Thymann T, Sangild PT, Nguyen DN. Gut and immune effects of bioactive milk factors in preterm pigs exposed to prenatal inflammation. *Am. J. Physiol. Gastrointest. Liver Physiol.* 2019;317(1):G67-G77.
130. Butel MJ, Roland N, Hibert A, Popot F, Favre A, Tessedre AC, Bensaada M, Rimbault A, Szyliet O. Clostridial pathogenicity in experimental necrotising enterocolitis in gnotobiotic quails and protective role of bifidobacteria. *J. Med. Microbiol.* 1998;47:391–399.
131. Lock JY, Carlson TL, Yu Y, Lu J, Claud EC, Carrier RL. Impact of Developmental Age, Necrotizing Enterocolitis Associated Stress, and Oral Therapeutic Intervention on Mucus Barrier Properties. *Sci. Rep.* 2020;10:6692.

132. Liu Y, Fatheree NY, Dingle BM, Tran DQ, Rhoads JM. *Lactobacillus reuteri* DSM 17938 changes the frequency of Foxp3⁺ regulatory T cells in the intestine and mesenteric lymph node in experimental necrotizing enterocolitis. *PLoS One* 2013;8:e56547.
133. Cilieborg MS, Bering SB, Ostergaard MV, Jensen ML, Krych L, Newburg DS, Sangild PT. Minimal short-term effect of dietary 2'-fucosyllactose on bacterial colonisation, intestinal function and necrotising enterocolitis in preterm pigs. *Br. J. Nutr.* 2016;116:834–841.
134. Rasmussen SO, Martin L, Ostergaard MV, Rudloff S, Roggenbuck M, Nguyen DN, Sangild PT, Bering SB. Human milk oligosaccharide effects on intestinal function and inflammation after preterm birth in pigs. *J. Nutr. Biochem.* 2017;40:141–154.
135. D'Souza A, Fordjour L, Ahmad A, Cai C, Kumar D, Valencia G, Aranda JV, Beharry KD. Effects of probiotics, prebiotics, and synbiotics on messenger RNA expression of caveolin-1, NOS, and genes regulating oxidative stress in the terminal ileum of formula-fed neonatal rats. *Pediatr. Res.* 2010;67:526–531.
136. D'Souza A, Cai CL, Kumar D, Cai F, Fordjour L, Ahmad A, Valencia G, Aranda JV, Beharry KD. Cytokines and Toll-like receptor signaling pathways in the terminal ileum of hypoxic/hyperoxic neonatal rats: Benefits of probiotics supplementation. *Am. J. Transl. Res.* 2012;4:187–197.
137. Clark JA, Doelle SM, Halpern MD, Saunders TA, Holubec H, Dvorak K, Boitano SA, Dvorak B. Intestinal barrier failure during experimental necrotizing enterocolitis: Protective effect of EGF treatment. *Am. J. Physiol. Gastrointest. Liver Physiol.* 2006;291:G938–G949.
138. MohanKumar K, Namachivayam K, Ho TTB, Torres BA, Ohls RK, Maheshwari A. Cytokines and growth factors in the developing intestine and during necrotizing enterocolitis. *Semin. Perinatol.* 2017;41:52–60.
139. Viscardi RM, Lyon NH, Sun CC, Hebel JR, Hasday JD. Inflammatory cytokine mRNAs in surgical specimens of necrotizing enterocolitis and normal newborn intestine. *Pediatr. Pathol. Lab. Med.* 1997;17:547–559.
140. Miyake H, Lee C, Seo S, Li B, Pierro A. Liver Organoids Generated from Mice with Necrotizing Enterocolitis Have Reduced Regenerative Capacity. *Eur. J. Pediatr. Surg.* 2020;30(1):79–84.
141. MohanKumar K, Kaza N, Jagadeeswaran R, Garzon SA, Bansal A, Kurundkar AR, Namachivayam K, Remon JI, Bandepalli CR, Feng X, et al. Gut mucosal injury in neonates is marked by macrophage infiltration in contrast to pleomorphic infiltrates in adult: Evidence from an animal model. *Am. J. Physiol. Gastrointest. Liver Physiol.* 2012;303:G93–G102.
142. Vincent D, Klinke M, Eschenburg G, Trochimiuk M, Appl B, Tiemann B, Bergholz R, Reinshagen K, Boettcher M. NEC is likely a NETs dependent process and markers of NETosis are predictive of NEC in mice and humans. *Sci. Rep.* 2018;8:12612.
143. Weitkamp JH, Koyama T, Rock MT, Correa H, Goettel JA, Matta P, Oswald-Richter, K, Rosen, M.J, Engelhardt, B.G, Moore, D.J, et al. Necrotising enterocolitis is characterised by disrupted immune regulation and diminished mucosal regulatory (FOXP3)/effector (CD4, CD8) T cell ratios. *Gut* 2013;62:73–82.
144. Ma F, Li S, Gao X, Zhou J, Zhu X, Wang D, Cai Y, Li F, Yang Q, Gu X, et al. Interleukin-6-mediated CCR9(+) interleukin-17-producing regulatory T cells polarization increases the severity of necrotizing enterocolitis. *EBioMedicine* 2019;44:71–85.
145. Cho SX, Berger PJ, Nold-Petry CA, Nold MF. The immunological landscape in necrotising enterocolitis. *Expert Rev. Mol. Med.* 2016;18:e12.
146. Hackam DJ, Sodhi CP. Toll-Like Receptor-Mediated Intestinal Inflammatory Imbalance in the Pathogenesis of Necrotizing Enterocolitis. *Cell. Mol. Gastroenterol. Hepatol.* 2018;6:229–238.e221.
147. Sodhi CP, Neal MD, Siggers R, Sho S, Ma C, Branca MF, Prindle T Jr, Russo AM, Afrazi A, Good M, et al. Intestinal epithelial Toll-like receptor 4 regulates goblet cell development and is required for necrotizing enterocolitis in mice. *Gastroenterology* 2012;143:708–718.e705.
148. Leaphart CL, Cavallo J, Gripar SC, Cetin S, Li J, Branca MF, Dubowski TD, Sodhi CP, Hackam DJ. A critical role for TLR4 in the pathogenesis of necrotizing enterocolitis by modulating intestinal injury and repair. *J. Immunol.* 2007;179:4808–4820.
149. Gripar SC, Sodhi CP, Richardson WM, Anand RJ, Gittes GK, Branca MF, Jakub A, Shi XH, Shah S, Ozolek JA, et al. Reciprocal expression and signaling of TLR4 and TLR9 in the pathogenesis and treatment of necrotizing enterocolitis. *J. Immunol.* 2009;182:636–646.

150. Nanthakumar N, Meng D, Goldstein AM, Zhu W, Lu L, Uauy R, Llanos A, Claud EC, Walker WA. The mechanism of excessive intestinal inflammation in necrotizing enterocolitis: An immature innate immune response. *PLoS One* 2011;6:e17776.
151. Cuna A, Sampath V. Genetic alterations in necrotizing enterocolitis. *Semin. Perinatol.* 2017;41:61–69.
152. Sampath V, Le M, Lane L, Patel AL, Cohen JD, Simpson PM, Garland JS, Hines RN. The NFKB1 (g.-24519delATTG) variant is associated with necrotizing enterocolitis (NEC) in premature infants. *J. Surg. Res.* 2011;169:e51-57.
153. Wolfs TG, Derikx JP, Hodin CM, Vanderlocht J, Driessen A, de Bruine AP, Bevins CL, Lasitschka F, Gassler N, van Gemert WG, et al. Localization of the lipopolysaccharide recognition complex in the human healthy and inflamed premature and adult gut. *Inflamm. Bowel Dis.* 2010;16:68–75.
154. Jenke AC, Zilbauer M, Postberg J, Wirth S. Human beta-defensin 2 expression in ELBW infants with severe necrotizing enterocolitis. *Pediatr. Res.* 2012;72:513–520.
155. Härtel C, Hartz A, Pagel J, Rupp J, Stein A, Kribs A, Müller A, Haase R, Gille C, Böttger R, et al. NOD2 Loss-of-Function Mutations and Risks of Necrotizing Enterocolitis or Focal Intestinal Perforation in Very Low-birth-weight Infants. *Inflamm. Bowel Dis.* 2016;22:249–256.
156. Caplan MS, Sun XM, Hseuh W, Hageman JR. Role of platelet activating factor and tumor necrosis factor-alpha in neonatal necrotizing enterocolitis. *J. Pediatrics* 1990;116:960–964.
157. Maheshwari A, Schelonka RL, Dimmitt RA, Carlo WA, Munoz-Hernandez B, Das A, McDonald SA, Thorsen P, Skogstrand K, Hougaard DM, et al. Cytokines associated with necrotizing enterocolitis in extremely-low-birth-weight infants. *Pediatr. Res.* 2014;76:100–108.
158. Benkoe T, Baumann S, Weninger M, Pones M, Reck C, Rebhandl W, Oehler R. Comprehensive evaluation of 11 cytokines in premature infants with surgical necrotizing enterocolitis. *PLoS One* 2013;8:e58720.
159. Edelson MB, Bagwell CE, Rozycki HJ. Circulating pro- and counterinflammatory cytokine levels and severity in necrotizing enterocolitis. *Pediatrics* 1999;103:766–771.
160. Rentea RM, Liedel JL, Fredrich K, Pritchard K Jr, Oldham KT, Simpson PM, Gourlay DM. Enteral intestinal alkaline phosphatase administration in newborns decreases iNOS expression in a neonatal necrotizing enterocolitis rat model. *J. Pediatr. Surg.* 2013;48:124–128.
161. Cuna A, Yu W, Menden HL, Feng L, Srinivasan P, Chavez-Bueno S, Ahmed I, Umar S, Sampath V. NEC-like intestinal injury is ameliorated by *Lactobacillus rhamnosus* GG in parallel with SIGIRR and A20 induction in neonatal mice. *Pediatr. Res.* 2020;88(4):546-555.
162. Rentea RM, Liedel JL, Fredrich K, Welak SR, Pritchard KA. Jr, Oldham KT, Simpson PM, Gourlay DM. Intestinal alkaline phosphatase administration in newborns decreases systemic inflammatory cytokine expression in a neonatal necrotizing enterocolitis rat model. *J. Surg. Res.* 2012;177:228–234.
163. Sánchez de Medina F, Romero-Calvo I, Mascaraque C, Martínez-Augustín O. Intestinal Inflammation and Mucosal Barrier Function. *Inflamm. Bowel Dis.* 2014;20:2394–2404.
164. Anderson JM, Van Itallie CM. Physiology and function of the tight junction. *Cold Spring Harb. Perspect. Biol.* 2009;1:a002584.
165. Halpern MD, Denning PW. The role of intestinal epithelial barrier function in the development of NEC. *Tissue Barriers* 2015;3:e1000707.
166. Anand RJ, Leaphart CL, Mollen KP, Hackam DJ. The role of the intestinal barrier in the pathogenesis of necrotizing enterocolitis. *Shock* 2007;27:124–133.
167. Schaart MW, de Bruijn AC, Bouwman DM, de Krijger RR, van Goudoever JB, Tibboel D, Renes IB. Epithelial functions of the residual bowel after surgery for necrotising enterocolitis in human infants. *J. Pediatr. Gastroenterol. Nutr.* 2009;49:31–41.
168. McElroy SJ, Prince LS, Weitkamp JH, Reese J, Slaughter JC, Polk DB. Tumor necrosis factor receptor 1-dependent depletion of mucus in immature small intestine: A potential role in neonatal necrotizing enterocolitis. *Am. J. Physiol. Gastrointest. Liver Physiol.* 2011;301:G656–G666.
169. Salzman NH, Polin RA, Harris MC, Ruchelli E, Hebra A, Zirin-Butler S, Jawad A, Martin Porter E, Bevins CL. Enteric defensin expression in necrotizing enterocolitis. *Pediatr. Res.* 1998;44:20–26.
170. Markasz L, Wanders A, Szekely L, Lilja HE. Diminished DEFA6 Expression in Paneth Cells Is Associated with Necrotizing Enterocolitis. *Gastroenterol. Res. Pr.* 2018;2018:7345426.

171. Gopalakrishna KP, Macadangdang BR, Rogers MB, Tometich JT, Firek BA, Baker R, Ji J, Burr AHP, Ma C, Good M, et al. Maternal IgA protects against the development of necrotizing enterocolitis in preterm infants. *Nat. Med.* 2019;25(7):1110-1115.
172. Moore SA, Nighot P, Reyes C, Rawat M, McKee J, Lemon D, Hanson J, Ma TY. Intestinal barrier dysfunction in human necrotizing enterocolitis. *J. Pediatr. Surg.* 2016;51:1907-1913.
173. Bein A, Eventov-Friedman S, Arbell D, Schwartz B. Intestinal tight junctions are severely altered in NEC preterm neonates. *Pediatr. Neonatol.* 2018;59:464-473.
174. Ares G, Buonpane C, Sincavage J, Yuan C, Wood DR, Hunter CJ. Caveolin 1 is Associated with Upregulated Claudin 2 in Necrotizing Enterocolitis. *Sci. Rep.* 2019;9:4982.
175. Wei J, Zhou Y, Besner GE. Heparin-binding EGF-like growth factor and enteric neural stem cell transplantation in the prevention of experimental necrotizing enterocolitis in mice. *Pediatr. Res.* 2015;78:29-37.
176. Chen CL, Yu X, James IO, Zhang HY, Yang J, Radulescu A, Zhou Y, Besner GE. Heparin-binding EGF-like growth factor protects intestinal stem cells from injury in a rat model of necrotizing enterocolitis. *Lab. Invest.* 2012;92:331-344.
177. Nair J, Lakshminrusimha S. Role of NO and other vascular mediators in the etiopathogenesis of necrotizing enterocolitis. *Front. Biosci.* 2019;11:9-28.
178. Murdoch EM, Sinha AK, Shanmugalingam ST, Smith GC, Kempley ST. Doppler flow velocimetry in the superior mesenteric artery on the first day of life in preterm infants and the risk of neonatal necrotizing enterocolitis. *Pediatrics* 2006;118:1999-2003.
179. Nowicki PT, Caniano DA, Hammond S, Giannone PJ, Besner GE, Reber KM, Nankervis CA. Endothelial nitric oxide synthase in human intestine resected for necrotizing enterocolitis. *J. Pediatr.* 2007;150:40-45.
180. Grishin A, Bowling J, Bell B, Wang J, Ford HR. Roles of nitric oxide and intestinal microbiota in the pathogenesis of necrotizing enterocolitis. *J. Pediatr. Surg.* 2016;51:13-17.
181. Ford H, Watkins S, Reblock K, Rowe M. The role of inflammatory cytokines and nitric oxide in the pathogenesis of necrotizing enterocolitis. *J. Pediatr. Surg.* 1997;32:275-282.
182. Nowicki PT, Reber KM, Giannone PJ, Nankervis CA, Hammond S, Besner GE, Caniano DA. Intestinal O₂ Consumption in Necrotizing Enterocolitis: Role of Nitric Oxide. *Pediatr. Res.* 2006;59:500-505.
183. Upperman JS, Potoka D, Grishin A, Hackam D, Zamora R, Ford HR. Mechanisms of nitric oxide-mediated intestinal barrier failure in necrotizing enterocolitis. *Semin. Pediatr. Surg.* 2005;14:159-166.
184. Nowicki PT, Dunaway DJ, Nankervis CA, Giannone PJ, Reber KM, Hammond SB, Besner GE, Caniano DA. Endothelin-1 in human intestine resected for necrotizing enterocolitis. *J. Pediatr.* 2005;146:805-810.
185. Günther C, Neumann H, Neurath MF, Becker C. Apoptosis, necrosis and necroptosis: Cell death regulation in the intestinal epithelium. *Gut* 2013;62:1062-1071.
186. Werts AD, Fulton WB, Ladd MR, Saad-Eldin A, Chen YX, Kovler ML, Jia H, Banfield EC, Buck R, Goerhing K, et al. A Novel Role for Necroptosis in the Pathogenesis of Necrotizing Enterocolitis. *Cell. Mol. Gastroenterol. Hepatol.* 2020;9(3):403-423.
187. Ates U, Gollu G, Kucuk G, Billur D, Bingol-Kologlu M, Yilmaz Y, Ozkan-Ulu H, Bayram P, Bagriacik E, Dindar H. Increase in pro-apoptotic Bax expression and decrease in anti-apoptotic Bcl-2 expression in newborns with necrotizing enterocolitis. *Arch. Argent. Pediatr.* 2016;114:243-247.
188. Neal MD, Sodhi CP, Dyer M, Craig BT, Good M, Jia H, Yazji I, Afrazi A, Richardson WM, Beer-Stolz D, et al. A critical role for TLR4 induction of autophagy in the regulation of enterocyte migration and the pathogenesis of necrotizing enterocolitis. *J. Immunol.* 2013;190:3541-3551.
189. Haq S, Grondin J, Banskota S, Khan WI. Autophagy: Roles in intestinal mucosal homeostasis and inflammation. *J. Biomed. Sci.* 2019;26:19.
190. Lu P, Struijs MC, Mei J, Witte-Bouma J, Korteland-van Male AM, de Bruijn AC, van Goudoever JB, Renes IB. Endoplasmic reticulum stress, unfolded protein response and altered T cell differentiation in necrotizing enterocolitis. *PLoS One* 2013;8:e78491.
191. Afrazi A, Branca MF, Sodhi CP, Good M, Yamaguchi Y, Egan CE, Lu P, Jia H, Shaffiey S, Lin J, et al. Toll-like receptor 4-mediated endoplasmic reticulum stress in intestinal crypts induces necrotizing enterocolitis. *J. Biol. Chem.* 2014;289:9584-9599.

192. Vieten D, Corfield A, Ramani P, Spicer R. Proliferative response in necrotising enterocolitis is insufficient to prevent disease progression. *Pediatr. Surg. Int.* 2006;22:50–56.
193. Clark JA, Lane RH, MacLennan NK, Holubec H, Dvorakova K, Halpern MD, Williams CS, Payne CM, Dvorak B. Epidermal growth factor reduces intestinal apoptosis in an experimental model of necrotizing enterocolitis. *Am. J. Physiol. Gastrointest. Liver Physiol.* 2005;288:G755–G762.
194. Yu Y, Shiou SR, Guo Y, Lu L, Westerhoff M, Sun J, Petrof EO, Claud EC. Erythropoietin protects epithelial cells from excessive autophagy and apoptosis in experimental neonatal necrotizing enterocolitis. *PLoS One* 2013;8:e69620.
195. Fundora JB, Guha P, Shores DR, Pammi M, Maheshwari A. Intestinal dysbiosis and necrotizing enterocolitis: Assessment for causality using Bradford Hill criteria. *Pediatr. Res.* 2020;87(2):235–248.
196. Pammi M, Cope J, Tarr PI, Warner BB, Morrow AL, Mai V, Gregory KE, Kroll JS, McMurtry V, Ferris MJ, et al. Intestinal dysbiosis in preterm infants preceding necrotizing enterocolitis: A systematic review and meta-analysis. *Microbiome* 2017;5:31.
197. Olm MR, Bhattacharya N, Crits-Christoph A, Firek BA, Baker R, Song YS, Morowitz MJ, Banfield JF. Necrotizing enterocolitis is preceded by increased gut bacterial replication, Klebsiella, and fimbriae-encoding bacteria. *Sci. Adv.* 2019;5:eaax5727.
198. Stinson LF, Boyce MC, Payne MS, Keelan JA. The Not-so-Sterile Womb: Evidence That the Human Fetus Is Exposed to Bacteria Prior to Birth. *Front. Microbiol.* 2019;10:1124–1124.
199. Westerbeek EA, van den Berg A, Lafeber HN, Knol J, Fetter WP, van Elburg RM. The intestinal bacterial colonisation in preterm infants: A review of the literature. *Clin. Nutr.* 2006;25:361–368.
200. Penders J, Thijs C, Vink C, Stelma FF, Snijders B, Kummeling I, van den Brandt PA, Stobberingh EE. Factors influencing the composition of the intestinal microbiota in early infancy. *Pediatrics* 2006;118:511–521.
201. Niemarkt HJ, De Meij TG, van Ganzewinkel CJ, de Boer NKH, Andriessen P, Hütten MC, Kramer BW. Necrotizing Enterocolitis, Gut Microbiota, and Brain Development: Role of the Brain-Gut Axis. *Neonatology* 2019;115:423–431.
202. Rudloff S, Kuntz S, Ostenfeldt Rasmussen S, Roggenbuck M, Sprenger N, Kunz C, Sangild PT, Brandt Bering S. Metabolism of Milk Oligosaccharides in Preterm Pigs Sensitive to Necrotizing Enterocolitis. *Front. Nutr.* 2019;6:23.
203. Heyman MB. Lactose intolerance in infants, children, and adolescents. *Pediatrics* 2006;118:1279–1286.
204. Book LS, Herbst JJ, Jung AL. Carbohydrate malabsorption in necrotizing enterocolitis. *Pediatrics* 1976;57:201–204.
205. Misselwitz B, Butter M, Verbeke K, Fox MR. Update on lactose malabsorption and intolerance: Pathogenesis, diagnosis and clinical management. *Gut* 2019;68:2080–2091.
206. Kien CL. Colonic fermentation of carbohydrate in the premature infant: Possible relevance to necrotizing enterocolitis. *J. Pediatr.* 1990;117:S52–S58.
207. Thymann T, Moller HK, Stoll B, Stoy AC, Buddington RK, Bering SB, Jensen BB, Olutoye OO, Siggers RH, Molbak L, et al. Carbohydrate maldigestion induces necrotizing enterocolitis in preterm pigs. *Am. J. Physiol. Gastrointest. Liver Physiol.* 2009;297:G1115–G1125.
208. Sangild PT. Gut responses to enteral nutrition in preterm infants and animals. *Exp. Biol. Med.* 2006;231:1695–1711.
209. Buddington RK, Sangild PT, Hance B, Huang EY, Black DD. Prenatal gastrointestinal development in the pig and responses after preterm birth. *J. Anim. Sci.* 2012;90:290–298.
210. Kulkarni S, Ganz J, Bayrer J, Becker L, Bogunovic M, Rao M. Advances in Enteric Neurobiology: The “Brain” in the Gut in Health and Disease. *J. Neurosci.* 2018;38:9346–9354.
211. Goyal RK, Hirano I. The enteric nervous system. *N. Engl. J. Med.* 1996;334:1106–1115.
212. Yoo BB, Mazmanian SK. The Enteric Network: Interactions between the Immune and Nervous Systems of the Gut. *Immunity* 2017;46:910–926.
213. Vergnolle N, Cirillo C. Neurons and Glia in the Enteric Nervous System and Epithelial Barrier Function. *Physiol. (Bethesda)* 2018;33:269–280.
214. Wedel T, Krammer HJ, Kuhnel W, Sigge W. Alterations of the enteric nervous system in neonatal necrotizing enterocolitis revealed by whole-mount immunohistochemistry. *Pediatr. Pathol. Lab. Med.* 1998;18:57–70.

215. Sigge W, Wedel T, Kuhnel W, Krammer HJ. Morphologic alterations of the enteric nervous system and deficiency of non-adrenergic non-cholinergic inhibitory innervation in neonatal necrotizing enterocolitis. *Eur. J. Pediatr. Surg.* 1998;8:87–94.
216. Zhou Y, Yang J, Watkins DJ, Boomer LA, Matthews MA, Su Y, Besner GE. Enteric nervous system abnormalities are present in human necrotizing enterocolitis: Potential neurotransplantation therapy. *Stem Cell. Res.* 2013;4:157.
217. Fagbemi AO, Torrente F, Puleston J, Lakhoo K, James S, Murch SH. Enteric neural disruption in necrotizing enterocolitis occurs in association with myenteric glial cell CCL20 expression. *J. Pediatr. Gastroenterol. Nutr.* 2013;57:788–793.
218. Bush TG. Enteric glial cells. An upstream target for induction of necrotizing enterocolitis and Crohn's disease? *Bioessays* 2002;24:130–140.
219. Chen W, Sun J, Kappel SS, Gormsen M, Sangild PT, Aunsholt L. Gut transit time, using radiological contrast imaging, to predict early signs of necrotizing enterocolitis. *Pediatr. Res.* 2021;89(1):127–133.
220. Latorre R, Sternini C, De Giorgio R, Greenwood-Van Meerveld B. Enteroendocrine cells: A review of their role in brain-gut communication. *Neurogastroenterol. Motil.* 2016;28:620–630.
221. Hodzic Z, Bolock AM, Good M. The Role of Mucosal Immunity in the Pathogenesis of Necrotizing Enterocolitis. *Front. Pediatrics* 2017;5:40.
222. Zhou Y, Wang Y, Olson J, Yang J, Besner GE. Heparin-binding EGF-like growth factor promotes neuronal nitric oxide synthase expression and protects the enteric nervous system after necrotizing enterocolitis. *Pediatr. Res.* 2017;82:490–500.
223. Zhang P, Lavoie PM, Lacaze-Masmonteil T, Rhahids M, Marc I. Omega-3 long-chain polyunsaturated fatty acids for extremely preterm infants: A systematic review. *Pediatrics* 2014; 134:120–134.
224. Collins CT, Makrides M, McPhee AJ, Sullivan TR, Davis PG, Thio M, Simmer K, Rajadurai VS, Travadi J, Berry MJ, et al. Docosahexaenoic Acid and Bronchopulmonary Dysplasia in Preterm Infants. *N. Engl. J. Med.* 2017;376:1245–1255.
225. Chi C, Buys N, Li C, Sun J, Yin C. Effects of prebiotics on sepsis, necrotizing enterocolitis, mortality, feeding intolerance, time to full enteral feeding, length of hospital stay, and stool frequency in preterm infants: A meta-analysis. *Eur. J. Clin. Nutr.* 2019;73:657–670.
226. Pammi M, Suresh G. Enteral lactoferrin supplementation for prevention of sepsis and necrotizing enterocolitis in preterm infants. *Cochrane Database Syst. Rev.* 2020;3:Cd007137.
227. Shah PS, Shah VS, Kelly LE. Arginine supplementation for prevention of necrotising enterocolitis in preterm infants. *Cochrane Database Syst. Rev.* 2017;4:Cd004339.
228. Moe-Byrne T, Brown JV, McGuire W. Glutamine supplementation to prevent morbidity and mortality in preterm infants. *Cochrane Database Syst. Rev.* 2016;4:Cd001457.
229. Foster JP, Seth R, Cole MJ. Oral immunoglobulin for preventing necrotizing enterocolitis in preterm and low birth weight neonates. *Cochrane Database Syst. Rev.* 2016;4:Cd001816.
230. Ananthan A, Balasubramanian H, Rao S, Patole S. Clinical Outcomes Related to the Gastrointestinal Trophic Effects of Erythropoietin in Preterm Neonates: A Systematic Review and Meta-Analysis. *Adv. Nutr.* 2018;9:238–246.
231. Hosseini M, Azampour H, Raeesi S, Behtari M, Valizadeh H, Saboohi R. The effects of enteral artificial amniotic fluid-containing erythropoietin on short term outcomes of preterm infants. *Turk. J. Pediatr.* 2019;61:392–398.
232. Omar OM, Massoud MN, Ghazal H, Hassouna H, Soma MF. Effect of enteral erythropoietin on feeding-related complications in preterm newborns: A pilot randomized controlled study. *Arab J. Gastroenterol.* 2020;21:37–42.
233. El-Ganzoury MM, Awad HA, El-Farrash RA, El-Gammasy TM, Ismail EA, Mohamed HE, Suliman SM. Enteral granulocyte-colony stimulating factor and erythropoietin early in life improves feeding tolerance in preterm infants: A randomized controlled trial. *J. Pediatr.* 2014;165:1140–1145.e1141.
234. Wardle SP, Hughes A, Chen S, Shaw NJ. Randomised controlled trial of oral vitamin A supplementation in preterm infants to prevent chronic lung disease. *Arch. Dis. Child. Fetal Neonatal Ed.* 2001;84:F9–F13.
235. Sun H, Cheng R, Wang Z. Early Vitamin A supplementation improves the outcome of retinopathy of prematurity in extremely preterm infants. *Retina* 2020;40:1176–1184.

236. Gray KD, Messina JA, Cortina C, Owens T, Fowler M, Foster M, Gbadegesin S, Clark RH, Benjamin DK Jr, Zimmerman KO, et al. Probiotic Use and Safety in the Neonatal Intensive Care Unit: A Matched Cohort Study. *J. Pediatr.* 2020;222:59-64.e1.
237. Xiong T, Maheshwari A, Neu J, Ei-Saie A, Pammi M. An Overview of Systematic Reviews of Randomized-Controlled Trials for Preventing Necrotizing Enterocolitis in Preterm Infants. *Neonatology* 2020;117(1):46-56.
238. Morgan RL, Preidis GA, Kashyap PC, Weizman AV, Sadeghirad B, Chang Y, Florez ID, Foroutan F, Shahid S, Zeraatkar D. Probiotics Reduce Mortality and Morbidity in Preterm, Low Birth Weight Infants: A Systematic Review and Network Meta-analysis of Randomized Trials. *Gastroenterology* 2020;159(2):467-480.
239. van den Akker CHP, van Goudoever JB, Szajewska H, Embleton ND, Hojsak I, Reid D, Shamir R. Probiotics for Preterm Infants: A Strain-Specific Systematic Review and Network Meta-analysis. *J. Pediatr. Gastroenterol. Nutr.* 2018;67:103-122.
240. van den Akker CHP, van Goudoever JB, Shamir R, Domellöf M, Embleton ND, Hojsak I, Lapillonne A, Mihatsch WA, Canani RB, Bronsky J, et al. Probiotics and Preterm Infants: A Position Paper by the ESPGHAN Committee on Nutrition and the ESPGHAN Working Group for Probiotics and Prebiotics. *J. Pediatr. Gastroenterol. Nutr.* 2020.
241. Manzoni P, Guardione R, Bonetti P, Priolo C, Maestri A, Mansoldo C, Mostert M, Anselmetti G, Sardei D, Bellettato M, et al. Lutein and zeaxanthin supplementation in preterm very low-birth-weight neonates in neonatal intensive care units: A multicenter randomized controlled trial. *Am. J. Perinatol.* 2013;30:25-32.
242. Serce Pehlevan O, Benzer D, Gursoy T, Karatekin G, Ovali F. Synbiotics use for preventing sepsis and necrotizing enterocolitis in very low birth weight neonates: A randomized controlled trial. *Clin. Exp. Pediatrics* 2020;63:226-231.
243. Indrio F, Riezzo G, Raimondi F, Bisceglia M, Cavallo L, Francavilla R. Effects of probiotic and prebiotic on gastrointestinal motility in newborns. *J. Physiol. Pharm.* 2009;60:27-31.
244. Mihatsch WA, Hoegel J, Pohlandt F. Prebiotic oligosaccharides reduce stool viscosity and accelerate gastrointestinal transport in preterm infants. *Acta Paediatr.* 2006;95:843-848.
245. Westerbeek EAM, Mørch E, Lafeber HN, Fetter WPF, Twisk JWR, Van Elburg RM. Effect of neutral and acidic oligosaccharides on fecal IL-8 and fecal calprotectin in preterm infants. *Pediatr. Res.* 2011;69:255-258.
246. Akin IM, Atasay B, Dogu F, Okulu E, Arsan S, Karatas HD, Ikinciogullari A, Turmen T. Oral lactoferrin to prevent nosocomial sepsis and necrotizing enterocolitis of premature neonates and effect on T-regulatory cells. *Am. J. Perinatol.* 2014;31:1111-1120.
247. Sevastiadou S, Malamitsi-Puchner A, Costalos C, Skouroliakou M, Briana DD, Antsaklis A, Roma-Giannikou E. The impact of oral glutamine supplementation on the intestinal permeability and incidence of necrotizing enterocolitis/septicemia in premature neonates. *J. Matern. Fetal Neonatal Med.* 2011;24:1294-1300.
248. Stratiki Z, Costalos C, Sevastiadou S, Kastanidou O, Skouroliakou M, Giakoumatou A, Petrohilou V. The effect of a bifidobacter supplemented bovine milk on intestinal permeability of preterm infants. *Early Hum. Dev.* 2007;83:575-579.
249. Serce Pehlevan O, Benzer D, Gursoy T, Aktas Cetin E, Karatekin G, Ovali MF. Cytokine responses to symbiotic and lactoferrin combination in very low birth weight neonates: A randomized control trial. *Arch. Argent. Pediatr.* 2020;118:e8-e15.
250. Nolan LS, Parks OB, Good M. A Review of the Immunomodulating Components of Maternal Breast Milk and Protection Against Necrotizing Enterocolitis. *Nutrients* 2019;12(1):14.
251. Manzoni P, Meyer M, Stolfi I, Rinaldi M, Cattani S, Pagni L, Romeo MG, Messner H, Decembrino L, Laforgia N, et al. Bovine lactoferrin supplementation for prevention of necrotizing enterocolitis in very-low-birth-weight neonates: A randomized clinical trial. *Early Hum. Dev.* 2014;90:S60-S65.
252. Gephart SM, Underwood MA, Rosito S, Kim JH, Caplan MS. Grading the evidence to identify strategies to modify risk for necrotizing enterocolitis. *Pediatr. Res.* 2020;88:41-47.
253. Ellis ZM, Tan HSG, Embleton ND, Sangild PT, van Elburg RM. Milk feed osmolality and adverse events in newborn infants and animals: A systematic review. *Arch. Dis. Child. Fetal Neonatal Ed.* 2019;104:F333.

254. ter Riet G, Korevaar DA, Leenaars M, Sterk PJ, Van Noorden CJ, Bouter LM, Lutter R, Elferink RP, Hooft L. Publication bias in laboratory animal research: A survey on magnitude, drivers, consequences and potential solutions. *Plos One* 2012;7:e43404.
255. van der Naald M, Wenker S, Doevendans PA, Wever KE, Chamuleau SAJ. Publication rate in preclinical research: A plea for preregistration. *Bmj Open Sci.* 2020;4:e100051.
256. Kilkenny C, Parsons N, Kadyszewski E, Festing MFW, Cuthill IC, Fry D, Hutton J, Altman DG. Survey of the quality of experimental design, statistical analysis and reporting of research using animals. *Plos One* 2009;4:e7824–e7824.
257. Sodhi C, Richardson W, Gribar S, Hackam DJ. The development of animal models for the study of necrotizing enterocolitis. *Dis. Model. Mech.* 2008;1:94–98.
258. Klinke M, Vincent D, Trochimiuk M, Appl B, Tiemann B, Reinshagen K, Pagerols Raluy L, Boettcher M. Development of an improved murine model of necrotizing enterocolitis shows the importance of neutrophils in NEC pathogenesis. *Sci. Rep.* 2020;10:8049.
259. Lu P, Sodhi CP, Jia H, Shaffiey S, Good M, Branca MF, Hackam DJ. Animal models of gastrointestinal and liver diseases. Animal models of necrotizing enterocolitis: Pathophysiology, translational relevance, and challenges. *Am. J. Physiol. Gastrointest. Liver Physiol.* 2014;306:G917–G928.
260. Kovler ML, Sodhi CP, Hackam DJ. Precision-based modeling approaches for necrotizing enterocolitis. *Dis. Model. Mech.* 2020;13(6):dmm044388.
261. Neu J. Necrotizing Enterocolitis: The Future. *Neonatology* 2020;117(2):240-244.
262. Neu J, Modi N, Caplan M. Necrotizing enterocolitis comes in different forms: Historical perspectives and defining the disease. *Semin. Fetal Neonatal Med.* 2018;23:370–373.
263. Senge, S, Ingano L, Freire R, Anselmo A, Zhu W, Sadreyev R, Walker WA, Fasano A. Human Fetal-Derived Enterospheres Provide Insights on Intestinal Development and a Novel Model to Study Necrotizing Enterocolitis (NEC). *Cell. Mol. Gastroenterol. Hepatol.* 2018;5:549–568.
264. Ashammakhi N, Nasiri R, Barros NR.d, Tebon P, Thakor J, Goudie M, Shamloo A, Martin MG, Khademhosseini A. Gut-on-a-chip: Current progress and future opportunities. *Biomaterials* 2020; 255:120196.

Supplemental materials

Table S2.1 Pubmed search.

Search title	Search terms used in Pubmed
general feeding interventions	((("feeding"[All Fields] OR "feedings"[All Fields] OR "feeds"[All Fields]) AND ("intervention s"[All Fields] OR "interventions"[All Fields] OR "interventive"[All Fields] OR "methods"[MeSH Terms] OR "methods"[All Fields] OR "intervention"[All Fields] OR "interventional"[All Fields])) OR ("nutrition s"[All Fields] OR "nutritional status"[MeSH Terms] OR ("nutritional"[All Fields] AND "status"[All Fields]) OR "nutritional status"[All Fields] OR "nutrition"[All Fields] OR "nutritional sciences"[MeSH Terms] OR ("nutritional"[All Fields] AND "sciences"[All Fields]) OR "nutritional sciences"[All Fields] OR "nutritional"[All Fields] OR "nutritionals"[All Fields] OR "nutritions"[All Fields] OR "nutritive"[All Fields]) AND ("intervention s"[All Fields] OR "interventions"[All Fields] OR "interventive"[All Fields] OR "methods"[MeSH Terms] OR "methods"[All Fields] OR "intervention"[All Fields] OR "interventional"[All Fields])) OR ("feeding"[All Fields] OR "feedings"[All Fields] OR "feeds"[All Fields]) OR ("nutrition s"[All Fields] OR "nutritional status"[MeSH Terms] OR ("nutritional"[All Fields] AND "status"[All Fields]) OR "nutritional status"[All Fields] OR "nutrition"[All Fields] OR "nutritional sciences"[MeSH Terms] OR ("nutritional"[All Fields] AND "sciences"[All Fields]) OR "nutritional sciences"[All Fields] OR "nutritional"[All Fields] OR "nutritionals"[All Fields] OR "nutritions"[All Fields] OR "nutritive"[All Fields]) AND ("necrotising enterocolitis"[All Fields] OR "enterocolitis, necrotizing"[MeSH Terms] OR ("enterocolitis"[All Fields] AND "necrotizing"[All Fields]) OR "necrotizing enterocolitis"[All Fields] OR ("necrotizing"[All Fields] AND "enterocolitis"[All Fields]) OR "NEC"[All Fields])
alkaline phosphatase	("alkaline phosphatase"[MeSH Terms] OR ("alkaline"[All Fields] AND "phosphatase"[All Fields]) OR "alkaline phosphatase"[All Fields] OR "ALP"[All Fields]) AND ("necrotising enterocolitis"[All Fields] OR "enterocolitis, necrotizing"[MeSH Terms] OR ("enterocolitis"[All Fields] AND "necrotizing"[All Fields]) OR "necrotizing enterocolitis"[All Fields] OR ("necrotizing"[All Fields] AND "enterocolitis"[All Fields]) OR "NEC"[All Fields])
epidermal growth factor heparin-binding EGF like growth factor	("EGF"[All Fields] OR ("epidermal growth factor"[MeSH Terms] OR ("epidermal"[All Fields] AND "growth"[All Fields] AND "factor"[All Fields]) OR "epidermal growth factor"[All Fields]) OR ("heparin binding egf like growth factor"[MeSH Terms] OR ("heparin binding"[All Fields] AND "egf like"[All Fields] AND "growth"[All Fields] AND "factor"[All Fields]) OR "heparin binding egf like growth factor"[All Fields] OR ("hb"[All Fields] AND "EGF"[All Fields]) OR "hb egf"[All Fields]) OR ("heparin binding egf like growth factor"[MeSH Terms] OR ("heparin binding"[All Fields] AND "egf like"[All Fields] AND "growth"[All Fields] AND "factor"[All Fields]) OR "heparin binding egf like growth factor"[All Fields] OR ("heparin"[All Fields] AND "binding"[All Fields] AND "EGF"[All Fields] AND "like"[All Fields] AND "growth"[All Fields] AND "factor"[All Fields]) OR "heparin binding egf like growth factor"[All Fields])) AND ("necrotising enterocolitis"[All Fields] OR "enterocolitis, necrotizing"[MeSH Terms] OR ("enterocolitis"[All Fields] AND "necrotizing"[All Fields]) OR "necrotizing enterocolitis"[All Fields] OR ("necrotizing"[All Fields] AND "enterocolitis"[All Fields]) OR "NEC"[All Fields])
erythropoietin	("erythropoietin"[MeSH Terms] OR "erythropoietin"[All Fields] OR "epoetin alfa"[MeSH Terms] OR ("epoetin"[All Fields] AND "alfa"[All Fields]) OR "epoetin alfa"[All Fields] OR "erythropoietins"[All Fields] OR "erythropoietin s"[All Fields] OR "EPO"[All Fields]) AND ("necrotising enterocolitis"[All Fields] OR "enterocolitis, necrotizing"[MeSH Terms] OR ("enterocolitis"[All Fields] AND "necrotizing"[All Fields]) OR "necrotizing enterocolitis"[All Fields] OR ("necrotizing"[All Fields] AND "enterocolitis"[All Fields]) OR "NEC"[All Fields])

Table S2.1 (continued)

exosomes	("exosomal"[All Fields] OR "exosomes"[MeSH Terms] OR "exosomes"[All Fields] OR "exosome"[All Fields] OR "exosomic"[All Fields] OR ("extracellular vesicles"[MeSH Terms] OR "extracellular"[All Fields] AND "vesicles"[All Fields]) OR "extracellular vesicles"[All Fields]) OR ("cell derived microparticles"[MeSH Terms] OR ("cell derived"[All Fields] AND "microparticles"[All Fields]) OR "cell derived microparticles"[All Fields] OR "microvesicle"[All Fields] OR "microvesicles"[All Fields])) AND ("necrotising enterocolitis"[All Fields] OR "enterocolitis, necrotizing"[MeSH Terms] OR ("enterocolitis"[All Fields] AND "necrotizing"[All Fields]) OR "necrotizing enterocolitis"[All Fields] OR ("necrotizing"[All Fields] AND "enterocolitis"[All Fields]) OR "NEC"[All Fields])
ganglioside	("gangliosides"[MeSH Terms] OR "gangliosides"[All Fields] OR "ganglioside"[All Fields] OR "gangliosidic"[All Fields] OR "GD3"[All Fields] OR "GM"[All Fields]) AND ("necrotising enterocolitis"[All Fields] OR "enterocolitis, necrotizing"[MeSH Terms] OR ("enterocolitis"[All Fields] AND "necrotizing"[All Fields]) OR "necrotizing enterocolitis"[All Fields] OR ("necrotizing"[All Fields] AND "enterocolitis"[All Fields]) OR "NEC"[All Fields])
glutamine	("Gln"[All Fields] OR ("glutamine"[MeSH Terms] OR "glutamine"[All Fields] OR "l glutamine"[All Fields]) OR ("glutamin"[All Fields] OR "glutamine"[MeSH Terms] OR "glutamine"[All Fields] OR "glutamine s"[All Fields] OR "glutamines"[All Fields])) AND ("necrotising enterocolitis"[All Fields] OR "enterocolitis, necrotizing"[MeSH Terms] OR ("enterocolitis"[All Fields] AND "necrotizing"[All Fields]) OR "necrotizing enterocolitis"[All Fields] OR ("necrotizing"[All Fields] AND "enterocolitis"[All Fields]) OR "NEC"[All Fields])
immunoglobulins	("immunoglobulin s"[All Fields] OR "immunoglobuline"[All Fields] OR "immunoglobulines"[All Fields] OR "immunoglobulins"[MeSH Terms] OR "immunoglobulins"[All Fields] OR "immunoglobulin"[All Fields] OR ("immunoglobulin g"[MeSH Terms] OR "immunoglobulin g"[All Fields] OR "igg"[All Fields]) OR ("immunoglobulin a"[MeSH Terms] OR "immunoglobulin a"[All Fields] OR "iga"[All Fields])) AND ("necrotising enterocolitis"[All Fields] OR "enterocolitis, necrotizing"[MeSH Terms] OR ("enterocolitis"[All Fields] AND "necrotizing"[All Fields]) OR "necrotizing enterocolitis"[All Fields] OR ("necrotizing"[All Fields] AND "enterocolitis"[All Fields]) OR "NEC"[All Fields])
insulin like growth factor	("somatomedins"[MeSH Terms] OR "somatomedins"[All Fields] OR ("insulin"[All Fields] AND "like"[All Fields] AND "growth"[All Fields] AND "factor"[All Fields]) OR "insulin like growth factor"[All Fields] OR "ILGF1"[All Fields] OR "IGF1"[All Fields]) AND ("necrotising enterocolitis"[All Fields] OR "enterocolitis, necrotizing"[MeSH Terms] OR ("enterocolitis"[All Fields] AND "necrotizing"[All Fields]) OR "necrotizing enterocolitis"[All Fields] OR ("necrotizing"[All Fields] AND "enterocolitis"[All Fields]) OR "NEC"[All Fields])
milk fat globule membrane	((("milk fat globule"[Supplementary Concept] OR "milk fat globule"[All Fields]) AND "membranal"[All Fields] OR "membrane s"[All Fields] OR "membraneous"[All Fields] OR "membranes"[MeSH Terms] OR "membranes"[All Fields] OR "membrane"[All Fields] OR "membranous"[All Fields])) OR ("milk fat globule"[Supplementary Concept] OR "milk fat globule"[All Fields]) AND ("necrotising enterocolitis"[All Fields] OR "enterocolitis, necrotizing"[MeSH Terms] OR ("enterocolitis"[All Fields] AND "necrotizing"[All Fields]) OR "necrotizing enterocolitis"[All Fields] OR ("necrotizing"[All Fields] AND "enterocolitis"[All Fields]) OR "NEC"[All Fields])

Table S2.1 (continued)

Search title	Search terms used in Pubmed
oligosaccharides	("gos"[All Fields] OR "FOS"[All Fields] OR ("oligosaccharides"[MeSH Terms] OR "oligosaccharides"[All Fields] OR "oligosaccharide"[All Fields] OR "oligosaccharidic"[All Fields]) AND ("necrotising enterocolitis"[All Fields] OR "enterocolitis, necrotizing"[MeSH Terms] OR "enterocolitis"[All Fields] AND "necrotizing"[All Fields]) OR "necrotizing enterocolitis"[All Fields] OR ("necrotizing"[All Fields] AND "enterocolitis"[All Fields]) OR "NEC"[All Fields])
osteopontin	("osteopontin"[MeSH Terms] OR "osteopontin"[All Fields] OR "osteopontine"[All Fields] OR "osteopontins"[All Fields] OR ("opt photonics news"[Journal] OR "opn"[All Fields])) AND ("necrotising enterocolitis"[All Fields] OR "enterocolitis, necrotizing"[MeSH Terms] OR "enterocolitis"[All Fields] AND "necrotizing"[All Fields]) OR "necrotizing enterocolitis"[All Fields] OR ("necrotizing"[All Fields] AND "enterocolitis"[All Fields]) OR "NEC"[All Fields])
platelet-activating factor acetylhydrolase	("PAF-AH"[All Fields] OR ("platelet activating factor"[MeSH Terms] OR ("platelet"[All Fields] AND "activating"[All Fields] AND "factor"[All Fields]) OR "platelet activating factor"[All Fields]) AND ("acetylhydrolase"[All Fields] OR "acetylhydrolases"[All Fields])) AND ("necrotising enterocolitis"[All Fields] OR "enterocolitis, necrotizing"[MeSH Terms] OR "enterocolitis"[All Fields] AND "necrotizing"[All Fields]) OR "necrotizing enterocolitis"[All Fields] OR ("necrotizing"[All Fields] AND "enterocolitis"[All Fields]) OR "NEC"[All Fields])
polyunsaturated fatty acid	("PUFA"[All Fields] OR ("fatty acids, unsaturated"[MeSH Terms] OR ("fatty"[All Fields] AND "acids"[All Fields] AND "unsaturated"[All Fields]) OR "unsaturated fatty acids"[All Fields] OR ("polyunsaturated"[All Fields] AND "fatty"[All Fields] AND "acid"[All Fields]) OR "polyunsaturated fatty acid"[All Fields]) OR ("fatty acids, omega 3"[MeSH Terms] OR "fatty"[All Fields] AND "acids"[All Fields] AND "omega 3"[All Fields]) OR "omega-3 fatty acids"[All Fields] OR "omega 3 fatty acids"[All Fields]) OR ("fatty acids, omega 6"[MeSH Terms] OR "fatty"[All Fields] AND "acids"[All Fields] AND "omega 6"[All Fields]) OR "omega-6 fatty acids"[All Fields] OR "omega 6 fatty acids"[All Fields]) OR ("long"[All Fields] AND "chain"[All Fields] OR "chain s"[All Fields] OR "chains"[All Fields]) AND ("fatty acids"[MeSH Terms] OR "fatty"[All Fields] AND "acids"[All Fields]) OR "fatty acids"[All Fields])) AND ("necrotising enterocolitis"[All Fields] OR "enterocolitis, necrotizing"[MeSH Terms] OR "enterocolitis"[All Fields] AND "necrotizing"[All Fields]) OR "necrotizing enterocolitis"[All Fields] OR ("necrotizing"[All Fields] AND "enterocolitis"[All Fields]) OR "NEC"[All Fields])
transforming growth factor β	("transforming growth factor beta"[MeSH Terms] OR ("transforming"[All Fields] AND "growth"[All Fields] AND "factor"[All Fields] AND "beta"[All Fields]) OR "transforming growth factor beta"[All Fields] OR "tgfbeta1"[All Fields] OR ("tgfbeta s"[All Fields] OR "tgfbetas"[All Fields] OR "transforming growth factor beta"[MeSH Terms] OR ("transforming"[All Fields] AND "growth"[All Fields] AND "factor"[All Fields] AND "beta"[All Fields]) OR "transforming growth factor beta"[All Fields] OR "tgfbeta"[All Fields])) AND ("necrotising enterocolitis"[All Fields] OR "enterocolitis, necrotizing"[MeSH Terms] OR "enterocolitis"[All Fields] AND "necrotizing"[All Fields]) OR "necrotizing enterocolitis"[All Fields] OR ("necrotizing"[All Fields] AND "enterocolitis"[All Fields]) OR "NEC"[All Fields])
vitamin A	("vitamin a"[MeSH Terms] OR "vitamin a"[All Fields] OR ("tretinoin"[MeSH Terms] OR "tretinoin"[All Fields] OR ("trans"[All Fields] AND "retinoic"[All Fields] AND "acid"[All Fields]) OR "all trans retinoic acid"[All Fields]) OR ("vitamin a"[MeSH Terms] OR "vitamin a"[All Fields] OR "retinol"[All Fields] OR "retinols"[All Fields] OR "retinoida"[All Fields] OR "retinoids"[MeSH Terms] OR "retinoids"[All Fields] OR "retinoid"[All Fields])) AND ("necrotising enterocolitis"[All Fields] OR "enterocolitis, necrotizing"[MeSH Terms] OR "enterocolitis"[All Fields] AND "necrotizing"[All Fields]) OR "necrotizing enterocolitis"[All Fields] OR ("necrotizing"[All Fields] AND "enterocolitis"[All Fields]) OR "NEC"[All Fields])

Table S2.1 (continued)

vitamin D	("vitamin d"[MeSH Terms] OR "vitamin d"[All Fields] OR "ergocalciferols"[MeSH Terms] OR "ergocalciferols"[All Fields] OR ("cholecalciferol"[MeSH Terms] OR "cholecalciferol"[All Fields] OR "cholecalciferols"[All Fields] OR "colecalfiferol"[All Fields]) OR ("ergocalciferols"[MeSH Terms] OR "ergocalciferols"[All Fields] OR "ergocalciferol"[All Fields]) OR "D2"[All Fields] OR "D3"[All Fields]) AND ("necrotising enterocolitis"[All Fields] OR "enterocolitis, necrotizing"[MeSH Terms] OR ("enterocolitis"[All Fields] AND "necrotizing"[All Fields]) OR "necrotizing enterocolitis"[All Fields] OR ("necrotizing"[All Fields] AND "enterocolitis"[All Fields]) OR "NEC"[All Fields])
-----------	--

Table S2.2 Embase search.

	Searches	Results
1	necrotizing enterocolitis/	12218
2	nutrition/	109194
3	feeding/	52256
4	2 or 3	158880
5	1 and 4	533
6	limit 5 to yr="1883-2020"	513
7	erythropoietin/	36171
8	1 and 7	105
9	limit 8 to yr="1883-2020"	102
10	alkaline phosphatase/	110896
11	1 and 10	79
12	limit 11 to yr="1883-2020"	79
13	glutamine/	41784
14	1 and 13	92
15	limit 14 to yr="1883-2020"	92
16	epidermal growth factor	41340
17	heparin binding epidermal growth factor	2781
18	16 or 17	43596
19	1 and 18	161
20	limit 19 to yr="1883-2020"	160
21	exosome/	32781
22	1 and 21	33
23	limit 22 to yr="1883-2020"	30
24	ganglioside/	9435
25	1 and 24	8
26	limit 25 to yr="1883-2020"	26
27	somatomedin/	16114
28	1 and 27	17
29	limit 28 to yr="1883-2020"	17
30	milk fat/	2925
31	1 and 30	10
32	limit 31 to yr="1883-2020"	9
33	osteopontin/	17679
34	1 and 33	8
35	limit 34 to yr="1883-2020"	8
36	oligosaccharide/	25624
37	1 and 36	113
38	limit 37 to yr="1883-2020"	110
39	polyunsaturated fatty acid/	22681

Table S2.2 (continued)

	Searches	Results
40	1 and 39	62
41	limit 40 to yr="1883-2020"	61
42	retinoic acid/	43088
43	1 and 42	12
44	limit 43 to yr="1883-2020"	12
45	transforming growth factor beta/	86269
46	1 and 45	59
47	limit 46 to yr="1883-2020"	58
48	vitamin D/	79604
49	1 and 48	57
50	limit 49 to yr="1883-2020"	56
51	Immunoglobulin/	120054
52	1 and 51	168
53	limit 52 to yr="1883-2020"	168
54	1 alkyl 2 acetylglycerophosphocholine esterase/	2314
55	1 and 54	19
56	limit 55 to yr="1883-2020"	19

Table S2.3 Cochrane library search.

	Searches	Results
#1	feeding intervention	9442
#2	nutritional intervention	13452
#3	Feeding	23499
#4	nutrition	55842
#5	necrotizing enterocolitis	1999
#6	NEC	998
#7	#1 OR #2 OR #3 OR #4	77042
#8	#5 OR #6	2344
#9	#7 AND #8	922
#10	#7 AND #8 with Cochrane Library publication date to Jan 2021, in Cochrane Reviews	185
#11	erythropoietin	4358
#12	EPO	2290
#13	#11 OR #12	4821
#14	#13 AND #8	44
#15	#13 AND #8 with Cochrane Library publication date to Jan 2021, in Cochrane Reviews	11
#16	alkaline phosphatase	5916
#17	ALPI	30
#18	#16 OR #17	4946
#19	#18 AND #8	30
#20	#18 AND #8 with Cochrane Library publication date to Jan 2021, in Cochrane Reviews	13
#21	Gln	325
#22	L-glutamine	241
#23	glutamine	2098
#24	#21 OR #22 OR #23	2159
#25	#24 AND #8	27
#26	#24 AND #8 with Cochrane Library publication date to Jan 2021, in Cochrane Reviews	7
#27	EGF	603
#28	epidermal growth factor	4834
#29	HB-EGF	16
#30	heparin-bindign EGF like growth factor	10
#31	#27 OR #28 OR #29 OR #30	5067

Table S2.3 (continued)

#32	#31 AND #8	6
#33	#31 AND #8 with Cochrane Library publication date to Jan 2021, in Cochrane Reviews	2
#34	exosomes	106
#35	extracellular vesicles	118
#36	microvesicles	48
#37	#34 OR #35 OR #36	250
#38	#37 AND #8	2
#39	#37 AND #8 with Cochrane Library publication date to Jan 2021, in Cochrane Reviews	0
#40	gangliosides	231
#41	GD3	27
#42	GM	15436
#43	#40 OR #31 OR #42	15654
#44	#43 AND #8	59
#45	#43 AND #8 with Cochrane Library publication date to Jan 2021, in Cochrane Reviews	16
#46	insulin like growth factor	3538
#47	ILGF1	0
#48	IGF1	245
#49	#46 OR #47 OR #48	3667
#50	#49 AND #8	29
#51	#49 AND #8 with Cochrane Library publication date to Jan 2021, in Cochrane Reviews	22
#52	milk fat globule membrane	61
#53	milk fat globule	78
#54	#52 OR #53	78
#55	#54 AND #8	2
#56	#54 AND #8 with Cochrane Library publication date to Jan 2021, in Cochrane Reviews	2
#57	osteopontin	232
#58	OPN	273
#59	#57 OR #58	429
#60	#59 AND #8	1
#61	#59 AND #8 with Cochrane Library publication date to Jan 2021, in Cochrane Reviews	0
#62	GOS	894
#63	FOS	505
#64	oligosaccharides	1012
#65	HMO	427
#66	#62 OR #63 OR #64 OR #65	2424
#67	#66 AND #8	30
#68	#66 AND #8 with Cochrane Library publication date to Jan 2021, in Cochrane Reviews	13
#69	PUFA	2024
#70	polyunsaturated fatty acid	2790
#71	omega 3 fatty acids	4973
#72	omega 6 fatty acids	2924
#73	long chain fatty acids	1748
#74	#69 OR #70 OR #71 OR #72 OR #73	7515
#75	#74 AND #8	33
#76	#74 AND #8 with Cochrane Library publication date to Jan 2021, in Cochrane Reviews	13
#77	vitamin A	27965
#78	all trans retinoic acid	413
#79	retinol	2262
#80	retinoids	504
#81	#77 OR #78 OR #79 OR #80	29410
#82	#81 AND #8	109
#83	#81 AND #8 with Cochrane Library publication date to Jan 2021, in Cochrane Reviews	44

Table S2.3 (continued)

	Searches	Results
#84	transforming growth factor beta	869
#85	TGFbeta1	234
#86	TGFbeta	447
#87	#84 OR #85 OR #86	1205
#88	#87 AND #8	2
#89	#87 AND #8 with Cochrane Library publication date to Jan 2021, in Cochrane Reviews	1
#90	vitamin D	17384
#91	cholecalciferol	3066
#92	ergocalciferol	354
#93	D2	4229
#94	D3	5590
#95	#90 OR #91 OR #92 OR #93 OR #94	22866
#96	#95 AND #8	76
#97	#95 AND #8 with Cochrane Library publication date to Jan 2021, in Cochrane Reviews	35
#98	immunoglobulins	2939
#99	IgG	5645
#100	IgA	4221
#101	#98 OR #99 OR #100	10801
#102	#101 AND #8	58
#103	#101 AND #8 with Cochrane Library publication date to Jan 2021, in Cochrane Reviews	22
#104	PAF-AH	24
#105	platelet-activating factor acetylhydrolase	28
#106	#104 OR #105	33
#107	#106 AND #8	0
#108	#106 AND #8 with Cochrane Library publication date to Jan 2021, in Cochrane Reviews	0

Table S2.4 Overview of RCTs that were not incorporated in one of the included meta-analyses and had a too small sample size (<50% of infants in the meta-analysis on the same intervention) to be included as separate trial.

Author and year	Type of study and sample size	In- and exclusion criteria	Control	Intervention	Effect on NEC incidence
Cui et al. 2019	single center RCT N=114 neonates	Inclusion: formula fed preterm infants admitted within 12h after birth to the First Neonatal Ward of the Shengjing Hospital of China Medical University, gestational age ≥ 30 and < 37 weeks; birthweight ≥ 1500 g and ≤ 2000 g, vital sign and hemodynamic parameters stable. Exclusion: congenital diseases, expected hospitalization < 2 weeks, maternal or neonatal antibiotics or probiotics administration before admission	no probiotics (N=57 neonates)	<i>Lactobacillus reuteri</i> DSM 17938, 1×10^8 CFU (5 drops) once daily, beginning with the first feeding until discharge from the hospital, <i>Lactobacillus reuteri</i> administration was stopped if enteral feeding was stopped due to feeding intolerance and resumed after feedings resumed (N=57 neonates)	NEC incidence control group 10.42% NEC incidence intervention group 2.22% (NS)
Gómez-Rodríguez et al. 2019	single center RCT N=90 neonates	Inclusion: preterm newborns, birthweight between 700 and 1500 g and gestational age < 33 weeks, no counter indication for enteral feeding in the first 7 days postnatally, inborn in tertiary healthcare from January 2014 to May 2015. Exclusion: birthweight > 1500 gram, Apgar score < 6 at 5 minutes, gastrointestinal malformations, patent ductus arteriosus with hemodynamic alterations and septic shock	single strain probiotic containing 1×10^9 CFU <i>Lactobacillus acidophilus boucardi</i> mixed in the feed each 24h during three weeks, starting from day 5 (N=45 neonates)	<i>multispecies probiotic containing 1×10^9 CFU Lactobacillus acidophilus, 4.4 \times 10^8 CFU Lactobacillus rhamnosus, 1 \times 10^9 CFU Lactobacillus casei, 1.76 \times 10^8 CFU Lactobacillus plantarum, 2.76 \times 10^7 CFU Bifidobacterium infantis and 6.6 \times 10^5 CFU Streptococcus thermophilus mixed in the feed each 24h during three weeks, starting from day 5 (N=45 neonates)</i>	1 infant developed NEC in the multispecies probiotic group, no infants developed NEC in the single strain probiotics group

Table S2.4 (continued)

Author and year	Type of study and sample size	In- and exclusion criteria	Control	Intervention	Effect on NEC incidence
Maamouri et al. 2016	single center RCT N=105 neonates	Inclusion: preterm neonates, gestational age <32 weeks, birth weight <1500 g, Apgar scores >7 at the NICU of the Qaem Hospital affiliated to the Mashhad University of Medical Sciences, Mashhad, Iran, informed consent	no enteral administration of L-glutamine (N=53 neonates)	L-glutamine, 0.3 g/kg/day divided in three doses, 5% solution, enterally administered from the 3 rd until the 28 th day of life (N=52 neonates)	OR 0.943 (95% CI 0.883-1.008) (NEC incidence)
Tarnow-Mordi 2020	multi center RCT N=1542 neonates	Inclusion: birth weight <1500 g, age <8 days Exclusion: lethal anomalies, late-onset sepsis before consent,	no pasteurized bovine lactoferrin added to feeds (N=771 neonates)	pasteurized bovine lactoferrin, 200 mg/kg, once daily added to formula feeding or breast milk, starting immediately after randomization and continued until 34 weeks postmenstrual age or for two weeks (whichever was longer) (N=771 neonates)	RR 1.09 (95% CI 0.63-1.9) (incidence stage II or III NEC)

Table S2.5 Overview included experimental animal studies on enteral feeding interventions for prevention of NEC.

Author and year	Model used	Control	Intervention	Sample size	Sample size / power calculation	Outcomes studied
Akisü et al. 1998	Balb/c mice (25-30 days old), NEC induction with one time hypoxia-reoxygenation (100% CO ₂ for 5 minutes followed by 100% O ₂ for 10 minutes), sacrifice after 4 hours	standard mouse chow (triglyceride composition: 45% saturated fatty acids, 40% monounsaturated fatty acids, 15% n-6 PUFA, 0% n-3 PUFA)	10% w/w fish oil supplemented mouse chow (triglyceride composition: 40% saturated fatty acids, 30% monounsaturated fatty acids, 18% EPA, 12% DHA), for 4 weeks prior to NEC induction	18 mice (N=6 per group)	not provided	histological NEC incidence/severity intestinal inflammation
Akisü et al. 2002	Balb/c mice (25-30 days old), NEC induction with one time hypoxia-reoxygenation (100% CO ₂ for 5 minutes followed by 100% O ₂ for 10 minutes), sacrifice after 4 hours	physiological saline, 1 mL by intraperitoneal injection immediately before NEC induction	L-arginine capsule in drinking water, 2 g/L, for 7 days prior to NEC induction L-carnitine solution in water, 50 mg/kg orally, for 7 days prior to NEC induction	28 mice (N=7 per group)	not provided	histological NEC incidence/severity vascular function / hypoxia-ischemia / free radical formation
Akisü et al. 2003	Balb/c mice (25-30 days old), NEC induction with one time hypoxia-reoxygenation (100% CO ₂ for 5 minutes followed by 100% O ₂ for 10 minutes), sacrifice after 4 hours	physiologic saline, 1 mL, by orogastric intubation immediately before NEC induction	L-glutamine in drinking water, 0.5 g/dL, for 3 days before NEC induction L-glutamine in drinking water, 3 g/dL, for 10 days before NEC induction	32 mice (N=8 per group)	not provided	histological NEC incidence/severity intestinal inflammation

Table S2.5 Overview included experimental animal studies on enteral feeding interventions for prevention of NEC.

Author and year	Model used	Control	Intervention	Sample size	Sample size / power calculation	Outcomes studied
Akisü et al. 1998	Balb/c mice (25-30 days old), NEC induction with one time hypoxia-reoxygenation (100% CO ₂ for 5 minutes followed by 100% O ₂ for 10 minutes), sacrifice after 4 hours	standard mouse chow (triglyceride composition: 45% saturated fatty acids, 40% monounsaturated fatty acids, 15% n-6 PUFA, 0% n-3 PUFA)	10% w/w fish oil supplemented mouse chow (triglyceride composition: 40% saturated fatty acids, 30% monounsaturated fatty acids, 18% EPA, 12% DHA), for 4 weeks prior to NEC induction	18 mice (N=6 per group)	not provided	histological NEC incidence/severity intestinal inflammation
Akisü et al. 2002	Balb/c mice (25-30 days old), NEC induction with one time hypoxia-reoxygenation (100% CO ₂ for 5 minutes followed by 100% O ₂ for 10 minutes), sacrifice after 4 hours	physiological saline, 1 mL, by intraperitoneal injection immediately before NEC induction	L-arginine capsule in drinking water, 2 g/L, for 7 days prior to NEC induction L-carnitine solution in water, 50 mg/kg orally, for 7 days prior to NEC induction	28 mice (N=7 per group)	not provided	histological NEC incidence/severity vascular function / hypoxia-ischemia / free radical formation
Akisü et al. 2003	Balb/c mice (25-30 days old), NEC induction with one time hypoxia-reoxygenation (100% CO ₂ for 5 minutes followed by 100% O ₂ for 10 minutes), sacrifice after 4 hours	physiologic saline, 1 mL, by orogastric intubation immediately before NEC induction	L-glutamine in drinking water, 0.5 g/dL, for 3 days before NEC induction L-glutamine in drinking water, 3 g/dL, for 10 days before NEC induction	32 mice (N=8 per group)	not provided	histological NEC incidence/severity intestinal inflammation

Table S2.5 (continued)

Autran et al. 2016	Sprague-Dawley rats (newborn), NEC induction with formula feeding (200 µL twice daily) and hypoxia (5% O ₂ , 95% N ₂ for 10 minutes) thrice daily for 4 days	Formula without HMO, GOS or sialylated GOS	HMO in formula, 10 mg/ml, simultaneous with NEC induction	95 rats (N=11-22 per group)	not provided	histological NEC incidence/severity
			GOS in formula, 8 mg/ml, simultaneous with NEC induction			
			sialylated GOS in formula, 500 µM, simultaneous with NEC induction			
			2'-FL in formula, 2 mg/ml, simultaneous with NEC induction			
Bergmann et al. 2013	C57BL/6 mice (newborn), NEC induction with inoculation with a standardized adult commensal bacteria mixture (10 ⁷ CFU) within 12 hours after birth, formula feeding (30 µL every 3 hours) and asphyxia (100% N ₂ for 1 minute) and cold exposure (4°C for 10 minutes) twice daily for 3 days	inoculation with vehicle	<i>Bifidobacterium infantis</i> strain BB-02 (human source), 3x10 ⁶ CFU in 20 µL in dextrose (immunofluorescence studies) or maltodextran (permeability studies, Western blot, histology), before NEC induction	not provided	not provided	histological NEC incidence/severity, intestinal barrier function
Butel et al. 1998	Germ-free quails (<i>coturnix</i> , <i>coturnix</i> subsp. <i>japonica</i>) (2 week old), NEC induction with colonization with fecal flora isolated from an infant with NEC and feeding with a 6-8% w/w lactose diet for 21 days	inoculation with a 10-fold dilution of fecal flora in 100 µL	<i>Bifidobacterium infantis</i> -longum strain CUETM 89-215 isolated from stool of a healthy premature infant, 10 ⁸ -viable cells/ml, 100 µL, simultaneous with NEC induction	59 quails (N=8-12 per group)	not provided	histological NEC incidence/severity, microbiome alterations

Table S2.5 (continued)

Author and year	Model used	Control	Intervention	Sample size	Sample size / power calculation	Outcomes studied
Cai et al. 2016	Sprague-Dawley rats (15 days old), NEC induction with asphyxia (100% N ₂ for 2 minutes) and cold exposure (4°C for 10 minutes) twice daily for 4 days	oral saline	astragaloside IV 25 mg/kg/d orally, simultaneous with NEC induction astragaloside IV 50 mg/kg/d orally, simultaneous with NEC induction astragaloside IV 75 mg/kg/d orally, simultaneous with NEC induction	40 rats (N=10 per group)	not provided	histological NEC incidence/severity intestinal inflammation systemic inflammation vascular function / hypoxia-ischemia / free radical formation
Cakir et al. 2018	Wistar rats (newborn), NEC induction with one time intraperitoneal LPS (1 mg/kg) on day 1, formula feeding (200 µL every 3h and increased by 100 µL daily if tolerated) and asphyxia (100% CO ₂ for 10 minutes), hyperoxia (97% O ₂ for 5 minutes) and cold exposure (4°C for 10 minutes) twice daily for 3 days	saline, 2 ml/kg, once daily, oral	ginger extract in water, 1000 mg/kg, once daily, simultaneous with NEC induction	30 rats (N=10 per group)	not provided	histological NEC incidence/severity NEC signs and symptoms intestinal inflammation
Caplan et al. 1997	Sprague-Dawley rats (newborn), NEC induction with formula feeding (100 µL every 3h and increased to 400 µL on day 4 if tolerated) and asphyxia (100% N ₂ for 50 seconds) followed by cold exposure (4°C for 10 minutes) twice daily for 4 days	25 µL dilution buffer in each feeding via orogastric tube	rPAF-AH, 80 U in 25 µL dilution buffer in each feeding via orogastric tube, the PAF-AH preparation had 0.8 mg/ml protein and approximately 4000 U/mg PAF-AH activity	52 rats (N=26 per group)	not provided	intestinal epithelial cell death histological NEC incidence/severity NEC survival

Table S2.5 (continued)

Caplan et al. 1999	Sprague-Dawley rats (newborn on day 21 of gestation), NEC induction with formula feeding (100 µL every 3h and increased to 400 µL on day 4 if tolerated) and asphyxia (100% N ₂ for 50 seconds) followed by cold exposure (4°C for 10 minutes) twice daily for 4 days	no administration of <i>Bifidobacterium infantis</i> . a second control group was used with administration of <i>Escherichia coli</i> , 10 ⁸ organisms, once daily, 30 minutes before asphyxia via orogastric tube	<i>Bifidobacterium infantis</i> (human source), 10 ⁸ organisms, once daily, 30 minutes before asphyxia via orogastric tube, simultaneous with NEC induction	51 rats (N=24-27 per group)	not provided	histological NEC incidence/severity NEC survival intestinal inflammation intestinal barrier function	
Caplan et al. 2001	Sprague-Dawley rats (newborn on day 21 of gestation), NEC induction with formula feeding (100 µL every 3h and increased to 300 µL on day 3 if tolerated) and asphyxia (100% N ₂ for 50 seconds) followed by cold exposure (4°C for 10 minutes) twice daily for 3 days	formula without PUFA and nucleotide supplementation (CMP 3.55 mg/100 g formula powder/200 mL water, UMP 6.2 mg/100 g formula powder/200 mL water, IMP 0.73 mg/100 g formula powder/200 mL water, AMP 0.18 mg/100 g formula powder/200 mL water, GMP 0.2 mg/100 g formula powder/200 mL water, GMP 0.2 mg/100 g formula powder/200 mL water, AMP 0.18 mg/100 g formula powder/200 mL water)	PUFA in formula, 34 mg/100 mL AA, 23 mg/100 mL DHA, simultaneous with NEC induction PUFA and nucleotides in formula, 34 mg/100 mL AA, 23 mg/100 mL DHA, CMP 15.62 mg/100 g formula powder/200 mL water, UMP 9.2 mg/100 g formula powder/200 mL water, IMP 3.06 mg/100 g formula powder/200 mL water, GMP 2.08 mg/100 g formula powder/200 mL water, AMP 03.57 mg/100 g formula powder/200 mL water, simultaneous with NEC induction	95 rats (N=23-24 per group)	not provided	histological NEC incidence/severity NEC survival intestinal inflammation intestinal barrier function vascular function / hypoxia-ischemia / free radical formation intestinal epithelial cell death	

Table S2.5 (continued)

Author and year	Model used	Control	Intervention	Sample size	Sample size / power calculation	Outcomes studied
Catala et al. 1999	Germ-free quails (<i>Coturnix coturnix</i> subsp. <i>japonica</i>) (2 week old), NEC induction with colonization with fecal flora isolated from an infant with NEC and feeding with a 6% w/w lactose diet for 21 days	control diet with 6% lactose w/w	diet of 3% FOS and 3% lactose w/w, simultaneous with NEC induction	80 quails (N=8-12 per group)	not provided	NEC signs and symptoms
Chen et al. 2012	Sprague-Dawley rats (newborn on day 21 of gestation), NEC induction with formula feeding and asphyxia (100% N ₂ for 90 seconds) and cold exposure (4°C for 10 minutes) thrice daily for 3 days	formula without recombinant human HB-EGF	recombinant human HB-EGF in formula, 800 µg/kg/dose, simultaneous with NEC induction	25 rats (N=5-10 per group)	not provided	intestinal barrier function intestinal epithelial proliferation
Chen et al. 2019	C57BL/6 mice (5-9 days old), NEC induction with enteral administration of LPS (4 mg/kg/day) once daily, formula feeding (50 µL/g thrice daily) and hypoxia (5% O ₂ for 10 minutes) thrice daily for 4 days	control formula	arginine in formula, 240 mg/kg/day, simultaneous with NEC induction	36 mice (N=8-11 per group)	not provided	enteric nervous system histological NEC incidence/severity intestinal inflammation
Cigsar et al. 2018	Wistar albino rats (newborn), NEC induction with formula feeding (200 µL twice daily) and asphyxia (100% CO ₂ for 10 minutes), hyperoxia (97% O ₂ for 10 minutes) and cold exposure (4°C for 10 minutes) twice daily for 3 days	no oral sesamol	97% sesamol orally, 100 mg/kg/dose, twice daily, simultaneous with NEC induction	34 rats (N=7-9 per group)	not provided	vascular function / hypoxia-ischemia / free radical formation histological NEC incidence/severity NEC signs and symptoms vascular function / hypoxia-ischemia / free radical formation intestinal epithelial cell death

Table S2.5 (continued)

	control formula	2'-FL in formula, 5 g/L, during minimal enteral feeding and full enteral feeding, simultaneous with NEC induction	33 pigs (N=16-17 per group)	Yes, power calculation based on estimated mean incidence and dispersion for NEC	histological NEC incidence/severity
Cilleborg et al. 2016	Preterm pigs (90% of gestational age, delivered by caesarian section), NEC induction with parental nutrition for the first 2 postnatal days (4-6 mL/kg/h) with minimal enteral feeding (2-3 mL/kg per 3 hours) and full enteral nutrition after 2 days with an oral bolus of 15 ml/kg formula every 3 hours for 3 days			incidence (69%, SEM 21%), estimated effect size of 30% and β 80%; required sample size 17	NEC signs and symptoms microbiome alterations digestion and absorption
Clark et al. 2005	Sprague-Dawley rats (newborn), NEC induction with formula feeding (100 μ L every 3-4 hours) and asphyxia (100% N ₂ for 1 minute) followed by cold exposure (4°C for 10 minutes) twice daily for 4 days	control cow-milk based formula (free of growth factors)	rat EGF in cow-milk based formula, 500 ng/mL, simultaneous with NEC induction	not provided	intestinal epithelial cell death / altered proliferation
Clark et al. 2006	Sprague-Dawley rats (newborn on day 21 of gestation), NEC induction with formula feeding (150 μ L every 5 hours) and asphyxia (100% N ₂ for 1 minute) followed by cold exposure (4°C for 10 minutes) twice daily for 4 days	control cow-milk based formula (free of growth factors)	rat EGF in cow-milk based formula, 500 ng/mL, simultaneous with NEC induction	not provided	NEC survival, intestinal barrier function
Coursodon-Boydell et al. 2012	Sprague-Dawley rats (newborn on day 21 of gestation), NEC induction with formula feeding (850 μ L every day in 6 feeds) and asphyxia (100% N ₂ for 1 minute) and cold exposure (4°C for 10 minutes) twice daily for 4 days	rat milk formula (0.0% conjugated linoleic acid, 20.9% n-6 PUFA, 3.5% n-3 PUFA)	1.5% pomegranate seed oil in rat milk formula (2.7% conjugated linoleic acid, 20.6% n-6 PUFA, 3.3% n-3 PUFA)	not provided	histological NEC incidence/severity NEC survival, intestinal inflammation intestinal epithelial proliferation

Table S2.5 (continued)

Author and year	Model used	Control	Intervention	Sample size	Sample size / power calculation	Outcomes studied
Cuna et al. 2020	C57BL6 mice (8-11 days old), NEC induction with one time intraperitoneal LPS (5 mg/kg) 12 hours before sacrifice, formula feeding (200 μ L/5 g body weight twice daily) and hypoxia (5% O ₂ for 2 minutes twice daily) for 3 days	vehicle, 0.1 mL, once daily for 2 days before NEC induction	<i>Lactobacillus rhamnosus</i> GG, 0.1 mL and 10 ⁷ CFU/mL, once daily for 2 days before NEC induction	unclear	not provided	intestinal inflammation intestinal barrier function intestinal epithelial cell death
Dilsiz et al. 2003	Sprague-Dawley rats (newborn), NEC induction with formula feeding three times a day for 4 days	formula without supplemented glutamine	glutamine (0.31 mg/kg/day) in formula feeding, simultaneous with NEC induction	40 rats (N=10 per group)	not provided	NEC signs and symptoms vascular function / hypoxia-ischemia / free radical formation NEC signs and symptoms NEC survival,
D'souza et al. 2010	Sprague-Dawley rats (newborn), NEC induction with formula feeding (200 μ L every three hours) for 4 days	formula without supplementation	<i>Saccharomyces Boulardii</i> 5 mg/mL in formula, simultaneous with NEC induction GOS/FOS in formula, simultaneous with NEC induction <i>Saccharomyces Boulardii</i> 5 mg/mL and GOS/FOS in formula, simultaneous with NEC induction	unclear	not provided	vascular function / hypoxia-ischemia / free radical formation NEC signs and symptoms NEC survival, vascular function / hypoxia-ischemia / free radical formation

Table S2.5 (continued)

D'Souza et al. 2012	Sprague-Dawley rats (newborn), NEC induction with formula feeding (200 µL every three hours), hyperoxia (50% O ₂) with brief periods of hypoxia (12% O ₂ for 1-2 minutes) every 4 (day 1), 5 (day 2) or 6 (day 3) hours.	formula without supplementation	<i>Saccharomyces Boulardii</i> undecar in formula, simultaneous with NEC induction GOS/FOS in formula, simultaneous with NEC induction	not provided	NEC signs and symptoms intestinal inflammation vascular function / hypoxia-ischemia / free radical formation
Dvorak et al. 2002	Sprague-Dawley rats (newborn), NEC induction with formula feeding and asphyxia (100% N ₂ for 1 minute) followed by cold exposure (4°C for 10 minutes) twice daily for 4 days	control cow-milk based formula (free of growth factors)	<i>Saccharomyces Boulardii</i> and GOS/FOS in formula, simultaneous with NEC induction	not provided	histological NEC incidence/severity NEC signs and symptoms
Dvorak et al. 2008	Sprague-Dawley rats (newborn, 1 day before scheduled birth), NEC induction with formula feeding and asphyxia (100% N ₂ for 1 minute) and cold exposure (4°C for 10 minutes) twice daily for 4 days	control cow-milk based formula (free of growth factors)	human HB-EGF in cow-milk based formula, 500 ng/mL, simultaneous with NEC induction rat EGF in cow-milk based formula, 500 ng/mL, simultaneous with NEC induction human HB-EGF, 500 ng/mL, and rat EGF, 500 ng/mL, in cow-milk based formula	not provided	histological NEC incidence/severity intestinal barrier intestinal epithelial cell death

Table S2.5 (continued)

Author and year	Model used	Control	Intervention	Sample size	Sample size / power calculation	Outcomes studied
Egan et al. 2016	C57BL/6 mice (7-8 days old), NEC induction with administration of enteric bacteria isolated from an infant with NEC (12.5 µL stool slurry in 1 mL formula), formula feeding and hypoxia (5% O ₂) twice daily for 4 days	no ATRA	ATRA, dissolved in 1:1 DMSO and corn oil, 6 mg/mL and 50 µg/mouse, once daily by gavage, simultaneous with NEC induction	unclear	not provided	histological NEC incidence/severity intestinal inflammation
Ergün et al. 2007	Wistar rats (newborn), NEC induction with formula feeding twice daily and hypoxia (5% O ₂ , 95% N ₂), thrice daily for 3 days	formula without resveratrol	resveratrol in formula, 15 mg/kg in every feed, simultaneous with NEC induction	27 rats (N=7-10 per group)	not provided	histological NEC incidence/severity NEC signs and symptoms
Fan et al. 2019	Sprague-Dawley rats (3-5 days old), NEC induction with Cronobacter sakazakii 1x 10 ⁹ CFU once per day, formula feeding (200 µL twice daily) and hypoxia (5% O ₂ and 95% N ₂ thrice daily) for 2 days	formula without <i>Bacteroides fragilis</i> strain ZY-312	<i>Bacteroides fragilis</i> strain ZY-312, 1x 10 ⁹ CFU in 200 µL formula, once daily starting 2 days before NEC induction	40 rats (N=10 per group)	not provided	vascular function / hypoxia-ischemia / free radical formation histological NEC incidence/severity NEC signs and symptoms NEC survival intestinal inflammation systemic inflammation intestinal barrier function vascular function / hypoxia-ischemia / free radical formation intestinal epithelial cell death

Table S2.5 (continued)

Feng et al. 2005	Sprague-Dawley rats (newborn), NEC induction with intragastric LPS (2 mg/kg) 8 hours after birth, formula feeding every 4 hours and hypoxia (100% N ₂ for 1 minute) followed by cold exposure (10 minutes at 4 °C) twice daily for 4 days	no HB-EGF	HB-EGF, 600 µg/kg, every 4 hours via orogastric feeding tube, simultaneous with NEC induction	not provided	histological NEC incidence/severity NEC survival intestinal barrier function
Feng et al. doi:10.1016/j.jpedsurg.2005.10.018 2006	Sprague-Dawley rats (newborn), NEC induction with intragastric LPS (2 mg/kg) 8 hours after birth, formula feeding (100 µL every 4 hours and increased to 400 µL per feed on day 4 if tolerated) and asphyxia (100% N ₂ for 1 minute) followed by cold exposure (4 °C for 10 minutes) twice daily for 4 days	no HB-EGF	HB-EGF, 600 µg/kg, every 4 hours via orogastric feeding tube, simultaneous with NEC induction	not provided	histological NEC incidence/severity NEC survival, intestinal barrier function
Feng et al. doi:10.1016/j.jpedsurg.2005.12.020 2006	Sprague-Dawley rats (newborn), NEC induction with intragastric administration of LPS (2 mg/kg) 8 hours after birth, formula feeding (100 µL every 4 hours and increased to 400 µL per feed on day 4 if tolerated) and asphyxia (100% N ₂ for 1 minute) followed by cold exposure (4 °C for 10 minutes) twice daily for 4 days	formula without HB-EGF	HB-EGF in formula, 600 µg/kg, every 4 hours via orogastric feeding tube, simultaneous with NEC induction	not provided	histological NEC incidence/severity intestinal epithelial cell death
Feng et al. 2007	Sprague-Dawley rats (newborn), NEC induction with intragastric administration of LPS (2 mg/kg) 8 hours after birth, formula feeding (100 µL every 4 hours and increased to 400 µL per feed on day 4 if tolerated) and asphyxia (100% N ₂ for 1 minute) followed by cold exposure (4 °C for 10 minutes) twice daily for 4 days	formula without HB-EGF	HB-EGF in formula, 600 µg/kg, every 4 hours via orogastric feeding tube, simultaneous with NEC induction	not provided	histological NEC NEC survival intestinal barrier function intestinal epithelial proliferation

Table S2.5 (continued)

Author and year	Model used	Control	Intervention	Sample size	Sample size / power calculation	Outcomes studied
Good et al. 2012	C57Bl/6 mice (10 days old), NEC induction with formula feeding (50 μ L/g body weight, 5 times a day) and hypoxia (5% O ₂ 95% N ₂ for 10 minutes) twice daily for 4 days	no amniotic fluid	amniotic fluid, 50 μ L/g, daily enteral, simultaneous with NEC induction	endotoxemia at least N=3 per group, for histology at least N=10 per group	not provided	histological NEC incidence/severity vascular function / hypoxia-ischemia / free radical formation intestinal epithelial proliferation histological NEC incidence/severity
Good et al. 2014	C57Bl/6 mice (7-10 days old), NEC induction with supplementation of enteric bacteria isolated from an infant with severe NEC (12.5 μ L stool slurry in 1 mL formula) in formula feeding (5 times a day) and hypoxia (5% O ₂ , 95% N ₂ for 10 minutes) twice daily for 4 days	no Lr-DNA, probiotics or CpG-DNA	Lr-DNA (microbial DNA purified from <i>Lactobacillus rhamnosus</i> HN001), 1 mg/kg/day by oral gavage, once daily for 4 days before NEC induction live <i>Lactobacillus rhamnosus</i> HN001, 3*10 ¹¹ CFU/kg/day by oral gavage, dose equivalent to 1 mg Lr-DNA/kg/day, once daily for 4 days before NEC induction UV-irradiated <i>Lactobacillus rhamnosus</i> HN001, 3*10 ¹¹ CFU/kg/day by oral gavage, dose equivalent to 1 mg Lr-DNA/kg/day, once daily for 4 days before NEC induction	at least N=10 per group	not provided	NEC signs and symptoms intestinal inflammation vascular function / hypoxia-ischemia / free radical formation

Table S2.5 (continued)

<p>Good et al. 2014</p> <p>Yorkshire piglets (newborn at day 105- 108 of gestation), NEC with supplementation of enteric bacteria isolated from an infant with surgical NEC (12.5 µL stool slurry in 1 mL formula) in formula feeding (15 mL/kg every 3 hours) for 4 days</p>	<p>no Lr-DNA or probiotics</p>	<p>Lr-DNA (microbial DNA purified from <i>Lactobacillus rhamnosus</i> HN001), 1 mg/kg/day by oral gavage, once daily, simultaneous with NEC induction</p>	<p>at least N=3 per group</p>	<p>not provided</p>	<p>histological NEC incidence/severity</p> <p>NEC signs and symptoms</p> <p>vascular function / hypoxia-ischemia / free radical formation</p>
<p>live <i>Lactobacillus rhamnosus</i> HN001, 3*10¹¹ CFU/kg/day by oral gavage, dose equivalent to 1 mg Lr-DNA/kg/day, once daily, simultaneous with NEC induction</p>					
<p>UV-irradiated <i>Lactobacillus rhamnosus</i> HN001, 3*10¹¹ CFU/kg/day by oral gavage, dose equivalent to 1 mg Lr-DNA/kg/day, once daily, simultaneous with NEC induction</p>					

Table S2.5 (continued)

Author and year	Model used	Control	Intervention	Sample size	Sample size / power calculation	Outcomes studied
Good et al. 2016	C57BL/6 mice (7-10 days old), NEC induction with supplementation of enteric bacteria isolated from an infant with severe NEC (12.5 µL stool slurry in 1 mL formula) in formula feeding (5 times a day) and hypoxia (5% O ₂ , 95% N ₂ for 10 minutes) twice daily for 4 days	formula without HMO 2'-FL	HMO 2'-FL, 5 mg/mL of formula, 0.25 mg/g, once daily, simultaneous with NEC induction	unclear	not provided	histological NEC incidence/severity NEC signs and symptom intestinal inflammation, vascular function / hypoxia-ischemia / free radical formation
Gunasekaran et al. 2019	Ctrl:CD11(CR) mice (14-16 days old), NEC induction with intraperitoneal injection of dithizone (83 mg/kg) diluted in ethanol/ammonium hydroxide, followed by gavage administration of 1x10 ⁸ CFU <i>Klebsiella pneumoniae</i> /kg (ATCC 10031), end of experiment 16 hours after intraperitoneal injection and 10 hours after bacterial administration	no sodium hyaluronate	sodium hyaluronate (35 kDa), 15 mg/kg, once daily for 3 days prior to induction of NEC and 1h prior to bacterial administration	unclear	not provided	microbiome alterations histological NEC incidence/severity NEC survival systemic inflammation intestinal barrier function
Halpern et al. 2003	Sprague-Dawley rats (newborn), NEC induction with formula feeding and asphyxia (100% N ₂ for 1 minute) followed by cold exposure (4°C for 10 minutes) twice daily for 4 days	rat milk substitute without growth factors	EGF in growth-factor-free rat milk substitute, 500 ng/mL, simultaneous with NEC induction	50 rats (N=15-18 per group)	not provided	histological NEC incidence/severity intestinal inflammation

Table S2.5 (continued)

He-Yang et al. 2020	Sprague-Dawley rats (newborn), NEC induction with formula feeding and hypoxia (5% O ₂ , 95% N ₂ for 10 minutes) and cold exposure (4 °C for 10 minutes) thrice daily for 3 days	formula without sialylated HMO	sialylated HMO (39.5% 6'-SL, 28.5% 3'-SL and 6.6% DSLNT) in formula, 1500 mg/L, simultaneous with NEC induction	38 rats (N=8-15 per group)	not provided	histological NEC incidence/severity
Hoang et al. 2018	C57BL/6 mice (newborn), NEC induction with formula feeding (100-200 µL, 4 times a day) and hypoxia (5% O ₂ , 95% N ₂ for 10 minutes) followed by cold exposure (4 °C for 5 minutes) thrice daily for 4 days	formula without bacterial strain	<i>Lactobacillus reuteri</i> 1.7938 in formula, 10 ⁶ CFU/g/day/mouse, simultaneous with NEC induction	59 mice (N=15-23 per group)	not provided	intestinal inflammation histological NEC incidence/severity
Isani et al. 2018	Sprague-Dawley rats (newborn), NEC induction with formula feeding (200 µL, every 8 hours) and hypoxia (5% O ₂ , 95% N ₂ for 10 minutes) after each feeding for 4 days	formula without supplementation or formula supplemented with empty soybean extract	human recombinant EGF from transgenic soybean in formula, 75 µg/kg/day, simultaneous with NEC induction	unclear	not provided	histological NEC incidence/severity NEC survival, intestinal barrier function
Jain et al. 2014	Sprague-Dawley rats (newborn at day 21.5 of gestation), NEC induction with formula feeding (200 µL starting 30 minutes after birth and every 4 hours and increased by 50 µL every 12 hours to a maximum of 300 µL) and hypoxia (5% O ₂ , 95% N ₂ for 1 minute) followed by cold exposure (4 °C for 10 minutes) twice daily for 4 days	formula without added substances formula with added BSA, 18 ng in total	30% v/v amniotic fluid in formula, simultaneous with NEC induction HGF in formula, 18 ng in total, simultaneous with NEC induction	amniotic fluid supplementation: 80 rats HGF supplementation: 58 rats	not provided	vascular function / hypoxia-ischemia / free radical formation histological NEC incidence/severity intestinal inflammation, vascular function / hypoxia-ischemia / free radical formation

Table S2.5 (continued)

Author and year	Model used	Control	Intervention	Sample size	Sample size / power calculation	Outcomes studied
Jantscher-Krenn et al. 2012	Sprague-Dawley rats (new born), NEC induction with formula feeding (200 μ L twice daily) and hypoxia (5% O ₂ , 95% N ₂ for 10 minutes) thrice daily for 4 days	formula without HMO	HMO in formula, 10 mg/mL, for the whole study period, simultaneous with NEC induction	N=8-26 rats per group	not provided	histological NEC incidence/severity NEC signs and symptoms NEC survival
			HMO in formula, 10 mg/mL, after the first 24 hours of NEC induction			
			HMO in formula, 10 mg/mL, for the first 24 hours after NEC induction only, simultaneous with NEC induction			
			formula supplemented with GOS (8 mg/mL), simultaneous with NEC induction			
			neutral HMO-containing (zero sialic acids) formula (10 mg/mL) for the whole study period			
			-1 HMO (one sialic acid) in formula, 10 mg/mL, for the whole study period, simultaneous with NEC induction			

Table S2.5 (continued)

Jantscher-Krenn et al. 2012	-2 HMO (two sialic acid) in formula, 10 mg/mL, for the whole study period, simultaneous with NEC induction		histological NEC incidence/severity
	-3 HMO (three sialic acid) in formula, 10 mg/mL, for the whole study period, simultaneous with NEC induction		intestinal inflammation
	-4 HMO (four sialic acid) in formula, 10 mg/mL, for the whole study period, simultaneous with NEC induction		systemic inflammation
Jing et al 2018	DSLNT in formula, 300 µM, simultaneous with NEC induction	60 rats (N=10 per group)	not provided
	Sprague-Dawley rats (newborn on day 21 of gestation), NEC induction with oral administration of LPS (4 mg/kg/day) on postnatal day 0 and 1, formula feeding (100 µL twice daily) and asphyxia (100% N ₂ for 90 seconds every 4 hours) for 4 days	formula without berberine	intestinal barrier function

Table S2.5 (continued)

Author and year	Model used	Control	Intervention	Sample size	Sample size / power calculation	Outcomes studied
Khalilova et al. doi: 10.1152/ajpg i.00141.2009 2009	Sprague-Dawley rats (newborn, 1 day before scheduled birth), NEC induction with formula feeding (total volume 850 μ L/day, 6 times a day) and asphyxia (100% N ₂ for 1 minute) followed by cold exposure (4 °C for 10 minutes) twice daily for 4 days	formula without bacterial strain	<i>Bifidobacterium bifidum</i> OLB6378 in formula, 5*10 ⁶ CFU per day, simultaneous with NEC induction	76 rats (N=16-30 per group)	not provided	histological NEC incidence/severity intestinal inflammation, intestinal barrier function
Khalilova et al. doi: 10.1203/PDR .0b013e3181 aa3198 2009	Sprague-Dawley rats (newborn, 1 day before scheduled birth), NEC induction with formula feeding (total volume 850 μ L/day) and asphyxia (100% N ₂ for 1 minute) followed by cold exposure (4 °C for 10 minutes) twice daily for 4 days	formula without rat EGF	rat EGF in formula, 500 ng/mL, simultaneous with NEC induction	82 rats (N=22-36 per group)	not provided	histological NEC incidence/severity
Khalilova et al. 2010	Sprague-Dawley rats (newborn, 1 day before scheduled birth), NEC induction with formula feeding (total volume 850 μ L/day, 6 times a day) and asphyxia (100% N ₂ for 1 minute) followed by cold exposure (4 °C for 10 minutes) twice daily for 4 days	Formula without <i>Bifidobacterium bifidum</i> strain OLB5378	<i>Bifidobacterium bifidum</i> strain OLB6378, 5*10 ⁶ CFU/mL per day in two feedings, simultaneous with NEC induction	76 rats (N=16-30 per group) for celecoxib experiments N=8 per group	not provided	histological NEC incidence/severity intestinal epithelial cell death
Li et al. 2019	C57BL/6 mice (5-9 days old), NEC induction with enteral administration of LPS (4 mg/kg/day) on postnatal day 6 and 7, formula feeding (50 μ L/g, thrice daily) and hypoxia (5% O ₂ for 10 minutes) thrice daily for 4 days	formula without bovine milk exosomes	bovine milk exosomes in formula, 1 μ L/ μ L, simultaneous with NEC induction	27 mice (N=9 per group)	not provided	histological NEC incidence/severity intestinal inflammation, intestinal barrier function

Table S2.5 (continued)

Li et al. 2020	C57BL/6 mice (5-9 days old), NEC induction with enteral administration of LPS (4 mg/kg/day) on postnatal day 6 and 7, formula feeding (50 μ L/g, thrice daily) and hypoxia (5% O ₂ for 10 minutes) thrice daily for 4 days	formula without HMO	HMO in formula, 20 mg/ml, 2% w/v, 2-3 mg HMO/g body weight/day, simultaneous with NEC induction	N=6-15 per group	not provided	histological NEC incidence/severity intestinal barrier function intestinal epithelial cell death / proliferation
Liu et al. 2012	Sprague-Dawley rats (newborn), NEC induction with formula feeding (100-200 μ L four times daily) and hypoxia (5% O ₂ , 95% N ₂ for 10 minutes) thrice daily for 3 days	formula without bacterial strain	<i>Lactobacillus reuteri</i> DSM 17938 in formula, 10 ⁶ CFU/g body weight/day, simultaneous with NEC induction <i>Lactobacillus reuteri</i> ATCC PTA 4659 in formula, 10 ⁶ CFU/g body weight/day, simultaneous with NEC induction	190 rats (N=17-46 per group)	not provided	histological NEC incidence/severity, NEC survival intestinal inflammation
Liu et al. 2013	Sprague-Dawley rats (newborn), NEC induction with formula feeding (100-200 μ L 5 times daily) and hypoxia (5% O ₂ , 95% N ₂ for 10 minutes) thrice daily for 3 days	formula without bacterial strain	<i>Lactobacillus reuteri</i> DSM 17938 in formula, 10 ⁶ CFU/g body weight/day, simultaneous with NEC induction	59 rats (N=15-22 per group)	not provided	NEC survival, intestinal inflammation
Liu et al. 2014	C57BL/6 mice (8-10 days old), NEC induction with formula feeding (200 μ L four times daily) and hypoxia (5% O ₂ , 95% N ₂ for 10 minutes) followed by cold exposure (4 °C for 5 minutes) twice daily for 4 days	formula without bacterial strain	<i>Lactobacillus reuteri</i> DSM 17938 in formula, 10 ⁶ CFU/g body weight/day, simultaneous with NEC induction	95 mice (N=16-36 per group)	not provided	histological NEC incidence/severity NEC survival intestinal inflammation

Table S2.5 (continued)

Author and year	Model used	Control	Intervention	Sample size	Sample size / power calculation	Outcomes studied
Liu et al. 2019	C57BL/6 mice (5-9 days old), NEC induction with administration of LPS, formula feeding and hypoxia for 4 days	no recombinant lactoferrin	recombinant lactoferrin, 0.3 g/kg/day, 6g/L, once daily by gavage from postnatal day 6 to 8	24 mice (N=7-9 per group)	not provided	histological NEC incidence/severity intestinal inflammation
Lock et al. 2020	Sprague-Dawley rats (newborn, 1 day before scheduled birth), NEC induction with 10 ⁷ CFU of both <i>Serratia marcescens</i> , <i>Klebsiella pneumoniae</i> and <i>Streptococcus viridans</i> in formula once daily, formula feeding (100 µL every 3 hours and increased to 250 µL over 5 days if tolerated) and hypoxia (5% O ₂ , 95% N ₂ for 10 minutes) every 8 hours for 5 days	formula without supplementation	egg white lysozyme in formula, 0.37 mg in 100 µL, 0.82 mg in 250 µL, simultaneous with NEC induction DHA in formula, 0.27 µL in 100 µL, 0.63 µL in 250 µL, simultaneous with NEC induction	60 rats (N=15-30 per group)	not provided	intestinal epithelial proliferation NEC survival, intestinal barrier function
Lu et al. 2007	Sprague-Dawley rats (newborn on day 21 of gestation), NEC induction with formula feeding (100 µL every 3 hours and increased to 300 µL every 3 hours over 3 days) and asphyxia (100% N ₂ for 50 seconds twice daily) for 3 days	formula without long-chain PUFA supplementation	AA and DHA in formula, AA 0.7% of total fatty acids, DHA 0.5% of total fatty acids, simultaneous with NEC induction egg phospholipids in formula, 0.7% AA of total fatty acids, 0.5% DHA of total fatty acids, simultaneous with NEC induction DHA in formula, 0.5% DHA of total fatty acids, simultaneous with NEC induction	352 rats (N=85-90 per group)	Yes, power calculation based on estimated NEC incidence (60%), estimated effect size of 50%, α 0.05 and β 0.8; required sample size 90	histological NEC incidence/severity intestinal inflammation

Table S2.5 (continued)

Lu et al. Chinese 2018	Sprague-Dawley rats (newborn on day 21 of gestation), NEC induction with formula feeding (100 µL every 4 hours and increased to 300 µL every 3 hours over 3 days), hypoxia (<1% O ₂ for 1 minute) followed by cold exposure (4 °C for 10 minutes) twice daily for 4 days	formula without <i>Bifidobacterium</i> mixture	<i>Bifidobacterium</i> mixture (<i>Bifidobacterium adolescentis</i> , <i>Bifidobacterium breve</i> and <i>Bifidobacterium bifidum</i>) in formula, 1.5*10 ¹⁰ CFU/ml, via gastric tube, once a day after cold exposure, simultaneous with NEC induction	40 rats (N=10 per group)	not provided	histological NEC incidence/severity intestinal barrier function
Lyu et al. 2020	C57BL/6 mice (5-6 weeks old), NEC induction with formula feeding and hypoxia (5% O ₂ , 95% N ₂ for 1 minute) followed by cold exposure (4 °C for 10 minutes) within 1 hour after feeding twice daily for 4 days	saline by gavage	vitamin D by gavage, 0.5 g/kg/day, simultaneous with NEC induction	32 mice (N=8 per group)	not provided	histological NEC incidence/severity NEC signs and symptoms intestinal inflammation, vascular function / hypoxia-ischemia / free radical formation
Maheshwari et al. 2011	Swiss-Webster mice (10-13 days old), NEC induction with formula feeding (200 µL/5 g body weight every 3 hours) and hypoxia (5% O ₂ for 2 minutes twice daily before feedings) for 4 days	no enteral TGF-β2	TGF-β2, 100 ng, single dose in the morning for 4 days, simultaneous with NEC induction	36 rats (N=18 per group)	Not provided	intestinal epithelial cell death / proliferation histological NEC incidence/severity

Table S2.5 (continued)

Author and year	Model used	Control	Intervention	Sample size	Sample size / power calculation	Outcomes studied
Matheson et al. 2014	Sprague-Dawley rats (newborn, 12 hours before scheduled birth), NEC induction with one time gastric administration of LPS (2 mg/kg), formula feeding (starting 100 μ L per feed, increased to 150 μ L per feed at 24 hours and to 200 μ L per feed at 48 hours, every 4-5 hours) and asphyxia (100% N ₂ for 1 minute) and cold exposure (4 °C for 10 minutes) twice daily for 2 days	formula without rat relaxin	rat relaxin in formula, 0.25 ng/0.1 mL in all feeds, simultaneous with NEC induction	48 rats (N=11-13 per group)	not provided	histological NEC incidence/severity NEC signs and symptoms vascular function / hypoxia-ischemia / free radical formation
Maynard et al. 2010	Sprague-Dawley rats (newborn, 1 day before scheduled birth), NEC induction with formula feeding (total volume 850 μ L/day, 6 times a day) and asphyxia (100% N ₂ for 1 minute) and cold exposure (4 °C for 10 minutes) twice daily for 4 days	control cow-milk based formula	rat EGF in cow-milk based formula, 500 ng/mL, simultaneous with NEC induction	60 rats (N=24-36 per group)	not provided	intestinal epithelial cell death
Miyake et al. 2019	C57BL/6 mice (5 days old), NEC induction with enteral administration of LPS (4 mg/kg/day), formula feeding (50 μ L/g, thrice daily) and hypoxia (5% O ₂ for 10 minutes, thrice daily) for 4 days	formula without human breast milk exosomes	human breast milk exosomes from raw milk in formula, simultaneous with NEC induction human breast milk exosomes from pasteurized milk in formula, simultaneous with NEC induction	undlear	not provided	histological NEC incidence/severity intestinal inflammation, intestinal barrier function

Table S2.5 (continued)

Møller et al. 2011	Preterm pigs (92% of gestational age, delivered by caesarian section), NEC induction with parenteral nutrition for the first 2 postnatal days (starting 4 ml/kg/h, after 12h 6 ml/kg/h) and enteral nutrition after 2 days with an oral bolus of 15 ml/kg formula every 3 hours for 1.5 day	deionized water (control for minimal enteral nutrition) control formula without supplementation of OPN, gangliosides or SL	bovine OPN, 2.22 g/L, minimal enteral dose of 5 mg/kg body weight pure OPN in sterile deionized water per 3 hours during parenteral nutrition and 2.2 g/L OPN in formula during full enteral nutrition, simultaneous NEC induction	47 pigs (N=5-13 per group)	not provided	histological NEC incidence/severity digestion and absorption
Nguyen et al. 2014	Preterm pigs (92% of gestational age, delivered by caesarian section), NEC induction with parenteral nutrition for the first 2 postnatal days (starting 4 ml/kg/h on day 1, 6 ml/kg/h on day 2) with minimal enteral feeding (3 mL/kg per 3 hours on day 1 and 5 mL/kg per 3 hours on day 2) and full enteral nutrition after 2 days with an oral bolus of 15 ml/kg formula every 3 hours for 2 days	formula without supplementation of bovine lactoferrin	gangliosides enriched bovine milk fraction in formula, 3 g/L resulting in 0.06 g/L gangliosides, simultaneous with start of enteral feeding SL enriched bovine milk fraction in formula, 60 g/L resulting in 8.7 g/L SL, simultaneous with start of enteral feeding bovine lactoferrin in formula, 10 g/L, during minimal enteral feeding, and full enteral feeding, simultaneous with NEC induction	28 pigs (N=13-15 per group)	not provided	histological NEC incidence/severity intestinal inflammation, intestinal barrier function digestion and absorption

Table S2.5 (continued)

Author and year	Model used	Control	Intervention	Sample size	Sample size / power calculation	Outcomes studied
Nguyen et al. 2016	Preterm pigs (90-92% of gestational age, delivered by caesarian section), NEC induction with parenteral nutrition for the first 2 postnatal days (starting 4 ml/kg/h on day 1, 6 ml/kg/h on day 2) with minimal enteral feeding (3 ml/kg per 3 hours on day 1 and 5 ml/kg per 3 hours on day 2) and full enteral nutrition after 2 days with an oral bolus of 15 ml/kg formula every 3 hours for 2 days	formula without supplementation of bovine lactoferrin	bovine lactoferrin in formula, 10 g/L, during minimal enteral feeding, and full enteral feeding, simultaneous with NEC induction	28 pigs (N=13-15 per group)	not provided	histological NEC incidence/severity intestinal epithelial cell death
Niño et al. 2017	C57BL/6 mice (7-8 days old), NEC induction with administration of enteric bacteria isolated from an infant with NEC in formula, formula feeding (5 times a day for 4 days) and hypoxia (5% O ₂ , 95% N ₂ for 10 minutes, twice daily) for 4 days	no ATRA	ATRA, dissolved in 1:1 DMSO and corn oil, final concentration 6 mg/ml, 50 µg/mouse, administered daily by gavage, simultaneous with NEC induction	at least N=5 per experimental group	not provided	histological NEC incidence/severity intestinal inflammation intestinal epithelial cell death / proliferation
Ohtsuka et al. 2011	Sprague-Dawley rats (newborn on day 20 of gestation), NEC induction with one time orogastric administration of formula (150 µL)	control maternal diet (soybean oil)	DHA enriched diet of mother, 49% DHA, 51% soybean oil of total fat, from day 7 to 20 of gestation, prior to NEC induction EPA enriched diet of mother, 49% EPA, 51% soybean oil of total fat, from day 7 to 20 of gestation, prior to NEC induction	6 pregnant rats (N=2 per group, resulting in N=20-28 pups per group, 11 control pups)	not provided	histological NEC incidence/severity NEC survival intestinal inflammation

Table S2.5 (continued)

Olson et al. 2016	Sprague-Dawley rats (newborn on day 21 of gestation), NEC induction with formula feeding (starting 100 µL per feed and advanced to 400 µL on day 4, 5 times a day) and asphyxia (100% N ₂ for 90 seconds) followed by cold exposure (4 °C for 10 minutes) thrice daily for 4 days	sterile water	<p><i>Lactobacillus reuteri</i> DSM 20016 in sterile water, 1*10⁸ CFU in 100 µL, once via oral gavage immediately after delivery, simultaneous with NEC induction</p> <p><i>Lactobacillus reuteri</i> DSM 20016 grown on unloaded dextranomer microspheres in sterile water, 1*10⁸ CFU in 100 µL, once via oral gavage immediately after delivery, simultaneous with NEC induction</p> <p><i>Lactobacillus reuteri</i> DSM 20016 grown on MRS broth loaded dextranomer microspheres in sterile water, 1*10⁸ CFU in 100 µL, once via oral gavage immediately after delivery, simultaneous with NEC induction</p>	168 rats (N=10-48 per group)	not provided	<p>histological NEC incidence/severity</p> <p>intestinal barrier function</p>
-------------------	--	---------------	--	------------------------------	--------------	---

Table S2.5 (continued)

Author and year	Model used	Control	Intervention	Sample size	Sample size / power calculation	Outcomes studied
Olson et al. 2018	Sprague-Dawley rats (newborn on day 20.5 of gestation), NEC induction with one time intragastric administration of LPS (2 mg/kg), formula feeding (starting 100 μ L per feed and advanced to 400 μ L on day 4, 5 times a day) and asphyxia (<1.5% O ₂ for 90 seconds) followed by cold exposure (4 °C for 10 minutes) thrice daily for 4 days	sterile 0.9% saline	<i>Lactobacillus reuteri</i> DSM 20016 in sterile 0.9% saline, 2*10 ⁸ CFU in 100 μ L, once via oral gavage immediately after delivery, simultaneous with NEC induction	279 rats (N=43-50 per group)	not provided	histological NEC incidence/severity NEC survival intestinal inflammation intestinal barrier function microbiome alterations
			<i>Lactobacillus reuteri</i> DSM 20016 grown on unloaded Sephadex microspheres in sterile 0.9% saline, 2*10 ⁸ CFU in 100 μ L, once via oral gavage immediately after delivery, simultaneous with NEC induction			
			<i>Lactobacillus reuteri</i> DSM 20016 grown on sucrose-loaded dextranomer microspheres in sterile 0.9% saline, 2*10 ⁸ CFU in 100 μ L, once via oral gavage immediately after delivery, simultaneous with NEC induction			

Table S2.5 (continued)

Olson et al. 2018	<p><i>Lactobacillus reuteri</i> DSM 20016 grown on maltose-loaded Sephadex microspheres in sterile 0.9% saline, 2*10⁸ CFU in 100 µL, once via oral gavage immediately after delivery, simultaneous with NEC induction</p>	<p>human breast milk extracellular vesicles in formula, 1*10⁸ with every feed, simultaneous with NEC induction</p>	<p>142 rats (N=13-70 per group)</p>	<p>not provided</p>	<p>histological NEC incidence/severity</p>
Pisano et al. 2020	<p>Sprague-Dawley rats (newborn on day 21 of gestation), NEC induction with one time intragastric administration of LPS (2 mg/kg) with the second feed, formula feeding (starting 100 µL per day and advanced with 100 µL per day to 400 µL on day 4, every 4 hours), hypoxia (<1.5% O₂ for 90 seconds) thrice daily and cold exposure (4 °C for 10 minutes) thrice daily for 4 days</p>	<p>sterile water intraperitoneal</p>	<p>not provided</p>	<p>not provided</p>	<p>histological NEC incidence/severity</p>
Quintanilla et al. 2014	<p>Sprague-Dawley rats (newborn), NEC induction with formula feeding (starting 150 µL per feed on day 1, 4 times daily), hypoxia (5% O₂, 95% N₂ for 10 minutes) thrice daily and cold exposure (4 °C for 10 minutes) thrice daily for 3 days</p>	<p>formula without surfactant protein A</p>	<p>42 rats (N=6-10 per group)</p>	<p>not provided</p>	<p>histological NEC incidence/severity NEC survival intestinal inflammation</p>

Table S2.5 (continued)

Author and year	Model used	Control	Intervention	Sample size	Sample size / power calculation	Outcomes studied
Radulescu et al. 2009	Sprague-Dawley rats (newborn on day 21.5 of gestation), NEC induction with one time intragastric administration of LPS (2 mg/kg) 8 hours after birth, formula feeding (starting 100 µL per feed and advanced as tolerated to 400 µL on day 4, every 4 hours), hypoxia (100% N ₂ for 1 minute) followed by cold exposure (4 °C for 10 minutes) twice daily for 4 days	formula without HB-EGF or EGF	dosing interval experiment: HB-EGF in formula, 800 µg/kg/dose, one / two / three / four or six times a day	203 rats (experiment administration frequency) 199 rats (dosage experiment)	not provided	histological NEC incidence/severity NEC survival
			<i>Escherichia coli</i> vs <i>Pichia pastoris</i> derived HB-EGF comparison experiment: HB-EGF derived from <i>Escherichia coli</i> in formula, 600 / 800 or 1000 µg/kg/dose, four or six times a day	120 rats (comparison HB-EGF and EGF) 137 rats (intervention starting directly after birth or later)		
			HB-EGF derived from <i>Pichia pastoris</i> in formula, 600 / 800 or 1000 µg/kg/dose, four or six times a day			
			HB-EGF and EGF comparison experiment: HB-EGF in formula, 800 µg/kg/dose EGF in formula, 800 µg/kg/dose EGF in formula, 570 µg/kg/dose (molarity equivalent to HB-EGF 800 µg/kg/dose)			

Table S2.5 (continued)

Radulescu et al. 2009	prophylactic vs therapeutic HB-EGF administration experiment: HB-EGF in formula, 800 µg/kg/dose, from first feeding 2h after birth or started at 12, 24, 48 or 72h after birth								
Ran-Ressler et al. 2011	Sprague-Dawley rats (newborn, 1 day before scheduled birth), NEC induction with formula feeding (total volume 850 µL/day, 6 times a day) and asphyxia (100% N ₂ for 1 minute) followed by cold exposure (4 °C for 10 minutes) twice daily for 4 days	rat formula without supplementation of BCFA	20% w/w BCFA mixture in rat formula, 25% iso-14:0, group	73 rats (N=15-35 per rat formula, 25% iso-14:0, group)	Yes, power calculation based on estimated mean and dispersion for NEC scores, α 0.05 and β 80%; required sample size 21	histological NEC incidence/severity			
Rasmussen et al. 2017	Preterm pigs (90-92% of gestational age, delivered by caesarian section), NEC induction with parenteral nutrition for the first 2 postnatal days (4-6 ml/kg/h) with minimal enteral feeding (3 ml/kg per 3 hours) and full enteral nutrition after 2 days with an oral bolus of 15 ml/kg formula every 3 hours for 2 days	control formula without HMO, but with maltodextrin (45-46 g/L)	4 different HMO in formula, 5.0 g/L in most of the experiments, 10 g/L during 4 days'	112 pigs (N=14-23 per group)	not provided	histological NEC incidence/severity	NEC signs and symptoms	intestinal inflammation	intestinal barrier function
	Preterm pigs (90-92% of gestational age, delivered by caesarian section), NEC induction with parenteral nutrition for the first 7 postnatal days (4-6 ml/kg/h) with minimal enteral feeding with slowly increasing amounts (3-17 mL/kg per 3 hours) and full enteral nutrition after 7 days with an oral bolus of 14-17 ml/kg formula every 3 hours for 4 days						NEC signs and symptoms	intestinal inflammation	intestinal epithelial proliferation
									microbiome alterations
									digestion and absorption

Table S2.5 (continued)

Author and year	Model used	Control	Intervention	Sample size	Sample size / power calculation	Outcomes studied
Ren et al. 2019	Preterm pigs (89-92% of gestational age, delivered by caesarian section), IA LPS from E. Coli 055:B5 1 mg in an area close to the mouth at 103 days of gestational age, NEC induction by parenteral nutrition (amount gradually decreasing from 96/ml/kg/day to 48 ml/kg/day) and enteral nutrition (gradually increasing from 24 ml/kg/day to 120 ml/kg/day) for 5 days	formula without supplemented OPN or CGMP	OPN in formula, 2.2 g/L, simultaneous with NEC induction CGMP in formula, 30 g/L, simultaneous with NEC induction	44 pigs (N=10-12 per group)	not provided	histological NEC incidence/severity intestinal inflammation, intestinal barrier function
Rentea et al. doi: 10.1016/j.jpedsurg.2012.03.018 2012	Sprague-Dawley rats (newborn, 1 day before scheduled birth), NEC induction with enteral administration of LPS (2 mg/kg LPS) per feed, formula feeding and hypoxia (5% O ₂ , 95% N ₂ for 10 minutes thrice daily) for 4 days	formula without supplemented IAP	IAP in formula, 0.4 U/kg, once daily, simultaneous with NEC induction IAP in formula, 4 U/kg, once daily, simultaneous with NEC induction IAP in formula, 40 U/kg, once daily, simultaneous with NEC induction	N=10-31 per group	not provided	histological NEC incidence/severity intestinal barrier function

Table S2.5 (continued)

<p>Rentea et al. doi: 10.1016/j.jss.2012.05.039 2012</p>	<p>Sprague-Dawley rats (newborn, 1 day before scheduled birth), NEC induction with enteral administration of LPS (2 mg/kg LPS) per feed, formula feeding every 4 hours and hypoxia (5% O₂, 95% N₂ for 10 minutes thrice daily) for 3 days</p>	<p>formula without supplemented IAP</p>	<p>IAP in formula, 0.4 U/kg, once daily, simultaneous with NEC induction</p> <p>IAP in formula, 4 U/kg, once daily, simultaneous with NEC induction</p> <p>IAP in formula, 40 U/kg, once daily, simultaneous with NEC induction</p>	<p>N=7-17 per group</p>	<p>not provided</p>	<p>systemic inflammation</p>
<p>Rentea et al. 2013</p>	<p>Sprague-Dawley rats (newborn, 1 day before scheduled birth), NEC induction with enteral administration of LPS (2 mg/kg LPS) per feed, formula feeding every 4 hours and hypoxia (5% O₂, 95% N₂ for 10 minutes) thrice daily for 1 day</p>	<p>formula without supplemented IAP</p>	<p>IAP in formula, 0.4 U/kg, once daily, simultaneous with NEC induction</p> <p>IAP in formula, 4 U/kg, once daily, simultaneous with NEC induction</p> <p>IAP in formula, 40 U/kg, once daily, simultaneous with NEC induction</p>	<p>at least N=7 per group</p>	<p>not provided</p>	<p>intestinal inflammation</p> <p>intestinal barrier function</p> <p>vascular function / hypoxia-ischemia / free radical formation</p>

Table S2.5 (continued)

Author and year	Model used	Control	Intervention	Sample size	Sample size / power calculation	Outcomes studied
Rudloff et al. 2019	Preterm pigs (90-92% of gestational age, delivered by caesarian section), NEC induction with parenteral nutrition for the first 2 postnatal days (4-6 ml/kg/h) with minimal enteral feeding (3 ml/kg per 3 hours) and full enteral nutrition after 2 days with an oral bolus of 15 ml/kg formula every 3 hours for 2 days	control formula without HMO, but with maltodextrin (45-46 g/L)	4 different HMO in formula, 5.0 g/L in most of the experiments, 10 g/L during 4 days' minimal enteral nutrition of the longer study period (0.16-0.64 g/kg/day during these 4 days), the 4 HMO cover the most abundant HMO in milk and represent the characteristic features of naturally occurring HMO, simultaneous with NEC induction	112 pigs (N=30-44 per group)	not provided	microbiome alterations
Satoh et al. 2016	Preterm pigs (90-92% of gestational age, delivered by caesarian section), NEC induction with parenteral nutrition for the first 7 postnatal days (4-6 ml/kg/h) with minimal enteral feeding with slowly increasing amounts (3-17 ml/kg per 3 hours) and full enteral nutrition after 7 days with an oral bolus of 14-17 ml/kg formula every 3 hours for 4 days	formula without <i>Bifidobacterium breve</i> M-16V	more than 25 different HMO in formula, 7.0 g/L, more than 25 HMO mimicking the naturally occurring HMO in human milk), simultaneous with NEC induction <i>Bifidobacterium breve</i> M-16V in formula, 6*10 ⁷ CFU per day	60 rats (N=17-23 per group)	not provided	histological NEC incidence/severity NEC survival intestinal inflammation intestinal barrier function intestinal epithelial cell death

Table S2.5 (continued)

Shen et al. 2019	Sprague-Dawley rats (newborn), NEC induction with formula feeding (200 µL every 4 hours on the first day, increasing with 50 µL in the subsequent day) and asphyxia (100% N ₂ for 1.5 minute) followed by cold stress (4 °C for 10 minutes) twice daily for 4 days	formula without supplemented lactadherin	lactadherin in formula, 10 µg/g/day, simultaneous with NEC induction	not provided	histological NEC incidence/severity NEC signs and symptoms NEC survival
Sheng et al. 2014	Sprague-Dawley rats (newborn on day 21.5 of gestation), NEC induction with formula feeding (100 µL every 4h and increased to 300-400 µL if tolerated) and asphyxia (100% N ₂ for 60 seconds) followed by cold exposure (4°C for 10 minutes) twice daily for 4 days	saline	human β defensin, 100 µg/kg in 100 µL, daily before asphyxia, simultaneous with NEC induction	68 rats (N=12-24 per group) not provided	intestinal barrier function histological NEC incidence/severity NEC signs and symptoms NEC survival
Shiou et al. 2011	Sprague-Dawley rats (newborn on day 20 of gestation), NEC induction with formula feeding (100 µL every 3 hours, incrementally increased to 250 µL) and hypoxia (5% O ₂ , 95% N ₂ for 10 minutes, thrice daily) for 5 days	formula without supplemented EPO or TGF-β	EPO in formula, 0.1 unit/mL, simultaneous with NEC induction TGF-β in formula, 30 ng/mL, simultaneous with NEC induction	132 rats (N=20-56 per group) not provided	intestinal barrier function histological NEC incidence/severity intestinal barrier function

Table S2.5 (continued)

Author and year	Model used	Control	Intervention	Sample size	Sample size / power calculation	Outcomes studied
Shiou et al. 2013	Sprague-Dawley rats (newborn on day 20 of gestation), NEC induction with 10 ⁷ CFU of both <i>Serratia marcescens</i> , <i>Klebsiella pneumoniae</i> and <i>Streptococcus viridans</i> , formula feeding every 3 hours and hypoxia (5% O ₂ , 95% N ₂ for 10 minutes, thrice daily) for 5 days	vehicle	TGF- β 1 in formula, 30 ng/ml, simultaneous with NEC induction	116 rats (N=20-48 per group)	not provided	histological NEC incidence/severity intestinal inflammation
Siggers et al. 2008	Preterm pigs (107d of gestational age, delivered by caesarian section), NEC induction with parenteral nutrition for the first 36 postnatal hours (starting 4 ml/kg/h, after 12h 6 ml/kg/h) and full enteral nutrition after 36 hours with an oral bolus of 15 ml/kg formula every 3 hours for 2 days	peptone water placebo	probiotic mixture in 1% peptone water, <i>Bifidobacterium animalis</i> DSM15954, <i>Lactobacillus acidophilus</i> DSM13241, <i>Lactobacillus casei</i> ATCC55544, <i>Lactobacillus pentosus</i> DSM14025 and <i>Lactobacillus plantarum</i> DSM13367 all strains 10 ⁸ CFU/gram viable lyophilized bacteria, total concentration of 5*10 ⁹ CFU/3 mL peptone water, 2 mL/kg birth weight administered every 6 hours during period of parenteral nutrition and every 3 hours during period of enteral nutrition	28 pigs (N=5-13 per group)	not provided	histological NEC incidence/severity microbiome alterations digestion and absorption

Table S2.5 (continued)

Siggers et al. 2013	<p>Preterm pigs (92% of gestational age, delivered by caesarian section), NEC induction with parenteral nutrition for the first 2 postnatal days (starting 4 ml/kg/h, after 12h 6 ml/kg/h) and full enteral nutrition after 2 days with an oral bolus of 15 ml/kg formula every 3 hours for 2 days</p> <p>Preterm pigs (92% of gestational age, delivered by caesarian section), NEC induction with exclusive parenteral nutrition for the first 2 postnatal days (starting 4 ml/kg/h, after 12h 6 ml/kg/h) and declining parenteral feeding and gradually increasing enteral nutrition after 2 days with an oral bolus of formula every 3 hours reaching 15 ml/kg after 9 hours for 2 days</p>	<p>formula without porcine amniotic fluid</p> <p>porcine amniotic fluid, 10 ml/kg pure bolus during parenteral nutrition every 3 hours and as water fraction (80%) in 15 ml/kg formula during full enteral nutrition, simultaneous with NEC induction</p> <p>porcine amniotic fluid, as water fraction (80%) in 15 ml/kg formula during full enteral nutrition, on postnatal day 3-4</p>	<p>30 pigs (N=7-13 per group)</p> <p>not provided</p>	<p>histological NEC incidence/severity</p> <p>NEC signs and symptoms</p> <p>intestinal inflammation</p> <p>vascular function / hypoxia-ischemia / free radical formation</p> <p>microbiome alterations</p> <p>digestion and absorption</p>
Sodhi et al. 2018	<p>C57BL/6J mice (7-8 days old), NEC induction with supplementation of enteric bacteria isolated from an infant with severe NEC (12.5 µL stool slurry in 1 mL formula) in formula feeding (50 µL/g, 5 times a day) and hypoxia (5% O₂, 95% N₂ for 10 minutes twice daily) for 4 days</p>	<p>control formula, 100% TAG-rich oils; mixture of 39% high oleic safflower oil, 29% soya oil and 27.9% coconut oil; 146 mg/L DHA, 312 mg/L AA</p> <p>pre-digested formula, 50% TAG-rich oils; 17.5% soybean NEFA, 20% 2-monoacylglycerol palmitate, 10.3% phospholipid lecithin, 34.8% high oleic safflower oil, 14.8% coconut oil, 135 mg/L DHA, 322 mg/L AA, simultaneous with NEC induction</p>	<p>at least N=8 per group</p> <p>not provided</p>	<p>histological NEC incidence/severity</p> <p>NEC signs and symptoms</p> <p>intestinal inflammation</p> <p>vascular function / hypoxia-ischemia / free radical formation</p>

Table S2.5 (continued)

Author and year	Model used	Control	Intervention	Sample size	Sample size / power calculation	Outcomes studied
Sodhi et al. 2018	very low fat formula, 161 mg/L DHA, 355 mg/L AA, fat replaced by lactose, simultaneous with NEC induction					
Sodhi et al. 2020	C57BL/6J mice (7-8 days old), NEC induction with supplementation of enteric bacteria isolated from an infant with severe NEC (12.5 µL stool slurry in 1 mL formula) in formula feeding (50 µL/g, 5 times a day) and hypoxia (5% O ₂ , 95% N ₂ for 10 minutes twice daily) immediately after feed for 4 days	formula without supplemented 2'-FL, 6'-SL, lactose or GOS	2'-FL in formula, 10 mg/kg, 200 µL/mouse, simultaneous with NEC induction 6'-SL in formula, 10 mg/kg, 200 µL/mouse, simultaneous with NEC induction lactose in formula, 10 mg/kg, 200 µL/mouse, simultaneous with NEC induction GOS in formula, 10 mg/kg, 200 µL/mouse, simultaneous with NEC induction	at least N= 5 per group	not provided	histological NEC incidence/severity NEC signs and symptoms intestinal inflammation vascular function / hypoxia-ischemia / free radical formation, intestinal epithelial cell death

Table S2.5 (continued)

Sodhi et al. 2020	Yorkshire piglets (~90% gestation, caesarian delivery), NEC with supplementation of enteric bacteria isolated from an infant with surgical NEC (12.5 µL stool slurry in 1 mL formula) in formula feeding (15 mL/kg every 3 hours) for 4 days	formula without supplemented 2'-FL or 6'-SL	2'-FL in formula, 10 mg/ml, simultaneous with NEC induction 6'-SL in formula, 10 mg/ml, simultaneous with NEC induction 2'-FL + 6'-SL in formula, 5 mg/ml each, simultaneous with NEC induction	at least N= 4 per group	not provided	histological NEC incidence/severity NEC signs and symptoms intestinal inflammation vascular function / hypoxia-ischemia / free radical formation, intestinal epithelial cell death histological NEC incidence/severity intestinal barrier function intestinal epithelial proliferation histological NEC incidence/severity NEC signs and symptoms intestinal inflammation vascular function / hypoxia-ischemia / free radical formation
Su et al. 2013	Friend Virus B-Type mice (newborn on day 18.5 of gestation), NEC induction with formula feeding (30 µL every 3 hours and increased to a maximum of 50 µL per feed at day 4) and asphyxia (100% N ₂ for 1 minute) and cold exposure (4 °C for 10 minutes) once daily for 4 days	formula without HB-EGF	HB-EGF in formula, 800 µg/kg/dose, added to each feed, simultaneous with NEC induction	182 mice (N=15-67 per group)	not provided	histological NEC incidence/severity intestinal barrier function intestinal epithelial proliferation
Tang et al. 2019	C57BL/6J mice (10 day old), NEC induction with formula feeding (300~500 µL/g, 5 times a day) and hypoxia (N ₂ 12 L/min for 1.5 minute) and cold exposure (4 °C for 10 minutes) thrice daily for 3 days	PBS	<i>Lactobacillus reuteri</i> DSM17938, 10 ⁶ CFU/g/day dissolved in PBS at 10 ⁷ CFU/mL, intragastric once every day, simultaneous with NEC induction	96 mice (N=32 per group)	not provided	histological NEC incidence/severity NEC signs and symptoms intestinal inflammation vascular function / hypoxia-ischemia / free radical formation

Table S2.5 (continued)

Author and year	Model used	Control	Intervention	Sample size	Sample size / power calculation	Outcomes studied
Tian et al. 2017	Sprague-Dawley rats (3 days old), NEC induction with formula feeding (150 μ L 4 times a day on day 1 and increased 100 μ L per feed per day) and hypoxia (100% N ₂ for 1.5 minute) followed by cold exposure (4 °C for 10 minutes) thrice daily for 3 days	Formula without supplemented IGF1	IGF1 in formula, 22 mg/L simultaneous with NEC induction	60 rats (N=20 per group)	not provided	histological NEC incidence/severity NEC signs and symptoms, intestinal inflammation
Wang et al. doi: 10.1002/mmf.r.201900262 2019	C57BL/6 mice (7 days old), NEC induction with enteral LPS (4 mg/kg/day) on postnatal day 7 (part of the animals), formula feeding (100-200 μ L every 8 hours) and hypoxia (5% O ₂ , 95% N ₂ for 10 minutes) followed by cold exposure (4 °C for 10 minutes) thrice daily for 3 days	formula without supplemented HMO	HMO in formula, 20 g/L simultaneous with NEC induction	90 mice (N=13-15 per group)	not provided	intestinal barrier function histological NEC incidence/severity NEC survival intestinal inflammation systemic inflammation
Wang et al. doi: 10.1002/mmf.r.201801247 2019	Sprague-Dawley rats (10 days old), NEC induction with formula feeding (50 μ L/8 body weight 3 times per day) and hypoxia (5% O ₂ , 95% N ₂ for 5 minutes twice daily) for 4 days	formula without supplemented human breast milk exosomes	human breast milk exosomes in formula, 200 μ g/mL, isolated from lactating mothers who had delivered preterm infants (24-36 weeks), simultaneous with NEC induction	unclear	not provided	intestinal epithelial proliferation histological NEC incidence/severity intestinal epithelial cell proliferation

Table S2.5 (continued)

Wang et al. 2020	C57BL/6 mice (7 days old), NEC induction with formula feeding (100-200 µL every 8 hours) and hypoxia (5% O ₂ , 95% N ₂ for 10 minutes) followed by cold exposure (4 °C for 10 minutes) thrice daily for 3 days	formula without supplemented HMO	HMO in formula, 5 g/L, simultaneous with NEC induction HMO in formula, 10 g/L, simultaneous with NEC induction HMO in formula, 20 g/L, simultaneous with NEC induction	70 mice (N=10-15 per group)	not provided	histological NEC incidence/severity NEC survival intestinal inflammation systemic inflammation intestinal epithelial cell death / proliferation intestinal barrier function enteric nervous system
Wei et al. doi:10.1038/pr.2015.63 2015	C57BL/6 mice (newborn), NEC induction with formula feeding (300 µL every 3 hours on day 1 and increased to a maximum of 500 µL per feed on day 4) and asphyxia (100% N ₂ for 1 minute) followed by cold exposure (4 °C for 10 minutes) twice daily for 4 days	formula without supplemented HB-EGF	HB-EGF in formula, 800 µg/kg per dose in each feed, simultaneous with NEC induction	246 mice (N=22-49 per group)	not provided	histological NEC incidence/severity intestinal inflammation histological NEC incidence/severity
Wei et al. doi: 10.1016/j.jss.2015.03.023 2015	C57BL/6 mice (newborn), NEC induction with formula feeding and hypoxia (5% O ₂ , 95% N ₂ for 1 minute) followed by cold exposure (4 °C for 10 minutes) twice daily for 4 days	formula without supplemented HB-EGF	HB-EGF in formula, 800 µg/kg per dose in each feed, simultaneous with NEC induction	92 mice (N=17-48 per group)	not provided	histological NEC incidence/severity intestinal inflammation
Whitehouse et al. 2010	Sprague-Dawley rats (newborn), NEC induction with formula feeding (200 µL thrice daily) supplemented with LPS IAP (2 mg/kg per feed, all or part of the feeds) and hypoxia (5% O ₂ for 10 minutes thrice daily) for 4 days	formula without supplemented bovine calf formula, four glycine units in the morning feed, simultaneous wit NEC induction	bovine calf IAP in formula, four glycine units in the morning feed, simultaneous wit NEC induction	89 rats (N=13-28 per group)	not provided	histological NEC incidence/severity

Table S2.5 (continued)

Author and year	Model used	Control	Intervention	Sample size	Sample size / power calculation	Outcomes studied
Wu et al. 2017	Sprague-Dawley rats (newborn on day 20-21 of gestation), NEC induction with formula feeding (150 μ L every 4 hours and increased to a maximum of 200 μ L per feed after 1 day if tolerated) and asphyxia (100% N ₂ for 1.5 minute) followed by cold exposure (4 °C for 10 minutes) twice daily for 3 days	formula without bacterial strain	<i>Bifidobacterium adolescentis</i> in formula, 1.0*10 ⁸ per day	45 rats (N=14-16 per group)	not provided	histological NEC incidence/severity NEC signs and symptoms NEC survival intestinal inflammation
Wu et al. 2019	C57BL/6 mice (5 days old), NEC induction with enteral administration of LPS (4 mg/kg/day) on postnatal day 6-7, formula feeding (50 μ L/g, thrice daily) and hypoxia (5% O ₂ for 10 minutes, thrice daily) for 5 days	lactose in formula, 2 mg/g/day	HMO from pooled mature breast milk in formula, 20 mg/mL (2% weight/volume), daily HMO intake 2-3 mg/g body weight, simultaneous with NEC induction	at least N=6 per group	not provided	histological NEC incidence/severity NEC signs and symptoms intestinal barrier function
Xiao et al. 2018	C57BL/6j mice (8 days old), NEC induction with formula feeding (every 4 hours) and asphyxia (100% N ₂ for 1 minute) followed by cold exposure (4 °C for 10 minutes) twice daily for 3 days	PBS	some experiments rutin hydrate, 0.5 mg/g body weight/day (protein disulfide isomerase antagonist) added to formula, simultaneous with NEC induction vitamin A, 20 IU, intragastric once daily from postnatal day 1-7, prior to NEC induction	24 mice (N=12 per group)	not provided	histological NEC incidence/severity intestinal inflammation, intestinal barrier function microbiome alterations

Table S2.5 (continued)

Xu et al. 2013	Sprague-Dawley rats (newborn), NEC induction with formula feeding (100 µL every 4 hours and increased if tolerated by 50 µL every 3 feeds to a maximum of 400 µL per feed on day 4) and asphyxia (100% N ₂ for 1 minute) followed by cold exposure (4 °C for 10 minutes) twice daily for 4 days	Formula without supplemented GD3	GD3 in formula, 15 µg/mL, simultaneous with NEC induction	90 rats (N=30 per group)	not provided	histological NEC incidence/severity NEC signs and symptoms intestinal inflammation
Yakut et al. 2020	Wistar rats (newborn), NEC induction with one time intraperitoneal LPS (1 mg/kg in distilled water from E. coli O111:B4) on the first day, formula feeding (starting 200 µL every 3 hours and daily increased by 100 µL if tolerated) and asphyxia (100 CO ₂ for 10 minutes), hyperoxia (97% O ₂ for 5 minutes) and cold exposure (4 °C for 5 minutes) twice daily for 3 days	distilled water	Foeniculum vulgare extract in distilled water, 200 mg/kg/day, 0.8 ml/kg/day, oral once daily, simultaneous with NEC induction	42 rats (N=12 per group)	not provided	histological NEC incidence/severity NEC signs and symptoms intestinal inflammation, vascular function / hypoxia-ischemia / free radical formation intestinal epithelial cell death histological NEC incidence/severity NEC signs and symptoms NEC survival intestinal barrier function
Yang et al. 2012	Sprague-Dawley rats (newborn on day 21.5 of gestation), NEC induction with formula feeding (starting 100 µL every 4 hours and increased to a maximum of 400 µL per feed on day 4) and asphyxia (100% N ₂ for 1 minute) followed by cold stress (4 °C for 10 minutes) twice daily for 4 days	Formula without supplemented HB-EGF	HB-EGF in formula, 800 µg/kg per dose in each feed, simultaneous with NEC induction	197 rats (N=10-43 per group)	not provided	histological NEC incidence/severity NEC signs and symptoms NEC survival intestinal barrier function

Table S2.5 (continued)

Author and year	Model used	Control	Intervention	Sample size	Sample size / power calculation	Outcomes studied
Yang et al. 2020	Sprague-Dawley rats (2 days old), NEC induction with enteral LPS (5 mg/ml) from day 3 of experiment (5 days old) and formula feeding (starting 200 µL every 4 hours and increased to 300 µL per feed) for 8 days	formula without supplementation of glutamine or MPLs	glutamine in formula, 200 mg/kg, simultaneous with NEC induction MPLs in formula, 50 mg/kg, simultaneous with NEC induction MPLs in formula, 100 mg/kg, simultaneous with NEC induction	72 rats (N=12 per group)	not provided	histological NEC incidence/severity NEC signs and symptoms intestinal inflammation intestinal epithelial cell death
Yin et al. 2020	Rats (newborn), NEC induction with hypoxia (5% O ₂ for 10 minutes) and hypothermia (8 °C for 10 minutes)	1% gum acacia solution	MPLs in formula, 200 mg/kg, simultaneous with NEC induction curcumin dissolved in 1% gum acacia solution, 20 mg/kg (low dose), orally administered	20 rats	not provided	histological NEC incidence/severity intestinal inflammation, intestinal epithelial cell death
Yu et al. 2009	Sprague-Dawley rats (newborn on day 21 of gestation), NEC induction with one time intragastric LPS (2 mg/kg) 8 hours after birth, formula feeding (100 µL every 4 hours and increased to a maximum of 400 µL per feed) and asphyxia (100% N ₂ for 1 minute) followed by cold exposure (4 °C for 10 minutes) twice daily for 1,2 or 3 days	formula without supplemented HB-EGF	curcumin dissolved in 1% gum acacia solution, 50 mg/kg (high dose), orally administered HB-EGF in formula, 800 µg/kg per dose in each feed, simultaneous with NEC induction	128 rats (N=63-65 per group)	not provided	histological NEC incidence/severity vascular function / hypoxia-ischemia / free radical formation

Table S2.5 (continued)

Yu et al. 2013	Sprague-Dawley rats (newborn, 1 day before scheduled birth), NEC induction with 10 ⁷ CFU of both <i>Serratia marcescens</i> , <i>Klebsiella pneumoniae</i> and <i>Streptococcus viridans</i> in 100 µL formula once daily, formula feeding (100 µL every 3 hours, incrementally increased to 250 µL) and hypoxia (5% O ₂ , 95% N ₂ for 10 minutes thrice daily) for 5 days	Formula without supplemented EPO	EPO in formula, 0.1 µg/mL, simultaneous with NEC induction	not provided	intestinal epithelial cell death
Yu et al. 2014	Sprague-Dawley rats (newborn), NEC induction with formula feeding (200 µL twice daily) and hypoxia (5% O ₂ , 95% N ₂ for 10 minutes thrice daily) for 4 days	formula without added HMO, GOS or synthetic disialyl glycans	HMO in formula, 2 mg/mL, simultaneous with NEC induction GOS in formula, 2 mg/mL, simultaneous with NEC induction	not provided	histological NEC incidence/severity
			DSLNT (synthetic disialyl glycan) in formula, 300 mg/ml, simultaneous with NEC induction		
			3''-sLNT (synthetic monosialyl glycan) in formula, 300 mg/ml, simultaneous with NEC induction		
			DS'LNT (synthetic disialyl glycan) in formula, 300 mg/ml, simultaneous with NEC induction		

Table S2.5 (continued)

Author and year	Model used	Control	Intervention	Sample size	Sample size / power calculation	Outcomes studied
Yu et al. 2014			GD3 (synthetic disialyl glycan) in formula, 300 mg/ml, simultaneous with NEC induction			
			DSLac (synthetic disialyl glycan) in formula, 300 mg/ml, simultaneous with NEC induction			
			HMO in formula, 10 mg/ml, simultaneous with NEC induction	139 rats (N=9-22 per group)	not provided	histological NEC incidence/severity
Yu et al. 2017	Sprague-Dawley rats (newborn), NEC induction with formula feeding (200 μ L twice daily) and hypoxia (5% O ₂ , 95% N ₂ for 10 minutes) thrice daily for 4 days	formula without added HMO or synthetic disialyl glycans	Neu5Gc-DS'LNT (synthetic disialyl glycan) in formula, 300 μ M, simultaneous with NEC induction			
			DS'LNT (synthetic disialyl glycan) in formula, 300 μ M, simultaneous with NEC induction			
			DSTa (synthetic disialyl glycan) in formula, 300 μ M, simultaneous with NEC induction			
			DSGalB (synthetic disialyl glycan) in formula, 300 μ M, simultaneous with NEC induction			

Table S2.5 (continued)

Yu et al. 2017			DSLNT (synthetic disialyl glycan) in formula, 300 µM, simultaneous with NEC induction		
Zhang et al. 2019	Sprague-Dawley rats (newborn), NEC induction with formula feeding (150 µL every 4 hours, incrementally increased to 300-400 µL per feed) and hypoxia (5% O ₂ , 95% N ₂ for 1.5 minute) followed by cold exposure (4 °C for 10 minutes) twice daily for 4 days	formula without supplemented MFGM	DSLNT (synthetic disialyl glycan) in formula, 300 µM, simultaneous with NEC induction MFGM in formula, 6 g/L, simultaneous with NEC induction MFGM in formula, 12 g/L, simultaneous with NEC induction	62 rats (N=12-20 per group)	not provided histological NEC incidence/severity NEC signs and symptoms NEC survival intestinal inflammation
Zhou et al. 2014	Sprague-Dawley rats (newborn on day 21 of gestation), NEC induction with formula feeding (starting 150 µL per feed every 4 hours, after 24h 200µL per feed), followed by asphyxia (N ₂ flow 10 L/minute, after reaching 0% O ₂ for 1.5 minute) and cold stress (4 °C for 10 minutes) twice daily for 3 days	formula without supplemented glutamine	glutamine in formula, 0.3g/kg, simultaneous with NEC induction	60 rats (N=20 per group)	not provided vascular function / hypoxia-ischemia / free radical formation histological NEC incidence/severity intestinal inflammation intestinal epithelial cell death

Table S2.5 (continued)

Author and year	Model used	Control	Intervention	Sample size	Sample size / power calculation	Outcomes studied
Zhou et al. 2015	Sprague-Dawley rats (newborn), NEC induction with intragastric LPS (30 mg/kg in sterile water) once daily and formula feeding (starting 100 µL per feed every 4 hours and increased with 50 µL every 12 hours with a maximum of 300 µL per feed) for 3 days	formula without Bifidobacterium microcapsules	Bifidobacterium microcapsules in formula, 1 *10 ¹⁰ CFU/ml, once daily, simultaneous with NEC induction	75 rats (N=15 per group)	not provided	histological NEC incidence/severity intestinal inflammation
Zhou et al. 2017	Sprague-Dawley rats (newborn on day 21 of gestation), NEC induction with one time intragastric LPS (2 mg/kg) 8 hours after birth, formula feeding and asphyxia (100% N ₂ for 1 minute) followed by cold exposure (4 °C for 10 minutes) twice daily for 4 days	formula without supplemented HB-EGF	HB-EGF in formula, 800 µg/kg per dose in each feed, simultaneous with NEC induction	at least N=3 per group	not provided	enteric nervous system alterations
Zhu et al. 2020	Sprague-Dawley rats (1 day old), NEC induction enteral administration of LPS (10 mg/kg) once daily, formula feeding (400 µL 4 times a day) and hypoxia (N ₂ flow 15 L/minute, after reaching 0% O ₂ for 1.5 minute) followed by cold exposure (4 °C for 10 minutes) twice daily for 3 days	no fish oil	fish oil, 35% DHA and EPA in total, 0.6 mL/100g/day, once daily for 7 days prior to NEC induction	96 rats (N=32 per group)	not provided	histological NEC incidence/severity NEC signs and symptoms intestinal inflammation intestinal epithelial cell death

AA: arachidonic acid; AMP, adenosine monophosphate; ATRA: all-trans retinoic acid; BCFA: branched chain fatty acids; CFU, colony forming units; CGMP: caseinoglycomacropeptide; CMP, Cytidine monophosphate; DHA: docosahexaenoic acid; DMSO, Dimethylsulfoxide; DSGalB, disialyl galactobiose; DSLINT, disialyl lacto-N-tetraose; DSLNnt, disialyl lacto-N-neotetraose; DS'LNT, a2-6-linked disialyl lacto-N-tetraose; DS'LNTnT, a2-6-linked disialyl lacto-N-tetraose; DSLac, disialyl lactose; DSTa, disialyl T-antigen tetraose; 3'''-sLNT, 3'''-sialyl lacto-N-neotetraose; EGF: epidermal growth factor; EPA: eicosapentaenoic acid; EPO: erythropoietin; 2'-FL: 2'-fucosyllactose; FOS, fructo-oligosaccharides; G-CSF: granulocyte colony-stimulating factor; GD3: ganglioside D3; GMP, guanosine monophosphate; GOS, galacto-oligosaccharides; HB-EGF: hemoglobin-binding EGF-like growth factor; HGF, hepatocyte growth factor; HMO: human milk oligosaccharides; IAP: intestinal alkaline phosphatase; IGF1: insulin-like growth factor 1; IMP, inosine monophosphate; LC-FOS: long chain fructo-oligosaccharides; MFGM: milk fat globule membrane; MPL: milk polar lipids; NEC: necrotizing enterocolitis; NEFA, non-esterified fatty acid; OPN: osteopontin; PAF-AH, platelet activating factor acetylhydrolase; PUFA: polyunsaturated fatty acids; SC-GOS: short chain galacto-oligosaccharides; SL: sialic acids; 6'-SL: 6'-sialyllactose; TAG, Triacylglycerol; TGF-β: transforming growth factor β; UMP, uridine monophosphate.

Table S2.6 Overview included clinical trials on enteral feeding interventions for prevention of NEC in human infants.

Author and year	Type of study and sample size	In- and exclusion criteria	Control	Intervention	Sample size / power calculation	Primary / secondary outcome measures
Akin et al. 2014	single center RCT N=50 neonates	Inclusion: in hospital born, birth weight <1500 g or gestational age <32 weeks at Ankara University School for Medicine between December 2009 and January 2011 Exclusion: lack of parental consent, severe congenital anomalies, severe perinatal asphyxia, expiring before allocation to treatment group in the first 72h	2 mL saline once a day throughout the hospitalization period after the baby reached 20 ml/kg/feeding/day feeding volume (N=25 neonates)	bovine lactoferrin, 200 mg/day throughout the hospitalization period after the baby reached 20 ml/kg/feeding/day feeding volume (N=25 neonates)	not provided	Primary outcome(s): tolerability and effectiveness of bovine lactoferrin 200 mg/day in the prevention of nosocomial sepsis, NEC and mortality Secondary outcome(s): effect of maturation and bovine lactoferrin on Treg levels
Collins et al. 2017	multi center RCT N=1205 neonates	Inclusion: infants <29 weeks that started on enteral feeding in the previous 3 days at one of 13 centers in Australia, New Zealand and Singapore from June 18th 2012 to September 30th 2015. Exclusion: lack of parental consent, major congenital or chromosomal anomalies, participating in another trial of fatty acid supplementation or receiving intravenous lipids containing fish oil or receiving breastmilk from a mother taking DHA supplements at a dose of more than 250 mg per day	soy emulsion emulsified with 1% lecithin and containing 20% total fat and 6% protein 0.5 mL of the soy emulsion contained 55 mg of linoleic acid, 5.7 mg of alpha-linolenic acid, 4.8 mg vitamin C and 0.01 mg vitamin E emulsion was enterally administered at dose of 0.17 ml/kg/body weight three times daily (total 0.5 ml/kg bodyweight/day) immediately before feeding via a naso-gastric orogastric tube (N=613 neonates)	DHA emulsion with a microencapsulated aqueous emulsion of fractionated tuna oil (70% of total oil as DHA in triglyceride form); emulsified 1% lecithin and containing 20% total fat and 6% protein 0.5 mL of the DHA emulsion contained 60 mg of DHA, 4 mg of EPA, 4.6 mg vitamin C, 0.05 mg vitamin E emulsion was enterally administered at dose of 0.17 ml/kg/body weight three times daily (total 0.5 ml/kg bodyweight/day) immediately before feeding via a nasogastric orogastric tube (N=592 neonates)	Yes, power calculation based on estimated absolute effect of 10 percent point and a 19% relative difference in incidence of bronchopulmonary dysplasia, power 90%; α 0.05; required sample size 1244 (622 per group)	Primary outcome(s): incidence of physiological bronchopulmonary dysplasia Secondary outcome(s): secondary respiratory outcomes, retinopathy of prematurity, intraventricular hemorrhage, sepsis, NEC and measures of safety and tolerance

Table S2.6 (continued)

Author and year	Type of study and sample size	In- and exclusion criteria	Control	Intervention	Sample size / power calculation	Primary / secondary outcome measures
El-Ganzoury et al. 2014	single center RCT N=90 neonates	Inclusion: gestational age \leq 33 weeks at the NICU of Ain-Shams University hospitals between March 2013 and March 2014. Exclusion: lack of parental consent, congenital or acquired anomalies of the gastrointestinal tract and previous use of cytokines or intravenous immunoglobulin.	1 mL of distilled water once daily (N=30 neonates)	recombinant EPO, single enteral daily dose of 80 IU/kg (N=20 neonates) recombinant G-CSF, single enteral daily dose of 4.5 μ g/kg (N=20 neonates) recombinant EPO, single enteral daily dose of 80 IU/kg, and recombinant G-CSF, single enteral daily dose of 4.5 μ g/kg (N=20 neonates)	Yes, power calculation based on mean total time to full enteral feeding of 35 +/- 5 days, estimated 30% relative difference time to full enteral feeding, power 80%; α 0.05; required sample size 20	Primary outcome(s): time to full enteral feeding Secondary outcome(s): weight gain, NEC incidence, NEC related death, length of hospital stay, hospital readmission, adverse effects of treatment
Hosseini et al. 2019	single center RCT N=150 neonates	Inclusion: gestational age \leq 28 weeks, birth weight <1250, appropriate for gestational age between June 21st 2016 and February 19th 2018. Exclusion: lack of parental consent, severe birth asphyxia, chromosome anomalies, congenital heart disease, congenital intestinal obstruction, omphalocele, gastroschisis, ml per os for more than 3 weeks	routine feeding without any administration (N=50 neonates)	all interventions started on the day of start of enteral feeding and continued until enteral intake reached 100 ml/kg/day or after a maximum of 7 days synthetic amniotic fluid (containing sodium chloride, sodium acetate, potassium chloride and G-CSF), 5 ml/kg/day (N=50 neonates) recombinant human EPO dissolved in synthetic amniotic fluid (containing sodium chloride, sodium acetate, potassium chloride and G-CSF) 4400 mU/ml (N=50 neonates) all interventions started 3 days after birth and were continued for 21 days	not provided	Primary/secondary outcome(s): gastric residual volume, vomiting, NEC (stage \geq 2), NEC requiring surgery, retinopathy of prematurity (stage 2 or 3), intraventricular hemorrhage (grade \geq 2), anemia of prematurity, late onset sepsis, mortality

Table 2.6 (continued)

Study	Design	Inclusion: healthy preterm neonates, appropriate for gestational age and normal Apgar score	Intervention	Control	Outcomes	Primary/secondary outcome(s)
Indrio et al. 2009	single center RCT N=49 neonates	Inclusion: healthy preterm neonates, appropriate for gestational age and normal Apgar score Exclusion: lack of parental consent, respiratory distress, congenital malformation, inborn errors of metabolism, proven sepsis or infection	prebiotic supplemented formula (0.8 g/dl of a mixture from SC-GOS and LC-FOS 9:1) for 30 days (N=10 neonates)	indistinguishable placebo formulation for 30 days (N=12 neonates) breastmilk fed control group (N=17 neonates)	not provided	Primary outcome(s): gastric electrical activity (propagation), gastric emptying, weight gain, adverse events
Manzoni et al. 2013	multi center RCT N=229 neonates	Inclusion: gestational age <32 weeks + 6 days, born within the study period Exclusion: lack of parental consent, admission >48 hours of life, death <72 hours of life and ophthalmic disease present at moment of randomization	oral carotenoids supplementation, 0.5 ml containing 0.14 mg lutein and 0.0006 mg of zeaxanthin, single daily oral dose starting from the first 48 hours of life until week 36 of corrected gestational age (N=113 neonates)	oral placebo supplementation, 0.5 mL glucose 5% (N=116 neonates)	Yes, power calculation based on pretrial retinopathy of prematurity incidence of 18%, estimated 66% relative difference in retinopathy of prematurity incidence by carotenoids supplementation, power 80%; α 0.05; required sample size 114	Primary outcome(s): incidence threshold retinopathy of prematurity, incidence bronchopulmonary dysplasia, incidence NEC and incidence NEC stage ≥ 2 Secondary outcome(s): incidence retinopathy of prematurity (all stage), intestinal perforation, late-onset sepsis, mortality prior to discharge, severe (grade 3 or 4) intraventricular hemorrhage, need for transfusion, liver failure

Table 2.6 (continued)

Author and year	Type of study and sample size	In- and exclusion criteria	Control	Intervention	Sample size / power calculation	Primary / secondary outcome measures
Manzoni et al. 2014	multi center RCT N=472	Inclusion: VLBW neonates younger than 3 days at tertiary care units in Italy and New Zealand Exclusion: lack of parental consent, ongoing antifungal prophylaxis, early onset	placebo (2 mL of a 5% glucose solution from day 3 once daily dissolved in milk for 6 (birth weight <1000 g) or 4 (birth weight 1001-1500g) weeks or until discharge (N=168 neonates)	bovine lactoferrin, 100 mg/day dissolved in milk, orally once daily from day 3 for 6 (birth weight <1000 g) or 4 (birth weight 1001-1500g) weeks or until discharge (N=153 neonates) bovine lactoferrin, 100 mg/day dissolved in milk, + Lactobacillus rhamnosus GG, 6*10 ⁹ CFU / day dissolved in milk, orally once daily from day 3 for 6 (birth weight <1000 g) or 4 (birth weight 1001-1500g) weeks or until discharge (N=151 neonates)	Yes, power calculation based on pretrial NEC incidence of 7%, estimated 66% relative difference in NEC incidence by supplementation, power 80%, α 0.05; required sample size 238 NB: due to lower incidence rate of NEC (5.4% instead of 7%) power fell to 54% for the bovine lactoferrin supplementation group and 97% for lactoferrin + Lactobacillus rhamnosus GG group	Primary outcome(s): NEC stage 22 and NEC or death Secondary outcome(s): overall mortality (not attributable to NEC)
Mihatsch et al. 2006	single center RCT N=20 neonates	Inclusion: healthy, stable, preterm infants with birthweight <1500 gram and full enteral feeding with preterm infant formula because breastmilk was unavailable Exclusion: lack of parental consent, anomalies that may interfere with feeding tolerance (cardiac defects, pulmonary diseases such as bronchopulmonary dysplasia, gastrointestinal diseases or chromosomal abnormalities)	standard preterm formula supplemented with placebo (1 g/dL, made from sachets with 0.9g GOS FOS and 1.8g maltodextrin) (N=10 neonates)	standard preterm formula supplemented with GOS FOS (1g/dL, GOS FOS 1:1, made from sachets with 0.9g GOS FOS and 0.9g maltodextrin) (N=10 neonates)	no power calculation performed (pilot study)	Primary outcome(s): stool viscosity, gastrointestinal transit time Secondary outcome(s): stool frequency and quality, stool pH, feeding volume, weight gain

Table S2.6 (continued)

Omar et al. 2020	single center, double-blind placebo controlled pilot study, N=120 neonates	Inclusion: gestational age ≤ 32 weeks at the NICU of a tertiary care hospital Exclusion: lack of parental consent, receiving chest compression or any medication during resuscitation, genetic syndromes or inborn errors of metabolism, major congenital defects, previous administration of parenteral growth factors or previous treatment with intravenous immunoglobulins	single daily dose of distilled water mixed with preterm formula (N=60 neonates)	enteral recombinant EPO, 0.88 IU/kg/day at concentration of 100 IU/ml in distilled water mixed with preterm formula, single enteral daily dose, starting at the day of enteral feeding until enteral intake of 150/ml/kg or after a maximum of 10 days (N=60 neonates)	Yes, a sample size of 30 patients per group was deemed sufficient for a pilot study with power of 80% and $\alpha 0.05$	Primary outcome(s): feeding tolerance (including day of successful start of enteral feeding). Secondary outcome(s): time to establish one-half, two-thirds and full enteral feedings, number of episodes of feeding intolerance, time to regain birth weight, incidence of NEC (stage ≥ 2), adverse effects
Serçe Pehlevan et al. 2020	single center RCT N=50 neonates doi: 10.5546/aap.2020.0.eng.e8	Inclusion: gestational age ≤ 32 weeks, admitted to the neonatology unit of the Zeynep Kamil Maternity and Children's Training and Research Hospital, Istanbul, Turkey, between July and September 2013 Exclusion: congenital anomalies, born to mothers with premature rupture of membranes or chorioamnionitis Excluded after randomization: mechanical ventilation for >7 days, culture proven sepsis at time of blood sampling, NEC, surgery, infants that died <30 days of life	placebo (distilled water 1 mL per dose, every 12 hours), added to breast milk or formula	1 mixture containing per sachet 8.2×10^8 <i>Lactobacillus rhamnosus</i> KCTC 12202BP, 4.1×10^8 <i>Lactobacillus plantarum</i> KCTC 10782BP, <i>Lactobacillus casei</i> KCTC 12398BP, <i>Bifidobacterium lactis</i> KCTC 11904BP, 383 mg FOS, 100 mg GOS and 2 mg bovine lactoferrin, 1/2 sachet every 12 hours added to breast milk or formula	Yes, with an estimated effect size of 0.75 SD, a power of 80% and $\alpha 0.05$, 24 patients were needed per group	Primary/secondary outcome(s): (IL5, IL10, IL17a, IFN γ)

Table S2.6 (continued)

Author and year	Type of study and sample size	In- and exclusion criteria	Control	Intervention	Sample size / power calculation	Primary / secondary outcome measures
Serce Pehlevan et al. doi: 10.3345/cep.2019.00381 2020	single center RCT N=208 neonates	Inclusion: gestational age ≥ 32 weeks, birth weight ≤ 1500 g, admitted to the neonatology unit of the Zeynep Kamil Maternity and Children's Training and Research Hospital/Istanbul, Turkey, between February 2012 and September 2013, survived to start of enteral feeding Exclusion: severe asphyxia (stage III), major congenital anomalies, fasted ≥ 3 weeks, death within first 14 postnatal days	placebo (distilled water 1 mL per dose, every 12 hours), added to breast milk or formula	1. mixture containing per sachet 8.2×10^8 <i>Lactobacillus rhamnosus</i> KCTC 12202BP, 4.1×10^8 <i>Lactobacillus plantarum</i> KCTC 10782BP, <i>Lactobacillus casei</i> KCTC 12398BP, <i>Bifidobacterium lactis</i> KCTC 11904BP, 383 mg FOS, 100 mg GOS and 2 mg bovine lactoferrin, 1/2 sachet every 12 hours added to breast milk or formula	Yes, power calculation based on pretrial NEC or late onset sepsis incidence of 31% and death or NEC incidence of 35%, estimated 50% difference in NEC/late onset sepsis or NEC/death incidence by supplementation, power 80%; α 0.05; required sample size of 104 for NEC or late onset sepsis and sample size of 92 for NEC or death not provided	Primary outcome(s): NEC stage ≥ 2 or culture proven late onset sepsis, NEC stage ≥ 2 or death Secondary outcome(s): time to reach 100 ml/kg/day of enteral feeding, oxygen dependency at 36 weeks, mortality before hospital discharge and duration of hospitalization
Sevastiadou et al. 2011	single center RCT N=101 neonates	Inclusion: formula fed, prematurely born infants admitted to the NICU of 'Alexandra' Regional General Hospital, Athens, Greece, between January 2007 and December 2008 with a GA < 34 weeks and birth weight < 2000 g Exclusion: lack of parental consent, major congenital or chromosomal anomalies, severe hypotension, severe perinatal distress (pH < 7 or hypoxia with bradycardia > 2 h), abdominal distention, signs of early NEC, receiving breast milk	isocaloric glucose-polymer powder with same color and smell as intervention powder (N=50 neonates)	enteral L-glutamin powder supplementation separate from formula, 3 times a day between 3 and 30 days of life, 0.3 g/kg/day diluted in water as a 10% solution (N=51 neonates)	not provided	Primary/secondary outcome(s): intestinal permeability, NEC incidence, sepsis

Table S2.6 (continued)

Stratiki et al. 2007	RCT N=75 neonates	Inclusion: gestational age between 27 and 37 gestational age, stable state, formula fed and not suffering from major deformities (congenital heart defects, bowel atresia)	formula without supplemented <i>Bifidobacterium lactis</i>	<i>Bifidobacterium lactis</i> in formula feeding, 2*10 ⁷ CFU/g milk powder, administered according to neonatal unit feeding protocol	Yes, based on data on lactulose / mannitol ratio from an earlier study, a sample size of 30 infants was considered adequate to detect a significant difference of lactulose / mannitol ratio following supplementation	Primary outcome(s): intestinal permeability Secondary outcome(s): somatic growth, tolerance, rates of sepsis and NEC
Sun et al. 2020	multi center RCT N=262 neonates	Inclusion: gestational age <28 weeks and <96 hours of age Exclusion: lack of parental consent, genetic metabolic disease, congenital major abnormalities, congenital TORCH infections with overt signs at birth, terminal stage illness (pH <7.0 or hypoxia with bradycardia >2 hours)	placebo solution with soybean oil with the same aspect as vitamin A solution (N=130 neonates)	Vitamin A, 1500 IU/day, solution was added to enteral feeds when minimal enteral feeding started until 28 days or discharge (N=132 neonates)	Yes, power calculation based on estimated 30% relative difference in retinopathy of prematurity incidence by supplementation, power 80%, α 0.05; required sample size 254	Primary outcome(s): composite of mortality or type 1 retinopathy of prematurity, bronchopulmonary dysplasia, serum vitamin A levels, sings of vitamin A toxicity, vomiting and intracranial pressure Secondary outcome(s): mortality, retinopathy of prematurity, sepsis, NEC stage ≥ 2 , severe intraventricular hemorrhage (grade ≥ 3), periventricular leukomalacia

Table S2.6 (continued)

Author and year	Type of study and sample size	In- and exclusion criteria	Control	Intervention	Sample size / power calculation	Primary / secondary outcome measures
Wardle et al. 2001	single center RCT N=154 neonates	Inclusion: <1000g birth weight and parental consent within the first 24 hours Exclusion: lack of parental consent, major life threatening congenital abnormality	daily dose of equal volume of an inert placebo solution (looking identical as the intervention) orally as a bolus through orogastric tube from postnatal day 1 until day 28 (N= 77 neonates)	vitamin A, daily dose of 5000 IU/kg (3000 µg/kg) orally as a bolus through orogastric tube from postnatal day 1 until day 28 (N= 77 neonates)	Yes, power calculation based on prior incidence of chronic lung disease death of 90% and of chronic lung disease in survivors of 83%, estimated risk reduction to 70% (chronic lung disease and death) and 50% (chronic lung disease), power 80%; α 0.05; required sample size 158	Primary outcome(s): requirement for supplementary oxygen at 28 days Secondary outcome(s): death before discharge, supplementary oxygen requirement at 36 weeks, retinopathy of prematurity requiring treatment, intraventricular hemorrhage with parenchymal involvement, patent ductus arteriosus requiring treatment, NEC requiring surgery and number of episodes of sepsis, adverse events Primary/secondary outcome(s): fecal calprotectin, fecal IL8
Westerbeek et al. 2011	single center RCT N=113 neonates	Inclusion: preterm infants <32 weeks GA and/or birthweight <1500 g admitted to the NICU of the VU University Medical Center, Amsterdam. Exclusion: >34 weeks GA, major congenital or chromosomal anomalies, imminent death, transfer to another hospital <48h after birth	placebo powder (maltodextrin) in increasing doses between d3 and d30 to a maximum of 1.5 g/kg added to breastmilk or preterm formula (without oligosaccharides) (N= 58 neonates)	72% SC-GOS, 8% LC-FOS, 20% AOS in increasing doses between d3 and d30 to a maximum of 1.5 g/kg added to breastmilk or preterm formula (without oligosaccharides) (N= 55 neonates)	Yes, the sample size of 113 was based on sample size calculation for the primary outcome of the main trial (serious infectious morbidity)	Primary/secondary outcome(s): number of episodes of sepsis, adverse events Primary/secondary outcome(s): fecal calprotectin, fecal IL8

RCT, randomized controlled trial; GA, gestational age; NEC, necrotizing enterocolitis; SC-GOS, short-chain galacto-oligosaccharides; LC-FOS, long-chain fructo-oligosaccharides; DHA, docosahexaenoic acid; EPA, eicosapentaenoic acid; EPO, erythropoietin; G-CSF, granulocyte colony-stimulating factor; AOS, acidic oligosaccharides.

Table S2.7 Overview included systematic reviews and meta-analysis on enteral feeding interventions for prevention of NEC in human infants.

Author and year	Type of study and sample size	Study selection criteria	Control	Intervention	Primary / secondary outcome measures	Evidence level and risk of bias according to authors meta-analysis
Van den Akker et al. 2018	systematic review and network meta-analysis N for NEC outcome = 43 studies and 10.651 neonates	RCTs reporting on only preterm infants or subgroup with preterm infants (<37 weeks GA), comparing probiotic treatment with placebo or no treatment or comparing different probiotic interventions, both single- or multiple strains included, available in English and fully published	placebo, usual care or head-to-head with different probiotic regime	probiotics single- or multiple-strain	Primary outcomes: well-described outcome reports of NEC, blood-culture proven late onset sepsis, postnatal age at reaching full enteral feeding, in-hospital mortality Secondary outcome: -	studies in general underpowered for NEC incidence as outcome measure, most strains only studied in a few trials, limited evidence for the most preterm infants
Ananthan et al. 2018	systematic review and meta-analysis N for NEC outcome (enteral administration) = 2 studies and 110 neonates	RCTs comparing recombinant EPO with placebo or standard treatment without recombinant EPO supplementation	placebo or standard treatment without EPO	recombinant EPO	Primary outcomes: incidence of NEC stage ≥2, any stage NEC Secondary outcomes: feeding intolerance, time to reach full feedings, late onset sepsis, bronchopulmonary dysplasia, mortality	the included trials for enteral administration were at risk for selection bias, reporting bias and other bias
Chi et al. 2019	systematic review and meta-analysis N for NEC outcome = 6 studies and 737 neonates	RCTs comparing prebiotics (SC-GOS, LC-FOS, pAOS, oligosaccharides, fructans, inulin or oligofructose) in low birth weight (<2500 g) or preterm (<37 weeks GA) infants with placebo, published in peer-reviewed journals from January 2020 until June 2018	placebo	prebiotics (SC-GOS, LC-FOS, pAOS, oligosaccharides, fructans, inulin or oligofructose)	Primary outcomes: incidence of sepsis, NEC and mortality Secondary outcomes: length of hospital stay, feeding intolerance, stool frequency	5 out of 6 included studies were judged to be of high quality, 1 study was of moderate quality

Table S2.7 (continued)

Author and year	Type of study and sample size	Study selection criteria	Control	Intervention	Primary / secondary outcome measures	Evidence level and risk of bias according to authors meta-analysis
Foster et al. 2016	systematic review and meta-analysis N for NEC outcome = 3 studies and 2095 neonates	RCTs and quasi-randomized controlled trials studying the use of oral immunoglobulins as prophylaxis against NEC in preterm (<37 weeks GA) and/or low birth weight (<2500 g) neonates	placebo or no treatment	oral immunoglobulins	Primary outcome: diagnosis of definite NEC during study period Secondary outcomes: suspected NEC during study period, surgery for NEC during study period, NEC related death, length of hospital stay, hospital readmission within the first year of life, days receiving total parenteral nutrition, growth and development in childhood, parental emotional and financial costs, adverse effects of treatment	low to very low quality of evidence; incomplete outcome data, high rate of non-compliance, unclear allocation concealment and imprecision
Moe-Byrne et al. 2016	systematic review and meta-analysis N for NEC outcome = 7 studies and 1172 neonates	RCTs and quasi-randomized controlled trials of glutamine supplementation in preterm neonates at any time from birth to discharge from hospital	no supplementation	enteral (or parenteral) glutamine supplementation from any time from birth until hospital discharge	Primary outcomes: death prior to hospital discharge, neurodevelopment Secondary outcomes: invasive infection during hospital admission, NEC during hospital admission	moderate quality of evidence; unexplained heterogeneity and funnel plot asymmetry

Table S2.7 (continued)

Author and year	Type of study and sample size	Study selection criteria	Control	Intervention	Primary / secondary outcome measures	Evidence level and risk of bias according to authors meta-analysis
Morgan et al. 2020	systematic review and network meta-analysis N for NEC outcome = 56 studies and 12738 neonates	RCTs with single- or multiple-strain probiotic (living bacteria) interventions for prevention of mortality or morbidity in preterm (<37 weeks GA) and/or low birth weight (<2500 gram) infants	placebo, formula, parenteral nutrition or no treatment	probiotics (living bacteria) single- or multiple-strain	Primary outcomes: all-cause mortality, severe NEC (stage ≥2), culture proven sepsis, hospitalization, time to reach full enteral feeds Secondary outcome: -	low to high certainty of evidence; data with low and moderate to high certainty of evidence are presented separately
Pammi et al. 2020	systematic review and meta-analysis N for NEC outcome = 7 studies and 4874 neonates	RCTs evaluating the effect of enteral lactoferrin administration at any dose or duration to prevent NEC (and sepsis) in preterm neonates	placebo or no intervention	enteral lactoferrin at any dose or duration	Primary outcomes: confirmed or suspected sepsis during hospital stay, NEC stage ≥2, all-cause mortality during hospital stay Secondary outcomes: neurological outcome at two years of age or alter, chronic lung disease in survivors, adverse outcomes, periventricular leukomalacia, duration of assisted ventilation through an endotracheal tube, length of hospital stay, posthoc analyses of bacterial infection, fungal infection, threshold retinopathy of prematurity and urinary tract infection	low certainty of evidence for NEC outcome; confidence in the effect estimate is limited, true effect may be substantially different from the estimate of the effect, risk of bias in the included trials and imprecision

Table S2.7 (continued)

Author and year	Type of study and sample size	Study selection criteria	Control	Intervention	Primary / secondary outcome measures	Evidence level and risk of bias according to authors meta-analysis
Shah et al. 2017	systematic review and meta-analysis N for NEC outcome = 3 studies and 285 neonates	RCTs and quasi-randomized controlled trials of arginine supplementation, administered orally or parenterally for at least seven days, in addition to intake with regular enteral/parenteral feeding	placebo or no treatment	enteral or parenteral arginine supplementation for at least 7 days	Primary outcome: NEC any stage and specific stages Secondary outcomes: death before discharge, death attributed to NEC, surgery for NEC, duration of total parenteral nutrition administration, plasma concentrations of arginine and glutamine, side effects of arginine supplementation	moderate certainty of evidence; future research likely will have an important impact on confidence in the estimate of effect and may change this estimate
Zhang et al. 2014	systematic review and meta-analysis N for NEC outcome = 5 studies and 900 neonates	observational studies or RCTs published until May 2013 that included infants <29 weeks GA that evaluated the relationship between n-3 long chain PUFA and major adverse neonatal outcomes	standard interventions, placebo or any other control levels of n-3 long chain PUFA exposure	any n-3 long chain PUFA exposure to the infant or any n-3 long chain PUFA supplementation directly to the infant or through the mother	Primary outcome: bronchopulmonary dysplasia free survival at 36 weeks postmenstrual age Secondary outcomes: death, duration of ventilation or oxygen support, length of hospitalization, occurrence of intraventricular hemorrhage, periventricular leukomalacia, NEC, infections, retinopathy of prematurity or hemodynamic significant patent ductus arteriosus	no separate quality analysis reported for the included studies

RCT, randomized controlled trial; GA, gestational age; NEC, necrotizing enterocolitis; EPO, erythropoietin; 5C-GOS, short chain galacto-oligosaccharides; LC-FOS, long chain fructo-oligosaccharides; PAOS: pectin-derived acidic oligosaccharides; PUFA, polyunsaturated fatty acids.

Table S2.8 Risk of bias assessment of the included experimental animal studies (SYRCLE's risk of bias tool).

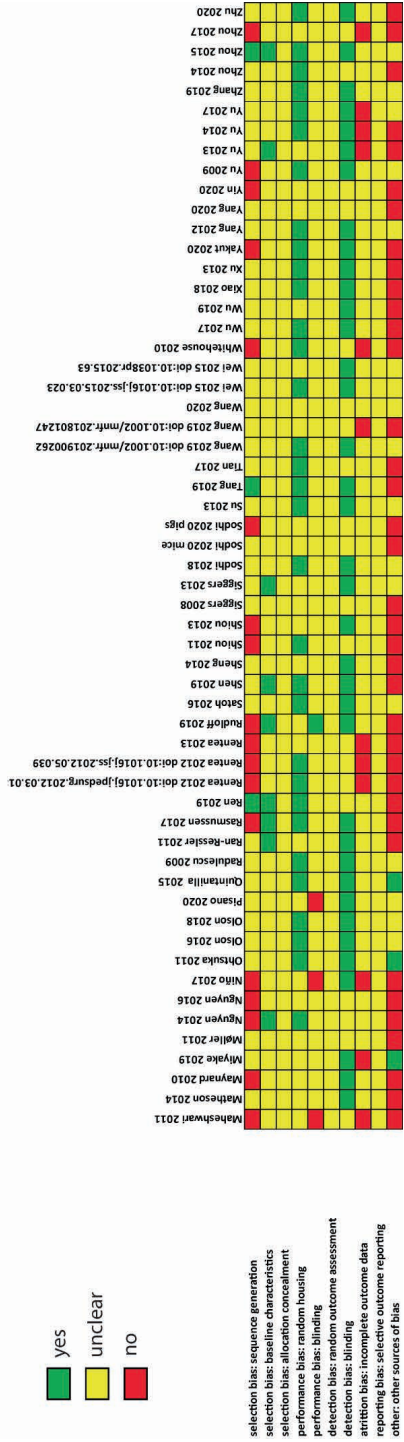


Table S2.9 Risk of bias assessment of the included RCTs (Jadad scoring system).

	Akin 2014	Collins 2017	El-Ganzoury 2014	Hosseini 2018	Indrio 2009	Manzoni 2013	Manzoni 2014	Mihatsch 2006	Omar 2020	Sere Pehlevan 2020 doi:10.5546/aap.2020.eng.8	Sere Pehlevan 2020 doi:10.3345/cep.2019.00381	Sevastidou 2011	Stratki 2007	Sun 2020	Wardle 2001	Westerbeek 2011
1) Was the study described as randomized	2	2	2	1	1	2	2	2	2	2	2	1	2	1	2	2
2) Was the study described as double-blind	2	2	2	0	2	2	2	2	2	2	2	2	2	2	2	2
3) Was there a description of withdrawals and dropouts	1	1	1	0	1	1	1	1	1	1	1	1	1	1	0	1
Total score	5	5	5	2	3	5	5	5	5	5	5	4	5	4	4	5

1) Was the study described as randomized

2) Was the study described as double-blind

3) Was there a description of withdrawals and dropouts

Total score

Table S2.10 Risk of bias assessment of the included RCTs (Jadad scoring system).

	Akker, van den 2018	Nanthan 2018	Chi 2018	Foster 2016	Moe-Byrne 2016	Morgan 2020	Pamiri 2020	Shah 2017	Zhang 2014
1) Was an 'a priori' design provided?	yes	can't answer	yes	yes	yes	yes	yes	yes	yes
2) Was there duplicate study selection and data extraction?	yes	yes	yes	yes	yes	yes	yes	yes	yes
3) Was a comprehensive literature search performed?	no	yes	yes	yes	yes	yes	yes	yes	yes
4) Was the status of publication (i.e. grey literature) used as an inclusion criterion?	no	yes	can't answer	yes	yes	yes	yes	yes	yes
5) Was a list of studies (included and excluded) provided?	no	no	no	yes	yes	can't answer	yes	no	no
6) Where the characteristics of the included studies provided?	yes	yes	yes	yes	yes	yes	yes	yes	yes
7) Was the scientific quality of the included studies assessed and documented?	yes	yes	yes	yes	yes	yes	yes	yes	yes
8) Was the scientific quality of the included studies used appropriately in formulating conclusions?	yes	yes	can't answer	yes	yes	yes	yes	yes	can't answer
9) Where their methods used to combine the findings of studies appropriate?	yes	yes	yes	yes	yes	yes	yes	yes	yes
10) Was the likelihood of publication bias assessed?	yes	yes	yes	yes	yes	yes	yes	yes	yes
10) Was the conflict of interest stated?	no	no	no	no	no	no	no	no	no

1) Was an 'a priori' design provided?

2) Was there duplicate study selection and data extraction?

3) Was a comprehensive literature search performed?

4) Was the status of publication (i.e. grey literature) used as an inclusion criterion?

5) Was a list of studies (included and excluded) provided?

6) Where the characteristics of the included studies provided?

7) Was the scientific quality of the included studies assessed and documented?

8) Was the scientific quality of the included studies used appropriately in formulating conclusions?

9) Where their methods used to combine the findings of studies appropriate?

10) Was the likelihood of publication bias assessed?

10) Was the conflict of interest stated?

Table S2.11 GRADE approach scoring of clinical studies.

Intervention	Limitations in study design or execution (risk of bias)	Inconsistency of results	Indirectness of evidence	Imprecision	Publication bias	Overall certainty of evidence (GRADE)
n-3 PUFA (NEC incidence all neonates)	-1	0	0	-1	0	Low
n-3 PUFA (NEC incidence neonates <32 weeks)	-1	0	0	-1	0	Low
DHA (NEC incidence)	0	0	0	-2	0	Low
probiotics (NEC incidence)	0	-1	0	-1	0	Low
lactoferrin (incidence stage II or III NEC)	-1	0	0	-1	0	Low
arginine (NEC incidence)	0	0	0	-1	0	Moderate
arginine (death due to NEC)	0	0	0	-2	0	Low
glutamine (NEC incidence)	0	0	0	-1	-1	Low
immunoglobulins, (NEC incidence)	-2	0	0	0	0	Low
immunoglobulins, (NEC surgery)	-2	0	0	-1	0	Low
immunoglobulins (death due to NEC)	-2	0	0	-1	0	Very low
EPO (incidence stage II or III NEC)	0	-1	0	-2	0	Very low
EPO (NEC incidence)	-1	-1	0	-2	0	Very low
EPO + G-CSF (NEC incidence)	0	0	0	-2	0	Low
G-CSF (NEC incidence)	0	0	0	-2	0	Low
G-CSF (in artificial amniotic fluid) (NEC incidence)	-1	0	0	-2	0	Very low
vitamin A (NEC incidence)	-1	0	0	-1	0	Low
probiotics Lactobacillus spp. and Bifidobacterium spp. (incidence stage II or III NEC)	0	0	-1	0	0	Moderate
probiotics Bifidobacterium animalis subsp. Lactis (incidence stage II or III NEC)	0	0	0	-1	0	Moderate
probiotics Lactobacillus reuteri (incidence stage II or III NEC)	0	0	-1	-1	0	Low
probiotics Lactobacillus rhamnosus (incidence stage II or III NEC)	0	0	0	-1	0	Moderate
probiotics combination of Lactobacillus spp., Bifidobacterium spp. and Enterococcus spp. (incidence stage II or III NEC)	-2	0	0	0	0	Low
probiotics combination of Bacillus spp. and Enterococcus spp. (incidence stage II or III NEC)	0	0	0	-1	0	Moderate
probiotics Bifidobacterium lactis Bb-12 or B-94 (NEC incidence)	0	0	0	-1	0	Moderate
probiotics Lactobacillus reuteri ATCC5730 or DSM17938 (NEC incidence)	0	0	-1	-1	0	Low
probiotics Lactobacillus rhamnosus GG (NEC incidence)	0	0	-1	-1	0	Low
probiotics combination of Bifidobacterium bifidum, Bifidobacterium infantis, Bifidobacterium longum and Lactobacillus acidophilus (NEC incidence)	0	0	0	-2	0	Low
probiotics combination of Bifidobacterium infantis Bb-02, Bifidobacterium lactis Bb-12 and Streptococcus thermophilus TH-4 (NEC incidence)	0	-1	0	-1	0	Low
probiotics Bifidobacterium longum 35624 and Lactobacillus rhamnosus GG (NEC incidence)	0	0	0	-2	0	Low
carotenoids (incidence stage II or III NEC)	0	0	0	-2	0	Low
mixture of probiotics, prebiotics and lactoferrin (NEC incidence)	0	0	0	-2	0	Low
mixture of probiotics, prebiotics and lactoferrin (incidence stage II or III NEC)	0	0	0	-2	0	Low

Part II

**Understanding NEC pathophysiology:
ENS alterations during chorioamnionitis and NEC**

Chapter 3

Chorioamnionitis induces enteric nervous system injury: effects of timing and inflammation in the ovine fetus

C. Heymans*, I.H. de Lange*, K. Lenaerts, L.C.G. Kessels, M. Hadfoune, G. Rademakers, V. Melotte, W. Boesmans, B.W. Kramer, A.H. Jobe, M. Saito, M.W. Kemp, W.G. van Gemert, and T.G.A.M. Wolfs

* Contributed equally

Molecular Medicine. 2020;26(1):82

Abstract

Background

Chorioamnionitis, inflammation of the chorion and amnion, which often results from intra-uterine infection, is associated with premature birth and contributes to significant neonatal morbidity and mortality, including necrotizing enterocolitis (NEC). Recently, we have shown that chronic chorioamnionitis is associated with significant structural enteric nervous system (ENS) abnormalities that may predispose to later NEC development. Understanding time point specific effects of an intra-amniotic (IA) infection on the ENS is important for further understanding the pathophysiological processes and for finding a window for optimal therapeutic strategies for an individual patient. The aim of this study was therefore to gain insight in the longitudinal effects of intra-uterine LPS exposure (ranging from 5 hours to 15 days before premature delivery) on the intestinal mucosa, submucosa, and ENS in fetal lambs by use of a well-established translational ovine chorioamnionitis model.

Materials and methods

We used an ovine chorioamnionitis model to assess outcomes of the fetal ileal mucosa, submucosa and ENS following IA exposure to one dose of 10 mg LPS for 5, 12 or 24 hours or 2, 4, 8 or 15 days.

Results

Four days of IA LPS exposure causes a decreased PGP9.5- and S100 β -positive surface area in the myenteric plexus along with submucosal and mucosal intestinal inflammation that coincided with systemic inflammation. These changes were preceded by a glial cell reaction with early systemic and local gut inflammation. ENS changes and inflammation recovered 15 days after the IA LPS exposure.

Conclusion

The pattern of mucosal and submucosal inflammation, and ENS alterations in the fetus changed over time following IA LPS exposure. Although ENS damage seemed to recover after prolonged IA LPS exposure, additional postnatal inflammatory exposure, which a premature is likely to encounter, may further harm the ENS and influence functional outcome. In this context, 4 to 8 days of IA LPS exposure may form a period of increased ENS vulnerability and a potential window for optimal therapeutic strategies.

Introduction

Chorioamnionitis, inflammation of the chorion and amnion during pregnancy, is associated with premature birth and contributes to significant neonatal morbidity and mortality¹⁻³. Chorioamnionitis typically results from a bacterial infection ascending through the birth canal². It is often clinically silent and therefore difficult to diagnose, but can nevertheless affect the developing fetus⁴. As the fetus swallows the amniotic fluid (AF), the intestine is directly exposed to bacterial components and inflammatory cytokines present in the AF, which can consequently cause gut injury and inflammation⁵. Moreover, during chorioamnionitis, the fetus can develop a fetal inflammatory response syndrome (FIRS), which is characterized by increased systemic interleukin 6 (IL-6) and interleukin 8 (IL-8) levels⁶. FIRS is an independent risk factor for considerable neonatal morbidity, including the postnatal intestinal disease necrotizing enterocolitis (NEC)^{4,7}. NEC has a high mortality of overall 25% with both significant short-term and long-term morbidity⁸. Severe intestinal inflammation is associated with NEC and can result in gut necrosis^{8,9}. Gut specimens from NEC patients contain alterations in the enteric nervous system (ENS) including a loss of neurons and glial cells¹⁰⁻¹³. The ENS resides in the intestinal wall and consists of two plexuses: the submucosal and myenteric plexus¹⁴. It operates autonomously and regulates diverse gastrointestinal functions such as motility, secretion, absorption, and maintenance of gut integrity¹⁴. ENS development is a complex process that requires coordinated migration, proliferation, and differentiation of the involved cell types, directed outgrowth of neurites and the establishment of an interconnected neuronal and glial cell network^{15,16}. Importantly, ENS development continues in the early postnatal period^{17,18}, during which it is shaped by amongst others immune cells, microbiota and enteral nutrition¹⁷.

Recently, we have shown in a preclinical ovine model that chronic chorioamnionitis is associated with significant structural ENS abnormalities¹⁹. Importantly, these alterations corresponded with those found in infants with NEC, indicating that ENS changes following chorioamnionitis may predispose to later NEC development¹⁹. Since inflammation is a dynamic process and the vulnerability of the fetus to injurious exposure during intra-uterine development varies, ENS alterations in response to inflammation can be time-dependent. As chorioamnionitis is often clinically silent and infants born after chorioamnionitis have been exposed to varying durations of intra-uterine inflammation, understanding time-dependent effects of intra-uterine inflammation on the ENS is clinically important to define optimal therapeutic strategies. Therefore, the aim of this study was to evaluate the time-dependent effects of 5 hour to 15 days of intra-uterine LPS exposure before premature delivery, on the intestinal submucosa, mucosa and ENS in fetal sheep.

Materials and methods

Animal model and experimental procedures

The experiments were approved by the animal ethics/care committee of the University of Western Australia (Perth, Australia; ethical approval number: RA/3/100/928).

The ovine model and experimental procedures were previously described^{6,20}. In brief, 52 time-mated merino ewes carrying singleton fetuses were randomly assigned to eight

different groups of six to seven animals. The pregnant ewes were IA injected under ultrasound guidance with 10 mg *Escherichia coli*-derived LPS (O55:B5; Sigma-Aldrich, St. Louis, MO, USA) dissolved in saline at 5, 12, or 24 hours, or 2, 4, 8 or 15 days before preterm delivery at 125 days of gestation (equivalent of 30-32 weeks of human gestation for the gut; term gestation in sheep around 150 days). The study design is based on the clinically relevant situation that the gestational age of the infant is known, but not the length of exposure to inflammation. Hence, all samples were collected at the same gestational age and inflammation was induced at various times before sampling. Of importance, with a half-life time of 1.7 days, LPS persists in AF and can still be detected at 15 days²¹. A group receiving IA injections of saline at variable gestational ages comparable to LPS injections, ranging from 5 hours to 15 days before preterm delivery, served as the controls (**Figure 3.1**).

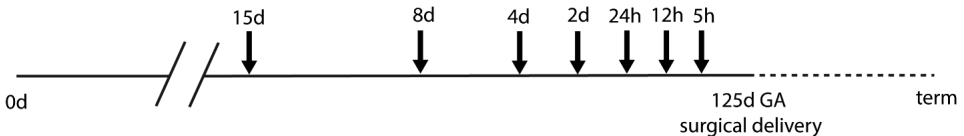


Figure 3.1 Study design. Pregnant ewes received an IA injection with 10 mg LPS at 5, 12, or 24 h or 2, 4, 8 or 15 days (black arrows) before preterm delivery at 122 days of gestation (term ~150 days). Control animals received an IA saline injection at comparable time points to LPS injections. Timing shown in gestational days.

Fetuses were delivered by cesarean section at 125 days of gestation and immediately euthanized with intravenous pentobarbitone (100 mg/kg). Fetuses of both sexes were used. At necropsy, the terminal ileum was sampled and fixed in 10% formalin or snap frozen. Formalin-fixed tissues were subsequently embedded in paraffin.

Antibodies

For immunohistochemistry, the following antibodies were used: polyclonal rabbit anti-myeloperoxidase ([MPO]; A0398, Dakocytomation, Glostrup, Denmark) for identification of neutrophils, polyclonal rabbit anti-bovine protein gene product 9.5 ([PGP9.5]; Z5116, Dakocytomation) for the detection of enteric neurons, polyclonal rabbit anti-doublecortin (Ab18723, Abcam, Cambridge, UK) for the detection of immature neurons, polyclonal rabbit anti-glial fibrillary acidic protein ([GFAP]; Zo334, Dakocytomation) for identification of activated enteric glial cells and polyclonal rabbit anti-S100 β (PA5-16257, Invitrogen, Carlsbad, CA, USA) which is considered a general marker of enteric glial cells.

The following secondary antibodies were used: peroxidase-conjugated polyclonal goat anti-rabbit (111-035-045, Jackson, WestGrove, PA, USA) (MPO), peroxidase-conjugated polyclonal swine anti-rabbit (P0399, DakoCytomation) (doublecortin) and BrightVision+ Poly-HRP-Anti Mouse/Rabbit IgG Biotin-free (ImmunoLogic, Duiven, the Netherlands) (PGP9.5), and biotin conjugated polyclonal swine anti-rabbit (E0353, DakoCytomation) (GFAP, S100 β).

Immunohistochemistry

Paraffin embedded formalin-fixed terminal ileum was cut into 4 μm sections. Following deparaffinization and rehydration, sections were incubated in 0.3% H₂O₂ diluted in phosphorylated buffer saline ([PBS]; pH 7.4) to block endogenous peroxidase activity. For PGP9.5, doublecortin and S100 β , antigen retrieval was achieved with citrate buffer. Non-specific binding was blocked for 30 minutes at room temperature with 10% normal goat serum (NGS) in PBS (MPO), 5% NGS in PBS (doublecortin), or 5% bovine serum albumin (BSA) in PBS (GFAP and S100 β) or for 10 minutes at room temperature with 20% fetal calf serum (FCS) in PBS (PGP9.5). Subsequently, sections were incubated with the primary antibody of interest for one hour (MPO) or overnight (others) followed by the secondary antibody for 30 minutes (MPO) or one hour (others). MPO, PGP9.5 and doublecortin were recognized using a peroxidase-conjugated secondary antibody; antibodies against GFAP and S100 β were detected with avidin-biotin complex (Vectastain Elite ABC kit, Bio-connect, Huissen, the Netherlands). Substrate staining was performed with 3-amino-9-ethylcarbazole ([AEC]; Merck, Darmstadt, Germany) (MPO), nickel-DAB (GFAP) or DAB (PGP9.5, doublecortin and S100 β). Hematoxylin (MPO, PGP9.5, doublecortin and S100 β) or nuclear fast red (GFAP) were used as nuclear counterstains.

Quantification of immunohistochemical stainings

The Ventana iScan HT slide scanner (Ventana Medical Systems, Oro Valley, AZ, USA) was used to scan stained tissue sections. With the use of Panoramic Viewer (version 1.15.4, 3DHISTECH, Budapest, Hungary), an overview picture of the transverse section of the ileum was taken. Two investigators blinded to the experimental groups counted the number of mucosal MPO-positive cells. Leica QWin Pro (version 3.4.0, Leica Microsystems, Mannheim, Germany) was used to calculate the mucosal surface area. The average number of mucosal MPO-positive cells corrected for total mucosal tissue surface area is reported as MPO-positive cells per area per animal. Secondly, random images of the submucosal layer were taken (200x). In five non-overlapping high power fields, the number of submucosal MPO-positive cells was counted by two investigators blinded to the experimental groups. The average number of submucosal MPO-positive cells per animal of the five power fields is reported as MPO-positive cells per area. For PGP9.5, doublecortin, GFAP and S100 β , the surface of positively stained areas in the submucosal and myenteric ganglia and total surface area of the muscle layer were measured (Leica QWin Pro version 3.4.0, Leica Microsystems, Mannheim, Germany) in five non-overlapping high-power fields. The area fraction was calculated by dividing the positively stained surface area by the total surface area of the muscle layer. The average area fraction of the five high-power fields per animal is given as fold increase over the control value. The control value will be stated at one. All area fraction measurements were performed by one investigator blinded to the study groups.

RNA extraction and real-time PCR

TRI reagent (Invitrogen)/chloroform extraction was used to extract RNA from snap frozen terminal ileum. Afterwards RNA was reverse transcribed into cDNA using sensifast cDNA

Synthese kit (Bioline, London, UK). Quantitative real-time PCR (qPCR) was performed with the specific primers in Sensimix SYBR & Fluorescein Kit (Bioline) using a 384-wells qPCR plate. qPCR reactions were performed in a LightCycler 480 Instrument (Roche Applied Science, Basel, Switzerland) for 45 cycles. Gene expression levels of tumor necrosis factor alpha (TNF- α), IL-8 and IL-10 were determined to assess terminal ileum inflammation. mRNA expression levels of neuronal nitric oxide synthase (nNOS) and choline acetyltransferase (CHAT) were determined to assess ENS motility signaling function. LinRegPCR software (version 2016.0, Heart Failure Research Center, Academic Medical Center, Amsterdam, the Netherlands) was used for qPCR data processing. The geometric mean of the expression levels of three reference genes (ribosomal protein S15 (RPS15), glyceraldehyde 3-phosphate dehydrogenase (GAPDH) and peptidylprolyl isomerase A (PPIA)) were calculated and used as a normalization factor. Data are expressed as fold increase over the control value. Sequences of the primers used are shown in **Table 3.1**.

Data analysis

Statistical analyses were performed using GraphPad Prism (version 6.01, GraphPad Software Inc., La Jolla, CA, USA). Data are presented as median with interquartile range. Differences between the groups and the controls were analyzed using a nonparametric Kruskal-Wallis test followed by Dunn's post hoc test. Differences are considered statistically significant at $p \leq 0.05$. Differences with a $p < 0.10$ are also taken into account because of the small study groups and because of potential biological relevance, and described as tendencies as previously described²². This assumption will decrease the chance of a type II error, but increases the chance of a type I error.

Table 3.1 Primer sequences.

Primer	Forward	Reverse
RPS15	5'-CGAGATGGTGGGCAGCAT-3'	5'-GCTTGATTCCACCTGGTTGA-3'
GAPDH	5'-GGAAGCTCACTGGCATGGC-3'	5'-CTTGCTTACCACCTTCTTG-3'
PPIA	5'-TTATAAAGGTTCTGCTTTCACAGAA-3'	5'-ATGGACTTGCCACCAGTACCA-3'
IL-8	5'-GTTCCAAGCTGGCTGTTGCT-3'	5'-GTGGAAGGTGTGGAATGTGTTT-3'
IL-10	5'-CATGGGCCTGACATCAAGGA-3'	5'-CGGAGGTCTTCAGCTTCTC-3'
TNF- α	5'-GCCGGAATACCTGGACTATGC-3'	5'-CAGGGCGATGATCCCAAAGTAG-3'
nNOS	5'-CGGCTTGGGGGTTATCAGT-3'	5'-TTGCCCCATTTCCACTCCTC-3'
CHAT	5'-CCGCTGGTATGACAAGTCCC-3'	5'-GCTGGTCTTACCATGTGCT-3'

Results

Chorioamnionitis induced intestinal inflammation

A statistically significant increase in MPO-positive cells was seen in the mucosa 4 and 8 days after IA LPS exposure, compared to control ($p < 0.05$; **Table 3.2**).

Table 3.2 Immune cells count in the mucosal layer.

	Control (n=6)	5h LPS (n=6)	12h LPS (n=7)	24h LPS (n=7)	2d LPS (n=6)	4d LPS (n=6)	8d LPS (n=7)	15d LPS (n=6)
MPO+ cell count	102	74	159	76	151	354*	332*	224
SD (±)	110	77	166	51	105	162	101	96

Values are expressed as median numbers of cells per square millimeter. SD: Standard deviation. Kruskal-Wallis test with Dunn's post hoc test was performed. * $p < 0.05$ compared to control.

In the submucosa, there was an increase of MPO-positive cells in animals exposed to 4 days of IA LPS, and submucosal MPO-positive cells still tended to be increased after 8 days of IA LPS exposure, compared to control ($p < 0.05$ and $p = 0.08$; **Figure 3.2**).

Examination of underlying cytokine levels revealed increased ileal IL-8 mRNA levels after 24 hours and 4 days of IA LPS exposure, compared to control (both $p < 0.05$; **Figure 3.3**). No differences were seen in IL-10 and TNF- α mRNA levels, compared to control (**Supplementary Figure S3.1**).

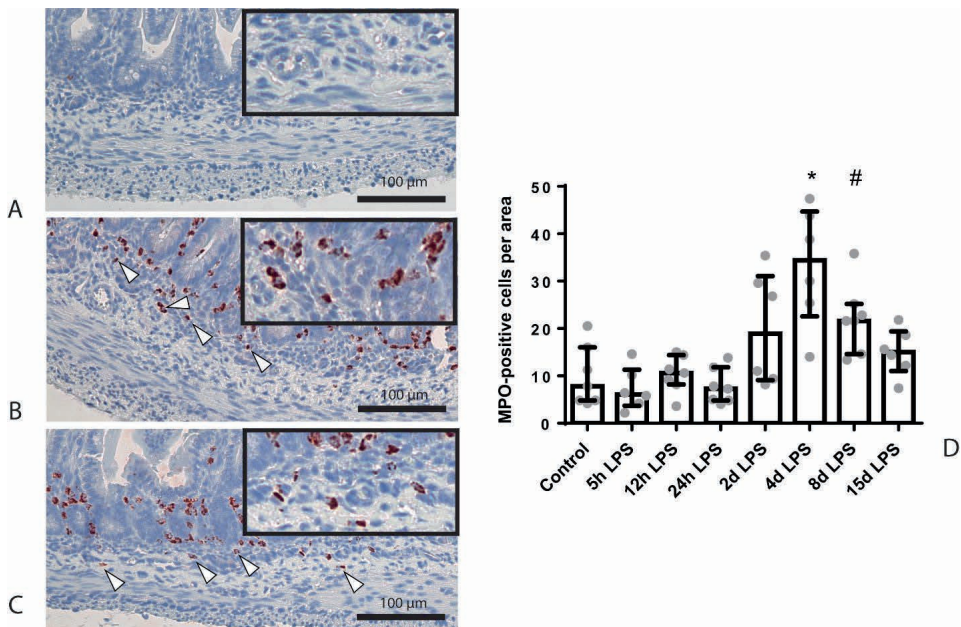


Figure 3.2 Representative images of submucosal neutrophil influx reflected by MPO-positive cell (indicated by white triangles) counts of the control (A), 4 days of IA LPS (B) and 8 days of IA LPS group (C). D: Increased MPO count in animals exposed to 4 and 8 days of IA LPS. * $p < 0.01$ compared to control. # $p = 0.08$ compared to control.

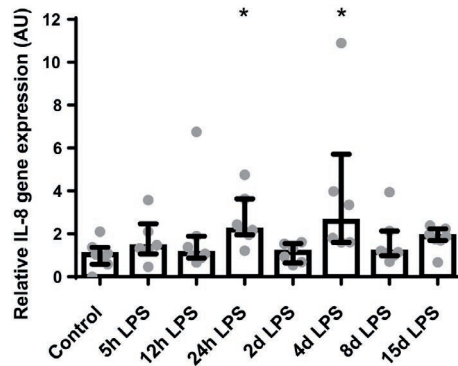


Figure 3.3 Relative gene expression of IL-8 in arbitrary unit (AU). Increased IL-8 gene expression in animals exposed to 24 hours and 4 days of IA LPS. * $p < 0.05$ compared to control.

Chorioamnionitis induced enteric nervous system alterations

The PGP9.5-positive and doublecortin-positive surface areas in the submucosal plexus were unchanged in all groups compared to control (**Supplementary Figure S3.2**). In the myenteric plexus, the PGP9.5-positive surface area was decreased after 4 days of IA LPS exposure, compared to control ($p < 0.05$; **Figure 3.4**).

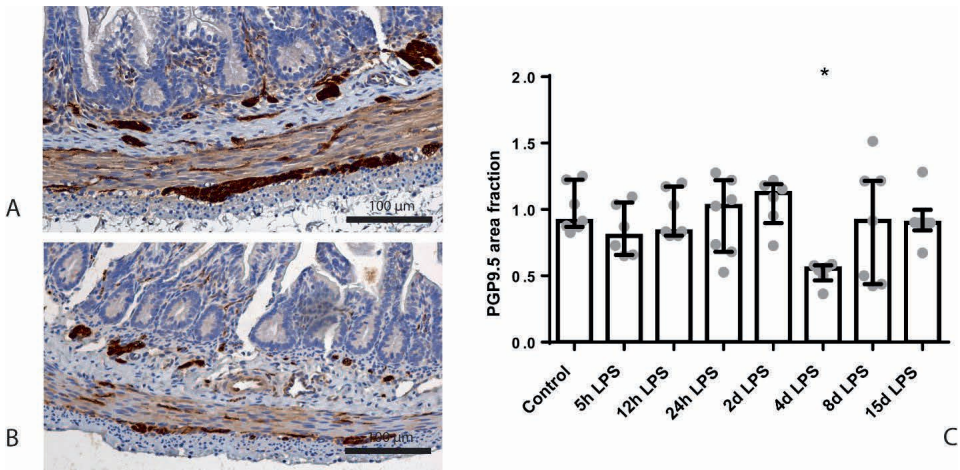


Figure 3.4 Representative images of PGP9.5 immunoreactivity in the submucosal and myenteric plexus of the control (A) and 4 days IA LPS group (B). Area fraction of PGP9.5 in the myenteric plexus (C) as fold increase over the control value. C: PGP9.5-positive surface area was decreased in animals exposed to 4 days of IA LPS. * $p < 0.05$ compared to control.

This reduction was resolved after 8 days of IA LPS exposure. At this time point, the doublecortin-positive surface area tended to be decreased in the myenteric plexus of LPS exposed animals, compared to control ($p = 0.07$; **Figure 3.5**).

In the submucosal plexus, no differences in the GFAP-positive surface areas were observed (**Supplementary Figure S3.3**), while in the myenteric plexus, the GFAP-positive surface area was increased in animals exposed to 2 days of IA LPS, compared to control ($p < 0.05$; **Figure 3.6**).

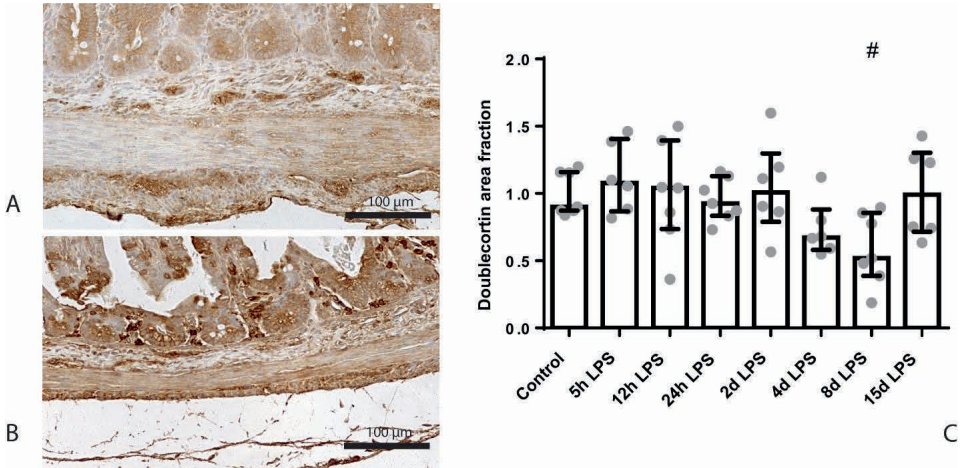


Figure 3.5 Representative images of doublecortin immunoreactivity in the submucosal and myenteric plexus of the control (A) and 8 days of IA LPS group (B). Area fraction of doublecortin in the myenteric plexus (C) as fold increase over the control value. C: Doublecortin-positive surface area tended to be decreased in animals exposed to 8 days of IA LPS. # $p = 0.07$ compared to control.

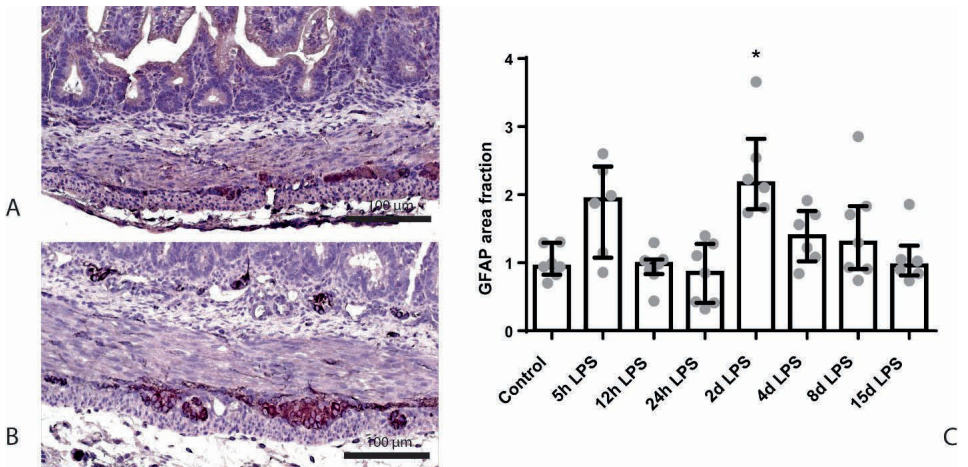


Figure 3.6 Representative images of GFAP immunoreactivity in the submucosal and myenteric plexus of the control (A) and 2 days of IA LPS group (B). Area fraction of GFAP in the myenteric plexus (C) as fold increase over the control value. C: GFAP-positive surface area in the myenteric plexus was increased in animals exposed to 2 days of IA LPS. * $p < 0.05$ compared to control.

The S100 β -positive surface area in the submucosal plexus tended to be decreased in animals exposed to 8 days of IA LPS, compared to control ($p=0.09$; **Figure 3.7**). In the myenteric plexus, the S100 β -positive surface area was decreased in animals exposed to 4 days of IA LPS, compared to control ($p<0.05$; **Figure 3.7**). No differences in nNOS and CHAT mRNA expression were observed between the groups (**Supplementary Figure S3.4**).

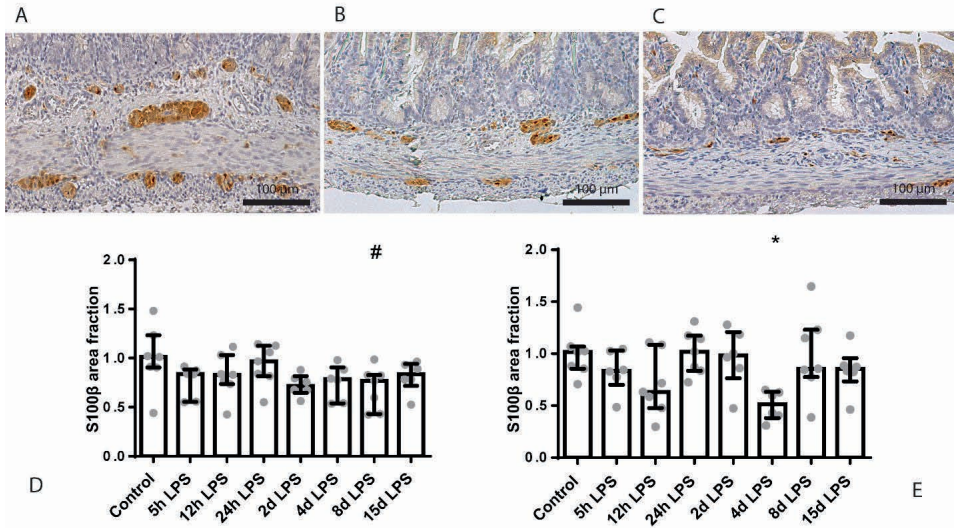


Figure 3.7 Representative images of S100 β immunoreactivity in the submucosal and myenteric plexus of the control (A), 4 days of IA LPS (B) and 8 days of IA LPS group (C). Area fraction of S100 β in the submucosal (D) and myenteric plexus (E) as fold increase over the control value. D: S100 β -positive surface area tended to be decreased in animals exposed to 8 days of IA LPS. # $p=0.09$ compared to control. E: S100 β -positive surface area is decreased in animals exposed to 4 days of IA LPS. * $p<0.05$ compared to control.

Discussion

In the current study, mucosal and submucosal intestinal inflammation were observed in the terminal ileum after 4 days of IA LPS exposure. On mRNA level, gut inflammation (IL-8) also occurs after 24 hours of IA LPS exposure, and this time point overlaps with the fetal systemic immune response, characterized by increased circulatory IL-6 levels⁶. *In utero* gastro-intestinal transit studies showed it takes approximately 24 hours for the swallowed AF to reach the mid-ileum (unpublished findings). Hence, this early inflammatory response in the terminal ileum is probably not caused by a local process, but solely the result of fetal systemic inflammation. In line, previous research in the same ovine model has shown that chorioamnionitis induced gut inflammation is the combined effect of direct gut exposure to LPS and a lung-mediated systemic inflammatory response⁵. It is possible that the early intestinal IL-8 peak contributes to the submucosal and mucosal increase of inflammatory cells at 4 days of IA LPS exposure through stimulation of chemotaxis²³.

Interestingly, the most evident signs of ENS alterations were also seen after 4 days, and after 8 days of IA LPS exposure. After 4 days IA LPS exposure, the myenteric plexus PGP9.5-positive surface area was decreased, indicating a loss of enteric neurons and/or reduction of PGP9.5 immunoreactivity of enteric nerve cells. Since the doublecortin-positive (immature neurons) surface area remained unchanged, this was probably the result of affected mature neurons. The reduced PGP9.5-positive surface area after 4 days of IA LPS exposure was recovered after 8 days of IA LPS exposure. The doublecortin-positive surface area tended to decrease at this time point. These findings might indicate that an initial loss of mature neurons is compensated by an accelerated maturation of immature neurons. Whether such an accelerated maturation is sufficient to fully compensate for the identified loss of neurons remains to be elucidated. These findings combined with the unaltered PGP9.5-positive and doublecortin-positive surface area after 2 and 7 days of IA LPS exposure in a previous study¹⁹, show that the ENS changes found are time-dependent and may recover following prolonged intra-uterine inflammation. Interestingly, in a previous study, a similar loss of mature neurons was observed after chronic IA exposure to UP, indicating that different inflammatory triggers can induce similar ENS damage¹⁹.

Enteric glial cells are important for neuronal maintenance, survival, and function²⁴, and are capable of generating enteric neurons in response to injury^{25,26}. In addition, enteric glia respond, in a manner similar as reactive astrogliosis in the central nervous system, to ENS injury and inflammation by changing both their morphology and their expression of key proteins such as GFAP^{27,28}. The neuronal loss in the myenteric plexus after four days of LPS exposure is accompanied with a reduced S100 β -positive surface area, likely representing a loss of glial cells and/or loss of S100 β immunoreactivity within glial cells, as was earlier described during chronic IA UP exposure¹⁹. Interestingly, this loss of neurons and glial cells is preceded by an increased myenteric plexus GFAP immunoreactivity after 2 days of LPS exposure. It is likely that the observed glial cell response results from fetal systemic inflammation and/or intestinal inflammation, since pro-inflammatory cytokines have been shown to induce GFAP expression in enteric glial cells²⁹. Moreover, as activated enteric glial cells can secrete various cytokines and other mediators involved in the infiltration and activation of immune cells^{30,31}, the observed glial cell reaction can contribute to the intestinal influx of neutrophils observed after 4 days of IA LPS exposure. Since a glial cell response in the context of intestinal inflammation can be destructive³² and eventually neuroregenerative³³, it is to date unclear whether it contributes to the loss of neurons and glial cells or is a protective mechanism that falls short with prolonged inflammation.

In this study, the most profound ENS changes were found in the myenteric plexus, rather than the submucosal plexus. This is in concordance with earlier findings in fetal lambs that were chronically IA exposed to UP¹⁹. Moreover, inflammation driven pathological changes of the ENS are more often found in the myenteric plexus than in the submucosal plexus³⁴. The mechanisms behind this apparent increased vulnerability of the myenteric plexus remain to be elucidated. At present, we can only speculate about the mechanisms responsible for the observed differences because multiple possible explanations are in play. First, since the ENS undergoes rapid structural growth *in utero*, the composition of the submucosal and myenteric plexus might be differently altered by the combination of ongoing developmental processes and LPS exposure. Alternatively, the migratory pattern of

cells in these plexi might be different during this essential developmental period of the ENS. Second, the macrophages in the plexus, which are in close proximity to neuronal cell bodies and nerve fibers, undergo differentiation towards a multitude of subsets depending on microenvironment but also depending on developmental stage and bacterial colonization. Our findings indicate that these cells play a role in the differential response of the submucosal and myenteric plexus, although the reason for that remains speculative. Notably, the transcriptional profiles of macrophages gradually differ from the lumen to the myenteric plexus. As a result, the macrophages closer to the lumen play an important role by sampling luminal bacteria and initiating adaptive immune responses to clear pathogenic bacteria, whereas macrophages in the muscularis, which are comparatively more distant from luminal stimulation, are primarily involved in tissue protection and regulation of the activity of enteric neurons and peristalsis^{35,36}. It is tempting to speculate that phenotypical differences of these immune cells following exposure to a bacterial stimulus in the different plexi are involved in the observed differences between the submucosal and myenteric plexus.

At present, it is unclear whether the observed changes have postnatal functional consequences. As the mRNA expression of CHAT and nNOS are unchanged, *in utero* motility signaling function could be unaltered. This confirms and extends previous findings in fetal lambs chronically IA exposed to UP¹⁹. The resolved inflammation and the recovery of (immature) neurons and glial cells after fifteen days of IA LPS exposure indicate that damage due to IA LPS exposure probably can be repaired *in utero*. Nevertheless, it is likely that a child that is born prematurely with ongoing inflammation due to FIRS will experience additional postnatal inflammatory stimuli such as mechanical ventilation³⁷ or sepsis³⁸. The effects of these postnatal exposures on the ENS should be studied in order to shed light on the long-term consequences of (intra-uterine) inflammation for ENS development and function. Notably, 4 to 8 days after the start of intra-uterine infection could very well be the window of vulnerability in which additional inflammation may have a higher impact as the ENS is already affected at this time point.

A limitation of this study is the relatively low number of animals per group, which is an unavoidable shortcoming of the translational large animal model. Secondly, the current set-up with the fixed moment of premature birth does not exclude a potential influence of gestational age at start of intra-uterine infection. Thirdly, in the current study we were unable to unravel the mechanisms behind the observed changes, as no serial sampling was applied following a specific injection time point.

In summary, submucosal intestinal inflammation was detected after 4 days of IA LPS exposure that coincided with gut mucosal and fetal systemic inflammation. At the same time point, a loss of PGP9.5 and S100 β immunoreactivity in the myenteric plexus was observed. These changes are preceded by a glial cell response with systemic inflammation and local gut inflammation. Although initial ENS damage seemed to recover after prolonged IA LPS exposure, additional postnatal inflammatory hits that a premature born child is likely to encounter may further harm the ENS and influence functional outcomes. In this context, 4 to 8 days after the start of an intra-uterine infection may be a window of increased ENS vulnerability, indicating that therapeutic interventions should ideally start before or at this time point.

References

1. Galinsky R, Polglase GR, Hooper SB, Black MJ, Moss TJ. The consequences of chorioamnionitis: preterm birth and effects on development. *J Pregnancy*. 2013;2013:412831.
2. Goldenberg RL, Hauth JC, Andrews WW. Intrauterine infection and preterm delivery. *N Engl J Med*. 2000;342(20):1500-7.
3. Kim CJ, Romero R, Chaemsaihong P, Chaiyasit N, Yoon BH, Kim YM. Acute chorioamnionitis and funisitis: definition, pathologic features, and clinical significance. *Am J Obstet Gynecol*. 2015;213(4 Suppl):S29-52.
4. Gantert M, Been JV, Gavilanes AW, Garnier Y, Zimmermann LJ, Kramer BW. Chorioamnionitis: a multiorgan disease of the fetus? *J Perinatol*. 2010;30 Suppl:S21-30.
5. Wolfs TG, Kramer BW, Thuijls G, Kemp MW, Saito M, Willems MG, Senthamarai-Kannan P, Newnham JP, Jobe AH, Kallapur SG. Chorioamnionitis-induced fetal gut injury is mediated by direct gut exposure of inflammatory mediators or by lung inflammation. *Am J Physiol Gastrointest Liver Physiol*. 2014;306(5):G382-93.
6. Gussenhoven R, Westerlaken RJJ, Ophelders D, Jobe AH, Kemp MW, Kallapur SG, Zimmermann LJ, Sangild PT, Pankratova S, Gressens P, Kramer BW, Fleiss B, Wolfs T. Chorioamnionitis, neuroinflammation, and injury: timing is key in the preterm ovine fetus. *J Neuroinflammation*. 2018;15(1):113.
7. Been JV, Lieveense S, Zimmermann LJ, Kramer BW, Wolfs TG. Chorioamnionitis as a risk factor for necrotizing enterocolitis: a systematic review and meta-analysis. *J Pediatr*. 2013;162(2):236-42 e2.
8. Neu J, Walker WA. Necrotizing enterocolitis. *N Engl J Med*. 2011;364(3):255-64.
9. Neu J, Pammi M. Necrotizing enterocolitis: The intestinal microbiome, metabolome and inflammatory mediators. *Semin Fetal Neonatal Med*. 2018.
10. Sigge W, Wedel T, Kuhnel W, Krammer HJ. Morphologic alterations of the enteric nervous system and deficiency of non-adrenergic non-cholinergic inhibitory innervation in neonatal necrotizing enterocolitis. *Eur J Pediatr Surg*. 1998;8(2):87-94.
11. Wedel T, Krammer HJ, Kuhnel W, Sigge W. Alterations of the enteric nervous system in neonatal necrotizing enterocolitis revealed by whole-mount immunohistochemistry. *Pediatr Pathol Lab Med*. 1998;18(1):57-70.
12. Fagbemi AO, Torrente F, Puleston J, Lakhoo K, James S, Murch SH. Enteric neural disruption in necrotizing enterocolitis occurs in association with myenteric glial cell CCL20 expression. *J Pediatr Gastroenterol Nutr*. 2013;57(6):788-93.
13. Zhou Y, Yang J, Watkins DJ, Boomer LA, Matthews MA, Su Y, Besner GE. Enteric nervous system abnormalities are present in human necrotizing enterocolitis: potential neurotransplantation therapy. *Stem Cell Res Ther*. 2013;4(6):157.
14. Furness JB. The enteric nervous system and neurogastroenterology. *Nat Rev Gastroenterol Hepatol*. 2012;9(5):286-94.
15. Rao M, Gershon MD. Enteric nervous system development: what could possibly go wrong? *Nat Rev Neurosci*. 2018;19(9):552-65.
16. Lake JI, Heuckeroth RO. Enteric nervous system development: migration, differentiation, and disease. *Am J Physiol Gastrointest Liver Physiol*. 2013;305(1):G1-24.
17. Hao MM, Foong JP, Bornstein JC, Li ZL, Vanden Berghe P, Boesmans W. Enteric nervous system assembly: Functional integration within the developing gut. *Dev Biol*. 2016;417(2):168-81.
18. Burns AJ, Roberts RR, Bornstein JC, Young HM. Development of the enteric nervous system and its role in intestinal motility during fetal and early postnatal stages. *Semin Pediatr Surg*. 2009;18(4):196-205.
19. Heymans C, de Lange IH, Hutten MC, Lenaerts K, de Ruijter NJE, Kessels L, Rademakers G, Melotte V, Boesmans W, Saito M, Usuda H, Stock SJ, Spiller OB, Beeton ML, Payne MS, Kramer BW, Newnham JP, Jobe AH, Kemp MW, van Gemert WG, Wolfs T. Chronic Intra-Uterine Ureaplasma parvum Infection Induces Injury of the Enteric Nervous System in Ovine Fetuses. *Front Immunol*. 2020;11:189.
20. Kuypers E, Wolfs TG, Collins JJ, Jellema RK, Newnham JP, Kemp MW, Kallapur SG, Jobe AH, Kramer BW. Intraamniotic lipopolysaccharide exposure changes cell populations and structure of the ovine fetal thymus. *Reprod Sci*. 2013;20(8):946-56.

21. Newnham JP, Kallapur SG, Kramer BW, Moss TJ, Nitsos I, Ikegami M, Jobe AH. Betamethasone effects on chorioamnionitis induced by intra-amniotic endotoxin in sheep. *Am J Obstet Gynecol.* 2003;189(5):1458-66.
22. Willems MG, Ophelders DR, Nikiforou M, Jellema RK, Butz A, Delhaas T, Kramer BW, Wolfs TG. Systemic interleukin-2 administration improves lung function and modulates chorioamnionitis-induced pulmonary inflammation in the ovine fetus. *Am J Physiol Lung Cell Mol Physiol.* 2016;310(1):L1-7.
23. Russo RC, Garcia CC, Teixeira MM, Amaral FA. The CXCL8/IL-8 chemokine family and its receptors in inflammatory diseases. *Expert Rev Clin Immunol.* 2014;10(5):593-619.
24. De Giorgio R, Giancola F, Boschetti E, Abdo H, Lardeux B, Neunlist M. Enteric glia and neuroprotection: basic and clinical aspects. *Am J Physiol Gastrointest Liver Physiol.* 2012;303(8):G887-93.
25. Joseph NM, He S, Quintana E, Kim YG, Nunez G, Morrison SJ. Enteric glia are multipotent in culture but primarily form glia in the adult rodent gut. *J Clin Invest.* 2011;121(9):3398-411.
26. Laranjeira C, Sandgren K, Kessar N, Richardson W, Potocnik A, Vanden Berghe P, Pachnis V. Glial cells in the mouse enteric nervous system can undergo neurogenesis in response to injury. *J Clin Invest.* 2011;121(9):3412-24.
27. Boesmans W, Lasrado R, Vanden Berghe P, Pachnis V. Heterogeneity and phenotypic plasticity of glial cells in the mammalian enteric nervous system. *Glia.* 2015;63(2):229-41.
28. Rosenbaum C, Schick MA, Wollborn J, Heider A, Scholz CJ, Cecil A, Niesler B, Hirrlinger J, Walles H, Metzger M. Activation of Myenteric Glia during Acute Inflammation In Vitro and In Vivo. *PLoS One.* 2016;11(3):e0151335.
29. von Boyen GB, Steinkamp M, Reinshagen M, Schafer KH, Adler G, Kirsch J. Proinflammatory cytokines increase glial fibrillary acidic protein expression in enteric glia. *Gut.* 2004;53(2):222-8.
30. Stoffels B, Hupa KJ, Snoek SA, van Bree S, Stein K, Schwandt T, Vilz TO, Lysson M, Veer CV, Kummer MP, Hornung V, Kalff JC, de Jonge WJ, Wehner S. Postoperative ileus involves interleukin-1 receptor signaling in enteric glia. *Gastroenterology.* 2014;146(1):176-87.e1.
31. Sharkey KA. Emerging roles for enteric glia in gastrointestinal disorders. *J Clin Invest.* 2015;125(3):918-25.
32. Brown IA, McClain JL, Watson RE, Patel BA, Gulbransen BD. Enteric glia mediate neuron death in colitis through purinergic pathways that require connexin-43 and nitric oxide. *Cell Mol Gastroenterol Hepatol.* 2016;2(1):77-91.
33. Belkind-Gerson J, Graham HK, Reynolds J, Hotta R, Nagy N, Cheng L, Kamionek M, Shi HN, Aherne CM, Goldstein AM. Colitis promotes neuronal differentiation of Sox2+ and PLP1+ enteric cells. *Sci Rep.* 2017;7(1):2525.
34. De Giorgio R, Guerrini S, Barbara G, Stanghellini V, De Ponti F, Corinaldesi R, Moses PL, Sharkey KA, Mawe GM. Inflammatory neuropathies of the enteric nervous system. *Gastroenterology.* 2004;126(7):1872-83.
35. Gabanyi I, Muller PA, Feighery L, Oliveira TY, Costa-Pinto FA, Mucida D. Neuro-immune Interactions Drive Tissue Programming in Intestinal Macrophages. *Cell.* 2016;164(3):378-91.
36. De Schepper S, Verheijden S, Aguilera-Lizarraga J, Viola MF, Boesmans W, Stakenborg N, Voytyuk I, Schmidt I, Boeckx B, Dierckx de Casterle I, Baekelandt V, Gonzalez Dominguez E, Mack M, Depoortere I, De Strooper B, Sprangers B, Himmelreich U, Soenen S, Guilliams M, Vanden Berghe P, Jones E, Lambrechts D, Boeckstaens G. Self-Maintaining Gut Macrophages Are Essential for Intestinal Homeostasis. *Cell.* 2018;175(2):400-15 e13.
37. Bose CL, Laughon MM, Allred EN, O'Shea TM, Van Marter LJ, Ehrenkranz RA, Fichorova RN, Leviton A, Investigators ES. Systemic inflammation associated with mechanical ventilation among extremely preterm infants. *Cytokine.* 2013;61(1):315-22.
38. Machado JR, Soave DF, da Silva MV, de Menezes LB, Etchebehere RM, Monteiro ML, dos Reis MA, Correa RR, Celes MR. Neonatal sepsis and inflammatory mediators. *Mediators Inflamm.* 2014;2014:269681.

Supplemental materials

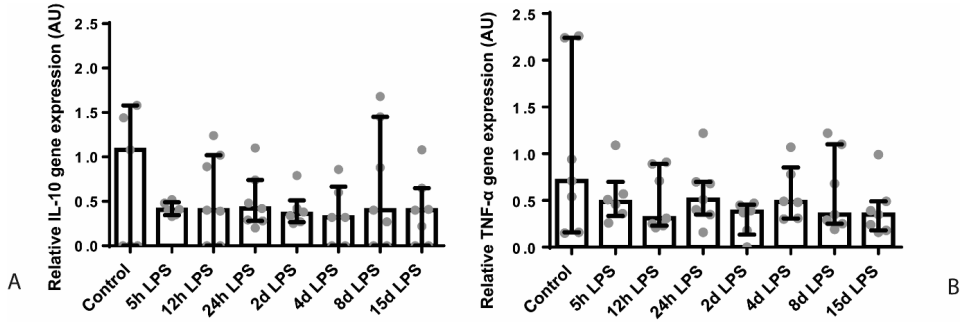


Figure S3.1 Relative gene expression of IL-10 and TNF- α in arbitrary unit (AU). No differences were seen in IL-10 and TNF- α mRNA levels, compared to control.

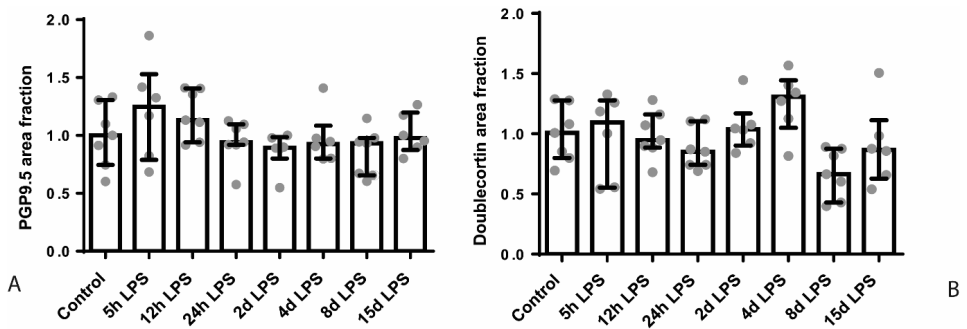


Figure S3.2 Area fraction of PGP9.5 (A) and doublecortin (B) in the submucosal plexus (C) as fold increase over the control value. The PGP9.5-positive and doublecortin-positive surface areas in the submucosal plexus were unchanged in all groups compared to control.

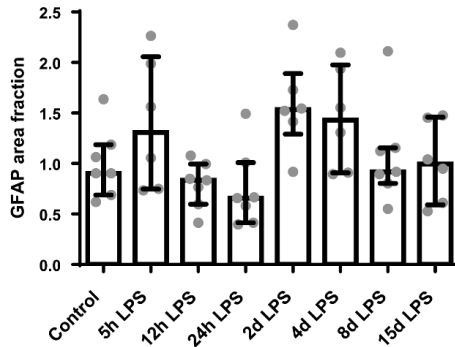


Figure S3.3 Area fraction of GFAP in the submucosal plexus as fold increase over the control value. No differences in the GFAP-positive surface areas were observed in the submucosal plexus compared to control.

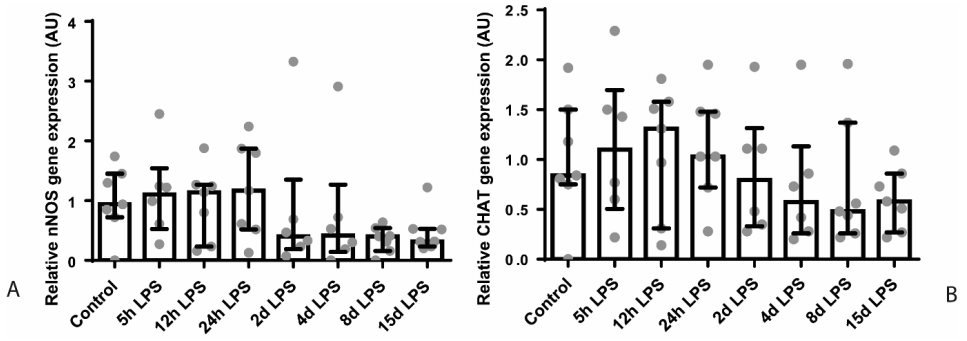


Figure S3.4 Relative gene expression of nNOS and CHAT in arbitrary unit (AU). No differences in nNOS and CHAT mRNA expression were observed between the groups.

Chapter 4

Chronic intra-uterine *Ureaplasma parvum* infection induces injury of the enteric nervous system in ovine fetuses

C. Heymans, I.H. de Lange, M.C. Hütten, K. Lenaerts, N.J.E. de Ruijter, L.C.G.A. Kessels,
G. Rademakers, V. Melotte, W. Boesmans, M. Saito, H. Usuda, S.J. Stock, O.B. Spiller,
M.L. Beeton, M.S. Payne, B.W. Kramer, J.P. Newnham, A.H. Jobe, M.W. Kemp,
W.G. van Gemert, and T.G.A.M. Wolfs

Frontiers in Immunology. 2020;11:189

Abstract

Background

Chorioamnionitis, inflammation of the fetal membranes during pregnancy, is often caused by intra-amniotic (IA) infection with single or multiple microbes. Chorioamnionitis can be either acute or chronic, and is associated with adverse postnatal outcomes of the intestine, including necrotizing enterocolitis (NEC). Neonates with NEC have structural and functional damage to the intestinal mucosa and the enteric nervous system (ENS), with loss of enteric neurons and glial cells. Yet, the impact of acute, chronic, or repetitive antenatal inflammatory stimuli on the development of the intestinal mucosa and ENS has not been studied. The aim of this study is therefore to investigate the effect of acute, chronic, and repetitive microbial exposure on the intestinal mucosa, submucosa and ENS in premature lambs.

Materials and methods

A sheep model of pregnancy was used in which the ileal mucosa, submucosa, and ENS were assessed following IA exposure to lipopolysaccharide (LPS) for 2 or 7 days (acute), *Ureaplasma parvum* (UP) for 42 days (chronic) or repetitive microbial exposure (42 days UP with 2 or 7 days LPS).

Results

IA LPS exposure for 7 days or IA UP exposure for 42 days caused intestinal injury and inflammation in the mucosal and submucosal layer of the gut. Repetitive microbial exposure did not further aggravate injury of the terminal ileum. Chronic IA UP exposure caused significant structural ENS alterations characterized by loss of PGP9.5 and S100 β immunoreactivity whereas these changes were not found after re-exposure of chronic UP-exposed fetuses to LPS for 2 or 7 days.

Conclusion

The *in utero* loss of PGP9.5 and S100 β immunoreactivity following chronic UP exposure corresponds with intestinal changes in neonates with NEC, and may therefore form a novel mechanistic explanation for the association of chorioamnionitis and NEC.

Introduction

Preterm birth is a common and major worldwide health issue, contributing to significant neonatal morbidity and mortality¹. Around one in every ten births is preterm, accounting for approximately 15 million premature newborns each year². Due to complications, over one million premature newborns will die shortly after birth^{3,4}. Chorioamnionitis, defined as inflammatory cell infiltration of fetal membranes, is frequently associated with preterm birth and typically occurs due to an ascending bacterial infection⁵⁻⁷ that can be acute or chronic⁸. Intra-uterine exposure of preterm infants to chorioamnionitis is associated with an increased risk of adverse neonatal outcomes^{9,10}, including necrotizing enterocolitis (NEC)^{9,11,12}. Adverse gastrointestinal outcomes have been associated with both systemic fetal inflammatory response syndrome (FIRS) and direct exposure of the gut to swallowed infected amniotic fluid^{11,13,14}. Chorioamnionitis can occur with intact membranes, which is common for genital mycoplasmas, such as *Ureaplasma* species (spp.), present in the lower genital tract of women^{6,15}. The *Ureaplasma* spp. can cause chronic chorioamnionitis that does not evoke a maternal response, but is still associated with adverse fetal outcomes¹⁶. In an experimental large animal model, we previously showed that an *Ureaplasma parvum* (UP) serovar 3 infection up to 14 days prior to delivery causes fetal gut inflammation with damaged villus epithelium, gut barrier loss and severe villus atrophy¹⁷.

The injury caused by intra-uterine *Ureaplasma* spp. exposure might derive from the direct inflammatory reaction, as well as from potential interactions with other inflammatory stimuli. Chorioamnionitis is often polymicrobial, as over 65% of positive amniotic fluid cultures lead to the identification of two or more pathogens⁷. In this context, we previously showed that cerebral and lung immune activation following intra-amniotic (IA) lipopolysaccharide (LPS) exposure was prevented when these animals were chronically pre-exposed to UP serovar 3^{18,19}. This illustrates that interactions between different microbes can occur, leading to organ-specific sensitization or preconditioning.

The enteric nervous system (ENS) consists of enteric neurons and glial cells, autonomously regulates gastrointestinal activity (i.e., secretion, absorption, and motility), and contributes to gut integrity²⁰. The formation of the ENS requires coordinated migration, proliferation, and differentiation of neural crest progenitors, directed neurite growth, and establishment of a network of interconnected neurons and glia^{21,22}. Although these processes mostly occur *in utero*, an important part of ENS development takes place postnatally^{23,24}. Neonates with NEC have structural and functional damage of the submucosal and myenteric plexus, including loss of enteric neurons and glial cells²⁵⁻²⁷. The involvement of chorioamnionitis in the induction of adverse intestinal outcomes including NEC combined with the presence of ENS abnormalities in NEC, prompted us to study the impact of an antenatal infection on the ENS.

The aim of this study was therefore to investigate the effect of acute IA exposure to LPS and chronic exposure to UP on the intestinal mucosa and ENS in fetal lambs using a well-established sheep model of chorioamnionitis. In addition, we investigated the potential interactions of repetitive IA microbial stimuli by acute exposure to LPS in ovine fetuses that were chronically pre-exposed to UP.

Materials and methods

Animal model and experimental procedures

All experiments were approved by the animal ethics committee of the University of Western Australia (Perth, Australia).

The animal model and experimental procedures were previously described¹⁸. Briefly, 39 date-mated merino ewes were randomly assigned to six different groups of between five and eight animals, to receive IA injections under ultrasound guidance. Verification of the IA injections was done by amniotic fluid electrolyte analysis. The date-mated pregnant ewes received an IA injection of an *in vitro* cultured strain HPA5 of UP serovar 3 (2×10^5 color-changing units [CCU])²⁸ 42 days prior to delivery (at 82 days of gestation, which corresponds to the second trimester in humans), or *E. coli*-derived LPS (O55:B5; Merck, Darmstadt, Germany), 10 mg in two mL of saline, 2 days or 7 days prior to delivery (at respectively 122 and 117 days of gestation). Previously, we have shown that the half-life time of LPS in the amniotic fluid is relatively long (1.7 days) and that the LPS amount is higher than the essential threshold of 1mg for at least 5 days^{29,30}. Chronic sustained UP infection was confirmed by positive culture of amniocentesis samples at intermediate time points and sterile amniotic fluid samples collected at caesarean delivery as previously described³¹. Two or 7 days LPS exposure (prior to caesarean delivery) represents an acute inflammatory challenge. To evaluate the combined effect between these inflammatory modalities, a subgroup of chronically UP infected ewes received IA LPS at 35 and 40 days post UP infection (i.e. 7 or 2 days LPS exposure prior to delivery following 42 days of UP infection). A group receiving IA injections of sterile saline (2 or 7 days prior to delivery; respectively 6 and 2 animals which were pooled) served as controls (**Figure 4.1**). Fetuses were surgically delivered at 124 ± 2 days of gestational age (term gestation in sheep = 150 days), equivalent of approximately 30 weeks of human gestation. After delivery, fetuses were euthanized with intravenous pentobarbital (100 mg/kg). For this experiment, fetuses of both sexes were used.

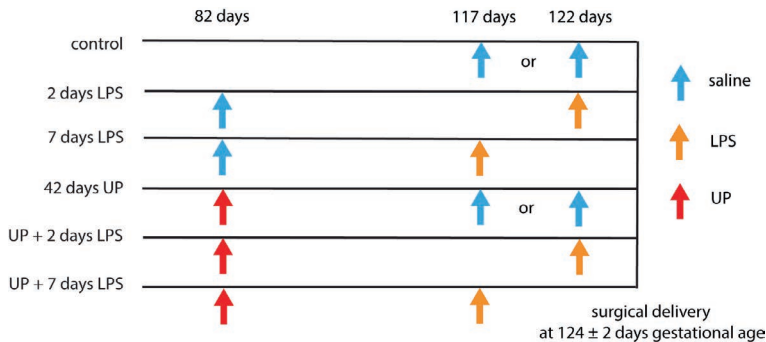


Figure 4.1 Different intervention study groups. All injections were delivered by ultrasound-guided amniocentesis. Timing shown in gestational days.

Sampling

During necropsy, blood and terminal ileum samples were collected. Ileum samples were fixed in 10% formalin and embedded in paraffin, or snap frozen in liquid nitrogen. Where insufficient paraffin-embedded material was available for study, additional material was generated by paraffin embedding snap frozen tissue samples: frozen tissue blocks were defrosted, fixed in 4% formaldehyde at room temperature overnight and transferred to 70% ethanol prior to embedding in paraffin with the use of a vacuum infiltration processor.

Antibodies

The following antibodies were used for immunohistochemistry: polyclonal rabbit anti-myeloperoxidase ([MPO]; A0398, Dakocytomation, Glostrup, Denmark) for identification of neutrophils, polyclonal rabbit anti-cluster of differentiation 3 ([CD3]; A0452, Dakocytomation) for the detection of T cells, polyclonal rabbit anti-bovine protein gene product 9.5 ([PGP9.5]; Z5116, Dakocytomation) for the detection of enteric neurons, polyclonal rabbit anti-doublecortin (Ab18723, Abcam, Cambridge, UK) for the detection of immature neurons, polyclonal rabbit anti-glial fibrillary acidic protein ([GFAP]; Zo334, Dakocytomation) to detect enteric glial cell reactivity/activation³² and polyclonal rabbit anti-S100 β (PA5-16257, Invitrogen, Carlsbad, CA, USA) as a marker for enteric glial cells.

The following secondary antibodies were used: peroxidase-conjugated polyclonal goat anti-rabbit (111-035-045, Jackson, WestGrove, PA, USA) (MPO), peroxidase-conjugated polyclonal swine anti-rabbit (P0399, DakoCytomation) (doublecortin) and BrightVision+ Poly-HRP-Anti Mouse/Rabbit IgG Biotin-free (ImmunoLogic, Duiven, the Netherlands) (PGP9.5), and biotin conjugated polyclonal swine anti-rabbit (E0353, DakoCytomation) (CD3, GFAP, S100 β).

Immunohistochemistry

Formalin-fixed terminal ileum was embedded in paraffin and 4 μ m sections were cut. After deparaffinization and rehydration, endogenous peroxidase activity was blocked with 0.3% H₂O₂ diluted in phosphate buffered saline ([PBS]; pH 7.4). Antigen retrieval was performed with citrate buffer for CD3, PGP9.5, doublecortin and S100 β stainings. Non-specific binding was blocked for 30 minutes at room temperature with 10% normal goat serum (NGS) in PBS (MPO), 5% NGS in PBS (doublecortin), or 5% bovine serum albumin (BSA) in PBS (CD3, GFAP and S100 β). For PGP9.5, non-specific binding was blocked for 10 minutes at room temperature with 20% fetal calf serum (FCS). Thereafter, sections were incubated with the primary antibody of interest and subsequently incubated with the respective secondary antibody. MPO, PGP9.5 and doublecortin were detected by using a peroxidase-conjugated secondary antibody and antibodies against CD3, GFAP and S100 β were detected with avidin-biotin complex (Vectastain Elite ABC kit, Bio-connect, Huissen, the Netherlands). Substrate staining was performed for MPO with 3-amino-9-ethylcarbazole ([AEC]; Merck, Darmstadt, Germany). Immunoreactivity for CD3 and GFAP was detected by using nickel-DAB. Immunoreactivity for PGP9.5, doublecortin and S100 β was detected by using DAB. Haematoxyline (MPO, PGP9.5, doublecortin and S100 β) or nuclear fast red (CD3 and GFAP) were used as counterstain for nuclei.

Qualitative analysis of damage of the terminal ileum

H&E slides were analyzed by two independent investigators blinded to the experimental setup, to assess damage of the terminal ileum. A scoring system from 0 to 4 was used to describe the severity of histological injury. Scoring was as follows: 0 no damage, 1 disrupted epithelial lining, but no loss of enterocytes, 2 disrupted epithelial lining, mild enterocyte loss from the villus tips, 3 disrupted epithelial lining, moderate enterocyte loss from villus tips, some debris in the lumen and 4 abundant enterocyte loss from villus tips, abundant debris in the lumen and severe shedding of villus tips.

Quantification of immunohistochemical stainings

The stained tissue sections were scanned with the Ventana iScan HT slide scanner (Ventana Medical Systems, Oro Valley, AZ, USA). Of these images, viewed with Panoramic Viewer (version 1.15.4, 3DHISTECH, Budapest, Hungary), random images of regions of interest were taken (200x).

Two investigators blinded to the study groups counted the MPO-positive and CD3-positive cells in three to five non-overlapping high-power fields in the mucosa and submucosa. The average MPO- and CD3-positive cells per area are reported for each animal. The percentage of area in the submucosal and myenteric ganglia positively stained for PGP9.5, doublecortin, GFAP and S100 β was determined in five non-overlapping high power fields using Leica QWin Pro software (version 3.4.0, Leica Microsystems, Mannheim, Germany) by an investigator blinded to the study groups. Relative area staining was calculated by dividing the positively stained areas of the ganglia of the submucosal or myenteric plexus by the total area of the muscle layer. The data are expressed as fold increase over the control value.

RNA extraction and quantitative real-time PCR

RNA was extracted from snap frozen terminal ileum tissue using TRI reagent (Invitrogen)/chloroform extraction. Isolated RNA was DNase treated to remove possible contamination with genomic DNA by using the RQ1 RNase-Free DNase kit (Promega, Madison, WI, USA) and afterwards reverse transcribed into cDNA using oligo(dT)12-18 primers (Invitrogen) and Moloney murine leukemia virus (M-MLV) reverse transcriptase (Invitrogen). Quantitative real-time PCR (qPCR) reactions were performed with a LightCycler 480 Instrument (Roche Applied Science, Basel, Switzerland) using the SensiMix™ SYBR® No-ROX Kit (Bioline, London, UK) for 45 cycles. mRNA levels of IL-1 β , IL-6, IL-10, tumor necrosis factor alpha (TNF- α) and interleukin-1 receptor-associated kinase 3 (IRAK3) were determined to assess inflammation of the terminal ileum. mRNA levels of neuronal nitric oxide synthase (nNOS) and choline acetyltransferase (CHAT) were determined to assess motility signaling functions of the ENS using LinRegPCR software (version 2016.0, Heart Failure Research Center, Academic Medical Center, Amsterdam, the Netherlands). The geometric mean of the mRNA levels of three reference genes (ribosomal protein S15 (RPS15), glyceraldehyde 3-phosphate dehydrogenase (GAPDH) and peptidylprolyl isomerase A (PPIA)) were calculated and used as a normalization factor. The data are expressed as fold increase over the control value. Primer sequences are shown in **Table 4.1**.

Table 4.1 Primer sequences.

Primer	Forward	Reverse
RPS15	5'-CGAGATGGTGGGCAGCAT-3'	5'-GCTTGATTCCACCTGGTTGA-3'
GAPDH	5'-GGAAGCTCACTGGCATGGC-3'	5'-CCTGCTTCACCACCTTCTTG-3'
PPIA	5'-TTATAAAGTTCTCTGTTTCACAGAA-3'	5'-ATGGACTGCCACCAGTACCA-3'
IL-1 β	5'-AGAATGAGCTGTTATTTGAGTTGATG-3'	5'-GTGAGAAATCTGCAGCTGGATGT-3'
IL-6	5'-ACATCGTCGACAAAATCTCTGCAA-3'	5'-GCCAGTGTCTCCTTGCTGTTT-3'
IL-10	5'-CATGGGCTGACATCAAGGA-3'	5'-CGGAGGGTCTTCAGCTTCTC-3'
TNF- α	5'-GCCGGAATACCTGGACTATGC-3'	5'-CAGGGCGATGATCCCAAAGTAG-3'
IRAK3	5'-AGTGTGTAGGTAACACAGCCC-3'	5'-TGCTGGTCATGCTTATGGCA-3'
nNOS	5'-CGGCTTTGGGGTTATCAGT-3'	5'-TTGCCCATTTCCACTCCTC-3'
CHAT	5'-CCGCTGGTATGACAAGTCCC-3'	5'-GCTGGTCTTCACCATGTGCT-3'

Data analysis

Data are presented as median with interquartile range. Statistical analyses were performed using GraphPad Prism (version 6.01, GraphPad Software Inc., La Jolla, CA, USA). A nonparametric Kruskal-Wallis test followed by Dunn's post hoc test was used to analyze statistically significant group differences. Differences were considered statistically significant at $p < 0.05$. Given the relatively small animal numbers per group, we also reported actual p -values between $p \geq 0.05$ and $p < 0.10$ and interpreted these as potentially biologically relevant. This assumption will decrease the chance of a type II error, but increases the chance of a type I error.

Results

Intestinal damage and inflammation in the terminal ileum due to chorioamnionitis

There was a higher intestinal damage score for all experimental groups, compared to control ($p < 0.005$ for 7d LPS group, $p < 0.05$ for 42d UP group and 42d UP + 7d LPS group and $p = 0.06$ for 42d UP + 2d LPS group all compared to control; **Figure 4.2**), except for the animals exposed to 2 days of LPS. Pre-exposure with UP did not augment mucosal injury in the LPS-treated groups.

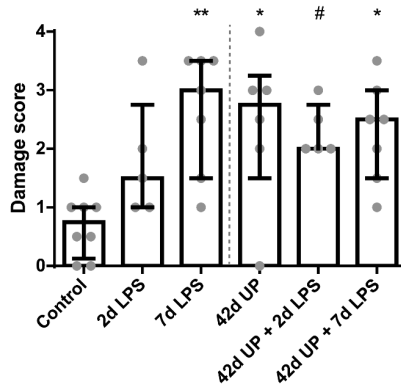


Figure 4.2 Increased mucosal injury in all groups, except for the animals exposed to 2 days LPS. # $p = 0.06$, * $p < 0.05$ and ** $p < 0.005$ compared to control.

A statistically significant increase in MPO-positive cells was seen in the mucosa 7 days after LPS exposure, compared to control ($p < 0.05$; **Figure 4.3**). Chronic UP infection also caused an elevation of mucosal MPO-positive cells, compared to control ($p = 0.08$; **Figure 4.3**). Furthermore, combining these two inflammatory insults resulted in an increased mucosal MPO-positive cell count compared to control ($p < 0.005$; **Figure 4.3**) and this experimental group tended to be increased when compared to the UP + two-day LPS-exposed group ($p = 0.07$; **Figure 4.3**). LPS exposure 2 days prior to delivery was insufficient to induce mucosal MPO-positive cell infiltration. Pre-exposure to UP in combination with LPS administration did not alter the number of mucosal MPO-positive cells, compared to LPS alone, both after 2 days and 7 days.

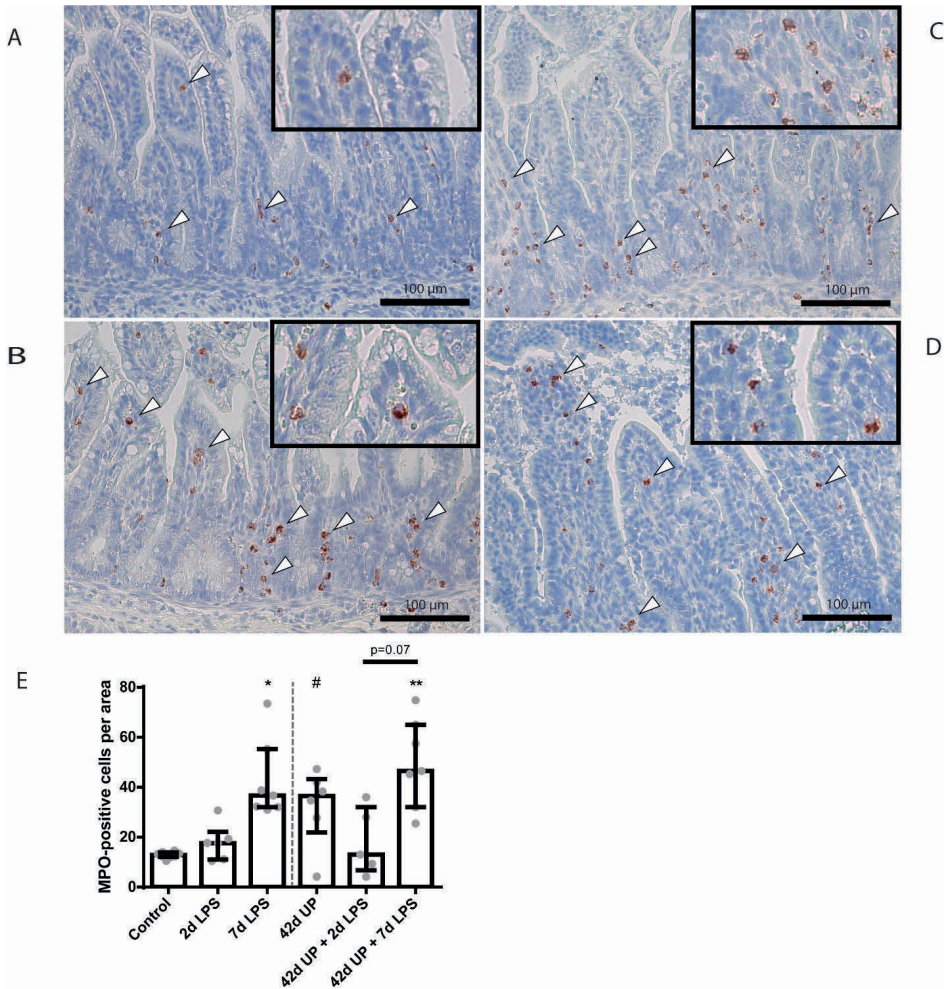


Figure 4.3 Representative images of mucosal neutrophil influx reflected by MPO-positive cell (indicated by white triangles) counts of the control (A), 7 days LPS (B), UP (C) and UP prior to 7 days LPS group (D). E: Increased MPO count in animals exposed to 7 days LPS, UP and UP prior to 7 days LPS. # $p = 0.08$, * $p < 0.01$, ** $p < 0.005$ compared to control.

While chronic UP infection and acute LPS exposure 2 days pre-delivery did not have any effect on mucosal CD3-positive T cell presence, those animals receiving LPS 7 days pre-delivery (both uninfected and chronic UP infected groups) as well as chronic UP infected animals receiving LPS 2 days pre-delivery all showed apparent elevated levels of CD3-positive T cell infiltration (**Figure 4.4**). However, the only comparison to achieve $p < 0.05$ significance was that of uninfected and chronic UP infected animals receiving LPS 2 days pre-delivery (**Figure 4.4**).

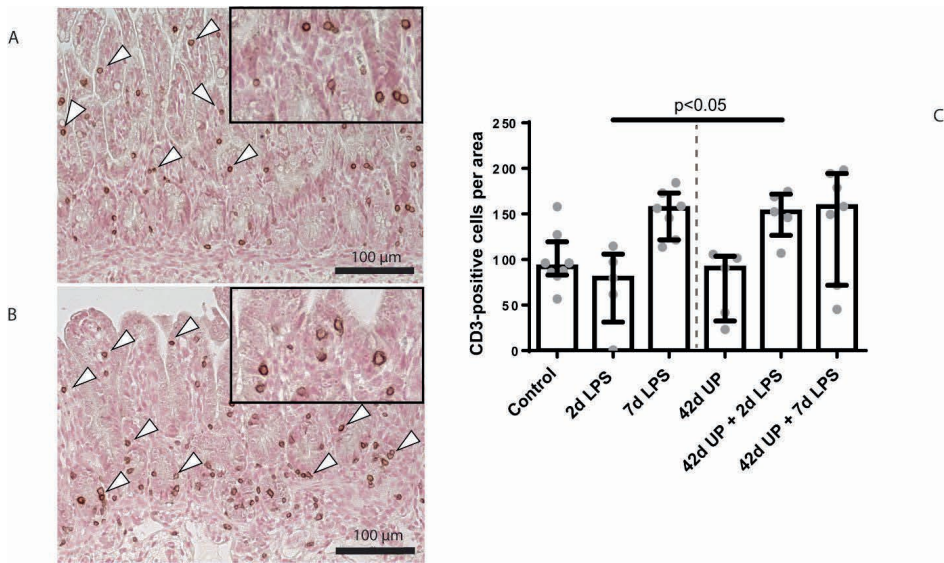


Figure 4.4 Representative images of mucosal T cell influx reflected by CD3-positive cell (indicated by white triangles) counts of the control (A) and UP prior to two-day LPS (B). C: Increased CD3 count in animals exposed to UP prior to 2 days LPS compared to the 2 days LPS group.

For investigation of submucosal inflammation, there was an increase of MPO-positive cells in the seven-day LPS group and submucosal MPO-positive cells tended to be increased in the chronic UP infection group, compared to control ($p < 0.05$ and $p = 0.06$; **Figure 4.5**). Additional acute LPS insult (2 or 7 days pre-delivery) in chronic UP infected animals resulted in increased variability and loss of significance in the MPO cell infiltration compared to 2 or 7 days of LPS alone.

The greatest increase of submucosal CD3-positive cells was observed in two-day LPS-exposed chronic UP infected animals, which was significantly increased compared to control or acute two-day LPS stimulation alone (both $p < 0.05$; **Figure 4.6**) and appeared more potent than in chronic UP infected animals receiving LPS at 7 days pre-delivery ($p = 0.08$; **Figure 4.6**).

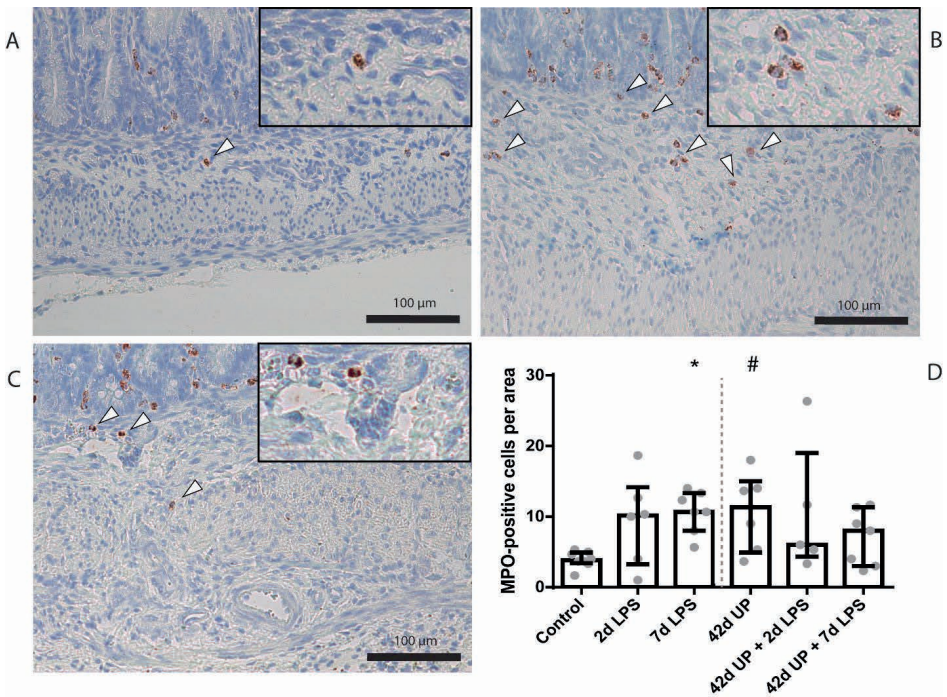


Figure 4.5 Representative images of submucosal neutrophil influx reflected by MPO-positive cell (indicated by white triangles) counts of the control (A), 7 days LPS (B) and UP (C). D: Increased MPO count in animals exposed to 7 days LPS and UP. # $p=0.06$, * $p<0.05$ compared to control.

Examination of underlying cytokine levels revealed increased IL-1 β mRNA levels only in uninfected or chronic UP infected animals when LPS was administered 2 days pre-delivery ($p<0.05$ compared to 7d LPS group; and $p<0.01$ compared to 42d UP group, $p<0.05$ compared to 42d UP + 7d LPS group and $p<0.05$ compared to control respectively; **Figure 4.7A**). Whereas IL-1 β mRNA levels had dropped to baseline again if LPS was administered 7 days pre-delivery (**Figure 4.7A**). IL-6 and IL-10 mRNA levels were not altered (data not shown) and the only group showing apparent TNF- α mRNA level elevation were the chronic UP infected animals additionally receiving LPS 2 days pre-delivery ($p=0.07$; **Figure 4.7B**).

IRAK3 mRNA levels were increased significantly only in animals exposed to 2 days of LPS alone compared to control ($p<0.05$; **Figure 4.7C**).

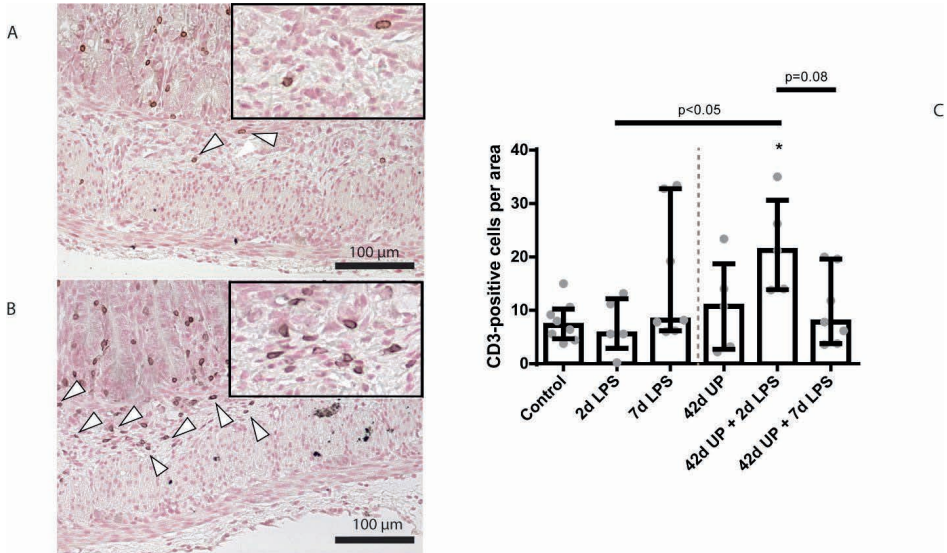


Figure 4.6 Representative images of submucosal T cell influx reflected by CD3-positive cell (indicated by white triangles) counts of the control (A) and UP prior to 2 days LPS group (B). C: Increased CD3 count in animals exposed to UP prior to 2 days LPS. * $p < 0.05$ compared to control.

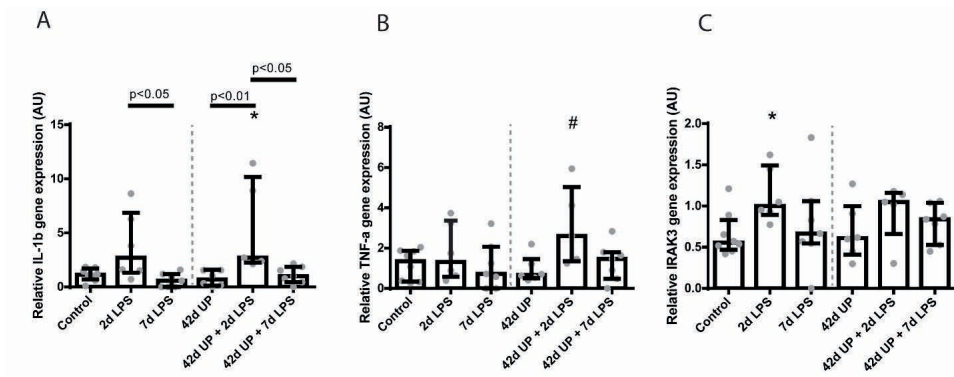


Figure 4.7 Relative mRNA levels of IL-1 β (A), TNF- α (B) and IRAK3 (C) in arbitrary unit (AU). A: Increased IL-1 β mRNA level in animals exposed to 2 days LPS and UP prior to 2 days LPS. * $p < 0.05$ compared to control. B: Increased TNF- α mRNA level in animals exposed to UP prior to 2 days LPS. # $p = 0.07$ compared to control. C: Increased IRAK3 mRNA level in animals exposed to 2 days LPS. * $p < 0.05$ compared to control.

ENS alterations in the terminal ileum due to chronic IA UP exposure

The PGP9.5-positive surface area in the submucosal plexus tended to be decreased in animals chronically infected for 42 days with UP, compared to control ($p=0.08$; **Figure 4.8**). Similarly, chronic UP infected animals had a diminished PGP9.5-positive surface area in the myenteric plexus ($p<0.05$; **Figure 4.8**).

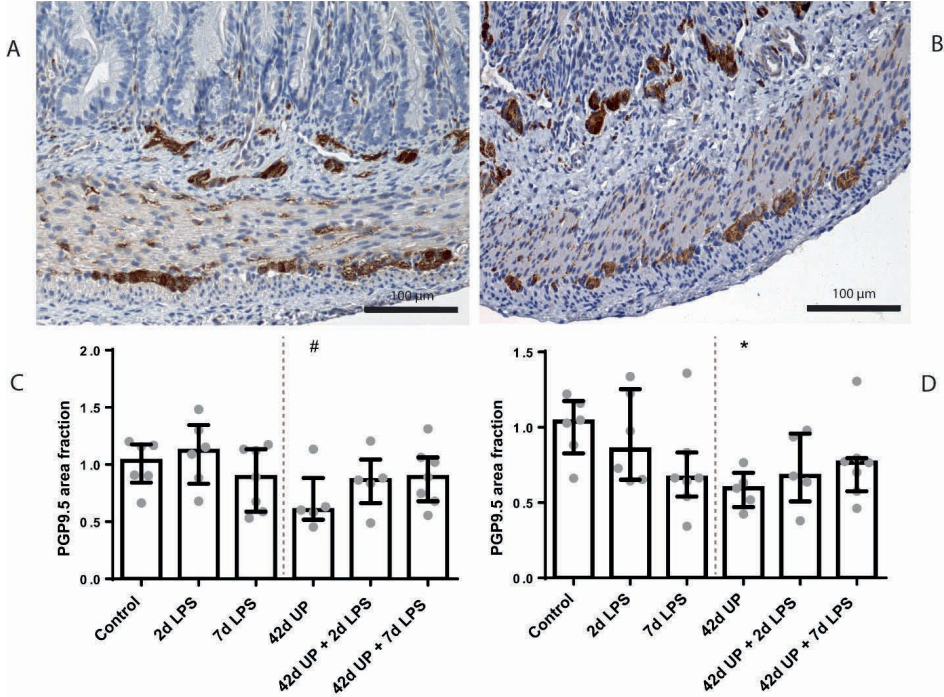


Figure 4.8 Representative images of PGP9.5 immunoreactivity in the submucosal and myenteric plexus of the control (A) and UP group (B). Area fraction of PGP9.5 in the submucosal plexus (C) and myenteric plexus (D) as fold increase over the control value. C: PGP9.5-positive surface area tended to be decreased in the submucosal plexus of animals exposed to UP. # $p=0.08$ compared to control. D: Decreased PGP9.5-positive surface area in the myenteric plexus of animals exposed to UP. * $p<0.05$ compared to control.

Doublecortin-positive surface areas were not altered in either the submucosal or the myenteric plexus (data not shown).

In the submucosal plexus, the GFAP-positive surface area tended to be increased in groups receiving LPS either 2 or 7 days pre-delivery, compared to control ($p=0.07$ and $p=0.09$; **Figure 4.9**), while in the myenteric plexus, the GFAP-positive surface area was only increased in the group receiving LPS 7 days pre-delivery, compared to control ($p<0.05$; **Figure 4.9**). For both of these regions, concomitant chronic infection by UP appeared to mute these effects.

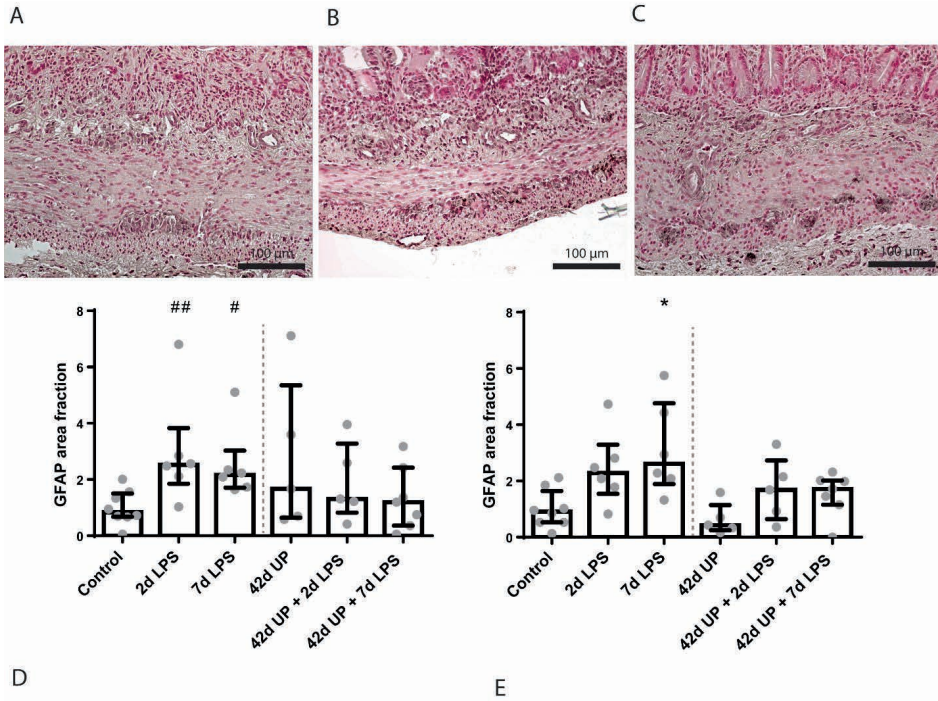


Figure 4.9 Representative images of GFAP immunoreactivity in the submucosal and myenteric plexus of the control (A), 2 days LPS (B) and 7 days LPS group (C). Area fraction of GFAP in the submucosal plexus (D) and myenteric plexus (E) as fold increase over the control value. D: GFAP-positive surface area tended to be increased in the submucosal plexus of animals exposed to 2 and 7 days LPS. ## $p=0.07$ and # $p=0.09$ compared to control. E: Increased GFAP-positive surface area in the myenteric plexus of animals exposed to 7 days LPS. * $p<0.05$ compared to control.

S100 β -positive surface areas were unaltered in the submucosal plexus for all conditions (data not shown), while in the myenteric plexus, the S100 β -positive surface area was significantly decreased in the chronic UP infected group, compared to control ($p<0.05$; **Figure 4.10**), but this effect appeared to be counteracted by acute stimulation by LPS at either 2 or 7 days pre-delivery.

No differences in nNOS and CHAT expression were observed between the groups (data not shown).

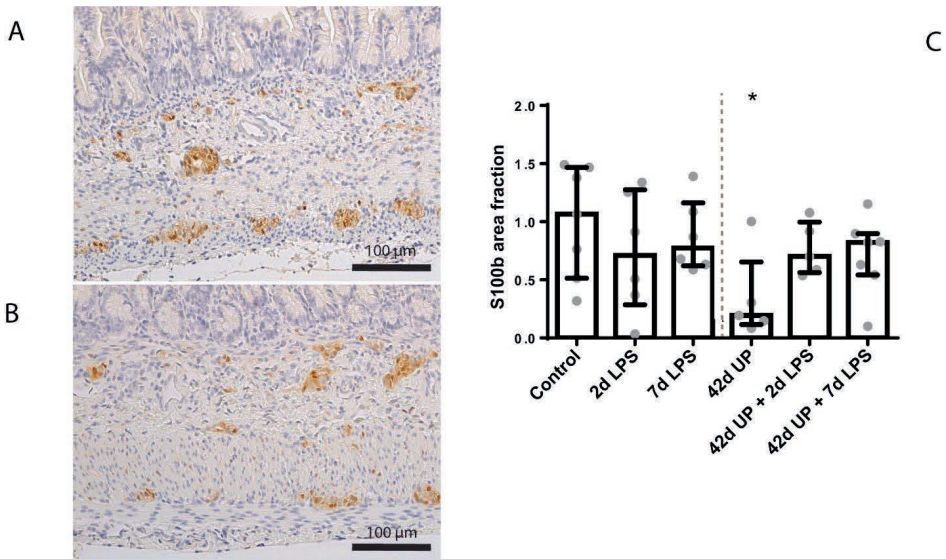


Figure 4.10 Representative images of S100 β immunoreactivity in the submucosal and myenteric plexus of the control (A) and UP group (B). Area fraction of S100 β in the myenteric plexus (C) as fold increase over the control value. C: S100 β -positive surface area was decreased in the myenteric plexus of animals exposed to UP. * $p < 0.05$ compared to control.

Discussion

In this study, we investigated the effect of acute, chronic, and combined microbial exposure as an antenatal infectious trigger (chorioamnionitis) on the mucosa, submucosa and ENS of the terminal ileum of premature lambs.

Both acute LPS and chronic UP exposure caused mucosal inflammation and injury to the terminal ileum. Although the inflammatory signature differed between these groups, mucosal injury was not aggravated in the combined exposure groups. Prenatal IA exposure to 7 days of LPS and to chronic 42-day infection by UP both provoked an influx of neutrophils (MPO-positive cells) in the intestine. By contrast, T cell (CD3-positive cells) numbers remained unaltered in the chronic UP and 2 day LPS groups compared to control group, but were increased in the UP + 2 day LPS-exposed animals, indicating a potential synergistic effect of both inflammatory stimuli in inducing an adaptive mucosal immune response. We observed a similar effect in the submucosa: while either LPS exposure or UP infection induced innate immune changes in the ileum, T cell alterations only occurred in the presence of combined UP and LPS exposure. Based on the current findings, we can only speculate on the mechanism behind this synergistic effect. In previous *in vitro* studies, signaling via Toll-like receptor (TLR) 1, 2 and 6 by *Ureaplasma* spp. increased LPS-mediated inflammation^{33,34}. Additionally, TNF- α mRNA levels tended to be increased in the UP infected animals receiving LPS 2 days pre-delivery, while TNF- α levels were not increased upon single exposure to either UP or LPS alone. By contrast, no synergistic effect of UP and LPS exposure on intestinal IL-1 β mRNA levels was found in the current study. This is

supported by our IRAK3 mRNA findings, a negative regulator of TLR signaling³⁵, which remained unaltered in combined exposure of UP infected animals to LPS. Based on these joined findings, it is tempting to speculate that UP + LPS induced upregulation of cell adhesion molecules, and consequently temporarily increased diapedesis, could at least in part be responsible for the observed increase in CD3-positive cells. The latter suggestion is supported by previous *in vitro* findings showing enhanced endothelial protein expression of the cell adhesion molecule CXCR7 following co-incubation with LPS and UP, which was not observed in independently UP or LPS-exposed cells³⁶.

Interestingly, other ovine studies have reported a suppressive immune effect in the premature lung and brain after chronic UP exposure prior to acute LPS exposure^{18,19}. Taken together, these data show that cells might be sensitized, preconditioned or remain unaffected following chronic UP infection, indicating organ dependent responses. The mechanisms responsible for organ specific effects of a second hit chorioamnionitis remain to be elucidated.

The ENS closely interacts with intestinal immune cells³⁷. As such, ENS alterations can both result from intestinal inflammation and modulate it^{38,39}. In this study, the most evident signs of ENS alterations were seen after chronic UP infection, which caused a reduced PGP9.5-positive surface area in both plexuses, likely representing a loss of enteric neurons. Alternatively, this might represent a loss of PGP9.5 immunoreactivity of enteric neurons. The doublecortin-positive (immature neurons) surface area in chronically UP-infected animals was unchanged, indicating that a decrease of mature neurons is responsible for the observed neuronal cell loss. As the period between 10 and 18 weeks of gestation is considered to be of paramount importance for both morphological and functional maturation of the ENS^{40,41}, one might assume that the timing of our inflammatory challenge during this vulnerable second trimester is the key determinant for the observed effects, rather than the nature of the microbial trigger. The loss of enteric neurons in the myenteric plexus following chronic UP infection coincides with a reduced S100 β -positive surface area, suggesting a reduced number of enteric glial cells. However, a reduction of S100 β immunoreactivity within glial cells could be involved in the observed effect as well. Enteric glial cells are known to contribute to neuronal maintenance, survival and function⁴². Interestingly, the S100 β -positive surface area was less reduced in the groups exposed to an additional LPS challenge in combination with chronic UP infection and the median of the PGP9.5-positive surface area was higher in these groups. In support, previous studies have shown that enteric glial cells are capable of generating enteric neurons in response to injury^{43,44}, indicating that glial cells could be the driving cells behind the loss or gain of neurons in our model. As a hallmark of their high level of cellular plasticity⁴⁵, enteric glia can respond to inflammatory cues and ENS damage by alternating their morphology and expression of key proteins such as GFAP, in a process similar to reactive astrogliosis^{46,47}. In this study, GFAP immunoreactivity was increased in both plexuses in the LPS-exposed animals, indicating that a glial response is induced by intestinal inflammation⁴⁸. An enteric glial cell response was not detected in chronic UP infected animals, despite signs of intestinal inflammation, suggesting normalization of GFAP levels within this period. Interestingly, pre-conditioning through chronic UP infection prevented GFAP upregulation in response to the overlapping second challenge with LPS in the glial cells in both plexuses, as no

altered GFAP immunoreactivity was seen following subsequent IA LPS exposure. Whether this is solely protective or can contribute to the ENS damage seen in chronic UP exposure is unclear, as activation of enteric glia in the context of intestinal inflammation has been described to be both destructive⁴⁹ and potentially neuroregenerative⁵⁰. We may conclude from the aforementioned findings that enteric glial cells are already able to react to inflammatory cues prenatally. Importantly, our results suggest that these cells play an important role in neuronal survival and neurogenesis in the intra-uterine setting.

At present, the postnatal consequences of the detected loss of mature neurons and glial cells following UP exposure in the second trimester remain unknown. A similar decrease in enteric neurons has been described in models of experimental colitis, which show that neuronal loss persists after recovery of inflammation⁵¹ and is accompanied by decreased colonic motility⁵². Based on these combined findings it is likely that the observed changes *in utero* will result in ENS dysfunction postnatally.

Interestingly, several studies describe intestinal changes in patients with acute NEC that are similar to those found after chronic UP infection, namely loss of both enteric neurons^{25-27,53} and glial cells²⁵⁻²⁷.

Moreover, it has been suggested that ablation of enteric glial cells may be an upstream target of NEC pathology⁵⁴. A potential causal role of the ENS in NEC pathophysiology is further supported by a rat study in which increased NEC survival and intestinal motility was associated with improvement of ENS changes, including an increase in enteric neurons²⁷. Collectively, our findings form a novel mechanistic explanation for the reported association of chorioamnionitis and NEC.

A limitation of this study is that it only enables us to study the effects of UP and LPS exposure at one timepoint, preventing us from dissecting the role of the different inflammatory triggers (LPS and UP) of inflammation duration (acute and chronic). In addition, group sizes are small, which is an inherent shortcoming of the translational ovine model used.

In summary, an acute inflammatory stimulus with LPS or a chronic inflammatory stimulus with UP causes intestinal injury and inflammation in the mucosal and submucosal layers of the gut. Combined overlapping microbial exposure does not aggravate injury of the terminal ileum. Most importantly, chronic UP infection causes structural ENS alterations characterized by PGP9.5 and S100 β immunoreactivity loss. Whether the observed ENS alterations result in functional abnormalities after birth remains to be elucidated. However, the observed changes *in utero* correspond with findings in neonates with NEC, which underlines the concept that NEC pathophysiology may already have its origin *in utero*.

References

1. Murphy SL, Mathews TJ, Martin JA, Minkovitz CS, Strobino DM. Annual Summary of Vital Statistics: 2013-2014. *Pediatrics*. 2017;139(6).
2. Howson CP, Kinney MV, McDougall L, Lawn JE, Born Too Soon Preterm Birth Action G. Born too soon: preterm birth matters. *Reprod Health*. 2013;10 Suppl 1:S1.
3. Blencowe H, Cousens S. Addressing the challenge of neonatal mortality. *Trop Med Int Health*. 2013;18(3):303-12.
4. Blencowe H, Cousens S, Oestergaard MZ, Chou D, Moller AB, Narwal R, Adler A, Vera Garcia C, Rohde S, Say L, Lawn JE. National, regional, and worldwide estimates of preterm birth rates in the year 2010 with time trends since 1990 for selected countries: a systematic analysis and implications. *Lancet*. 2012;379(9832):2162-72.
5. Galinsky R, Polglase GR, Hooper SB, Black MJ, Moss TJ. The consequences of chorioamnionitis: preterm birth and effects on development. *J Pregnancy*. 2013;2013:412831.
6. Goldenberg RL, Hauth JC, Andrews WW. Intrauterine infection and preterm delivery. *N Engl J Med*. 2000;342(20):1500-7.
7. Tita AT, Andrews WW. Diagnosis and management of clinical chorioamnionitis. *Clin Perinatol*. 2010;37(2):339-54.
8. Peng CC, Chang JH, Lin HY, Cheng PJ, Su BH. Intrauterine inflammation, infection, or both (Triple I): A new concept for chorioamnionitis. *Pediatr Neonatol*. 2018;59(3):231-7.
9. Silwedel C, Speer CP, Glaser K. Ureaplasma-associated prenatal, perinatal, and neonatal morbidities. *Expert Rev Clin Immunol*. 2017;13(11):1073-87.
10. Viscardi RM. Ureaplasma species: role in diseases of prematurity. *Clin Perinatol*. 2010;37(2):393-409.
11. Been JV, Lieveense S, Zimmermann LJ, Kramer BW, Wolfs TG. Chorioamnionitis as a risk factor for necrotizing enterocolitis: a systematic review and meta-analysis. *J Pediatr*. 2013;162(2):236-42 e2.
12. Okogbule-Wonodi AC, Gross GW, Sun CC, Agthe AG, Xiao L, Waites KB, Viscardi RM. Necrotizing enterocolitis is associated with ureaplasma colonization in preterm infants. *Pediatr Res*. 2011;69(5 Pt 1):442-7.
13. Wolfs TG, Jellema RK, Turrisi G, Becucci E, Buonocore G, Kramer BW. Inflammation-induced immune suppression of the fetus: a potential link between chorioamnionitis and postnatal early onset sepsis. *J Matern Fetal Neonatal Med*. 2012;25 Suppl 1:8-11.
14. Wolfs TG, Kramer BW, Thuijls G, Kemp MW, Saito M, Willems MG, Senthamarai-Kannan P, Newnham JP, Jobe AH, Kallapur SG. Chorioamnionitis-induced fetal gut injury is mediated by direct gut exposure of inflammatory mediators or by lung inflammation. *Am J Physiol Gastrointest Liver Physiol*. 2014;306(5):G382-93.
15. Kataoka S, Yamada T, Chou K, Nishida R, Morikawa M, Minami M, Yamada H, Sakuragi N, Minakami H. Association between preterm birth and vaginal colonization by mycoplasmas in early pregnancy. *J Clin Microbiol*. 2006;44(1):51-5.
16. Sweeney EL, Dando SJ, Kallapur SG, Knox CL. The Human Ureaplasma Species as Causative Agents of Chorioamnionitis. *Clin Microbiol Rev*. 2017;30(1):349-79.
17. Wolfs TG, Kallapur SG, Knox CL, Thuijls G, Nitsos I, Polglase GR, Collins JJ, Kroon E, Spierings J, Shroyer NF, Newnham JP, Jobe AH, Kramer BW. Antenatal ureaplasma infection impairs development of the fetal ovine gut in an IL-1-dependent manner. *Mucosal Immunol*. 2013;6(3):547-56.
18. Gussenhoven R, Ophelders D, Kemp MW, Payne MS, Spiller OB, Beeton ML, Stock SJ, Cillero-Pastor B, Barre FPY, Heeren RMA, Kessels L, Stevens B, Rutten BP, Kallapur SG, Jobe AH, Kramer BW, Wolfs T. The Paradoxical Effects of Chronic Intra-Amniotic Ureaplasma parvum Exposure on Ovine Fetal Brain Development. *Dev Neurosci*. 2017;39(6):472-86.
19. Kallapur SG, Kramer BW, Knox CL, Berry CA, Collins JJ, Kemp MW, Nitsos I, Polglase GR, Robinson J, Hillman NH, Newnham JP, Chougnat C, Jobe AH. Chronic fetal exposure to Ureaplasma parvum suppresses innate immune responses in sheep. *J Immunol*. 2011;187(5):2688-95.
20. Furness JB. *The Enteric Nervous System*. Blackwell Publishing, Oxford (2006). 2006.
21. Lake JJ, Heuckeroth RO. Enteric nervous system development: migration, differentiation, and disease. *Am J Physiol Gastrointest Liver Physiol*. 2013;305(1):G1-24.

22. Rao M, Gershon MD. Enteric nervous system development: what could possibly go wrong? *Nat Rev Neurosci.* 2018;19(9):552-65.
23. Burns AJ, Roberts RR, Bornstein JC, Young HM. Development of the enteric nervous system and its role in intestinal motility during fetal and early postnatal stages. *Semin Pediatr Surg.* 2009;18(4):196-205.
24. Hao MM, Foong JP, Bornstein JC, Li ZL, Vanden Berghe P, Boesmans W. Enteric nervous system assembly: Functional integration within the developing gut. *Dev Biol.* 2016;417(2):168-81.
25. Sigge W, Wedel T, Kuhnel W, Krammer HJ. Morphologic alterations of the enteric nervous system and deficiency of non-adrenergic non-cholinergic inhibitory innervation in neonatal necrotizing enterocolitis. *Eur J Pediatr Surg.* 1998;8(2):87-94.
26. Wedel T, Krammer HJ, Kuhnel W, Sigge W. Alterations of the enteric nervous system in neonatal necrotizing enterocolitis revealed by whole-mount immunohistochemistry. *Pediatr Pathol Lab Med.* 1998;18(1):57-70.
27. Zhou Y, Yang J, Watkins DJ, Boomer LA, Matthews MA, Su Y, Besner GE. Enteric nervous system abnormalities are present in human necrotizing enterocolitis: potential neurotransplantation therapy. *Stem Cell Res Ther.* 2013;4(6):157.
28. Moss TJ, Knox CL, Kallapur SG, Nitsos I, Theodoropoulos C, Newnham JP, Ikegami M, Jobe AH. Experimental amniotic fluid infection in sheep: effects of *Ureaplasma parvum* serovars 3 and 6 on preterm or term fetal sheep. *Am J Obstet Gynecol.* 2008;198(1):122 e1-8.
29. Kramer BW, Moss TJ, Willet KE, Newnham JP, Sly PD, Kallapur SG, Ikegami M, Jobe AH. Dose and time response after intraamniotic endotoxin in preterm lambs. *Am J Respir Crit Care Med.* 2001;164(6):982-8.
30. Newnham JP, Kallapur SG, Kramer BW, Moss TJ, Nitsos I, Ikegami M, Jobe AH. Betamethasone effects on chorioamnionitis induced by intra-amniotic endotoxin in sheep. *Am J Obstet Gynecol.* 2003;189(5):1458-66.
31. Miura Y, Payne MS, Keelan JA, Noe A, Carter S, Watts R, Spiller OB, Jobe AH, Kallapur SG, Saito M, Stock SJ, Newnham JP, Kemp MW. Maternal intravenous treatment with either azithromycin or solithromycin clears *Ureaplasma parvum* from the amniotic fluid in an ovine model of intrauterine infection. *Antimicrob Agents Chemother.* 2014;58(9):5413-20.
32. Rao M, Nelms BD, Dong L, Salinas-Rios V, Rutlin M, Gershon MD, Corfas G. Enteric glia express proteolipid protein 1 and are a transcriptionally unique population of glia in the mammalian nervous system. *Glia.* 2015;63(11):2040-57.
33. Manimtim WM, Hasday JD, Hester L, Fairchild KD, Lovchik JC, Viscardi RM. *Ureaplasma urealyticum* modulates endotoxin-induced cytokine release by human monocytes derived from preterm and term newborns and adults. *Infect Immun.* 2001;69(6):3906-15.
34. Shimizu T, Kida Y, Kuwano K. *Ureaplasma parvum* lipoproteins, including MB antigen, activate NF- κ B through TLR1, TLR2 and TLR6. *Microbiology.* 2008;154(Pt 5):1318-25.
35. Kobayashi K, Hernandez LD, Galan JE, Janeway CA, Jr., Medzhitov R, Flavell RA. IRAK-M is a negative regulator of Toll-like receptor signaling. *Cell.* 2002;110(2):191-202.
36. Silwedel C, Speer CP, Haarmann A, Fehrholz M, Claus H, Buttmann M, Glaser K. Novel insights into neuroinflammation: bacterial lipopolysaccharide, tumor necrosis factor alpha, and *Ureaplasma* species differentially modulate atypical chemokine receptor 3 responses in human brain microvascular endothelial cells. *J Neuroinflammation.* 2018;15(1):156.
37. Yoo BB, Mazmanian SK. The Enteric Network: Interactions between the Immune and Nervous Systems of the Gut. *Immunity.* 2017;46(6):910-26.
38. Brierley SM, Linden DR. Neuroplasticity and dysfunction after gastrointestinal inflammation. *Nat Rev Gastroenterol Hepatol.* 2014;11(10):611-27.
39. Margolis KG, Gershon MD. Enteric Neuronal Regulation of Intestinal Inflammation. *Trends Neurosci.* 2016;39(9):614-24.
40. Fekete E, Resch BA, Benedeczyk I. Histochemical and ultrastructural features of the developing enteric nervous system of the human foetal small intestine. *Histol Histopathol.* 1995;10(1):127-34.
41. Fekete E, Bagyánszki M, Resch BA. Prenatal development of the myenteric plexus in the human fetal small intestine. *Acta Biol Szeged [Internet].* 2000;44(1-4):3-19.

42. De Giorgio R, Giancola F, Boschetti E, Abdo H, Lardeux B, Neunlist M. Enteric glia and neuroprotection: basic and clinical aspects. *Am J Physiol Gastrointest Liver Physiol*. 2012;303(8):G887-93.
43. Joseph NM, He S, Quintana E, Kim YG, Nunez G, Morrison SJ. Enteric glia are multipotent in culture but primarily form glia in the adult rodent gut. *J Clin Invest*. 2011;121(9):3398-411.
44. Laranjeira C, Sandgren K, Kessaris N, Richardson W, Potocnik A, Vanden Berghe P, Pachnis V. Glial cells in the mouse enteric nervous system can undergo neurogenesis in response to injury. *J Clin Invest*. 2011;121(9):3412-24.
45. Boesmans W, Lasrado R, Vanden Berghe P, Pachnis V. Heterogeneity and phenotypic plasticity of glial cells in the mammalian enteric nervous system. *Glia*. 2015;63(2):229-41.
46. Chow AK, Gulbransen BD. Potential roles of enteric glia in bridging neuroimmune communication in the gut. *Am J Physiol Gastrointest Liver Physiol*. 2017;312(2):G145-G52.
47. Rosenbaum C, Schick MA, Wollborn J, Heider A, Scholz CJ, Cecil A, Niesler B, Hirrlinger J, Walles H, Metzger M. Activation of Myenteric Glia during Acute Inflammation In Vitro and In Vivo. *PLoS One*. 2016;11(3):e0151335.
48. Cirillo C, Sarnelli G, Turco F, Mango A, Grosso M, Aprea G, Masone S, Cuomo R. Proinflammatory stimuli activates human-derived enteroglia cells and induces autocrine nitric oxide production. *Neurogastroenterol Motil*. 2011;23(9):e372-82.
49. Brown IA, McClain JL, Watson RE, Patel BA, Gulbransen BD. Enteric glia mediate neuron death in colitis through purinergic pathways that require connexin-43 and nitric oxide. *Cell Mol Gastroenterol Hepatol*. 2016;2(1):77-91.
50. Belkind-Gerson J, Graham HK, Reynolds J, Hotta R, Nagy N, Cheng L, Kamionek M, Shi HN, Aherne CM, Goldstein AM. Colitis promotes neuronal differentiation of Sox2+ and PLP1+ enteric cells. *Sci Rep*. 2017;7(1):2525.
51. Linden DR, Couvrette JM, Ciolino A, McQuoid C, Blaszyk H, Sharkey KA, Mawe GM. Indiscriminate loss of myenteric neurones in the TNBS-inflamed guinea-pig distal colon. *Neurogastroenterol Motil*. 2005;17(5):751-60.
52. Boyer L, Ghoreishi M, Templeman V, Vallance BA, Buchan AM, Jevon G, Jacobson K. Myenteric plexus injury and apoptosis in experimental colitis. *Auton Neurosci*. 2005;117(1):41-53.
53. Fagbemi AO, Torrente F, Puleston J, Lakhoo K, James S, Murch SH. Enteric neural disruption in necrotizing enterocolitis occurs in association with myenteric glial cell CCL20 expression. *J Pediatr Gastroenterol Nutr*. 2013;57(6):788-93.
54. Bush TG. Enteric glial cells. An upstream target for induction of necrotizing enterocolitis and Crohn's disease? *Bioessays*. 2002;24(2):130-40.

Chapter 5

Alterations of the enteric nervous system and intestinal motility in a mouse model of necrotizing enterocolitis

I.H. de Lange*, C. Heymans*, I.G. De Plaen, E. Managlia, X. Yan, K. Lenaerts,
L.C.G.A. Kessels, J.P.M. Derikx, W.G. van Gemert, and T.G.A.M. Wolfs

* contributed equally

Abstract

Background

Necrotizing enterocolitis (NEC), characterized by severe intestinal inflammation and in later stages bowel necrosis, is one of the most common intestinal emergencies in premature neonates. Alterations of the enteric nervous system (ENS) and immature intestinal motility are associated with NEC in babies and large animal models. Since experimental mouse NEC models are important for understanding NEC pathophysiology, it is essential to study ENS in these models of NEC. To this end, we studied the ENS and intestinal transit in a well-characterized mouse NEC model.

Materials and methods

NEC was induced in newborn C57BL/6 mice by formula feeding, supplementation of oral commensal bacteria and LPS, asphyxia and cold stress. Mature neurons (NeuN), immature neurons (doublecortin), glial cells (S100 β), presynaptic vesicles (synaptophysin) and intestinal transit were studied in a time window from 24h to 72h of exposure to the NEC protocol.

Results

An early increase in glial cells was observed in the submucosal plexus at 24h in pups exposed to the NEC protocol. Also, mice in the experimental NEC group at different times examined (7-72h) had more mature neurons and glial cells and an increase in presynaptic vesicles in the submucosal and myenteric plexus compared to controls. At 24h, intestinal transit was increased, whereas a decrease of the intestinal motility was detected at 48h.

Conclusion

As glial cell alterations were the first to emerge following NEC protocol exposure, glial cell changes may be a driving force behind later ENS alterations. The time-dependent changes in intestinal motility could not be fully explained by histological data, indicating that functional read outs of gut motility are of importance when studying ENS changes in NEC.

Introduction

Necrotizing enterocolitis (NEC), characterized by severe intestinal inflammation and—in later stages—bowel necrosis, is one of the most common intestinal emergencies in premature neonates¹. It affects around 5 to 10% of very low birth weight infants and incidences are rising, which is primarily caused by improved early survival rates of premature newborns^{2,3}. Mortality generally ranges from 15 to 30%, but increases up to 50% for extremely low birth weight babies treated surgically^{1,4,5}. Infants that do survive are at increased risk for long-term morbidities such as growth retardation^{6,7} and neurodevelopmental delay^{8,9}.

The pathogenesis of NEC is multifactorial and still incompletely understood; however, immaturity of the intestinal immune system and abnormal bacterial colonization are clearly involved in the etiology of the excessive inflammation^{1,10}. In addition, immature gut motility is regarded as a risk factor for NEC development¹⁰. Consistently, alterations of the enteric nervous system (ENS) are associated with NEC; in intestinal specimens from infants with NEC, structural ENS abnormalities including loss of neurons and enteric glial cells have been found^{11–13}. In addition, reduced expression of neuronal nitric oxide synthase (nNOS) and choline acetyltransferase (CHAT), markers for motility signaling functions of the ENS, during acute NEC suggest a functional impairment of the ENS¹⁴. Finally, several studies indicate that ENS alterations and dysmotility are involved in NEC pathophysiology; in a preterm pig NEC model¹⁵ and a mouse NEC model¹⁶ motility changes were observed prior to intestinal inflammation and NEC development. Additionally, pharmacological recovery of gut motility in a mouse NEC model reduced NEC severity¹⁶.

The ENS autonomously regulates gastrointestinal activity, including secretion, absorption, and motility and it contributes to gut integrity^{17,18}. Furthermore, it is involved in the shaping of the mucosal immune system and the intestinal microbiome^{17,19}. Development of the ENS requires a complex coordinated migration, proliferation and differentiation of neural crest progenitors, directed neurite growth, and establishment of a network of glial cells and interconnected neurons^{20,21}. In premature neonates the ENS is still immature²⁰, reflected by immature migrating motor complexes and mixing motor patterns²⁰, and ENS development continues postnatally under the influence of several neurotrophins such as cell line-derived nerve growth factor (GDNF)^{20,22}. As NEC research in infants is notably difficult for ethical reasons and as it is subjected to many clinical confounding factors, animal models of NEC are frequently used^{23,24}. Interestingly, ENS alterations in conjunction with altered intestinal motility remain essentially unstudied in models of NEC. To bridge this knowledge gap, we studied the ENS and intestinal transit over time in a well-established mouse NEC model²⁵.

Materials and methods

Experimental design

The animal studies were approved by the Northwestern University Institutional Animal Care and Use Committee (Chicago, IL, USA) and the National Research Council's guide for the care and use of laboratory animals was followed. Male and female C57BL/6 mice from

Jackson Laboratory (Bar Harbor, ME, USA) were housed in a barrier facility and dams were mated overnight to obtain timed pregnancies. After natural delivery, less than 24h-old pups (from each litter) were randomly assigned to the two experimental groups: control and NEC. Birth weight was recorded and was similar between the groups. Mouse pups assigned to the NEC group were separated from the dams and placed in a humidified 37°C incubator. NEC was induced as previously described²⁵. Briefly, at the initiation of the study period, 10⁸ CFU of standardized commensal bacteria including 5 mg/kg LPS were administered by orogastric gavage within 24h after birth. Thereafter, enteral feeding by orogastric gavage was initiated and repeated every 3h. Pups were fed with Esbilac (PetAg, Hampshire, IL, USA) formula (33 g dissolved in 100 mL water), 30, 40 and 50 µL on day 1, 2 and 3 respectively. In addition, pups were exposed to a short period of asphyxia (100% nitrogen for 60 seconds) followed by cold stress (4 degrees for 10 minutes) twice daily. Pups remaining with the dams and being dam fed during the entire study period served as controls. Mouse pups were continuously monitored for signs of distress (abdominal distension, lethargy, respiratory distress) and pups were euthanized by decapitation if severe distress was present. Those surviving were euthanized at the end of the 72h study period. Time of death or euthanasia was documented and a 72h survival curve was defined. Subgroups of pups were euthanized after 24h and 48h to study early changes of the ENS following NEC protocol exposure. After euthanasia, intestines were collected and fixed with 10% buffered formalin for histological analyses. Pups found dead were excluded from the analyses. The remaining 85 mouse pups (72h experiments) were used for the 72h survival and histological analyses (control: n=28 and NEC protocol: n=57). For the 24h experiment, 18 mouse pups were used for histological analyses (control: n=10 and NEC protocol: n=8) and 28 mouse pups for mRNA analyses (control: n=13 and NEC protocol: n=15; of note, due to limited RNA yields, not all genes could be tested for all animals). In addition, 29 mouse pups were used for analysis of intestinal transit at 24h (control: n=8 and NEC: n=9) and 48h (control: n=5 and NEC: n=7).

Antibodies

The following primary antibodies were used for immunohistochemistry: polyclonal rabbit anti-doublecortin (Ab18723, Abcam, Cambridge, UK) to detect immature neurons, monoclonal mouse anti-neuronal nuclear protein (NeuN) (clone A60, IHCR1001, Merck, Darmstadt, Germany) to identify mature neurons, polyclonal rabbit anti-S100β (PA5-16257, ThermoFisher, Waltham, MA, USA) for the detection of glial cells and monoclonal rabbit anti-synaptophysin (Ab32127, Abcam, Cambridge, UK) for the identification of pre-synaptic vesicles. Secondary antibodies used were: biotin-conjugated polyclonal donkey anti-rabbit (711-065-152, Jackson, West Grove, PA, USA) (for detection of doublecortin), biotin conjugated polyclonal goat anti-mouse (E0433, DakoCytomation, Glostrup, Denmark) (for detection of NeuN) and biotin-conjugated polyclonal swine anti-rabbit (E0353 DakoCytomation, Glostrup, Denmark) (for detection of S100β and synaptophysin).

Histochemical stainings and histological analysis

Formalin-fixed intestine was embedded in paraffin and 4-µm sections were cut. A Haematoxylin and Eosin (H&E) staining was performed to determine the NEC severity stage

as explained below. H&E slides were scored on severity of intestinal histological injury as previously described.²⁵ In short, H&E slides were assessed by two independent investigators blinded to the experimental groups (X.Y. and I.G.D.P.) to determine the intestinal damage score based on the area of worst injury. The following scoring system was used as previously described²⁵: Grade 0: intact villi; 1: superficial epithelial cell sloughing; 2: mid-villus necrosis; 3: complete villus necrosis; 4: transmural necrosis. Mice with damage scores ≥ 2 were considered to have NEC.

Immunohistochemistry

After deparaffinization and rehydration of paraffin-embedded sections, endogenous peroxidase activity was blocked with 0.3% H₂O₂ diluted in phosphorylated buffer saline (PBS). Heat-mediated antigen retrieval was performed by boiling in 10 mM sodium-citrate buffer (pH 6.0). Non-specific binding was blocked for 30 minutes at room temperature with 5% bovine serum albumin (BSA) in PBS (doublecortin, NeuN and S100 β), or 5% normal goat serum (NGS) in PBS (synaptophysin). Thereafter, sections were incubated with the primary antibody of interest and subsequently incubated with the selected secondary antibody. The primary antibodies were visualized with an avidin-biotin complex (Vectastain Elite ABC kit, Bio-connect, Huissen, the Netherlands). Immunoreactivity for doublecortin and S100 β was detected by using diaminobenzidine (DAB). Immunoreactivity for NeuN and synaptophysin was detected by using nickel-3, 3'-DAB. Haematoxylin (doublecortin and S100 β) or nuclear fast red (NeuN and synaptophysin) were used as counterstain.

Analyses of immunohistochemical stainings

The stained tissue sections were scanned with the Ventana iScan HT slide scanner (Ventana Medical Systems, Oro Valley, AZ, USA). Of these images, viewed with Ventana Image Viewer (version 3.1.4, Ventana Medical Systems, Oro Valley, AZ, USA), random snapshots of cross sections of the small intestine were taken (200x).

Doublecortin (immature neurons), NeuN (mature neurons), S100 β (glial cells) and synaptophysin (presynaptic vesicles) were studied as markers for the ENS. Doublecortin, NeuN, S100 β and synaptophysin positively stained areas in the submucosal and myenteric ganglia were measured in five non-overlapping high power fields by calculating the area fraction (%) with Leica QWin Pro (version 3.4.0, Leica Microsystems, Mannheim, Germany). The area fraction was calculated by dividing the positively stained areas in the ganglia of the submucosal or myenteric plexus by the total surface of the muscle layer. The average area fraction per high-power field per animal is given. The area fractions were measured by an investigator blinded to the study groups.

Intestinal transit

Mice included for the intestinal transit experiment were subjected to the same experimental set-up as described above. At 24h after subjection to the NEC protocol (control: n=8 and NEC: n=9) and at 48h after subjection to the NEC protocol (control: n=5 and NEC: n=7), both NEC pups and littermate dam fed controls were gavaged with 20 μ l of 5% Evans Blue (in 1.5% carboxymethylcellulose) after 4h of fasting. Pups were euthanized

10 minutes after gavage and the total length of the intestine and the length covered by Evans Blue dye were measured (colon excluded). The intestinal transit was expressed as the percentage of small intestinal length covered by Evans Blue (**Figure S5.1**).

Real-time qPCR

To determine mRNA expression of several genes involved in neurotransmitter formation and reuptake (SERT, TPH2, CHAT and nNOS) and genes involved in ENS development (RET and GDNF) in dam fed controls and mice exposed to the NEC protocol for 24h, RNA isolation from full-wall thickness intestinal samples and RT-qPCR were performed as previously described²⁶. Briefly, following sacrifice, mice intestines were preserved in RNAprotect Tissue Reagent (Qiagen, Valencia, CA, USA). Tissues were homogenized and RNA was isolated with the Qiagen RNeasy Mini Kit (Qiagen, Valencia, CA, USA). Prior to RT-qPCR, cDNA was synthesized using the cDNA Archive kit (Life Technologies, Carlsbad, CA, USA). Subsequently, real-time PCR was performed using Power SYBR Green 2X master mix (Life Technologies) for cDNA amplification and run on an ABI 7500 Fast real-time PCR System (Applied Biosystems, Foster City, CA, USA) (95°C for 10 min, followed by 40 cycles of 95°C for 15 seconds, then 60°C for 60 seconds). An overview of the primers that were used is presented in **Table 5.1**. The mRNA expression of the housekeeping gene GAPDH was used for data normalization.

Table 5.1 Primer sequences.

Primer	Forward	Reverse
GAPDH	5'-GAACGGATTGGCCGTATTG-3'	5'-TGAGTGGAGTCATACTGGAACATGT-3'
SERT	5'-CCGAGAGCTCTCAGTCTTGT-3'	5'-CCCTGACTAGCTCTTGGTTCTTG-3'
TPH2	5'-CAACTGCGGGCGTATGG-3'	5'-TCGAAAAGAGCATGCTTCAA-3'
CHAT	5'-CCCTGCAGAAAAGCTCTTG-3'	5'-CCAGTATTCAGAGACCCAATTGG-3'
nNOS	5'-GGTCTTCGGGTGTCGACAA-3'	5'-GCACGTCTGTACATATTTCTTTGG-3'
RET	5'-GAAGGCGAGTTTGAAAAGTTG-3'	5'-TGGGAGGCGTTTTCTTTCAG-3'
GDNF	5'-GTGACTCCAATATGCTGAAGATTATC-3'	5'-TCAGTCTTTAATGGTGGCTTGAA-3'

Statistical analyses

Statistical analyses were performed using GraphPad Prism 6.01 (GraphPad Prism, La Jolla, CA, USA). 72h survival was analysed by log-rank test and NEC severity scoring with a Mann-Whitney U test. For the immunohistochemical read-outs from the 72h experiment, data were tested for normality with the D'Agostino and Pearson omnibus normality test. Differences among two groups were measured with an unpaired T-test for normally distributed data (NeuN myenteric plexus, S100 β myenteric plexus, synaptophysin myenteric plexus, doublecortin both plexuses) or Mann-Whitney U test for non-normally distributed data (other read-outs). Immunohistochemical read-outs for the 24h experiment, transit time and mRNA expression read-outs were analysed with a Mann-Whitney U test. Finally, correlation between postnatal age / survival duration and ENS outcomes for the 72h experiment were analysed with Spearman Rank-order Correlation with IBM SPSS Statistics Version 27.0 (IBM Corporation, Armonk, NY, USA). Differences are regarded statistically

significant at $p \leq 0.05$. Data are presented as mean with standard deviation (SD; normally distributed data) or median with interquartile range (IQR; non-normally distributed data).

Results

Historical NEC severity scoring and 72h survival

The animals subjected to the NEC protocol had an increased histological NEC severity score ($p < 0.0001$; **Figure 5.1**) and a significant lower survival than control animals ($p < 0.0001$; **Figure 5.2**). Of the 57 mouse pups subjected to the NEC protocol, 21 developed NEC (histological NEC severity score ≥ 2).

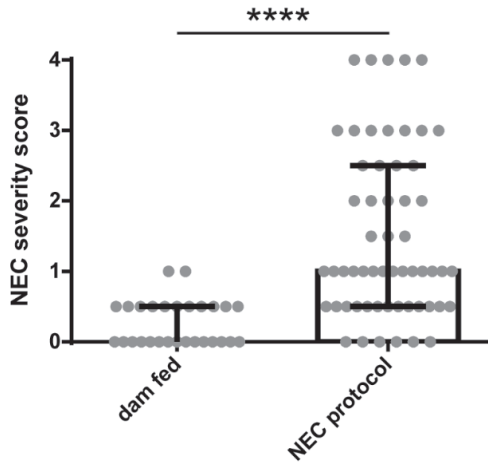


Figure 5.1 Histological NEC severity score of the 72h experiment. H&E slides were scored on a 0 to 4 scale for intestinal damage (25). NEC severity score was increased in animals subjected to the NEC protocol, compared to dam fed animals. Data points represent individual mouse pups. **** $p \leq 0.0001$.

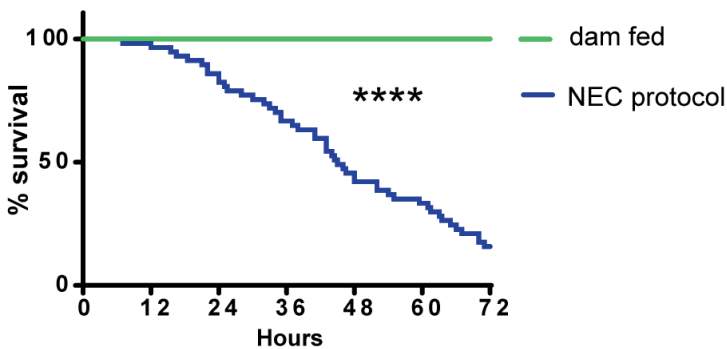


Figure 5.2 Survival analysis of the 72h experiment. The animals subjected to the NEC protocol ($n=57$) had a significant lower survival than control animals ($n=28$). **** $p \leq 0.0001$.

ENS alterations: neurons (NeuN, doublecortin)

Compared to control animals (**Figure 5.3A**), the NeuN-positive surface area (mature neurons) was increased in animals subjected to the NEC protocol in the 72h experiment (**Figure 5.3B**), in both the submucosal plexus ($p \leq 0.05$; **Figure 5.3C**) and the myenteric plexus ($p \leq 0.001$; **Figure 5.3D**). No differences were observed in NeuN-positive surface area between control and NEC protocol exposed animals at 24h (**Figure 5.3E, 5.3F**). The doublecortin-positive surface area (immature neurons) was unaltered by NEC protocol exposure in the 72h and the 24h experiment in both plexuses (**Figure S5.2**).

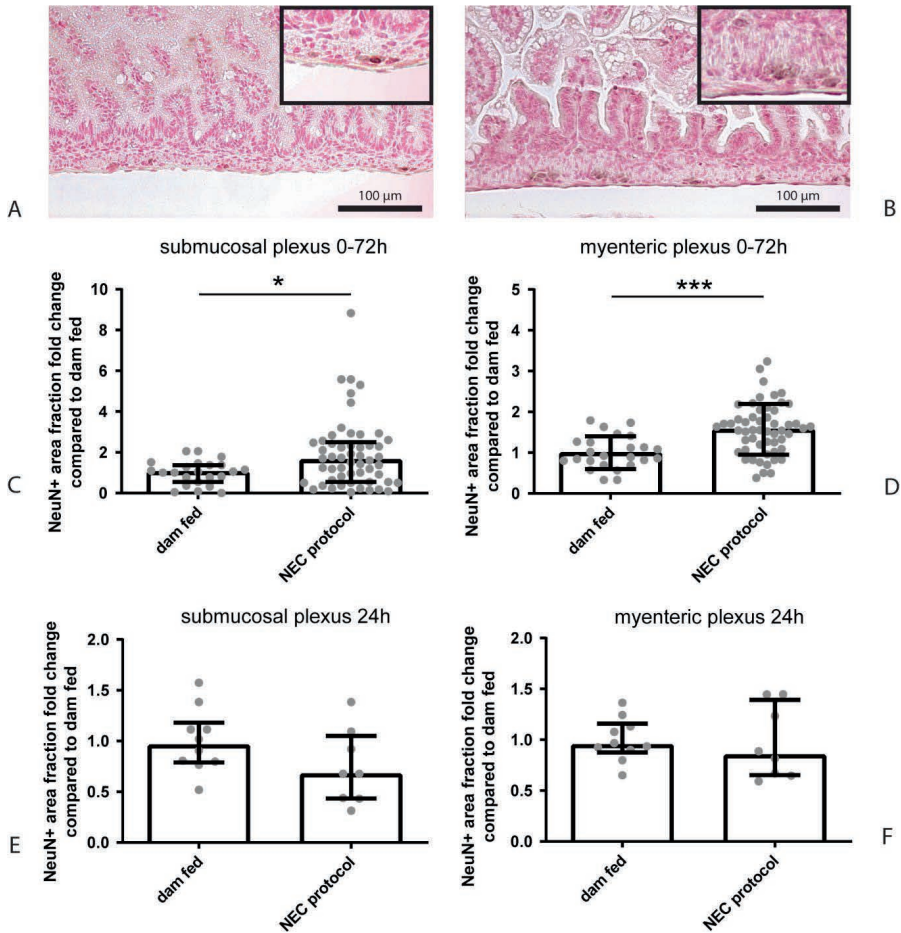


Figure 5.3 Representative images of NeuN immunoreactivity in the submucosal and myenteric plexus of control animals (A) and animals subjected to the NEC protocol (B). NeuN positive surface area was increased in the submucosal (C) and myenteric plexus (D) of animals subjected to the NEC protocol in the 72h experiment compared to the control group. NeuN-positive surface area was unaltered in the submucosal (E) and myenteric plexus (F) of animals subjected to the NEC protocol for 24h compared to the control group. Data points represent individual mouse pups. Scale bars indicate 100 μm . * $p \leq 0.05$, *** $p \leq 0.001$.

ENS alterations: glial cells (S100 β)

Compared to controls (**Figure 5.4A, 5.4C, 5.4D**) S100 β immunoreactivity (glial cell marker) increased following NEC protocol exposure in both the submucosal and the myenteric plexus in the 72h experiment ($p \leq 0.001$ and $p \leq 0.05$ respectively; **Figure 5.4B, 5.4C, 5.4D**). At 24h, increased S100 β immunoreactivity was also observed in the submucosal plexus ($p \leq 0.01$; **Figure 5.4E**), but not in the myenteric plexus (**Figure 5.4F**), following NEC protocol exposure compared to dam fed controls.

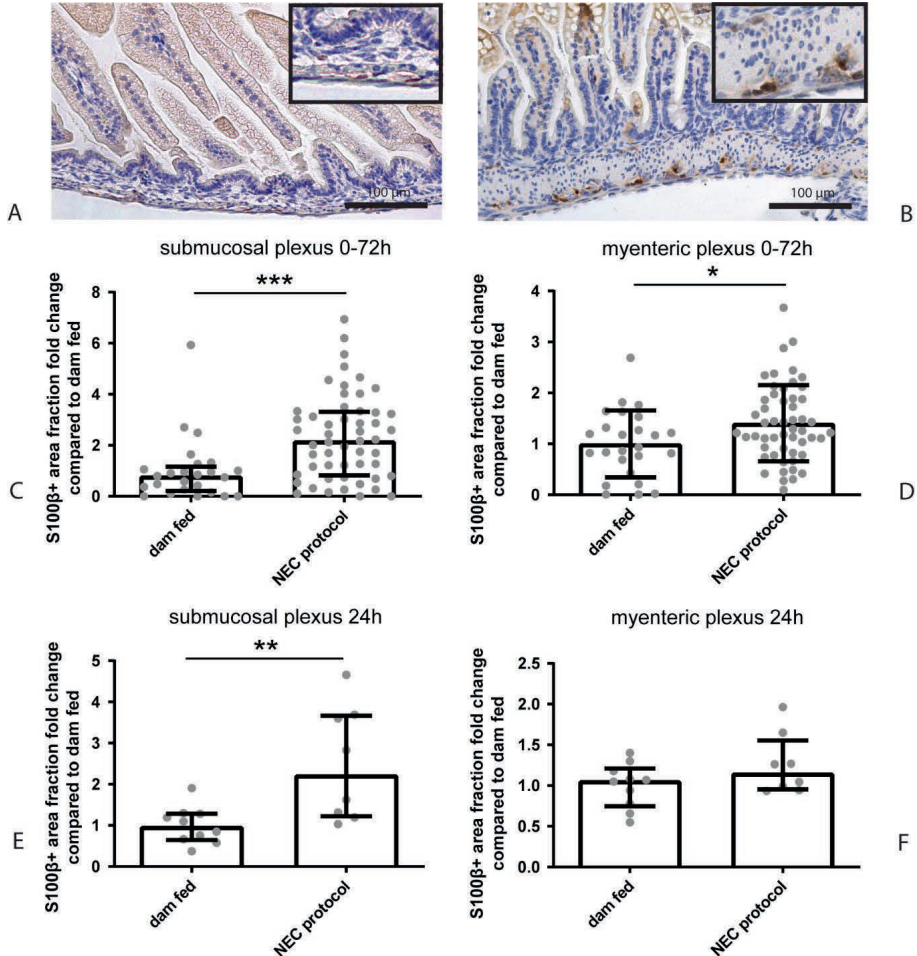


Figure 5.4 Representative images of S100 β immunoreactivity in the submucosal and myenteric plexus of control animals (A) and animals subjected to the NEC protocol (B). S100 β -positive surface area was increased in the submucosal (C) and myenteric plexus (D) of animals subjected to the NEC protocol in the 72h experiment compared to the control group. S100 β -positive surface area was increased in the submucosal (E), but not in the myenteric plexus (F) of animals subjected to the NEC protocol at 24h compared to the control group. Data points represent individual mouse pups. Scale bars indicate 100 μm . * $p \leq 0.05$, ** $p \leq 0.01$, *** $p \leq 0.001$.

ENS alteration: presynaptic vesicles (synaptophysin)

Synaptophysin was used as a marker for presynaptic vesicles. Compared to controls (**Figure 5.5A**), synaptophysin immunoreactivity was increased in animals exposed to the NEC protocol in the 72h experiment (**Figure 5.5B**) in both the submucosal ($p \leq 0.0001$; **Figure 5.5C**) and the myenteric plexus ($p \leq 0.0001$; **Figure 5.5D**). After 24h, no differences were observed in synaptophysin immunoreactivity between the groups (**Figure 5.5E-5.5F**).

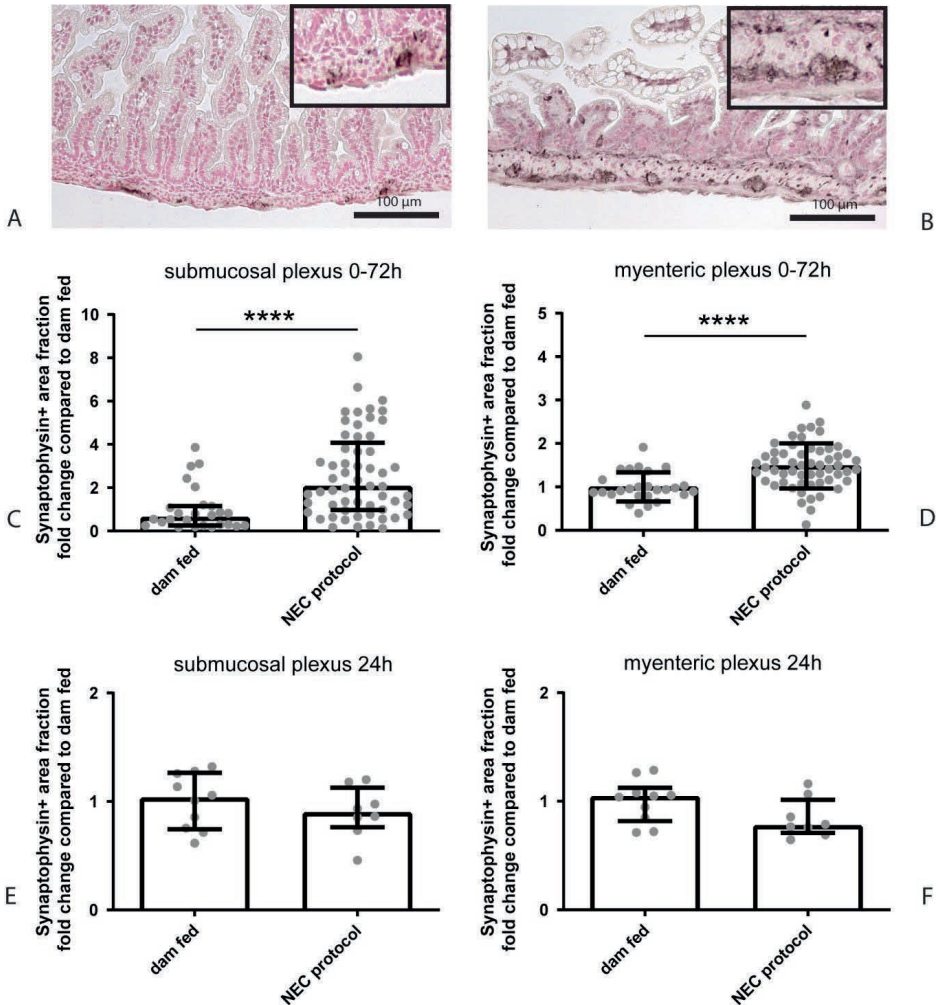


Figure 5.5 Representative images of synaptophysin immunoreactivity in the submucosal and myenteric plexus of control animals (A) and animals subjected to the NEC protocol (B). Synaptophysin-positive surface area was increased in the submucosal (C) and myenteric plexus (D) of animals subjected to the NEC protocol in the 72h experiment compared to the control group. Synaptophysin-positive surface area in submucosal (E) and myenteric plexus (F) was not affected by NEC protocol exposure in the 24h experiment in the 24h experiment in mouse pups. Scale bars indicate 100 µm. **** $p \leq 0.0001$.

Intestinal transit

The intestinal transit was increased in animals 24h after subjection to the NEC protocol, compared to control ($p \leq 0.01$; **Figure 5.6A**). At 48h after subjection to the NEC protocol, the intestinal transit was decreased, compared to control ($p \leq 0.05$; **Figure 5.6B**).

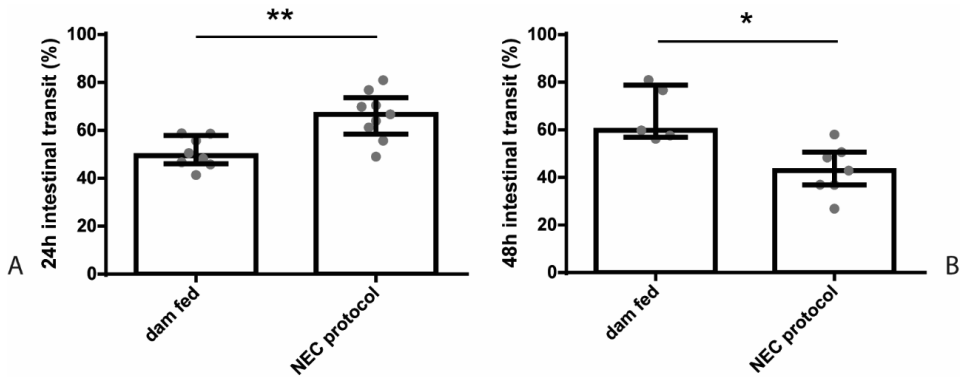


Figure 5.6 Intestinal transit expressed as the percentage of small intestinal length covered by Evans Blue. The intestinal transit was increased in animals 24h after subjection to the NEC protocol, compared to controls (A). After 48h exposure to the NEC protocol, intestinal transit was decreased compared to controls (B). Data points represent individual mouse pups. * $p \leq 0.05$, ** $p \leq 0.01$

Formation and reuptake of neurotransmitters and RET / GDNF expression

mRNA expression of genes involved in formation and reuptake of neurotransmitters was studied in animals exposed to the NEC protocol for 24h to shed light on the increased intestinal transit at this time point. mRNA expression of SERT (serotonin reuptake transporter) decreased following NEC protocol exposure ($p \leq 0.05$; **Figure 5.7A**). mRNA expression of TPH2 (tryptophan hydroxylase, involved in serotonin formation in the ENS), CHAT (choline acetyltransferase, involved in acetylcholine formation) and nNOS (neuronal nitric oxide synthase, involved in NO formation) remained unaltered following NEC protocol exposure compared to controls (**Figure 5.7B-5.7D**). Last, GDNF and its receptor RET were studied for their role in ENS development²⁷. No differences were observed in RET or GDNF mRNA expression in mice that were exposed to the NEC protocol for 24h compared to dam fed controls (**Figure 5.7E-5.7F**).

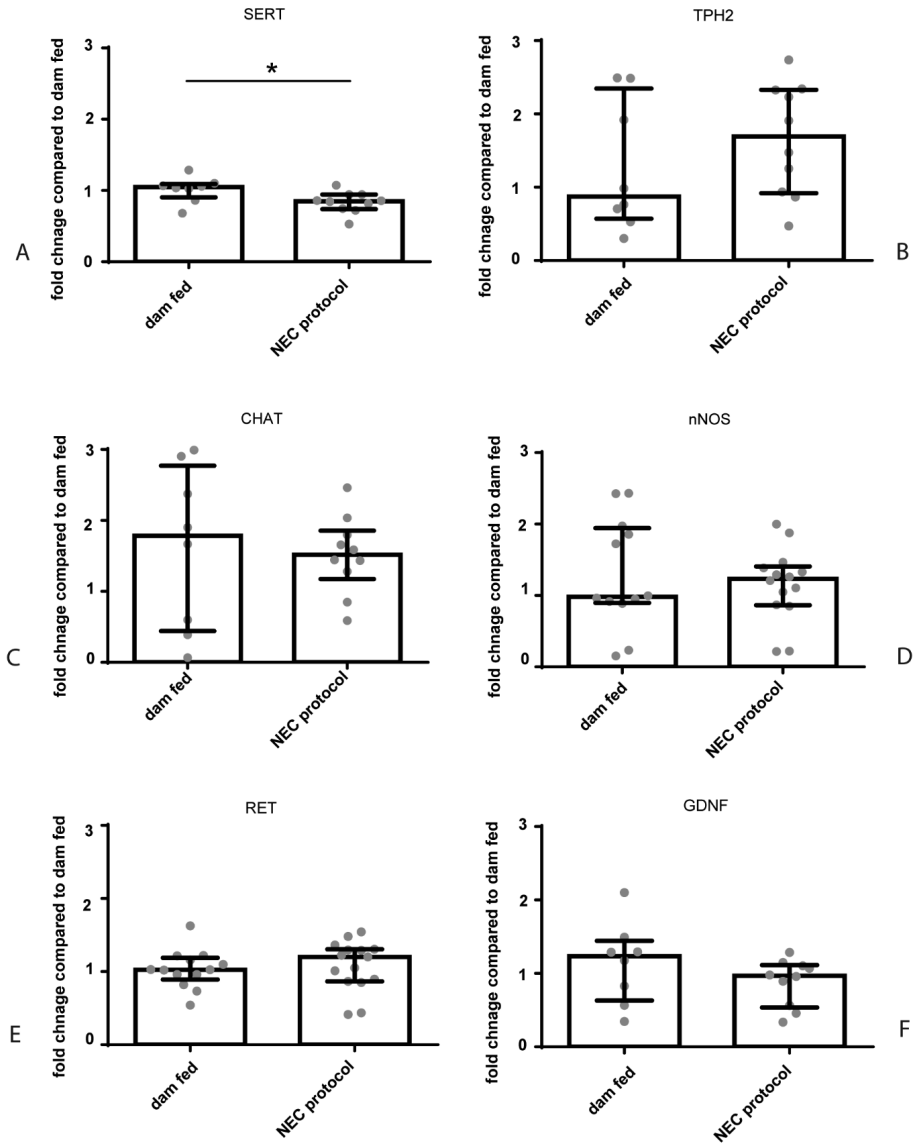


Figure 5.7 mRNA expression of various genes involved in formation and reuptake of neurotransmitters and enteric nervous system development in the 24h experiment. mRNA expression of SERT decreased after 24h of NEC protocol exposure compared to controls (A). mRNA expression of TPH2, CHAT, nNOS, RET and GDNF remained unaltered after 24h NEC protocol exposure compared to controls (B-F). Data are reported as relative expression compared to dam fed controls (set at 1). Data points represent individual mouse pups. * $p \leq 0.05$

Discussion

In the current study, we investigated the ENS and intestinal transit in a well-established mouse NEC model in which NEC was induced in newborn C57BL/6 mice by formula feeding, oral commensal bacteria with LPS supplementation, asphyxia and cold stress.

Key findings of the current study are the increase in mature neurons (NeuN) and enteric glial cells (S100 β) in the mice subjected to the NEC protocol in the 72h experiment, which were accompanied by an increase in presynaptic vesicles (synaptophysin). Enteric glial cells are increasingly recognized for their regulatory function in gastrointestinal homeostasis and their neuroprotective capacities during inflammation^{28,29}. Ablation of enteric glial cells in a transgenic mouse model leads to a fulminant jejuno-ileitis, resembling NEC, with degeneration of myenteric plexus neurons³⁰ and has recently been linked to increased NEC severity¹⁶. Thus, the increased S100 β surface area in the NEC protocol exposed mice is probably a compensatory response of glial cells to intestinal inflammation that was previously shown in this NEC model³¹. Since glial cell alterations emerged before (i.e., at 24h) and paralleled (i.e., in the 72h experiment) neuronal changes, the increased numbers of glial cells may be a driving force behind the increase of neurons and presynaptic vesicles. Although the complex cross-talk between enteric glial cells and ENS neurons is incompletely understood³², neurotrophic factors released by glial cells, such as glial-cell line derived neurotrophic factor (GDNF) and brain derived neurotrophic factor (BDNF) are clearly involved in their interaction^{33,34}. GDNF is involved in the development of the ENS^{20,27} and its protein expression is upregulated during inflammation³⁵, as is induced during this experimental NEC protocol³¹. It has been implicated to promote neuronal proliferation³³ and *in vitro* work from Bottner et al., reports that stimulating a rat enteric nerve cell culture with GDNF increased synaptophysin mRNA expression³⁶. BDNF was reported to reduce inflammation mediated apoptosis of enteric glial cells *in vitro*³⁷. Moreover, a recent study by Kovler et al. observed that BDNF expression was reduced in human and experimental NEC, and that administration of BDNF in a mouse NEC model rescued intestinal motility, decreased intestinal TLR4 signalling and inflammation and improved histological gut outcome¹⁶. Future studies are needed to unravel the role of neurotrophic factors in ENS changes in the neonatal setting and the time course of these changes. Interestingly, increased synaptophysin immunoreactivity was previously also observed *in utero* in the context of perinatal asphyxia³⁸, a known risk factor for NEC development³⁹. Whether the increased presence of presynaptic vesicles during NEC alters ENS signalling and whether this plays a role in intestinal motility changes and intestinal injury during NEC development remain to be elucidated.

Our findings are in accordance with observations of hyperplasia of glial cells and hypertrophy and hyperplasia of neuronal cell bodies in inflammatory bowel disease, characterized by intestinal inflammation, but typically no necrosis⁴⁰. By contrast, other studies on ENS abnormalities in NEC, both in human specimen¹¹⁻¹³ and a rat NEC model^{13,41} report a loss of both glial cells and neurons, with the most severe lesions in the regions prone to intestinal ischemia¹². A reduction of neurons was also reported in a mouse NEC model with a different NEC induction protocol, with amongst others a longer exposure time to the experimental NEC protocol of 96h⁴². Importantly, findings of ENS alterations in

human NEC are based on specimens obtained during surgery and/or post-mortem, and may not be representative for changes in early and/or less severe NEC in infants. Based on these combined findings, it is tempting to speculate that our data may represent a relatively milder disease state with an ENS response that predisposes to glial cell and neuronal loss at a later time point. This suggests that different rodent NEC models and different durations of post NEC induction follow up can be used to gain longitudinal insight in the ENS changes during NEC pathophysiology. To extrapolate these findings to the clinical setting, functional ENS analyses, such as measurements of transit time and intestinal motility are of vital importance.

We observed an increased intestinal transit in animals subjected to the NEC protocol for 24h, indicating increased intestinal motility. This most likely results from an immunological host response and subsequent diarrhoea⁴³⁻⁴⁶ rather than structural alterations of the ENS, since no differences were observed in synaptophysin immunoreactivity at 24h and the mRNA expression of genes related to neurotransmitter formation were unaltered. Decreased mRNA expression of SERT (serotonin reuptake transporter) at 24h could be involved, since it is associated with increased synaptic levels of serotonin, a neurotransmitter that is important for gastrointestinal motility⁴⁷. Nevertheless, other intestinal cell types besides than neurons express SERT⁴⁸, including enterocytes, and, in the current study set-up, we cannot dissect which cell types are responsible for the overall decrease in SERT mRNA.

Next to its potential role in altering intestinal motility, downregulation of SERT and increased serotonin signalling could contribute to NEC pathogenesis, as genetic deletion of SERT increased intestinal inflammation and systemic manifestations in a mouse NEC model⁴⁸ and some clinical cases of NEC have been related to maternal use of selective serotonin reuptake inhibitors⁴⁹. Of note, the effect of serotonin on intestinal inflammation depends on its cellular source; whereas TPH1 knock-out mice, which lack serotonin production by enterochromaffin cells, were protected against experimental colitis⁵⁰, TPH2 knock-out mice, which lack neuronal serotonin production, were more severely affected⁵¹. Downregulation of SERT mRNA expression in our model likely results from inflammation, as it has previously been described in the epithelium of IBD patients with active disease compared to controls^{52,53} and in human colon organoids upon TNF α administration⁵².

In contrast to the increased intestinal motility at 24h, intestinal transit decreased at 48h of exposure to the NEC protocol. This suggests that neuronal signalling function is disturbed following prolonged exposure to the NEC protocol, despite the presence of sufficient amounts of presynaptic vesicles (i.e., increased synaptophysin immunoreactivity in NEC protocol exposed animals in the 72h experiment). Additional studies are needed to unravel the mechanisms behind the reduced intestinal motility following exposure to the NEC protocol. Moreover, it highlights that including a functional assay of gut motility is of importance when studying ENS changes in NEC.

A limitation of this study is that, due to the size of the mouse intestines, we could not distinguish between the different anatomical parts of the small intestine, or varying disease severities within parts of a single intestine. In addition, the translation of these rodent findings into the clinic is challenging as biopsies from NEC patients, that are available for research, exclusively reflect children with the most severe phenotype of the NEC spectrum.

Last, animals in the 72h NEC experiment, with a survival ranging from 7h till 72h, were compared with a dam fed control group composed of animals that all survived 72h, suggesting postnatal age may be a confounding factor in this comparison. However, almost all ENS markers examined in the 72h NEC group correlated weakly and positively with postnatal age, except for two markers in which this correlation was negative (NeuN positive area fraction in the myenteric plexus and Doublecortin positive area fraction in the myenteric plexus) and very weak (**Table S5.1**). These findings suggest the differences between the 72h NEC group and the dam fed group are caused by NEC protocol exposure rather than their difference in postnatal age.

In summary, in this experimental NEC model, subjection to the experimental NEC protocol was associated with an increase of mature neurons, glial cells and increased presence of presynaptic vesicles in the submucosal and myenteric plexus and time-dependant changes in intestinal motility.

Since glial cell changes commenced early following NEC protocol exposure, glial cell changes may be a driving force behind later ENS alterations. The current histological data cannot fully explain the observed changes in motility, thus, additional studies are needed to unravel the mechanisms underlying these functional changes. Last, since our findings differ from those in clinical NEC biopsies but are in accordance with findings in IBD patients, the ENS changes in this NEC model seem to represent a relatively milder disease state within the clinical NEC spectrum, with an ENS response that precedes glial cell and neuronal loss.

References

1. Lin PW, Stoll BJ. Necrotising enterocolitis. *Lancet*. 2006;368(9543):1271-83.
2. Ahle M, Drott P, Andersson RE. Epidemiology and trends of necrotizing enterocolitis in Sweden: 1987-2009. *Pediatrics*. 2013;132(2):e443-51.
3. Heida FH, Stolwijk L, Loos MH, van den Ende SJ, Onland W, van den Dungen FA, et al. Increased incidence of necrotizing enterocolitis in the Netherlands after implementation of the new Dutch guideline for active treatment in extremely preterm infants: Results from three academic referral centers. *J Pediatr Surg*. 2017;52(2):273-6.
4. Blakely ML, Lally KP, McDonald S, Brown RL, Barnhart DC, Ricketts RR, et al. Postoperative outcomes of extremely low birth-weight infants with necrotizing enterocolitis or isolated intestinal perforation: a prospective cohort study by the NICHD Neonatal Research Network. *Ann Surg*. 2005;241(6):984-9; discussion 9-94.
5. Hull MA, Fisher JG, Gutierrez IM, Jones BA, Kang KH, Kenny M, et al. Mortality and management of surgical necrotizing enterocolitis in very low birth weight neonates: a prospective cohort study. *J Am Coll Surg*. 2014;218(6):1148-55.
6. Hintz SR, Kendrick DE, Stoll BJ, Vohr BR, Fanaroff AA, Donovan EF, et al. Neurodevelopmental and growth outcomes of extremely low birth weight infants after necrotizing enterocolitis. *Pediatrics*. 2005;115(3):696-703.
7. Hong CR, Fullerton BS, Mercier CE, Morrow KA, Edwards EM, Ferrelli KR, et al. Growth morbidity in extremely low birth weight survivors of necrotizing enterocolitis at discharge and two-year follow-up. *J Pediatr Surg*. 2018;53(6):1197-202.
8. Rees CM, Piirro A, Eaton S. Neurodevelopmental outcomes of neonates with medically and surgically treated necrotizing enterocolitis. *Archives of disease in childhood Fetal and neonatal edition*. 2007;92(3):F193-F8.
9. Schulzke SM, Deshpande GC, Patole SK. Neurodevelopmental outcomes of very low-birth-weight infants with necrotizing enterocolitis: a systematic review of observational studies. *Arch Pediatr Adolesc Med*. 2007;161(6):583-90.
10. Neu J, Walker WA. Necrotizing enterocolitis. *N Engl J Med*. 2011;364(3):255-64.
11. Sigge W, Wedel T, Kuhnel W, Krammer HJ. Morphologic alterations of the enteric nervous system and deficiency of non-adrenergic non-cholinergic inhibitory innervation in neonatal necrotizing enterocolitis. *Eur J Pediatr Surg*. 1998;8(2):87-94.
12. Wedel T, Krammer HJ, Kuhnel W, Sigge W. Alterations of the enteric nervous system in neonatal necrotizing enterocolitis revealed by whole-mount immunohistochemistry. *Pediatr Pathol Lab Med*. 1998;18(1):57-70.
13. Zhou Y, Yang J, Watkins DJ, Boomer LA, Matthews MA, Su Y, et al. Enteric nervous system abnormalities are present in human necrotizing enterocolitis: potential neurotransplantation therapy. *Stem Cell Res Ther*. 2013;4(6):157-.
14. Zhou Y, Yang J, Watkins DJ, Boomer LA, Matthews MA, Su Y, et al. Enteric nervous system abnormalities are present in human necrotizing enterocolitis: potential neurotransplantation therapy. *Stem Cell Res Ther*. 2013;4(6):157.
15. Chen W, Sun J, Kappel SS, Gormsen M, Sangild PT, Aunsholt L. Gut transit time, using radiological contrast imaging, to predict early signs of necrotizing enterocolitis. *Pediatr Res*. 2020.
16. Kovler ML, Gonzalez Salazar AJ, Fulton WB, Lu P, Yamaguchi Y, Zhou Q, et al. Toll-like receptor 4-mediated enteric glia loss is critical for the development of necrotizing enterocolitis. *Sci Transl Med*. 2021;13(612):eabg3459.
17. Goyal RK, Hirano I. The enteric nervous system. *N Engl J Med*. 1996;334(17):1106-15.
18. von Boyen GB, Steinkamp M, Reinshagen M, Schafer KH, Adler G, Kirschs J. Proinflammatory cytokines increase glial fibrillary acidic protein expression in enteric glia. *Gut*. 2004;53(2):222-8.
19. Yoo BB, Mazmanian SK. The Enteric Network: Interactions between the Immune and Nervous Systems of the Gut. *Immunity*. 2017;46(6):910-26.
20. Burns AJ, Roberts RR, Bornstein JC, Young HM. Development of the enteric nervous system and its role in intestinal motility during fetal and early postnatal stages. *Semin Pediatr Surg*. 2009;18(4):196-205.

21. Lake JJ, Heuckeroth RO. Enteric nervous system development: migration, differentiation, and disease. *Am J Physiol Gastrointest Liver Physiol*. 2013;305(1):G1-24.
22. Rodrigues DM, Li AY, Nair DG, Blennerhassett MG. Glial cell line-derived neurotrophic factor is a key neurotrophin in the postnatal enteric nervous system. *Neurogastroenterol Motil*. 2011;23(2):e44-56.
23. Sulistyono A, Rahman A, Biouss G, Antounians L, Zani A. Animal models of necrotizing enterocolitis: review of the literature and state of the art. *Innov Surg Sci*. 2018;3(2):87-92.
24. Ganji N, Li B, Lee C, Filler R, Pierro A. Necrotizing Enterocolitis: State of the Art in Translating Experimental Research to the Bedside. *Eur J Pediatr Surg*. 2019;29(4):352-60.
25. Tian R, Liu SX, Williams C, Soltau TD, Dimmitt R, Zheng X, et al. Characterization of a necrotizing enterocolitis model in newborn mice. *Int J Clin Exp Med*. 2010;3(4):293-302.
26. Liu SX, Tian R, Baskind H, Hsueh W, De Plaen IG. Platelet-activating factor induces the processing of nuclear factor-kappaB p105 into p50, which mediates acute bowel injury in mice. *Am J Physiol Gastrointest Liver Physiol*. 2009;297(1):G76-81.
27. Pawloski V, Schmidt MHH. Neuron-Glia Interaction in the Developing and Adult Enteric Nervous System. *Cells*. 2020;10(1).
28. Sharkey KA. Emerging roles for enteric glia in gastrointestinal disorders. *J Clin Invest*. 2015;125(3):918-25.
29. Margolis KG, Gershon MD. Enteric Neuronal Regulation of Intestinal Inflammation. *Trends Neurosci*. 2016;39(9):614-24.
30. Bush TG, Savidge TC, Freeman TC, Cox HJ, Campbell EA, Mucke L, et al. Fulminant jejuno-ileitis following ablation of enteric glia in adult transgenic mice. *Cell*. 1998;93(2):189-201.
31. Managlia E, Liu SXL, Yan X, Tan XD, Chou PM, Barrett TA, et al. Blocking NF-kappaB Activation in Ly6c(+) Monocytes Attenuates Necrotizing Enterocolitis. *Am J Pathol*. 2019;189(3):604-18.
32. Boesmans W, Martens M, Weltens N, Hao M, Tack J, Cirillo C, et al. Imaging neuron-glia interactions in the enteric nervous system. *Front Cell Neurosci*. 2013;7:183.
33. Cortés D, Carballo-Molina OA, Castellanos-Montiel MJ, Velasco I. The Non-Survival Effects of Glial Cell Line-Derived Neurotrophic Factor on Neural Cells. *Front Mol Neurosci*. 2017;10:258-.
34. Hansebout CR, Su C, Reddy K, Zhang D, Jiang C, Rathbone MP, et al. Enteric glia mediate neuronal outgrowth through release of neurotrophic factors. *Neural Regen Res*. 2012;7(28):2165-75.
35. von Boyen GB, Schulte N, Pflüger C, Spaniol U, Hartmann C, Steinkamp M. Distribution of enteric glia and GDNF during gut inflammation. *BMC Gastroenterol*. 2011;11:3.
36. Bottner M, Harde J, Barrenschee M, Hellwig I, Vogel I, Ebsen M, et al. GDNF induces synaptic vesicle markers in enteric neurons. *Neurosci Res*. 2013;77(3):128-36.
37. Steinkamp M, Schulte N, Spaniol U, Pflüger C, Hartmann C, Kirsch J, et al. Brain derived neurotrophic factor inhibits apoptosis in enteric glia during gut inflammation. *Medical science monitor : international medical journal of experimental and clinical research*. 2012;18(4):BR117-22.
38. Nikiforou M, Willburger C, de Jong AE, Kloosterboer N, Jellema RK, Ophelders DRMG, et al. Global hypoxia-ischemia induced inflammation and structural changes in the preterm ovine gut which were not ameliorated by mesenchymal stem cell treatment. *Molecular medicine (Cambridge, Mass)*. 2016;22:244-57.
39. Fox TP, Godavitarne C. What really causes necrotising enterocolitis? *ISRN Gastroenterol*. 2012;2012:628317-.
40. Geboes K, Collins S. Structural abnormalities of the nervous system in Crohn's disease and ulcerative colitis. *Neurogastroenterol Motil*. 1998;10(3):189-202.
41. Zhou Y, Wang Y, Olson J, Yang J, Besner GE. Heparin-binding EGF-like growth factor promotes neuronal nitric oxide synthase expression and protects the enteric nervous system after necrotizing enterocolitis. *Pediatr Res*. 2017;82(3):490-500.
42. Wei J, Zhou Y, Besner GE. Heparin-binding EGF-like growth factor and enteric neural stem cell transplantation in the prevention of experimental necrotizing enterocolitis in mice. *Pediatr Res*. 2015;78(1):29-37.
43. Wirthlin DJ, Cullen JJ, Spates ST, Conklin JL, Murray J, Caropreso DK, et al. Gastrointestinal transit during endotoxemia: the role of nitric oxide. *J Surg Res*. 1996;60(2):307-11.

44. Hellstrom PM, al-Saffar A, Ljung T, Theodorsson E. Endotoxin actions on myoelectric activity, transit, and neuropeptides in the gut. Role of nitric oxide. *Dig Dis Sci.* 1997;42(8):1640-51.
45. Cullen JJ, Doty RC, Ephgrave KS, Hinkhouse MM, Broadhurst K. Changes in intestinal transit and absorption during endotoxemia are dose dependent. *J Surg Res.* 1999;81(1):81-6.
46. Cullen JJ, Mercer D, Hinkhouse M, Ephgrave KS, Conklin JL. Effects of endotoxin on regulation of intestinal smooth muscle nitric oxide synthase and intestinal transit. *Surgery.* 1999;125(3):339-44.
47. Li Z, Chalazonitis A, Huang Y-y, Mann JJ, Margolis KG, Yang QM, et al. Essential Roles of Enteric Neuronal Serotonin in Gastrointestinal Motility and the Development/Survival of Enteric Dopaminergic Neurons. *The Journal of Neuroscience.* 2011;31(24):8998.
48. Gross Margolis K, Vittorio J, Talavera M, Gluck K, Li Z, Iuga A, et al. Enteric serotonin and oxytocin: endogenous regulation of severity in a murine model of necrotizing enterocolitis. *Am J Physiol Gastrointest Liver Physiol.* 2017;313(5):G386-g98.
49. Stiskal JA, Kulin N, Koren G, Ho T, Ito S. Neonatal paroxetine withdrawal syndrome. *Arch Dis Child Fetal Neonatal Ed.* 2001;84(2):F134-5.
50. Ghia JE, Li N, Wang H, Collins M, Deng Y, El-Sharkawy RT, et al. Serotonin has a key role in pathogenesis of experimental colitis. *Gastroenterology.* 2009;137(5):1649-60.
51. Gershon MD. Serotonin is a sword and a shield of the bowel: serotonin plays offense and defense. *Trans Am Clin Climatol Assoc.* 2012;123:268-80.
52. Jørandli JW, Thorsvik S, Skovdahl HK, Kornfeld B, Sæterstad S, Gustafsson BI, et al. The serotonin reuptake transporter is reduced in the epithelium of active Crohn's disease and ulcerative colitis. *Am J Physiol Gastrointest Liver Physiol.* 2020;319(6):G761-g8.
53. Tada Y, Ishihara S, Kawashima K, Fukuba N, Sonoyama H, Kusunoki R, et al. Downregulation of serotonin reuptake transporter gene expression in healing colonic mucosa in presence of remaining low-grade inflammation in ulcerative colitis. *J Gastroenterol Hepatol.* 2016;31(8):1443-52.

Supplementary materials

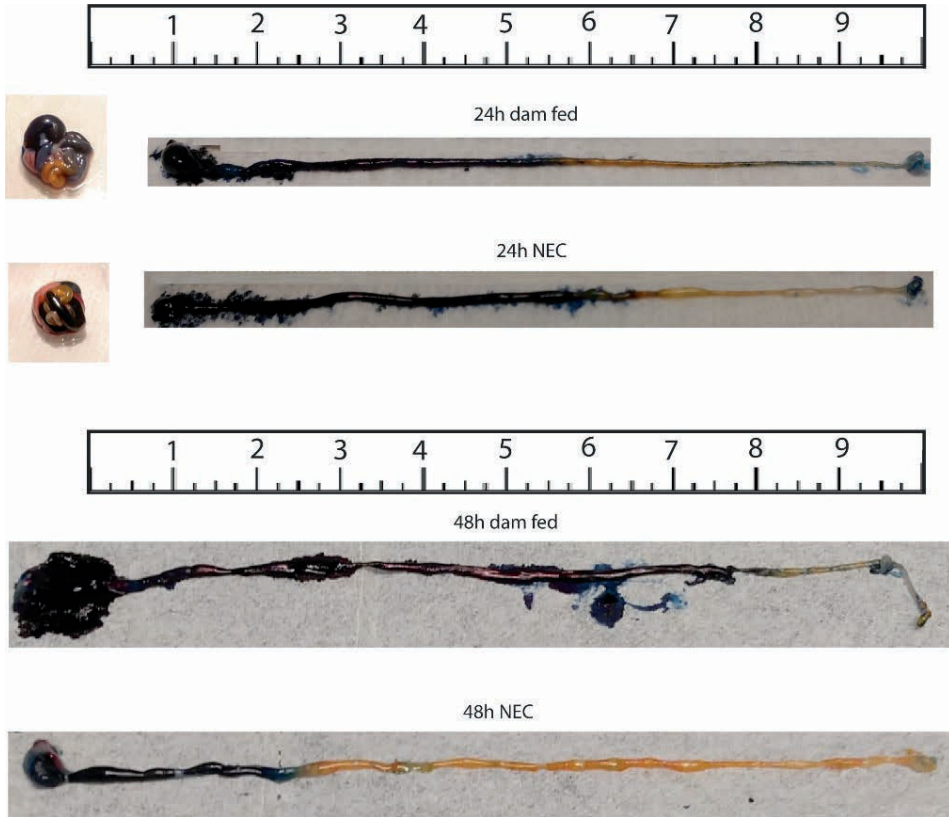


Figure S5.1 Measurement of intestinal transit in mouse pups after 24h and 48h with % Evans Blue.

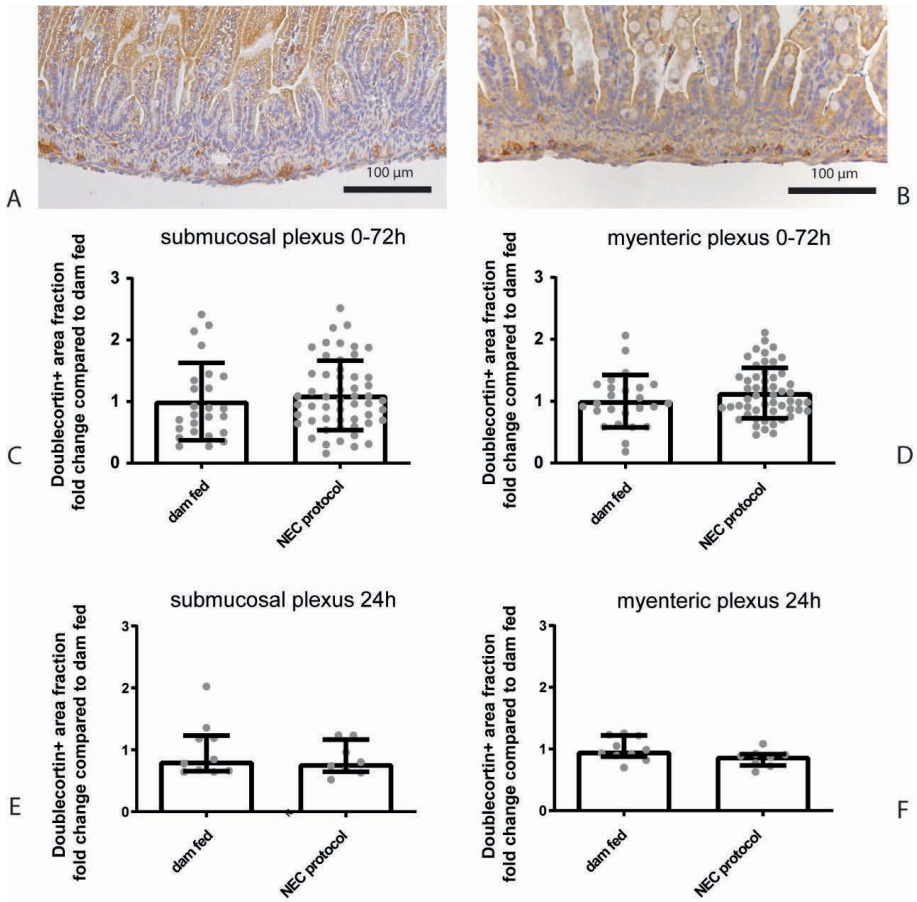


Figure S5.2 Representative images of doublecortin immunoreactivity in the submucosal and myenteric plexus of control animals (A) and animals subjected to the NEC protocol (B). No difference was observed in doublecortin immunoreactivity in the submucosal or the myenteric plexus in the 72h experiment (C, D) or at 24h (E, F). Data points represent individual mouse pups. Scale bars indicate 100 μ m.

Table S5.1 Spearman's Rho correlation coefficient of the correlation between animal postnatal age / survival duration and histological ENS outcomes in the NEC protocol exposed animals in the 72h experiment.

	Correlation with animal postnatal age / survival duration
NeuN positive area fraction submucosal plexus	0.251
NeuN positive area fraction myenteric plexus	-0.055
Doublecortin positive area fraction submucosal plexus	0.426
Doublecortin positive area fraction myenteric plexus	-0.106
S100 β positive area fraction submucosal plexus	0.264
S100 β positive area fraction myenteric plexus	0.109
Synaptophysin positive area fraction submucosal plexus	0.362
Synaptophysin positive area fraction myenteric plexus	0.191

Part III

**Understanding NEC pathophysiology:
mucus barrier alterations during
chorioamnionitis and NEC**

Chapter 6

Intestinal goblet cell loss during chorioamnionitis in fetal lambs: mechanistic insights and postnatal implications

C. van Gorp, I.H. de Lange, K.R.I. Massy, L. Kessels, A.H. Jobe, J.P.M. Cleutjens,
M.W. Kemp, M. Saito, H. Usada, J. Newnham, M. Hütten, B.W. Kramer,
L.J. Zimmermann, and Tim G.A.M. Wolfs

Int J Mol Sc. 2021;22(4):1946

Abstract

Chorioamnionitis, an important cause of preterm birth, is linked to necrotizing enterocolitis (NEC). NEC is characterized by a disrupted mucus barrier, goblet cell loss, and endoplasmic reticulum (ER) stress of the intestinal epithelium. These findings prompted us to investigate the mechanisms underlying goblet cell alterations over time in an ovine chorioamnionitis model. Fetal lambs were intra-amniotically (IA) exposed to lipopolysaccharides (LPS) for 5, 12, or 24 h, or 2, 4, 8, or 15 d before premature delivery at 125 d gestational age (GA). Gut inflammation, the number, distribution, and differentiation of goblet cells, ER stress, and apoptosis were measured. We found a biphasic reduction in goblet cell numbers 24 h–2 d after, and 15 d after IA LPS exposure. The second decrease of goblet cell numbers was preceded by intestinal inflammation, apoptosis, and crypt ER stress, and increased SAM-pointed domain-containing ETS transcription factor (SPDEF)-positive cell counts. Our combined findings indicated that ER stress drives apoptosis of maturing goblet cells during chorioamnionitis, ultimately reducing goblet cell numbers. As similar changes have been described in patients suffering from NEC, these findings are considered to be clinically important for understanding the predecessors of NEC, and targeting ER stress in this context is interesting for future therapeutics.

Introduction

Chorioamnionitis is an important risk factor for preterm birth and contributes to neonatal morbidity and mortality¹. This antenatal condition, caused by intra-amniotic exposure to microorganisms and their toxic components (e.g., lipopolysaccharides (LPS)), is defined as inflammatory cell infiltration in the fetal membranes (chorion and amnion) and the amniotic cavity¹. During chorioamnionitis, the fetus is exposed to an infectious environment and this can initiate a fetal inflammatory response syndrome (FIRS), which is characterized by elevated systemic interleukin (IL)-6 and IL-8 concentrations^{2,3}. In addition, the contaminated amniotic fluid (AF) is swallowed by the fetus and thereby directly affects the fetal gut. From previous studies that used preclinical chorioamnionitis models, it is known that intrauterine inflammation/ infection (caused by, e.g., LPS or *Ureaplasma* species) is associated with intestinal inflammation and concomitant developmental disruptions and gastrointestinal injury⁴⁻⁹. Accordingly, chorioamnionitis is a risk factor for adverse postnatal intestinal outcomes, including necrotizing enterocolitis (NEC)¹⁰⁻¹². NEC is a severe intestinal disease that is characterized by intestinal inflammation and, in severe stages, necrosis¹³. Hence, NEC is associated with a high mortality rate of up to 50%^{12,13}.

Intestinal goblet cells produce and secrete mucins that are an important part of the mucus barrier, which forms the first passive line of defense against infiltration of bacteria and bacterial-derived products^{14,15}. Importantly, in a murine study by Elgin et al., reduced goblet cell numbers were observed at birth as a result of maternal-induced fetal inflammation, indicating chorioamnionitis may already disrupt the mucus barrier⁷. In addition, neonates with NEC experience intestinal mucosal barrier disruption. This is characterized by a reduced number of mucin-2 (MUC2)-positive goblet cells and reduced production of mucins, which compromises the mucus barrier¹⁶⁻¹⁸. This disrupted mucus barrier allows bacteria to reach the intestinal epithelium and aggravate intestinal inflammation¹⁸. Intestinal goblet cells derive from intestinal stem cells that reside near the bottom of the intestinal crypt¹⁹. These stem cells constantly yield transit-amplifying daughter cells that proliferate and differentiate while migrating from the crypts into the lower part of the intestinal villi²⁰. Once fully differentiated, intestinal goblet cells continue to migrate towards the villus tips where they finally die and shed into the intestinal lumen²⁰.

Intestinal epithelial endoplasmic reticulum (ER) stress is a mechanism involved in NEC pathophysiology that may underlie the loss of goblet cells in NEC^{21,22}. During ER stress, unfolded proteins accumulate in the ER lumen and binding immunoglobulin protein (BiP) initiate an unfolded protein response (UPR) to resolve the unfolded protein synthesis^{23,24}. If the UPR is unable to process the accumulation of unfolded proteins, apoptosis is induced through various pathways including the upregulation of transcription factor C/enhancer binding protein homologous protein (CHOP)²⁵. Goblet cells are sensitive to ER stress due to their secretory nature and the large size of mucins that are folded in the ER²⁶⁻²⁸. ER stress in goblet cells typically arises during intestinal inflammation²⁵, which can trigger goblet cells to both synthesize and secrete mucins^{27,29}. Post translation, mucins are transported to the ER for protein folding²⁵, and consequently, an increased mucin production during inflammation can lead to an accumulation of unfolded proteins in the ER and subsequent ER stress²⁸. In human specimens from infants with NEC, UPR activation was associated with intestinal

inflammation, increased morphological damage, and worse outcome²¹. In addition, knockout of important ER stress pathways prevented NEC development in a mouse model of NEC²².

Currently, the time dependent changes and mechanisms that underlie goblet cell alterations following chorioamnionitis remain unknown. To address these mechanistic questions, we longitudinally studied the effects of chorioamnionitis by intra-amniotically (IA) administering LPS at different time points (5, 12, and 24 h, and 2, 4, 8, and 15 d) before premature delivery.

Materials and methods

Experimental design

Animal experiments were approved by the Animal Ethics/Care Committee of the University of Western Australia (Perth, Australia; ethical approval number: RA/3/100/928; approval date 1 January 2010). The study design was previously published^{2,30}. Briefly, singleton fetuses from time-mated merino crossbred ewes were randomly assigned to eight study groups. IA saline (controls; 0.9% saline solution) or IA LPS injections (10 mg *Escherichia coli*-derived LPS; O55:B5; Sigma–Aldrich, St. Louis, MO) were performed under ultrasound guidance at 5, 12, or 24 h, or 2, 4, 8, or 15 d before preterm delivery at 125 d gestational age (GA), which is for the gut comparable to approximately 27–30 weeks of human GA (term ~150 d GA) (Figure 6.1). IA LPS administration has previously been shown to induce inflammation of the chorion and amnion and influx of inflammatory cells in the amniotic fluid that correlates well with human chorioamnionitis³¹. The half-life time of IA-administered LPS is relatively long (1.7 days) and the LPS remains detectable until 15 d after IA injection³¹. Because no differences between various durations of saline exposure were found within the control group, all the saline animals were pooled into one control group. Directly after preterm delivery (125 d GA), the lambs were euthanized by intravenous injection of pentobarbitone (100 mg/kg, Valaber, Pitman–Moore, Australia). Distal ileum tissue was collected post-mortem for analyses. The involved investigators were blinded to treatment allocation during data analyses.

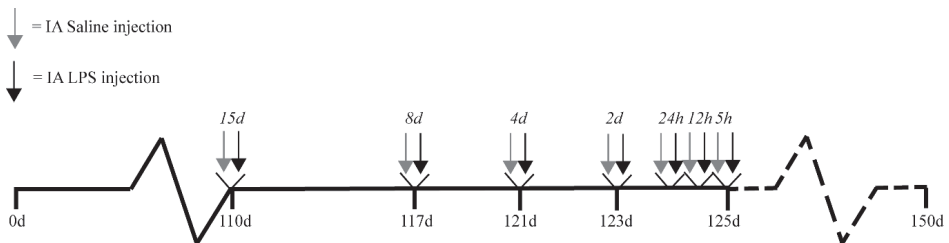


Figure 6.1 **Study design.** Singleton fetuses from time-mated merino crossbred ewes were randomly assigned to eight different study groups. IA saline or LPS (10mg *Escherichia coli*-derived LPS) injections were given at seven different time points (5, 12, or 24 h, or 2, 4, 8, or 15 d) before preterm delivery at 125 d gestational age (GA0 (~150d GA is term)). Saline-exposed animals were pooled within one control group. Abbreviations: IA, intra-amniotic.

Antibodies

The following antibodies were used: Polyclonal rabbit antibody against human myeloperoxidase (MPO) (A0398, Dakocytomation, Glostrup, Denmark); polyclonal rabbit anti-muc2c3 (kindly provided by the University of Gothenburg, Gothenburg, Sweden); polyclonal rabbit anti-SAM-pointed domain containing ETS transcription factor (SPDEF) (ab197375, abcam, Cambridge, United Kingdom); monoclonal rabbit anti-BiP (C50B12, cell signaling technology, Leiden, the Netherlands); monoclonal mouse anti-CHOP (clone 9C8, MA1-250, Thermo Fisher Scientific, Waltham, MA, USA), and polyclonal rabbit anti-cleaved caspase-3 (CC3) (asp175) (9661, cell signaling technology, Leiden, the Netherlands).

Secondary antibodies used were: Peroxidase-conjugated goat anti-rabbit (111-035-045, Jackson, West Grove, PA, USA), biotin-conjugated rabbit anti-mouse (E0413, DakoCytomation, Glostrup, Denmark), and biotin-conjugated swine anti-rabbit (E0353, DakoCytomation, Glostrup, Denmark).

Alcian Blue/Periodic Acid–Schiff (AB/PAS)

AB/PAS was used as a general marker for mature (e.g., glycosylated) mucins^{32,33}. Distal ileum tissue was fixated in 4% paraformaldehyde and embedded in paraffin and 4- μ m sections were cut with a microtome (Leica RM2235). Sections were stained with Alcian blue (8GC work-solution, 66011-500ML-F, Sigma–Aldrich, St. Louis, MO) for 30 min at room temperature (RT) followed by incubation in periodic acid (PA, 0.5%) for 5 min. After washing, slides were stained with Schiff's reagent (3952016-500ML, Sigma–Aldrich, St. Louis, MO) for 15 min. Stained slides were scanned using Ventana IScan (Ventana Medical System, Inc., Tucson, AZ). The number of AB/PAS-positive cells was manually counted with the use of Ventana Image Viewer (v3.1.4, Ventana Medical System, Inc., Tucson, AZ), and the number of positive cells per mm² of ileal surface area was calculated after ileal surface area measurements with the use of Qwin Pro software (v3.4.0, Leica Microsystem, Wetzlar, Germany).

Immunohistochemistry

MPO was used as a marker for inflammation. MUC2 immunoreactivity was analyzed as an additional goblet cell marker; the antibody used detects both immature (not O-glycosylated) and mature (O-glycosylated) mucins. SPDEF was used to assess goblet cell differentiation^{34,35,36}. BiP and CHOP staining were performed to study intestinal epithelial ER stress and CC3 to assess apoptosis. After tissue fixation in 4% paraformaldehyde and paraffin embedding, 4- μ m thick ileal sections were cut and were used to perform immunohistochemical studies. Endogenous peroxidase activity was blocked with 0.3% H₂O₂ dissolved in phosphate buffered saline (PBS) for 20 min. For MUC2, SPDEF, BiP, CHOP, and CC3, antigen retrieval was applied by boiling the slides in 10 mM sodium citrate buffer (pH 6.0). Aspecific binding sites were blocked with 4% normal goat serum (MPO, SPDEF) or 5% bovine serum albumin (MUC2, BiP, CHOP, CC3) for 30 min at room temperature (RT). Ileal sections were incubated with primary antibody for 1 h at RT (MPO) or incubated overnight at 4°C (MUC2, SPDEF, BiP, CHOP, and CC3). Subsequently, slides were incubated with peroxidase-conjugated (MPO) or biotin-conjugated (MUC2, SPDEF, BiP, CHOP, and CC3)

secondary antibodies at RT. MPO-positive cells were visualized using 3-amino-9-ethylcarbazole (AEC, Sigma–Aldrich, St. Louis, MO, USA); MUC2 and CC3 were detected with nickel-3, 3'-diaminobenzidine (NiDAB, Sigma Aldrich, St. Louis, MO, USA), and SDPEF, BiP, and CHOP were visualized using 3, 3'-diaminobenzidine (DAB, Sigma Aldrich, St. Louis, MO, USA). (Nuclear) counterstaining was performed with hematoxylin (MPO), nuclear fast red (MUC2 and CC3), or AB/PAS (SPDEF).

For MPO, SPDEF, MUC2, CHOP, and CC3, positive cells were manually counted in two ileal cross sections with the use of Ventana Image Viewer (v3.1.4, Ventana Medical System, Inc., Tucson, AZ) and corrected for ileal surface area with the use of Qwin Pro software (v3.4.0, Leica Microsystem, Wetzlar, Germany). Only good cross-sections through the full crypt-villus axis were used. The number of cells was depicted as number of cells per mm² ileal surface area and the average count per sheep was presented. Because (developing) goblet cells migrate from the crypt bottom towards the villus tips over time²⁰, we considered the anatomical location of goblet cells and ER stress of importance for understanding the underlying mechanisms involved. We therefore analyzed the MUC2-positive cell count and CHOP-positive cell count in ileal crypts, the lower villi, the middle villi, and the tips of the villi, and corrected this for the adequate tissue surface area (**Supplementary Figure S6.1**). Ileal crypts were selected based on tissue morphology. The ileal villi were divided in three parts (lower villi, middle villi, and villi tips) that were all one third of the average villus length. For BiP, staining intensity was also analyzed in the ileal crypts, the lower villi, the middle villi, and the tips of the villi (**Supplementary Figure S6.1**) in two ileal cross sections with the following scoring system: No staining was scored as 0, mild staining was indicated as 1, moderate staining was scored as 2, and intense staining intensity was indicated with a score of 3.

Statistical analysis

Statistical analyses were performed with GraphPad Prism Software (v6.0, Graphpad Software INC., La Jolla, CA, USA). Data are displayed as median with interquartile range (IQR) for all readouts. A Kruskal–Wallis test followed by Dunn's post hoc test was used to test statistically significant differences between the different groups. Differences were interpreted as statistically significant at $p \leq 0.05$. Given the relatively small number of animals per group, p -values between 0.05 and 0.10 were reported in exact numbers and were regarded as potentially biologically relevant, as previously described^{2,8,37}. This assumption decreased the chance of a false negative finding, but increased the chance of false positive results.

Results

Intestinal inflammation

To investigate intestinal inflammation in fetal lambs after IA LPS exposure, myeloperoxidase (MPO)-positive cells were counted in the distal ileum (**Figure 6.2**). Compared to control fetuses (**Figure 6.2A**), the number of MPO-positive cells increased ($p \leq 0.05$) at 4 and 8 d after

IA LPS exposure (Figure 6.2B–D) and remained high until 15 d after LPS exposure ($p=0.06$) (Figure 6.2D).

Goblet cell number and distribution

To assess alterations in goblet cell numbers and distribution, Alcian blue (AB)/periodic acid–Schiff (PAS)- and mucin-2 (MUC2)-positive cells were identified in the distal ileum (Figures 6.3 and 6.4). Compared to control animals (Figure 6.3A,D), the number of mature goblet cells, indicated by AB/PAS-positive cells, tended to be reduced at 24 h after ($p=0.10$) (Figure 6.3B,D) and 2 d after ($p=0.07$) (Figure 6.3D) IA LPS exposure. This reduction was normalized ($p\leq 0.05$) in the 8-d LPS exposure group (Figure 6.3D). A second decrease ($p\leq 0.05$) in the number of goblet cells was observed at 15 d after IA LPS exposure compared to control ($p=0.09$) and the 8-d LPS exposure group ($p\leq 0.05$) (Figure 6.3C,D).

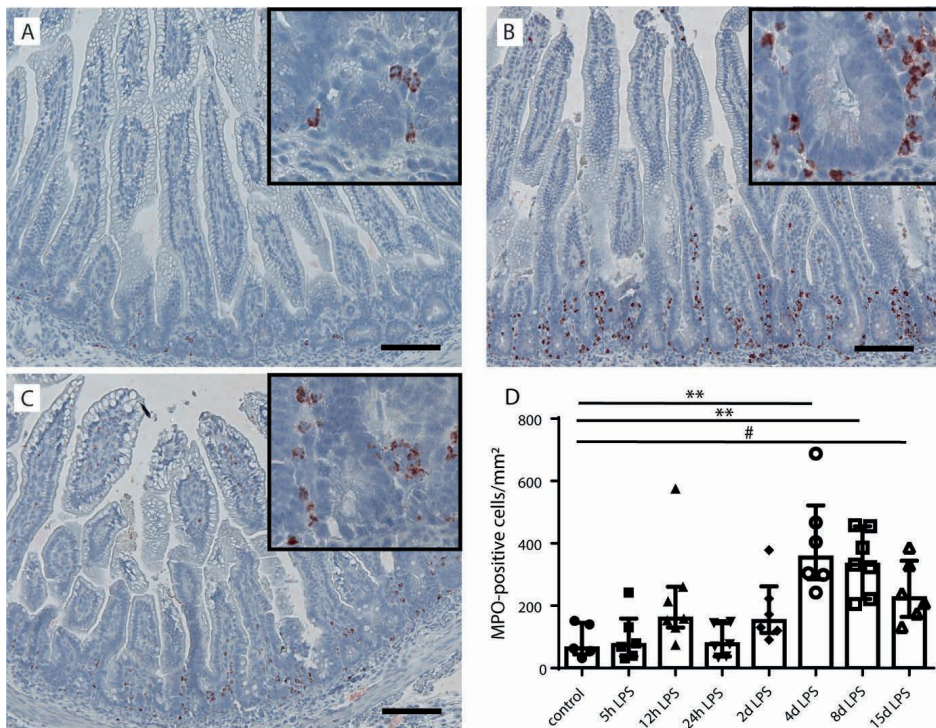


Figure 6.2 The number of myeloperoxidase (MPO)-positive cells per mm² ileal surface area in the distal ileum of fetal lambs after intra-amniotic (IA) lipopolysaccharides (LPS) exposure. Few MPO-positive cells were detected in the distal ileum of control fetuses (A, D). The number of MPO-positive cells increased at 4 (B, D) and 8 d (C, D) and still tended to be increased at 15 d after IA LPS exposure (D). In all groups, MPO-positive cells were mainly detected near the intestinal crypts. Each data point represents the MPO-positive cell count of one lamb. Data are displayed as median with interquartile range. Scale bars indicate 100 μ m. ** $p < 0.01$; # $0.05 < p \leq 0.10$. Abbreviations: MPO, myeloperoxidase.

No statistically significant group differences were found with regard to total MUC2-positive cell counts (**Supplementary Figure S6.2**). Interestingly, the presence of AB/PAS-positive cells largely paralleled that of MUC2-positive cells in the villi tips; the number of MUC2-expressing cells tended to be increased in the villi tips of the distal ileum ($p=0.09$) at 8 d after IA LPS exposure compared to 24 h after IA LPS exposure (**Figure 6.4A,B,D**). At 15 d after IA LPS exposure, the number of MUC2-positive cells tended to be reduced ($p=0.10$) compared to 8 d after IA LPS exposure (**Figure 6.4C,D**). No differences were observed in MUC2-positive cell counts in ileal crypts, lower villi, and middle villi (data not shown).

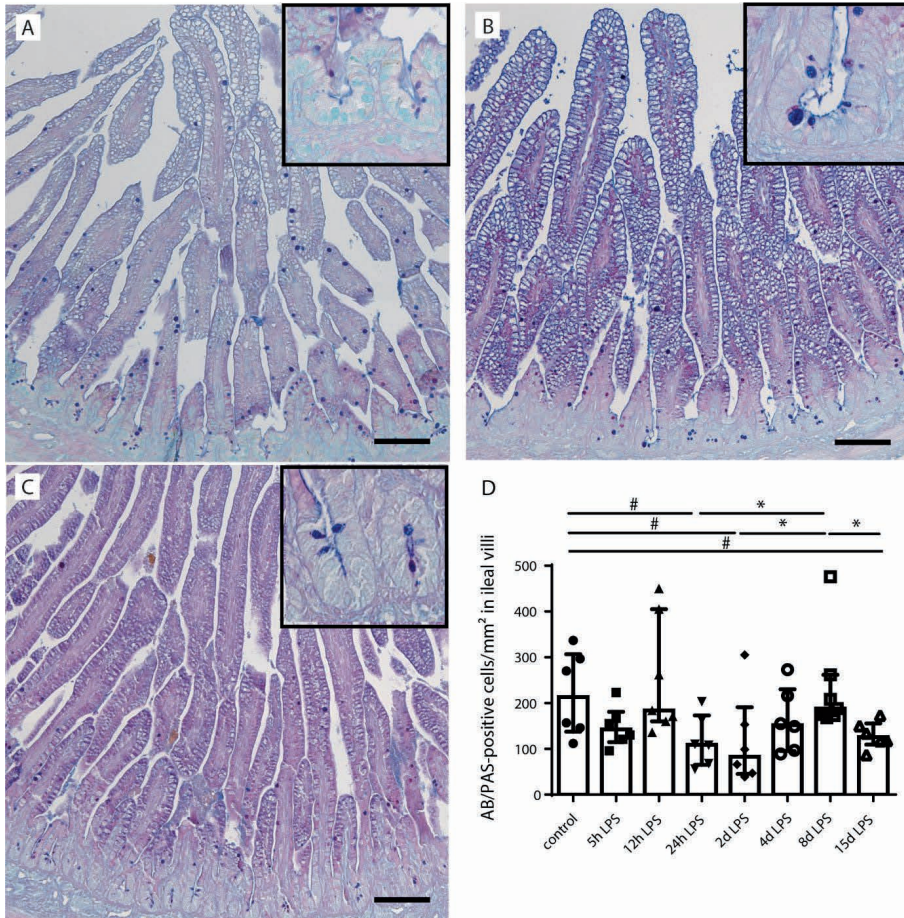


Figure 6.3 The number of Alcian blue (AB)/periodic acid–Schiff (PAS)-positive cells per mm² surface area in distal ileum of premature lambs. The number of AB/PAS-positive cells in control lambs (A). This number tended to be decreased at 24 h (B, D) and 2 d (D) after IA LPS exposure. The number of AB/PAS-positive cells was normalized at 8 d after IA LPS exposure (D). However, a second reduction in the number of AB/PAS-positive cells was observed 15 d after LPS exposure (C, D). Each data point represents the AB/PAS-positive cell count of one lamb. Data are displayed as median with interquartile range. Scale bars indicate 100 μ m. * $p < 0.05$, # $0.05 < p < 0.10$. Abbreviations: AB/PAS; Alcian blue/periodic acid–Schiff.

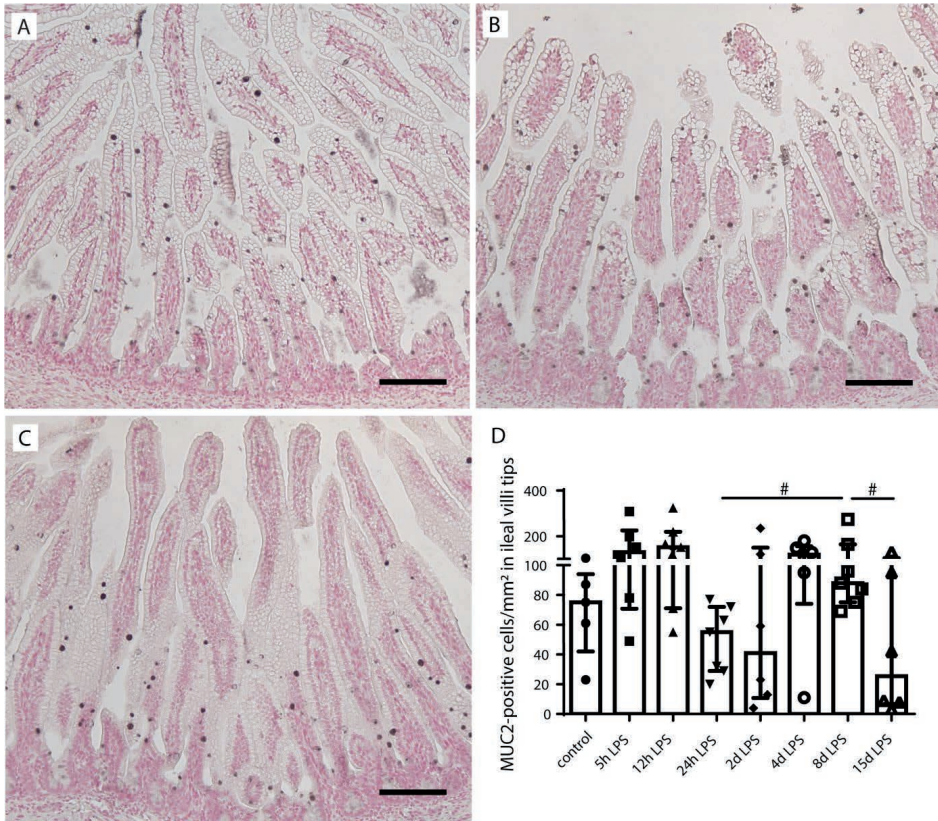


Figure 6.4 Mucin-2 (MUC2)-positive cell count in ileal villi tips of premature lambs. MUC2-positive cells in the distal ileum of control lambs (A, D). MUC2-positive cells tended to be increased in the 8 d after LPS group (B) compared to the 24 h after LPS exposure group (D). This increase in the 8-d LPS group tended to be reduced at 15 d after LPS exposure (C, D). MUC2-positive goblet cells were counted in the villi tips, and the count was corrected for ileal villi tip surface (cells/mm²) for all treatment groups. Each data point represents the MUC2-positive cell count of one lamb. Data are displayed as median with interquartile range. Scale bars indicate 100 μ m. # 0.05 < p \leq 0.10. Abbreviations: MUC2; mucin-2.

Intestinal epithelial cell death

As apoptosis is associated with intestinal inflammation³⁸ and may explain the loss of goblet cells following chorioamnionitis, intestinal epithelial apoptosis (cleaved-caspase 3 (CC3)) was studied (Figure 6.5). The number of CC3-positive cells was elevated from 2 d after IA LPS exposure onwards and normalized at 15 d after IA LPS exposure, with the highest count at 4 d after IA LPS exposure compared to controls ($p < 0.05$) (Figure 6.5A–D). Apoptosis was mainly detected in the lower villi region (Figure 6.5B). Increased cell death did not cause villus atrophy (Supplementary Figure S6.3), which indicates loss of goblet cells relative to enterocytes following IA infection.

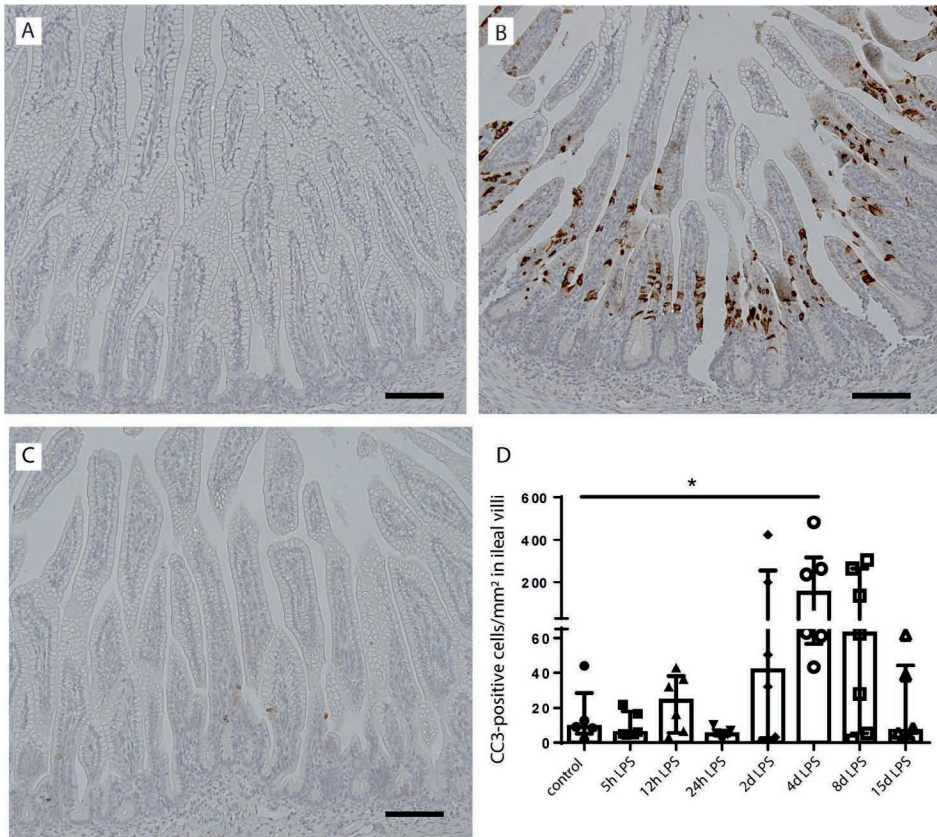


Figure 6.5 Presence of intestinal epithelial cell death in the distal ileum of premature lambs. In the control group, low counts of cleaved caspase 3 (CC3)-positive cells were found (A, D). The number of CC3-positive cells was statistically significantly increased at 4 d after IA LPS exposure compared to controls (B, D). At the other timepoints, including 15 d after IA LPS (C), no statistically significant increase in apoptosis was observed (D). The number of CC3-positive cells was corrected for ileal surface (cells/mm²) for all treatment groups. Each data point represents the CC3-positive cell count of one lamb. Data are displayed as median with interquartile range. Scale bars indicate 100 μ m. * $p < 0.05$. Abbreviations: CC3; cleaved-caspase 3.

Goblet cell differentiation

In addition to apoptosis, goblet cell differentiation was studied as a potential mechanism that underlies the reduced number of goblet cells. SAM-pointed domain-containing ETS transcription factor (SPDEF)-positive cells, counterstained with AB/PAS were counted in all groups (Figure 6.6). The number of SPDEF-positive cells was increased at 4 d after IA LPS exposure ($P = 0.09$) and this increase reached statistical significance at 8 d after IA LPS exposure compared to controls ($p \leq 0.05$) (Figure 6.6B,D). At 15 d after IA LPS exposure, the SPDEF-positive cell count still tended to be increased ($p = 0.06$) (Figure 6.6C, D). For all time points, most SPDEF-positive cells were observed in the lower villi region.

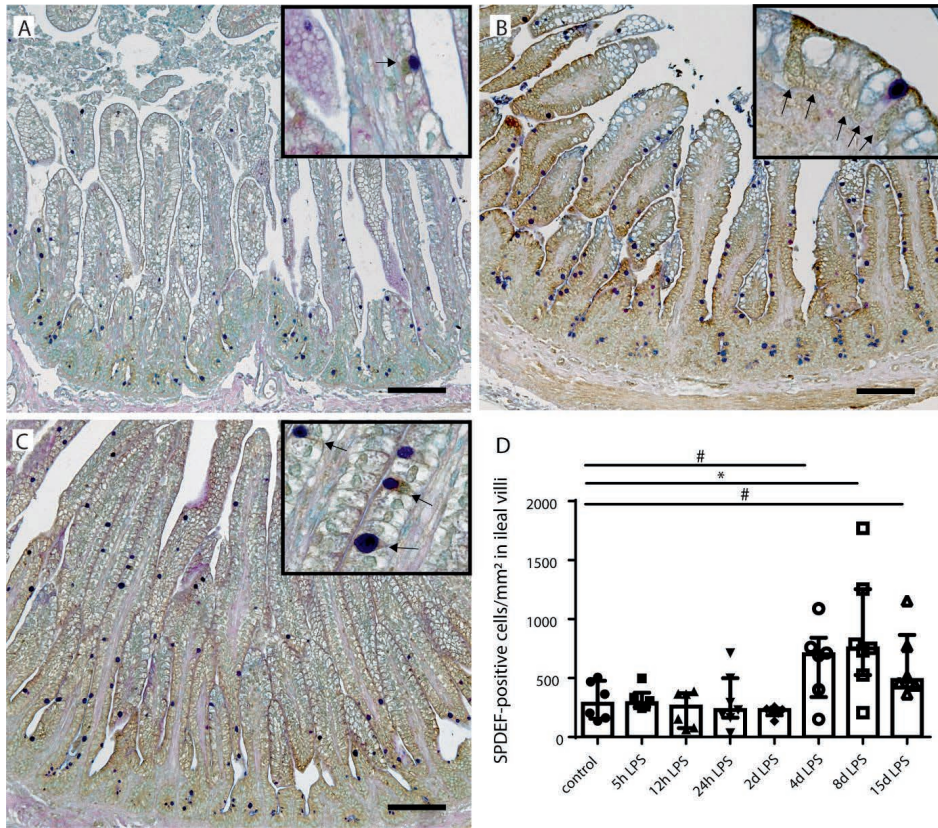


Figure 6.6 Number of SAM-pointed domain-containing ETS transcription factor (SPDEF)-positive goblet cells per mm² surface area. In control fetuses, some SPDEF positive goblet cells were detected (A, D). The number of SDPEF-positive goblet cells (indicated by black arrows in inserts) was statistically significantly increased at 8 d after (B, D), and still tended to be increased at 15 d after (C, D) IA LPS exposure compared to the controls. Each data point represents the SPDEF-positive cell count of one lamb. Data are displayed as median with interquartile range. Scale bars indicate 100 μ m. * $p < 0.05$; # $0.05 < p < 0.10$. Abbreviations: SPDEF; SAM-pointed domain. 2.5. ER-Stress in Distal Ileum of Premature Lambs.

ER-Stress in Distal Ileum of Premature Lambs

To study the underlying mechanism behind alterations in goblet cell numbers, differentiation, and distribution, the BiP expression pattern and CHOP-positive cell counts in the ileal crypt-villi axis were studied (Figure 6.7). BiP is an ER chaperone protein that under physiological conditions prevents inositol-requiring protein 1 α (IRE1 α) signaling²⁴. However, under ER stress, a condition which secretory cells including goblet cells are especially vulnerable to, BiP accumulates and dissociates from IRE1 α , thereby initiating the unfolded protein response²⁴. In control fetuses, BiP immunoreactivity is mainly present in the lower villi region of the crypt-villus axis (Figure 6.7A,D). The BiP expression pattern changed at 4 d after IA LPS exposure, where BiP immunoreactivity was detected in the ileal crypts (Figure

6.7B,D). Interestingly, BiP expression pattern was also changed in the 15 d after LPS group. In contrast to the crypt expression at 4 d after IA LPS exposure, the 15-d pattern was characterized by increased BiP immunoreactivity in the villi tips (**Figure 6.7C,D**).

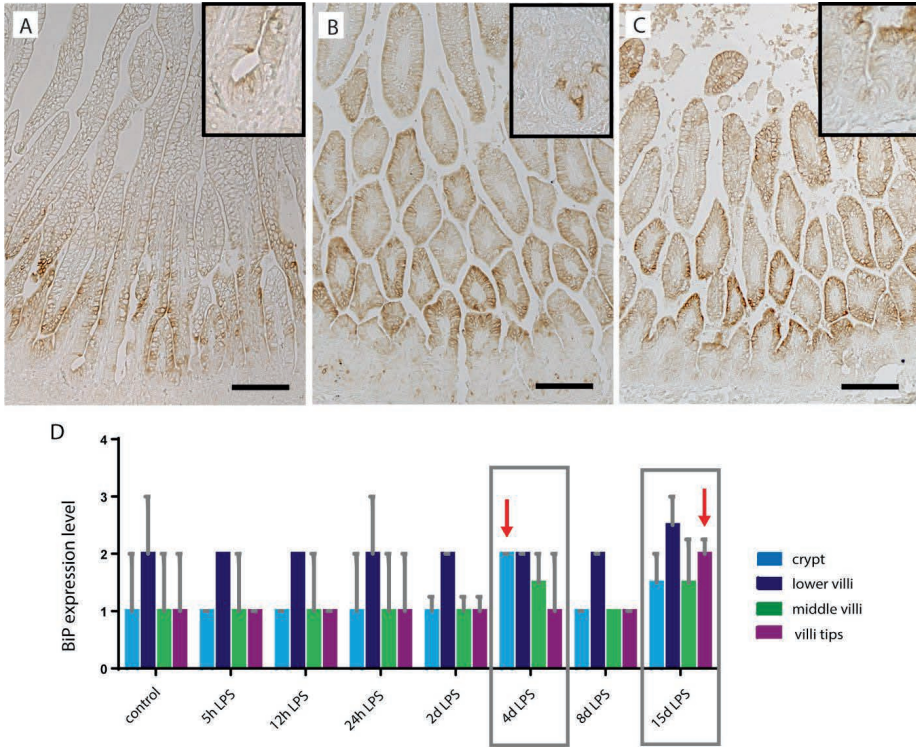


Figure 6.7 Binding immunoglobulin protein (BiP) expression pattern along crypt-villus axis in distal ileum of premature lambs. BiP was mainly expressed in the lower villi region, localized above the crypts, in the control fetuses (A, D). This expression pattern was changed in the 4 d after LPS group when BiP immunoreactivity was increased in the ileal crypts (indicated by arrow) (B, D), and at 15 d after IA LPS exposure, when BiP immunoreactivity was increased in the ileal villi tips (indicated by arrow) (C, D). BiP expression pattern was scored as follows: 0 = no BiP expression; 1 = mild BiP expression; 2 = moderate BiP expression; and 3 = intense BiP expression for all treatment groups. Data are displayed as median with interquartile range. Scale bars indicate 100 μ m. Abbreviations: BiP; binding immunoglobulin protein.

CHOP is associated with ER stress-induced apoptosis, which indicates progression of ER stress²⁵. The number of CHOP-positive cells was increased in the whole crypt-villus axis following IA LPS, but predominantly highest in the intestinal crypt (Figure 6.8A–E).

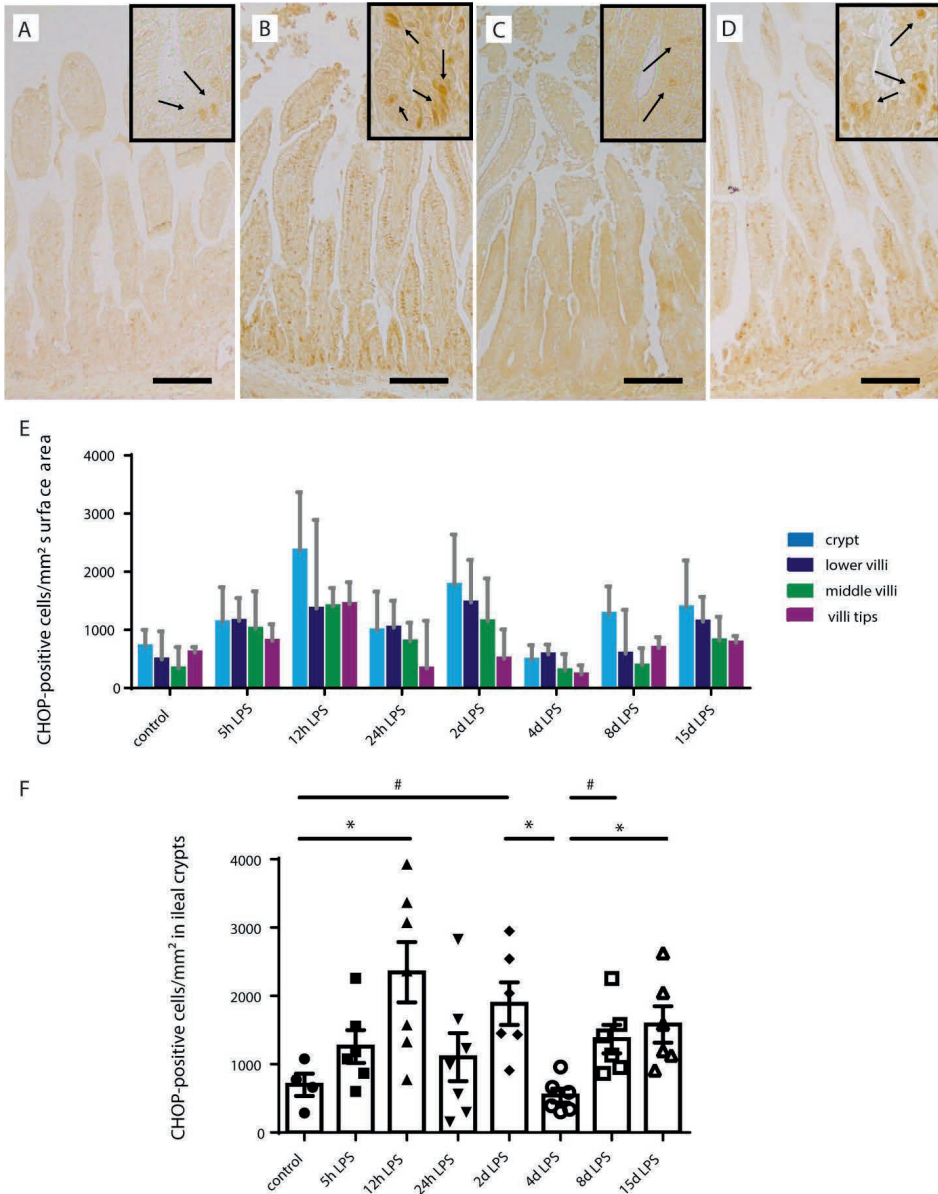


Figure 6.8 Number of transcription factor C/enhancer binding protein homologous protein (CHOP)-positive intestinal epithelial cells per mm² surface area. In all groups, the number of CHOP-positive intestinal epithelial cells (indicated by black arrows in inserts) per mm² surface area

was highest in the intestinal crypts (A–E). From 5 h onwards, the number of CHOP-positive cells was elevated, with the highest counts at 12 h ($p<0.05$) (B, F) and 2 d ($p=0.08$) (F) after IA LPS exposure compared to controls. At 4 d after IA LPS exposure, the CHOP-positive intestinal epithelial cell counts normalized (C, F). A second increase in CHOP-positive intestinal epithelial cell count was observed at 8 ($p=0.08$) (F) and 15 d ($p<0.05$) after IA LPS exposure (D, F). Each data point represents the CHOP-positive cell count of one lamb. Data are displayed as median with interquartile range. Scale bars indicate 100 μm . * $p\leq 0.05$; # $0.05<p\leq 0.10$. Abbreviations: CHOP; transcription factor C/enhancer binding protein homologous protein.

Increased CHOP-positive cell counts in the intestinal crypt were present from 5 h after IA LPS exposure onwards, with the highest CHOP-positive cell numbers at 12 h ($p<0.05$) (**Figure 6.8B,D**) and 2 d ($p=0.08$) (**Figure 6.8F**) after IA LPS exposure compared to controls. At 4 d after IA LPS exposure, CHOP-positive cell counts in the intestinal crypt were normalized (**Figure 6.8C,F**). Interestingly, a second increase of CHOP-positive cell numbers was observed at 8 ($p=0.08$) (**Figure 6.8F**) and 15 d ($p<0.05$) after IA LPS exposure (**Figure 6.8D,F**).

Discussion

In the current study, we investigated the effects of LPS-induced chorioamnionitis on the number, distribution, and differentiation of goblet cells. In addition, we studied whether intestinal inflammation, intestinal epithelial ER stress and apoptosis are mechanistically involved.

LPS-induced chorioamnionitis was observed to cause a biphasic decrease in goblet cell counts. The first reduction coincided with early systemic inflammation 24 h after IA LPS exposure (IL6)² and intestinal inflammation at 24 h (IL8)³⁹ and 2 d (macrophages)⁴⁰ after IA LPS exposure that we observed in earlier published studies of the same experiment. It is therefore probably caused by emptying of goblet cell secretory vesicles as a natural response to acute inflammation²⁹. Secretion of mucins by the goblet cells will result in decreased volume of the goblet cell theca and therefore can reduce goblet cell counts on analysis of the AB/PAS staining. While it could alternatively be due to goblet cell loss, the unaltered SPDEF immunoreactivity and the lack of apoptosis within this period do not support this scenario. Of note, the number of SPDEF-positive cells was higher than the number of AB/PAS-positive cells in all experimental groups. Several factors could explain this apparent discrepancy. First, mucus secretion lowers the amount of AB/PAS-positive cells counted. Second, developing goblet cells, which already express SPDEF³⁴, have no theca or small theca sizes and, thus, are likely to be AB/PAS-negative. This latter notion is supported by the high SPDEF-positive cell counts in the lower villi region and could be related to normal intestinal development of the fetus. Future studies are needed to discern why a relatively large amount of cells in the lower villi region express SPDEF in utero.

Interestingly, the initial reduction in goblet cell numbers was restored at 8 d after IA LPS exposure, indicating that the effects of acute inflammation on goblet cell numbers were compensated. This compensation could be explained by the increase in goblet cell differentiation (increased SPDEF immunoreactivity) at 4 and 8 d after IA LPS exposure that is most likely triggered by inflammation. Accordingly, intraperitoneal administration of the pro-inflammatory cytokine TNF α caused an increase in mRNA level of the goblet cell

differentiation marker SPDEF in neonatal mice¹⁷. In addition, the pro-inflammatory cytokine IL-1 β induced SPDEF mRNA levels in human bronchial epithelial cells⁴¹. Moreover, the IL-1 β -induced increase in MUC5 protein expression and secretion, the main mucin of lung goblet cells, was strongly reduced in SPDEF-deficient mice⁴¹, which suggests that SPDEF has an important role in upregulating mucus production and secretion in mucosal tissue upon inflammation.

Importantly, at 15 d after IA LPS exposure, the reduction of AB/PAS-positive cell counts in combination with reduced numbers of MUC2 positive cells at the villus tips indicates that a loss of mature goblet cells was involved in the second wave of reduced goblet cell counts. Moreover, the absence of villus atrophy strongly suggests this loss was goblet cell-specific (e.g., greater loss of goblet cells than enterocytes). Three scenarios might be responsible for the observed loss of mature goblet cells: First, chorioamnionitis-driven intestinal inflammation might induce cell death of mature goblet cells. However, since in the villus tips neither apoptosis nor epithelial damage was present, this scenario is not likely. Second, disturbed goblet cell differentiation by altered programming of maturing goblet cells may be involved. Yet, this concept is not supported by the finding that the number of SPDEF-positive cells was not decreased 15 d after IA LPS exposure. Finally, cell death of maturing cells that prevents the formation of mature goblet cells could be responsible. This latter concept is supported by our findings of increased apoptosis in the lower villus region, since apoptosis is often present in the crypt and in the villi tips, but it rarely occurs in the lower villi⁴². Collectively, our combined findings indicate that prolonged antenatal LPS exposure triggers a loss of mature goblet cells through cell death of maturing goblet cells, potentially predisposing to postnatal pathologies.

The increase in intestinal inflammation and intestinal epithelial ER stress in the crypts provide insight into the potential mechanisms behind the apoptosis in the lower villus region. Mild ER stress is important for the development of secretory cells⁴³. Consequently, BiP expression is naturally present in the lower villus region⁴⁴, which is important for terminal differentiation of goblet cells¹⁹. However, from 5 h until 4 d after IA LPS exposure, ER stress emerged in the intestinal crypts. The identified ER stress in the crypts was considered to be injurious, as a study by Afrazi et al. reports ER stress in LGR5-positive stem cells to be associated with apoptosis within the intestinal crypt and an increased NEC severity²². Besides stem cells, Paneth cells, which are vital for stem cell maintenance, may be subject to crypt ER stress⁴⁵. Thus, ER stress in crypt intestinal epithelial cells can either directly or through stem cell dysfunction affect maturing goblet cells and result in apoptosis in the lower villus region following migration from the crypts. We consider inflammation to be the driving force behind ER stress and subsequent intestinal epithelial apoptosis, leading to reduced numbers of mature goblet cells. Intestinal inflammation and ER stress are bidirectionally linked. Intestinal inflammation can induce ER stress²⁵, and intestinal epithelial ER stress can aggravate intestinal inflammation, indirectly through disturbance of the mucus layer and Paneth cell secretion²⁵ and directly by UPR-initiated inflammatory signals^{25,46}. Thus, in the current study, we proposed—as an underlying mechanism of the observed loss of mature goblet cells—a vicious circle of inflammation and ER stress that leads to apoptosis of maturing goblet cells.

Importantly, similar changes have been described in patients suffering from NEC^{16-18,22}, which suggests that a loss of goblet cells in utero may predispose to NEC development. Reduced goblet cell numbers are associated with a disturbed mucus layer⁴⁷ and, thus, a reduced intestinal barrier function, which makes a neonate upon birth more vulnerable during the crucial period of microbial colonization. In addition, the increase of CHOP-positive cells in the crypt at 8–15 d after IA LPS exposure implies that the intestine is prone to a second wave of apoptosis, either following ongoing (intrauterine) inflammation or after additional postnatal inflammatory hits such as mechanical ventilation⁴⁸ or sepsis⁴⁹. This concept is supported by recent findings in a murine chorioamnionitis model in which chorioamnionitis not only induced goblet cell loss in utero, but also predisposed to further reduced goblet cell numbers following a postnatal inflammatory hit⁷.

Of note, several nutritional interventions, such as epidermal growth factor (EGF), heparin-binding EGF-like growth factor, insulin-like growth factor 1, human milk oligosaccharides (HMO), and bovine and human breast milk exosomes, have been shown to influence goblet cells and mucus barrier function in animal NEC models⁵⁰⁻⁵⁵. ER stress may be a crucial mechanism involved. Enteral administration of bovine milk exosomes reduced intestinal injury and inflammation, and prevented a loss of goblet cells in a murine NEC model⁵³. Importantly, treatment with these bovine milk exosomes also increased the number of cells positive for GRP94⁵³, an ER chaperone protein that is important for goblet cell maintenance⁵⁶. Likewise, supplementation of formula with human milk oligosaccharides (HMO) reduced murine NEC injury and prevented a loss of goblet cells, concomitant with an increased protein expression of the ER chaperone proteins BiP and protein disulfide isomerase (PDI)⁵⁵. Moreover, administration of the PDI inhibitor rutin abolished the HMO effects on intestinal injury and goblet cell numbers, which shows that ER stress plays a crucial role in the pharmacological effect of HMO in NEC⁵⁵. We have previously shown that a nutritional intervention with plant sterols can already positively affect the gut outcome in chorioamnionitis in utero⁸. Targeting in utero alterations of the mucus barrier with nutritional interventions is therefore a promising topic for future research.

An important strength of the current study is the longitudinal study set-up, which allowed us to gain mechanistic insight regarding the goblet cell alterations observed. A limitation is the low number of animals per treatment group, which is inherent to the large animal model used. In addition, our study set-up did not rule out an effect of gestational age at the start of IA LPS exposure.

In summary, we reported a biphasic reduction in goblet cell counts after IA LPS exposure. Whereas the first reduction wave could be explained by mucin secretion, the second resulted from loss of mature goblet cells that was strongly linked with intestinal inflammation, ER stress, and concomitant apoptosis. Our combined findings indicate that ER stress-driven apoptosis of maturing goblet cells gives rise to reduced goblet cell numbers in chorioamnionitis. As in utero goblet cell loss has been experimentally shown to persist postnatally and predisposes to further disruption of goblet cells following additional inflammatory hits⁷, chorioamnionitis-driven goblet cell loss may play a role in NEC pathophysiology and potentially in other adverse gut outcomes. In this context, ER stress is an interesting target for future therapeutics.

References

1. Kim CJ, Romero R, Chaemsaitong, P, Chaiyasit N, Yoon BH, Kim YM. Acute chorioamnionitis and funisitis: Definition, pathologic features, and clinical significance. *Am J Obstet Gynecol* 2015;213: S29–S52.
2. Gussenhoven R, Westerlaken RJJ, Ophelders D, Jobe AH, Kemp MW, Kallapur SG, Zimmermann LJ, Sangild PT, Pankratova S, Gressens P, et al. Chorioamnionitis, neuroinflammation, and injury: Timing is key in the preterm ovine fetus. *J Neuroinflammation* 2018;15:113.
3. Gotsch F, Romero R, Kusanovic JP, Mazaki-Tovi S, Pineles BL, Erez O, Espinoza J, Hassan SS. The fetal inflammatory response syndrome. *Clin Obstet Gynecol* 2007;50:652–83.
4. Nguyen DN, Thymann T, Goericke-Pesch SK, Ren S, Wei W, Skovgaard K, Damborg P, Brunse A, van Gorp C, Kramer BW, et al. Prenatal Intra-Amniotic Endotoxin Induces Fetal Gut and Lung Immune Responses and Postnatal Systemic Inflammation in Preterm Pigs. *Am J Pathol* 2018;188:2629–43.
5. Nikiforou M, Vanderlocht J, Chougnat CA, Jellema RK, Ophelders DR, Joosten M, Kloosterboer N, Senden-Gijsbers BL, Germeraad WT, Kramer BW, et al. Prophylactic Interleukin-2 Treatment Prevents Fetal Gut Inflammation and Injury in an Ovine Model of Chorioamnionitis. *Inflamm Bowel Dis* 2015;21:2026–38.
6. Wolfs TG, Buurman WA, Zoer B, Moonen RM, Derikx JP, Thuijls G, Villamor E, Gantert M, Garnier Y, Zimmermann LJ, et al. Endotoxin induced chorioamnionitis prevents intestinal development during gestation in fetal sheep. *PLoS One* 2009;4:e5837.
7. Elgin TG, Fricke EM, Gong H, Reese J, Mills DA, Kalantera KM, Underwood MA, McElroy SJ. Fetal exposure to maternal inflammation interrupts murine intestinal development and increases susceptibility to neonatal intestinal injury. *Dis Models Mech* 2019;12:dmm040808.
8. van Gorp C, de Lange IH, Spiller OB, Dewez F, Cillero Pastor B, Heeren RMA, Kessels L, Kloosterboer N, van Gemert WG, Beeton ML, et al. Protection of the Ovine Fetal Gut against *Ureaplasma*-Induced Chorioamnionitis: A Potential Role for Plant Sterols. *Nutrients* 2019;11:968.
9. Heymans C, de Lange IH, Hütten MC, Lenaerts K, de Ruijter NJE, Kessels L, Rademakers G, Melotte V, Boesmans W, Saito M, et al. Chronic Intra-Uterine *Ureaplasma parvum* Infection Induces Injury of the Enteric Nervous System in Ovine Fetuses. *Front Immunol* 2020;11:189.
10. Been JV, Lievens S, Zimmermann LJ, Kramer BW, Wolfs TG. Chorioamnionitis as a risk factor for necrotizing enterocolitis: A systematic review and meta-analysis. *J Pediatr* 2013;162:236–42 e2.
11. Gantert M, Been JV, Gavilanes AW, Garnier Y, Zimmermann LJ, Kramer BW. Chorioamnionitis: A multiorgan disease of the fetus? *J Perinatol* 2010;30:S21–S30.
12. Neu J, Walker WA. Necrotizing enterocolitis. *N Engl J Med* 2011;364:255–64.
13. Hall NJ, Eaton S, Pierro A. Royal Australasia of Surgeons Guest Lecture. Necrotizing enterocolitis: Prevention, treatment, and outcome. *J Pediatr Surg* 2013;48:2359–67.
14. Johansson ME, Sjoval H, Hansson GC. The gastrointestinal mucus system in health and disease. *Nat Rev Gastroenterol Hepatol* 2013;10:352–61.
15. Pelaseyed T, Bergstrom JH, Gustafsson JK, Ermund A, Birchenough GM, Schutte A, van der Post S, Svensson F, Rodriguez-Pineiro AM, Nystrom EE, et al. The mucus and mucins of the goblet cells and enterocytes provide the first defense line of the gastrointestinal tract and interact with the immune system. *Immunol Rev* 2014;260:8–20.
16. Schaart MW, de Bruijn AC, Bouwman DM, de Krijger RR, van Goudoever JB, Tibboel D, Renes IB. Epithelial functions of the residual bowel after surgery for necrotizing enterocolitis in human infants. *J Pediatr Gastroenterol Nutr* 2009;49:31–41.
17. McElroy SJ, Prince LS, Weitkamp JH, Reese J, Slaughter JC, Polk DB. Tumor necrosis factor receptor 1-dependent depletion of mucus in immature small intestine: A potential role in neonatal necrotizing enterocolitis. *Am J Physiol Gastrointest Liver Physiol* 2011;301:G656–66.
18. Halpern MD, Denning PW. The role of intestinal epithelial barrier function in the development of NEC. *Tissue barriers* 2015;3:e1000707.
19. van der Flier LG, Clevers H. Stem cells, self-renewal, and differentiation in the intestinal epithelium. *Annu Rev Physiol* 2009;71:241–60.

20. Sato T, Clevers H. Growing self-organizing mini-guts from a single intestinal stem cell: Mechanism and applications. *Science* 2013;340:1190–4.
21. Lu P, Struijs MC, Mei J, Witte-Bouma J, Korteland-van Male AM, de Bruijn ACJM, van Goudoever JB, Renes IB. Endoplasmic reticulum stress, unfolded protein response and altered T cell differentiation in necrotizing enterocolitis. *PLoS One* 2013;8:e78491.
22. Afrazi A, Branca MF, Sodhi CP, Good M, Yamaguchi Y, Egan CE, Lu P, Jia H, Shaffiey S, Lin J, et al. Toll-like receptor 4-mediated endoplasmic reticulum stress in intestinal crypts induces necrotizing enterocolitis. *J Biol Chem* 2014;289:9584–99.
23. Ron D, Walter P. Signal integration in the endoplasmic reticulum unfolded protein response. *Nat Rev Mol Cell Biol* 2007;8:519–29.
24. Hetz C. The unfolded protein response: Controlling cell fate decisions under ER stress and beyond. *Nat Rev Mol Cell Biol* 2012;13:89–102.
25. McGuckin MA, Eri RD, Das I, Lourie R, Florin TH. ER stress and the unfolded protein response in intestinal inflammation. *Am J Physiol Gastrointest Liver Physiol* 2010;298:G820–32.
26. Li B, Zani A, Lee C, Zani-Ruttenstock E, Zhang Z, Li X, Ip W, Gonska T, Pierro A. Endoplasmic reticulum stress is involved in the colonic epithelium damage induced by maternal separation. *J Pediatr Surg* 2016;51:1001–4.
27. Cornick S, Tawiah A, Chadee K. Roles and regulation of the mucus barrier in the gut. *Tissue barriers* 2015;3:e982426.
28. Birchenough GM, Johansson ME, Gustafsson JK, Bergstrom JH, Hansson GC. New developments in goblet cell mucus secretion and function. *Mucosal Immunol* 2015;8:712–9.
29. Kim YS, Ho SB. Intestinal goblet cells and mucins in health and disease: Recent insights and progress. *Cur Gastroenterol Rep* 2010;12:319–30.
30. Kuypers E, Wolfs TG, Collins JJ, Jellema RK, Newnham JP, Kemp MW, Kallapur SG, Jobe AH, Kramer BW. Intraamniotic lipopolysaccharide exposure changes cell populations and structure of the ovine fetal thymus. *Reprod Sci* 2013;20:946–56.
31. Newnham JP, Kallapur SG, Kramer BW, Moss TJ, Nitsos I, Ikegami M, Jobe AH. Betamethasone effects on chorioamnionitis induced by intra-amniotic endotoxin in sheep. *Am J Obstet Gynecol* 2003;189:1458–66.
32. Yamabayashi S. Periodic acid-Schiff-alcian blue: A method for the differential staining of glycoproteins. *Histochem J* 1987;19:565–71.
33. Hurd EA, Holmén JM, Hansson GC, Domino SE. Gastrointestinal mucins of Fut2-null mice lack terminal fucosylation without affecting colonization by *Candida albicans*. *Glycobiology* 2005;15: 1002–7.
34. Gregorieff A, Stange DE, Kujala P, Begthel H, van den Born M, Korving J, Peters PJ, Clevers H. The ets-domain transcription factor Spdef promotes maturation of goblet and paneth cells in the intestinal epithelium. *Gastroenterology* 2009;137:1333–45.
35. Chen G, Korfhagen TR, Xu Y, Kitzmiller J, Wert SE, Maeda Y, Gregorieff A, Clevers H, Whitsett JA. SPDEF is required for mouse pulmonary goblet cell differentiation and regulates a network of genes associated with mucus production. *J Clin Invest* 2009;119:2914–24.
36. Noah TK, Kazanjian A, Whitsett J, Shroyer NF. SAM pointed domain ETS factor (SPDEF) regulates terminal differentiation and maturation of intestinal goblet cells. *Exp Cell Res* 2010;316:452–65.
37. Willems MG, Ophelders DR, Nikiforou M, Jellema RK, Butz A, Delhaas T, Kramer BW, Wolfs TG. Systemic interleukin-2 administration improves lung function and modulates chorioamnionitis-induced pulmonary inflammation in the ovine fetus. *Am J Physiol Lung Cell Mol Physiol* 2016;310: L1–L7.
38. Günther C, Neumann H, Neurath MF, Becker C. Apoptosis, necrosis and necroptosis: Cell death regulation in the intestinal epithelium. *Gut* 2013;62:1062–71.
39. Heymans C, de Lange IH, Lenaerts K, Kessels L, Rademakers G, Melotte V, Boesmans W, Kramer BW, Jobe AH, et al. Chorioamnionitis induces enteric nervous system injury: Effects of timing and inflammation in the ovine fetus. *Mol Med* 2020;26:82.
40. Heymans C, den Dulk M, Lenaerts K, Heij LR, de Lange IH, Hadfoune M, van Heugten C, Kramer BW, Jobe AH, Saito M, et al. Chorioamnionitis induces hepatic inflammation and time-dependent changes of the enterohepatic circulation in ovine fetuses. *Sci Rep* 2021;11:10331.

41. Chen G, Sun L, Kato T, Okuda K, Martino MB, Abzhanova A, Lin JM, Gilmore RC, Batson BD, O'Neal YK, et al. IL-1 β dominates the promucin secretory cytokine profile in cystic fibrosis. *J Clin Invest* 2019;129:4433–50.
42. Negroni A, Cucchiara S, Stronati L. Apoptosis, Necrosis, and Necroptosis in the Gut and Intestinal Homeostasis. *Mediators Inflamm* 2015;2015:250762.
43. Asada R, Saito A, Kawasaki N, Kanemoto S, Iwamoto H, Oki M, Miyagi H, Izumi S, Imaizumi K. The endoplasmic reticulum stress transducer OASIS is involved in the terminal differentiation of goblet cells in the large intestine. *J Biol Chem* 2012;287:8144–53.
44. Heijmans J, van Lidth de Jeude JF, Koo BK, Rosekrans SL, Wielenga MCB, van de Wetering M, Ferrante M, Lee AS, Onderwater JJM, Paton JC, et al. ER Stress Causes Rapid Loss of Intestinal Epithelial Stemness through Activation of the Unfolded Protein Response. *Cell Rep* 2013;3:1128–39.
45. Clevers HC, Bevins CL. Paneth cells: Maestros of the small intestinal crypts. *Annu Rev Physiol* 2013; 75:289–311.
46. Zhang K, Kaufman RJ. From endoplasmic-reticulum stress to the inflammatory response. *Nature* 2008;454:455–62.
47. Grondin JA, Kwon YH, Far PM, Haq S, Khan WI. Mucins in Intestinal Mucosal Defense and Inflammation: Learning From Clinical and Experimental Studies. *Front. Immunol.* 2020;11:2054.
48. Bose CL, Laughon MM, Allred EN, O'Shea TM, Van Marter LJ, Ehrenkranz RA, Fichorova RN, Leviton A. Systemic inflammation associated with mechanical ventilation among extremely preterm infants. *Cytokine* 2013;61:315–22.
49. Machado JR, Soave DF, da Silva MV, de Menezes LB, Etchebehere RM, Monteiro ML, dos Reis MA, Correa RR, Celes MR. Neonatal sepsis and inflammatory mediators. *Mediators Inflamm* 2014;2014: 269681.
50. Dvorak B, Khailova L, Clark JA, Hosseini DM, Arganbright KM, Reynolds CA, Halpern MD. Comparison of epidermal growth factor and heparin-binding epidermal growth factor-like growth factor for prevention of experimental necrotizing enterocolitis. *J Pediatr Gastroenterol Nutr* 2008; 47:11–8.
51. Clark JA, Doelle SM, Halpern MD, Saunders TA, Holubec H, Dvorak K, Boitano SA, Dvorak B. Intestinal barrier failure during experimental necrotizing enterocolitis: Protective effect of EGF treatment. *Am J Physiol Gastrointest Liver Physiol* 2006;291:G938–49.
52. Tian F, Liu GR, Li N, Yuan G. Insulin-like growth factor I reduces the occurrence of necrotizing enterocolitis by reducing inflammatory response and protecting intestinal mucosal barrier in neonatal rats model. *Eur Rev Med Pharmacol Sci* 2017;21:4711–9.
53. Li B, Hock A, Wu RY, Minich A, Botts SR, Lee C, Antounians L, Miyake H, Koike Y, Chen Y, et al. Bovine milk-derived exosomes enhance goblet cell activity and prevent the development of experimental necrotizing enterocolitis. *PLoS One* 2019;14:e0211431.
54. Miyake H, Lee C, Chusilp S, Bhalla M, Li B, Pitino M, Seo S, O'Connor DL, Pierro A. Human breast milk exosomes attenuate intestinal damage. *Pediatr Surg Int* 2020;36:155–63.
55. Wu RY, Li B, Koike Y, Maattanen P, Miyake H, Cadete M, Johnson-Henry KC, Botts SR, Lee C, Abrahamsson TR, et al. Human Milk Oligosaccharides Increase Mucin Expression in Experimental Necrotizing Enterocolitis. *Mol Nutr Food Res* 2019;63:e1800658.
56. Liu B, Staron M, Hong F, Wu BX, Sun S, Morales C, Crosson CE, Tomlinson S, Kim I, Wu D, et al. Essential roles of grp94 in gut homeostasis via chaperoning canonical Wnt pathway. *Proc. Natl Acad Sci U S A* 2013;110:6877–82.

Supplementary materials

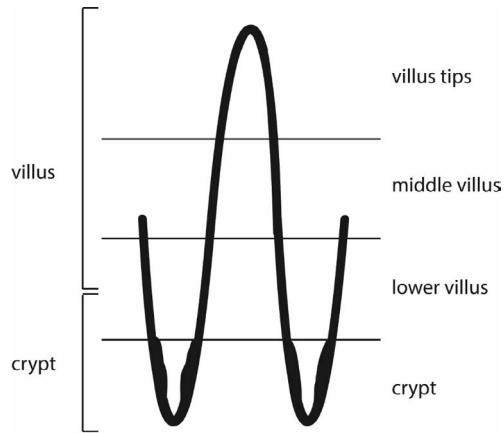


Figure S6.1 Division of crypt-villus axis in crypt, lower villus, middle villus and villus tips.

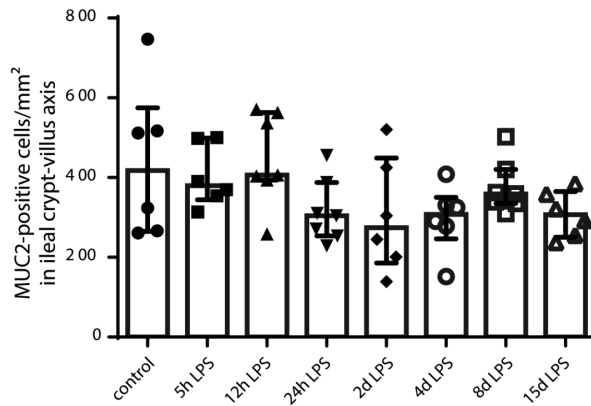


Figure S6.2 Total MUC2-positive cell counts in intestinal crypt-villus axis. No statistically significant changes were observed between the different treatment groups. Each data point represents the MUC2-positive cell count of one lamb. Data are displayed as median with interquartile range.

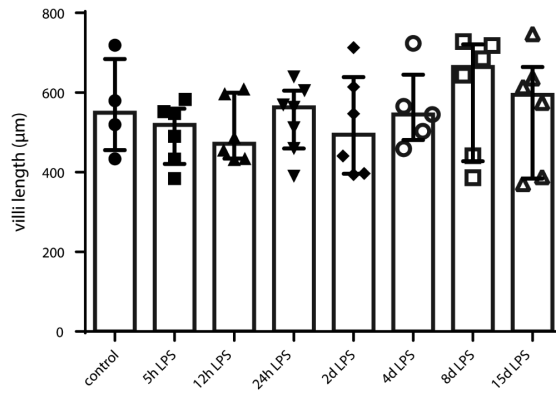


Figure S6.3 Villus length measurements of all experimental groups. No statistically significant changes were observed between the different treatment groups. Each data point represents the villus length of one lamb. Data are displayed as median with interquartile range.

Chapter 7

**Antenatal *Ureaplasma parvum* infection induces
ovine small intestinal goblet cell abnormalities:
a strong link with NEC pathology**

C. van Gorp, I.H. de Lange, M.C. Hütten, C. López-Iglesias, K.R.I. Massy, L. Kessels,
B.W. Kramer, W.J. van de Wetering, O.B. Spiller, G.M.H. Birchenough, W.G. van Gemert,
L.J.I. Zimmermann, and T.G.A.M. Wolfs

Abstract

Disruption of the intestinal mucus barrier and intestinal epithelial endoplasmic reticulum (ER) stress contribute to necrotizing enterocolitis (NEC) development in neonates. Previously, we observed loss of intestinal goblet cells and increased intestinal epithelial ER stress already during pregnancy in the course of chorioamnionitis. Here, we investigated how chorioamnionitis affects goblet cells by assessing their functional and cellular characteristics. Importantly, goblet cell features are compared with those in clinical NEC biopsies and gestation matched controls.

Fetal lambs were intra-amniotically (IA) infected with *Ureaplasma parvum* serovar 3, the main microorganism clinically associated with chorioamnionitis, for 7 days from 122d gestational age (GA) until 129d GA (equivalent to 30-32 weeks' human GA). After preterm delivery, mucus thickness, goblet cell numbers, gut inflammation, epithelial proliferation and apoptosis and intestinal epithelial ER stress were investigated in the terminal ileum. In addition, goblet cell morphological alterations (TEM) were studied and compared to human NEC samples.

Ileal mucus thickness and the number of goblet cells were elevated following IA UP exposure compared to controls. Increased pro-apoptotic ER stress, detected by CHOP-positive cell counts and disrupted organelle morphology of secretory cells in the intestinal epithelium, was observed in IA UP exposed animals. Importantly, comparable cellular morphological alterations were observed in the ileum from NEC patients.

In conclusion, our data indicate that UP-driven chorioamnionitis leads to a thickened ileal mucus layer, which may be caused by mucus hypersecretion from goblet cells. As these observations were associated with pro-apoptotic ER stress and organelle disruption, mucus barrier alterations seem to take place at the expense of goblet cell resilience and therefore may predispose to detrimental outcomes of the premature ileum. The remarkable overlap of these *in utero* findings with observations in the ileum of NEC patients underscores its clinical relevance.

Introduction

Ureaplasma parvum (UP) is frequently isolated from the amniotic fluid (AF) and uterine membranes of women with chorioamnionitis¹. Chorioamnionitis is characterized by an inflammatory cell influx to fetal membranes and an important cause of preterm birth². Although it's often clinically silent, it can affect the foetus through direct contact with the contaminated amniotic fluid³ and via systemic inflammation in the foetus called fetal inflammatory response syndrome (FIRS). We previously showed in an ovine chorioamnionitis model that UP-induced chorioamnionitis caused intestinal inflammation, injury and developmental disruptions^{4,5}. Consequently, chorioamnionitis and FIRS are associated with increased neonatal morbidity and mortality^{6,7} including necrotizing enterocolitis (NEC)⁸. NEC is a severe gut disease, affecting premature neonates, that is characterized by intestinal inflammation and necrosis when the disease progresses⁹. Mortality generally ranges from 20-30% and survivors are at risk of long-term morbidities including short-bowel syndrome and neurodevelopmental delays⁹.

Despite being an important research topic in the neonatology for years, NEC pathophysiology is still incompletely understood. One previously described contributing factor is disruption of the intestinal mucus barrier with goblet cell loss and reduced mucin production¹⁰⁻¹². In a healthy gut, a mucus layer is generated by gel-forming mucins that are secreted by goblet cells, separates the intestinal epithelium from the gut lumen and prevents bacteria from adhering to the epithelial surface¹⁰. Upon disruption, bacteria reach the intestinal epithelial cells and trigger inflammation¹⁰. In previous preclinical chorioamnionitis studies using lipopolysaccharides (LPS) as inflammatory stimulus, it was observed that chorioamnionitis induces goblet cell loss *in utero*, suggesting mucus barrier alterations may, at least in part, form a mechanistic explanation for the association between chorioamnionitis and NEC^{13,14}. Additionally, goblet cell loss was found to be associated with intestinal inflammation, intestinal epithelial endoplasmic reticulum (ER) stress and apoptosis¹⁴. These combined findings suggest that impaired development of mature goblet cells by ER stress driven apoptosis was mechanistically involved¹⁴. Importantly, ER stress is causally linked with the pathophysiology of intestinal diseases, including inflammatory bowel disease¹⁵ and NEC^{16,17}. A key function of the ER is the folding of proteins following ribosomal protein synthesis. If the ER's capacity to fold proteins is exceeded, ER stress occurs and the unfolded protein response (UPR) will be initiated by binding immunoglobulin protein (BiP) to support ER stress resolution^{18,19}. Once the UPR is not able to resolve ER stress, apoptosis will be induced through, amongst other mechanisms, upregulation of transcription factor C/enhancer binding protein homologous protein (CHOP)²⁰.

Here we investigated how goblet cells are affected by UP-induced chorioamnionitis by examining cellular mechanisms including ER stress and by in depth analysis of goblet cell characteristics in the terminal ileum with transmission electron microscopy (TEM). Moreover, we studied the functional consequences for the ileal mucus layer. Importantly, we compared morphological goblet cells alterations during chorioamnionitis with those in clinical ileal NEC biopsies and gestation matched controls.

Materials and methods

Experimental design

Experiments were approved by the animal experimentation committee of Maastricht University (registration number PV2015-005-02). The ovine model used and experimental procedures have been described in detail previously^{5,21}. The study design is presented in **Supplementary Figure S7.1**. Ten time-mated Texel ewes carrying twin foetuses were randomly assigned (per twin) to two groups of eight to ten animals. One lamb was appointed to a different experiment and one lamb was excluded because of a humane endpoint. At 122d gestational age (GA), ewes (both amniotic sacs) were intra-amniotically (IA) injected with viable *Ureaplasma parvum* serovar-3 (HPA5 strain, 10⁷ color changing units (CCU)) or saline (controls). Foetuses were delivered preterm via caesarean section at 129d GA (term ~150d GA), equivalent to approximately 30-32 weeks of human gastrointestinal development, and subsequently euthanized. Euthanasia and tissue sampling procedures are described in **Supplementary File S7.1**.

Alcian Blue/Periodic Acid Schiff (AB-PAS)

AB-PAS was used as marker for mature (e.g., glycosylated) mucins^{22,23}. Staining was performed on 4 µm thick Carnoy fixated (MUC2) terminal ileum sections as previously described¹⁴ with the exception of a shorter incubation with Alcian blue of 15 minutes in the current study.

Immunohistochemistry

For immunohistochemical stainings, 4 µm thick paraffin embedded paraformaldehyde fixated (Ki67, CC3, CHOP, IBA1 and BiP) or Carnoy's solution fixated (MUC2) terminal ileum sections were used. Staining procedures were described previously²¹ and are summarized in **Supplementary File S7.2**. Antibodies used are listed in **Supplementary Table S7.1**.

Analysis of stained sections (AB-PAS and immunohistochemistry)

Stained sections were scanned using Ventana IScan (Ventana Medical System, Inc., Tucson, AZ). Cells that were positively stained for AB-PAS, CC3, CHOP, Ki67 and MUC2 were counted in a semi-automated fashion with the use of QuPath quantitative pathology and bioimage analysis software version 0.20 (University of Edinburgh, Edinburgh, UK)²⁴. For AB-PAS, BiP and MUC2, lower villus, middle villus and villus tips were analysed separately as previously described¹⁴ to investigate regional differences. For BiP and CHOP, crypts were analysed separately. Crypts were not analysed for AB-PAS and MUC2, since these markers are expressed by goblet cells and Paneth cells. Mucosal surface area and IBA1 positively stained surface area (macrophages) were measured in Leica QWin Pro version 3.4.0 (Leica Microsystems). Positive cell count and positively stained surface area were corrected for mucosal surface area and presented as positive cell count per mm² ileal surface area or percentage of positively stained ileal surface area. Quantitative analyses were performed by one investigator blinded to experimental groups. Qualitative assessment of BiP staining intensity was assessed by two independent blinded researchers. The scoring system used was previously reported¹⁴, 0: no staining, 1: mild staining, 2: moderate staining, 3: intense staining.

RNA isolation, cDNA synthesis and RT-qPCR

Snap frozen terminal ileum was lysed, homogenized and RNA was isolated with the RNeasy Mini Kit (#74104, Qiagen, Hilden, Germany). cDNA was synthesized with the SensiFast cDNA synthesis kit (BIO-65054, Bioline, London, UK). Real-time (RT) qPCR was performed with the SensiMix SYBR Hi-Rox kit (QT605-05, Bioline) and LightCycler-580 Instrument (Roche Applied Science, Basel, Switzerland). Ovine specific primers were used (**Supplementary Table S7.2**). RT-qPCR data processing was performed with LinRegPCR software (version 2016.0, Heart Failure Research Center, Academic Medical Center, Amsterdam, the Netherlands). The geometric mean of three housekeeping genes (ovRPS15, GAPDH and YWHAZ) was used for data normalization. Delta CT values were used for statistical analyses. Data are presented as fold change compared controls (calculated from delta-delta CT values).

Mucus thickness measurements

After sacrifice, fresh ileal tissue was stored in ice-cold Krebs buffer (NaHCO₃ 24.9 mM, KH₂PO₄ 1.2 mM, MgSO₄·7H₂O 1.1 mM, KCl 4.7 mM, NaCl 118.2 mM and CaCl₂·2H₂O 2.5 mM) and kept at 4°C until measurement of mucus thickness within 3 hours after sample collection. Ileal mucus thickness measurements were based on a method developed at the University of Gothenburg, Sweden²⁵ and are described in detail in **Supplementary File S7.3** and **Supplementary Figure S7.2**.

Human intestinal sample collection

We collected gut samples and clinical data of five paediatric patients undergoing ileal resection for acute NEC (patient 1-3), stoma reversal after NEC (patient 4) and stoma reversal after meconium ileus (patient 5). Patients were born prematurely and treated at the neonatal intensive care unit during surgery. The study was approved by the Medical Ethical Committee of Maastricht University Medical Centre (registration number 16-5-185). All parents gave written informed consent. After tissue removal, ileum was kept on ice and fixated in Karnovsky's fixative for TEM analysis.

Transmission electron microscopy (TEM)

For TEM, ileum samples from randomly selected fetal lambs (N=5 controls and N=6 UP exposed lambs), human NEC (N=3) and human control tissue (N=2) were prepared for imaging as described in Supplementary File S7.1. Following tissue processing and cutting, ultrathin sections were mounted on Formvar-coated copper grids and stained with 2% uranyl acetate in 50% ethanol and lead citrate. We imaged stained sections of all EM fixed ileal samples using a Tecnai G2 Spirit transmission electron microscope with a CCD Eagle 4kx4k camera (Thermo Fisher Scientific).

Statistics

We used graphPad Prism Software (v6.0, GraphPad software inc., La Jolla, CA, USA) for statistical analysis. We tested for statistical significance between the groups with a Mann-Whitney U test. Differences were regarded as statistically significant at p<0.05. Data are displayed as median and interquartile range (IQR) for all outcome measures.

Results

Mucus layer thickness in distal ileum of premature lambs

To assess the consequences of IA UP exposure for the small intestinal mucus layer, distal ileal mucus thickness was measured. Ileal mucus thickness was increased in animals, IA exposed to UP for 7 days compared to controls ($p < 0.05$) (**Figure 7.1A**). No differences in villus length were observed between groups (**Supplementary Figure S7.3**), suggesting the mucus layer was also increased relative to villus length following UP exposure.

Presence of goblet cells expressing mature mucins and their distribution in distal ileum of premature lambs

AB-PAS- and MUC2-positive cells were identified in the distal ileum to assess alterations in goblet cell numbers and their expression of the major intestinal gel-forming mucin, since such goblet cell changes could contribute to the increased mucus layer thickness. Compared to controls (**Figure 7.1B**), the number of AB-PAS-positive cells was increased in the lower villus (**Figure 7.1C, 7.1D**), middle villus (**Figure 7.1C, 7.1E**) and total villus (**Figure 7.1C, 7.1F**) of IA UP exposed animals (all $p < 0.05$). In the upper villus region, AB-PAS-positive cell counts did not differ between groups (**Supplementary Figure S7.4**). The number of MUC2-positive cells did not differ between groups in all regions analysed (**Supplementary Figure S7.5**). Collectively, these findings suggest that the number of goblet cells (AB-PAS-positive) was increased following IA UP exposure. However, this increase was not linked to additional MUC2-positive cells, indicating the increased numbers of goblet cells might reflect cells producing alternative gel-forming mucins²⁶.

Signs of mild inflammation in the distal ileum of premature lambs

Intestinal inflammation was investigated as potential mechanism underlying the observed increased mucus layer thickness and goblet cell alterations. After 7d of IA UP exposure, 7 out of 8 UP exposed animals had IBA1 positive surface area (macrophages) above median control level (**Figure 7.2A, 7.2B, 7.2C**), versus 5 out of 10 control animals (**Figure 7.2A, 7.2C**) and the median percentage IBA1-positive surface area was 1.2% higher following UP exposure (74% relative difference). Regarding TNF α mRNA expression, 6 out of 8 UP exposed animals had delta CT values below median control delta CT values with a difference in median expression of 1.65 CT value (~214% median relative increase of mRNA expression) (**Figure 7.2D**), and for TGF β mRNA expression 5 out of 8 UP exposed animals had delta CT levels below median control values (**Figure 7.2E**) with a difference in median expression of 0.95 CT value (~93% median relative increase of mRNA expression). Collectively, these data indicate mild inflammation of the terminal ileum after 7 days of IA UP exposure.

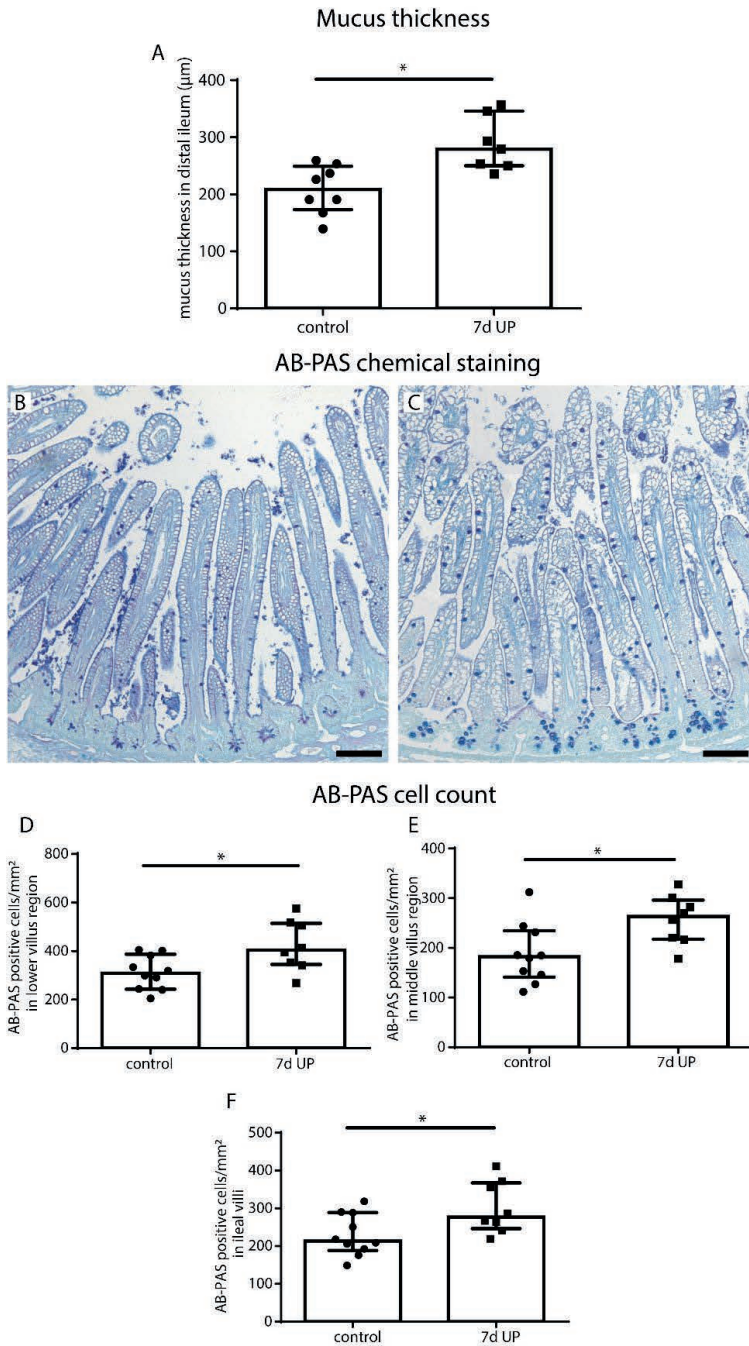


Figure 7.1 Mucus layer thickness, the number of AB-PAS-positive cells per mm² surface area in distal ileum of premature lambs. Compared to control lambs, mucus layer thickness was increased in

7d UP exposed animals (A). Compared to control lambs (B), the number of AB-PAS positive cells was increased in UP exposed lambs (C) in the lower villus region (D), middle villus region (E) and in the total villi (F). Each data point represents the mucus layer thickness or average cell of one lamb. Data are displayed as median with interquartile range. Scale bar indicates 100 μ m. * $p < 0.05$. Abbreviations: AB-PAS: alcian blue / periodic acid Schiff, IA: intra-amniotic, UP: *Ureaplasma parvum*.

ER-stress and intestinal epithelial apoptosis and proliferation in distal ileum of premature lambs

Intestinal epithelial levels of ER stress were investigated because increased mucus layer thickness could result from enhanced mucus secretion by goblet cells, which could induce ER stress. Expression levels of BiP, an important initiator of the UPR to resolve ER stress^{18,19}, were in both groups highest in the lower villus region, but did not differ between controls (Figure 7.3A, 7.3C) and IA UP exposed animals (Figure 7.3B, 7.3C). In contrast, the number of cells positive for CHOP, a driver of ER stress induced apoptosis²⁰, was increased in ileal crypts (Figure 7.3E, 7.3F) and ileal villi (Figure 7.3E, 7.3G) of IA UP exposed lambs compared to controls (Figure 7.3D, 7.3F, 7.3G).

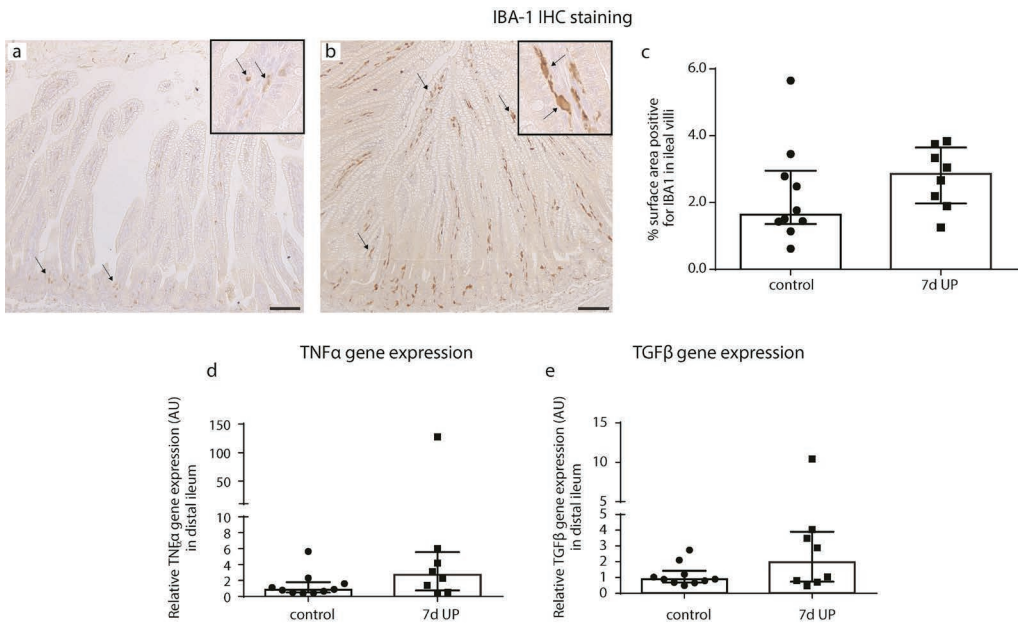


Figure 7.2 Inflammation in the ileum of premature lambs. Mild inflammation was detected in IA UP exposed animals compared to controls, although none of the comparisons reached statistical significance. A mild increase in IBA1 positive surface area (macrophages) (black arrows) (A, B, C), TNF α mRNA expression (D) and TGF β mRNA expression (E) was detected in the ileum of IA UP exposed lambs compared to controls. Each data point represents the average positive surface area or relative mRNA expression of one lamb. Data are displayed as median with interquartile range. Scale bar indicates 100 μ m. Abbreviations: IA: intra-amniotic, IBA1: ionized calcium-binding adaptor molecule 1, TNF α : tumor necrosis factor α , TGF β : transforming growth factor β , UP: *Ureaplasma parvum*.

Subsequently, we studied whether the observed ER stress lead to increased intestinal epithelial apoptosis and whether intestinal epithelial proliferation was altered. Compared to controls (**Figure 7.3H, 7.3K**), the number of apoptotic cells (CC3-positive cell count) was not statistically significantly altered in IA UP exposed animals (**Figure 7.3I, 7.3J, 7.3K**). Apoptosis was primarily detected in the intestinal crypts (**Figure 7.3H, 7.3I**). Of note, two IA UP exposed animals had high amounts of apoptotic cells and in these animals, apoptosis was mainly detected in the lower villus region (**Figure 7.3J**). No differences in intestinal epithelial proliferation (Ki67-positive cell counts, **Supplementary Figure S7.6**) were detected.

Thus, 7 days of IA UP exposure was associated with pro-apoptotic ER stress and potential increased apoptosis at a later time point.

Cellular morphological alterations in distal ileum of premature lambs – TEM

We performed TEM to investigate whether the elevated epithelial ER stress levels were associated with cellular morphological alterations in the fetal ileum. Interestingly, most pronounced differences were observed in secretory cell types (Goblet cells and Paneth cells) in the crypt to villus transition region. In UP exposed animals, in ~60% of the crypts-villi axes affected secretory cells were present in this region, whereas secretory cells of control animals and non-secretory cells in both groups (data not shown) were seldomly altered. In affected secretory cells, the mitochondria show an elongated morphology with abundant parallel cristae perpendicular to the mitochondria membrane in control animals (**Figure 7.4A**), while mitochondria in IA UP exposed animals are globular shaped, contain less electron dense matrix and have altered cristae morphology and organization (**Figure 7.4B**). The rough endoplasmic reticulum (RER) cisternae show a wide range of sizes and shapes in control animals, from almost parallel membranes with thin spaces in between (**Figure 7.4C**) to ovoidal shapes with wider intramembrane spaces (**Figure 7.4A**), which are both considered structurally normal. In contrast, in the IA UP exposed animals, the RER does not have recognizable cisternae, but contains big spaces filling the cytoplasm (**Figure 7.4D**). Regarding the Golgi apparatus, the differences between control and IA UP exposed animals concern to the dimensions of the saccules, which are clearly swollen in UP exposed animals (**Figure 7.4E, 7.4F**). Thus, whereas mitochondria, RER and Golgi apparatus are structurally normal in control animals, these organelles are morphologically disrupted in the secretory cells in the transition region from crypt to villus of IA UP exposed animals. In addition, in this region, cells with necrotic characteristics were exclusively detected in the lumen of IA UP exposed animals (**Figure 7.4G, 7.4H**). In the base of the crypts, no morphological alterations of secretory cell types, including Paneth cells (**Supplementary Figure S7.7**), were detected.

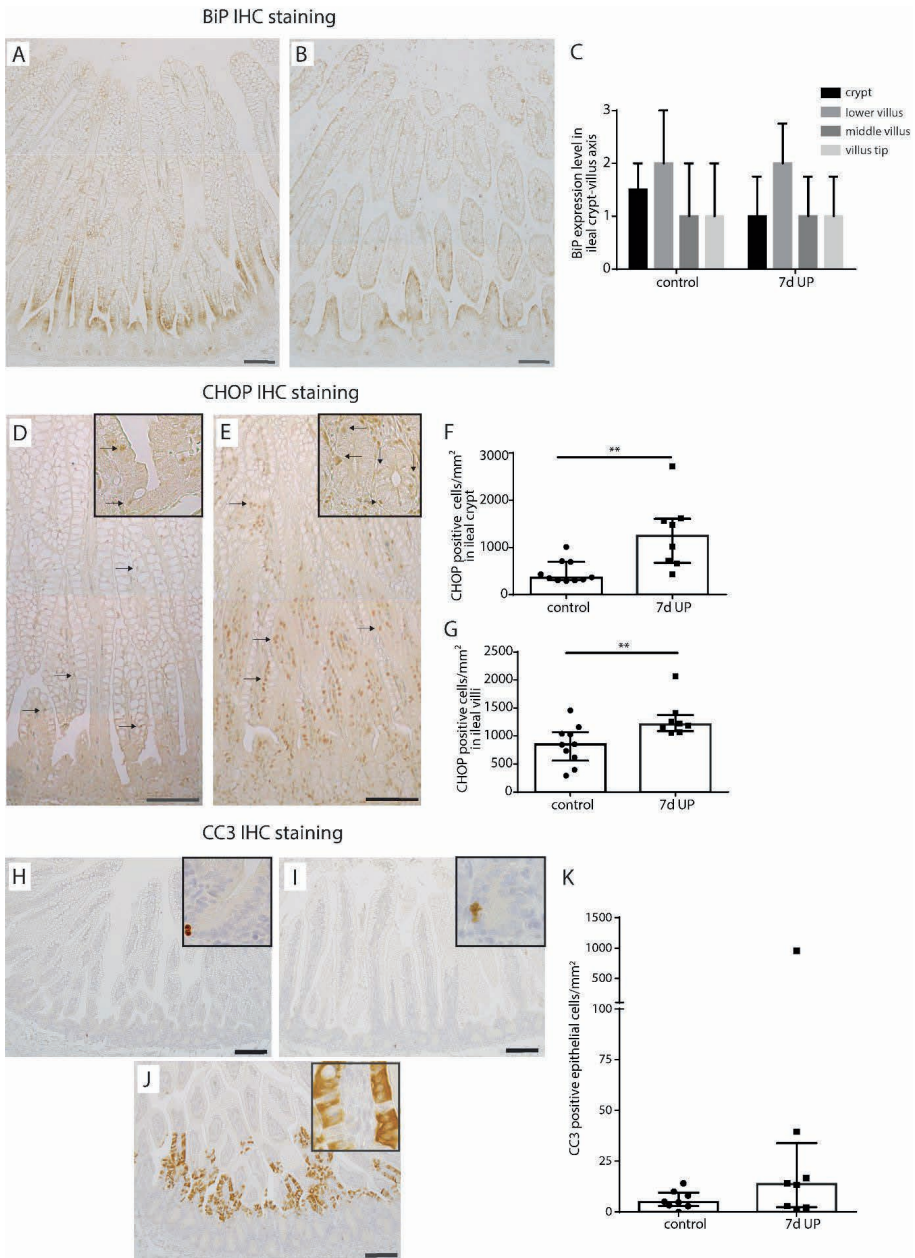


Figure 7.3 BiP expression pattern along crypt-villus axis, the number of CHOP-positive cells per mm² surface area and the number of CC3-positive cells per mm² surface area in distal ileum of premature lambs. The BiP expression pattern of controls (A, C) was comparable to that of IA UP exposed lambs (B, C). Compared to controls (D, F, G), CHOP positive cell count was increased after 7d UP exposure in ileal crypts (E, F) and ileal villi (E, G). The CC3-positive cell count was not

statistically significant different between control (H, K) and IA UP exposed animals (I, J, K). However, two IA UP exposed animals had high CC3-positive cell counts and these cells were detected in the lower villus region (J, K). Each data point represents the average CHOP- or CC3-positive cell count of one lamb. Data are displayed as median with interquartile range. Scale bar indicates 100 μm . ** $p < 0.01$. Abbreviations: BiP: binding immunoglobulin protein, CC3: cleaved caspase 3, CHOP: C/enhancer binding protein homologous protein, IA: intra-amniotic, UP: *Ureaplasma parvum*.

Morphological differences at cellular level were also observed in the villus region (**Figure 7.5**). At organelle level, mitochondria and RER were, structurally normal in enterocytes of control animals, with organelle morphologies similar to those observed in the transition region from crypt to villus (**Figure 7.5A, 7.5C**), whereas these organelles were morphologically disrupted in epithelial cells of ~60% of the villi of IA UP exposed animals (**Figure 7.5B, 7.5D**). In addition, in small intestinal enterocytes of control animals, small vacuoles were found (**Figure 7.5E**), which corresponds to the intestinal cell morphology of fetal enterocytes.²⁷ Remarkably, larger vacuoles were observed in enterocytes of UP exposed animals (**Figure 7.5F**). Secretory cells were structurally normal in both the control group and in UP exposed animals (data not shown).

Collectively, 7 days of IA UP exposure was associated with overt cellular morphological alterations of secretory cells in the transition region from crypt to villus and of enterocytes in the villus region.

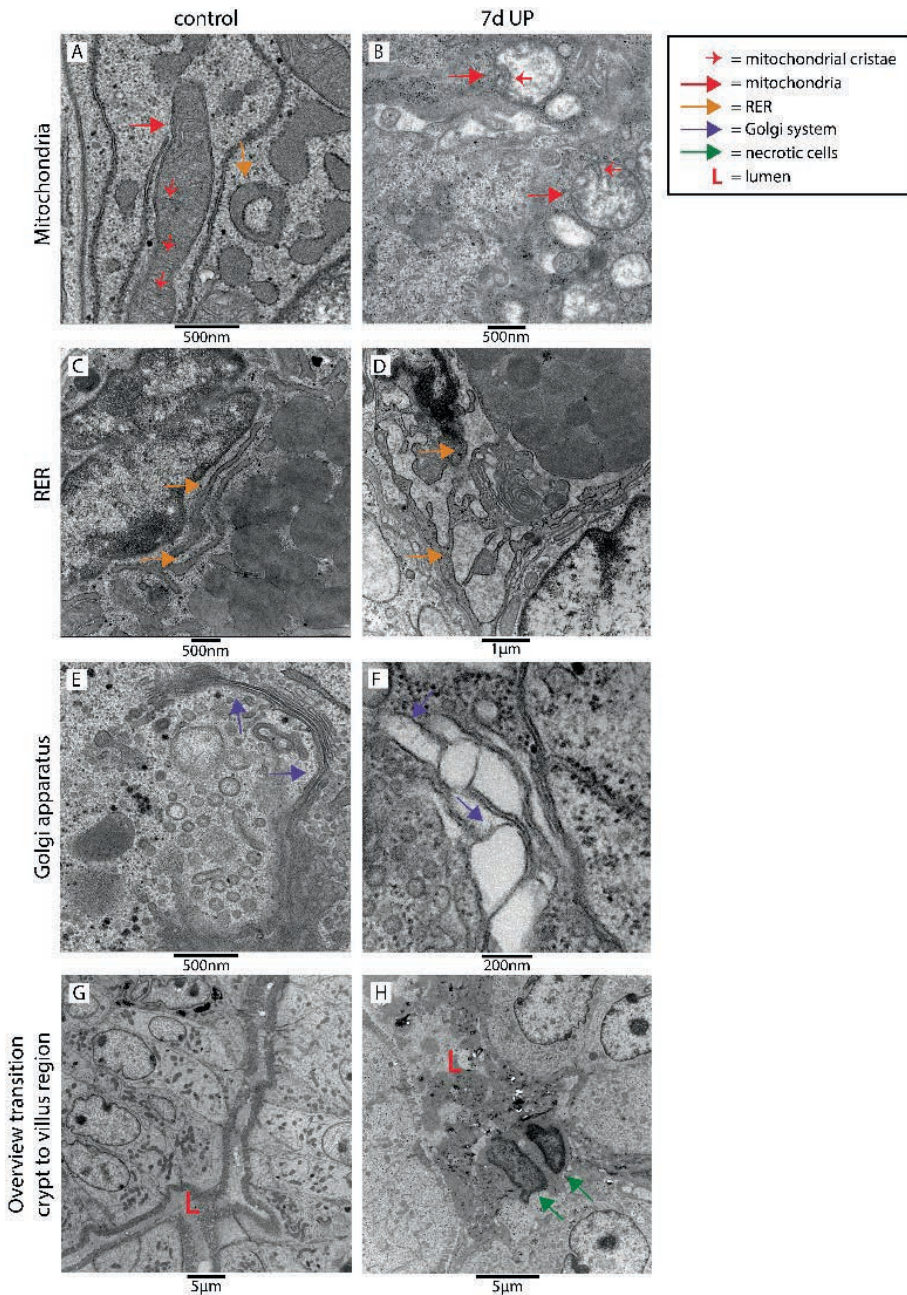


Figure 7.4 Organelle and cellular morphology of secretory cells (goblet cells and Paneth cells) in the crypt to villus transition region in the distal ileum of premature lambs imaged with TEM. In control animals, mitochondria (A; red arrows, cristae indicated by small red arrows), RER (C; orange arrows) and Golgi apparatus (E; purple arrows) of secretory cells had a structurally

normal appearance. In IA UP exposed animals, these organelles were morphologically disrupted (B, D, F). In addition, cells with necrotic characteristics (green arrows) were observed in the lumen (L) of IA UP exposed animals (H), but not in controls (G). Abbreviations: IA: intra-amniotic, L: lumen, RER: rough endoplasmic reticulum, TEM: transmission electron microscopy, UP: *Ureaplasma Parvum*.

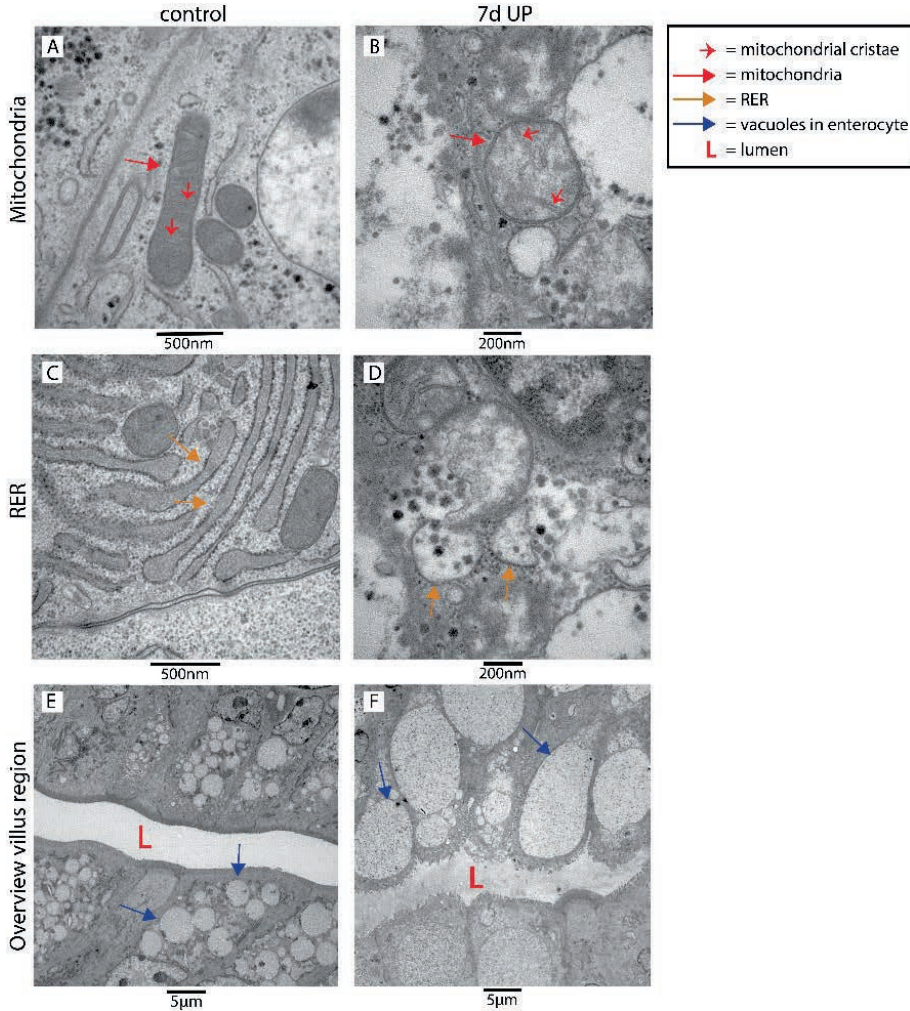


Figure 7.5 Organelle and cellular morphology of enterocytes in the villus region in the distal ileum of premature lambs imaged with TEM. Mitochondria (A; red arrows, mitochondrial cristae indicated by small red arrows) and RER (C; orange arrows) of enterocytes were normal in control animals. In IA UP exposed animals these organelles were morphologically disrupted (B, D). In addition, enterocytes containing small vacuoles (blue arrows) were observed in control animals (E), whereas larger vacuoles were detected in IA UP exposed lambs (F). Abbreviations: IA: intra-amniotic, L: lumen, RER: rough endoplasmic reticulum, TEM: transmission electron microscopy, UP: *Ureaplasma Parvum*.

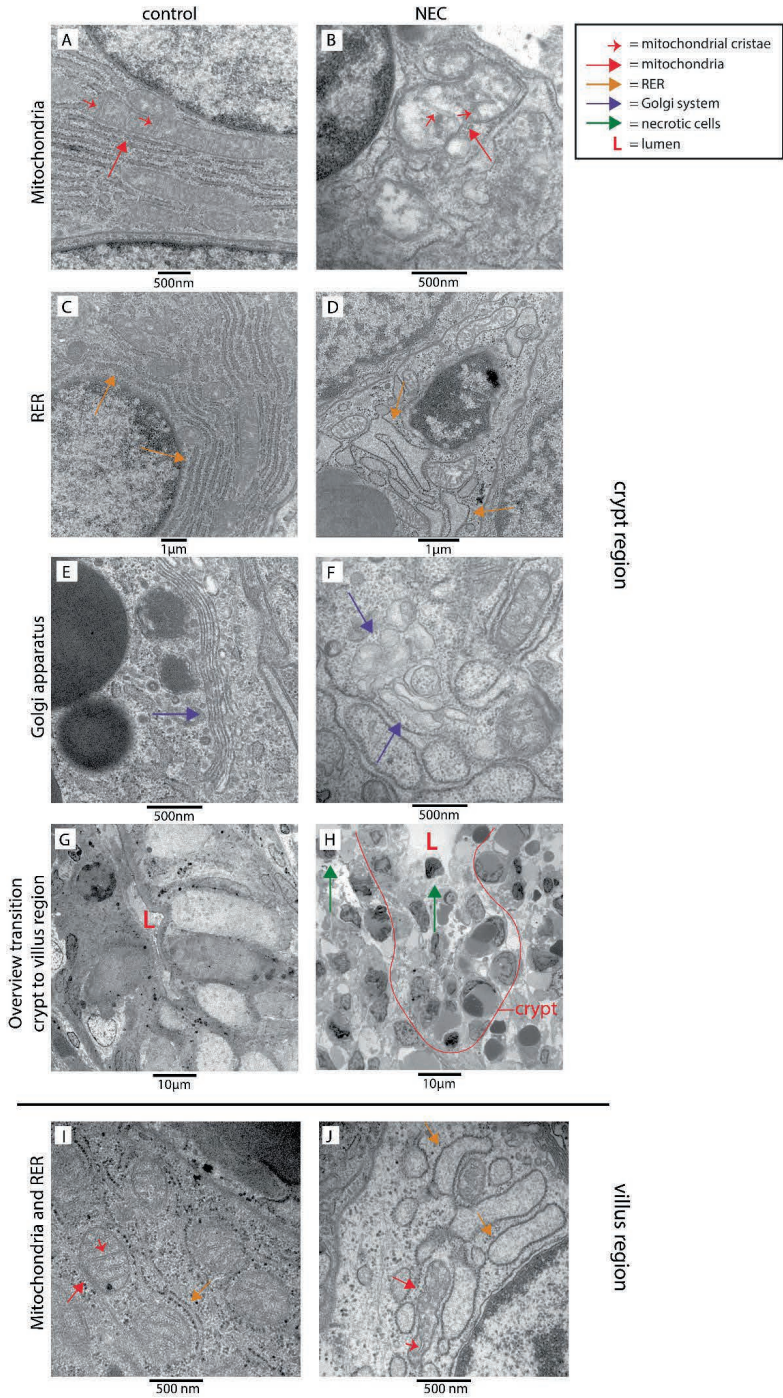


Figure 7.6 Organelle and cellular morphology of enterocytes and secretory cells (goblet cells and Paneth cells) in the ileal crypt region and villus region of NEC patients and controls detected with TEM. Mitochondria (red arrows; mitochondrial cristae indicated by small red arrows), RER (orange arrows) and the Golgi apparatus (purple arrows) of epithelial and secretory cells were normal in the crypt region of control infants (A, C, E), but morphologically disrupted in the NEC patients (B, D, F). Interestingly, compared to control ileal samples (G), large amounts of intestinal cells with necrotic characteristics (green arrows) were present in the crypts of NEC patients (H). Similarly, mitochondria (red arrows, mitochondrial cristae are indicated by small red arrows) and RER (orange arrows) appeared normal in goblet cells and enterocytes in the ileum of control infants (I), whereas these organelles were morphologically disrupted in goblet cells and enterocytes in the ileum from NEC patients (J). Abbreviations: L: lumen, NEC: necrotizing enterocolitis, RER: rough endoplasmic reticulum, TEM: transmission electron microscopy.

Cellular morphological alterations in distal ileum of NEC patients and controls – TEM

To investigate whether cellular changes comparable to those in UP exposed animals are present in the ileum of NEC patients, TEM was performed on ileal samples of NEC patients and gestation matched controls. Consistent with our findings in IA UP exposed animals, mitochondria, RER and Golgi apparatus were morphologically disrupted in the transition region from crypt to villus in the ileum of NEC patients (**Figure 7.6B, 7.6D, 7.6F**) compared to controls (**Figure 7.6A, 7.6C, 7.6E**). However, in NEC patients, changes were observed in all cell types, the cellular morphological alterations were present in all crypt-villus axes and extended to the whole crypt (compared to crypt to villus transition region in UP exposed animals). In addition, the organisation of the crypt region was completely disrupted in most ileal crypts, with presence of a large amount of necrotic cells (**Figure 7.6H**), compared to controls (**Figure 7.6G**). Interestingly, in crypts that were not fully disrupted, the number of Paneth cells was reduced and Paneth cell granule intensity was diminished in the base of the crypts of NEC patients compared to control ileal samples (**Supplementary Figure 7.6**).

Villi were largely necrotic in ileal NEC samples. Comparable to the findings in IA UP exposed animals, mitochondria and RER of enterocytes, but also goblet cells, were morphologically disrupted in all the remaining villi of NEC patients (**Figure 7.6J**), whereas a normal organelle appearance was observed in control samples (**Figure 7.6I**).

Collectively, there is remarkable overlap between the cellular morphological alterations observed in the ileum of NEC patients and those observed in the ovine terminal ileum following IA UP exposure.

Discussion

Key findings of the current study are increased numbers of goblet cells and increased mucus layer thickness, which may be caused by mucus hypersecretion, in the distal ileum of premature lambs following UP-induced chorioamnionitis, demonstrating that goblet cells respond to a microbial trigger already *in utero*. These mucus barrier alterations were associated with pro-apoptotic intestinal epithelial ER stress and cellular morphological disruptions that largely overlap with the observations in the ileum of NEC patients. This

indicates that, although the increased mucus layer thickness at the short term could be favorable, antenatal UP exposure poses a large burden on the resilience of goblet cells and therefore may predispose to detrimental outcomes of the premature ileum.

Although, at the time point of premature delivery, no gut injury (villus atrophy) and alterations in intestinal epithelial proliferation were detected and no increase of intestinal epithelial cell death (CC3) was observed in the majority of UP exposed animals, UP exposure caused considerable disruptions on cellular level. Interestingly, pro-apoptotic ER stress, which probably results from mucus hypersecretion, seems to be an important mechanism contributing to hampered goblet cell resilience. CHOP-positive cell counts were increased following UP exposure and the observed cellular morphological alterations are indicative of ER stress. Moreover, pro-apoptotic intestinal epithelial ER stress was previously observed at a later time point in the course of LPS-induced chorioamnionitis and was paralleled by reduced goblet cell numbers¹⁴. Together, these findings supports that UP is not just an innocent bystander during chorioamnionitis but contributes to its pathophysiology¹. One might argue that the fact that the increased CHOP immunoreactivity was not accompanied by altered BiP expression at the studied time point contradicts the involvement of ER stress. However, in an earlier study in fetal sheep we observed that BiP and CHOP immunoreactivity did not peak at the same moment following intra-uterine inflammation¹⁴. Of note, overt organelle disruptions of both crypt and villi were only detected in 4 out of 6 UP exposed animals studied by TEM and there was also pronounced variability in other studied parameters. This reflects the variable phenotype of infants prenatally exposed to UP in the clinical setting²⁸, which to date is not fully understood, but has been associated with the magnitude of the host response²⁹.

The clinical relevance of the antenatal findings in our translational model is substantiated by comparable findings in clinical biopsies from NEC patients compared to matched controls. In ileal samples from patients with NEC, morphological alterations on organelle level (as assessed by TEM analysis) that were observed in secretory cells of the intestinal crypts largely overlapped with our findings in UP-induced chorioamnionitis (morphologically disrupted RER and mitochondria). In clinical NEC tissues however, these changes were present in all crypt-villus axes and extended to the whole crypt instead of predominantly in the transition region from crypt to villus. This could be related to the more severe nature of NEC, its multifactorial origin, including the influence of the microbiome and exposure to enteral nutrition, and the longer duration of pro-inflammatory insults when compared to our antenatal pre-clinical setting. Importantly, even temporal disturbance of resilience of intestinal goblet cells could predispose the vulnerable infant to injury following additional pro-inflammatory hits, such as sepsis³⁰ and mechanical ventilation³¹, and may in part explain the association between chorioamnionitis and postnatal development of NEC.

Increased mucus layer thickness is likely caused by an increased secretion of mucus by goblet cells. Alternatively, other factors, such as increased ion secretion or altered mucus proteolysis, could be involved in the increased mucus layer thickness following IA UP exposure^{32,33}.

UP induced inflammation could underlie the increased expression of mature mucins by goblet cells and the postulated increased mucus secretion rate, as several pro-inflammatory cytokines have been reported to induce mucus secretion³⁴. Consistently, (mild)

inflammation was detected at the time point of delivery in this study and we have previously shown intestinal inflammation in comparable ovine studies^{5,21}. Moreover, direct contact between UP and intestinal goblet cells could trigger mucus release by UP-induced activation of Toll-like receptors (TLRs)³⁵. In the mouse colon, sentinel goblet cells have been described at the entrance of intestinal crypts that secrete MUC2 upon endocytosis of a TLR2/1 ligand and subsequently promote mucus release from adjacent reactive goblet cells³⁶. Interestingly, several findings support the concept that the thicker mucus layer observed in the distal ileum may result from a similar mechanism. First, goblet cells present in the transition region from crypt to villus display a cellular morphology (observed with TEM) of ER stress (disrupted RER and Golgi apparatus) and oxidative stress (disrupted mitochondria), whereas this phenotype was less pronounced in goblet cells in the villus region. These observations are considered to be causally linked to the observed increased mucin production, as mucins are processed by the ER and the Golgi apparatus and ER stress and oxidative stress can give rise to a vicious cycle^{20,37}. Reactive oxygen species (ROS) can disturb ER protein folding and ER stress can increase ROS formation directly through oxidative protein folding in the ER and indirectly through mitochondrial uptake of Ca²⁺ released from the ER³⁷. Second, in the transition region from crypt to villus, cells with necrotic characteristics were observed that may represent sentinel goblet cells that were expelled into the intestinal lumen following mass mucus secretion^{36,38}.

Interestingly, cellular changes (as assessed by TEM analysis) and increased pro-apoptotic levels of ER stress (CHOP) were also detected in intestinal villi, suggesting that, besides goblet cells, enterocytes are affected by intrauterine inflammation. In control animals, vacuolated enterocytes were observed, which is a hallmark of fetal enterocytes that results from amniotic fluid macromolecule uptake²⁷. In UP exposed animals however, these vacuoles were much larger. Although the precise nature of this observation remains to be elucidated, similar findings were described in a murine NEC model³⁹. That study suggested that these vacuoles were giant lysosomes resulting from lysosomal overloading due to excessive endocytosis and autophagy and these structures were implicated to be involved in NEC pathophysiology³⁹. In addition, we observed morphologically disrupted organelles (RER and mitochondria) in vacuolated enterocytes as well, indicating elevated levels of ER stress in the villus region. Whether this ER stress is causally related to the presence of larger vacuoles is an interesting topic for future research.

In conclusion, UP-induced chorioamnionitis increased the number of goblet cells, which may be related to an increased mucus secretion rate and subsequent increased ileal mucus layer thickness. It is likely these changes take place at the expense of goblet cell resilience, as they were associated with pro-apoptotic intestinal epithelial ER stress and the presence of cellular morphological changes largely overlapped with the observations of the ileum from NEC patients. Interestingly, intrauterine inflammation also negatively affected enterocytes. Even temporal disruption of intestinal goblet cell and enterocyte resilience could predispose the vulnerable infant to injury following additional pro-inflammatory hits and may in part explain the association between chorioamnionitis and NEC. Therefore, timely initiation of interventions that may support intestinal recovery after chorioamnionitis, such as enteral feeding intervention⁴⁰, could aid in preserving a healthy mucus barrier and preventing NEC development.

References

1. Sweeney EL, Dando SJ, Kallapur SG, et al. The Human Ureaplasma Species as Causative Agents of Chorioamnionitis. *Clinical microbiology reviews* 2017;30:349-379.
2. Thomas W, Speer CP. Chorioamnionitis: important risk factor or innocent bystander for neonatal outcome? *Neonatology* 2011;99:177-187.
3. Gantert M, Been JV, Gavilanes AW, et al. Chorioamnionitis: a multiorgan disease of the fetus? *Journal of perinatology : official journal of the California Perinatal Association* 2010;30 Suppl:S21-30.
4. Heymans C, de Lange IH, Hütten MC, et al. Chronic Intra-Uterine Ureaplasma parvum Infection Induces Injury of the Enteric Nervous System in Ovine Fetuses. *Frontiers in immunology* 2020;11:189.
5. Wolfs TG, Kallapur SG, Knox CL, et al. Antenatal ureaplasma infection impairs development of the fetal ovine gut in an IL-1-dependent manner. *Mucosal immunology* 2013;6:547-556.
6. Gotsch F, Romero R, Kusanovic JP, et al. The fetal inflammatory response syndrome. *Clinical obstetrics and gynecology* 2007;50:652-683.
7. Sprong KE, Mabenge M, Wright CA, et al. Ureaplasma species and preterm birth: current perspectives. *Critical reviews in microbiology* 2020;46:169-181.
8. Been JV, Lievense S, Zimmermann LJ, et al. Chorioamnionitis as a risk factor for necrotizing enterocolitis: a systematic review and meta-analysis. *The Journal of pediatrics* 2013;162:236-242.e232.
9. Neu J, Walker WA. Necrotizing enterocolitis. *The New England journal of medicine* 2011;364:255-264.
10. Halpern MD, Denning PW. The role of intestinal epithelial barrier function in the development of NEC. *Tissue barriers* 2015;3:e1000707.
11. McElroy SJ, Prince LS, Weitkamp JH, et al. Tumor necrosis factor receptor 1-dependent depletion of mucus in immature small intestine: a potential role in neonatal necrotizing enterocolitis. *American journal of physiology Gastrointestinal and liver physiology* 2011;301:G656-666.
12. Schaart MW, de Bruijn AC, Bouwman DM, et al. Epithelial functions of the residual bowel after surgery for necrotising enterocolitis in human infants. *Journal of pediatric gastroenterology and nutrition* 2009;49:31-41.
13. Elgin TG, Fricke EM, Gong H, et al. Fetal exposure to maternal inflammation interrupts murine intestinal development and increases susceptibility to neonatal intestinal injury. *Disease models & mechanisms* 2019; 12.
14. van Gorp C, de Lange IH, Massy KRI, et al. Intestinal Goblet Cell Loss during Chorioamnionitis in Fetal Lambs: Mechanistic Insights and Postnatal Implications. *International journal of molecular sciences* 2021;22.
15. Coleman OI, Haller D. ER Stress and the UPR in Shaping Intestinal Tissue Homeostasis and Immunity. *Frontiers in immunology* 2019;10:2825.
16. Afrazi A, Branca MF, Sodhi CP, et al. Toll-like receptor 4-mediated endoplasmic reticulum stress in intestinal crypts induces necrotizing enterocolitis. *The Journal of biological chemistry* 2014;289:9584-9599.
17. Lu P, Struijs MC, Mei J, et al. Endoplasmic reticulum stress, unfolded protein response and altered T cell differentiation in necrotizing enterocolitis. *PloS one* 2013;8:e78491.
18. Hetz C. The unfolded protein response: controlling cell fate decisions under ER stress and beyond. *Nature reviews Molecular cell biology* 2012;13:89-102.
19. Ron D, Walter P. Signal integration in the endoplasmic reticulum unfolded protein response. *Nature reviews Molecular cell biology* 2007;8:519-529.
20. McGuckin MA, Eri RD, Das I, et al. ER stress and the unfolded protein response in intestinal inflammation. *American journal of physiology Gastrointestinal and liver physiology* 2010;298:G820-832.
21. van Gorp C, de Lange IH, Spiller OB, et al. Protection of the Ovine Fetal Gut against Ureaplasma-Induced Chorioamnionitis: A Potential Role for Plant Sterols. *Nutrients* 2019;11.
22. Yamabayashi S. Periodic acid-Schiff-alcian blue: a method for the differential staining of glycoproteins. *The Histochemical journal* 1987;19:565-571.
23. Hurd EA, Holmén JM, Hansson GC, et al. Gastrointestinal mucins of Fut2-null mice lack terminal fucosylation without affecting colonization by *Candida albicans*. *Glycobiology* 2005;15:1002-1007.

24. Bankhead P, Loughrey MB, Fernández JA, et al. QuPath: Open source software for digital pathology image analysis. *Scientific Reports* 2017;7:16878.
25. Gustafsson JK, Ermund A, Johansson MEV, et al. An ex vivo method for studying mucus formation, properties, and thickness in human colonic biopsies and mouse small and large intestinal explants. *American journal of physiology Gastrointestinal and liver physiology* 2012;302:G430-G438.
26. Hasnain SZ, Evans CM, Roy M, et al. Muc5ac: a critical component mediating the rejection of enteric nematodes. *The Journal of experimental medicine* 2011;208:893-900.
27. Skrzypek T, Szymańczyk S, Ferenc K, et al. The contribution of vacuolated foetal-type enterocytes in the process of maturation of the small intestine in piglets. Invited review. *J Anim Feed Sci* 2018;27:187-201.
28. Waites KB, Katz B, Schelonka RL. Mycoplasmas and ureaplasmas as neonatal pathogens. *Clinical microbiology reviews* 2005;18:757-789.
29. Sweeney EL, Dando SJ, Kallapur SG, et al. The Human Ureaplasma Species as Causative Agents of Chorioamnionitis. *Clinical microbiology reviews* 2016;30:349-379.
30. Machado JR, Soave DF, da Silva MV, et al. Neonatal sepsis and inflammatory mediators. *Mediators of inflammation* 2014;2014:269681.
31. Bose CL, Laughon MM, Allred EN, et al. Systemic inflammation associated with mechanical ventilation among extremely preterm infants. *Cytokine* 2013;61:315-322.
32. Gustafsson JK, Ermund A, Ambort D, et al. Bicarbonate and functional CFTR channel are required for proper mucin secretion and link cystic fibrosis with its mucus phenotype. *The Journal of experimental medicine* 2012;209:1263-1272.
33. Nyström EEL, Birchenough GMH, van der Post S, et al. Calcium-activated Chloride Channel Regulator 1 (CLCA1) Controls Mucus Expansion in Colon by Proteolytic Activity. *EBioMedicine* 2018;33:134-143.
34. Cornick S, Tawiah A, Chadee K. Roles and regulation of the mucus barrier in the gut. *Tissue barriers* 2015;3:e982426-e982426.
35. Triantafilou M, De Glanville B, Aboklaish AF, et al. Synergic activation of toll-like receptor (TLR) 2/6 and 9 in response to Ureaplasma parvum & urealyticum in human amniotic epithelial cells. *PloS One* 2013;8:e61199.
36. Birchenough GM, Nyström EE, Johansson ME, et al. A sentinel goblet cell guards the colonic crypt by triggering Nlrp6-dependent Muc2 secretion. *Science (New York, NY)* 2016;352:1535-1542.
37. Cao SS, Kaufman RJ. Endoplasmic reticulum stress and oxidative stress in cell fate decision and human disease. *Antioxidants & redox signaling* 2014;21:396-413.
38. Zhang M, Wu C. The relationship between intestinal goblet cells and the immune response. *Bioscience Reports* 2020;40.
39. Yamoto M, Alganabi M, Chusilp S, et al. Lysosomal overloading and necrotizing enterocolitis. *Pediatric Surgery International* 2020;36:1157-1165.
40. de Lange IH, van Gorp C, Eeftinck Schattenkerk LD, et al. Enteral Feeding Interventions in the Prevention of Necrotizing Enterocolitis: A Systematic Review of Experimental and Clinical Studies. *Nutrients* 2021;13:1726.

Supplementary materials

Supplementary file 7.1: Euthanasia and tissue sampling procedures

Directly after birth, lambs were euthanized by intravenous sodium-pentobarbital (200 mg/kg) administration. Samples of terminal ileum were collected and fixed in 4% paraformaldehyde, Carnoy's solution (60% methanol (31721.M1, Thermo Fisher Scientific, Waltham, MA, USA), 30% chloroform (22711324, VWR Chemicals, Radnor, PA, USA) and 10% glacial acetic acid (20102292, VWR Chemicals)) and Karnovsky's fixative (2.5% glutaraldehyde and 2% paraformaldehyde in sodium cacodylate 0.1M, pH 7.4), snap frozen in liquid nitrogen and used directly for measurements of mucus thickness. Paraformaldehyde and Carnoy's solution fixed tissues were subsequently embedded in paraffin and 4 µm thick sections were cut with a microtome (RM2235, Leica Microsystems) for Alcian Blue/Periodic Acid Schiff (AB-PAS) stainings and immunohistochemical stainings. Terminal ileum samples for TEM analysis fixated with Karnovsky's fixative were stored in 2% paraformaldehyde in phosphate buffer (PB) at 4°C. Tissue was rinsed with sodium cacodylate 0.1M, fixated at 4°C with 1% osmium tetroxide in sodium cacodylate 0.1M containing 0.8% potassium ferrocyanide and dehydrated with ethanol. Thereafter, tissue was infiltrated with Epon resin for 48h, embedded and polymerized for 48h at 60°C. Ultrathin sections were cut using an Ultracut UC6 ultramicrotome (Leica Microsystems).

Supplementary file 7.2: Immunohistochemical stainings procedures

Tissue sections were deparaffinised and rehydrated. Thereafter, sections were incubated in 0.3% H₂O₂ diluted in phosphatase buffered saline (PBS) to block endogenous peroxidase activity. We performed antigen retrieval by boiling sections in a 10 mM sodium-citrate buffer (pH 6.0) for 10 minutes for Ki67, CC3, CHOP, IBA1, MUC2 and BiP. Nonspecific bindings sites were blocked by incubating the sections in 5% BSA in PBS (BiP, CC3, CHOP, Ki67, MUC2; 30 minutes at RT) or 4% normal goat serum (NGS) in PBS (IBA1; 30 minutes at RT). Subsequently, sections were incubated with the primary antibody of interest at 4°C overnight (BiP, CC3, CHOP, IBA1, Ki67, MUC2). After washing, sections were incubated with the appropriate secondary antibody which was biotin-conjugated for BiP, CC3, CHOP, Ki67, IBA1 and MUC2. Secondary antibody signal was enhanced with an avidin-biotin complex formation using a standard kit (Vectastain Elite ABC kit, PK6100, Maravai LifeSciences, San Diego, CA, USA). Immunoreactivity for BiP, CC3, CHOP, IBA1, Ki67 and MUC2 were visualized with 3,3'-diaminobenzidine tetrahydrochloride (DAB, Thermo Fisher Scientific, Waltham, MA, USA). Counterstaining of nuclei was performed with haematoxylin (CC3, IBA1, Ki67). No counterstaining was performed for BiP, CHOP and MUC2.

Supplementary file 7.3: Mucus measurement technique

Tissue was stretched on a silicone elastomere coated petridish with the apical side up and black dyed polystyrene microspheres of 10 µm (24294-2, Polysciences, Warrington, US) were added to the apical surface to visualize the mucus layer. The distance between charcoal bead clusters between the villi and the tissue surface with a microneedle. These microneedles were generated in house with a Flaming/brown micropipette puller model P-

87 (Sutter Instruments, Novato, CA, USA) from borosilica standard wall capillaries (GC150F-10, 30-0057, Harvard Apparatus, Holliston, US) and had a 1.5 mm outer diameter, 0.86 mm inner diameter and $\sim 25 \mu\text{m}$ tip diameter. Needles were attached to a custom made micro-manipulator (Debets Mechanical Support, Stein, The Netherlands) in a 45-degree angle. Vertical thickness of the mucus layer was calculated by multiplying the distance between the charcoal beads and the crypt bottom measured with the 45-degree angled needle with $\cos 45$.^{1,2} The measurement set-up is presented in **Supplementary Figure S7.2**.

1. Gustafsson JK, Ermund A, Johansson MEV, et al. An ex vivo method for studying mucus formation, properties, and thickness in human colonic biopsies and mouse small and large intestinal explants. *American journal of physiology Gastrointestinal and liver physiology* 2012;302:G430-G438.
2. Strugala V, Allen A, Dettmar PW, et al. Colonic mucin: methods of measuring mucus thickness. *The Proceedings of the Nutrition Society* 2003;62:237-243.

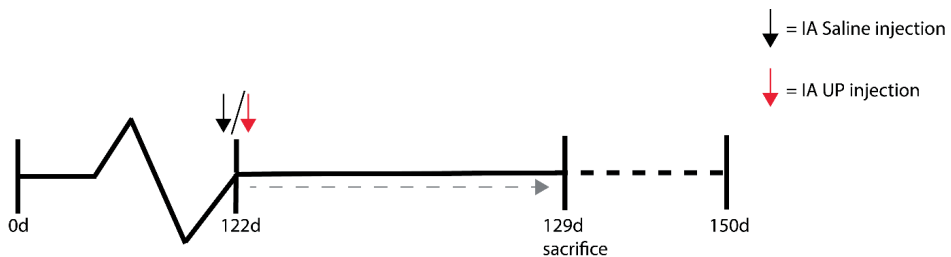


Figure S7.1 Study design. Twin foetuses from time-mated Texel ewes were randomly assigned to one of two treatment groups. An IA injection with saline or *Ureaplasma parvum* serovar 3 (107 color changing units) was administered at 122d of GA (term is ~ 150 d GA). At 129d GA, 7 days after IA injection, animals were sacrificed. Abbreviations: GA, gestational age; IA, intra-amniotic; UP: *Ureaplasma parvum*.

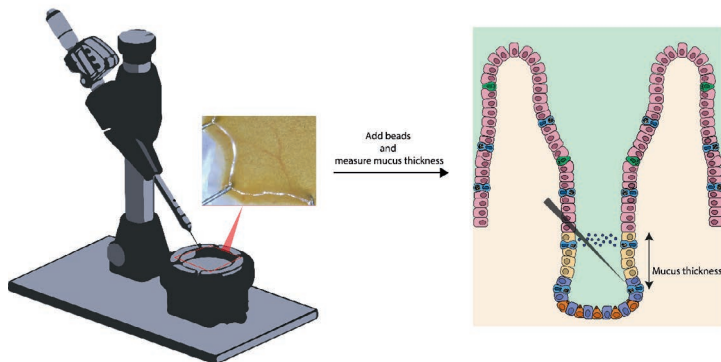


Figure S7.2 Mucus measurement methodology. Fresh ileal tissue was stretched with the apical side up. Charcoal particles were added apically to visualize the mucus layer. Thereafter, mucus layer thickness was measured by determining the 45-degree distance between the particles and the intestinal tissue surface with a microneedle attached to our custom made micro-manipulator. Vertical mucus thickness was calculated.

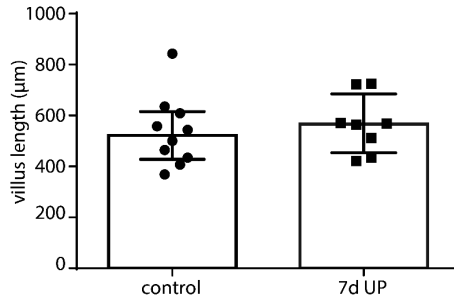


Figure S7.3 Villus length (μm) in distal ileum of premature lambs. No differences were observed in villus length between control and IA UP exposed animals. Data are displayed as median with interquartile range. Abbreviations: IA: intra-amniotic, UP: *Ureaplasma parvum*.

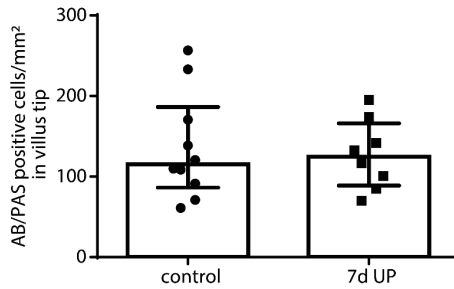


Figure S7.4. Number of AB-PAS-positive cells per mm^2 in the villus tip of control and IA UP exposed distal ileum of premature lambs. No differences in AB-PAS-positive cell count were detected between the two groups. Each data point represents the AB-PAS-positive cell count of one lamb. Data are displayed as median with interquartile range. Abbreviations: AB-PAS: alcian blue / periodic acid Schiff, IA: intra-amniotic, UP: *Ureaplasma parvum*.

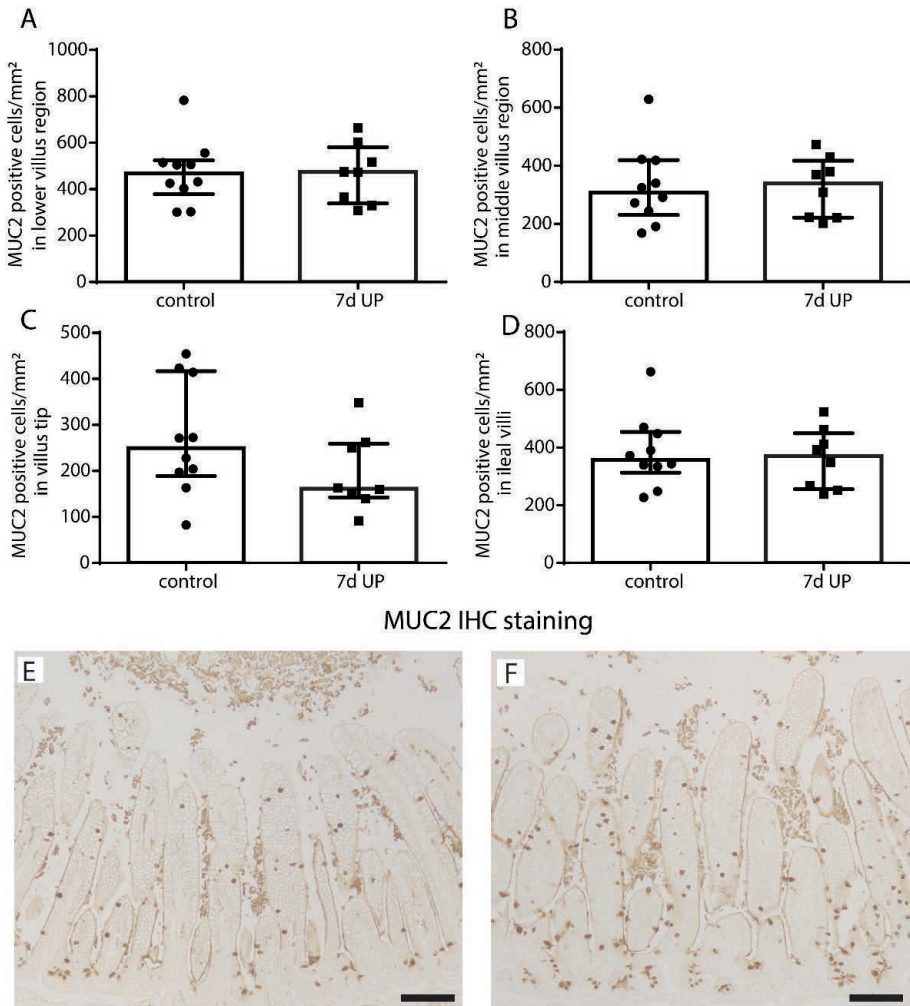


Figure S7.5 Number of MUC2-positive cells per mm² in the different villus regions of control and IA UP exposed distal ileum of premature lambs. No differences in MUC2-positive cell count in the lower villus region (A), middle villus region (B), villus tip (C) and total villus (D) were observed between controls (E) and lambs in the 7d IA UP group (F). Each data point represents the MUC2-positive cell count of one lamb. Data are displayed as median with interquartile range. Abbreviations: IA: intra-amniotic, MUC2: Mucin 2, UP: *Ureaplasma parvum*.

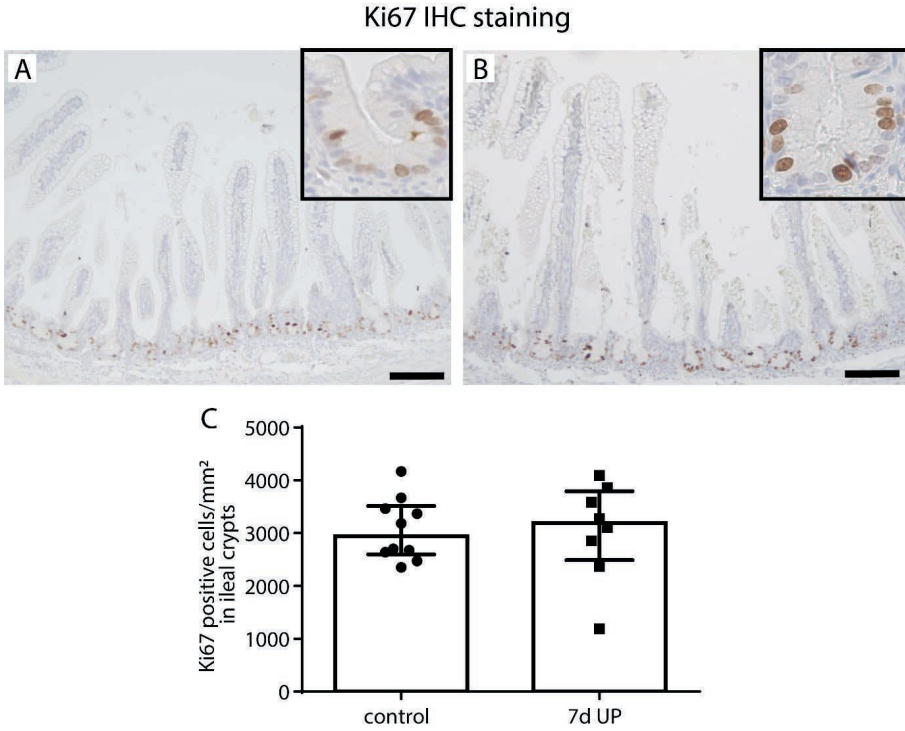


Figure S7.6 The number of Ki67-positive cells per mm² surface area in distal ileum of premature lambs. No differences were observed in the number of Ki67-positive cells in the crypts of control (A, C) and IA UP exposed (B, C) lambs. Data are displayed as median with interquartile range. Scale bar indicates 100 μ m. Abbreviations: CC3: cleaved caspase 3, IA: intra-amniotic, UP: *Ureaplasma parvum*.

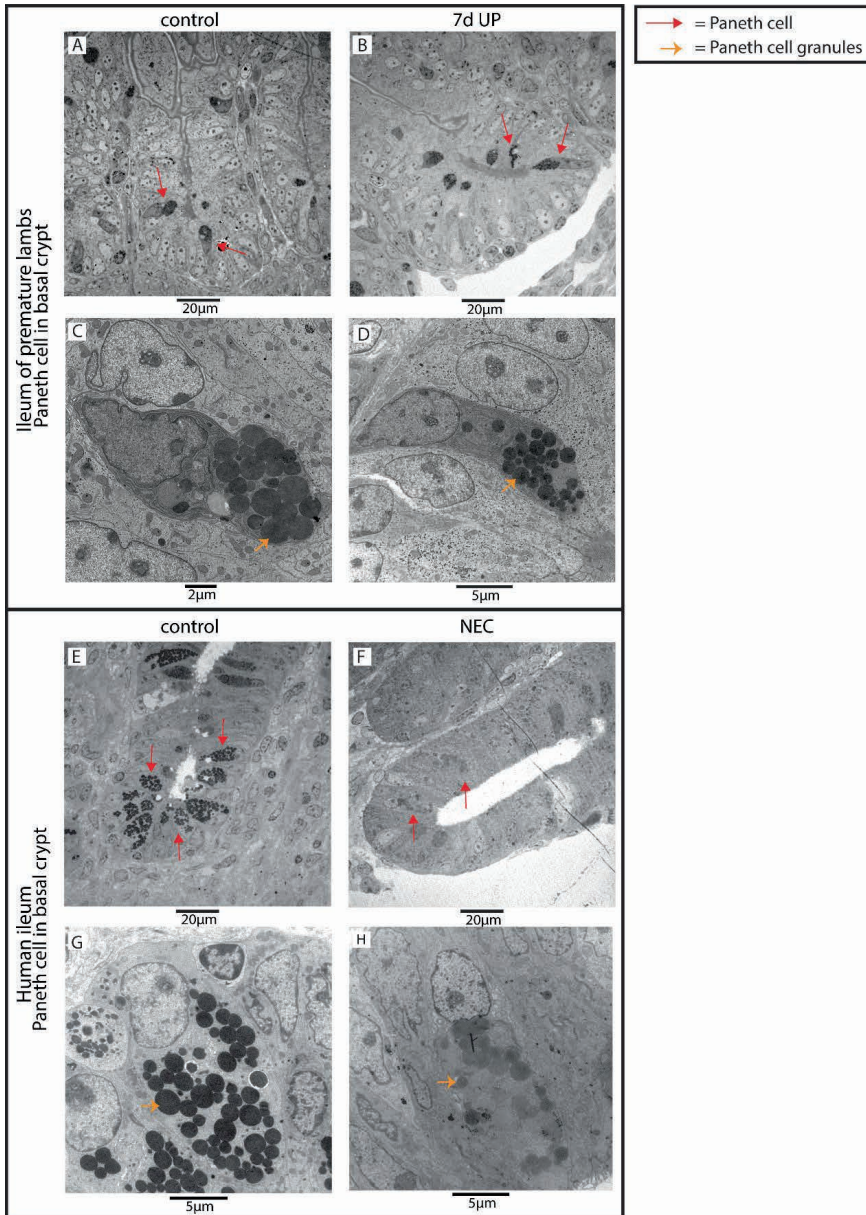


Figure S7.7 Paneth cells in basal crypts of premature lambs and human neonates, imaged with TEM. No differences were observed in number of Paneth cells (red arrows) and Paneth cell granule intensity (orange arrows) in the ileal crypts of control (A, C) and IA UP exposed lambs (B, D). Interestingly, compared to control infants (E, G), the number of Paneth cells (red arrows) was reduced and the intensity of the granules (orange arrows) was diminished in NEC patients (F, H). Abbreviations: IA: intra-amniotic, NEC: necrotizing enterocolitis, TEM: transmission electron microscopy, UP: *Ureaplasma parvum*.

Table S7.1 Antibodies used.

Primary antibodies used:
monoclonal rabbit anti-BiP (C50B12 #3177 Cell Signaling Technology, Danvers, MA, USA)
polyclonal rabbit anti-Ki67 (ab15580, abcam, Cambridge, United Kingdom)
polyclonal rabbit anti-CC3 (ASP 175, #9661 Cell Signaling Technology)
monoclonal mouse anti-CHOP (9C8, MA1-250, Invitrogen, Carlsbad, CA, USA)
polyclonal rabbit anti-IBA1 (019-19741, Fujifilm Wako Chemicals Europe, Neuss, Germany)
polyclonal rabbit anti-SPDEF (ab197375, abcam)
polyclonal rabbit anti-mucin 2 (MUC2c3) kindly provided by Gunnar Hansson, University of Gothenburg, Gothenburg, Sweden
Secondary antibodies used:
biotin-conjugated polyclonal swine anti-rabbit (E0353, DakoCytomation, Glostrup, Denmark) (BiP, CC3, IBA1, MUC2, SPDEF),
biotin-conjugated donkey anti-rabbit (#711-065-152, Jackson ImmunoResearch, Cambridgeshire, UK) (Ki67)
biotin-conjugated polyclonal rabbit anti-mouse (E0413, DakoCytomation, Glostrup, Denmark) (CHOP)

Table S7.2 Sequences of primers used.

Primer	Forward	Reverse
Housekeeping genes		
ovRPS15	5'-CGAGATGGTGCCAGCAT-3'	5'-GCTTGATTCCACCTGGTTGA-3'
GAPDH	5'-ATGCCTCCTGCACCACCA-3'	5'-ATGCCCTCCACGATGCCAA-3'
YWHAZ	5'-TGAACCTCCCTGAGAAAGCC-3'	5'-TCCGATGTCCACAATGTCAAGT-3'
Genes of interest		
TNF α	5'-GCCGGAATACCTGGACTATGC-3'	5'-CAGGGCGATGATCCCAAAGTAG-3'
TGF β	5'-AAAAGAAGCTGTGTTCTGCA-3'	5'-GACCTTGCTGACTGTGTGTC-3'

Abbreviations: ovRPS15: ovine ribosomal protein S15, GAPDH, glyceraldehyde 3-phosphate dehydrogenase, YWHAZ: 14-3-3 protein zeta/delta.

Part **IV**

**Towards better strategies for the prevention of NEC
with enteral feeding interventions**

Chapter 8

Protection of the ovine fetal gut against *Ureaplasma*-induced chorioamnionitis: a potential role for plant sterols

C. van Gorp*, I.H. de Lange*, O.B. Spiller, F. Dewez, B. Cillero Pastor, R.M.A. Heeren,
L. Kessels, N. Kloosterboer, W.G. van Gemert, M.L. Beeton, S.J. Stock, A.H. Jobe,
M.S. Payne, M.W. Kemp, L.J. Zimmermann, B.W. Kramer, J. Plat, and T.G.A.M. Wolfs

* Contributed equally

Nutrients 2019;11(5):968.

Abstract

Chorioamnionitis, clinically most frequently associated with *Ureaplasma*, is linked to intestinal inflammation and subsequent gut injury. No treatment is available to prevent chorioamnionitis-driven adverse intestinal outcomes. Evidence is increasing that plant sterols possess immune-modulatory properties. Therefore, we investigated the potential therapeutic effects of plant sterols in lambs intra-amniotically (IA) exposed to *Ureaplasma*. Fetal lambs were IA exposed to *Ureaplasma parvum* (*U. parvum*, UP) for six days from 127 d–133 d of gestational age (GA). The plant sterols β -sitosterol and campesterol, dissolved with β -cyclodextrin (carrier), were given IA every two days from 122 d–131 d GA. Fetal circulatory cytokine levels, gut inflammation, intestinal injury, enterocyte maturation, and mucosal phospholipid and bile acid profiles were measured at 133 d GA (term 150 d). IA plant sterol administration blocked a fetal inflammatory response syndrome. Plant sterols reduced intestinal accumulation of proinflammatory phospholipids and tended to prevent mucosal myeloperoxidase-positive (MPO) cell influx, indicating an inhibition of gut inflammation. IA administration of plant sterols and carrier diminished intestinal mucosal damage, stimulated maturation of the immature epithelium, and partially prevented *U. parvum*-driven reduction of mucosal bile acids. In conclusion, we show that β -sitosterol and campesterol administration protected the fetus against adverse gut outcomes following UP-driven chorioamnionitis by preventing intestinal and systemic inflammation.

Introduction

Preterm birth is the leading cause of neonatal mortality and morbidity, and it accounts for 35% of neonatal deaths worldwide¹. Annually, 15 million children are born prematurely, an incidence that is still increasing². Chorioamnionitis, defined as inflammatory cell infiltration of fetal membranes, is an important cause of preterm birth³. During chorioamnionitis, contaminated amniotic fluid (AF) is swallowed by the fetus, consequently infecting the gastrointestinal system. We have previously studied the effects of chorioamnionitis on the fetal gut in a translational ovine chorioamnionitis model that is of relevance to human pathology because of the close resemblance between the developmental biology and physiology of human and ovine fetuses⁴. In this model, intra-amniotic (IA) infections with micro-organisms and inflammatory mediators (lipopolysaccharide (LPS)) can induce gut inflammation and subsequent gut injury and developmental alterations^{5,6}. Accordingly, chorioamnionitis is associated with an increased risk of postnatal intestinal pathologies, such as necrotizing enterocolitis (NEC), which is known for its high mortality and morbidity rates⁷⁻⁹. In addition, chorioamnionitis is associated with the fetal inflammatory response syndrome (FIRS), which is characterized by increased IL-6 concentrations in fetal blood and is an independent risk factor for severe neonatal morbidity¹⁰.

Currently, no treatments are able to prevent intestinal inflammation and its sequelae following chorioamnionitis or to consequently prevent postnatal intestinal disorders⁹. Plant sterols, also known as phytosterols, are a dietary component derived from vegetable oils, fruits, nuts, and grains¹¹. They were first evaluated in the atherosclerosis field for their cholesterol-lowering effects¹². In addition, their immune-regulatory potential has been increasingly recognized¹³. Recently, these plant sterols were shown to possess anti-inflammatory properties in the context of intestinal inflammatory diseases such as inflammatory bowel disease¹⁴⁻¹⁶. Interestingly, this was recently confirmed in a small pilot study in fetal lambs, in which intestinal inflammation and mucosal injury following IA LPS exposure were prevented by plant sterol treatment¹⁷.

This pilot study prompted us to conduct the current in-depth study, in which chorioamnionitis was induced by viable *U. parvum* serovar 3, the micro-organism most frequently associated with chorioamnionitis. UP, a mycoplasma present in the female urogenital tract¹⁸, inflicts a milder hit than LPS does. Nevertheless, UP colonization in preterm infants has been found to increase NEC incidence twofold, with a gestational age-adjusted odds ratio (OR) of 2.47 (95% CI, 1.13–5.43)^{19,20}, making UP a clinically relevant stressor.

We IA-administered a mixture of β -sitosterol and campesterol, the two most common plant sterols in nature¹¹, as a treatment prior to IA injection of UP serovar 3. The effects of plant sterol treatment in the context of UP-induced chorioamnionitis were investigated by studying circulatory cytokine levels, fetal gut inflammation, intestinal delivery of the plant sterols, and intestinal injury and maturation.

Materials and methods

Experimental design

The animal studies were approved by the Animal Ethics Committee of the University of Western Australia (Perth, Australia), and the National Research Council's guide for the care and use of laboratory animals was followed. Time-mated Merino cross-breed ewes with singleton fetuses were randomly assigned to the 6 study groups. A total number of 50 animals were used, based on a power analysis with intestinal inflammation as the primary outcome.

Following drop-outs, the group size for data analyses was six to seven animals per group (**Figure 8.1**). Animals were group-housed with a 12-h dark/light cycle and had ad libitum access to food and water. Animal welfare was assessed daily by qualified personnel. The experiment was reported to be in compliance with the ARRIVE (Animal Research: Reporting of In Vivo Experiments) guidelines²¹.

To investigate whether plant sterols can be used as a nutritional intervention in utero to improve fetal outcomes in the context of chorioamnionitis, we deliberately chose IA administration, since the pharmacokinetics of plant sterols in sheep are to date unclear. In addition, several findings have supported the concept that plant sterol availability to the fetus is determined by the maternal diet. First, plant sterols are not synthesized by animals and humans and are exclusively gained through the diet²²: The natural presence of plant sterols in AF thus implies that maternal diet-derived plant sterols reach the AF^{23,24}. Second, the plant sterol transporter NPC1L1 is present in the human placenta^{22,25}. Finally, a meta-analysis from Ras et al. reported that oral plant sterol administration increases plasma plant sterol concentrations²⁶. Therefore, increasing plant sterol levels in the maternal diet is clinically the most relevant route of administration.

Therefore, we enriched the AF of pregnant ewes as a model for AF enrichment following maternal oral plant sterol intake. A mixture of β -sitosterol (70%) and campesterol (30%) (total of 0.6 mg/mL) dissolved in a carrier, 18% 2-hydroxypropyl- β -cyclodextrin (H107, Sigma Aldrich, St. Louis, MO, USA) in saline, carrier in saline, or saline alone was injected IA at 122 d of gestational age (GA), five days before IA UP injection. This dosage was chosen to supplement endogenous plant sterol concentration, starting with a twofold increase. Since the plant sterol mixture was hydrophobic, the carrier β -cyclodextrin was essential in dissolving the plant sterols (transport). Animals were injected every two days with additional IA injections containing saline or a plant sterol mixture until 131 d GA. AF samples were collected every 2 days from 122 d GA until preterm delivery at 133 d GA. Viable *U. parvum* serovar 3 (107 color changing units (CCUs)) or saline was given IA at 127 d of gestational age (GA). UP was grown in vitro and injected into the AF under ultrasound guidance as reported previously²⁷. AF sampled at 133 d GA was cultured for UP enumeration²⁸. Colonization of UP was not detected in the AF of controls. Fetuses were delivered preterm by caesarean section at 133 d GA (150 d \sim term), which is (with regard to the gut) comparable to 33–34 weeks of human gestation. Lambs were euthanized directly after delivery by an intravenous injection of pentobarbitone (100 mg/kg, Valaberb, Pitman-Moore, Australia). Distal ileum and blood samples for obtaining plasma were collected

postmortem. The investigators involved in the data analyses were blinded to treatment allocation.

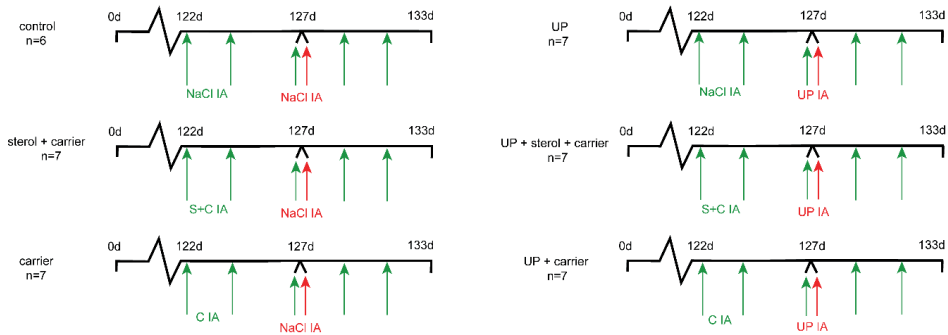


Figure 8.1 Experimental design. Animals were randomly assigned to six study groups of six to seven animals. Plant sterols dissolved with a carrier (C) (β -cyclodextrin) were given by intra-amniotic (IA) injection at 122 d of gestational age (GA), before onset of chorioamnionitis. Plant sterol injections were repeated every 2 days until 131 d GA, followed by premature delivery at 133 d GA. *U. parvum* serovar 3 (10^7 color changing units (CCUs)) was given by IA injection at 127 d GA to induce chorioamnionitis. Control groups had saline injections. Two groups received the carrier (β -cyclodextrin) IA without plant sterols to assess the carrier separately from the plant sterols. C, carrier; IA, intra-amniotic; S, plant sterols; UP, *U. parvum*.

Antibodies

The following antibodies were used: polyclonal rabbit antibody against human myeloperoxidase (MPO) (A0398, DakoCytomation, Glostrup, Denmark) and cluster of differentiation 3 (CD3) (A0452, DakoCytomation, Glostrup, Denmark), monoclonal rabbit antibody against human fork head box P3 (FoxP3) (clone eBio7979, 14-7979-82, eBioscience, San Diego, CA, USA), ovine interleukin-6 (IL-6) (MAB1004, Millipore, Darmstadt, Germany), and ovine IL-8 (MAB1044 Millipore, Darmstadt, Germany). Antibodies against intestinal fatty acid binding protein (I-FABP) were kindly provided by the Department of Surgery, Maastricht University Medical Centre, the Netherlands. Secondary antibodies were the following: biotin-conjugated rabbit antimouse (E0413, DakoCytomation, Glostrup, Denmark), swine antirabbit (E0353, DakoCytomation, Glostrup, Denmark), and peroxidase-conjugated goat antirabbit (111-035-045, Jackson, West Grove, PA, USA). Detection antibodies against IL-6 (AB1839, Millipore, Darmstadt, Germany) and IL-8 (AB1840, Millipore, Darmstadt, Germany) were used.

ELISA

Plasma I-FABP concentrations were assessed by ELISA. A high-sensitivity ELISA kit was kindly provided by the Department of Surgery, Maastricht University Medical Centre, the Netherlands. The protocol used was as described previously²⁹. Circulatory IL-6 and IL-8 concentrations were measured to assess whether systemic inflammation was present as previously described³⁰. Briefly, a 96-well plate (ELISA 96-well, Greiner Bio One) was precoated with 100 μ l of IL-6 (5 μ g/mL) or IL-8 (5 μ g/mL) antibodies overnight at 4°C. After

incubation and washing, nonspecific binding sites were blocked. For the standard curve, protein standards were prepared by two-step serial dilutions of recombinant IL-6 or IL-8 (ImmunoChemistry Technologies, Bloomington, MN, USA). Diluted plasma samples and protein standards were added in duplicate and incubated for 2 h at 37°C. After washing, detection antibodies were added for one hour at room temperature (RT). Detection antibodies against IL-6 or IL-8 were detected using a peroxidase-conjugated antibody and 3, 3', 5, 5'-tetramethylbenzidine (TMB) substrate solution (Sigma Aldrich, St. Louis, MO, USA).

Immunohistochemistry

We fixed distal ileum in 4% paraformaldehyde, embedded it in paraffin, and cut 4-um sections with a Leica RM2235 microtome to perform immunohistochemistry studies. Intestinal mucosal damage and morphological changes were assessed using hematoxylin and eosin staining (H&E). Per animal, a histological score was assigned to the intestinal section by 2 blinded investigators. The following scoring system (from no injury to severe injury) was developed to describe the severity of histological injury: no damage, mild damage (disrupted epithelial lining, but no loss of enterocytes), moderate damage (disrupted epithelial lining, moderate enterocyte loss from the villus tips), or severe damage (a disrupted epithelial lining, abundant enterocyte loss from villus tips).

Sections were stained for CD3, FoxP3, MPO, and I-FABP as described previously⁶. Briefly, endogenous peroxidase activity was blocked with 0.3% H₂O₂ in phosphate-buffered saline. For CD3, antigen retrieval was performed by boiling in 10 mM of sodium-citrate buffer (pH 6.0) for 10 min. Blocking of nonspecific binding sites was performed with normal goat serum (MPO) or bovine serum albumin (CD3, FoxP3, I-FABP) for 30 min at room temperature. Subsequently, slides were incubated with the primary antibody of interest for one hour at room temperature (MPO) or overnight at 4°C (CD3, FoxP3, I-FABP). After washing, slides were incubated with biotin-conjugated (CD3, FoxP3) or peroxidase-conjugated secondary antibodies (MPO, I-FABP). MPO and I-FABP positivity was visualized with 3-amino-9-ethylcarbazole (AEC, Sigma Aldrich, St. Louis, MO, USA). CD3- and FoxP3-positive cells were detected using nickel-3, 3'-diaminobenzidine (Sigma Aldrich, St. Louis, MO, USA). Nuclei were counterstained with hematoxylin (MPO and I-FABP) or with nuclear fast red (CD3 and FoxP3). The number of MPO-, CD3-, and Foxp3-positive cells were counted per high power fields (100x) using a light microscope (Leica Microsystem CTG, type DFC295) and ImageJ (1.52b software, National Institutes of Health, USA). For MPO, the number of MPO+ cells present in the villi was determined separately, and the percentage of MPO+ cells in the villi compared to the total MPO+ cell count was determined. The average value of five representative high power fields was used for the analyses.

Gas–Liquid Chromatography–Mass Spectrometry (GC-MS)

Plant sterols (β -sitosterol and campesterol), cholesterol and cholesterol precursor (desmosterol and lathosterol) concentrations in plasma (lathosterol), and AF samples (demosterol and lathosterol) were measured using gas chromatography–mass spectrometry as described previously¹².

Matrix-Assisted Laser Desorption Ionization Mass Spectrometry Imaging

To study the distribution and changes in intestinal lipid profiles in more detail, molecular analysis of the distal ileum ($n=3$ per group) was performed by matrix-assisted laser desorption ionization mass spectrometry imaging (MALDI-MSI). After sampling, the intestinal tissues of all treatment groups (control, sterol + carrier, carrier, 6-d UP, 6-d UP + sterol + carrier, and 6-d UP + carrier) were frozen in liquid nitrogen, and cryo-sections of 10 μm were cut in a cryostat (Leica CM3050S, Amsterdam, the Netherlands). The tissue sections were deposited on indium tin oxide conductive slides (Delta Technologies, USA) and stored at -20°C . A matrix solution consisting of norharman (7 mg/mL) in 2:1 chloroform/methanol was sprayed on top of the tissue sections by using a TM-Sprayer M3 (HTX Technologies Carrboro, NC, USA). The imaging experiments were performed with a Bruker RapifleX MALDI TissueTyper in reflectron mode (Bruker Daltonik GmbH, Germany) at a raster size of 80 μm . Data were acquired in positive ion mode in the mass range m/z 300–1600 and in negative ion mode in the mass range m/z 350–1600. Each tissue section was used for both polarities, with an offset of 40 μm in the X/Y directions. High spatial resolution experiments were performed using 5 mg/mL of α -cyano-4-hydroxycinnamic acid (Sigma Aldrich, St. Louis, MO, USA) in 70% acetonitrile and 0.2% trifluoroacetic acid and were sprayed with a SunCollect sprayer (SunChrom). Data were acquired in positive mode with a MALDI HDMS SYNAPT G2-Si mass spectrometer (Waters, Manchester, UK) with a modified MALDI source unit, which achieves a laser spot 15 μm in diameter at a spatial resolution of 20 μm^{31} . Lipid identifications were obtained using a high-mass resolution MALDI-MSI Orbitrap Elite Hybrid Ion trap mass spectrometer (Thermo Fisher Scientific, Bremen, Germany). Tandem Mass Spectrometry (MS/MS) spectra (**Table S8.1**, **Table S8.2**) were submitted to the ALEX123 lipid database (<http://alex123.info/ALEX123/MS.php>). To study differences between all conditions, principal component analyses (PCAs) and discriminant analysis (DA) were performed. Both the PCAs and DA were performed by using an in-house built ChemomeTricks toolbox for MATLAB version 2014a (MathWorks, Natick, MA, USA). For analyzing lipid patterns in the intestinal epithelium, luminal lipid signals were excluded from the data analyses. Only for an analysis of β -cyclodextrin presence were luminal signals included.

Statistics

Statistical analyses were performed using GraphPad Prism software (version v6.0, GraphPad Software Inc., La Jolla, CA, USA). Data are presented as the median with an interquartile range (IQR) for all read-outs, except for the damage score, where only the median is presented. A nonparametric Kruskal–Wallis test followed by Dunn’s post hoc test was used to analyze significant differences between the groups. Differences were regarded as statistically significant at $p<0.05$: p -values ≤ 0.1 were interpreted as biologically relevant, as previously described³².

Results

Systemic and Intestinal Inflammation

Systemic Inflammation

Plant sterol treatment before and during UP exposure significantly lowered systemic IL-6 concentrations compared to UP-exposed animals ($p < 0.05$) (**Figure 8.2**). No significant changes were observed in IL-8 plasma concentrations among the several treatment groups (**Supplementary Figure S8.1**).

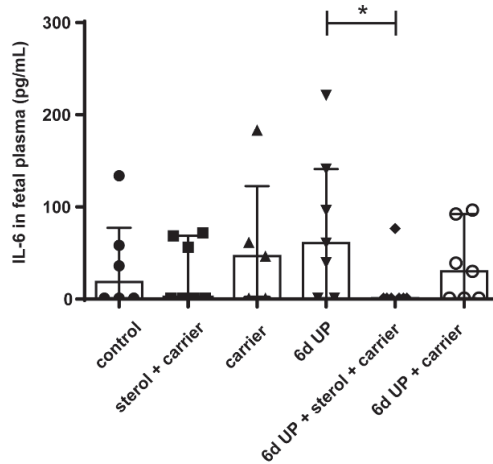


Figure 8.2 Circulatory IL-6 levels in fetuses of 133 d GA. Plant sterols significantly inhibited circulatory IL-6 levels. * $p < 0.05$. GA, gestational age; UP, *U. parvum*.

Intestinal inflammation

The percentage of MPO-positive cells that migrated into the villi in the distal ileum increased significantly after 6 d of UP exposure ($p < 0.05$) compared to control animals (**Figure 8.3A,B,D**). This increase tended to be reduced ($p = 0.10$) by plant sterols (**Figure 8.3C,D**). The number of FoxP3+ and CD3+ cells did not differ with statistical significance between the experimental groups (**Figure 8.4A,B**). The FoxP3+/CD3+ ratio tended to be reduced in fetuses exposed to UP ($p = 0.06$), which was not restored by plant sterol treatment. Remarkably, plant sterol treatment alone also tended to reduce the FoxP3+/CD3+ ratio ($p = 0.09$) (**Figure 8.4C**).

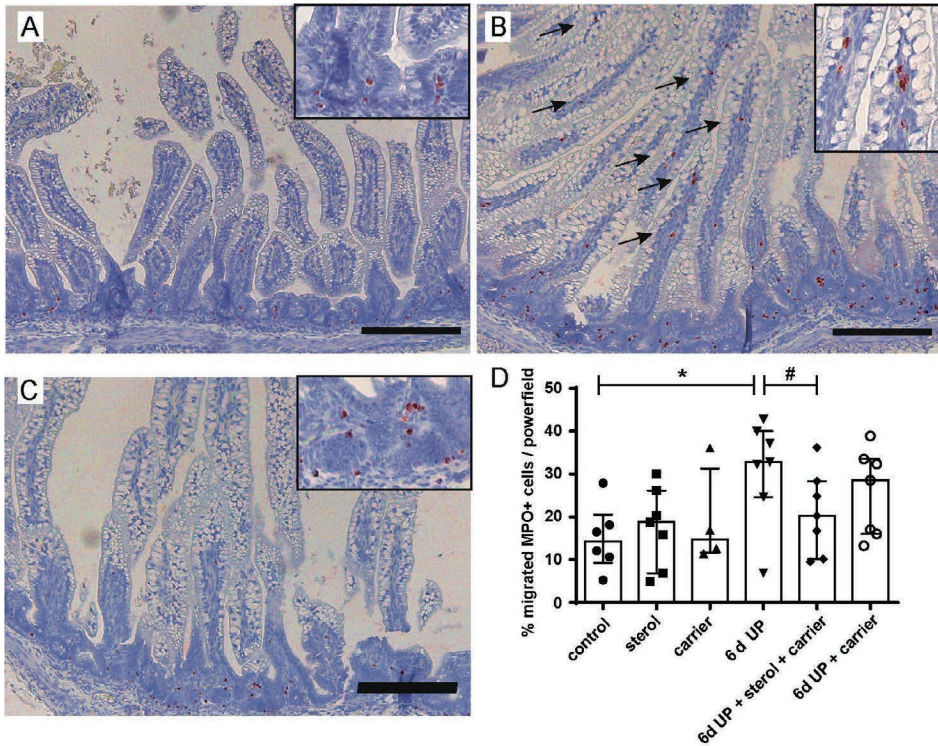


Figure 8.3 Immunohistochemical distribution of MPO-positive cells. (A) In control fetuses, MPO-positive cells were predominantly located in the lower crypt region. (B) After 6 d of UP exposure, the percentage of migrated MPO-positive cells (indicated by black arrows) increased compared to control fetuses. (C) An influx of MPO-positive cells in the villi tended to be prevented after treatment with plant sterols. (D) The total number of MPO-positive cells and the number of migrated MPO-positive cells were counted per high-power field, and the mean value of the count in five representative high-power fields is given. Scale bar indicates 200 μm . * $p < 0.05$; # $0.05 < p < 0.10$. MPO, myeloperoxidase; UP, *U. parvum*

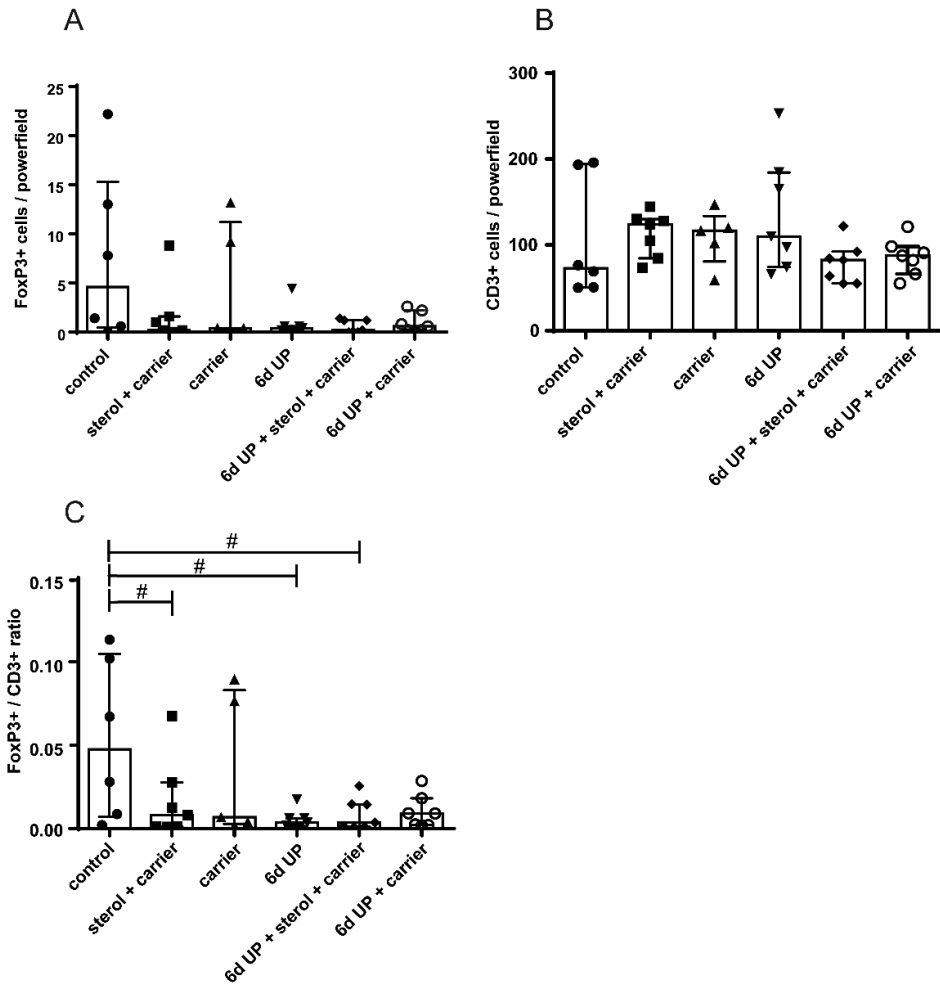


Figure 8.4 The number of CD3-positive cells, FoxP3-positive cells, and the FoxP3+/CD3+ ratio in the distal ileum of preterm lambs. (A) FoxP3-positive cells and (B) CD3-positive cells are displayed for all treatment groups. No significant differences were observed. (C) The FoxP3+/CD3+ ratio tended to be reduced in fetuses of the sterol + carrier, 6-d UP, and 6-d UP + sterol + carrier groups. The number of CD3+ and FoxP3+ cells were counted per high-power field, and the mean value of the count in five representative high-power fields is given. # 0.05 < p < 0.10. CD3, cluster of differentiation 3; FoxP3, fork head box P3; UP, *U. parvum*

UP and sterol concentrations in amniotic fluid

UP infection was confirmed by the presence of UP in the AF of ewes injected with UP (**Supplementary Figure S8.2**). No statistically significant differences were observed in UP CCUs between the three treatment groups. No UP CCUs were present in the AF of animals that were not injected with UP.

IA concentrations of β -sitosterol in the sterol group increased with repeated doses and were statistically significantly ($p < 0.05$) elevated compared to controls at 133 d GA, indicating the accumulation of β -sitosterol over time with IA delivery (**Figure 8.5A**). Here, β -sitosterol concentrations were not statistically significantly increased in the 6-d UP group treated with plant sterols at 133 d GA. The AF campesterol concentration tended to be increased ($p=0.09$) at 133 d GA in ewes that were treated with IA plant sterols compared to control ewes (**Figure 8.5B**). Campesterol was not statistically significantly elevated in the AF of ewes that were exposed to UP and plant sterols at 133 d GA. No statistically significant differences were found in lathosterol, desmosterol, and cholesterol concentrations in the AF between treatment groups (**Supplementary Figure S8.3**).

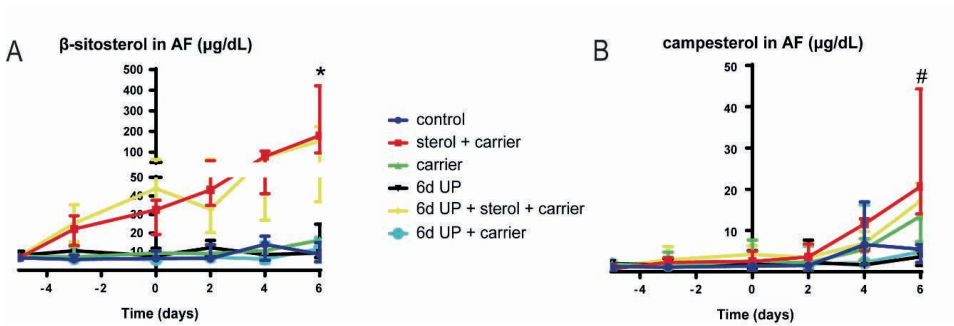


Figure 8.5 AF concentrations of β -sitosterol and campesterol. AF samples were taken every two days from 122 d GA until preterm delivery at 133 d GA. (A) AF concentrations of β -sitosterol were significantly increased at day 11 in the sterol + carrier group. (B) AF concentrations of campesterol tended to be increased at day 11 in the sterol + carrier group. Day 0 (122 d GA) is the start of plant sterol treatment, day 5 (127 d GA) is the day of intra-amniotic UP injection, and day 11 (133 d GA) is the moment of preterm delivery. * $p < 0.05$; # $0.05 < p < 0.10$. AF, amniotic fluid; GA, gestational age; UP, *U. parvum*

Sterol concentrations in fetal plasma

Fetal plasma concentrations of β -sitosterol and campesterol in the sterol-supplemented groups were not significantly elevated at 133 d GA compared to the other groups (**Figure 8.6A,B**). Lathosterol concentrations were statistically significantly decreased after 6 d of UP exposure with plant sterol treatment ($p < 0.05$) and tended to be decreased after 6 d of UP exposure alone ($p = 0.10$) compared to the control animals (**Figure 8.6C**). The changes in plasma lathosterol concentrations did not result in altered plasma cholesterol concentrations in the different experimental groups (**Figure 8.6D**).

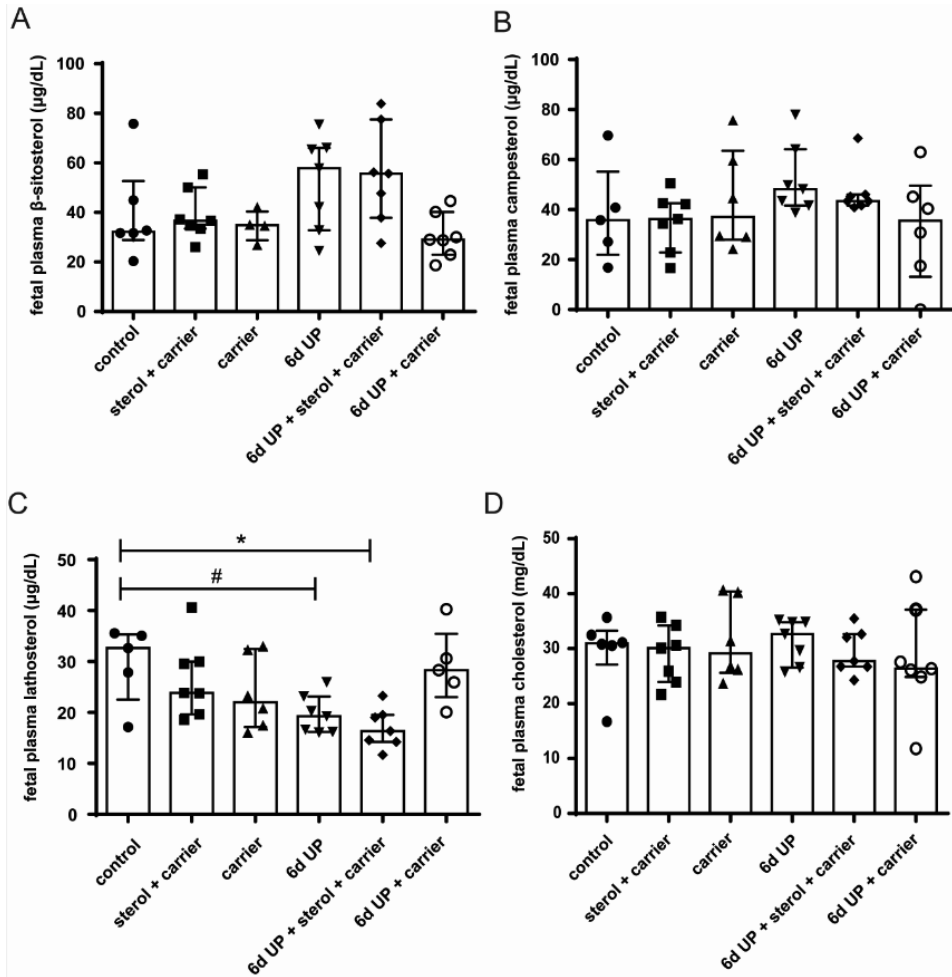


Figure 8.6 Circulatory β -sitosterol, campesterol, lathosterol (cholesterol precursor), and cholesterol levels in lambs of 133 d GA (preterm delivery). No significant differences were found for β -sitosterol (A) and campesterol (B) in all treatment groups. (C) UP exposure with and without plant sterol treatment reduced lathosterol plasma concentrations compared to controls. (D) Plasma cholesterol concentrations were not affected by UP exposure and/or plant sterol treatment. * $p < 0.05$; # $0.05 < p < 0.10$. GA, gestational age; UP, *U. parvum*.

Intestinal damage and gut maturation

Enterocyte loss at the villi tips in H&E stained ileal tissue, indicating moderate to severe intestinal damage, was found in five out of seven of the 6-d UP-exposed lambs, compared to one out of six controls (**Figure 8.7A,B**; **Supplementary Figure S8.4**). Intestinal damage was partly blocked by the administration of plant sterols (only two out of six had moderate to severe damage) and the carrier (three out of seven had moderate to severe damage) (**Figure**

8.7C,D; Supplementary Figure S8.4). No changes were observed in fetal plasma concentrations of I-FABP (**Supplementary Figure S8.5**), a small protein present in the cytoplasm of mature enterocytes. Furthermore, the sizes of enterocyte vacuoles were increased in all experimental groups when compared to control animals (**Figure 8.7A–D**).

To assess enterocyte maturation, the distribution of I-FABP was analyzed in the distal ileum. I-FABP expression was altered in the 6-d UP-exposed fetuses compared to controls, as expression was more localized in the intestinal crypts (**Figure 8.8A,B**). This disturbed I-FABP distribution was partially restored by carrier administration (**Figure 8.8C**) as well as by plant sterol treatment (**Figure 8.8D**).

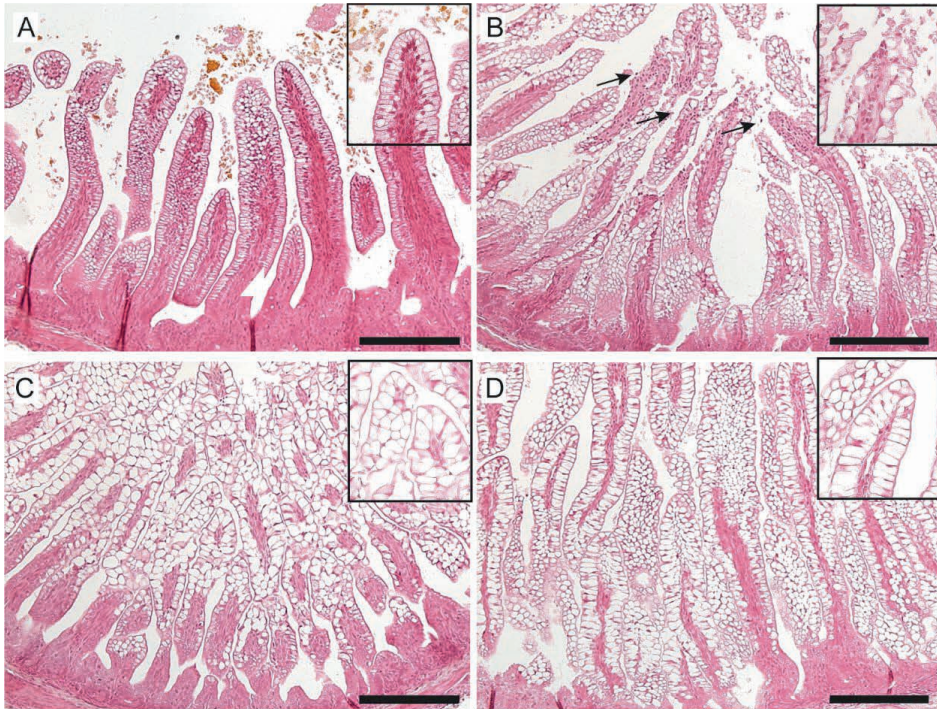


Figure 8.7 Evaluation of morphological changes and enterocyte vacuolization in the distal ileum of preterm lambs by H&E staining in control (A), UP-exposed (B), UP + carrier-exposed (C), and UP + sterol + carrier-exposed fetal lambs (D). Injury of the villi tips (arrows) was observed after 6 d UP exposure, which was prevented by carrier and/or sterol + carrier treatment. The size of the vacuoles within the enterocytes was increased in all experimental groups and most profoundly in UP + carrier and UP + sterol + carrier animals. Scale bar indicates 200 μm . H&E, hematoxylin and eosin; UP, *U. parvum*.

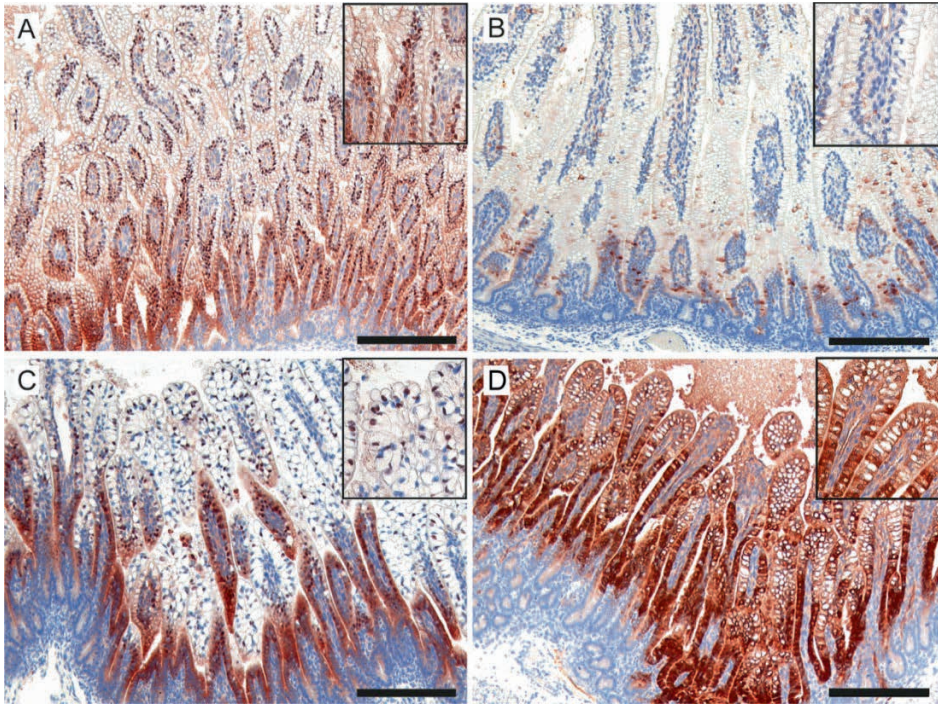


Figure 8.8 Expression pattern of I-FABP in the ileal gut. (A) In control fetuses, I-FABP expression was present along the crypt–villi axis. (B) This pattern was disrupted in UP-exposed lambs, where I-FABP expression was more localized in the intestinal crypts. (C) The I-FABP expression pattern was restored in most preterm lambs treated with the carrier, without and with (D) plant sterols with a pattern comparable to that seen in the control intestinal samples. Scale bar indicates 200 μ m. I-FABP, intestinal fatty acid binding protein; UP, *U. parvum*.

Changes in lipid profiles in the fetal gut

MALDI-MSI was used for the following reasons: 1) to study changes in the morphological appearance of the vacuolated enterocytes after plant sterol treatment, 2) as an additional read-out for inflammation, and 3) to confirm that plant sterols were delivered in the fetal intestinal lumen following IA plant sterol administration. Interestingly, lipid composition was changed after 6 d UP exposure compared to the other treatment groups and was characterized by an increased presence of different phosphatidylcholines (PCs) and sphingomyelins (SMs), as the first discriminant function (DF1) shows (**Figure 8.9A–C**).

A clear accumulation of m/z 782.58 PC 34:1 [M+Na]⁺ was detected in the 6-d UP group compared to the control situation (**Figure 8.9C**). Furthermore, m/z 810.60 PC 36:1 [M + Na]⁺ and m/z 725.57 SM 34:1 [M+Na]⁺ were also enriched in the 6-d UP group lipid profile (**Figure 8.9B**). These UP-induced changes of the intestinal lipidome were partially reduced by plant sterols and/or the carrier (**Figure 8.9D–G**). The carrier was characterized by m/z 1331.52 [M+Na]⁺ and was confirmed by tandem MS³³. Other peaks related to the carrier, such as m/z 1273.48, m/z 1389.55, and m/z 1447.59, were also detected in the intestinal epithelium of the sterol + carrier, carrier, UP + sterol + carrier, and UP + carrier groups (**Figure 8.9F,G**). The presence of the carrier was mainly detected in the intestinal lumen in all carrier and plant sterol groups (sterol + carrier, carrier, 6-d UP + sterol + carrier, and 6-d UP + carrier), but not in the control and 6-d UP groups (**Figure 8.10**), showing intraluminal delivery and subsequent uptake in the distal ileum.

Lipid species, including phosphatidylinositols (PIs) and bile acids (BAs), were identified in the negative ion mode by using MALDI-MSI (**Figure 8.11**). In line with the results in the positive ion mode, the most profound lipidome changes were detected in the UP-exposed animals (**Figure 8.11A**). More precisely, a higher abundance of m/z 885.58 PI 38:4 [M-H]⁻ and a strong reduction of dihydroxy BA m/z 498.29 taurodeoxycholic acid/taurochenodeoxycholic acid [M-H]⁻ (TCDA/TCDCDA) and trihydroxy BA m/z 514.29 [M-H]⁻ taurocholic acid (TCA) following UP infection were found, which were indicative of a proinflammatory environment and a reduced BA status (**Figure 8.11A,B**). These UP-induced lipidome and BA changes detected in the negative ion mode were partially prevented by plant sterol and/or carrier administration (**Figure 8.11C–F**).

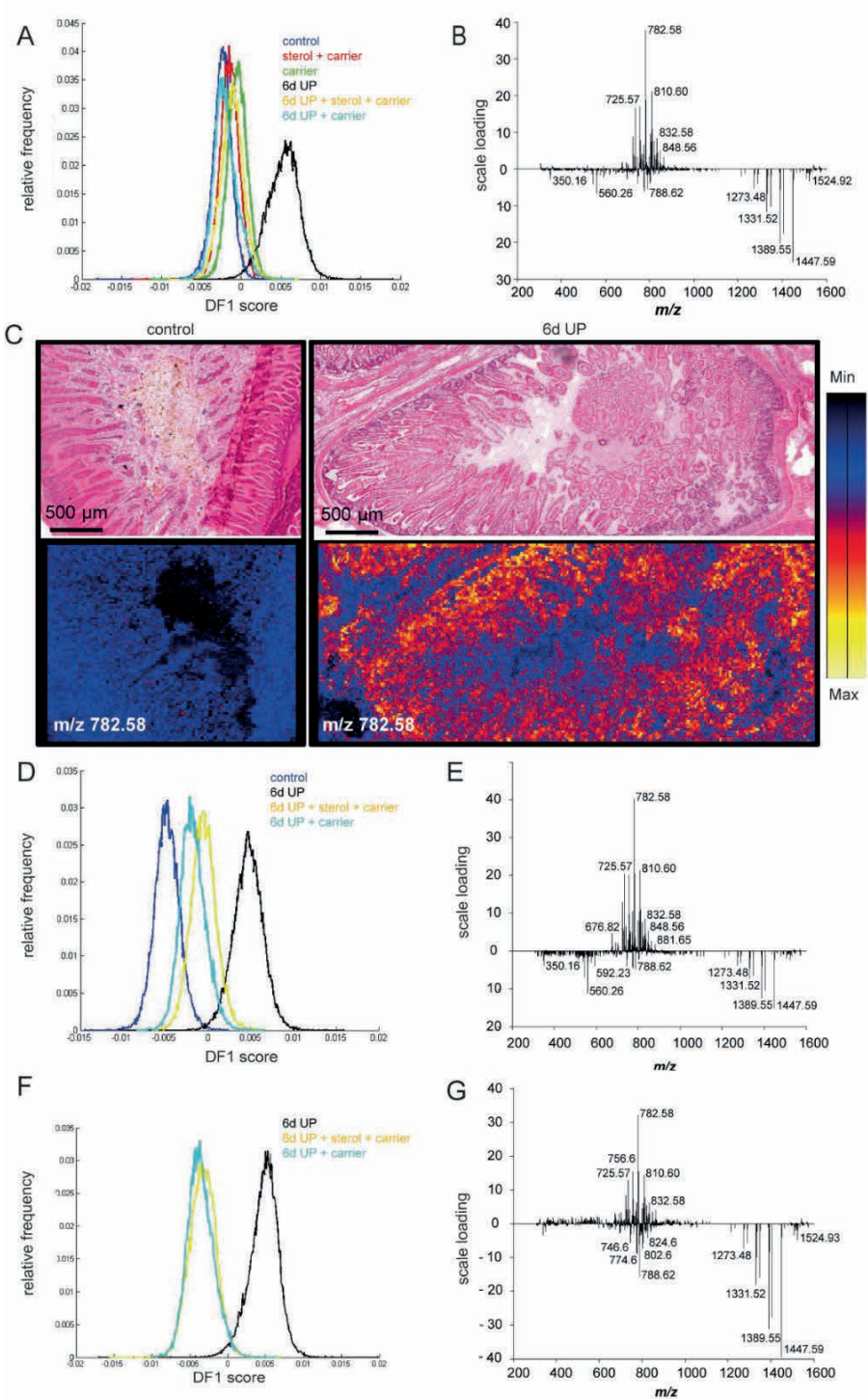


Figure 8.9 Matrix-assisted laser desorption ionization mass spectrometry imaging performed in positive ion mode followed by principal component analysis. The first discriminant function is shown. (A) Intestinal lipid composition was changed after 6 d UP exposure compared to the other treatment groups, (B, C) with increased presence of different PCs and SMs in the 6-d UP group, including m/z 782.58 PC 34:1 [M+Na]⁺, m/z 810.60 PC 36:1 [M+Na]⁺, and m/z 725.57 SM 34:1 [M+Na]⁺. (D,E,F,G) These UP-induced changes in the intestinal lipidome were partially normalized by plant sterols and/or the carrier. The carrier (2-hydroxypropyl- β -cyclodextrin), characterized by m/z 1331.52 [M+Na]⁺, m/z 1389.55, and m/z 1447.59, was detected in the intestinal epithelium of the 6-d UP + sterol + carrier and the 6-d UP + carrier groups. PCs, phosphocholines; SMs, sphingomyelins; UP, *U. parvum*.

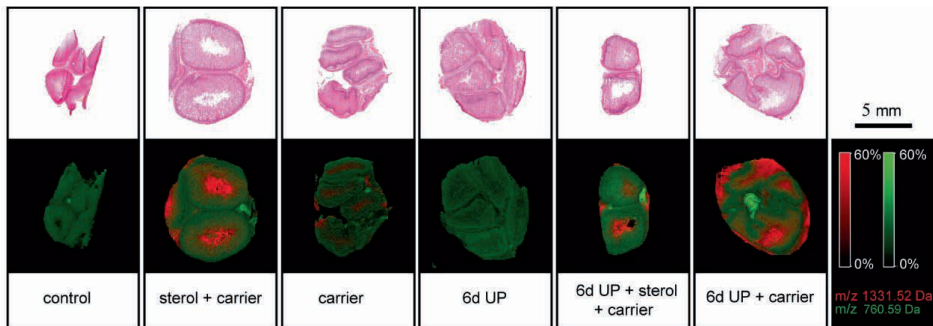


Figure 8.10 Presence of the carrier, indicated by m/z 1331.52 [M+Na]⁺, was detected in the intestinal lumen in the carrier, 6-d UP + carrier, sterol + carrier, and 6-d UP + sterol + carrier groups, but not in the control and 6-d UP groups. m/z 760.59 [M+H]⁺ was a homogenously distributed PC lipid present in the intestinal epithelial layer. Scale bar indicates 5 mm. PCs, phosphocholines; UP, *U. parvum*

Discussion

An important finding was that IA plant sterol administration decreased the fetal systemic inflammatory response (circulatory IL-6 levels) during UP-driven chorioamnionitis. This corresponds with a study from Bouic et al. showing that a systemic inflammatory response following excessive exercise (increased serum IL-6 concentrations) was prevented by supplementing ultramarathon athletes with capsules containing a mixture of plant sterols^{34,35}. This decrease in systemic inflammation was supported by work from Nashed et al., who showed that splenocytes cultured from plant sterol-treated apo E-knockout mice reduced the production of IL-6 upon stimulation with LPS³⁶.

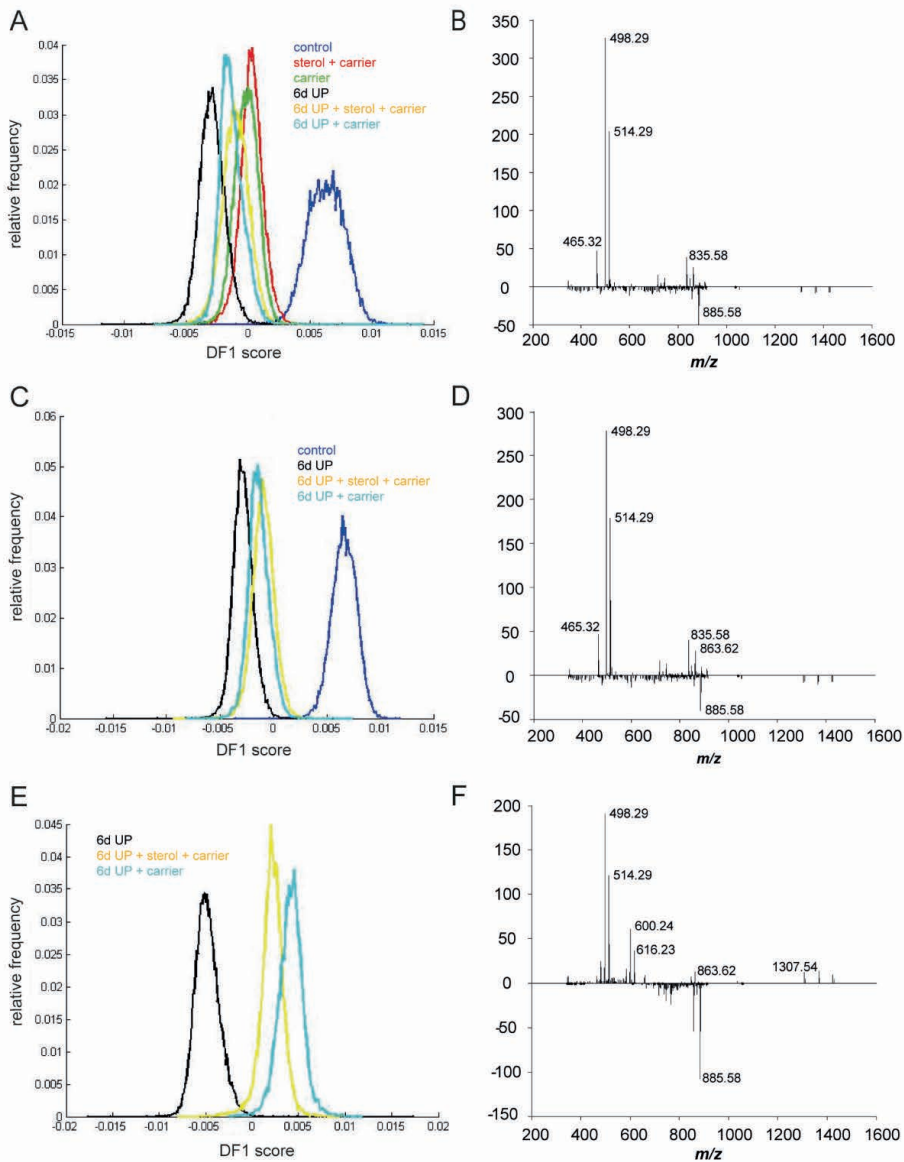


Figure 8.11 Matrix-assisted laser desorption ionization mass spectrometry imaging performed in negative ion mode followed by principal component analysis. The first discriminant function is shown. (A) 6-d UP group animals showed an altered lipid profile compared to the other treatment groups, (B) with a higher abundance of m/z 885.58 PI 38:4 [M-H]⁻ and a reduced presence of m/z 498.29 [M-H]⁻ dihydroxy BA TCDA/TCDA and m/z 514.29 [M-H]⁻ trihydroxy BA TCA. (C,D,E,F) In the 6-d UP + sterol and 6-d UP + sterol + carrier groups, UP-induced lipidome and BA changes were partially prevented with a profile comparable to the controls. BA, bile acid; PI, phosphatidylinositol; TCA, taurocholic acid; TCDA, taurodeoxycholic acid; TCDA, taurochenodeoxycholic; UP, *U. parvum*.

In addition, our data suggest that IA plant sterol treatment partially modulates fetal intestinal inflammation in response to UP infection. This result is supported by a recent pilot study in which we showed that IA plant sterol administration completely prevented mucosal neutrophil infiltration in ovine fetuses IA exposed to LPS instead of UP¹⁷. In this study, IA LPS exposure provoked excessive inflammation and severe epithelial injury. Such severe injury might be a prerequisite to better detect the protective effects of plant sterols. In an earlier study of UP-induced chorioamnionitis, we reported that intestinal inflammation after IA UP exposure was characterized by an imbalance between regulatory T-cells (Treg) and effector T-cells³⁷. This was confirmed in the current study, where we observed a trend toward a reduced FoxP3+/CD3+ ratio with UP exposure. In our experiments, IA plant sterol administration tended to decrease the FoxP3+/CD3+ ratio, indicating that IA plant sterol administration may suppress the number of intestinal Tregs. Other studies have also reported the effects of plant sterols on Treg cell numbers, although both increased and decreased Treg numbers have been observed. More precisely, Te Velde et al. found an increase in Treg numbers and a decrease in total T-cell numbers in the colon in a murine T-cell transfer colitis model after dietary plant sterol enrichment¹⁴. De Smet et al. showed that oral administration of plant sterols reduced both Treg numbers and T-cell numbers in the jejunum of healthy volunteers with a concomitant reduction in T-cell-associated gene expression³⁸. This variation illustrates that the effect of plant sterols on T-cells is determined by the underlying pathophysiology, intestinal region, timing of the intervention, duration, and nature of the inflammatory stimulus and developmental stage.

Since plant sterols are known to influence cholesterol metabolism, which may be relevant to fetal/neonatal growth and development³⁹, cholesterol and cholesterol precursor concentrations in AF and plasma were studied. No changes were seen in AF and fetal plasma in the plant sterol group compared to the control group, indicating that plant sterol administration did not disturb systemic cholesterol concentrations or cholesterol synthesis in the fetus. The reason for the increased size of enterocyte vacuoles following plant sterol and carrier supplementation remains unknown. Interestingly, UP administration did reduce endogenous cholesterol synthesis, as reflected by reduced fetal plasma lathosterol concentrations. The mechanisms by which IA UP exposure can influence endogenous cholesterol synthesis are currently unclear. The disturbance of endogenous cholesterol synthesis was not prevented by plant sterol administration.

In this study, we found an enrichment of phospholipids (i.e., phosphatidylcholines, sphingomyelins, and phosphatidylinositol)^{40–43} present in the cell membrane and involved in diverse cell signaling processes following IA UP exposure. Interestingly, similar changes in the cerebral lipodome were found by Gussenhoven et al. in ovine fetuses after two days of IA LPS exposure, and these changes were indicative of an inflammation-induced “diseased” lipid profile⁴⁴. Although such lipid disturbances have been associated with detrimental effects on the central nervous system, immune system, and skeletal muscles⁴⁵, the significance for the intestine is still unknown⁴⁶.

Besides changes in phospholipids, BAs were reduced in UP-exposed animals. BAs are critical to the facilitation of dietary lipid absorption, intestinal antimicrobial defense^{47,48}, and regulation of gastrointestinal motility^{49,50}. A reduction of intestinal BA following antenatal UP exposure might therefore subvert lipid malabsorption, microbial defense, and intestinal

motility, which are known risk factors for NEC development⁵¹⁻⁵³. In line with this theory, an increased incidence of NEC has been associated with UP infections^{19,20}.

Interestingly, in this study, plant sterols and/or the carrier reduced mucosal damage and stimulated the maturation of enterocytes. Based on these data, we cannot define to what extent plant sterols and/or the carrier are responsible for protective gut barrier/maturation effects, but several findings have indicated that the effects are plant sterol-specific. First, as we recently showed, plant sterol administration, but not the carrier, prevented severe damage to the fetal gut following LPS-induced chorioamnionitis¹⁷. Second, plant sterols prevent systemic inflammation, which is a known inducer of gut integrity loss.

In this short-term proof of concept study, repetitive IA plant sterol injections induced a gradual increase in AF plant sterol concentrations. This ultimately led to a 10-fold increase, which is likely higher than can be expected following maternal oral administration of plant sterols. Further studies are thus needed to explore the potential beneficial effects of a maternal oral nutritional intervention with β -sitosterol and campesterol on the fetus over time.

In our study, we found therapeutic effects of the carrier β -cyclodextrin that were milder, but which recapitulated the effects of β -cyclodextrin + plant sterols. Overlapping working mechanisms of both plant sterols and β -cyclodextrin may explain these findings: β -cyclodextrin has previously been shown to exert anti-inflammatory effects in the field of atherosclerosis⁵⁴⁻⁵⁶, mediated (among other things) by an increase in liver-X-receptor (LXR) target gene expression⁵⁶. Interestingly, plant sterols are also known activators of LXRs⁵⁷, and LXR signaling has been implicated in playing a role in experimental colitis and inflammatory bowel disease^{58,59}. As more prominent and exclusive effects of plant sterols are seen when compared to carrier-only-treated animals, it is tempting to speculate that plant sterols target LXR-independent pathways, which remains to be further elucidated.

Conclusions

In conclusion, we showed in this proof of concept study that IA β -sitosterol and campesterol administration prevented fetal systemic and intestinal inflammation. Moreover, the combined results from the LPS- and UP-induced chorioamnionitis models showed that plant sterols have the potential to prevent intestinal mucosal injury. Future studies are required to investigate the pharmacokinetics of plant sterols in the fetus following maternal intake during human pregnancy to further dissect the role of plant sterols and the carrier in the protection of the fetal gut and ultimately unravel the clinical potential of plant sterols in the perinatal context.

References

1. Liu L, Oza S, Hogan D, Chu Y, Perin J, Zhu J, Lawn, JE, Cousens S, Mathers C, Black, RE. Global, regional, and national causes of under-5 mortality in 2000–15: an updated systematic analysis with implications for the Sustainable Development Goals. *Lancet* 2016;388:3027–3035.
2. Blencowe H, Cousens S, Oestergaard MZ, Chou D, Moller AB, Narwal R, Adler A, Garcia CV, Rohde S, Say L, et al. National, regional, and worldwide estimates of preterm birth rates in the year 2010 with time trends since 1990 for selected countries: a systematic analysis and implications. *Lancet* 2012;379:2162–2172.
3. Kim CJ, Romero R, Chaemsaitong P, Chaiyasit N, Yoon BH, Kim YM. Acute Chorioamnionitis and Funisitis: Definition, Pathologic Features, and Clinical Significance. *Am J Obstet Gynecol* 2015;213: S29–S52.
4. Wolfs TG, Jellema RK, Turrisi G, Becucci E, Buonocore G, Kramer BW. Inflammation-induced immune suppression of the fetus: a potential link between chorioamnionitis and postnatal early onset sepsis. *Matern-Fetal Neonatal Med* 2012;25:8–11.
5. Wolfs TGAM, Buurman WA, Zoer B, Moonen RMJ, Derikx JPM, Thuijls G, Villamor E, Gantert M, Garnier Y, Zimmermann LJ, et al. Endotoxin Induced Chorioamnionitis Prevents Intestinal Development during Gestation in Fetal Sheep. *PLoS One* 2009;4:e5837.
6. Wolfs TG, Kallapur SG, Knox CL, Thuijls G, Nitsos I, Polglase GR, Collins JJ, Kroon E, Spierings J, Shroyer NF, et al. Antenatal ureaplasma infection impairs development of the fetal ovine gut in an IL-1-dependent manner. *Mucosal Immunol* 2013;6:547–556.
7. Been JV, Lievense S, Zimmermann LJ, Kramer BW, Wolfs TG. Chorioamnionitis as a Risk Factor for Necrotizing Enterocolitis: A Systematic Review and Meta-Analysis. *J Pediatr* 2013;162:236–242.e2.
8. Gantert M, Been JV, Gavilanes AW, Garnier Y, Zimmermann LJ, Kramer BW. Chorioamnionitis: a multiorgan disease of the fetus?. *J Perinatol* 2010;30:S21–S30.
9. Neu J, Walker WA. Necrotizing Enterocolitis. *New Engl. J Med* 2011;364:255–264.
10. Gotsch F, Romero R, Kusanovic JP, Mazaki-Tovi S, Pineles BL, Erez O, Espinoza J, Hassan SS. The Fetal Inflammatory Response Syndrome. *Clin Obstet Gynecol* 2007;50:652–683.
11. Gylling H, Plat J, Turley S, Ginsberg HN, Ellegård L, Jessup W, Jones PJ, Lütjohann D, Maerz W, Masana L, et al. Plant sterols and plant stanols in the management of dyslipidaemia and prevention of cardiovascular disease. *Atherosclerosis* 2014;232:346–360.
12. De Jong A, Plat J, Lütjohann D, Mensink RP. Effects of long-term plant sterol or stanol ester consumption on lipid and lipoprotein metabolism in subjects on statin treatment. *Br J Nutr* 2008;100:937–941.
13. Brüll F, De Smet E, Mensink RP, Vreugdenhil A, Kerksiek A, Lütjohann D, Wesseling G, Plat J. Dietary plant stanol ester consumption improves immune function in asthma patients: results of a randomized, double-blind clinical trial. *Am J Clin Nutr* 2016;103:444–453.
14. Velde AAT, Brüll F, Heinsbroek SEM, Meijer SL, Lütjohann D, Vreugdenhil A, Plat J, Velde AT. Effects of Dietary Plant Sterols and Stanol Esters with Low- and High-Fat Diets in Chronic and Acute Models for Experimental Colitis. *Nutrients* 2015;7:8518–8531.
15. Aldini R, Micucci M, Cevenini M, Fato R, Bergamini C, Nanni C, Cont M, Camborata C, Spinozzi S, Montagnani M, et al. Antiinflammatory Effect of Phytosterols in Experimental Murine Colitis Model: Prevention, Induction, Remission Study. *PLoS One* 2014;9:e108112.
16. Lee IA, Kim EJ, Kim DH. Inhibitory Effect of β -Sitosterol on TNBS-Induced Colitis in Mice. *Planta Med* 2012;78:896–898.
17. Plat J, Baumgartner S, Vanmierlo T, Lütjohann D, Calkins KL, Burrin DG, Guthrie G, Thijs C, Te Velde AA, Vreugdenhil ACE, et al. Plant-based sterols and stanols in health & disease: "Consequences of human development in a plant-based environment?". *Prog Lipid Res* 2019; 74:87-102
18. Goldenberg RL, Andrews WW, Hauth JC. Intrauterine Infection and Preterm Delivery. *New Engl J Med* 2000;342:1500–1507.
19. Viscardi RM. Ureaplasma species: role in neonatal morbidities and outcomes. *Arch. Dis. Child.-Fetal Neonatal Ed* 2014;99:F87–92.

20. Okogbule-Wonodi AC, Gross GW, Sun CCJ, Agthe AG, Xiao L, Waites KB, Viscardi RM, Okogbule-Wonodi GWGAC. Necrotizing Enterocolitis is associated with Ureaplasma Colonization in Preterm Infants *Pediatr Res* 2011;69:442–447.
21. Kilkenny C, Browne W, Cuthill IC, Emerson M, Altman DG. Animal research: Reporting in vivo experiments: The ARRIVE guidelines. *Br J Pharmacol* 2010;160:1577–1579.
22. Calpe-Berdiel L, Escolà-Gil JC, Blanco-Vaca F. New insights into the molecular actions of plant sterols and stanols in cholesterol metabolism. *Atherosclerosis* 2009;203:18–31.
23. Baardman ME, Erwich JJH, Berger RM, Hofstra RM, Kerstjens-Frederikse WS, Lütjohann D, Plösch T. The origin of fetal sterols in second-trimester amniotic fluid: endogenous synthesis or maternal-fetal transport?. *Am J Obstet Gynecol* 2012;207:202.e19–e25.
24. Amaral C, Gallardo E, Rodrigues R, Leite RP, Quelhas D, Tomaz C, Cardoso M. Quantitative analysis of five sterols in amniotic fluid by GC–MS: Application to the diagnosis of cholesterol biosynthesis defects. *J Chromatogr B* 2010;878:2130–2136.
25. Burke KT, Colvin PL, Myatt L, Graf GA, Schroeder F, Woollett LA. Transport of maternal cholesterol to the fetus is affected by maternal plasma cholesterol concentrations in the Golden Syrian hamster. *J Lipid Res* 2009;50:1146–1155.
26. Ras RT, Hiemstra H, Lin Y, Vermeer MA, Duchateau GS, Trautwein EA. Consumption of plant sterol-enriched foods and effects on plasma plant sterol concentrations – A meta-analysis of randomized controlled studies. *Atherosclerosis* 2013;230:336–346.
27. Moss TJ, Knox CL, Kallapur SG, Nitsos I, Theodoropoulos C, Newnham JP, Ikegami M, Jobe AH. Experimental amniotic fluid infection in sheep: effects of Ureaplasma parvum serovars 3 and 6 on preterm or term fetal sheep. *Am J Obstet Gynecol* 2008;198:122.e1–e8.
28. Miura Y, Payne MS, Keelan JA, Noe A, Carter S, Watts R, Spiller OB, Jobe AH, Kallapur SG, Saito M, et al. Maternal Intravenous Treatment with either Azithromycin or Solithromycin Clears Ureaplasma parvum from the Amniotic Fluid in an Ovine Model of Intrauterine Infection. *Antimicrob Agents Chemother* 2014;58:5413–5420.
29. Dello SAWG, Reisinger KW, Van Dam RM, Bemelmans MHA, Van Kuppevelt TH, Broek MAJVD, Damink SWMO, Poeze M, Buurman WA, DeJong CHC. Total Intermittent Pringle Maneuver during Liver Resection Can Induce Intestinal Epithelial Cell Damage and Endotoxemia. *Plos One* 2012;7: e30539.
30. Tanaka T, Narazaki M, Kishimoto T. IL-6 in Inflammation, Immunity, and Disease. *Cold Spring Harb Perspect Biol* 2014;6:a016295.
31. Barré F, Rocha B, Dewez F, Towers M, Murray P, Claude E, Cillero-Pastor B, Heeren R, Porta Siegel T. Faster raster matrix-assisted laser desorption/ionization mass spectrometry imaging of lipids at high lateral resolution. *Int J Mass Spectrom* 2019;437:38–48.
32. Willems MG, Ophelders DR, Nikiforou M, Jellema RK, Butz A, Delhaas T, Kramer BW, Wolfs TG. Systemic interleukin-2 administration improves lung function and modulates chorioamnionitis-induced pulmonary inflammation in the ovine fetus. *Am J Physiol Cell Mol Physiol* 2016;310:1–3107.
33. Jiang H, Sidhu R, Fujiwara H, De Meulder M, De Vries R, Gong Y, Kao M, Porter FD, Yanjanin NM, Carillo-Carasco N, et al. Development and validation of sensitive LC-MS/MS assays for quantification of HP- β -CD in human plasma and CSF. *J Lipid Res* 2014;55:1537–1548.
34. Bouic P, Clark A, Lamprecht J, Freestone M, Pool E, Liebenberg R, Kotze D, Van Jaarsveld P. The Effects of B-Sitosterol (BSS) and B-Sitosterol Glucoside (BSSG) Mixture on Selected Immune Parameters of Marathon Runners: Inhibition of Post Marathon Immune Suppression and Inflammation. *Int J Sports Med* 1999;20:258–262.
35. Camus G, Deby-Dupont G, Duchateau J, Deby C, Pincemail J, Lamy M. Are similar inflammatory factors involved in strenuous exercise and sepsis?. *Intensiv Care Med* 1994;20:602–610.
36. Nashed B, HayGlass KT, Moghadasian MH, Yeganeh B. Antiatherogenic Effects of Dietary Plant Sterols Are Associated with Inhibition of Proinflammatory Cytokine Production in Apo E-KO Mice. *J Nutr* 2005;135:2438–2444.
37. Wolfs TG, Kallapur SG, Polglase GR, Pillow JJ, Nitsos I, Newnham JP, Chougnnet CA, Kroon E, Spierings J, Willems CH, et al. IL-1 α mediated chorioamnionitis induces depletion of FoxP3+ cells and ileal inflammation in the ovine fetal gut. *PLoS One* 2011;6:e18355.

38. De Smet E, Mensink RP, Boekschoten MV, De Ridder R, Germeraad WTV, Wolfs TGAM, Plat J. An acute intake of plant stanol esters alters immune-related pathways in the jejunum of healthy volunteers. *Br J Nutr* 2015;113:794–802.
39. Woollett L, Heubi JE. Endotext: Fetal and Neonatal Cholesterol Metabolism. De Groot LJ, Chrousos G, Dungan K, Feingold KR, Grossman A, Hershman JM, Koch C, Korbonits M, McLachlan R, New M, et al. Eds. MDText.com, Inc.: South Dartmouth, MA, USA, 2000.
40. Furse S, De Kroon AIPM. Phosphatidylcholine's functions beyond that of a membrane brick. *Mol Membr Boil* 2015;32:117–9.
41. Ohanian J, Ohanian V. Sphingolipids in mammalian cell signalling. *Cell Mol Life Sci* 2001;58: 2053–68.
42. Payrastré B, Missy K, Giuriato S, Bodin S, Plantavid M, Gratacap MP. Phosphoinositides : key players in cell signalling, in time and space. *Cell Signal* 2001;13:377–87.
43. Pike LJ. Lipid rafts: bringing order to chaos. *J Lipid Res* 2003;44:655–67.
44. Gussenhoven R, Ophelders DR, Kemp MW, Payne MS, Spiller OB, Beeton ML, Stock SJ, Cillero-Pastor B, Barré FP, Heeren RM, et al. The paradoxical effects of chronic intra-amniotic *Ureaplasma parvum* exposure on ovine fetal brain development. *Dev Neurosci* 2017;39:472–86.
45. Adibhatla RM, Hatcher JF. Role of Lipids in Brain Injury and Diseases. *Futur Lipidol* 2007;2:403–22.
46. Tallima H, El Ridi R. Arachidonic acid: Physiological roles and potential health benefits—A review. *J Adv Res* 2018;11:33–41.
47. Hofmann AF, Eckmann L. How bile acids confer gut mucosal protection against bacteria. *Proc Natl Acad Sci U S A* 2006;103:4333–4.
48. Begley M, Gahan CG, Hill C. The interaction between bacteria and bile. *FEMS Microbiol Rev* 2005; 29:625–51.
49. Marin JJG, Macias RIR, Briz O, Banales JM, Monte MJ. Bile Acids in Physiology, Pathology and Pharmacology. *Drug Metab* 2015;17:4–29.
50. Bajor A, Gillberg PG, Abrahamsson H. Bile acids: short and long term effects in the intestine. *Scand J Gastroenterol* 2010;45:645–64.
51. Berseth C. Gestational evolution of small intestine motility in preterm and term infants. *J Pediatr* 1989;115:646–51.
52. Niño DF, Sodhi CP, Hackam DJ. Necrotizing enterocolitis: new insights into pathogenesis and mechanisms. *Nat Rev Gastroenterol Hepatol* 2016;13:590–600.
53. Warner BB, Deych E, Zhou Y, Hall-Moore C, Weinstock GM, Sodergren E, Shaikh N, Hoffmann J, Linneman L, Hamvas A, et al. Gut bacteria dysbiosis and necrotising enterocolitis in very low birthweight infants: a prospective case-control study. *Lancet* 2016;387:1928–36.
54. Atger VM, Moya MDLL, Stoudt GW, Rodriguez WV, Phillips MC, Rothblat GH. Cyclodextrins as catalysts for the removal of cholesterol from macrophage foam cells. *J Clin Investig* 1997;99: 773–80.
55. Liu SM, Cogny A, Kockx M, Dean RT, Gaus K, Jessup W, Kritharides L. Cyclodextrins differentially mobilize free and esterified cholesterol from primary human foam cell macrophages. *J Lipid Res* 2003;44:1156–66.
56. Zimmer S, Grebe A, Bakke SS, Bode N, Halvorsen B, Ulas T, Skjelland M, De Nardo D, Labzin LI, Kerkusiek A, et al. Cyclodextrin promotes atherosclerosis regression via macrophage reprogramming. *Sci Transl Med* 2016;8:333ra50.
57. Plat J, Nichols JA, Mensink RP. Plant sterols and stanols: effects on mixed micellar composition and LXR (target gene) activation. *J Lipid Res* 2005;46:2468–76.
58. Jakobsson T, Vedin LL, Hassan T, Ventecléf N, Greco D, D'Amato M, Treuter E, Gustafsson JA, Steffensen KR. The oxysterol receptor LXR β protects against DSS- and TNBS-induced colitis in mice. *Mucosal Immunol* 2014;7:1416–28.
59. Andersen V, Christensen J, Ernst A, Jacobsen BA, Tjonneland A, Krarup HB, Vogel U. Polymorphisms in NF- κ B, PXR, LXR, PPAR γ and risk of inflammatory bowel disease. *World J Gastroenterol* 2011;17:197–206.

Supplementary materials

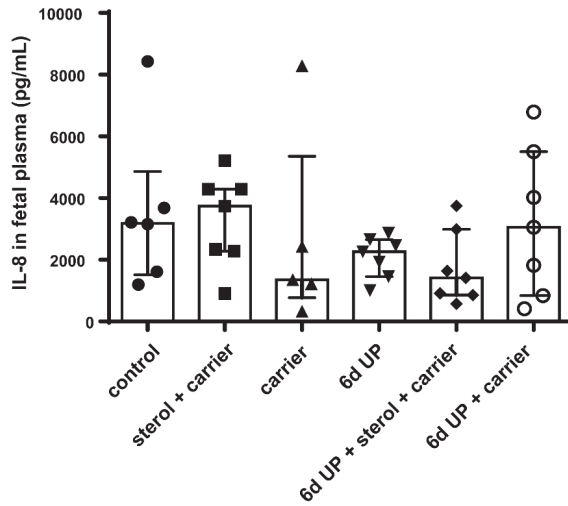


Figure S8.1 Circulatory IL-8 levels in fetuses of 133d GA. No significant changes were found between the treatment groups. UP: Ureaplasma.

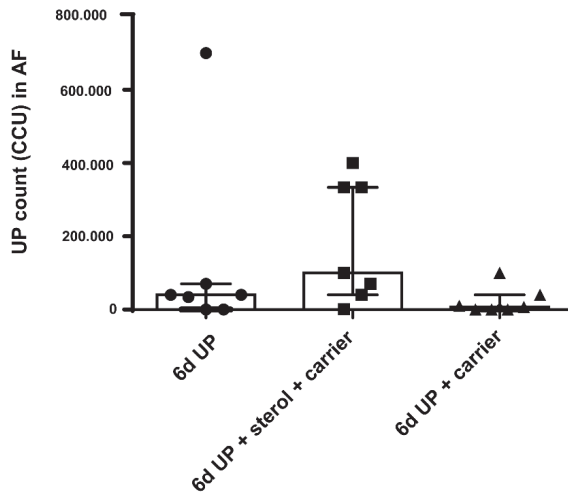


Figure S8.2 Ureaplasma parvum titers measured in AF samples taken at 133d GA. UP was only found in AF of animals injected with UP. No statistical differences were found between the different treatment groups. AF: amniotic fluid; CCU: color changing unit; GA: gestational age; UP: Ureaplasma.

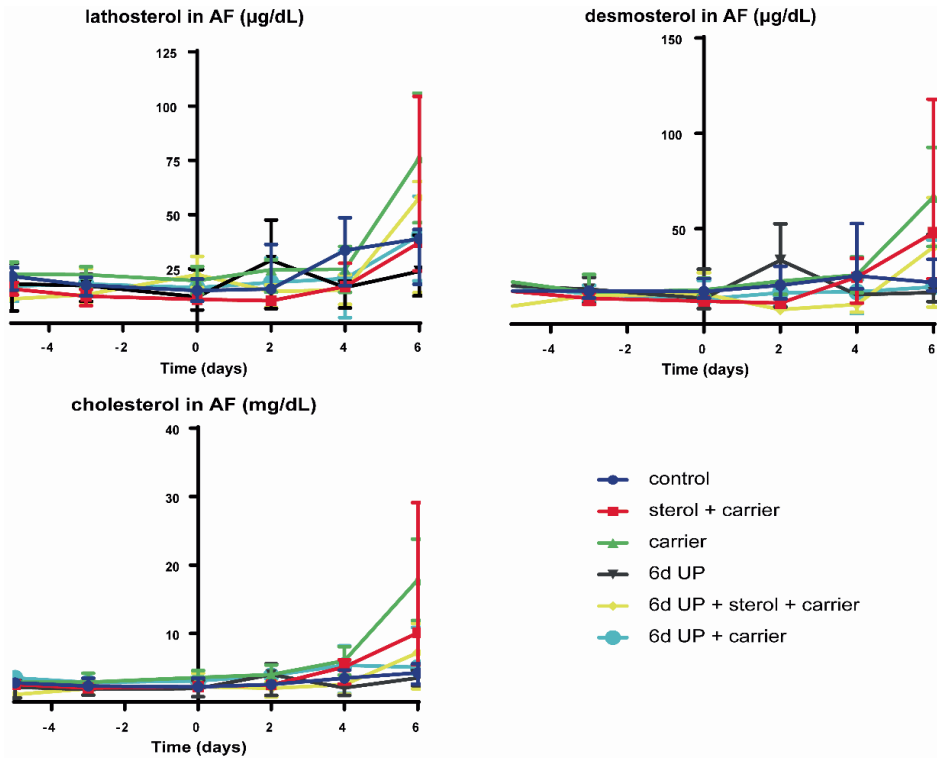


Figure S8.3 AF concentrations of cholesterol precursors (lathosterol, desmosterol) and cholesterol. At day 11, no significant differences were found for lathosterol (A), desmosterol (B) and cholesterol (C) in all treatment groups. Day 0 (122d GA) is the start of plant sterol treatment, day 5 (127d GA) is the day of intra-amniotic UP injection and day 11 (133d GA) is the moment of preterm delivery. AF: amniotic fluid; GA: gestational age; UP: Ureaplasma.

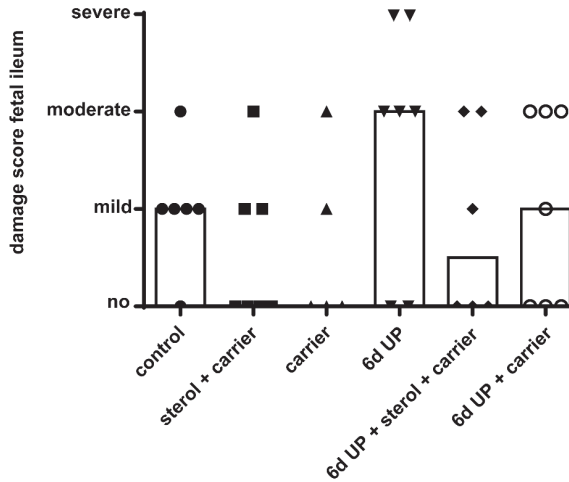


Figure S8.4 Evaluation of damage in the distal ileum of preterm lambs by H&E staining. Intestinal sections were judged as no damage (no damage visible), mild damage (apical epithelial integrity not complete, but no apparent loss of enterocytes), moderate damage (apical epithelial integrity not complete, loss of some enterocytes from the villus tips) or severe damage (apical epithelial integrity not complete, abundant loss of enterocytes from villus tips). The 6d UP group had more moderate to severe intestinal damage than the other experimental groups. H&E: hematoxylin and eosin; UP: Ureaplasma.

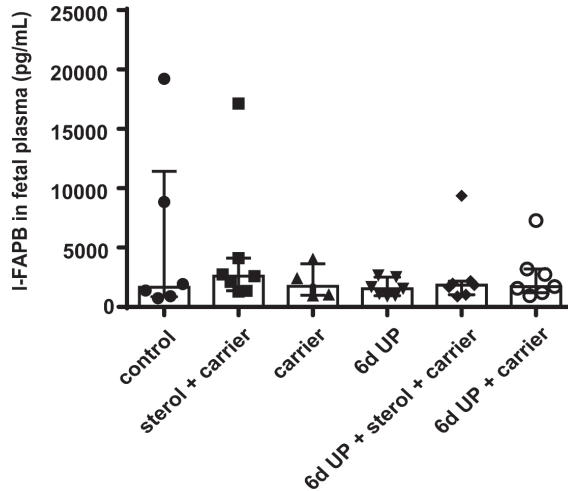


Figure S8.5 Circulatory I-FAPB levels in fetuses of 133d GA. No significant changes were found between all treatment groups. I-FAPB: intestinal fatty acid binding protein; UP: Ureaplasma.

Table S8.1 Identification of phosphocholines, sphingomyelins, phosphatidylinositol and bile acids.

Mass-to-charge ratio <i>m/z</i>	Exact mass	Δm (ppm)	Lipid assignment	Adduct	Fragment ions (<i>m/z</i>)
725.5587	725.5567	2.75	SM (34:1)	[M+Na] ⁺	184.0 (phosphocholine head group), 542.5 (loss of phosphocholine ion, $\Delta m=183$), 666.5 (loss of trimethylamine, $\Delta m=59$)
760.5868	760.5850	2.36	PC (34:1)	[M+H] ⁺	184.0 (phosphocholine head group), 577.5 (loss of phosphocholine ion, $\Delta m=183$), 701.5 (loss of trimethylamine, $\Delta m=59$)
782.5692	782.5670	2.8	PC (34:1)	[M+Na] ⁺	184.0 (phosphocholine head group), 577.5 (loss of phosphocholine ion + Na ⁺), 599.5 (loss of phosphocholine ion, $\Delta m=183$), , 723.5 (loss of trimethylamine, $\Delta m=59$)
810.6006	810.5983	2.83	PC (36:1)	[M+Na] ⁺	184.0 (phosphocholine head group), 605.5 (loss of phosphocholine ion + Na ⁺), 627.5 (loss of phosphocholine ion, $\Delta m=183$), , 751.5 (loss of trimethylamine, $\Delta m=59$)
885.5423	885.5498	8.46	PI (38:4)	[M-H] ⁻	581.3 (loss of FA, $\Delta m=304$), 241,0 PI(241)
498.2901	498.2895	1.2	Taurodeoxycholic acid (TDCA)	[M-H] ⁻	79.96 [SO ₃] ⁻ , 106.9 [C ₂ H ₃ O ₃ S] ⁻ , 124 [C ₂ H ₆ NO ₃ S] ⁻
514.2848	514.2844	0.7	Taurocholic acid (TCA)	[M-H] ⁻	79.96 [SO ₃] ⁻ , 106.9 [C ₂ H ₃ O ₃ S] ⁻ , 124 [C ₂ H ₆ NO ₃ S] ⁻

Table S8.2 Identification of the carrier (2-hydroxypropyl- β -cyclodextrin).

	Mass-to-charge ratio <i>m/z</i> on tissue	Mass-to-charge ratio <i>m/z</i> standard	Δm (ppm)
Parent ion	1331.4856	1331.4854	0.15
	1169.4324	1169.4323	0.09
	1007.3794	1007.3794	0
	949.3375	949.3374	0.10
MS/MS fragments	845.3264	845.3266	0.23
	787.2846	787.2849	0.38
	729.2427	729.2428	0.14
	683.2736	683.2738	0.29
	625.2317	625.2318	0.16
	567.1898	567.1903	0.88
	463.1787	463.1787	0
	405.1369	405.1371	0.49
	304.2464	304.2434	9.86

Chapter 9

Hypoxia-driven changes in a human intestinal organoid model and the protective effects of hydrolyzed whey

I.H. de Lange, C. van Gorp, K.R.I. Massy, L. Kessels, N. Kloosterboer, A. Bjørnshave,
M. Stampe Ostenfeld, J.G.M.C. Damoiseaux, J.P.M. Derikx,
W.G. van Gemert, and T.G.A.M. Wolfs

Abstract

Many whey proteins, peptides and protein-derived amino acids have been suggested to improve gut health, through their anti-oxidant, anti-microbial, barrier protective and immune modulating effects. Interestingly, although the degree of hydrolysis influences peptide composition and thereby biological function, this important aspect is often overlooked. In the current study, we aimed to investigate effects of whey protein fractions with different degrees of enzymatic hydrolysis on the intestinal epithelium in health and disease with a novel 2D human intestinal organoid (HIO) monolayer model. In addition, we aimed to assess antimicrobial activity and immune effects of the whey protein fractions.

Human intestinal organoids were cultured from adult small intestines and a model enabling apical administration of nutritional components during hypoxia-induced intestinal inflammation and normoxia (control) in crypt-like and villus-like HIO was established. Subsequently, potential beneficial effects of whey protein isolate (WPI) and two whey protein hydrolysates with a 27.7% degree of hydrolysis (DH28) and a 50.9% degree of hydrolysis (DH51) were assessed. In addition, possible immune modulatory effects on human peripheral immune cells and anti-microbial activity on four microbial strains of the whey protein fractions were investigated.

Exposure to DH28 prevented paracellular barrier loss of crypt-like HIO following hypoxia-induced intestinal inflammation with a concomitant decrease in HIF1 α mRNA expression. While WPI increased Treg numbers and Treg expression of CD25 and CD69 and reduced CD4+ T cell proliferation, no antimicrobial effects were observed.

The observed biological effects were differentially mediated by diverse whey protein fractions, indicating that (the degree of) hydrolysis influences their biological effects. Moreover, these newly described insights provide important opportunities to improve immune tolerance, prevent or treat several intestinal diseases and promote intestinal health.

Conflict of interest statement

This study was financially supported by and whey protein fractions were provided by Arla Foods Ingredients, Viby J., Denmark. Arla Food Ingredients was not involved in the experimental design, (statistical) analysis, data presentation, or decision to publish.

Introduction

Whey is an important co-product of the dairy industry that has long been viewed as refuge¹. However, over the years whey proteins and peptides have increasingly been regarded as useful compounds with considerable nutritional value and beneficial biological functions^{1,2}. Major whey proteins in cow milk such as β -lactoglobulin, α -lactoglobulin, glycomacropeptide and lactoferrin are examples of valuable constituents for human health¹⁻⁴. Whey proteins are added to infant formula to mimic the higher whey to casein protein ratio of ~90:10% in human colostrum and ~60:40% in mature human milk⁴, since breast milk, and the protein composition herein, is considered the gold standard for infant feeding. Moreover, specific whey proteins such as α -lactoglobulin are used in infant formulas⁴, because of their high content of essential amino acids and, after digestion, occurrence of biologically active peptides³. Extensively hydrolyzed formulas and free amino acid formulas are given to infants with cow milk allergy⁵. Although supportive evidence remains lacking, (partially) hydrolyzed formulas are used in atopic infants to prevent allergy, or in preterm infants for their perceived benefits in the reduction of feeding intolerance and necrotizing enterocolitis (NEC) incidence^{6,7}.

In the adult context, whey proteins or their hydrolysates may improve muscle protein synthesis^{8,9} and muscle recovery following resistance training¹⁰, may aid in preventing sarcopenia in the elderly¹¹, and could improve metabolic health^{12,13}. Moreover, many whey proteins, peptides and whey protein-derived amino acids have been suggested to improve gut health, for instance through their anti-inflammatory, anti-oxidant, anti-microbial, barrier protective and immune modulating effects¹⁴⁻¹⁸. Importantly, in some studies in experimental colitis models, high amounts of dietary free amino acids were associated with increased intestinal inflammation^{19,20}, suggesting (too) high amounts of free amino acids could be harmful.

Collectively, these findings make whey protein and well-balanced (partial) whey protein hydrolysates interesting candidates for prevention or treatment of several intestinal diseases that have considerable impact on human health across all ages and are characterized by inflammation, intestinal barrier loss and oxidative stress, such as inflammatory bowel disease (IBD)^{14,21-23}, intestinal ischemia reperfusion injury (IRI)²⁴ and NEC^{15,25}.

The diverse beneficial effects of whey proteins can be attributed to the easy absorption of whey protein²⁶, the easy digestion and postulated faster absorption of whey protein hydrolysates^{27,28}, the high content of essential and branched chain amino acids in whey²⁹ and to beneficial effects of various whey protein derived peptides^{29,30}. Many whey peptides, which are derived from whey proteins following hydrolysis by commercial or gastrointestinal enzymes, are regarded as bioactive and are described to display a broad range of biological effects, such as antioxidant and antimicrobial activity²⁹. Bioactive whey protein-derived peptides vary in size and weight, ranging from several to >15 amino acids and from ~300 Da to ~1500 Da²⁹. Interestingly, although, together with protein source, the degree and technique of hydrolysis determines peptide content and could thereby alter biological function³¹⁻³³, the aspect of degree of hydrolysis (DH) is often overlooked when beneficial effects of whey proteins and peptides are assessed.

In the current study, we aimed to perform a comprehensive screening of whey protein isolate (WPI) and two whey protein hydrolysates with 27.7% degree of hydrolysis (DH28) and 50.9% degree of hydrolysis (DH51), to investigate their effect on the intestinal epithelium in health and disease. To this end, a novel 2D human intestinal organoid (HIO) monolayer model, which enabled apical exposure of the human intestinal epithelium to the different whey protein fractions, was adapted to allow for testing of nutritional interventions in a healthy setting and during hypoxia mediated intestinal inflammation and was used for screening of the effect of the whey protein fractions. In addition, the effect of the different whey protein fractions on peripheral immune cells, on two well-described pathogenic strains³⁴⁻³⁶ (i.e. *Escherichia coli* and *Staphylococcus aureus*) and two probiotic strains (i.e. *Lactobacillus rhamnosus* and *Bifidobacterium longum*)^{37,38} relevant for human (gut) health was investigated.

Materials and methods

Human tissues and ethics

Healthy small-intestinal tissue samples were collected from patients undergoing pancreaticoduodenectomy at Maastricht University Medical Centre or RWTH Aachen University Hospital. The study has been approved by the medical ethical committee of both participating centers (METC 16-4-185 and EK 206/09) and written informed consent was obtained. Five HIO lines, derived from small intestine of donors ranging from 50-82 years, 3 males and 2 females, were used for this study, of which four were used for model development and three were used for whey fraction comparison.

Small intestinal crypt isolation

The protocol for small intestinal crypt isolation and subsequent formation of HIOs was adapted from Sato et al.³⁹. After collection from the operating theater, small intestinal tissue was kept in AdDF+++ medium (Advanced DMEM/F12 (12634028, Thermo Fisher Scientific, Waltham, MA, USA) supplemented with 10 mM HEPES buffer solution (15630056, Thermo Fisher Scientific), 1x GlutaMAX supplement (35050038, Thermo Fisher Scientific) and 1x Antibiotic Antimycotic solution (A5955, Sigma Aldrich, St. Louis, MO, USA) at 4°C for a maximum of 5 hours. Subsequently, tissue was washed, muscle layer was stripped off and tissue was cut into fragments of 4-5 mm. Tissue fragments were washed with ice cold chelation buffer (5.6 mM Na₂HPO₄ (7558-79-4, Merck Millipore, Burlington, MA, USA); 8 mM KH₂PO₄ (7778-77-0, Merck Millipore); 96 mM NaCl (7647-14-5, Merck Millipore); 1.6 mM KCl (7447-40-7, Merck Millipore); 44 mM sucrose (57-50-1, Merck Millipore); 54.8 mM D-sorbitol (S1876, Sigma Aldrich); 80 ug/mL DL-dithiothreitol (D0632, Sigma Aldrich) and incubated in 0.5M EDTA (46-034-Cl, Corning Incorporated, Corning, NY, USA) in chelation buffer for 90 minutes on a rotating platform at 4°C. EDTA in chelation buffer was removed and tissue fragments were firmly resuspended in the ice cold chelation buffer with a 10 mL pipette. After settling down of tissue fragments, supernatant was removed and kept on ice. This procedure was repeated ~10 times until the supernatant was clear. The different stored fractions were evaluated with light microscopy and fractions with isolated crypts

were put through a 100 µm strainer (43-50100-51, pluriSelect Life Science, Leipzig, Germany) and pooled in a 50 mL tube with 10% fetal bovine serum (FBS) (F7524, Sigma Aldrich). The combined fractions were spun down at 300 g for 5 minutes at 4°C. The pellet with isolated crypts was then suspended in cultrex reduced growth factor Basement Membrane Extract type 2 (BME) (3533-010-02, Bio-Techne, Minneapolis, MIN, USA) and plated in 40 µL drops on a pre-heated 24-wells plate (662160, Greiner Bio-One, Kremsmünster, Austria). After solidification of the BME drops for 30 minutes, normal HIO growth medium (GM) was added, 500 µL per well, and HIOs were cultured in a 37°C incubator (21% O₂, 5% CO₂).

3D HIO maintenance

GM was replaced every 3-7 days and HIOs were passaged ~1:5 every 7-14 days. For passaging, GM was removed and replaced by ice cold PBS (10010023, Thermo Fisher Scientific). BME drops were mechanically disrupted by scratching with a pipette tip and the BME dissolved in ice-cold PBS was collected in a 15 mL tube. HIO were then spun down at 400 g for 5 minutes at 4°C and supernatant was removed. The pellet was dissolved in 2 mL 1x TrypLE Express Enzyme (12605010, Thermo Fisher Scientific) supplemented with 10 µM Y-27632 dihydrochloride rho-k-inhibitor (HY-10583, Bio-Connect, Huissen, The Netherlands) and incubated for 1.5 minutes at 37°C. Thereafter, HIO were mechanically disrupted with a narrowed Pasteur's pipette (612-1799, VWR International, Radnor, PA, USA). Dissociated HIOs were washed with 10 mL AdDF+++, spun down at 400G for 5 minutes at 4°C, dissolved in fresh BME and added to a new 24 wells plate. For long term storage, HIOs were frozen in ice-cold Recovery Cell Culture Freezing Medium (12648010, Thermo Fisher Scientific) and kept in liquid nitrogen. All experiments were performed with HIOs recovered from liquid nitrogen. HIOs from passage numbers 3-15 were used.

HIO culture medium

GM was used for HIO maintenance and for studying HIOs in a crypt-like phenotypical state. GM consisted of AdDF+++ (Advanced DMEM/F12 (12634028, Thermo Fisher Scientific) supplemented with 10 mM HEPES buffer solution (15630056, Thermo Fisher Scientific), 1x GlutaMAX supplement (35050038, Thermo Fisher Scientific) and 1x Antibiotic Antimycotic Solution (A5955, Sigma Aldrich), supplemented with 50% v/v Wnt3a conditioned medium, 20% v/v Rspodin-1 conditioned medium, 10% v/v Noggin conditioned medium, 1x B27 supplement (17504044, Thermo Fisher Scientific), 1x N2 supplement (17502001, Thermo Fisher Scientific), 1.25 mM N-acetyl-cysteine (NAC) (A9165, Sigma Aldrich), 50 ng/mL recombinant human epidermal growth factor (EGF) (AF-100-15, Peprotech, Rocky Hill, IL, USA), 10 nM [Leu15]-Gastrin (G9145, Sigma Aldrich), 10 mM nicotinamide (N5535, Sigma Aldrich), 500 nM A83-01 (2939, Tocris Bioscience, Bristol, UK), 10 µM SB202190 (S7067, Sigma Aldrich), 10 µM Y-27632 dihydrochloride rho-k-inhibitor (HY-10583, Bio-Connect) and 1% Antibiotic Antimycotic Solution (A5955, Sigma Aldrich) (end concentration including Antibiotic Antimycotic Solution in AdDF+++). Wnt3a conditioned medium was in-house made with L cells stably transfected with pCDNA3.1Zeo- mouse Wnt3a, the basic medium was DMEM (31966, Thermo Fisher Scientific) supplemented with 10% FBS (F7524, Sigma

Aldrich) and 1% penicillin-streptomycin (15140122, Thermo Fisher Scientific), (end concentration 100 U/mL penicillin and 100 µg/mL streptomycin). Rspodin1 conditioned medium was in-house made with HEK-293 cells stably transfected with a plasmid carrying the gene for mouse Rspodin1, the basic medium was AdDF+++. Noggin conditioned medium was in-house made with HEK-293 cells stably transfected with a plasmid carrying the gene for mouse Noggin, the basic medium was AdDF+++. Differentiation medium (DM) was used to induce differentiation in the HIOs and generate a villus-like phenotype and was adapted from the composition described by Van Dussen et al. and Kozuka et al.^{40,41}. In differentiation medium, A83-01, SB202190, NAC and Nicotinamide were omitted. In addition, the concentrations of Wnt3a, Rspodin and Noggin conditioned medium were decreased to 5% v/v, 2% v/v and 1% v/v, respectively. Besides, the γ -secretase inhibitor DAPT 10 µM (D5942, Sigma Aldrich) was added to the differentiation medium for inhibition of Notch signaling.

HIO monolayer culture

To increase accessibility of the apical side of the HIO epithelial cells, a monolayer culture model was used, in which the apical side of the enterocyte orients upwards⁴⁰. Single cells used for monolayer seeding were derived from full grown 3D cultured HIOs. Briefly, GM was removed and ice-cold PBS was used to harvest the HIOs in BME. HIOs were then spun down at 400 G for 5 minutes at 4°C and supernatant was removed. The pellet was dissolved in 1x TrypLE Express Enzyme (12605010, Thermo Fisher Scientific) supplemented with 10 µM Y-27632 dihydrochloride rho-k-inhibitor (HY-10583, Bio-Connect) and incubated for 9 minutes at 37°C. Thereafter, HIO were mechanically disrupted with a narrowed Pasteur's pipette (612-1799, VWR International). Dissociated HIOs were washed with 10 mL AdDF+++, spun down at 400G for 5 minutes at 4°C, dissolved in GM and filtered with a 40 µm strainer (43-50040-51, pluriSelect Life Science) to remove large HIO fragments. The cell suspension was added to a 96 well plate (0030 730.119, Eppendorf, Hamburg, Germany) (RNA isolation HIO experiments) or to a µ-Slide (81506, Ibidi, Fitchburg, WI, USA) that were pre-coated with a 1% BME in PBS solution for at least 1 hour, 100 µL per well (96 well plate) or 40 µL per well (µ-Slide). For monolayers in a 96 well plate, another 200 µL GM was added following adhesion of the cells, giving a total volume of 300 µL GM per well. Medium was refreshed every 1-3 days. Apical-basolateral orientation of the enterocytes with the apical side upwards was confirmed by immunofluorescent detection of ZO1 above the cell nucleus (z-stack) (**Supplementary Figure S9.1**).

Immunofluorescence staining of HIO monolayers

Monolayers for immunofluorescent (IF) staining of Ki67, cleaved caspase 3 (CC3) and zona-occludens 1 (ZO1) were cultured in a µ-Slide (81506, Ibidi). After finishing the experiment, medium was removed and HIO monolayers were fixed with 4% paraformaldehyde for 20 minutes. Following fixation, monolayers were washed with PBS and cells were permeabilized by incubation in 0.1% Triton-X in 1% bovine serum albumin (BSA)/PBS for 20 minutes. Thereafter, monolayers were washed and aspecific binding was blocked by incubation with 5% BSA/PBS (CC3) or 10% normal goat serum (NGS)/PBS (ZO1). For IF

staining of Ki67, no block step was performed. Monolayers were incubated with the primary antibody of interest overnight at 4°C. The following primary antibodies were used: polyclonal rabbit anti-Ki67 (ab15580, Abcam, Cambridge, UK), polyclonal rabbit anti-CC3 (ASP 175, #9661 Cell Signaling Technology, Danvers, MA, USA) and polyclonal rabbit anti-ZO1 (61-7300, Thermo Fisher Scientific). Monolayers were again washed with PBS and incubated with the secondary antibody, polyclonal donkey anti-rabbit Alexa 488 (A-21206, Thermo Fisher Scientific), for 1 hour at room temperature. Thereafter, monolayers were washed again with PBS and incubated with DAPI (200 µg/mL) (D9542, Sigma Aldrich) for 5 minutes. After a final washing step with PBS and RiOs water, fluorescence mounting medium (S3023, Agilent, Santa Clara, CA, USA) was added to the µ-Slide wells to preserve an optimal fluorescent signal. Slides were imaged within 2 days after staining with a LEICA DMI 4000 confocal microscope (Leica Microsystems, Wetzlar, Germany). Ki67 immunofluorescence was expressed as the percentage of cells that was positively stained for Ki67. Total number of cells (determined by amount of DAPI positive nuclei) and cells positively stained for Ki67 were counted semi-automatically with QuPath quantitative pathology and bioimage analysis software version 0.20 (University of Edinburgh, Edinburgh, UK)⁴². CC3 immunoreactivity was expressed as the surface area positively stained for CC3. Total surface area (determined by DAPI positive nuclei surface area) and the area positively stained for CC3 were calculated with Image J software (version 1.51s, National Institutes of Health, USA).

Measurement of paracellular barrier function of 3D HIO

Paracellular barrier function of 3D HIOs was assessed with a method adapted from Xu et al.⁴³. To this end, 3D HIOs were seeded in 10 µL BME drops in a µ-Slide (81506, Ibidi) and 17% v/v FITC-D4 (FD4, Thermo Fisher Scientific) was added to the experimental medium for 24 hours. Translocation of FITC-D4 from the basolateral to the apical side of the 3D HIO was imaged with a LEICA DMI 4000 confocal microscope (Leica Microsystems) and a luminal:basolateral ratio (L:BL ratio) of the fluorescent signal was calculated with Image J software (version 1.51s, National Institutes of Health, USA). For 3D HIO cultured under normoxic conditions, 10 HIOs per group per donor were included. For 3D HIOs cultured under hypoxic conditions this number was increased to 15 organoids per group per donor because of the higher biological variance.

Human PBMC isolation and culture

Human peripheral blood mononuclear cells (PBMCs) from buffy coats from four adult donors derived from Sanquin Blood Bank (number NVT0526.01) were washed with PBS and counted. Cells assigned for later flow cytometry analyses were labeled with 3 µM 5(6)-carboxyfluorescein diacetate succinyl ester (CFSE) (C34554, Thermo Fisher Scientific) in 0.1% BSA/PBS for 7 minutes at 37°C. For T-cell activation, anti-Biotin MACSiBead Particles loaded with human antibodies against CD2, CD3 and CD28 were used (T cell Activation/Expansion Kit, 130-091-441, Miltenyi Biotec, Bergisch Gladbach, Germany) according to the manufacturer's instructions (2.5*10⁶ loaded Anti-Biotin MACSiBead Particles per 5*10⁶ PBMCs). PBMCs (both T-cell-activated and non-T-cell-activated) were

cultured in TexMACS Medium (130-097-196, Miltenyi Biotec) with a starting density of ~300.000 cells/well in a round bottom 96 well plate (CLS3799, Sigma Aldrich). PBMCs were cultured in a 37°C incubator (21% O₂, 5% CO₂). After 48h, culture plates were shaken every 24h on a shaker plate for 10 minutes (improved CFSE signal during flow cytometry analysis).

Flow cytometry analysis of human PBMC

Non-activated human PBMCs were stained for detection of CD3, CD4, CD8, CD25, CD69 and CD127 according to the manufacturer's protocol. Activated human PBMCs were stained for detection of CD3, CD4 and CD8 according to the manufacturer's protocol. In addition, a live-dead marker (LIVE/DEAD™ Fixable Aqua Dead Cell Stain Kit, for 405 nm excitation, L34965, Thermo Fisher Scientific) and CFSE labeling were incorporated in both panels. The following antibodies were used for non-activated PBMC experiments: monoclonal mouse-anti CD3 V450 (clone UCHT1, 561812, BD Biosciences, Franklin Lakes, NJ, USA), monoclonal mouse anti-CD4 PerCP-Cy™5.5 (clone SK3, 332772, BD Biosciences), monoclonal mouse anti-CD8 APC-H7 (clone SK1, 641400, BD Biosciences), monoclonal mouse anti-CD25 PE-Cy™7 (clone 2A3, 335824, BD Biosciences), monoclonal mouse anti-CD69 PE (clone FN50, 555531, BD Biosciences) and monoclonal mouse anti-CD127 APC (clone eBioRDR5, 17-1278-42, Thermo Fisher). Antibodies used for activated PBMC experiments were: monoclonal mouse anti-CD3 APC-H7 (clone SK7, 641415, BD Biosciences), monoclonal mouse anti-CD4 PerCP-Cy™5.5 (clone SK3, 332772, BD Biosciences) and monoclonal mouse-anti CD8 PE-Cy™7, (clone SK1, 335822, BD Biosciences). Stained cells were acquired on a FACS Canto II (BD Biosciences) flow cytometer equipped with FACS Diva software (version 6.1.2; BD Biosciences).

For both the unactivated experiment and the T-cell activated experiment, single cells were selected from PBMCs in forward and side scatter and live cells were selected with a live-dead marker. From this population, the CD3+ cells were gated and the amount of CD4+ and CD8+ cells was determined. In unactivated PBMCs, the percentage of Treg (CD4+CD25^{high}CD127^{low} T cells) was calculated from the population of live CD4+ T cells. In addition, the percentage of Treg that is CD69+ was calculated and the Mean Fluorescent Intensity (MFI) of CD25 of the total population of Treg was measured. In T-cell activated PBMCs, the percentages of live CD4+ T cells and of live CD8+ T cells that proliferated were calculated.

RNA isolation and quantitative real-time PCR

RNA from HIO monolayers and human PBMCs was isolated with the RNeasy plus Micro kit (74034, Qiagen, Hilden, Germany) according to the manufacturer's instructions. The RNA concentration of the samples was determined using the NanoDrop™ 1000 Spectrophotometer. Subsequently, cDNA was synthesized with the SensiFAST™ cDNA Synthesis Kit (BIO-65053, Meridian Bioscience, Cincinnati, OH, USA). Quantitative real-time PCR was performed on the LifeCycler® 480 qPCR machine (Roche Molecular Systems, Inc.) with a three-step program for 40 cycles and SensiMix SYBR Hi-ROX Kit (QT605-05, Meridian Bioscience, Cincinnati, OH, USA) was used for cDNA amplification. 5 ng cDNA was used per reaction with a primer concentration of 250 nM (both for forward and reverse primer). An overview of the primers that were used is presented in **Table 9.1**. RT-qPCR data was

analyzed using LinRegPCR software (version 2016.0). The geometric mean of the three housekeeping genes (beta-actin, glyceraldehyde 3-phosphate dehydrogenase (GAPDH) and 14-3-3 protein zeta/delta (YWHAZ) for HIO monolayer experiments and CD3 epsilon (CD3e), GAPDH and YWHAZ for PBMC experiments) was used for data normalization.

Table 9.1 Primer sequences.

Primer	Forward	Reverse
β-actin	5'-ATTGCCGACAGGATGCAGAAG-3'	5'-TTGCTGATCCACATCTGCTGG-3'
GAPDH	5'-GGAAGCTCACTGGCATGGC-3'	5'-CCTGCTTACCACCTTCTTG-3'
YWHAZ	5'-TGAACTCCCCTGAGAAAGCC-3'	5'-TCCGATGCCACAATGTCAAGT-3'
CD3e	5'-TGCTGCTGGTTACTACTGGA-3'	5'-GGATGGGCTCATAGTCTGGG-3'
IL8	5'-GCCGGAATACCTGGACTATGC-3'	5'-TTCCTTGGGGTCCAGACAGA-3'
OLFM4	5'-TGGACAGAGTGGAACGCTTG-3'	5'-TCAGAGCCACGATTTCTCGG-3'
LYS	5'-GATAACATCGTGATGCTGTAGCT-3'	5'-CATGCCACCCATGCTCTAATG-3'
IFABP	5'-ACGGACAGACAATGGAAACGA-3'	5'-ACTGTGCGCCAAGAATAATGC-3'
MUC2	5'-CTACTGGTGTGAGTCCAAGG-3'	5'-GGCACTGGAGGAATAAACTG-3'
PEPT1	5'-TGTCACCGCCATCTACCATA-3'	5'-CCACGAGTCGGCGATAAGAG-3'
LAT2	5'-AGGCTGGAACCTTCTGAATTACG-3'	5'-ACATAAGCGCATTGGCAAAGA-3'
HIF1a	5'-ATCCATGTGACCATGAGGAAATG-3'	5'-TCGGCTAGTTAGGGTACACTTC-3'
IL4	5'-AGTGTCTTCTCATGGTGGC-3'	5'-CACCGAGTTGACCGTAACAG-3'
IL17	5'-CACTTTGCCTCCAGATCAC-3'	5'-ACCAATCCAAAAGGTCCTC-3'
IFNγ	5'-TGGCTTTTACGCTCTGCATC-3'	5'-CCGCTACATCTGAATGACCTG-3'
TNFα	5'-TCAATCGGCCGACTATCTC-3'	5'-CAGGGCAATGATCCCAAAGT-3'
IL10	5'-TCCCTGTGAAAACAAGACA-3'	5'-ATAGAGTCGCCACCCTGATG-3'
Foxp3	5'-CACCTGGCTGGGAAATGG-3'	5'-GGAGCCCTTGTCGGATGAT-3'

Microbiology experiments

The effects of whey protein fractions on the growth of two pathogenic bacteria strains (*Escherichia coli* ATCC 25922, *Staphylococcus aureus* ATCC 29213) and two probiotic bacterial strains (*Lactobacillus rhamnosus* and *Bifidobacterium longum*) was investigated. These strains were plated onto blood-agar plates (BD Biosciences, Franklin Lakes, NJ, USA) and incubated overnight at conditions described in **Table 9.2**. A single colony from each culture plate was used to inoculate the appropriate medium (**Table 9.2**). Subsequently, cultures were grown overnight in a shaker. Thereafter, saturated bacterial suspensions were diluted in their medium to a concentration of 10⁴-10⁵ CFU/ml and 100 μL of each suspension was added to 100 μL of a 10-fold serial whey protein fraction dilutions (200 μg/mL to 0.002 μg/mL) in a round-bottom 96 well plate (650185, Greiner Bio-One). Medium without addition of the whey protein fraction was used as a growth control. In addition, as control for growth inhibition, 100 μL of each bacterial suspension was mixed with 100 μL medium supplemented with an antibiotic as described in **Table 9.2**. After incubation, the optical density at 600 nm (OD) of the plates was measured in a Victor³ 1420 Multilabel Counter (Perkin-Elmer, Waltham, MA, USA).

Table 9.2 Culture medium and antibiotic used as growth inhibition control for included bacterial strains.

Strain	Culture medium	Antibiotic used as growth inhibition control
<i>Escherichia coli</i> ATCC 25922	BHI	colistin (2 µg/mL)
<i>Staphylococcus aureus</i> ATCC 29213	BHI	ampicillin (50 µg/mL)
<i>Lactobacillus rhamnosis</i>	BHI	erythromycin (10 µg/mL)
<i>Bifidobacterium longum</i>	MRS (+0.05% cystein)	erythromycin (10 µg/mL)

Abbreviations: ATCC, American Type Culture Collection; BHI, brain heart infusion; MRS, De Man, Rogosa and Sharpe agar.

Whey protein isolate and whey protein hydrolysates

WPI, DH28 and DH51 were provided by Arla Foods Ingredients Group P/S, Viby J., Denmark. For organoid experiments, WPI, DH28 and DH51 were mixed with AdDF+++ at a stock concentration of 6.82 mg/mL (GM experiments) or 1.15 mg/mL (DM experiments). For PBMC experiments, fractions were mixed with TexMACS medium at a stock concentration of 5 mg/mL. Stock solutions were filtered with a 0.22 µm strainer and kept at 4°C in the dark during the duration of the experiment. For final experiments in organoids and PBMCs, stocks were diluted till a final concentration of 1 mg/mL in the appropriate medium. This concentration was based on earlier studies in which (whey) protein compounds were tested on (human) intestinal epithelial cells⁴⁴⁻⁴⁷ and PBMCs^{48,49} *in vitro*. For microbiology experiments, WPI, DH28 and DH51 were diluted in the appropriate medium and serial dilutions ranging from 200 µg/mL to 0.002 µg/mL were used. Information about the intervention composition is displayed in **Table 9.3** and in **Supplementary Table S9.1**.

Table 9.3 Composition of interventions.

Product	WPI	DH28	DH51
Protein (%)	90.0	86.5	85.1
Lactose (%)	0.05	0.10	0.09
Fat (%)	0.10	0.10	0.07
Ash (%)	4.0	3.3	4.9
Mn (Da)	N/A	593	333
Mw (Da)	N/A	914	581
<375 Da (%)		16.1	37.3
375-750 Da (%)		35.9	36.4
750-1250 Da (%)		24.6	19.4
1250-2500 Da (%)		21.4	6.6
>2500 Da (%)		2.1	0.3
DH (%)		27.7	50.9
FAA (%)	0.0	0.5	29.0

Abbreviations: Mn, number average molecular weight; Mw, weight average molecular weight; DH, degree of hydrolysis; FAA, free amino acids.

Experimental set-up

An overview of the experimental set-up is displayed in **Figure 9.1**. Additional experiments for model development are described in **Supplementary Figure S9.2**. Following monolayer seeding, HIO monolayers were cultured with GM for 3-7 days to reach ~80-90% confluence. Thereafter, monolayers were cultured for 36h with GM or 12h with DM (healthy setting qPCR/immunofluorescence experiments and diseased setting qPCR experiments). Subsequently, GM/DM with WPI, DH28 or DH51 was added to the cells. GM/DM without added WPI, DH28 or DH51 was used as control. To induce hypoxia mediated intestinal inflammation, monolayers were placed in a hypoxic incubator (1% O₂, 5% CO₂ and 37°C) for 24h (GM) or 48h (DM qPCR experiments). A longer hypoxia period was chosen for DM cultured HIO monolayers than for GM cultured HIO monolayers as DM cultured HIO were observed to be less sensitive to the effects of hypoxia (unpublished observations). For immunofluorescence monolayer experiments, the hypoxic period was shortened to 24h (and the normoxic pre-culture with DM prolonged from 12h to 36h) as too many cells were lost during the washing steps of the immunofluorescence staining following 48h hypoxia. After hypoxia, HIO monolayers were directly processed for RNA isolation or fixed for immunofluorescence staining to prevent a longer period of re-oxygenation. 3D HIO for paracellular barrier experiments were grown for 4-10d before start of experiment. GM with FITC-D4 and with WPI, DH28 or DH51 was added 24h before imaging. GM with FITC-D4 but without added WPI, DH28 or DH51 served as control. To induce barrier loss, 3D HIOs were placed in the hypoxic incubator (1% O₂, 5% CO₂ and 37°C) for 16h. HIOs were imaged within 2 hours of removal from the hypoxic incubator to minimize the effects of re-oxygenation. For barrier experiments, a hypoxia time of 16h was chosen, instead of 24h in other experiments, as this gave a steady loss of barrier function in the hypoxic organoids, while retaining a good barrier function in the normoxic controls, and this allowed for pre-incubation of the whey protein fractions before start of hypoxia within a total experimental duration of 24 hours. Microbiology experiments were conducted for 16h (*Escherichia coli* and *Streptococcus aureus*) or 36h (*Lactobacillus rhamnosus* and *Bifidobacterium longum*) under circumstances physiological to the studied strain (aerobic for *Escherichia coli* and *Streptococcus aureus*; anaerobic for *Lactobacillus rhamnosus* and *Bifidobacterium longum*). PBMCs were cultured for 5 days in absence or presence of WPI, DH28 and DH51 before flow cytometry analyses and RNA isolation.

Statistical analyses

We performed statistical analyses with GraphPad Prism (Version 9, GraphPad Software Inc., La Jolla, CA, USA). Data are presented as median with interquartile range for all read-outs except for microbiology experiment data, which is presented as mean and standard deviation. For qPCR results, delta CT values were used for statistical analyses. qPCR data is presented as fold change compared to the control group (calculated from delta-delta CT values by $2^{-\Delta\Delta CT}$). Differences between groups for experiments regarding HIO model development were analyzed with a Mann-Whitney U test (two groups compared) or a Kruskal Wallis followed by Dunn's post hoc test (more than two groups compared). Experiments with comparison of the different whey fractions (both HIO monolayer

experiments and PBMC experiments) were analyzed with a Friedman test followed by Dunn's posthoc test. Barrier experiments with the different whey fractions were analyzed with a Kruskal Wallis followed by Dunn's post hoc test. Last, data from microbiology experiments were analyzed with a two-way ANOVA with a Tukey post hoc test. Differences are considered statistically significant at $p \leq 0.05$. Differences with a p-value > 0.05 and ≤ 0.10 are reported as trend.

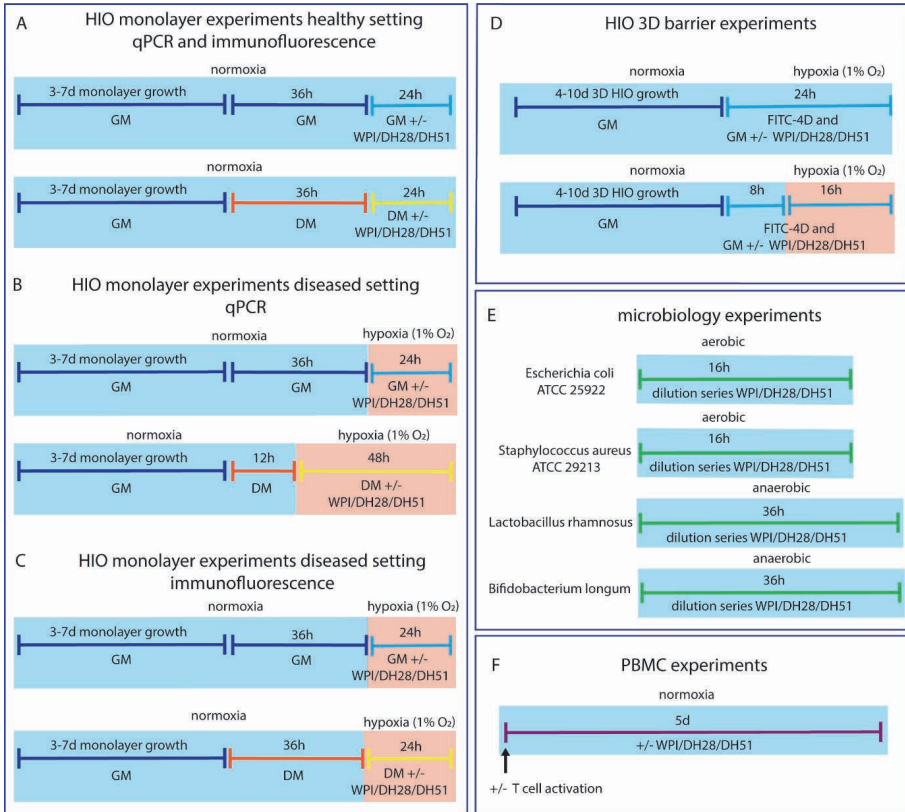


Figure 9.1 Experimental set-up of the different experiments performed. Light blue blocks indicate physiological culture conditions; light red blocks indicate a diseased (hypoxic) setting. A. For HIO monolayer experiments in a healthy setting (normoxia) analysed by qPCR and immunofluorescence, HIO monolayers were cultured for 3-7d prior to the onset of the experiment. At start of experiment, crypt like-organoids were cultured with GM for 36h, followed by 24h incubation with GM with or without added WPI, DH28 or DH51. Villus-like organoids were cultured with DM for 36h and subsequently for 24h with DM with or without added WPI, DH28 or DH51. B. For HIO monolayer experiments in a diseased setting (hypoxia) analysed by qPCR, HIO monolayers were cultured for 3-7d prior to the onset of the experiment. At start of experiment, crypt like-organoids were cultured with GM for 36h, followed by 24h incubation in a hypoxic incubator (1% O₂) with GM with or without added WPI, DH28 or DH51. Villus-like organoids were cultured with DM for 12h and subsequently for 48h in a hypoxic incubator (1% O₂) with DM with or without added WPI, DH28 or DH51. C. For HIO monolayer experiments in a diseased setting (hypoxia) analysed by immunofluorescence staining, HIO

monolayers were cultured for 3-7d prior to the onset of the experiment. At start of experiment, crypt like-organoids were cultured with GM for 36h, followed by 24h incubation in a hypoxic incubator (1% O₂) with GM with or without added WPI, DH28 or DH51. Villus-like organoids were cultured with DM for 36h and subsequently for 24h in a hypoxic incubator (1% O₂) with DM with or without added WPI, DH28 or DH51. D. For paracellular barrier experiments with 3D crypt-like HIO, HIO were cultured for 4-10d prior to the onset of the experiment. 24h before analyses, FITC-D4 was added to the GM with or without supplemented WPI, DH28 or DH51. 3D HIO tested in a normoxic setting remained in the 21% O₂ incubator until analysis, whereas HIO tested in a hypoxic setting were transferred to a hypoxic incubator (1% O₂) 16h prior to analysis. E. The four different strains used in the microbiology experiments were cultured aerobic (*Escherichia coli* and *Staphylococcus aureus*) or anaerobic (*Lactobacillus rhamnosus* and *Bifidobacterium longum*) depending circumstances physiological to the strain used for 16h (*Escherichia coli* and *Staphylococcus aureus*) or 36h (*Lactobacillus rhamnosus* and *Bifidobacterium longum*) in presence or absence of different concentrations of WPI, DH28 or DH51. F. PBMCs were activated or non-activated at start of culture with anti-Biotin MACSiBead Particles loaded with human antibodies against CD2, CD3 and CD28. Thereafter, cells were cultured with or without added WPI, DH28 or DH51 for 5 days before analyses.

Results

Model development

Differentiation from crypt-like to villus-like HIO monolayers

To induce differentiation towards a villus-like phenotype, HIO monolayers were cultured with DM for 60h. This decreased the mRNA expression of crypt cell markers OLFM4 (stem cell marker; $p \leq 0.05$) and LYZ (Paneth cell marker, $p \leq 0.01$) compared to GM cultured controls (**Figure 9.2A**). Concomitantly, mRNA expression of villus cell markers MUC2 (goblet cell marker; $p \leq 0.01$) was increased and PEPT1 tended to be increased (di-/tri-peptide transporter, enterocyte marker; $p = 0.07$) in DM cultured monolayers compared to GM cultured monolayers (**Figure 9.2A**). No differences were observed in mRNA expression of IFABP (enterocyte marker) and LAT2 (neutral amino acid transporter) in DM versus GM cultured monolayers (**Figure 9.2A**). DM culturing increased intestinal epithelial apoptosis (CC3 immunoreactivity) compared to GM cultured controls ($p \leq 0.05$; **Figure 9.2B**). In addition, after 60h of DM culturing, intestinal epithelial proliferation (Ki67 immunoreactivity) was completely lost, whereas proliferating cells were still present in GM cultured HIO monolayers (**Figure 9.2C**).

Effect of hypoxia on crypt-like HIO monolayers and 3D HIO

Hypoxia was used to induce a diseased phenotype in the crypt-like HIO, since it is an important factor contributing to the pathogenesis of IBD⁵⁰, IRI⁵¹ and NEC⁵². Exposure of crypt like (GM cultured) HIO monolayers to hypoxia (1% O₂) for 24 hours increased mRNA expression of the pro-inflammatory cytokine IL8 and decreased the mRNA expression of OLFM4 ($p \leq 0.05$), LYZ ($p \leq 0.05$) and PEPT1 ($p \leq 0.0001$) compared to normoxic controls (**Figure 9.3A**). mRNA expression of LAT2 and Hypoxia Inducible Factor 1 alpha (HIF1A, hypoxia regulated transcription factor) were unaltered (**Figure 9.3A**). Importantly, however, mRNA expression of HIF1A (both hypoxia regulated transcription factors) appeared to peak at an earlier time point following the onset of hypoxia (**Supplementary Figure 9.3**). Exposure to hypoxia increased intestinal epithelial apoptosis (CC3 immunoreactivity, **Figure 9.3B**) and proliferation (Ki67 immunoreactivity, **Figure 9.3C**) in crypt-like HIO monolayers compared to

normoxic controls ($p \leq 0.01$), indicating increased epithelial cell turnover. In addition, 24h exposure to hypoxia caused disruption of ZO1 protein expression (**Figure 9.3D**), characterized by unequal division of ZO1 protein across the cell-cell surface and focal ZO1 accumulation. Last, after 16h of hypoxia, the paracellular barrier function of 3D crypt-like HIO was diminished compared to normoxic controls (increased L:BL ratio in FITC-D4 paracellular barrier assay, **Figure 9.3E**). For this experiment, 16h of hypoxia was chosen as this gave a steady loss of barrier function in the hypoxic organoids, while normoxic controls retaining a good barrier function, and concurrently allowed for pre-incubation of the nutritional components before start of hypoxia within a 24 hour study period.

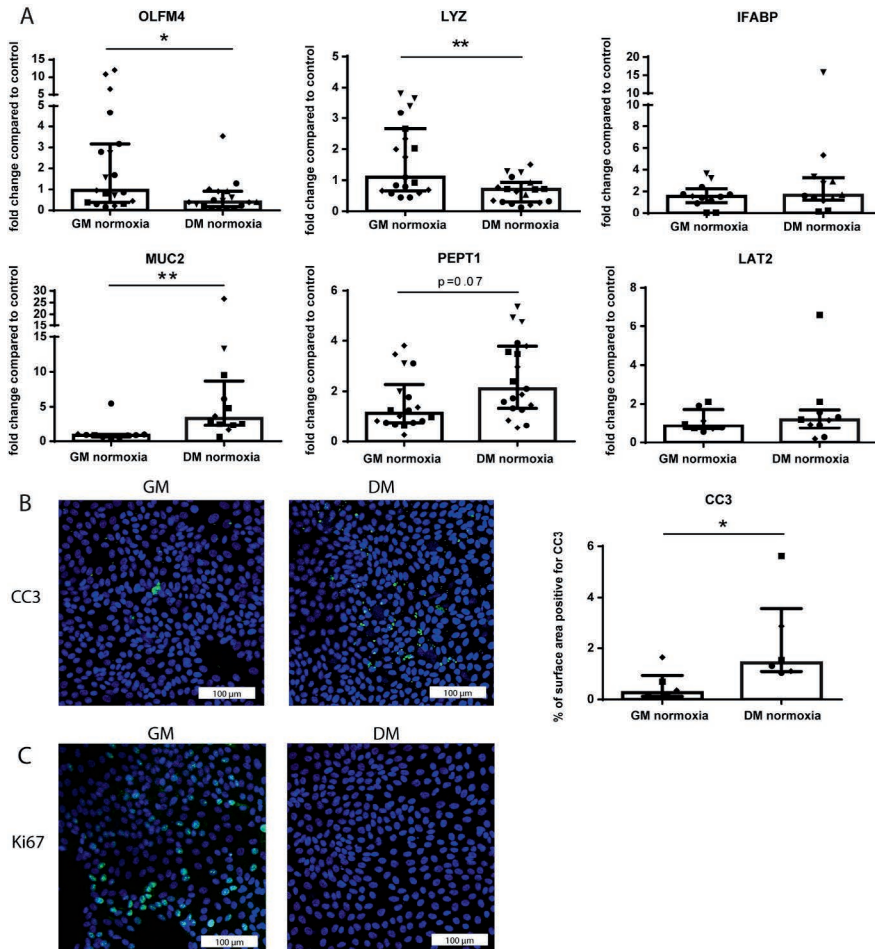


Figure 9.2 Effects of 60h culturing with DM on HIO monolayers compared GM cultured controls. A. mRNA expression of crypt cell markers OLFM4 (stem cells) and LYZ (Paneth cells), villus cell markers IFABP (enterocytes), MUC2 (Goblet cells) and PEPT1 (enterocytes) and LAT2 (amino acid transporter). Data are reported as relative expression compared to GM (set at 1) and displayed as median with interquartile range. Results were obtained from three different HIO

donors (depicted by different data point symbols). * $p \leq 0.05$, ** $p \leq 0.01$. **B.** Representative images of immunofluorescence staining of CC3 in HIO monolayers cultured with GM or DM for 60h and analysis of the % of surface area positive for CC3 in both groups. Data are displayed as median with interquartile range. Results were obtained from three different HIO donors (depicted by different data point symbols). Scale bars indicate 100 μm . * $p \leq 0.05$. **C.** Representative images of immunofluorescence staining of Ki67 in HIO monolayers cultured with GM or DM for 60h. Data are displayed as median with interquartile range. Results were obtained from three different HIO donors (depicted by different data point symbols). Scale bars indicate 100 μm . Abbreviations: OLFM4, olfactomedin 4; LYZ, lysozyme; IFABP, intestinal fatty acid binding protein; MUC2, mucin 2; PEPT1, peptide transporter 1; LAT2, L-type amino acid transporter 2; CC3, cleaved caspase 3.

Effect of hypoxia on villus-like HIO monolayers

Hypoxia was used to induce a diseased phenotype in villus-like HIO as well. A longer hypoxia period of 48 hours was chosen for DM cultured HIO monolayers compared to GM cultured HIO monolayers as DM cultured HIO were observed to be less sensitive to the effects of hypoxia (unpublished observations). In villus-like HIO (DM cultured), exposure to hypoxia (1% O_2) for 48 hours increased mRNA expression of IL8 ($p \leq 0.05$) and decreased the mRNA expression of OLFM4 ($p \leq 0.01$) and PEPT1 ($p \leq 0.001$) compared to normoxic controls (**Figure 9.4A**). Additionally, mRNA expression of HIF1A ($p \leq 0.05$) was decreased after 48h of hypoxia compared to normoxic controls (**Figure 9.4A**), which may result from the effect of negative feedback loops on its expression following prolonged hypoxia^{53,54}. mRNA expression of LYZ and LAT2 were unaltered following hypoxia at the studied time point (**Figure 9.4A**). Exposing villus-like HIO monolayers to hypoxia for 24h mildly disrupted ZO1 protein expression (**Figure 9.4C**), characterized by focal ZO1 protein accumulation. In addition, 24h of hypoxia caused an increase in intestinal epithelial apoptosis (CC3 immunoreactivity), although this increase did not reach statistical significance (**Figure 9.4B**).

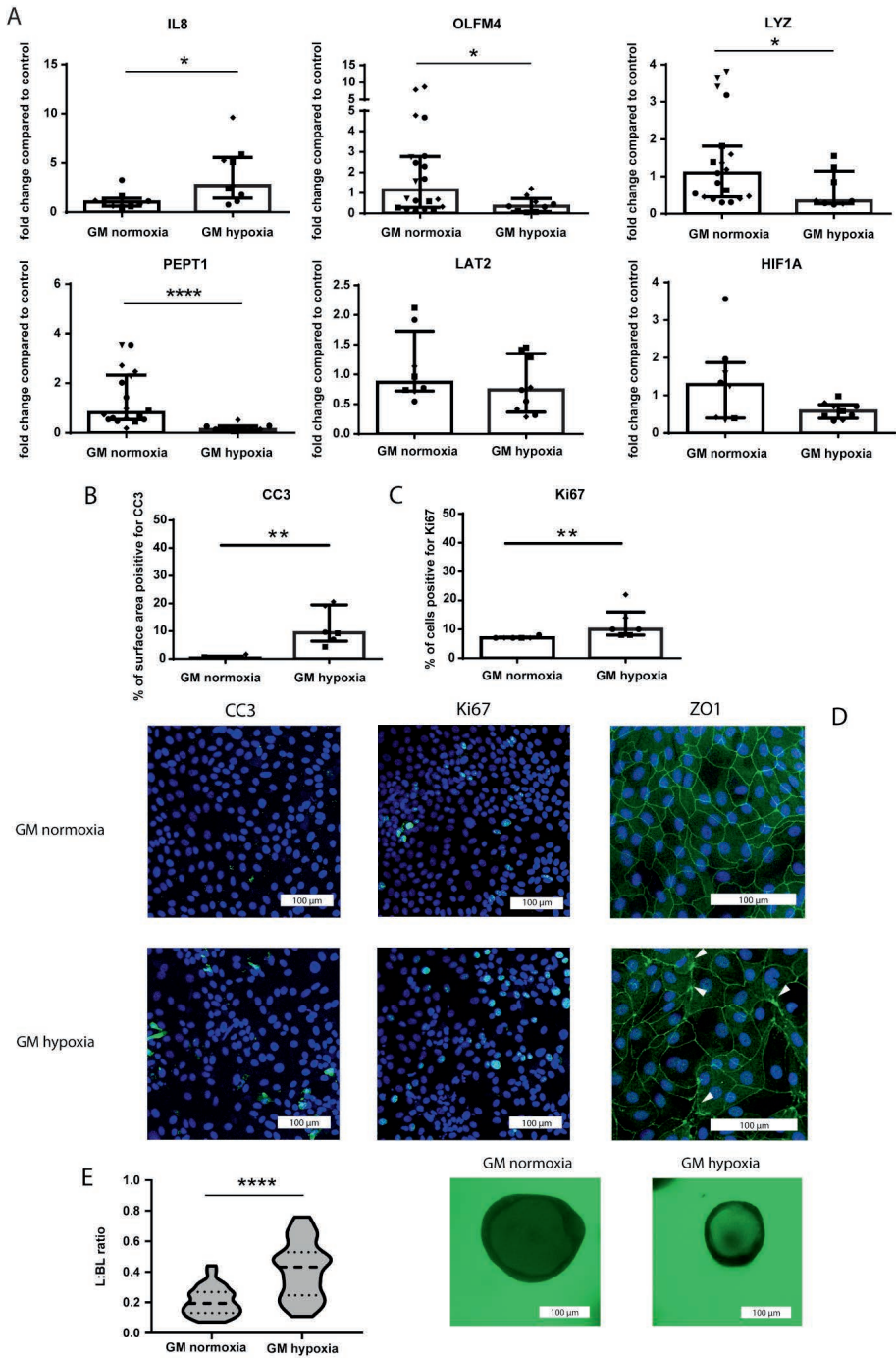


Figure 9.3 **Effects of hypoxia on crypt-like (GM cultured) HIO (monolayer and 3D cultured).** A. mRNA expression of IL8 (pro-inflammatory cytokine), OLFM4 (stem cells), LYZ (Paneth cells), PEPT1 (di/tri-peptide transporter), LAT2 (amino acid transporter) and HIF1A (hypoxia regulated transcription factor). Data are reported as relative expression compared to normoxia (set at 1) and displayed as median with interquartile range. Results were obtained from three different HIO donors (depicted by different data point symbols). * $p \leq 0.05$, **** $p \leq 0.0001$. B. Analysis of the % of surface area positive for CC3 and representative images from immunofluorescence staining of CC3 in crypt-like HIO monolayers exposed to hypoxia for 24h compared to normoxic controls. Data are displayed as median with interquartile range. Results were obtained from three different HIO donors (depicted by different data point symbols). Scale bars indicate 100 μm . ** $p \leq 0.01$. C. Analysis of the % of cells positive for Ki67 and representative images from immunofluorescence staining of Ki67 in crypt-like HIO monolayers exposed to hypoxia for 24h compared to normoxic controls. Data are displayed as median with interquartile range. Results were obtained from three different HIO donors (depicted by different data point symbols). Scale bars indicates 100 μm . ** $p \leq 0.01$. D. Representative images from immunofluorescence staining of ZO1 in crypt-like HIO monolayers exposed to hypoxia for 24h compared to normoxic controls. Results were obtained from three different HIO donors. Scale bars indicate 100 μm . E. FITC-D4 paracellular barrier assay with representative images of crypt-like 3D HIO exposed to hypoxia for 16h compared to controls. FITC-D4 fluorescence intensity is expressed as a luminal (L) to basolateral (BL) ratio. Per group, at least 10 HIO were measured in three different donors. Scale bars indicate 100 μm . **** $p \leq 0.0001$. Abbreviations: IL8, interleukin 8; OLFM4, olfactomedin 4; LYZ, lysozyme; PEPT1, peptide transporter 1; LAT2, L-type amino acid transporter 2; HIF1A, hypoxia inducible factor 1 alpha; CC3, cleaved caspase 3; ZO1, zona occludens 1.

Differential effect of hypoxia on crypt-like and villus-like HIO monolayers and 3D HIO

Villus-like HIO, both 3D and monolayer cultured, displayed less damage following exposure to hypoxia than crypt-like HIO. Both in crypt-like and villus-like HIO monolayers, hypoxia led to increased intestinal epithelial cell death (CC3 immunoreactivity) (**Figure 9.5A**). However, the increase was less pronounced in villus-like HIO monolayers than in crypt-like HIO monolayers (**Figure 9.5A**). Comparably, 16h of hypoxia exposure caused substantially less loss of paracellular barrier function in villus-like 3D HIO than in crypt-like 3D HIO (**Figure 9.5B**). This difference in vulnerability to hypoxia was not abrogated by removal of the antioxidant NAC from GM, addition of NAC to DM or replacement of the surplus of AdDF+++ in DM by the DMEM medium used for the production of Wnt3a conditioned medium (**Figure 9.5B**).

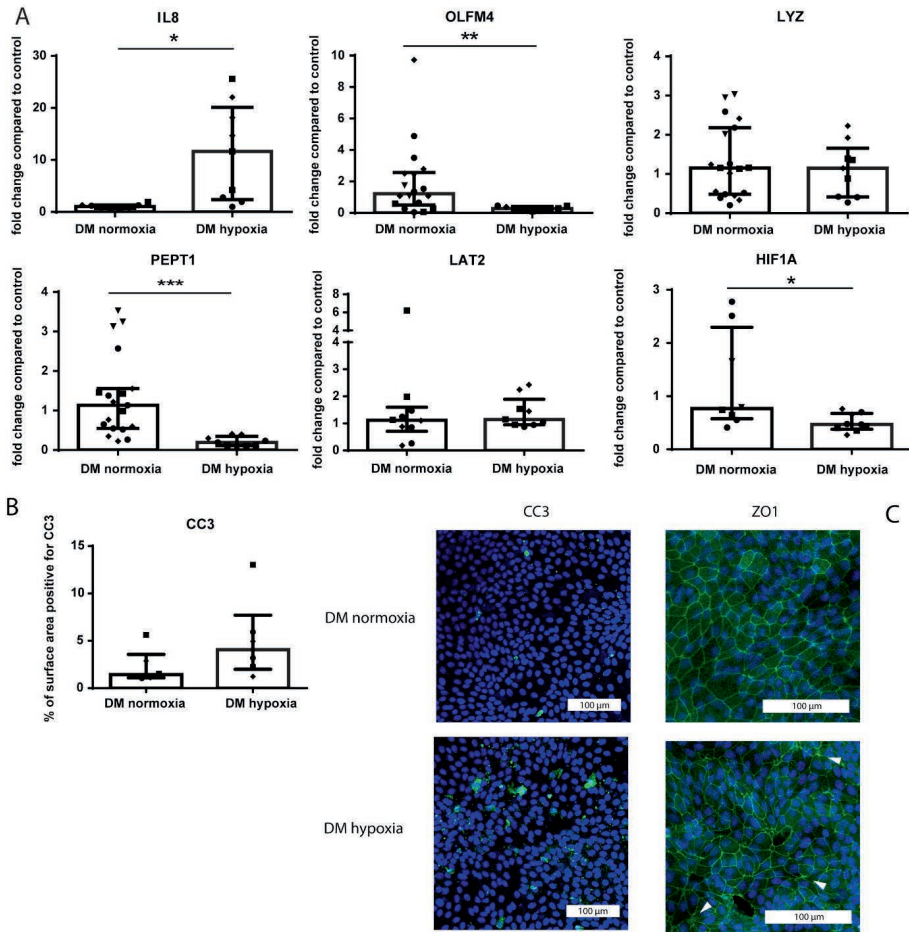


Figure 9.4 Effects of hypoxia on villus-like (DM cultured) HIO (monolayer cultured). A. mRNA expression of IL8 (pro-inflammatory cytokine), OLFM4 (stem cells), LYZ (Paneth cells), PEPT1 (di/tri-peptide transporter), LAT2 (amino acid transporter) and HIF1A (hypoxia regulated transcription factor) following 48h of hypoxia (1% O₂) in villus-like HIO monolayers. Data are reported as relative expression compared to normoxia (set at 1) and displayed as median with interquartile range. Results were obtained from three different HIO donors (depicted by different data point symbols). * p \leq 0.05, **p \leq 0.01, ***p \leq 0.001. B. Analysis of the % of surface area positive for CC3 and representative images from immunofluorescence staining of CC3 in villus-like HIO monolayers exposed to hypoxia for 24h compared to normoxic controls. C. Representative images from immunofluorescence staining of ZO1 in villus-like HIO monolayers exposed to hypoxia for 24h compared to normoxic controls. Results were obtained from three different HIO donors. Scale bars indicate 100 μ m. Data are displayed as median with interquartile range. Results were obtained from three different HIO donors (depicted by different data point symbols). Scale bars indicate 100 μ m. Abbreviations: IL8, interleukin 8; OLFM4, olfactomedin 4; LYZ, lysozyme; PEPT1, peptide transporter 1; LAT2, L-type amino acid transporter 2; HIF1A, hypoxia inducible factor 1 alpha; ZO1, zona occludens 1; CC3, cleaved caspase 3.

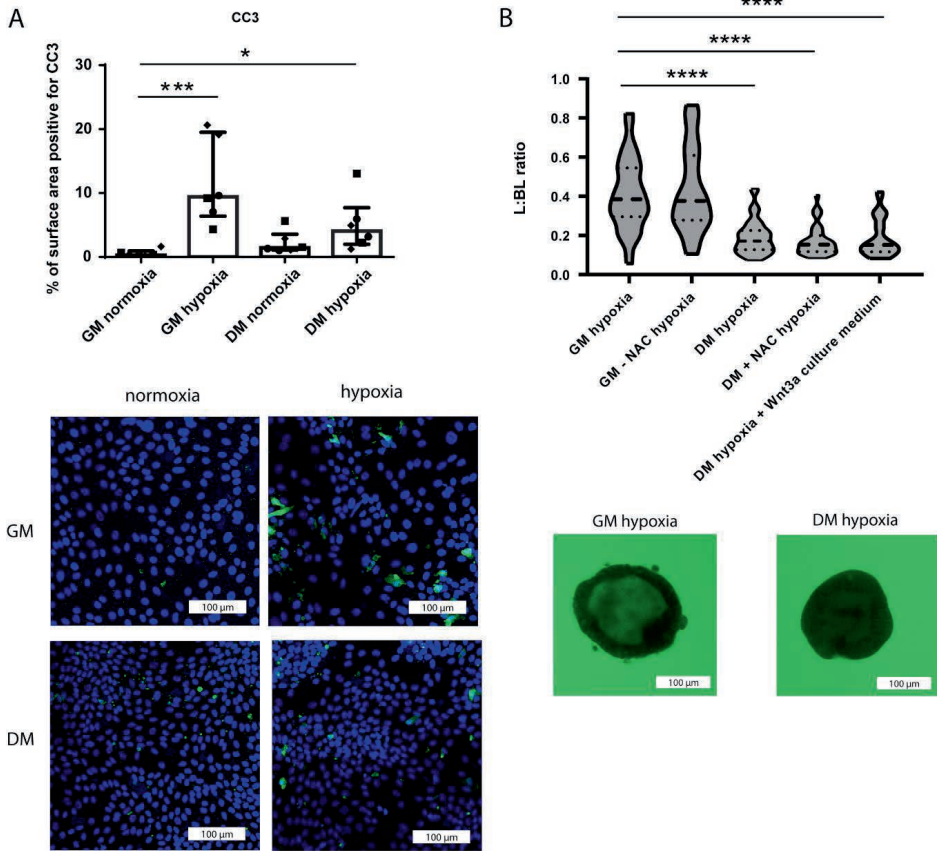


Figure 9.5 Differential effect of hypoxia on crypt-like and villus-like HIO (3D and monolayer cultured). A. Analysis of the % of surface area positive for CC3 and representative images from immunofluorescence staining of CC3 in crypt-like and villus-like HIO monolayers exposed to hypoxia for 24h compared to normoxic controls. Data are displayed as median with interquartile range. Results were obtained from three different HIO donors (depicted by different data point symbols). Scale bars indicate 100 μ m. B. FITC-D4 paracellular barrier assay of crypt-like (GM cultured) and villus-like (DM cultured) 3D HIO exposed to hypoxia for 16h, in presence or absence of NAC and following replacement of the surplus of AddF+++ in DM by the DMEM medium used for the production of Wnt3a conditioned medium. Representative images of crypt-like (GM cultured) and villus-like (DM cultured) 3D HIO exposed to hypoxia for 16h. FITC-D4 fluorescence intensity is expressed as a luminal (L) to basolateral (BL) ratio. Per group, 15 HIO were measured in 3 different donors. Scale bars indicate 100 μ m. * p ≤0.5, *** p ≤0.001, **** p ≤0.0001. Abbreviations: CC3, cleaved caspase 3.

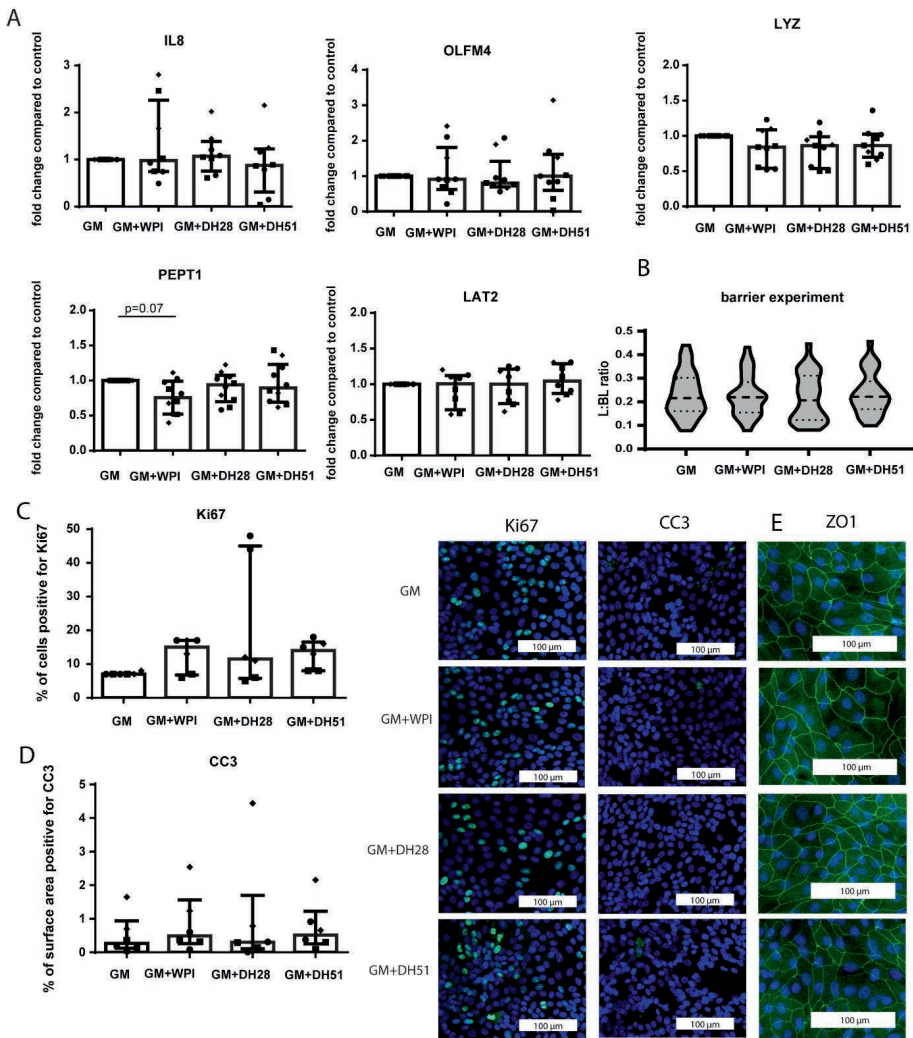


Figure 9.6 Effect of WPI, DH28 and DH51 on crypt-like HIO (monolayer and 3D cultured) in a healthy setting (normoxia). A. mRNA expression of IL8 (pro-inflammatory cytokine), OLFM4 (stem cells), LYZ (Paneth cells), PEPT1 (di/tri-peptide transporter) and LAT2 (amino acid transporter) in crypt-like HIO monolayers following 24h exposure to WPI, DH28 or DH51 compared to control. Data are reported as relative expression compared to control (set at 1) and displayed as median with interquartile range. Results were obtained from three different HIO donors (depicted by different data point symbols). B. FITC-D4 paracellular barrier assay of crypt-like 3D HIO exposed to WPI, DH28 or DH51 for 24h compared to controls. FITC-D4 fluorescence intensity is expressed as a luminal (L) to basolateral (BL) ratio. Per group, 10 HIO were measured in three different donors. C. Analysis of the % of cells positive for Ki67 and representative images from immunofluorescence staining of Ki67 in crypt-like HIO monolayers exposed to WPI, DH28 or DH51 for 24h compared to controls. Data are displayed as median with interquartile range. Results were obtained from three different HIO donors (depicted by different data point symbols). Scale bars indicates 100 μ m. D. Analysis of the % of surface area positive for CC3 and representative images from immunofluorescence staining of CC3 in crypt-like HIO monolayers exposed to WPI, DH28 or DH51 for 24h compared to controls. Data are displayed as median with interquartile range. Results were obtained from three different HIO donors (depicted by different data point symbols). Scale bars indicates 100 μ m.

representative images from immunofluorescence staining of CC3 in crypt-like HIO monolayers exposed to WPI, DH28 or DH51 for 24h compared to controls. Data are displayed as median with interquartile range. Results were obtained from three different HIO donors (depicted by different data point symbols). Scale bars indicate 100 μm . E. Representative images from immunofluorescence staining of ZO1 in crypt-like HIO monolayers exposed to WPI, DH28 or DH51 for 24h compared to controls. Results were obtained from three different HIO donors. Scale bars indicate 100 μm . Abbreviations: IL8, interleukin 8; OLFM4, olfactomedin 4; LYZ, lysozyme; PEPT1, peptide transporter 1; LAT2, L-type amino acid transporter 2; CC3, cleaved caspase 3, ZO1, zona occludens 1; WPI, whey protein isolate; DH28, whey protein hydrolysate with 28% degree of hydrolysis; DH51, whey protein hydrolysate with 51% degree of hydrolysis.

Comprehensive screening of whey protein fractions

Effect of WPI, DH28 and DH51 on crypt-like HIO (monolayer and 3D cultured) in a healthy setting (normoxia)

In a healthy setting (normoxia), 24h exposure to the different whey fractions of crypt-like HIO monolayers did not alter the mRNA expression of IL8, OLFM4, LYZ or LAT2 (**Figure 9.6A**). PEPT1 mRNA expression tended to be decreased by exposure to WPI, but this difference did not reach statistical significance ($p=0.07$) (**Figure 9.6A**). Paracellular barrier function of 3D HIO was unaltered by the different whey fractions under normoxic conditions (**Figure 9.6B**). In addition, exposure to the different whey fractions did not alter the amount of proliferating intestinal epithelial cells (Ki67 immunoreactivity) (**Figure 9.6C**), the level of intestinal epithelial apoptosis (**Figure 9.6D**) or ZO1 protein expression (**Figure 9.6E**).

Effect of WPI, DH28 and DH51 on villus-like HIO (monolayer and 3D cultured) in a healthy setting (normoxia)

Exposing villus-like HIO monolayers for 24h to WPI, DH28 or DH51 did not alter the mRNA expression of IL8, OLFM4 or PEPT1 (**Figure 9.7A**) compared to controls in a healthy setting (normoxia). LAT2 mRNA expression was moderately but statistically significantly decreased by WPI ($p\leq 0.05$, **Figure 9.7A**). In addition, LYZ mRNA expression tended to be decreased by DH51 ($p=0.05$, **Figure 9.7A**). Exposure to the different whey fractions in a healthy setting (normoxia) did not alter the level of intestinal epithelial apoptosis (**Figure 9.7B**) or ZO1 protein expression (**Figure 9.7C**).

Effect of WPI, DH28 and DH51 on crypt-like HIO (monolayer and 3D cultured) in a diseased setting (hypoxia)

In a diseased setting (24h exposure to hypoxia), 24h exposure to DH28 and DH51 increased the mRNA expression of stem cell marker OLFM4 (both $p\leq 0.01$) (**Figure 9.8A**) in crypt-like HIO monolayers. Exposure to DH28 concomitantly decreased the mRNA expression of HIF1A ($p\leq 0.05$) (**Figure 9.8A**). In addition, exposure to WPI increased the mRNA expression of PEPT1 ($p\leq 0.05$) (**Figure 9.8A**). mRNA expression of IL8, LYZ and LAT2 were unaffected by exposure to WPI, DH28 or DH51 in crypt-like hypoxic HIO monolayers. The amount of proliferating intestinal epithelial cells (Ki67 immunoreactivity) tended to be increased by exposure to DH28, although this increase did not reach statistical significance ($p=0.08$)

(Figure 9.8B). The level of intestinal epithelial apoptosis (CC3 immunoreactivity) was not changed by addition of WPI, DH28 or DH51 (Figure 9.8C) to the GM, nor was the ZO1 protein expression (Figure 9.8D). Importantly, however, paracellular barrier function was improved by exposure to DH28 ($p \leq 0.05$) (Figure 9.8E).

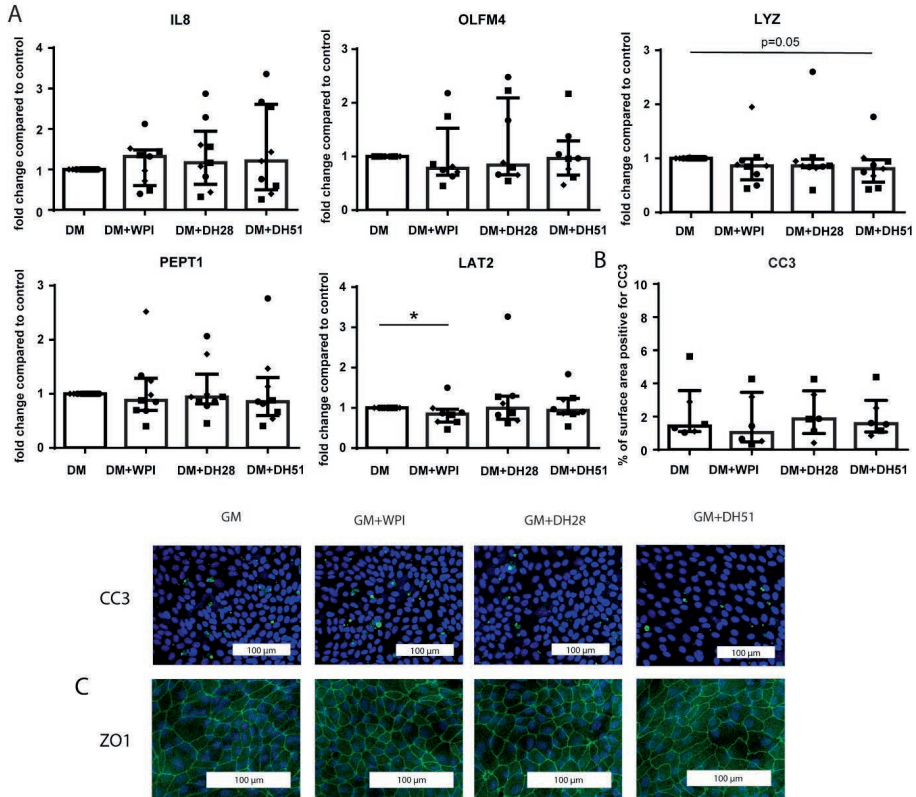


Figure 9.7 Effect of WPI, DH28 and DH51 on villus-like HIO (monolayer cultured) in a healthy setting (normoxia). A. mRNA expression of IL8 (pro-inflammatory cytokine), OLFM4 (stem cells), LYZ (Paneth cells), PEPT1 (di/tri-peptide transporter) and LAT2 (amino acid transporter) in villus-like HIO monolayers following 24h exposure to WPI, DH28 or DH51 compared to control. Data are reported as relative expression compared to control (set at 1) and displayed as median with interquartile range. Results were obtained from 3 different HIO donors (depicted by different data point symbols). * $p \leq 0.05$. B. Analysis of the % of surface area positive for CC3 and representative images from immunofluorescence staining of CC3 in villus-like HIO monolayers exposed to WPI, DH28 or DH51 for 24h compared to controls. Data are displayed as median with interquartile range. Results were obtained from 3 different HIO donors (depicted by different data point symbols). Scale bars indicate 100 μm . E. Representative images from immunofluorescence staining of ZO1 in villus-like HIO monolayers exposed to WPI, DH28 or DH51 for 24h compared to controls. Results were obtained from 3 different HIO donors. Scale bars indicate 100 μm . Abbreviations: IL8, interleukin 8; OLFM4, olfactomedin 4; LYZ, lysozyme; PEPT1, peptide transporter 1; LAT2, L-type amino transporter 2; CC3, cleaved caspase 3; WPI, whey protein isolate; DH28, whey protein hydrolysate with 28% degree of hydrolysis; DH51, whey protein hydrolysate with 51% degree of hydrolysis.

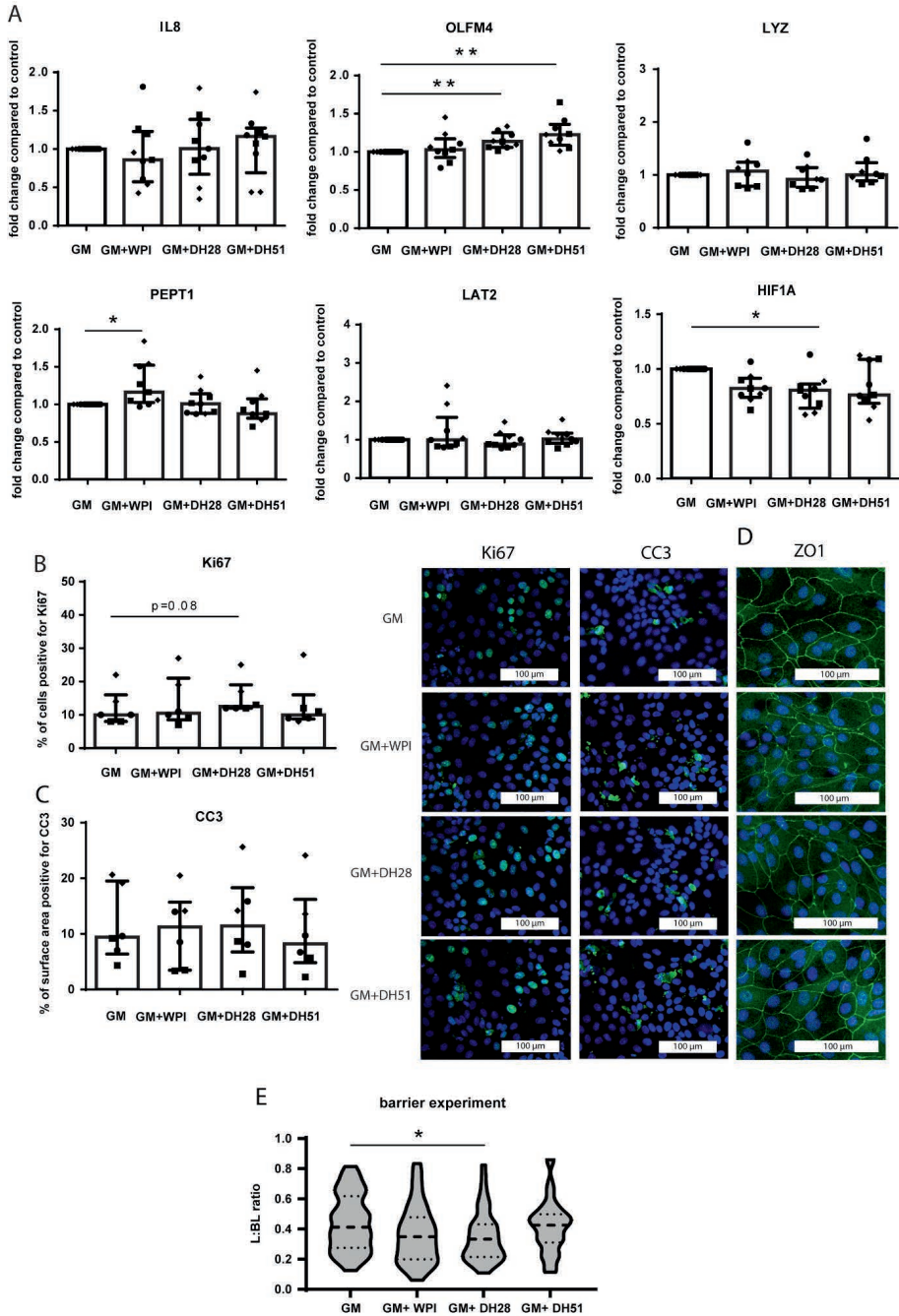


Figure 9.8 Effect of WPI, DH28 and DH51 on crypt-like HIO (monolayer and 3D cultured) in a diseased setting (hypoxia). A. mRNA expression of IL8 (pro-inflammatory cytokine), OLFM4 (stem cells),

LYZ (Paneth cells), PEPT1 (di/tri-peptide transporter), LAT2 (amino acid transporter) and HIF1A (hypoxia regulated transcription factor) in crypt-like HIO monolayers exposed to hypoxia (24h) and to WPI, DH28 or DH51 (24h) compared to control. Data are reported as relative expression compared to control (set at 1) and displayed as median with interquartile range. Results were obtained from 3 different HIO donors (depicted by different data point symbols). * $p \leq 0.05$, ** $p \leq 0.01$. B. Analysis of the % of cells positive for Ki67 and representative images from immunofluorescence staining of Ki67 in crypt-like HIO monolayers exposed to hypoxia (24h) and to WPI, DH28 or DH51 (24h) compared to controls. Data are displayed as median with interquartile range. Results were obtained from three different HIO donors (depicted by different data point symbols). Scale bars indicates 100 μm . C. Analysis of the % of surface area positive for CC3 and representative images from immunofluorescence staining of CC3 in crypt-like HIO monolayers exposed to hypoxia (24h) and to WPI, DH28 or DH51 (24h) compared to controls. Data are displayed as median with interquartile range. Results were obtained from three different HIO donors (depicted by different data point symbols). Scale bars indicate 100 μm . D. Representative images from immunofluorescence staining of ZO1 in crypt-like HIO monolayers exposed to hypoxia (24h) and to WPI, DH28 or DH51 (24h) compared to controls. Results were obtained from three different HIO donors. Scale bars indicate 100 μm . E. FITC-D4 paracellular barrier assay of crypt-like 3D HIO exposed to hypoxia (16h) and to WPI, DH28 or DH51 (24h) compared to controls. FITC-D4 fluorescence intensity is expressed as a luminal (L) to basolateral (BL) ratio. Per group, 15 HIO were measured in three different donors. * $p \leq 0.05$. Abbreviations: IL8, interleukin 8; OLFM4, olfactomedin 4; LYZ, lysozyme; PEPT1, peptide transporter 1; LAT2, L-type amino acid transporter 2; HIF1A, hypoxia inducible factor 1 alpha; ZO1, zona occludens 1; CC3, cleaved caspase 3; WPI, whey protein isolate; DH28, whey protein hydrolysate with 28% degree of hydrolysis; DH51, whey protein hydrolysate with 51% degree of hydrolysis.

Effect of WPI, DH28 and DH51 on villus-like HIO (monolayer and 3D cultured) in a diseased setting (hypoxia)

In a diseased setting (48h exposure to hypoxia), 48h exposure to DH51 increased the mRNA expression of stem cell marker OLFM4 ($P \leq 0.05$) (**Figure 9.9A**) in villus-like HIO monolayers. HIF1A mRNA expression was reduced by exposure to DH28 ($P \leq 0.05$) (**Figure 9.9A**). The different whey fractions did not alter the mRNA expression of IL8, LYZ, PEPT1 and LAT2 (**Figure 9.9A**). The level of intestinal epithelial apoptosis (CC3 immunoreactivity) was not changed by addition of WPI, DH28 or DH51 (**Figure 9.9B**) to the DM for 24h in a diseased setting (24h hypoxia). Last, ZO1 protein expression was not affected by administration of WPI, DH28 or DH51 (24h) during hypoxia (24h) (**Figure 9.9C**).

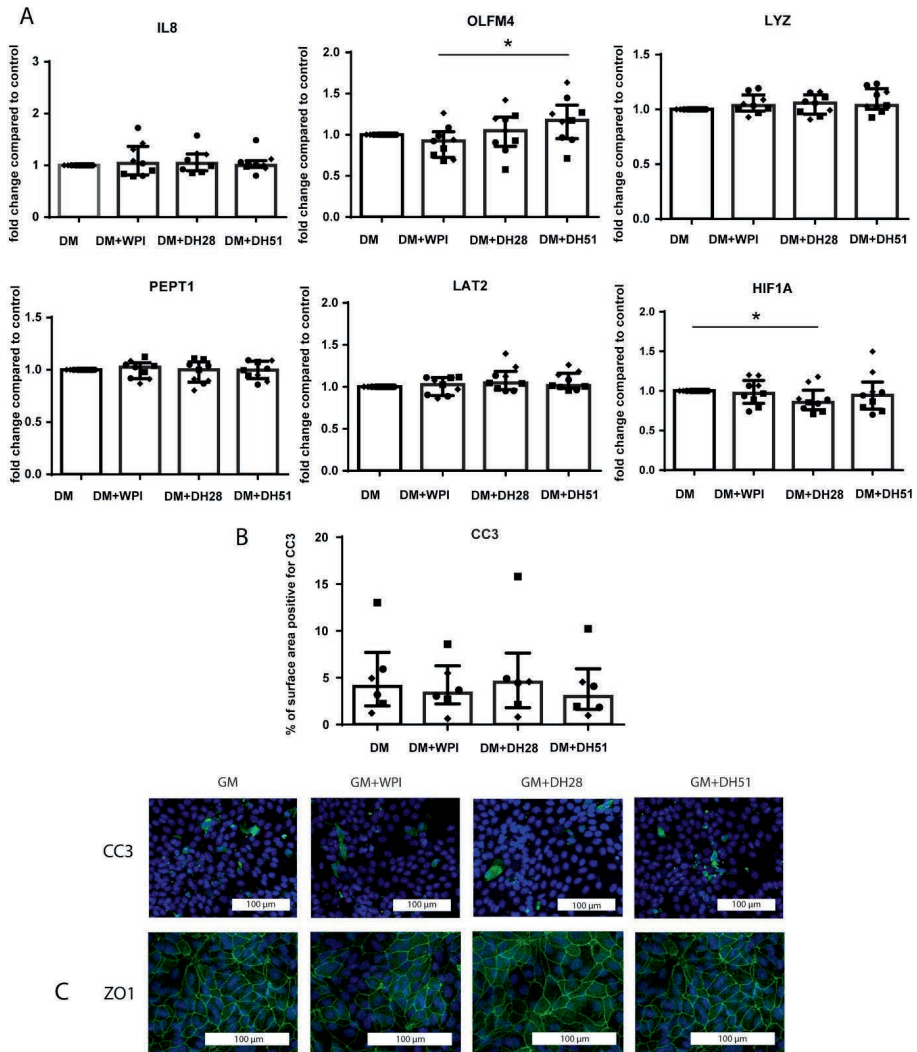


Figure 9.9 Effect of WPI, DH28 and DH51 on villus-like HIO (monolayer cultured) in a diseased setting (hypoxia). A. mRNA expression of IL8 (pro-inflammatory cytokine), OLFM4 (stem cells), LYZ (Paneth cells), PEPT1 (di/tri-peptide transporter), LAT2 (amino acid transporter) and HIF1A (hypoxia regulated transcription factor) in villus-like HIO monolayers exposed to hypoxia (48h) and to WPI, DH28 or DH51 (48h) compared to control. Data are reported as relative expression compared to control (set at 1) and displayed as median with interquartile range. Results were obtained from 3 different HIO donors (depicted by different data point symbols). * $p < 0.05$. B. Analysis of the % of surface area positive for CC3 and representative images from immunofluorescence staining of CC3 in villus-like HIO monolayers exposed to hypoxia (24h) and to WPI, DH28 or DH51 (24h) compared to controls. Data are displayed as median with interquartile range. Results were obtained from 3 different HIO donors (depicted by different data point symbols). Scale bars indicate 100 μm . C. Representative images from

immunofluorescence staining of ZO1 in villus-like HIO monolayers exposed to hypoxia (24h) and to WPI, DH28 or DH51 (24h) compared to controls. Results were obtained from 3 different HIO donors. Scale bars indicate 100 μm . Abbreviations: IL8, interleukin 8; OLFM4, olfactomedin 4; LYZ, lysozyme; PEPT1, peptide transporter 1; LAT2, L-type amino acid transporter 2; HIF1A, hypoxia inducible factor 1 alpha; CC3, cleaved caspase 3; ZO1, zona occludens 1; WPI, whey protein isolate; DH28, whey protein hydrolysate with 28% degree of hydrolysis; DH51, whey protein hydrolysate with 51% degree of hydrolysis.

Effect of WPI, DH28 and DH51 on T cell subsets and T cell proliferation

We studied the effect of WPI, DH28 and DH51 on regulatory T cells (Treg) with flow cytometric analysis of unactivated PBMCs cultured with or without the different experimental fractions for 5 days (**Supplementary Figure S9.4**). WPI increased the percentage of Treg (CD4+CD25^{high}CD127^{low} T cells) within the population of CD4+ T cells ($p \leq 0.001$, **Figure 9.10A**). This finding was supported by an increased FoxP3 mRNA expression in this group ($p \leq 0.01$, **Figure 9.10B**). In addition, incubation with WPI increased the percentage of CD69+ T cells within the population of Treg and increased the CD25 expression (MFI) of Treg ($p \leq 0.01$ and $p \leq 0.001$ respectively, **Figure 9.10C, D**). The percentage of CD69+ T cells in Treg was also increased by incubation with DH28 ($p \leq 0.05$, **Figure 9.10C**). These findings prompted us to study the effects of WPI, DH28 and DH51 on T cell proliferation of T-cell activated PBMCs (**Supplementary Figure S9.5**). Incubation with WPI, but not DH28 or DH51, decreased the percentage of CD4+ T cells proliferating ($p \leq 0.01$) (**Figure 9.10E, Supplementary Figure S9.5**). CD8+ T cell proliferation also tended to be decreased by exposure to WPI ($p = 0.08$, **Supplementary Figure S9.5**).

Effect of WPI, DH28 and DH51 on PBMC cytokine expression and activation makers

Cytokine mRNA expression was studied in human PBMCs in which T-cells were activated and that were cultured with or without the different experimental fractions for 5 days. Upon T-cell activation, incubation of PBMCs with DH51 tended to decrease the IL10 mRNA expression (Treg cytokine, $p = 0.08$) (**Figure 9.11A**). Incubation with DH28 increased the mRNA expression of IFN γ (Th1 cytokine, $p \leq 0.05$, **Figure 9.11A**) and IFN γ relative to IL4 (IFN γ -IL4 z-score difference, Th1-Th2 balance, $P \leq 0.0001$, **Figure 9.11B**) compared to incubation with WPI (**Figure 9.11B**). mRNA expression of TNF α (Th1 cytokine), IL17A (Th17 cytokine) and IL4 (Th2 cytokine) was not affected by incubation with WPI, DH28 or DH51 (**Figure 9.11A**).

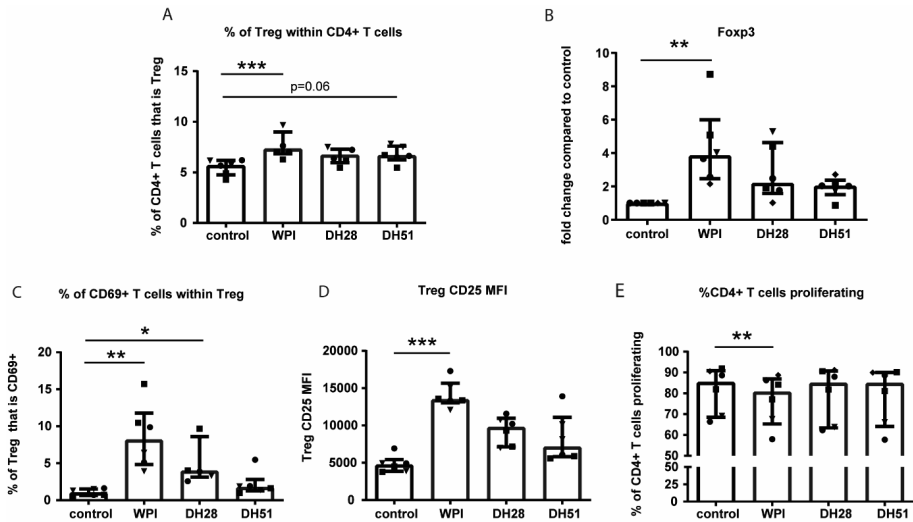


Figure 9.10 Number and CD25 and CD69 expression of CD4+CD25^{high}CD127^{low} Treg in unactivated PBMCs, and proliferation of CD4+ T cells in T-cell activated PBMCs following incubation with WPI, DH28 or DH51. A. The percentage of Treg (CD4+CD25^{high}CD127^{low} T cells) within the population of CD4+ T cells in unactivated PBMCs incubated with or without WPI, DH28 or DH51 for 5 days. Data are displayed as median with interquartile range. ***p<0.001 Results were obtained from three different PBMC donors (depicted by different data point symbols). B. mRNA expression of FoXP3 in unactivated PBMCs incubated with or without WPI, DH28 or DH51 for 5 days. Data are reported as relative expression compared to control (set at 1) and displayed as median with interquartile range. Results were obtained from four different PBMC donors (depicted by different data point symbols). **p<0.01 C. Percentage of CD69+ T cells within the population of Treg in unactivated PBMCs incubated with or without WPI, DH28 or DH51 for 5 days. Data are displayed as median with interquartile range. *p<0.05, **p<0.01 Results were obtained from three different PBMC donors (depicted by different data point symbols). D. CD25 expression (MFI) of Treg in unactivated PBMCs incubated with or without WPI, DH28 or DH51 for 5 days. Data are displayed as median with interquartile range. ***p<0.001 Results were obtained from three different PBMC donors (depicted by different data point symbols). E. The percentage of CD4+ cells proliferating in T-cell activated PBMCs incubated with or without WPI, DH28 or DH51 for 5 days. Results were obtained from four different PBMC donors (depicted by different data point symbols). Data are displayed as median with interquartile range. **p<0.001 Abbreviations: CD4, cluster of differentiation 4; FoXP3, forkhead box P3; CD25, cluster of differentiation 25; CD69, cluster of differentiation 69; CD127, cluster of differentiation 127; WPI, whey protein isolate; DH28, whey protein hydrolysate with 28% degree of hydrolysis; DH51, whey protein hydrolysate with 51% degree of hydrolysis; MFI mean fluorescent intensity.

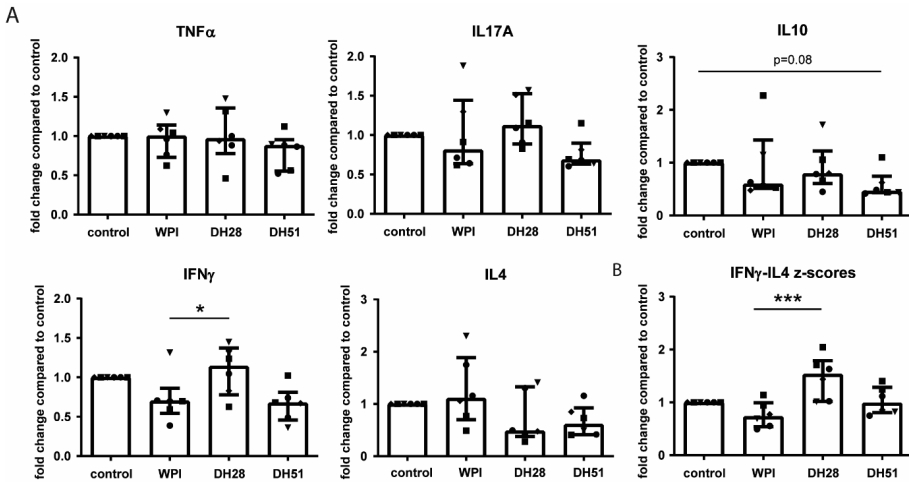


Figure 9.11 mRNA expression of various cytokines in T-cell activated PBMCs following incubation with WPI, DH28 or DH51. A. mRNA expression of TNF α (Th1 cytokine), IL17A (Th17 cytokine), IL-10 (regulatory T cell cytokine), IFN γ (Th1 cytokine) and IL4 (Th2 cytokine) in T-cell activated PBMCs incubated with or without WPI, DH28 or DH51 for 5 days. Data are reported as relative expression compared to control (set at 1) and displayed as median with interquartile range. Results were obtained from four different PBMC donors (depicted by different data point symbols). * $p \leq 0.05$. B. mRNA expression of IFN γ relative to IL4 (IFN γ -IL4 z-scores, Th1-Th2 balance) in T-cell activated PBMCs incubated with or without WPI, DH28 or DH51 for 5 days. Data are reported as relative expression compared to control (set at 1) and displayed as median with interquartile range. Results were obtained from three different HIO donors (depicted by different data point symbols). Results were obtained from four different PBMC donors (depicted by different data point symbols). *** $p \leq 0.001$. Abbreviations: TNF α , tumor necrosis factor alpha; IL17A, interleukin 17A; IL10, interleukin 10; IFN γ , interferon gamma; IL4, interleukin 4; WPI, whey protein isolate; DH28, whey protein hydrolysate with 28% degree of hydrolysis; DH51, whey protein hydrolysate with 51% degree of hydrolysis.

Effect of WPI, DH28 and DH51 on four microbial strains

Effects of WPI, DH28 and DH51 of two pathogenic (*Escherichia coli* and *Staphylococcus aureus*) and two probiotic (*Lactobacillus rhamnosus* and *Bifidobacterium longum*) microbial strains were investigated with a serial dilutions growth inhibition test. WPI, DH28 and DH51 did not change growth of *Escherichia coli*, *Staphylococcus aureus*, *Lactobacillus rhamnosus* and *Bifidobacterium longum* (Figure 9.12).

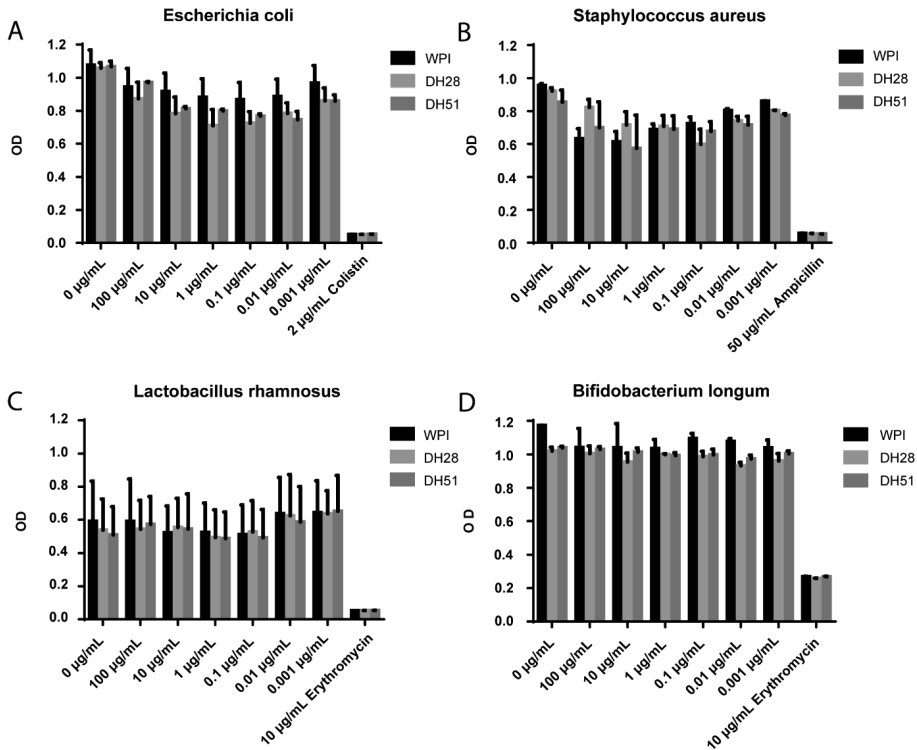


Figure 9.12 Absence of inhibition of growth of *Escherichia coli*, *Staphylococcus aureus*, *Lactobacillus rhamnosus* and *Bifidobacterium longum* by incubation with WPI, DH28 or DH51. Data are presented as mean and standard deviation of two independent measurements. Abbreviations: OD, optical density; WPI, whey protein isolate; DH28, whey protein hydrolysate with 28% degree of hydrolysis; DH51, whey protein hydrolysate with 51% degree of hydrolysis.

Discussion

In the current study, we extended a validated HIO monolayer culture model^{40,41,55} to facilitate screening of the effects of (nutritional) substances including whey protein fractions with different degrees of hydrolysis on undifferentiated and differentiated epithelial cells in a healthy and a diseased state. In line with findings in earlier studies^{40,41}, replacing the normal growth medium (GM) with a differentiation medium (DM) changed the HIO phenotype from crypt-like to villus-like, and, in accordance with the *in vivo* situation, completely blocked intestinal epithelial proliferation, thereby enabling nutritional intervention studies on the complete crypt-villus axis. Moreover, the HIO monolayer model allowed apical administration of the whey protein fractions. Exposure to hypoxia induced a 'diseased state' in the HIO, characterized by intestinal epithelial inflammation (IL8 increase), increased intestinal epithelial apoptosis (CC3) and intestinal barrier loss, reflected by disturbed expression of the tight junction protein ZO1 and, in crypt-like 3D HIOs, a loss of paracellular barrier function. In addition, mRNA expression of the enterocyte marker PEPT1

(crypt-like and villus-like), the stem cell marker OLFM4 (crypt-like and villus-like) and Paneth cell marker LYZ (crypt-like) were reduced by exposure to hypoxia, which is considered to reflect cellular damage along the crypt-villus axis. Importantly, these combined characteristics are an essential part of the pathophysiology of several diseases affecting the intestine, such as IBD^{50,56}, IRI⁵¹ and NEC^{52,57}, indicating the 'diseased state' induced by hypoxia in this HIO model is potentially very relevant for studying the effect of nutritional interventions in a broad set of gastrointestinal diseases.

Interestingly, we observed that villus-like (DM-cultured) HIOs were less sensitive to the effects of hypoxia than crypt-like (GM-cultured) HIOs. This effect was already observed within 24h after replacing GM with DM and was independent of the presence of the antioxidant NAC or the percentage of AdDF+++ in the medium. This suggests that the sensitivity of the HIO intestinal epithelial cells to hypoxia is, amongst others, determined by their differentiation status, or, alternatively, by the presence of medium components directly related to differentiation status, such as Wnt3a. Differences in energy metabolism of undifferentiated (i.e., stem cells and transit amplifying cells) versus differentiated intestinal epithelial cells are likely involved. Analogous to the Warburg effect in cancer cells, highly proliferating cells such as intestinal stem cells largely depend on aerobic glycolysis, whereas differentiated cells rely more on oxidative phosphorylation^{58,59}. Wnt signaling appears to be an important factor modifying this metabolic phenotype^{59,60}. Importantly, differentiated organoids are described to have reduced oxygen consumption rates compared to undifferentiated organoids⁶¹, which is not surprising considering the oxygen gradient along the crypt-villus axis and the physiological hypoxia that is present in the lumen of the intestine⁶². Differences in the metabolic adaptation to hypoxia could also be involved, since Kip et al. previously showed on protein level that crypt-like and villus-like HIOs differentially adapt their mitochondrial metabolism during hypoxia⁶³. Recapitulating, it is important to take the differentiation status of HIOs into account when developing a hypoxia-based HIO model and to study nutritional interventions both in crypt-like and villus-like HIO.

Following successful model development, this HIO model was used as a screening tool to study the effect of whey protein isolate (WPI) and two whey protein hydrolysates with a 28% degree of hydrolysis (DH28) and a 51% degree of hydrolysis (DH51) on the intestinal epithelium in health and disease.

A key finding is that addition of DH28 protected the paracellular barrier function of crypt-like HIO during hypoxia. A possible explanation for this observation is DH28-driven increased intestinal epithelial proliferation. However, this should be interpreted with caution; although the increased proliferation following DH28 exposure may be biologically relevant, differences between the groups did not meet conventional levels of statistical significance ($p=0.08$). Findings at the studied time point did not provide an alternative explanation for the protection of paracellular barrier function. However, we cannot rule out the possibility that factors such as reduction of apoptosis or improvement of tight junction integrity are involved at an earlier moment.

Improvement of paracellular barrier function could be causally linked to the reduced HIF1 α mRNA expression that was detected in both crypt-like and villus-like HIOs following DH28 exposure. The HIF complex, including its hypoxia inducible subunit HIF1 α , is important for cellular adaptation to hypoxia via regulation of a broad range of cellular processes such

as angiogenesis, adaptation of metabolism and cell survival⁶⁴. Besides, HIF1 α signaling is important for maintenance of intestinal barrier function via regulation of tight junction integrity⁶⁵. However, it can contribute to several disease mechanisms⁶⁶, such as intestinal inflammation and gut barrier loss⁶⁷, during prolonged and/or severe hypoxia. HIF1 α signaling is directly controlled by cellular oxygen tension through hydroxylation of HIF1 α by oxygen dependent prolyl-hydroxylase domain containing enzymes (PHD) and subsequent protein breakdown (68). Besides this direct regulation, several metabolic intermediates including reactive oxygen species (ROS) increase HIF1 α signaling, both via direct stabilization of HIF1 α through PHD inhibition and via multiple indirect mechanisms^{68,69}. Given the effect of ROS formation on HIF1 α signaling, antioxidant peptides that have been described to be present in whey protein fractions are likely involved in the downregulation of HIF1 α mRNA following DH28 exposure²⁹. Alternatively, Sirtuin1 (SIRT1), as an important regulator of HIF1 α signaling⁷⁰, and ROS⁷¹ might be involved in the observed HIF1 α reduction and barrier protection following exposure to DH28. This scenario is consistent with earlier findings of SIRT1-mediated protection of the intestinal barrier following LPS-induced inflammation *in vitro*, with concomitant downregulation of HIF1 α protein expression and activity⁷², and with upregulation of SIRT1 by whey protein⁷³. These hypotheses are summarized in **Supplementary Figure S9.6**.

Another evident observation is the increase on mRNA level of the stem cell marker OLFM4 following exposure to DH28 and DH51 in crypt-like (DH28 and DH51) and villus-like (DH51) HIOs under hypoxic conditions. Since the expression of other cell specific markers such as the Paneth cell marker LYZ did not change following exposure to the whey protein fractions, it is likely that the increase in OLFM4 mRNA represents an increased expression per cell rather than an increase in stem cell numbers. As OLFM4 mRNA expression was downregulated during hypoxia in both crypt-like and villus-like HIOs and OLFM4 is important for mucosal defense and acts as an anti-inflammatory molecule in IBD, these findings are potentially relevant for human translation⁷⁴⁻⁷⁶.

On immune cell level, exposure to WPI increased the percentage of Treg in the CD4+ T cell population in unactivated PBMCs, whereas this was not observed following exposure to DH28 or DH51. In addition, the expression of CD25 and CD69 by Treg was increased by incubation with WPI. Interestingly, CD69 expression was previously shown to increase IL10 expression by Treg and their suppressive capacities in mice^{77,78}. In addition, adoptive cell transfer of CD69+ Treg, but not of CD69- Treg or CD69+ Treg from IL10^{-/-} mice, reduced DSS-induced colitis severity in mice⁷⁷, suggesting WPI exposure may increase immune tolerance via induction of Treg with enhanced suppressive capacities. These findings prompted us to study the effects of WPI on T cell proliferation in T-cell activated PBMCs. In line with our Treg observations, WPI decreased the proliferation of CD4+ T cells following T-cell activation. These findings confirm and extend findings in earlier studies; enteral administration of a bovine whey protein extract stimulated the generation of Treg *in vivo* in a murine asthma model⁷⁹ and oral treatment with a formula enriched with WPI improved oral tolerance to ovalbumin in mice⁸⁰. Importantly, in these studies, effects of whey protein could be largely attributed to the presence of TGF β within the whey protein fraction^{79,80}. TGF β consists of a group of 12.7-25 kDa proteins that is virtually absent following hydrolysis⁸⁰ and is of importance for immune tolerance and Treg induction and

function^{81,82}. Thus, TGF β could be an important factor in the observed changes in Treg numbers and expression profile and the reduced CD4+ T cell proliferation following WPI exposure in the current study. Of note, orally administered TGF β was observed to retain its biological effect in intestinal mucosa and was associated with increased serum TGF β levels in mice⁸³, which underscores the potential relevance of our *in vitro* findings for the *in vivo* situation. Interestingly, also T cell cytokine mRNA expression profile was differentially altered by exposure to the different whey protein fractions; DH28 exposure increased the relative expression of IFN γ to IL4 compared to WPI, suggesting DH28 exposure may shift the Th1-Th2 balance more towards a Th1 phenotype. If preserved *in vivo*, these *in vitro* findings could be of clinical relevance. Reduction of CD4+ T cell proliferation and induction of Treg by WPI administration could be used in the infants in the prevention of NEC, which is characterized by decreased proportion of Treg⁸⁴, or in the context of atopic diseases⁸⁵. For adults, these findings could be relevant for several immune mediated diseases with increasing prevalence, such as IBD or autoimmune diseases^{86,87}. Additionally, shifting the Th1-Th2 balance towards a Th1 phenotype could be beneficial in both infants and adults based on several determinants, such as disease state⁸⁸⁻⁹⁰, age⁹¹ and atopic predisposition⁹², which will be addressed in adjacent studies.

A limitation of the current study set-up is that the different whey protein fractions were administered basolaterally during the paracellular barrier function experiments, which could limit the bioactive effect of the whey protein fractions in case these depend on cellular uptake of di- or tri-peptides or on receptors that are solely expressed at the apical surface of the enterocyte. Another limitation is that, although effects of the whey protein fractions on peripheral immune cells and microbial strains were investigated, experiments with interaction between intestinal epithelial cells, immune cells and microbial strains were not performed. One might argue that direct administration of the whey protein fractions to PBMCs limits the relevance of these findings to enteral administration of these fractions *in vivo*, in which PBMCs are separated from the intestinal lumen by the gut epithelium. However, a recent *in vitro* study using intestinal tissue of 7-week-old pig in an Using chamber model demonstrated that, although in small amounts, whey oligopeptides with a molecular weight of up to ~4000 dalton (median ~1500 dalton) could pass the intestinal epithelial barrier⁹³. In addition, several mechanisms of antigen sampling exist in the small intestine, such as uptake by dendritic cells protruding in the intestinal lumen, suggesting direct influence of luminal content on local and systemic immune homeostasis⁹⁴. To gain further insight in the relevance of our findings in this proof-of-concept study for the infant context, a head-to-head comparison with organoids derived from fetal or neonatal tissue and PBMCs derived from cord blood would be of added value. Last, in the current study set-up, effects of gastrointestinal digestion were not accounted for, which should be addressed by in future studies.

In summary, in the current study we successfully developed a HIO model that enables screening of apically administered (nutritional) substances on intestinal epithelial cells, representing the full-crypt villus axis, during health and hypoxia-mediated intestinal inflammation. Comprehensive screening of different whey protein fractions revealed that protection of paracellular barrier function, downregulation of HIF1 α and upregulation of stem cell marker OLFM4 during hypoxia-mediated inflammation, increase of Treg numbers,

alteration of their CD25 and CD69 expression profile and reduction of CD4+ T cell proliferation were differentially mediated by the different fractions, indicating that (degree of) hydrolysis determines their biological effects. Therefore, this should be taken into account when choosing specific nutritional products in a clinical and/or preventative setting and in future studies assessing biological effects of whey proteins/peptides. WPI could be used for the prevention and treatment of immune mediated diseases that may benefit from an increase of Treg or inhibition of CD4+ T cell proliferation. Given the protection of paracellular barrier function by DH28 during hypoxia mediated intestinal inflammation, DH28 forms a promising candidate for preventing or treating several intestinal diseases and promoting intestinal health.

References

1. Smithers GW. Whey and whey proteins—From ‘gutter-to-gold’. *Int Dairy J.* 2008;18(7):695-704.
2. Madureira AR, Pereira CI, Gomes AMP, Pintado ME, Xavier Malcata F. Bovine whey proteins - Overview on their main biological properties. *Food Res Int.* 2007;40(10):1197-1211.
3. Layman DK, Lönnerdal B, Fernstrom JD. Applications for α -lactalbumin in human nutrition. *Nutr Rev.* 2018;76(6):444-460.
4. Fenelon MA, Hickey RM, Buggy A, McCarthy N, Murphy EG. Chapter 12 - Whey Proteins in Infant Formula. In: Deeth HC, Bansal N, editors. *Whey Proteins*: Academic Press; 2019:439-494.
5. American Academy of Pediatrics. Committee on Nutrition. Hypoallergenic infant formulas. *Pediatrics.* 2000;106(2 Pt 1):346-349.
6. Boyle RJ, Ierodiakonou D, Khan T, Chivinge J, Robinson Z, Geoghegan N, et al. Hydrolysed formula and risk of allergic or autoimmune disease: systematic review and meta-analysis. *BMJ.* 2016;352:i974.
7. Ng DHC, Klassen JR, Embleton ND, McGuire W. Protein hydrolysate versus standard formula for preterm infants. *The Cochrane database of systematic reviews.* 2019;7(7):Cd012412.
8. Pennings B, Boirie Y, Senden JM, Gijsen AP, Kuipers H, van Loon LJ. Whey protein stimulates postprandial muscle protein accretion more effectively than do casein and casein hydrolysate in older men. *Am J Clin Nutr.* 2011;93(5):997-1005.
9. Tang JE, Moore DR, Kujbida GW, Tarnopolsky MA, Phillips SM. Ingestion of whey hydrolysate, casein, or soy protein isolate: effects on mixed muscle protein synthesis at rest and following resistance exercise in young men. *Journal of applied physiology (Bethesda, Md: 1985).* 2009;107(3):987-992.
10. Davies RW, Carson BP, Jakeman PM. The Effect of Whey Protein Supplementation on the Temporal Recovery of Muscle Function Following Resistance Training: A Systematic Review and Meta-Analysis. *Nutrients.* 2018;10(2).
11. Liao Y, Peng Z, Chen L, Zhang Y, Cheng Q, Nüssler AK, et al. Prospective Views for Whey Protein and/or Resistance Training Against Age-related Sarcopenia. *Aging Dis.* 2019;10(1):157-173.
12. Badely M, Sepandi M, Samadi M, Parastouei K, Taghdir M. The effect of whey protein on the components of metabolic syndrome in overweight and obese individuals; a systematic review and meta-analysis. *Diabetes Metab Syndr.* 2019;13(6):3121-3131.
13. Wirunsawanya K, Upala S, Jaruvongvanich V, Sanguankeo A. Whey Protein Supplementation Improves Body Composition and Cardiovascular Risk Factors in Overweight and Obese Patients: A Systematic Review and Meta-Analysis. *J Am Coll Nutr.* 2018;37(1):60-70.
14. Sprong RC, Schonewille AJ, van der Meer R. Dietary cheese whey protein protects rats against mild dextran sulfate sodium-induced colitis: role of mucin and microbiota. *J Dairy Sci.* 2010;93(4): 1364-1371.
15. Chatterton DE, Nguyen DN, Bering SB, Sangild PT. Anti-inflammatory mechanisms of bioactive milk proteins in the intestine of newborns. *Int J Biochem Cell Biol.* 2013;45(8):1730-1747.
16. Schaafsma G. Health issues of Whey Proteins: 3. Gut Health Promotion. *Current Topics in Nutraceutical Research.* 2007;5(1):29-34.
17. Hering NA, Andres S, Fromm A, van Tol EA, Amasheh M, Mankertz J, et al. Transforming growth factor- β , a whey protein component, strengthens the intestinal barrier by upregulating claudin-4 in HT-29/B6 cells. *J Nutr.* 2011;141(5):783-789.
18. Xiao K, Jiao L, Cao S, Song Z, Hu C, Han X. Whey protein concentrate enhances intestinal integrity and influences transforming growth factor- β 1 and mitogen-activated protein kinase signalling pathways in piglets after lipopolysaccharide challenge. *Br J Nutr.* 2016;115(6):984-993.
19. Diederer K, Li JV, Donachie GE, de Meij TG, de Waart DR, Hakvoort TBM, et al. Exclusive enteral nutrition mediates gut microbial and metabolic changes that are associated with remission in children with Crohn's disease. *Sci Rep.* 2020;10(1):18879.
20. Souza AL, Fiorini Aguiar SL, Gonçalves Miranda MC, Lemos L, Freitas Guimaraes MA, Reis DS, et al. Consumption of Diet Containing Free Amino Acids Exacerbates Colitis in Mice. *Front Immunol.* 2017;8:1587.
21. Triantafyllidis JK, Tzouvala M, Triantafyllidis E. Enteral Nutrition Supplemented with Transforming Growth Factor- β , Colostrum, Probiotics, and Other Nutritional Compounds in the Treatment of Patients with Inflammatory Bowel Disease. *Nutrients.* 2020;12(4):1048.

22. Cui Y, Zhu C, Ming Z, Cao J, Yan Y, Zhao P, et al. Molecular mechanisms by which casein glycomacropeptide maintains internal homeostasis in mice with experimental ulcerative colitis. *PLoS One*. 2017;12(7):e0181075-e.
23. Hvas CL, Dige A, Bendix M, Wernlund PG, Christensen LA, Dahlerup JF, et al. Casein glycomacropeptide for active distal ulcerative colitis: a randomized pilot study. *Eur J Clin Invest*. 2016;46(6):555-563.
24. Yamaguchi M, Uchida M. Alpha-lactalbumin suppresses interleukin-6 release after intestinal ischemia/reperfusion via nitric oxide in rats. *Inflammopharmacology*. 2007;15(1):43-47.
25. de Lange IH, van Gorp C, Eeftinck Schattenkerk LD, van Gemert WG, Derikx JPM, Wolfs TGAM. Enteral Feeding Interventions in the Prevention of Necrotizing Enterocolitis: A Systematic Review of Experimental and Clinical Studies. *Nutrients*. 2021;13(5):1726.
26. Boirie Y, Dangin M, Gachon P, Vasson MP, Maubois JL, Beaufrère B. Slow and fast dietary proteins differently modulate postprandial protein accretion. *Proc Natl Acad Sci U S A*. 1997;94(26):14930-14935.
27. Manninen AH. Protein hydrolysates in sports nutrition. *Nutr Metab (Lond)*. 2009;6(1):38.
28. Morifuji M, Ishizaka M, Baba S, Fukuda K, Matsumoto H, Koga J, et al. Comparison of different sources and degrees of hydrolysis of dietary protein: effect on plasma amino acids, dipeptides, and insulin responses in human subjects. *J Agric Food Chem*. 2010;58(15):8788-8797.
29. Brandelli A, Daroit DJ, Corrêa APF. Whey as a source of peptides with remarkable biological activities. *Food Res Int*. 2015;73:149-161.
30. Nielsen SD, Beverly RL, Qu Y, Dallas DC. Milk bioactive peptide database: A comprehensive database of milk protein-derived bioactive peptides and novel visualization. *Food Chem*. 2017;232:673-682.
31. Silvestre MPC, da Silva MC, de Souza MWS, Silva VDM, de Aguiar MJB, Silva MR. Hydrolysis degree, peptide profile and phenylalanine removal from whey protein concentrate hydrolysates obtained by various proteases. *Int J Food Sci Technol*. 2013;48(3):588-595.
32. Morais HA, Silvestre MPC, Silva VDM, Silva MR, Simoes e Silva AC, Silveira JN. Correlation between the Degree of Hydrolysis and the Peptide Profile of Whey Protein Concentrate Hydrolysates: Effect of the Enzyme Type and Reaction Time. *American Journal of Food Technology*. 2013;8(1):1-16.
33. Iskandar MM, Lands LC, Sabally K, Azadi B, Meehan B, Mawji N, et al. High Hydrostatic Pressure Pretreatment of Whey Protein Isolates Improves Their Digestibility and Antioxidant Capacity. *Foods (Basel, Switzerland)*. 2015;4(2):184-207.
34. Poolman JT, Anderson AS. *Escherichia coli* and *Staphylococcus aureus*: leading bacterial pathogens of healthcare associated infections and bacteremia in older-age populations. *Expert review of vaccines*. 2018;17(7):607-618.
35. Coggins SA, Wynn JL, Weitkamp J-H. Infectious Causes of Necrotizing Enterocolitis. *Clin Perinatol*. 2015;42(1):133-154.
36. Price LB, Hungate BA, Koch BJ, Davis GS, Liu CM. Colonizing opportunistic pathogens (COPs): The beasts in all of us. *PLoS Pathog*. 2017;13(8):e1006369-e.
37. Capurso L. Thirty Years of *Lactobacillus rhamnosus* GG: A Review. *J Clin Gastroenterol*. 2019;53 Suppl 1:S1-s41.
38. Arbolea S, Watkins C, Stanton C, Ross RP. Gut Bifidobacteria Populations in Human Health and Aging. *Front Microbiol*. 2016;7:1204.
39. Sato T, Stange DE, Ferrante M, Vries RG, Van Es JH, Van den Brink S, et al. Long-term expansion of epithelial organoids from human colon, adenoma, adenocarcinoma, and Barrett's epithelium. *Gastroenterology*. 2011;141(5):1762-1772.
40. VanDussen KL, Marinsshaw JM, Shaikh N, Miyoshi H, Moon C, Tarr PI, et al. Development of an enhanced human gastrointestinal epithelial culture system to facilitate patient-based assays. *Gut*. 2015;64(6):911-920.
41. Kozuka K, He Y, Koo-McCoy S, Kumaraswamy P, Nie B, Shaw K, et al. Development and Characterization of a Human and Mouse Intestinal Epithelial Cell Monolayer Platform. *Stem cell reports*. 2017;9(6):1976-1990.
42. Bankhead P, Loughrey MB, Fernández JA, Dombrowski Y, McArt DG, Dunne PD, et al. QuPath: Open source software for digital pathology image analysis. *Sci Rep*. 2017;7(1):16878.

43. Xu P, Becker H, Elizalde M, Masclee A, Jonkers D. Intestinal organoid culture model is a valuable system to study epithelial barrier function in IBD. *Gut*. 2018;67(10):1905-1906.
44. Zimmermann C, Eaton AD, Lanter BB, Roper J, Hurley BP, Delaney B. Extended exposure duration of cultured intestinal epithelial cell monolayers in characterizing hazardous and non-hazardous proteins. *Food Chem Toxicol*. 2018;115:451-459.
45. Kobayashi C, Inagaki M, Nohara M, Fukuoka M, Xijier, Yabe T, et al. The effects of denatured major bovine whey proteins on the digestive tract, assessed by Caco-2 cell differentiation and on viability of suckling mice. *J Dairy Res*. 2021;88(2):221-225.
46. Inagaki M, Kawai S, Ijier X, Fukuoka M, Yabe T, Iwamoto S, et al. Effects of heat treatment on conformation and cell growth activity of alpha- lactalbumin and beta-lactoglobulin from market milk. *Biomed Res*. 2017;38(1):53-59.
47. Arbizu S, Chew B, Mertens-Talcott SU, Noratto G. Commercial whey products promote intestinal barrier function with glycomacropeptide enhanced activity in downregulating bacterial endotoxin lipopolysaccharides (LPS)-induced inflammation in vitro. *Food Funct*. 2020;11(7):5842-5852.
48. Kiewiet MBG, Dekkers R, Gros M, van Neerven RJJ, Groeneveld A, de Vos P, et al. Toll-like receptor mediated activation is possibly involved in immunoregulating properties of cow's milk hydrolysates. *PLoS One*. 2017;12(6):e0178191.
49. Rodríguez-Carrio J, Fernández A, Riera FA, Suárez A. Immunomodulatory activities of whey β -lactoglobulin tryptic-digested fractions. *Int Dairy J*. 2014;34(1):65-73.
50. Chang JT. Pathophysiology of Inflammatory Bowel Diseases. *N Engl J Med*. 2020;383(27):2652-2664.
51. Grootjans J, Lenaerts K, Buurman WA, Dejong CHC, Derikx JPM. Life and death at the mucosal-luminal interface: New perspectives on human intestinal ischemia-reperfusion. *World J Gastroenterol*. 2016;22(9):2760-2770.
52. Neu J, Walker WA. Necrotizing enterocolitis. *N Engl J Med*. 2011;364(3):255-264.
53. Cavadas MAS, Mesnieres M, Crifo B, Manresa MC, Selfridge AC, Scholz CC, et al. REST mediates resolution of HIF-dependent gene expression in prolonged hypoxia. *Sci Rep*. 2015;5:17851-.
54. Bruning U, Cerone L, Neufeld Z, Fitzpatrick SF, Cheong A, Scholz CC, et al. MicroRNA-155 promotes resolution of hypoxia-inducible factor 1 α activity during prolonged hypoxia. *Mol Cell Biol*. 2011;31(19):4087-4096.
55. Noel G, Baetz NW, Staab JF, Donowitz M, Kovbasnjuk O, Pasetti MF, et al. A primary human macrophage-enteroid co-culture model to investigate mucosal gut physiology and host-pathogen interactions. *Sci Rep*. 2017;7:45270.
56. Blander JM. On cell death in the intestinal epithelium and its impact on gut homeostasis. *Current opinion in gastroenterology*. 2018;34(6):413-419.
57. Lin PW, Stoll BJ. Necrotising enterocolitis. *Lancet*. 2006;368(9543):1271-1283.
58. Vander Heiden MG, Cantley LC, Thompson CB. Understanding the Warburg effect: the metabolic requirements of cell proliferation. *Science (New York, NY)*. 2009;324(5930):1029-1033.
59. Stringari C, Edwards RA, Pate KT, Waterman ML, Donovan PJ, Gratton E. Metabolic trajectory of cellular differentiation in small intestine by Phasor Fluorescence Lifetime Microscopy of NADH. *Sci Rep*. 2012;2:568.
60. Urbauer E, Rath E, Haller D. Mitochondrial Metabolism in the Intestinal Stem Cell Niche-Sensing and Signaling in Health and Disease. *Frontiers in cell and developmental biology*. 2020;8:602814.
61. Okkelman IA, Neto N, Papkovsky DB, Monaghan MG, Dmitriev RI. A deeper understanding of intestinal organoid metabolism revealed by combining fluorescence lifetime imaging microscopy (FLIM) and extracellular flux analyses. *Redox biology*. 2020;30:101420.
62. Zheng L, Kelly CJ, Colgan SP. Physiologic hypoxia and oxygen homeostasis in the healthy intestine. A Review in the Theme: Cellular Responses to Hypoxia. *American journal of physiology Cell physiology*. 2015;309(6):C350-C360.
63. Kip AM, Soons Z, Mohren R, Duivenvoorden AAM, Röth AAJ, Cillero-Pastor B, et al. Proteomics analysis of human intestinal organoids during hypoxia and reoxygenation as a model to study ischemia-reperfusion injury. *Cell Death Dis*. 2021;12(1):95.
64. Dengler VL, Galbraith M, Espinosa JM. Transcriptional regulation by hypoxia inducible factors. *Crit Rev Biochem Mol Biol*. 2014;49(1):1-15.

65. Muenchau S, Deutsch R, de Castro IJ, Hielscher T, Heber N, Niesler B, et al. Hypoxic Environment Promotes Barrier Formation in Human Intestinal Epithelial Cells through Regulation of MicroRNA 320a Expression. *Mol Cell Biol.* 2019;39(14):e00553-18.
66. Semenza GL. HIF-1: mediator of physiological and pathophysiological responses to hypoxia. *J Appl Physiol.* 2000;88(4):1474-1480.
67. Kannan KB, Colorado I, Reino D, Palange D, Lu Q, Qin X, et al. Hypoxia-inducible factor plays a gut-injurious role in intestinal ischemia reperfusion injury. *American journal of physiology Gastrointestinal and liver physiology.* 2011;300(5):G853-G861.
68. Greer SN, Metcalf JL, Wang Y, Ohh M. The updated biology of hypoxia-inducible factor. *EMBO J.* 2012;31(11):2448-2460.
69. Movafagh S, Crook S, Vo K. Regulation of hypoxia-inducible factor-1 α by reactive oxygen species: new developments in an old debate. *J Cell Biochem.* 2015;116(5):696-703.
70. Lim JH, Lee YM, Chun YS, Chen J, Kim JE, Park JW. Sirtuin 1 modulates cellular responses to hypoxia by deacetylating hypoxia-inducible factor 1 α . *Mol Cell.* 2010;38(6):864-878.
71. Liang D, Zhuo Y, Guo Z, He L, Wang X, He Y, et al. SIRT1/PGC-1 pathway activation triggers autophagy/mitophagy and attenuates oxidative damage in intestinal epithelial cells. *Biochimie.* 2020;170:10-20.
72. Bai M, Lu C, An L, Gao Q, Xie W, Miao F, et al. SIRT1 relieves Necrotizing Enterocolitis through inactivation of Hypoxia-inducible factor (HIF)-1 α . *Cell cycle (Georgetown, Tex).* 2020;19(16):2018-2027.
73. Hwang JS, Han SG, Lee CH, Seo HG. Whey Protein Attenuates Angiotensin II-Primed Premature Senescence of Vascular Smooth Muscle Cells through Upregulation of SIRT1. *Korean J Food Sci Anim Resour.* 2017;37(6):917-925.
74. Liu W, Rodgers GP. Olfactomedin 4 expression and functions in innate immunity, inflammation, and cancer. *Cancer Metastasis Rev.* 2016;35(2):201-212.
75. Wang XY, Chen SH, Zhang YN, Xu CF. Olfactomedin-4 in digestive diseases: A mini-review. *World J Gastroenterol.* 2018;24(17):1881-1887.
76. Gersemann M, Becker S, Nuding S, Antoni L, Ott G, Fritz P, et al. Olfactomedin-4 is a glycoprotein secreted into mucus in active IBD. *Journal of Crohn's & colitis.* 2012;6(4):425-434.
77. Yu L, Yang F, Zhang F, Guo D, Li L, Wang X, et al. CD69 enhances immunosuppressive function of regulatory T-cells and attenuates colitis by prompting IL-10 production. *Cell Death Dis.* 2018;9(9):905.
78. Cortés JR, Sánchez-Díaz R, Bovolenta ER, Barreiro O, Lasarte S, Matesanz-Marín A, et al. Maintenance of immune tolerance by Foxp3⁺ regulatory T cells requires CD69 expression. *J Autoimmun.* 2014;55:51-62.
79. Chen JH, Huang PH, Lee CC, Chen PY, Chen HC. A bovine whey protein extract can induce the generation of regulatory T cells and shows potential to alleviate asthma symptoms in a murine asthma model. *Br J Nutr.* 2013;109(10):1813-1820.
80. Holvoet S, Perrot M, de Groot N, Prioult G, Mikogami T, Verhasselt V, et al. Oral Tolerance Induction to Newly Introduced Allergen is Favored by a Transforming Growth Factor- β -Enriched Formula. *Nutrients.* 2019;11(9):2210.
81. Wan YY, Flavell RA. TGF- β and regulatory T cell in immunity and autoimmunity. *J Clin Immunol.* 2008;28(6):647-659.
82. Zhang L, Yi H, Xia XP, Zhao Y. Transforming growth factor- β : an important role in CD4⁺CD25⁺ regulatory T cells and immune tolerance. *Autoimmunity.* 2006;39(4):269-276.
83. Ando T, Hatsushika K, Wako M, Ohba T, Koyama K, Ohnuma Y, et al. Orally administered TGF- β is biologically active in the intestinal mucosa and enhances oral tolerance. *J Allergy Clin Immunol.* 2007;120(4):916-923.
84. Weitkamp JH, Koyama T, Rock MT, Correa H, Goettel JA, Matta P, et al. Necrotising enterocolitis is characterised by disrupted immune regulation and diminished mucosal regulatory (FOXP3)/effector (CD4, CD8) T cell ratios. *Gut.* 2013;62(1):73-82.
85. Durrant DM, Metzger DW. Emerging roles of T helper subsets in the pathogenesis of asthma. *Immunol Invest.* 2010;39(4-5):526-549.
86. Chen ML, Sundrud MS. Cytokine Networks and T-Cell Subsets in Inflammatory Bowel Diseases. *Inflamm Bowel Dis.* 2016;22(5):1157-1167.

87. Hirahara K, Nakayama T. CD4+ T-cell subsets in inflammatory diseases: beyond the Th1/Th2 paradigm. *Int Immunol*. 2016;28(4):163-171.
88. Farmer DG, Ke B, Shen X-D, Kaldas FM, Gao F, Watson MJ, et al. Interleukin-13 protects mouse intestine from ischemia and reperfusion injury through regulation of innate and adaptive immunity. *Transplantation*. 2011;91(7):737-743.
89. Imam T, Park S, Kaplan MH, Olson MR. Effector T Helper Cell Subsets in Inflammatory Bowel Diseases. *Front Immunol*. 2018;9:1212-.
90. Ren S, Pan X, Gao F, Sangild PT, Nguyen DN. Prenatal inflammation suppresses blood Th1 polarization and gene clusters related to cellular energy metabolism in preterm newborns. *FASEB J*. 2020;34(2):2896-2911.
91. Debock I, Flamand V. Unbalanced Neonatal CD4(+) T-Cell Immunity. *Front Immunol*. 2014;5:393-.
92. Magnan AO, Mély LG, Camilla CA, Badier MM, Montero-Julian FA, Guillot CM, et al. Assessment of the Th1/Th2 paradigm in whole blood in atopy and asthma. Increased IFN-gamma-producing CD8(+) T cells in asthma. *Am J Respir Crit Care Med*. 2000;161(6):1790-1796.
93. Ozorio L, Mellinger-Silva C, Cabral LMC, Jardim J, Boudry G, Dupont D. The Influence of Peptidases in Intestinal Brush Border Membranes on the Absorption of Oligopeptides from Whey Protein Hydrolysate: An Ex Vivo Study Using an Ussing Chamber. *Foods (Basel, Switzerland)*. 2020;9(10):1415.
94. Schulz O, Pabst O. Antigen sampling in the small intestine. *Trends Immunol*. 2013;34(4):155-161.

Supplementary materials

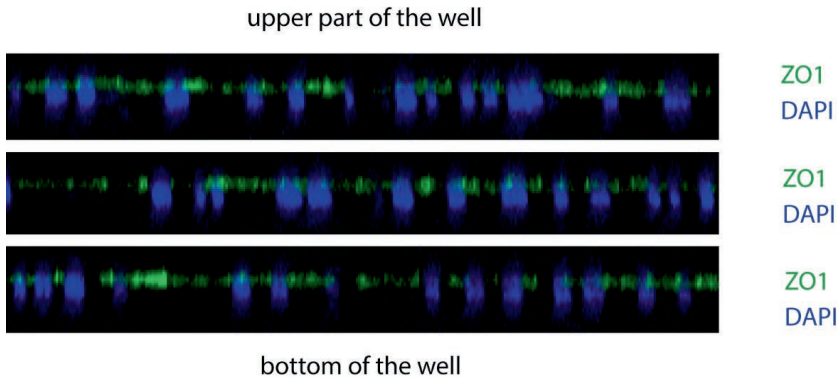


Figure S9.1 Apical – basolateral orientation of human intestinal epithelial cells in the HIO monolayer model with the apical side facing the upper part of the well was detected through localization of ZO1 (green) relative to the cell nucleus (DAPI, blue).

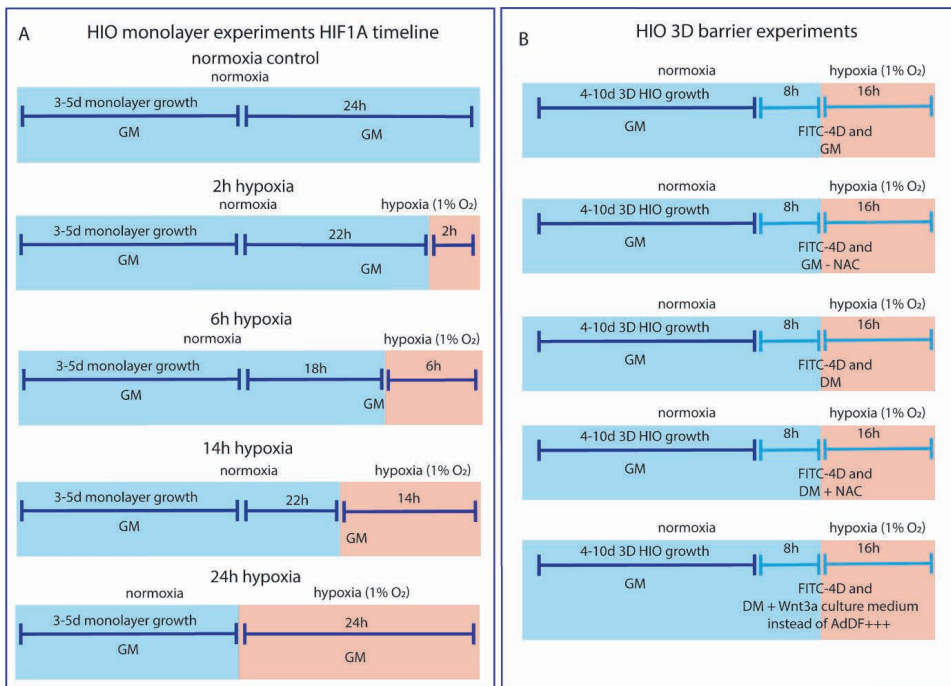


Figure S9.2 Experimental set-up of the experiment assessing HIF1A mRNA expression over time during hypoxia and additional 3D paracellular barrier experiments for HIO model development. **A.** For assessing HIF1A mRNA expression over time during hypoxia in crypt-like HIO monolayers, HIO monolayers were cultured for 3-5d prior to the onset of the experiment. Subsequently, organoids were cultured with GM for an additional 24h and exposed to 0h, 2h, 6h, 14h or 24h

of hypoxia (1% O₂) before end-of-experiment. B. For additional paracellular barrier experiments with 3D crypt-like and villus-like HIO, HIO were cultured with GM for 4-10d prior to the onset of the experiment. 24h before analyses, FITC-D4 was added to the GM or DM with or without supplemented NAC. In addition, in one group DM was used in which the surplus of AdDF+++ was replaced by the DMEM medium used for the production of Wnt3a conditioned medium. All groups were exposed to 16h of hypoxia (1% O₂) prior to analysis.

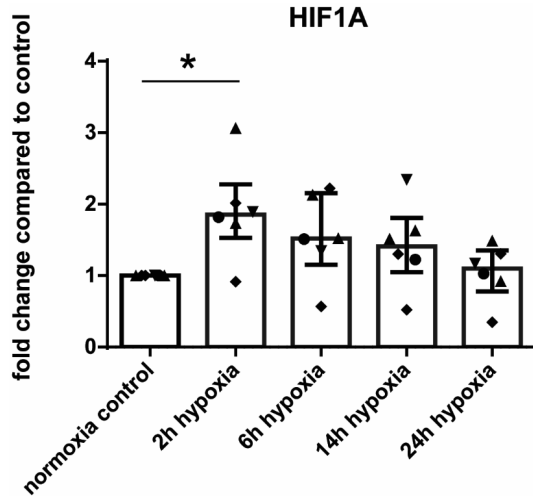


Figure S9.3 mRNA expression of HIF1A over time during hypoxia (2h, 6h, 14h and 24h of hypoxia) compared to a normoxic control in crypt-like HIO monolayers. Data are reported as relative expression compared to control (set at 1) and displayed as median with interquartile range. Results were obtained from 3 different HIO donors (depicted by different data point symbols).

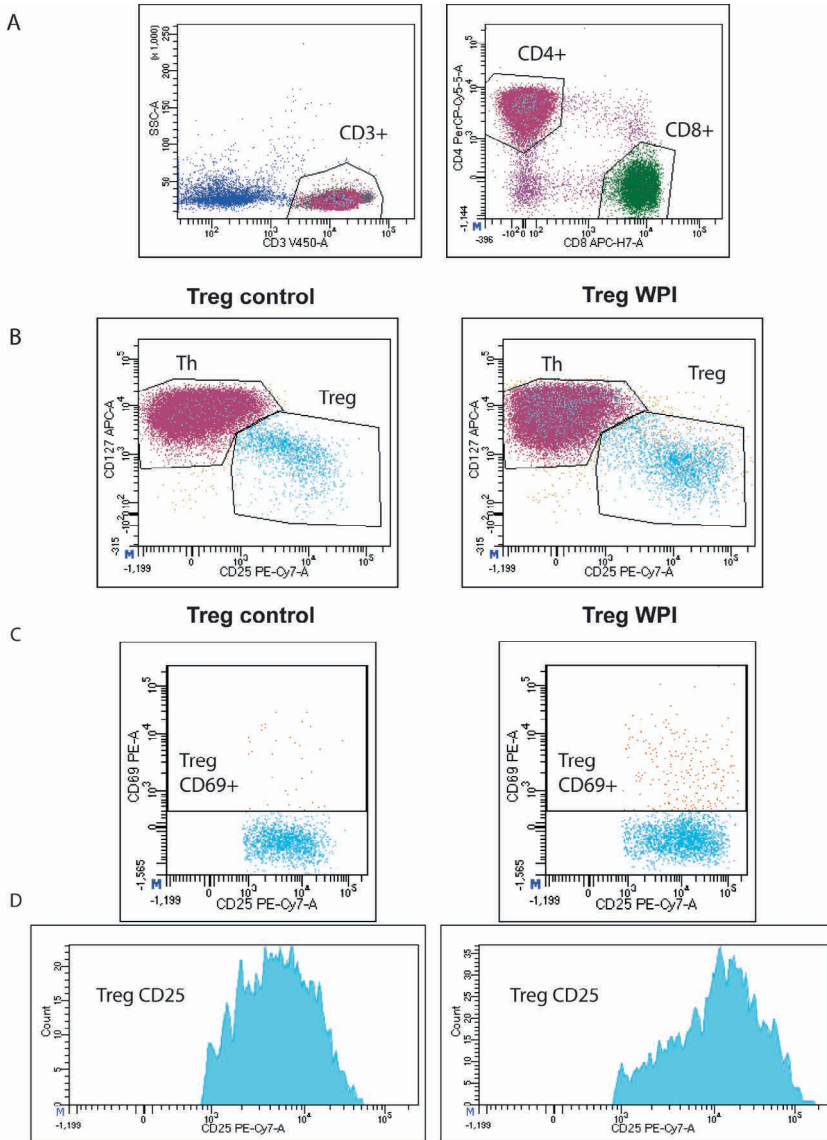


Figure S9.4 Measurement of the number and CD25 and CD69 expression of CD4+CD25highCD127low Treg in non-activated PBMCs and proliferation A. Single cells were selected from PBMCs in forward and side scatter and live cells were selected with a live-dead marker. From this population, the CD3+ cells were picked and the amount of CD4+ and CD8+ cells was determined. Within the population of CD4+ T cells, CD25 and CD127 expression was determined and the percentage of CD4+CD25highCD127low Treg was measured. B. Relative to controls, incubation with WPI increased the percentage of CD4+ T cells that is Treg. C. Relative to controls, incubation with WPI increased the % of Treg that is CD69+. D. Relative to controls, incubation with WPI increased the CD25 expression of Treg (CD25 MFI). Abbreviations: CD3, cluster of differentiation 3; CD4, cluster of differentiation 4; CD8, cluster of differentiation 8; WPI, whey protein isolate; MFI, mean fluorescent intensit.

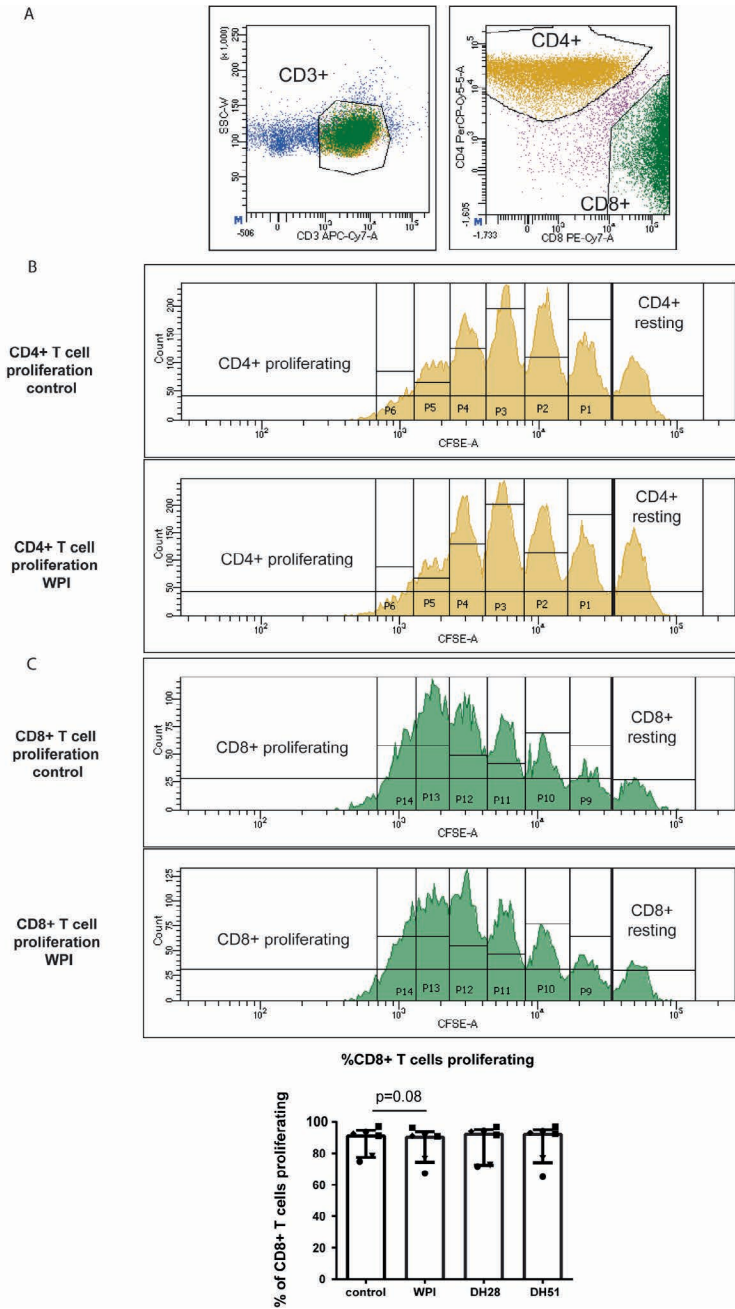


Figure S9.5 Measurement of the proliferation of CD4+ and CD8+ T cells in T-cell activated PBMCs. A. Single cells were selected from PBMCs in forward and side scatter and live cells were selected with a live-dead marker. From this population, the CD3+ cells were picked and the

amount of CD4+ and CD8+ cells was determined. B. Within the population of CD4+ T cells the percentage of proliferating cells was determined with a CFSE proliferation assay. Incubation with WPI for 5 days decreased CD4+ T cell proliferation. C. Within the population of CD8+ T cells the percentage of proliferating cells was determined with a CFSE proliferation assay. Incubation with WPI for 5 days tended to decrease CD8+ T cell proliferation. Results were obtained from four different PBMC donors (depicted by different data point symbols). Abbreviations: CD3, cluster of differentiation 3; CD4, cluster of differentiation 4; CD8, cluster of differentiation 8; WPI, whey protein isolate.

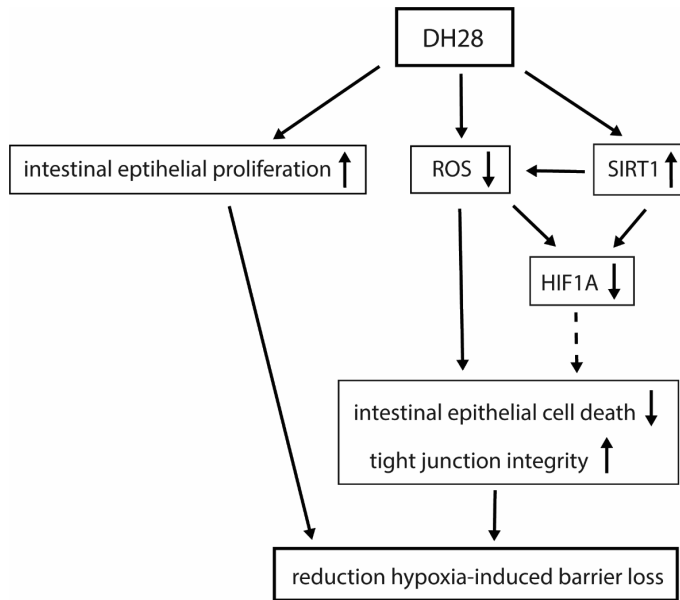


Figure S9.6 Hypotheses regarding the mechanisms behind DH28 mediated protection against hypoxia-induced intestinal barrier loss.

Table S9.1 Composition of interventions.

FAA distribution (mg/100g powder)	WPI	DH28	DH51
Alanine		44,3	1250
Arginine		<10	1050
Asparagine		17,2	1650
Aspartic acid		12,2	1020
Cystine		<10	179
Glutamine		<10	1050
Glutamic acid		69,4	1050
Glycine		<10	113
Histidine		11,9	748
Isoleucine		15,3	2370
Leucine		102	5420
Lysine		53,5	3990
Methionine		11,3	1200
Phenylalanine		57,3	1660
Proline		<10	35,9
Serine		28,9	1160
Threonine		33,4	1600
Tryptophane		20,2	410
Tyrosine		29,6	993
Valine		34,9	2110
FAA distribution (g/100 g AA)	WPI	DH28	DH51
Alanine	4,91	5,39	5,43
Arginine	1,88	1,75	1,78
Asparagine+Aspartic acid	10,99	11,44	11,29
Cystine	2,4	2	2,15
Glutamine+Glutamic acid	16,9	18,93	18,41
Glycine	1,58	1,53	1,51
Histidine	1,52	1,53	1,57
Isoleucine	6,43	6,28	6,84
Leucine	10,08	9,6	9,60
Lysine	9,28	9,71	9,83
Methionine	2,13	2,22	2,08
Phenylalanine	2,81	2,36	2,39
Proline	6,56	5,98	5,62
Serine	4,89	4,74	4,74
Threonine	7,34	7,38	7,35
Tryptophane	1,85	1,27	1,24
Tyrosine	2,74	2,3	2,31
Valine	5,71	5,61	5,87

Abbreviations: AA, amino acids, FAA, free amino acids, WPI, whey protein isolate; DH28, whey protein hydrolysate with 28% degree of hydrolysis; DH51, whey protein hydrolysate with 51% degree of hydrolysis.

Part V

Conclusions, perspectives and impact

Chapter 10

Summary and general discussion

Summary and general discussion

Preterm birth, defined as birth before 37 weeks of gestation, is a major worldwide health issue¹. It is an important cause of neonatal mortality and morbidity, and begets considerable economic burden on society². Preterm birth often results from inflammation of the fetal membranes (i.e., chorioamnionitis), which is most frequently caused by microbial invasion of the uterine cavity³. It can progress to intra-uterine infection or inflammation³ and this can subsequently give rise to a systemic inflammatory response syndrome in the fetus (FIRS)^{4,5}. Importantly, chorioamnionitis and FIRS are, independently of premature birth, risk factors for adverse neonatal outcomes^{6,7}, such as the neonatal gastrointestinal emergency necrotizing enterocolitis (NEC)⁸. NEC is characterized by severe intestinal inflammation that often proceeds to necrosis. It is associated with considerable mortality and long-term morbidity^{9,10}, including neurodevelopmental delays¹¹. Although factors such as immature intestinal motility and diminished intestinal (mucus) barrier function are clearly involved, NEC pathophysiology remains incompletely understood¹². Accordingly, treatment of NEC has thus far been largely symptomatic¹². Breast milk feeding is an important factor in reducing NEC risk¹³, mainly because breast milk contains many bioactive components that modulate mechanisms involved in NEC pathogenesis, such as intestinal barrier function and gut inflammation¹⁴⁻¹⁶. Unfortunately, mothers' (own) milk is not available to all preterm neonates¹⁷, and donor milk is not a full-fledged alternative¹⁸. Therefore, the development of nutritional interventions that incorporate (combinations of) bioactive human breast milk components hold great promise as a novel preventative strategy to reduce NEC incidence and severity.

In this thesis, I focused on elements that all contribute to a novel framework for the improvement of such preventive nutritional interventions through acknowledgement on the multifactorial pathophysiology of NEC and its postulated prenatal onset. This was achieved by:

1. mapping the current state of evidence on effectiveness and disease-mechanism-specific effects of enteral feeding interventions in the prevention of NEC and identifying ways to improve the research on this topic (**chapter 2**);
2. enhancing the understanding of NEC pathophysiology by investigating the effects of chorioamnionitis and NEC on the enteric nervous system (ENS) and intestinal mucus barrier (**chapter 3-7**);
3. investigating the effects of an *in utero* enteral feeding intervention on the fetal gut affected by chorioamnionitis (**chapter 8**);
4. developing a novel, human intestinal organoid model for screening of (combinations of) nutritional interventions in the context of hypoxia-induced intestinal inflammation and studying the effects of (hydrolyzed) whey in this model (**chapter 9**).

Enteral feeding interventions for NEC prevention: current state of evidence

In **chapter 2**, we systematically reviewed the current state of evidence on enteral feeding interventions in the prevention of NEC. We showed that experimental animal studies provide a large amount of evidence for the beneficial effects of specific enteral feeding interventions in the prevention of NEC incidence and mortality, and for the favorable effect of many interventions on a broad range of pathophysiological mechanisms of NEC. Knowledge derived from animal studies of the effects of enteral feeding interventions on the pathophysiological mechanisms of NEC is of especially great value, as these read-outs are often difficult to study in neonates. In contrast to the comprehensive evidence from animal studies, few enteral feeding interventions (probiotics and arginine) have been shown to be effective in (meta-analyses of) clinical trials. There are several reasons underlying the difficult translation from animal models to clinical practice. These include animal-experiment-related factors such as suboptimal assessment of bias, unclear certainty of evidence, suboptimal modelling of NEC, and the start of (preventive) interventions simultaneously with experimental NEC induction. Factors related to clinical trials are also in play; many clinical trials are not adequately powered, and NEC as clinical diagnosis is not always clearly defined. Dose and administration regimen are seldom studied, and it is unclear how these variables in animal studies can be translated to the neonate. Last, combinations of different nutritional components are only sporadically studied, whereas this is likely to be of pivotal importance, given the complex composition of breast milk and the multifactorial nature of NEC pathophysiology.

Strategies to overcome the current pitfalls in NEC research have been incorporated in this thesis and include improving our understanding of NEC pathophysiology (**chapter 3-7**), studying preventative enteral feeding interventions at an earlier moment (i.e., *in utero*) (**chapter 8**) and developing a human-tissue-based, experimental organoid model that enables medium- to high-throughput screening of (combinations) of nutritional interventions (**chapter 9**).

Effects of pro-inflammatory hits on the fetal and neonatal gut: beyond intestinal inflammation

Previous experiments in an ovine chorioamnionitis model have shown that intra-amniotic (IA) inflammation induced by IA exposure to either lipopolysaccharides (LPS)¹⁹⁻²¹, IL1 α ²² or *Ureaplasma parvum* (UP)²³ provokes fetal intestinal inflammation. Additionally, depending on the trigger and length of exposure, chorioamnionitis causes mucosal damage with villus damage or villus atrophy^{20,21,23}. Effects of chorioamnionitis on the fetal gut beyond intestinal inflammation and histological injury were previously reported in studies using sheep chorioamnionitis models; intra-amniotic inflammation was associated with impaired tight junction maturation in LPS-induced¹⁹⁻²¹, IL1 α -induced²² and UP-induced chorioamnionitis²³. UP-induced chorioamnionitis reduced intestinal epithelial proliferation and negatively affected epithelial differentiation and enterocyte maturation²³, whereas increased intestinal epithelial proliferation was observed following intra-uterine LPS exposure²¹. Last, intra-uterine LPS exposure was found to be associated with vascular dysfunction¹⁹. In the current thesis, we expanded and deepened the understanding of the effects of chorioamnionitis on

the fetal gut beyond intestinal inflammation by studying its effects on two factors very relevant to NEC pathogenesis: the ENS and the intestinal mucus barrier. Moreover, we studied postnatal ENS alterations in a murine NEC model and related our mucus barrier findings to alterations observed in clinical NEC biopsies.

Effects of perinatal inflammatory hits on the enteric nervous system

In **chapter 3**, we studied, in an ovine chorioamnionitis model, the effects of intra-uterine LPS exposure on the fetal ENS over time. In this study, we observed that the immunoreactivity of mature neurons (PGP9.5) was decreased in the myenteric plexus at 4 days after IA LPS exposure, with a concomitant decrease of glial cell immunoreactivity (S100 β). These changes were preceded by and overlapped with fetal intestinal and systemic inflammation²⁴. Of note, structural alterations of the ENS were normalized 15 days after IA LPS exposure. In **chapter 4**, we compared the effects of an acute IA exposure to LPS (2 days or 7 days) with chronic IA exposure to UP (42 days) or combined exposure (2 days or 7 days LPS and 42 days UP) on the fetal ENS, since chorioamnionitis is often polymicrobial. In accordance with the ENS alterations observed after 4d IA LPS exposure in **chapter 3**, chronic UP exposure caused a reduction in mature neurons (PGP9.5) in the myenteric plexus, and, to a lesser extent, in the submucosal plexus. Enteric glial cells (S100 β) were also decreased in the myenteric plexus by chronic UP exposure, whereas acute (7 days) LPS exposure induced reactive enteric gliosis (increased GFAP immunoreactivity). Both acute LPS exposure and chronic UP exposure caused intestinal injury and mucosal and submucosal inflammation, although the signature of gut inflammation differed between the groups. In **chapter 5**, we studied postnatal changes to the ENS longitudinally in a murine NEC model. In contrast to our *in utero* findings, in this study an increase of mature neurons (NeuN) was observed in both the submucosal and the myenteric plexus after 72 hours of exposure to the experimental NEC protocol, which was preceded and accompanied by increased numbers of enteric glial cells (S100 β). In addition, functional changes to the ENS were studied; whereas 24 hours of exposure to the NEC protocol increased intestinal transit, transit was decreased after 48 hours of NEC protocol exposure.

A common denominator of the three studies in **chapter 3**, **4** and **5** is the fact that the enteric glial cell responses paralleled that of mature enteric neurons, both when the number of enteric neurons decreased (**chapter 3** and **4**) and increased (**chapter 5**). Enteric glial cells not only provide structural support to enteric neurons, but are also involved in neuroprotection and neuronal maintenance via mechanisms such as release of glutathione and release of neurotrophic factors, including glial cell-line derived neurotrophic factor (GDNF)²⁵ and brain-derived neurotrophic factor (BDNF)²⁶. They act as antigen-presenting cells and modulate the mucosal immune response^{27,28}. In response to inflammation, enteric glial cells proliferate, upregulate their expression of GFAP in a process called reactive enteric gliosis, and can produce pro-inflammatory cytokines²⁹. Additionally, enteric glial cells were observed to increase oxidative stress during intestinal inflammation through production of NO^{28,30,31}, possibly contributing to neuronal cell death³⁰. Thus, besides their well-documented protective role, enteric glial cells may augment local inflammation and induce neuronal loss, as was previously described for astrocytes, their central nervous system

equivalents³². Whether the enteric glial cells play a protective or detrimental role in the studies incorporated in this thesis and the human setting remains to be elucidated. The paralleled alterations of S100 β (glial cells) and PGP9.5/NeuN (neurons) immunoreactivity in **chapter 3, 4 and 5** and previous findings of increased NEC severity in glia-deficient mice (33) support the former. However, in the *in utero* setting, reactive enteric gliosis (increased GFAP protein expression) was observed during acute (LPS-mediated) inflammation (**chapter 3 and 4**) and prior to the loss of enteric neurons (**chapter 3**), which suggests reactive enteric gliosis may contribute to neuronal loss following prolonged inflammation. Alternatively, this could reflect a compensatory mechanism of enteric glial cells falling short with prolonged inflammation. Of note, enteric glial cells display broad morphological and functional heterogeneity and extensive phenotypical plasticity³⁴ and the response of different enteric glial subtypes to perinatal inflammation may differ. Future studies that investigate the role of enteric glial cells during perinatal inflammatory stress are of great interest, given the potential role of enteric glial cells in the neuronal changes associated with this inflammatory stress, their importance for other processes in the gut, such as regulation of mucosal immunity and gut barrier integrity³⁵, and the possibility to modulate enteric glial cells with breast milk components³⁶.

Another overarching finding is that *in utero* alterations were more pronounced for the myenteric plexus than the submucosal plexus (**chapter 3 and 4**), whereas the plexuses were more or less equally affected after postnatal inflammatory hits in a murine NEC model (**chapter 5**). The differential *in utero* vulnerability of both plexuses may be attributed to several factors. First, it could be related to differences in enteric glial cell³⁴ or neuronal³⁷ phenotypes (in both plexuses). Second, differential responses of macrophages that reside in close proximity of the neuronal plexus may also be involved. Macrophage transcriptional profile^{38,39}, cell morphology³⁹ and cell dynamics³⁹ differ depending on their anatomical location in the intestinal wall and depletion of these cells contributes to neuronal apoptosis in both submucosal and myenteric plexus³⁸. Last, since myenteric plexus development precedes that of the submucosal plexus by approximately 3 weeks⁴⁰, the developmental stage may be a determinant for the differences in *in utero* vulnerability of both plexuses. However, this is less likely since differences in vulnerability were detected with microbial triggers administered at largely different gestational ages (i.e., ~121 days GA in **chapter 3**, and 82 days GA in **chapter 4**). Why both plexuses are affected in the postnatal setting following NEC protocol exposure is currently unclear. However, it is likely that the combination of pro-inflammatory hits of the experimental NEC protocol, their severity, or the presence of non-microbial triggers such as hypoxia and formula feeding are involved.

Importantly, both the acute and long-term functional consequences of *in utero* ENS alterations are at the moment unknown. In **chapter 3** and **chapter 4**, mRNA expression of nNOS (which produces the neurotransmitter NO) and CHAT (which produces the neurotransmitter acetylcholine) were unaffected by intra-uterine inflammation, suggesting ENS function might be unaltered at the moment of sacrifice. However, since such a broad range of neuronal subtypes and neurotransmitters is involved in the diverse ENS functions^{37,41}, functional measures such as gut motility assays are indispensable to accurately estimate functional outcome and should be incorporated in future studies that assess ENS alterations following perinatal inflammatory stress. This notion is further

supported by the poor correlation between histological ENS alterations and acute functional outcome in the murine NEC model used in **chapter 5**. Long-term consequences of perinatal ENS alterations do not only depend on functional changes in the acute setting, but also on the potential of the ENS to recover from initial damage. Although a decrease in enteric neurons, associated with decreased colonic motility⁴², has been described to persist after recovery of inflammation and mucosal damage in an experimental colitis model⁴³, the fetal and neonatal ENS are still developing and therefore may display enhanced plasticity compared to the adult setting. In line with this concept, ENS changes were observed to normalize over time in the course of LPS-induced chorioamnionitis in **chapter 3**. By contrast, the presence of ENS alterations after 42 days of IA UP infection in **chapter 4**, shows that ENS alterations can persist long after onset of intra-uterine inflammation. Thus, additional studies are needed to assess longitudinal and postnatal changes of the ENS following intra-uterine inflammation and to determine the influence of microbial trigger(s) involved and the moment of onset and duration of inflammation.

Effects of perinatal inflammatory hits on goblet cells and the intestinal mucus barrier

In **chapter 6**, longitudinal goblet cell changes in the terminal ileum following intra-uterine LPS exposure were assessed in an ovine chorioamnionitis model. In this study, we observed a biphasic reduction in goblet cell numbers at 24 hours to 2 days and 15 days after IA LPS-exposure. Whereas the first reduction is considered to be caused by mucus secretion, the second reduction was preceded by intestinal inflammation, increased intestinal epithelial endoplasmic reticulum (ER) stress (increased BiP and CHOP immunoreactivity) in the crypts and apoptosis in the lower villus region, which implies that this decrease results from ER-stress-driven apoptosis of maturing goblet cells. In **chapter 7**, we studied the mucus barrier changes, including mucus thickness as a functional measure, in the terminal ileum 7 days after IA UP administration. UP exposure induced mucus hypersecretion and thereby increased mucus layer thickness. These alterations were associated with increased pro-apoptotic intestinal epithelial ER stress (increased CHOP-positive cell counts) and secretory cell organelle disruptions, indicating that the mucus barrier alterations take place at the expense of goblet cell resilience. This concept was further strengthened by the remarkable overlap of our data with findings of organelle disruption in the terminal ileum of infants with NEC. Of note, although no increase of intestinal epithelial apoptosis was observed in the group of UP-exposed animals, two of the UP-exposed animals showed apoptosis in the same pattern in the lower villus region as previously observed following IA LPS exposure in **chapter 6**, suggesting that similar pathophysiological mechanisms may be involved in both studies.

Results in **chapters 6** and **7** show that goblet cells in the terminal ileum do respond to intra-uterine microbial triggers and are already capable of increasing mucus layer thickness *in utero*. Although this may be beneficial in the short run to prevent microbes from approaching the epithelium, our data suggest this comes at the expense of goblet cell resilience and may lead to a loss of goblet cells.

Additionally, our findings in **chapters 6 and 7** indicate that increased intestinal epithelial ER stress, which ultimately leads to apoptosis, is probably an important mechanism that contributes to gross disruption and loss of goblet cells in the *in utero* setting. This work extends previous findings showing that stem cells⁴⁴ and enterocytes⁴⁵ were affected by ER stress in experimental NEC studies. We also observed organelle disruptions indicative of ER stress in enterocytes in **chapter 7**. However, alterations were more pronounced on goblet cell level in our study. This can likely be attributed to the fact that secretory cells including goblet cells are relatively sensitive to ER stress due to their secretory nature and the complexity of their excretory proteins (mucins)⁴⁶. Intestinal epithelial ER stress is considered to contribute to NEC pathophysiology. Namely, increased intestinal epithelial ER stress and apoptosis were previously observed in the ileum of NEC patients^{44,47} and (genetic) downregulation of important ER stress pathways, including CHOP, decreased NEC severity in a murine NEC model^{44,45}. Outside the perinatal field, intestinal epithelial ER stress is involved in the pathophysiology of other gut diseases that are characterized by hypoperfusion and inflammation and in which goblet cells play an important role⁴⁸⁻⁵⁰, such as inflammatory bowel disease (IBD)^{51,52} and intestinal ischemia reperfusion injury (IRI)⁵³. Importantly, enteral nutritional interventions, such as human milk oligosaccharides (HMO) and bovine milk exosomes, have previously been shown to modulate intestinal epithelial ER stress and concomitantly prevent goblet cell loss and intestinal injury in experimental NEC models^{54,55}. Similarly, several enteral feeding interventions, such as glutamine^{56,57}, berberine⁵⁸ or chitosan oligosaccharide⁵⁹ ameliorated intestinal ER stress and apoptosis and improved intestinal outcome in experimental models of colitis^{56,58}, IRI⁵⁷ and nutrient deprivation stress induced intestinal injury⁵⁹. Together, these studies show that enteral nutritional interventions are capable of modulating ER stress and improving intestinal outcome, making them an interesting target for future research in the perinatal context.

For net barrier function, not only mucus thickness is of importance, but also mucus quality. Mucus quality is dependent on posttranscriptional modification of the mucins by glycosylation, sialylation, and the formation of disulfide bonds^{60,61}, which largely take place in the endoplasmic reticulum and the Golgi system, and, thus, may be affected during ER stress. Studies in IBD patients and experimental colitis models have shown that colon mucus quality is impaired in active disease and may also be hampered during remission in a subset of patients⁶². Currently, the effects of perinatal intestinal inflammation on mucus quality are unclear; this would be another interesting subject for future studies.

Effects of perinatal inflammatory hits on the fetal and neonatal enteric nervous system and mucus barrier: lessons learned

Collectively, our combined findings in **chapter 3-7** show that structural ENS alterations, disruption and loss of goblet cells, and mucus barrier alterations in response to pro-inflammatory hits already occur *in utero* and in early postnatal life. This supports the hypothesis that damage to the ENS and goblet cells contributes to NEC pathophysiology and strengthens the paradigm that NEC pathophysiology has its origins *in utero* in at least a subset of infants. Additionally, it indicates that early (i.e., *in utero* or early postnatal) preventative treatments targeted at improving ENS and goblet cell outcomes are probably

beneficial for NEC prevention and could be a useful add-on to, already extensively studied, postnatal interventions.

Although fetuses and neonates have large developmental plasticity⁶³ and are likely to recover over time from initial damage to the ENS and goblet cells, such as observed for the ENS in **chapter 3**, there is an inevitable window of increased vulnerability in which initial damage has not yet recovered. Of note, the major alterations of the ENS and mucus barrier we observed in this thesis did not develop and recover at the same moment after a pro-inflammatory hit; ENS changes were most pronounced after ~4 days of IA LPS exposure (**chapter 3**), whereas goblet cell loss was observed in the same animals only at 15 days of IA LPS exposure (**chapter 6**). This indicates such a window of increased vulnerability may be quite broad. During this time window, additional pro-inflammatory hits that a premature born neonate is likely to encounter, such as mechanical ventilation⁶⁴ and sepsis⁶⁵, and other impactful postnatal events such as microbial colonization and introduction of enteral feeding, may tip the balance towards NEC development more easily. In this context, addition of (targeted) preventative enteral feeding interventions as counteracting protective measure could contribute to prevention of NEC development.

Protecting the gut against perinatal stress: when to intervene?

An important question in enteral feeding interventions for the prevention of NEC is: when should such an intervention be initiated? Because intestinal alterations that probably predispose to postnatal NEC development already take place *in utero* following chorioamnionitis, enteral feeding interventions should ideally start as early as possible, namely *in utero*. Since the fetus swallows amniotic fluid during pregnancy⁶⁶, we investigated in a proof-of-concept study (**chapter 8**) whether (preventative) enrichment of the amniotic fluid with plant sterols, through IA administration of plant sterols with a carrier, could reduce systemic inflammation and improve intestinal outcome following 6 days of IA UP exposure. Plant sterols were chosen because they were previously shown to have anti-inflammatory effects in the context of IBD^{67,68}, to downregulate T-cell functions in the intestine of healthy volunteers⁶⁹ and to prevent chorioamnionitis induced fetal gut inflammation and mucosal injury following intra-amniotic administration in a pilot study⁶⁸. Moreover, since plant sterols cross the placenta⁷⁰, they can be administered orally to pregnant women to safely enrich the amniotic fluid in the future. In the current study, we observed that IA administration of plant sterols successfully increased plant sterol concentrations in the amniotic fluid, without altering fetal plasma plant sterol or cholesterol levels, which underscores the safety of this intervention. In addition, this therapy was associated with decreased fetal systemic inflammation, intestinal inflammation and mucosal damage. Collectively, we showed that *in utero* enteral feeding interventions can improve fetal (intestinal) outcomes. In addition, we identified plant sterols as nutritional components that could be clinically relevant for the prevention or treatment of FIRS.

Although direct intra-amniotic administration of nutritional components is currently not clinically feasible due to the risk of miscarriage and infection associated with amniocentesis, enrichment of the amniotic fluid can be safely achieved through modulation of the maternal diet, as many nutritional components pass the placenta⁷¹. Importantly, before clinical

studies of *in utero* interventions, pre-clinical safety studies are necessary. In addition, pharmacokinetic studies are required to determine at which dose nutritional components should be administered to reach therapeutic concentrations in the amniotic fluid, taking into account factors such as pregnancy duration and placental health⁷². As alternative to an *in utero* start, preventative enteral feeding interventions should start as soon as possible after birth to optimally use the therapeutic window of opportunity before NEC onset⁷³. Understanding the dynamics of intestinal inflammation and its sequelae following intra-uterine inflammation may aid in choosing the optimal moment of intervention. Although findings in **chapter 3, 4, 6** and **7** already provide some meaningful information, additional research is needed. Non-invasive markers of gut health could aid in studying the course of chorioamnionitis without using large amounts of laboratory animals and extensive research funds.

Protecting the gut against perinatal stress: in whom to intervene?

A second question is: in which infants or pregnant women should we intervene? Enteral feeding interventions could be used as universal preventative measure, i.e., for all pregnant women or all neonates, however, this requires very high safety standards and makes it more difficult to achieve sufficient effect size and a favorable benefit-cost ratio (both economically and non-economically)⁷⁴. Plant sterols could, in the future, serve as such a general intervention for pregnant women. They have, amongst others due to their natural occurrence in plant-based foods⁷⁵, a beneficial safety profile⁷⁶, can be administered orally to pregnant women because they pass over the placenta⁷⁰, have potential to be cost-effective⁷⁷ and are already used as dietary additives⁷⁸. Alternatively, plant sterols or other interventions could be embedded targeted, based on individual risk assessment. Risk assessment can be based on maternal risk factors, such as a medical history of preterm birth^{79,80} or chorioamnionitis⁸¹, or fetal/neonatal risk factors, such as gestational age at birth, perinatal asphyxia or confirmed chorioamnionitis or FIRS. Additionally, biomarkers or biomarker-based prediction models can be used. Although chorioamnionitis is often clinically silent and therefore difficult to diagnose before birth, a recent proof-of-concept study in sheep has shown that volatile organic compounds (VOCs) in exhaled breath can potentially be used for early detection of chorioamnionitis⁸². In addition, many studies have focused on early detection of NEC, through general and tissue-specific biomarkers in blood, stool or urine such as CRP⁸³, calprotectin⁸³, IFABP⁸³, VOCs^{84,85}, and DNA methylation patterns⁸⁶. The overall sensitivity and specificity of individual markers is still insufficient for clinical use^{83,87}, but the field is rapidly developing and new –omics technologies combined with bioinformatics software aides in developing new diagnostic algorithms^{88,89}.

Protecting the gut against perinatal stress: how to intervene?

Which nutritional components should be incorporated in a preventive intervention for NEC depends on several factors. First of all, the timing of (the start of) the intervention in relation to gestational age of the fetus or infant and the onset of risk factors such as chorioamnionitis could be a determining factor. In addition, the pathophysiological mechanisms involved are paramount. Since several nutritional components act on different

pathophysiological mechanisms (**chapter 2**), the ideal mix of components is determined by their mechanisms of action and possible synergistic effects. For instance, GDNF and BDNF, both present in breast milk^{90,91}, support ENS development⁹² and, in an experimental neonatal rat model of axotomy-induced neuronal cell death, displayed synergistic neuronal survival promoting effects⁹³, making combined administration of GDNF and BDNF an interesting approach for the prevention of ENS damage. When nutritional interventions are added to donor breast milk, known differences between donor milk and mothers' own milk can be considered as well, such as lower amounts of nutrients that are lost by pasteurization¹⁸. Similarly, when added to formula feeding, differences between human milk and formula should be taken into account⁹⁴. Additionally, characteristics of the individual child are important; for instance, the fatty acid requirements of infants are dependent on their genotype of fatty acid desaturase genes⁹⁵, and human milk oligosaccharide expression in breast milk varies in accordance with the mother's Lewis blood group and secretory status⁹⁶. A practical issue that needs attention is the effects of gastrointestinal processing^{97,98}, which changes during postnatal development. Thus, ideally, the mix of nutritional components is determined on an individual level and adapted over time (personalized medicine).

Human intestinal organoids as in vitro screening model for enteral nutritional interventions

To facilitate screening of the effects of (combinations of) nutritional components on the gut in a healthy or a diseased state, we developed a novel human intestinal organoid model (**chapter 9**). In this model, we used hypoxia as trigger for gut inflammation, intestinal epithelial apoptosis and gut barrier loss, since hypoxia is an important factor that contributes to the pathophysiology of several intestinal diseases such as NEC⁹⁹, IBD¹⁰⁰ and IRI¹⁰¹. To allow apical administration of the nutritional components of interest, human intestinal organoids were cultured in monolayers. In addition, culture medium of the organoids was adapted to mimic a crypt-like and villus-like phenotype, thereby aiding investigation of the effect of nutritional components along the full crypt-villus axis. Besides model development, we tested the effect of non-hydrolyzed, moderately hydrolyzed, and extensively hydrolyzed whey protein as potential beneficial nutritional interventions, both in the organoid model as well as in four relevant microbial strains and peripheral immune cells. Interestingly, biological effects were differentially mediated by the different whey protein fractions; moderately hydrolyzed whey improved paracellular barrier function of the organoids and concomitantly decreased mRNA expression of HIF1 α , whereas non-hydrolyzed whey protein decreased CD4+ T cell proliferation and shifted Th1-Th2 balance towards a Th1 phenotype on mRNA level. Collectively, these results demonstrate that the novel organoid model enables rapid screening of (combinations of) nutritional components. In addition, these findings indicate that whey proteins possess biologically relevant capacities to promote gut health and that the degree of hydrolysis of proteins is key for their biological effect and should, thus, be considered during the development of a nutritional intervention.

The current human intestinal organoid model provides a good basis for medium- to high-throughput screening purposes. Nevertheless, several aspects of the model can be improved. First, co-culture of the human intestinal organoids with immune cells^{102,103}, microbes^{104,105} and enteric nervous system¹⁰⁶ can further improve translational relevance. The effect of several nutritional components probably depends on non-epithelial mechanisms and on the communication between the intestinal epithelium and adjacent systems. For instance, HMO mainly work via modulation of the infant's microbiome and immune system¹⁰⁷, and their effects will not or only minimally be detected in absence of these elements. Importantly, these initial limitations of the organoid model can partially be overcome by separate experiments with immune cells or microbial strains, as we demonstrated in **chapter 9**. Moreover, as the field of organoid technology is rapidly developing, co-cultures that enable investigation of the interaction between intestinal epithelium and other parts of the intestinal micro-environment^{108,109} are feasible in future studies. Second, cell culture conditions can be optimized. Whereas human intestinal organoids are traditionally cultured with 21% oxygen, like we did in **chapter 9**, the *in vivo* phenotype may be better reflected at oxygen concentrations closer to the natural oxygen tension in the intestine (physioxia)^{110,111}. Third, because our current model is based on cells derived from adult intestinal tissue, our results cannot be translated one-to-one to the perinatal context. Although little is known about the differences between adult, neonatal and fetal human small intestinal organoids, these may very well exist. Human-fetal-tissue-derived organoids were observed to have an altered gene expression profile compared to adult-tissue-derived organoids regarding maturation, gut barrier function and innate immunity, and they responded differently to LPS exposure¹¹². Whereas DNA methylation patterns remained relatively stable during long-term culture in adult and pediatric human intestinal organoids, fetal intestinal organoids were reported to undergo DNA methylation changes that correspond with *in vitro* maturation¹¹³. In addition, pediatric and adult organoids were recently observed to have different maturation features and increased paracellular permeability compared to organoids of adult origin¹¹⁴. Thus, future experiments with organoids cultured from neonatal or fetal intestinal tissue could increase the translational value of our current findings to the perinatal context. Importantly, the feasibility of a pediatric-tissue-based intestinal organoid model for assessing nutritional interventions was recently demonstrated in a paper by Noel et al.¹¹⁴. Fourth, culturing organoids from small intestinal tissue of patients with acute NEC or patients recovered from NEC is potentially interesting. To date, increasing evidence suggests that at least part of a diseased state is preserved when organoids are cultured at low passage numbers from patients with IBD^{115,116}, indicating this may also be the case for organoids derived from patients with NEC. However, culturing organoids from highly inflamed or necrotic tissue is difficult. Using tissue from infants that recovered from NEC and have been operated for intestinal strictures or stoma removal could be an alternative, as this approach at least covers the known genetic predisposition to NEC¹¹⁷. Last, the field of intestinal organoids and related *in vitro* models is rapidly developing and novel bioengineering techniques such as cell cultures on 3D scaffolds, with multicellular architecture and with micro-perfusion (e.g., gut-on-a-chip models¹¹⁸) could aid in reducing model heterogeneity while even more closely approaching the actual *in vivo* situation^{119,120}. Importantly, however, the complexity of the *in*

vitro model should be well balanced with its manageability and associated costs, to ensure its application as medium- to high-throughput screenings model.

Conclusions

In this thesis, we have shown that enteral nutritional interventions are highly promising for the prevention of NEC and that novel strategies that focus on its postulated prenatal onset as well as its multifactorial pathogenesis are vital for enhancing the development of such nutritional interventions. We have demonstrated—in an ovine model—that chorioamnionitis-induced ENS alterations and gross goblet cell disruptions that are considered to predispose to postnatal NEC development already occur *in utero*. These changes were of a greater magnitude than researchers have demonstrated so far, and underscore that the effects of intra-uterine inflammation on the fetal gut extend beyond mere intestinal inflammation. Moreover, we have established—in a preclinical proof-of-concept study—that an intra-uterine enteral feeding intervention with plant sterols can improve fetal systemic and intestinal outcomes, which indicates that the detrimental effects of chorioamnionitis can be addressed at the earliest possible moment (*i.e.*, *in utero*). Last, to enhance recognition of the multifactorial pathogenesis of NEC in the development of nutritional interventions, we have developed a novel human intestinal organoid model that enables screening of (combinations of) nutritional components in both health and disease. Even though more research on the synergistic effects of nutritional components, pharmacokinetics and clinical safety is required before novel interventions can be implemented in clinical practice, we are confident that the studies in this thesis contribute to a novel framework for the development of clinically effective preventative enteral feeding interventions for NEC in the future, by us or by other researchers.

References

1. Harrison MS, Goldenberg RL. Global burden of prematurity. *Semin Fetal Neonatal Med.* 2016;21(2):74-79.
2. Frey HA, Klebanoff MA. The epidemiology, etiology, and costs of preterm birth. *Semin Fetal Neonatal Med.* 2016;21(2):68-73.
3. Kim CJ, Romero R, Chaemsaithong P, Chaiyasit N, Yoon BH, Kim YM. Acute chorioamnionitis and funisitis: definition, pathologic features, and clinical significance. *Am J Obstet Gynecol.* 2015;213(4 Suppl):S29-52.
4. Peng CC, Chang JH, Lin HY, Cheng PJ, Su BH. Intrauterine inflammation, infection, or both (Triple I): A new concept for chorioamnionitis. *Pediatr Neonatol.* 2018;59(3):231-237.
5. Gotsch F, Romero R, Kusanovic JP, Mazaki-Tovi S, Pineles BL, Erez O, et al. The fetal inflammatory response syndrome. *Clin Obstet Gynecol.* 2007;50(3):652-683.
6. Gantert M, Been JV, Gavilanes AW, Garnier Y, Zimmermann LJ, Kramer BW. Chorioamnionitis: a multiorgan disease of the fetus? *J Perinatol.* 2010;30 Suppl:S21-30.
7. Tang Q, Zhang L, Li H, Shao Y. The fetal inflammation response syndrome and adverse neonatal outcomes: a meta-analysis. *J Matern Fetal Neonatal Med.* 2019:1-13.
8. Been JV, Lieveense S, Zimmermann LJ, Kramer BW, Wolfs TG. Chorioamnionitis as a risk factor for necrotizing enterocolitis: a systematic review and meta-analysis. *J Pediatr.* 2013;162(2):236-42 e2.
9. Jacob J, Kamitsuka M, Clark RH, Kelleher AS, Spitzer AR. Etiologies of NICU deaths. *Pediatrics.* 2015;135(1):e59-65.
10. Fitzgibbons SC, Ching Y, Yu D, Carpenter J, Kenny M, Weldon C, et al. Mortality of necrotizing enterocolitis expressed by birth weight categories. *J Pediatr Surg.* 2009;44(6):1072-1075; discussion 5-6.
11. Schulzke SM, Deshpande GC, Patole SK. Neurodevelopmental outcomes of very low-birth-weight infants with necrotizing enterocolitis: a systematic review of observational studies. *Arch Pediatr Adolesc Med.* 2007;161(6):583-90.
12. Lin PW, Stoll BJ. Necrotizing enterocolitis. *Lancet.* 2006;368(9543):1271-1283.
13. Lucas A, Cole TJ. Breast milk and neonatal necrotizing enterocolitis. *Lancet.* 1990;336(8730): 1519-1523.
14. Thai JD, Gregory KE. Bioactive Factors in Human Breast Milk Attenuate Intestinal Inflammation during Early Life. *Nutrients.* 2020;12(2).
15. Andreas NJ, Kampmann B, Mehring Le-Doare K. Human breast milk: A review on its composition and bioactivity. *Early Hum Dev.* 2015;91(11):629-635.
16. Chatterton DE, Nguyen DN, Bering SB, Sangild PT. Anti-inflammatory mechanisms of bioactive milk proteins in the intestine of newborns. *Int J Biochem Cell Biol.* 2013;45(8):1730-1747.
17. Wilson E, Edstedt Bonamy A-K, Bonet M, Toome L, Rodrigues C, Howell EA, et al. Room for improvement in breast milk feeding after very preterm birth in Europe: Results from the EPICE cohort. *Matern Child Nutr.* 2018;14(1):e12485.
18. Colaizy TT. Effects of milk banking procedures on nutritional and bioactive components of donor human milk. *Semin Perinatol.* 2021:151382.
19. Wolfs TG, Buurman WA, Zoer B, Moonen RM, Derikx JP, Thuijls G, et al. Endotoxin induced chorioamnionitis prevents intestinal development during gestation in fetal sheep. *PLoS One.* 2009;4(6):e5837.
20. Nikiforou M, Vanderlocht J, Chougnat CA, Jellema RK, Ophelders DR, Joosten M, et al. Prophylactic Interleukin-2 Treatment Prevents Fetal Gut Inflammation and Injury in an Ovine Model of Chorioamnionitis. *Inflamm Bowel Dis.* 2015;21(9):2026-2038.
21. Wolfs TG, Kramer BW, Thuijls G, Kemp MW, Saito M, Willems MG, et al. Chorioamnionitis-induced fetal gut injury is mediated by direct gut exposure of inflammatory mediators or by lung inflammation. *Am J Physiol Gastrointest Liver Physiol.* 2014;306(5):G382-393.
22. Wolfs TG, Kallapur SG, Polglase GR, Pillow JJ, Nitsos I, Newnham JP, et al. IL-1 α mediated chorioamnionitis induces depletion of FoxP3 $^{+}$ cells and ileal inflammation in the ovine fetal gut. *PLoS One.* 2011;6(3):e18355.

23. Wolfs TG, Kallapur SG, Knox CL, Thuijls G, Nitsos I, Polglase GR, et al. Antenatal ureaplasma infection impairs development of the fetal ovine gut in an IL-1-dependent manner. *Mucosal Immunol.* 2013;6(3):547-556.
24. Gussenhoven R, Westerlaken RJJ, Ophelders D, Jobe AH, Kemp MW, Kallapur SG, et al. Chorioamnionitis, neuroinflammation, and injury: timing is key in the preterm ovine fetus. *J Neuroinflammation.* 2018;15(1):113.
25. De Giorgio R, Giancola F, Boschetti E, Abdo H, Lardeux B, Neunlist M. Enteric glia and neuroprotection: basic and clinical aspects. *Am J Physiol Gastrointest Liver Physiol.* 2012;303(8):G887-893.
26. Hansebout CR, Su C, Reddy K, Zhang D, Jiang C, Rathbone MP, et al. Enteric glia mediate neuronal outgrowth through release of neurotrophic factors. *Neural Regen Res.* 2012;7(28):2165-2175.
27. Rühl A, Nasser Y, Sharkey KA. Enteric glia. *Neurogastroenterol Motil.* 2004;16 Suppl 1:44-49.
28. Turco F, Sarnelli G, Cirillo C, Palumbo I, De Giorgi F, D'Alessandro A, et al. Enteroglial-derived S100B protein integrates bacteria-induced Toll-like receptor signalling in human enteric glial cells. *Gut.* 2014;63(1):105-115.
29. Lomax AE, Fernández E, Sharkey KA. Plasticity of the enteric nervous system during intestinal inflammation. *Neurogastroenterol Motil.* 2005;17(1):4-15.
30. Brown IA, McClain JL, Watson RE, Patel BA, Gulbransen BD. Enteric glia mediate neuron death in colitis through purinergic pathways that require connexin-43 and nitric oxide. *Cellular and molecular gastroenterology and hepatology.* 2016;2(1):77-91.
31. Cirillo C, Sarnelli G, Esposito G, Grosso M, Petruzzelli R, Izzo P, et al. Increased mucosal nitric oxide production in ulcerative colitis is mediated in part by the enteroglial-derived S100B protein. *Neurogastroenterol Motil.* 2009;21(11):1209-e112.
32. Colombo E, Farina C. Astrocytes: Key Regulators of Neuroinflammation. *Trends Immunol.* 2016;37(9):608-620.
33. Kovler ML, Gonzalez Salazar AJ, Fulton WB, Lu P, Yamaguchi Y, Zhou Q, et al. Toll-like receptor 4-mediated enteric glia loss is critical for the development of necrotizing enterocolitis. *Sci Transl Med.* 2021;13(612):eabg3459.
34. Boesmans W, Lasrado R, Vanden Berghe P, Pachnis V. Heterogeneity and phenotypic plasticity of glial cells in the mammalian enteric nervous system. *Glia.* 2015;63(2):229-241.
35. Seguella L, Gulbransen BD. Enteric glial biology, intercellular signalling and roles in gastrointestinal disease. *Nature reviews Gastroenterology & hepatology.* 2021;18(8):571-587.
36. Fichter M, Klotz M, Hirschberg DL, Waldura B, Schofer O, Ehnert S, et al. Breast milk contains relevant neurotrophic factors and cytokines for enteric nervous system development. *Mol Nutr Food Res.* 2011;55(10):1592-1596.
37. Furness JB. Types of neurons in the enteric nervous system. *J Auton Nerv Syst.* 2000;81(1-3):87-96.
38. De Schepper S, Verheijden S, Aguilera-Lizarraga J, Viola MF, Boesmans W, Stakenborg N, et al. Self-Maintaining Gut Macrophages Are Essential for Intestinal Homeostasis. *Cell.* 2018;175(2):400-15.e13.
39. Gabanyi I, Muller PA, Feighery L, Oliveira TY, Costa-Pinto FA, Mucida D. Neuro-immune Interactions Drive Tissue Programming in Intestinal Macrophages. *Cell.* 2016;164(3):378-391.
40. Rao M, Gershon MD. Enteric nervous system development: what could possibly go wrong? *Nat Rev Neurosci.* 2018;19(9):552-65.
41. Furness JB, Callaghan BP, Rivera LR, Cho HJ. The enteric nervous system and gastrointestinal innervation: integrated local and central control. *Adv Exp Med Biol.* 2014;817:39-71.
42. Boyer L, Ghoreishi M, Templeman V, Vallance BA, Buchan AM, Jevon G, et al. Myenteric plexus injury and apoptosis in experimental colitis. *Auton Neurosci.* 2005;117(1):41-53.
43. Linden DR, Couvrette JM, Ciolino A, McQuoid C, Blaszyk H, Sharkey KA, et al. Indiscriminate loss of myenteric neurons in the TNBS-inflamed guinea-pig distal colon. *Neurogastroenterol Motil.* 2005;17(5):751-760.
44. Afrazi A, Branca MF, Sodhi CP, Good M, Yamaguchi Y, Egan CE, et al. Toll-like receptor 4-mediated endoplasmic reticulum stress in intestinal crypts induces necrotizing enterocolitis. *J Biol Chem.* 2014;289(14):9584-9599.

45. Li P, Fu D, Sheng Q, Yu S, Bao X, Lv Z. TUDCA attenuates intestinal injury and inhibits endoplasmic reticulum stress-mediated intestinal cell apoptosis in necrotizing enterocolitis. *Int Immunopharmacol.* 2019;74:105665.
46. McGuckin MA, Eri RD, Das I, Lourie R, Florin TH. ER stress and the unfolded protein response in intestinal inflammation. *Am J Physiol Gastrointest Liver Physiol.* 2010;298(6):G820-32.
47. Lu P, Struijs MC, Mei J, Witte-Bouma J, Korteland-van Male AM, de Bruijn AC, et al. Endoplasmic reticulum stress, unfolded protein response and altered T cell differentiation in necrotizing enterocolitis. *PLoS One.* 2013;8(10):e78491.
48. Grootjans J, Hundscheid IH, Lenaerts K, Boonen B, Renes IB, Verheyen FK, et al. Ischaemia-induced mucus barrier loss and bacterial penetration are rapidly counteracted by increased goblet cell secretory activity in human and rat colon. *Gut.* 2013;62(2):250-258.
49. Johansson ME, Hansson GC. The goblet cell: a key player in ischaemia-reperfusion injury. *Gut.* 2013;62(2):188-189.
50. Grondin JA, Kwon YH, Far PM, Haq S, Khan WI. Mucins in Intestinal Mucosal Defense and Inflammation: Learning From Clinical and Experimental Studies. *Front Immunol.* 2020;11:2054.
51. Luo K, Cao SS. Endoplasmic reticulum stress in intestinal epithelial cell function and inflammatory bowel disease. *Gastroenterology research and practice.* 2015;2015:328791-.
52. Hosomi S, Kaser A, Blumberg RS. Role of endoplasmic reticulum stress and autophagy as interlinking pathways in the pathogenesis of inflammatory bowel disease. *Current opinion in gastroenterology.* 2015;31(1):81-88.
53. Grootjans J, Hodin CM, de Haan JJ, Derikx JP, Rouschop KM, Verheyen FK, et al. Level of activation of the unfolded protein response correlates with Paneth cell apoptosis in human small intestine exposed to ischemia/reperfusion. *Gastroenterology.* 2011;140(2):529-39.e3.
54. Li B, Hock A, Wu RY, Minich A, Botts SR, Lee C, et al. Bovine milk-derived exosomes enhance goblet cell activity and prevent the development of experimental necrotizing enterocolitis. *PLoS One.* 2019;14(1):e0211431.
55. Wu RY, Li B, Koike Y, Maattanen P, Miyake H, Cadete M, et al. Human Milk Oligosaccharides Increase Mucin Expression in Experimental Necrotizing Enterocolitis. *Mol Nutr Food Res.* 2019;63(3):e1800658.
56. Crespo I, San-Miguel B, Prause C, Marroni N, Cuevas MJ, González-Gallego J, et al. Glutamine treatment attenuates endoplasmic reticulum stress and apoptosis in TNBS-induced colitis. *PLoS One.* 2012;7(11):e50407.
57. Xu H, Liu G, Gu H, Wang J, Li Y. Glutamine protects intestine against ischemia-reperfusion injury by alleviating endoplasmic reticulum stress induced apoptosis in rats. *Acta Cir Bras.* 2020;35(1):e202000104-e.
58. Yan S, Yingchao L, Zhangliu W, Xianli R, Si L, Siyi N, et al. Effect of Berberine from *Coptis chinensis* on Apoptosis of Intestinal Epithelial Cells in a Mouse Model of Ulcerative Colitis: Role of Endoplasmic Reticulum Stress. *Evid Based Complement Alternat Med.* 2020;2020:3784671.
59. Fang T, Yao Y, Tian G, Chen D, Wu A, He J, et al. Chitosan oligosaccharide attenuates endoplasmic reticulum stress-associated intestinal apoptosis via the Akt/mTOR pathway. *Food Funct.* 2021.
60. Pelaseyed T, Bergström JH, Gustafsson JK, Ermund A, Birchenough GM, Schütte A, et al. The mucus and mucins of the goblet cells and enterocytes provide the first defense line of the gastrointestinal tract and interact with the immune system. *Immunol Rev.* 2014;260(1):8-20.
61. McGuckin MA, Lindén SK, Sutton P, Florin TH. Mucin dynamics and enteric pathogens. *Nature Reviews Microbiology.* 2011;9(4):265-278.
62. Johansson ME, Gustafsson JK, Holmén-Larsson J, Jabbar KS, Xia L, Xu H, et al. Bacteria penetrate the normally impenetrable inner colon mucus layer in both murine colitis models and patients with ulcerative colitis. *Gut.* 2014;63(2):281-291.
63. Hanson MA, Gluckman PD. Early developmental conditioning of later health and disease: physiology or pathophysiology? *Physiol Rev.* 2014;94(4):1027-1076.
64. Bose CL, Laughon MM, Allred EN, O'Shea TM, Van Marter LJ, Ehrenkranz RA, et al. Systemic inflammation associated with mechanical ventilation among extremely preterm infants. *Cytokine.* 2013;61(1):315-322.

65. Machado JR, Soave DF, da Silva MV, de Menezes LB, Etchebehere RM, Monteiro ML, et al. Neonatal sepsis and inflammatory mediators. *Mediators Inflamm.* 2014;2014:269681.
66. Rogido M, Griffin I. Macronutrient Digestion and Absorption in the Preterm Infant. *NeoReviews.* 2019;20(1):e25-e36.
67. te Velde AA, Brull F, Heinsbroek SE, Meijer SL, Lutjohann D, Vreugdenhil A, et al. Effects of Dietary Plant Sterols and Stanol Esters with Low- and High-Fat Diets in Chronic and Acute Models for Experimental Colitis. *Nutrients.* 2015;7(10):8518-8531.
68. Plat J, Baumgartner S, Vanmierlo T, Lutjohann D, Calkins KL, Burrin DG, et al. Plant-based sterols and stanols in health & disease: "Consequences of human development in a plant-based environment?". *Prog Lipid Res.* 2019;74:87-102.
69. De Smet E, Mensink RP, Boekschoten MV, de Ridder R, Germeraad WT, Wolfs TG, et al. An acute intake of plant stanol esters alters immune-related pathways in the jejunum of healthy volunteers. *Br J Nutr.* 2015;113(5):794-802.
70. Vuorio AF, Miettinen TA, Turtola H, Oksanen H, Gylling H. Cholesterol metabolism in normal and heterozygous familial hypercholesterolemic newborns. *J Lab Clin Med.* 2002;140(1):35-42.
71. Lager S, Powell TL. Regulation of nutrient transport across the placenta. *Journal of pregnancy.* 2012;2012:179827.
72. Gaccioli F, Lager S. Placental Nutrient Transport and Intrauterine Growth Restriction. *Front Physiol.* 2016;7:40.
73. Yee WH, Soraisham AS, Shah VS, Aziz K, Yoon W, Lee SK. Incidence and timing of presentation of necrotizing enterocolitis in preterm infants. *Pediatrics.* 2012;129(2):e298-304.
74. Dodge KA. Annual Research Review: Universal and targeted strategies for assigning interventions to achieve population impact. *J Child Psychol Psychiatry.* 2020;61(3):255-267.
75. Jaceldo-Siegl K, Lutjohann D, Sirirat R, Mashchak A, Fraser GE, Haddad E. Variations in dietary intake and plasma concentrations of plant sterols across plant-based diets among North American adults. *Mol Nutr Food Res.* 2017;61(8).
76. Laitinen K, Isolauri E, Kaipiainen L, Gylling H, Miettinen TA. Plant stanol ester spreads as components of a balanced diet for pregnant and breast-feeding women: evaluation of clinical safety. *Br J Nutr.* 2009;101(12):1797-1804.
77. Law M. Plant sterol and stanol margarines and health. *BMJ (Clinical research ed).* 2000;320(7238):861-864.
78. Fransen HP, de Jong N, Wolfs M, Verhagen H, Verschuren WM, Lutjohann D, et al. Customary use of plant sterol and plant stanol enriched margarine is associated with changes in serum plant sterol and stanol concentrations in humans. *J Nutr.* 2007;137(5):1301-1306.
79. McManemy J, Cooke E, Amon E, Leet T. Recurrence risk for preterm delivery. *Am J Obstet Gynecol.* 2007;196(6):576.e1-6; discussion .e6-7.
80. Esplin MS, O'Brien E, Fraser A, Kerber RA, Clark E, Simonsen SE, et al. Estimating recurrence of spontaneous preterm delivery. *Obstet Gynecol.* 2008;112(3):516-523.
81. Laibl VR, Sheffield JS, Roberts S, McIntire DD, Wendel GD, Jr. Recurrence of clinical chorioamnionitis in subsequent pregnancies. *Obstet Gynecol.* 2006;108(6):1493-1497.
82. Ophelders D, Boots AW, Hütten MC, Al-Nasiry S, Jellema RK, Spiller OB, et al. Screening of Chorioamnionitis Using Volatile Organic Compound Detection in Exhaled Breath: A Pre-clinical Proof of Concept Study. *Frontiers in pediatrics.* 2021;9:617906.
83. Ng PC. An update on biomarkers of necrotizing enterocolitis. *Semin Fetal Neonatal Med.* 2018;23(6):380-386.
84. Wright H, Bannaga AS, Iriarte R, Mahmoud M, Arasaradnam RP. Utility of volatile organic compounds as a diagnostic tool in preterm infants. *Pediatr Res.* 2020.
85. Berkhout DJC, Niemarkt HJ, de Boer NKH, Benninga MA, de Meij TGJ. The potential of gut microbiota and fecal volatile organic compounds analysis as early diagnostic biomarker for necrotizing enterocolitis and sepsis in preterm infants. *Expert Rev Gastroenterol Hepatol.* 2018;12(5):457-470.
86. Good M, Chu T, Shaw P, Nolan LS, McClain L, Chamberlain A, et al. Neonatal necrotizing enterocolitis-associated DNA methylation signatures in the colon are evident in stool samples of affected individuals. *Epigenomics.* 2021;13(11):829-844.

87. Terrin G, Stronati L, Cucchiara S, De Curtis M. Serum Markers of Necrotizing Enterocolitis: A Systematic Review. *J Pediatr Gastroenterol Nutr.* 2017;65(6):e120-e32.
88. Picaud JC, De Magistris A, Mussap M, Corbu S, Dessi A, Noto A, et al. Urine NMR Metabolomics Profile of Preterm Infants With Necrotizing Enterocolitis Over the First Two Months of Life: A Pilot Longitudinal Case-Control Study. *Frontiers in molecular biosciences.* 2021;8:680159.
89. Agakidou E, Agakidis C, Gika H, Sarafidis K. Emerging Biomarkers for Prediction and Early Diagnosis of Necrotizing Enterocolitis in the Era of Metabolomics and Proteomics. *Frontiers in pediatrics.* 2020;8:602255.
90. Martysiak-Żurowska D, Puta M, Kielbratowska B, Wesołowska A. Neurotrophic Factors in Human Milk in Early Lactation and the Effect of Holder and Microwave Pasteurization on Their Concentrations. *J Pediatr Gastroenterol Nutr.* 2021;72(6):900-905.
91. Li R, Xia W, Zhang Z, Wu K. S100B protein, brain-derived neurotrophic factor, and glial cell line-derived neurotrophic factor in human milk. *PLoS One.* 2011;6(6):e21663.
92. Gianino S, Grider JR, Cresswell J, Enomoto H, Heuckeroth RO. GDNF availability determines enteric neuron number by controlling precursor proliferation. *Development.* 2003;130(10):2187-2198.
93. Vejsada R, Tseng JL, Lindsay RM, Acheson A, Aebischer P, Kato AC. Synergistic but transient rescue effects of BDNF and GDNF on axotomized neonatal motoneurons. *Neuroscience.* 1998;84(1):129-139.
94. Hageman JHJ, Keijer J, Dalsgaard TK, Zeper LW, Carrier F, Feitsma AL, et al. Free fatty acid release from vegetable and bovine milk fat-based infant formulas and human milk during two-phase in vitro digestion. *Food Funct.* 2019.
95. Salas Lorenzo I, Chisaguano Tonato AM, de la Garza Puentes A, Nieto A, Herrmann F, Dieguez E, et al. The Effect of an Infant Formula Supplemented with AA and DHA on Fatty Acid Levels of Infants with Different FADS Genotypes: The COGNIS Study. *Nutrients.* 2019;11(3):602.
96. Totten SM, Zivkovic AM, Wu S, Ngyuen U, Freeman SL, Ruhaak LR, et al. Comprehensive profiles of human milk oligosaccharides yield highly sensitive and specific markers for determining secretor status in lactating mothers. *J Proteome Res.* 2012;11(12):6124-6133.
97. Bourlieu C, Menard O, Bouzerzour K, Mandalari G, Macierzanka A, Mackie AR, et al. Specificity of infant digestive conditions: some clues for developing relevant in vitro models. *Crit Rev Food Sci Nutr.* 2014;54(11):1427-1457.
98. Dallas DC, Underwood MA, Zivkovic AM, German JB. Digestion of Protein in Premature and Term Infants. *Journal of nutritional disorders & therapy.* 2012;2(3):112.
99. Perrone S, Tataranno ML, Santacroce A, Negro S, Buonocore G. The role of oxidative stress on necrotizing enterocolitis in very low birth weight infants. *Curr Pediatr Rev.* 2014;10(3):202-207.
100. Cummins EP, Crean D. Hypoxia and inflammatory bowel disease. *Microbes Infect.* 2017;19(3): 210-221.
101. Eltzschig HK, Eckle T. Ischemia and reperfusion—from mechanism to translation. *Nat Med.* 2011;17(11):1391-1401.
102. Noel G, Baetz NW, Staab JF, Donowitz M, Kovbasnjuk O, Pasetti MF, et al. A primary human macrophage-enteroid co-culture model to investigate mucosal gut physiology and host-pathogen interactions. *Sci Rep.* 2017;7:45270.
103. Staab JF, Lemme-Dumit JM, Latanich R, Pasetti MF, Zachos NC. Co-Culture System of Human Enteroids/Colonoids with Innate Immune Cells. *Curr Protoc Immunol.* 2020;131(1):e113.
104. Puschhof J, Pleguezuelos-Manzano C, Martinez-Silgado A, Akkerman N, Saftien A, Boot C, et al. Intestinal organoid cocultures with microbes. *Nat Protoc.* 2021.
105. Rubert J, Schweiger PJ, Mattivi F, Tuohy K, Jensen KB, Lunardi A. Intestinal Organoids: A Tool for Modelling Diet-Microbiome-Host Interactions. *Trends Endocrinol Metab.* 2020;31(11):848-858.
106. Levin DE, Mandal A, Fleming MA, Bae KH, Gerry B, Moore SR. Intestinal crypt-derived enteroid coculture in presence of peristaltic longitudinal muscle myenteric plexus. *Biology methods & protocols.* 2021;6(1):bpaa027.
107. Thum C, Wall CR, Weiss GA, Wang W, Szeto IM, Day L. Changes in HMO Concentrations throughout Lactation: Influencing Factors, Health Effects and Opportunities. *Nutrients.* 2021;13(7).
108. Obata Y, Pachnis V. The Effect of Microbiota and the Immune System on the Development and Organization of the Enteric Nervous System. *Gastroenterology.* 2016;151(5):836-844.

109. Soderholm AT, Pedicord VA. Intestinal epithelial cells: at the interface of the microbiota and mucosal immunity. *Immunology*. 2019;158(4):267-280.
110. Ferguson DCJ, Smerdon GR, Harries LW, Dodd NJF, Murphy MP, Curnow A, et al. Altered cellular redox homeostasis and redox responses under standard oxygen cell culture conditions versus physioxia. *Free Radic Biol Med*. 2018;126:322-333.
111. Skovdahl HK, Gopalakrishnan S, Svendsen TD, Granlund AVB, Bakke I, Ginbot ZG, et al. Patient Derived Colonoids as Drug Testing Platforms-Critical Importance of Oxygen Concentration. *Front Pharmacol*. 2021;12:679741.
112. Senger S, Ingano L, Freire R, Anselmo A, Zhu W, Sadreyev R, et al. Human Fetal-Derived Enterospheres Provide Insights on Intestinal Development and a Novel Model to Study Necrotizing Enterocolitis (NEC). Cellular and molecular gastroenterology and hepatology. 2018;5(4):549-68.
113. Kraiczky J, Nayak KM, Howell KJ, Ross A, Forbester J, Salvestrini C, et al. DNA methylation defines regional identity of human intestinal epithelial organoids and undergoes dynamic changes during development. *Gut*. 2017.
114. Noel G, In JG, Lemme-Dumit JM, DeVine LR, Cole RN, Guerrero AL, et al. Human Breast Milk Enhances Intestinal Mucosal Barrier Function and Innate Immunity in a Healthy Pediatric Human Enteroid Model. *Frontiers in cell and developmental biology*. 2021;9:685171.
115. Niklinska-Schirtz BJ, Venkateswaran S, Anbazhagan M, Kolachala VL, Prince J, Dodd A, et al. Ileal derived organoids from Crohn's disease patients show unique transcriptomic and secretomic signatures. *Cellular and molecular gastroenterology and hepatology*. 2021.
116. Ojo BA, VanDussen KL, Rosen MJ. The Promise of Patient-Derived Colon Organoids to Model Ulcerative Colitis. *Inflamm Bowel Dis*. 2021.
117. Cuna A, George L, Sampath V. Genetic predisposition to necrotizing enterocolitis in premature infants: Current knowledge, challenges, and future directions. *Semin Fetal Neonatal Med*. 2018;23(6):387-393.
118. De Fazio L, Beghetti I, Bertuccio SN, Marsico C, Martini S, Masetti R, et al. Necrotizing Enterocolitis: Overview on In Vitro Models. *Int J Mol Sci*. 2021;22(13).
119. Creff J, Malaquin L, Besson A. In vitro models of intestinal epithelium: Toward bioengineered systems. *J Tissue Eng*. 2021;12:2041731420985202-.
120. Kakni P, Hueber R, Knoops K, López-Iglesias C, Truckenmüller R, Habibovic P, et al. Intestinal Organoid Culture in Polymer Film-Based Microwell Arrays. *Advanced biosystems*. 2020;4(10):2000126.

Chapter 11

Scientific and societal impact

Scientific and societal impact

This chapter reflects on the scientific and societal impact of this thesis, and on the ways the target audience can be informed of and engaged with the main results of this thesis, in order to promote future use of the acquired knowledge.

Research field and aims of this thesis

Each year, around 15 million babies are born prematurely, i.e., before 37 weeks of pregnancy¹. Although more and more of these babies survive, premature birth remains the leading cause of death for infants below 5 years of age¹. In addition, surviving children often have long-term health problems, especially if they are born extremely preterm (before 28 weeks of gestational age) or severely preterm (between 28 and 31 weeks of gestational age)². An important reason for preterm birth is inflammation or infection of the membranes covering the inside of the uterus, which is called chorioamnionitis³. Chorioamnionitis is often accompanied by inflammation of the amniotic fluid and even of the fetal blood and tissues⁴, which further increase the risk of death of the infant and major health concerns^{5,6}. Importantly, since many diseases of premature babies are influenced by risk factors during pregnancy, such as chorioamnionitis, it is suggested that the development of such diseases may start before birth^{6,7}. One of these diseases is necrotizing enterocolitis (NEC)⁸. NEC is characterized by severe inflammation of the intestines and, in later stages, death of intestinal tissue⁹. Why and how NEC develops is currently insufficiently clarified, but it is known that multiple factors such as loss of intestinal barrier function and altered intestinal motility contribute to NEC development¹⁰. NEC affects around 7% of infants who are treated at the neonatal intensive care unit (NICU). About 15-30% of infants with NEC die from it¹⁰, and this number increases up to 50% in infants that need to be treated surgically¹¹. In addition, children who do survive are at risk of long-term health consequences such as problems with digestion and absorption of nutrition¹¹ and disturbed brain development¹⁰. Importantly, besides being a major health issue, both premature birth and its sequelae pose a considerable economic burden on society. NICU care is expensive and a multitude of these costs are caused by the life-long care for individuals with preterm-birth-related long-term health consequences^{12,13}. Direct health-care costs of NEC have been estimated to range from \$70,000 to \$180,000 per infant^{14,15}. In addition, quality of life of both the infant and his or her parents (and further family) is negatively affected^{16,17}.

Despite having been studied for years, NEC treatment remains largely symptomatic and difficult to majorly improve, amongst others due to the rapid onset and aggressive disease course of NEC⁹. Consequently, the field of NEC research has, over the past decades, aimed at developing new preventative approaches^{9,18}. In this context, breast milk and breast milk components are promising, since NEC cases are reduced by 10-fold when only human milk is fed to the infants, and by 3- to 5-fold when human milk feeding is combined with feeding of infant formula¹⁹. The protective role of breast milk can be explained by the large number of bioactive components present in breast milk that collectively act on several disease mechanisms involved in NEC development²⁰⁻²². Unfortunately, mothers' own milk is not always available for infants treated at the NICU^{23,24} and donor milk, which is increasingly being used, is not a full-fledged alternative^{25,26}. Thus, the development of nutritional

interventions containing (combinations of) bioactive human breast milk components holds great promise for the prevention of NEC. As many years of research into feeding interventions have not majorly reduced NEC occurrence yet, alternative research strategies are desired. Therefore, in the current thesis, we aimed to provide a framework for the improvement of preventative feeding interventions for NEC, by applying novel strategies that specifically acknowledge the fact that NEC is caused by multiple factors and that NEC development may already start before birth.

Direct relevance of the key findings in this thesis

In this thesis, we provided an overview of the current state of evidence regarding feeding interventions for the prevention of NEC. This work provides (future) researchers with an interest in enteral feeding interventions for NEC, with a summary of what has already been done and which biological effects (such as reduction of intestinal inflammation and improved gut barrier function) were previously attributed to nutritional components. This information is also relevant for researchers looking into other diseases marked by similar disease mechanisms that may benefit from feeding interventions with such biological effects, such as inflammatory bowel disease (IBD)²⁷. We demonstrated that although a large number of positive results were observed in experimental animal studies, only scarce interventions were successful in clinical trials, and we identified various aspects that can explain this difference. Important reasons include that most studies start interventions postnatally, which may be (too) late, and the fact that the NEC development is incompletely understood. Moreover, most studies mainly looked at single component interventions, whereas, given the complex composition of breast milk and the multifactorial origin of NEC, interventions using combinations of nutritional components are more likely to be successful. These challenges were addressed in the studies incorporated in this thesis and this knowledge can be used to improve future (pre-)clinical studies in the field of neonatology and NEC and in other (bio)medical fields that face similar challenges.

We observed that alterations in the nervous system of the gut, which is, amongst others, responsible for bowel movements, and the intestinal mucus barrier, are found already before birth as a consequence of chorioamnionitis. Moreover, our studies provided indications on which disease mechanism could be involved. Since these alterations and potential mechanistic explanations correspond to findings in NEC, this knowledge contributes to a better understanding of NEC development and supports the concept that NEC development may start before birth. This could benefit researchers who are designing future studies to unravel NEC development, and strengthens the idea that feeding interventions before birth may be useful to improve outcomes after birth. In addition, scientists in other fields may benefit from the knowledge acquired, since the implicated disease mechanisms are generic for multiple diseases in neonates or in the gut, such as perinatal brain injury^{28,29}, IBD^{30,31}, and intestinal ischemia reperfusion injury (IRI)^{32,33}.

We reported, in a proof-of-concept study, that a prenatal feeding intervention with plant sterols (food components present in plant cell membranes) by administration in the amniotic fluid, reduced inflammation in the fetal blood and improved gut outcome. As far as we know, this is the first study to report that the fetus can be targeted perinatally with a

feeding intervention to improve gut health. This first study could pave the way for future studies addressing health problems of the prematurely born neonate at the earliest possible moment, namely before it is born, by modulation of the nutrition of pregnant women. Of note, although we performed this study in the context of gut inflammation and NEC, plant sterols and other interventions could also be relevant for other diseases associated with blood inflammation of the fetus, such as bronchopulmonary dysplasia (chronic lung disease)⁵ and brain injury around birth⁵. In a broader context, our study once again shows that the composition of the amniotic fluid, which is partially determined by maternal diet, is important for the health of the fetus. This concept is vital for health care staff, such as obstetricians, midwives, neonatologists, and dieticians, but also for the mother/parents-to-be. Additionally, this information could be relevant for the government and health insurance companies, since they can promote a healthy lifestyle via legislation and/or public campaigns.

Last, we developed a human intestinal organoid model for the screening of nutritional interventions in the context of intestinal health and disease. In this model, we successfully tested the effect of hydrolyzed ('digested') and non-hydrolyzed ('non-digested') whey proteins as potential beneficial feeding intervention. Such a screening model is key for adjusting future research into preventative feeding interventions for NEC from single interventions, which have not been very successful over the years, to combinations of interventions, of which more promising effects can be expected. In addition, this approach can reduce the number of laboratory animals used. Given the findings in this thesis, plant sterols and whey protein are interesting candidates to be incorporated in such a combined nutritional intervention. The work described here forms a solid basis for further extending such organoid models, by creating organoid co-cultures with immune cells, microbes or cells from the nervous system of the gut in future studies. Such (extended) organoid models can be useful for other researchers developing (nutritional) interventions in the context of NEC and other gastrointestinal diseases such as IBD and IRI. In addition, techniques used in this model can be applied in other studies that use (human intestinal) organoids.

Potential long-term relevance of the key findings in this thesis

The work described in this thesis provides new scientific insights and adds points of departure for follow-up studies and future clinical trials. The knowledge acquired can, in the long run, contribute to the development of novel enteral feeding interventions that effectively prevent NEC as well as NEC-related death and long-term health consequences. Neonatal intensive care is very expensive, although it is much more cost effective compared to adult health care¹³. If enteral feeding interventions are effective in improving survival and reducing the duration of NICU stay, they are likely to reduce neonatal intensive care costs¹³. Importantly, environmental circumstances including nutrition in the first 1000 days of life are increasingly recognized as an important determinant for lifelong health^{34,35} and more and more studies support interaction between development of the gut and other organs such as the brain and the lung³⁶⁻³⁸. In line with these findings, breastfeeding is, amongst others, linked to reduced risk of childhood obesity^{39,40}, type 2 diabetes^{39,41}, IBD⁴², and

asthma⁴³. This indicates that development of novel enteral feeding interventions can promote health beyond the gut and beyond the neonatal period.

Dissemination of knowledge to target groups

The direct impact of this thesis is mainly scientific; thus the main target group is the scientific community. Dissemination to this group has taken place and will take place in the future via scientific publications in international peer-reviewed journals and via presentations at (inter)national congresses. All published studies incorporated in this thesis have been published in open-access journals and are thereby freely available to the general public. A second target group that could benefit from the knowledge acquired in this thesis comprises health care staff, such as pediatricians and neonatologists, perinatologists and obstetricians, pediatric surgeons, midwives, and dieticians. Currently, this mainly concerns the general concept that NEC development may already start before birth, and that fetal and neonatal health are influenced by amniotic fluid composition. However, if the knowledge acquired supports better enteral feeding intervention studies for NEC in the future, it could in the long run lead to adjustment of clinical guidelines and improvement of neonatal intensive care. Healthcare staff can be updated about the content of this thesis via clinical congresses, presentations during teaching moments in the hospital, and during peer consultation.

A last target group is formed by (future) parents of premature neonates or infants with NEC, and their loved ones. In the first place, they may take comfort in the thought that efforts are being made to improve the outcome of their child and future children. Ultimately, this group directly benefits from this research by improved health care. This target group can be reached via patient organizations and platforms, such as the European Foundation for the Care of Newborn Infants (EFCNI), Care4Neo and Kleine Kanjers, and via (local) fundraisers in the field, such as Strong Babies and Kinderonderzoeksfonds Limburg.

References

1. Harrison MS, Goldenberg RL. Global burden of prematurity. *Semin Fetal Neonatal Med.* 2016;21(2):74-79.
2. Goldenberg RL, Culhane JF, Iams JD, Romero R. Epidemiology and causes of preterm birth. *Lancet.* 2008;371(9606):75-84.
3. Goldenberg RL, Hauth JC, Andrews WW. Intrauterine infection and preterm delivery. *N Engl J Med.* 2000;342(20):1500-1507.
4. Kim CJ, Romero R, Chaemsaitong P, Chaiyasit N, Yoon BH, Kim YM. Acute chorioamnionitis and funisitis: definition, pathologic features, and clinical significance. *Am J Obstet Gynecol.* 2015;213(4 Suppl):S29-52.
5. Tang Q, Zhang L, Li H, Shao Y. The fetal inflammation response syndrome and adverse neonatal outcomes: a meta-analysis. *J Matern Fetal Neonatal Med.* 2019:1-13.
6. Gantert M, Been JV, Gavilanes AW, Garnier Y, Zimmermann LJ, Kramer BW. Chorioamnionitis: a multiorgan disease of the fetus? *J Perinatol.* 2010;30 Suppl:S21-30.
7. Watson SN, McElroy SJ. Potential Prenatal Origins of Necrotizing Enterocolitis. *Gastroenterol Clin North Am.* 2021;50(2):431-444.
8. Been JV, Lievens S, Zimmermann LJ, Kramer BW, Wolfs TG. Chorioamnionitis as a risk factor for necrotizing enterocolitis: a systematic review and meta-analysis. *J Pediatr.* 2013;162(2):236-242 e2.
9. Neu J, Walker WA. Necrotizing enterocolitis. *N Engl J Med.* 2011;364(3):255-264.
10. Lin PW, Stoll BJ. Necrotizing enterocolitis. *Lancet.* 2006;368(9543):1271-1283.
11. Murthy K, Yanowitz TD, DiGeronimo R, Dykes FD, Zaniletti I, Sharma J, et al. Short-term outcomes for preterm infants with surgical necrotizing enterocolitis. *J Perinatol.* 2014;34(10):736-740.
12. Frey HA, Klebanoff MA. The epidemiology, etiology, and costs of preterm birth. *Semin Fetal Neonatal Med.* 2016;21(2):68-73.
13. Cheah IGS. Economic assessment of neonatal intensive care. *Translational pediatrics.* 2019;8(3):246-256.
14. Bisquera JA, Cooper TR, Berseth CL. Impact of necrotizing enterocolitis on length of stay and hospital charges in very low birth weight infants. *Pediatrics.* 2002;109(3):423-428.
15. Ganapathy V, Hay JW, Kim JH. Costs of necrotizing enterocolitis and cost-effectiveness of exclusively human milk-based products in feeding extremely premature infants. *Breastfeed Med.* 2012;7(1):29-37.
16. Amin R, Knezevich M, Lingongo M, Szabo A, Yin Z, Oldham KT, et al. Long-term Quality of Life in Neonatal Surgical Disease. *Ann Surg.* 2018;268(3):497-505.
17. McAndrew S, Acharya K, Westerdahl J, Brousseau DC, Panepinto JA, Simpson P, et al. A Prospective Study of Parent Health-Related Quality of Life before and after Discharge from the Neonatal Intensive Care Unit. *J Pediatr.* 2019;213:38-45.e3.
18. Gordon PV, Swanson JR, Attridge JT, Clark R. Emerging trends in acquired neonatal intestinal disease: is it time to abandon Bell's criteria? *J Perinatol.* 2007;27(11):661-671.
19. Lucas A, Cole TJ. Breast milk and neonatal necrotizing enterocolitis. *Lancet.* 1990;336(8730): 1519-2153.
20. Thai JD, Gregory KE. Bioactive Factors in Human Breast Milk Attenuate Intestinal Inflammation during Early Life. *Nutrients.* 2020;12(2).
21. Andreas NJ, Kampmann B, Mehring Le-Doare K. Human breast milk: A review on its composition and bioactivity. *Early Hum Dev.* 2015;91(11):629-635.
22. Chatterton DE, Nguyen DN, Bering SB, Sangild PT. Anti-inflammatory mechanisms of bioactive milk proteins in the intestine of newborns. *Int J Biochem Cell Biol.* 2013;45(8):1730-1747.
23. Cregan MD, De Mello TR, Kershaw D, McDougall K, Hartmann PE. Initiation of lactation in women after preterm delivery. *Acta Obstet Gynecol Scand.* 2002;81(9):870-877.
24. Heller N, Rüdiger M, Hoffmeister V, Mense L. Mother's Own Milk Feeding in Preterm Newborns Admitted to the Neonatal Intensive Care Unit or Special-Care Nursery: Obstacles, Interventions, Risk Calculation. *Int J Environ Res Public Health.* 2021;18(8).
25. Colaizy TT. Effects of milk banking procedures on nutritional and bioactive components of donor human milk. *Semin Perinatol.* 2021:151382.

26. Sánchez Luna M, Martin SC, Gómez-de-Orgaz CS. Human milk bank and personalized nutrition in the NICU: a narrative review. *Eur J Pediatr.* 2021;180(5):1327-1333.
27. Pigneur B, Ruemmele FM. Nutritional interventions for the treatment of IBD: current evidence and controversies. *Therap Adv Gastroenterol.* 2019;12:1756284819890534.
28. Bueter W, Dammann O, Leviton A. Endoplasmic reticulum stress, inflammation, and perinatal brain damage. *Pediatr Res.* 2009;66(5):487-494.
29. Ophelders D, Gussenhoven R, Klein L, Jellema RK, Westerlaken RJJ, Hütten MC, et al. Preterm Brain Injury, Antenatal Triggers, and Therapeutics: Timing Is Key. *Cells.* 2020;9(8).
30. Seguela L, Gulbransen BD. Enteric glial biology, intercellular signalling and roles in gastrointestinal disease. *Nature reviews Gastroenterology & hepatology.* 2021;18(8):571-587.
31. Coleman OI, Haller D. ER Stress and the UPR in Shaping Intestinal Tissue Homeostasis and Immunity. *Front Immunol.* 2019;10(2825).
32. Kaser A, Tomczak M, Blumberg RS. "ER stress(ed out)!": Paneth cells and ischemia-reperfusion injury of the small intestine. *Gastroenterology.* 2011;140(2):393-396.
33. Mendes CE, Palombit K, Vieira C, Silva I, Correia-de-Sá P, Castelucci P. The Effect of Ischemia and Reperfusion on Enteric Glial Cells and Contractile Activity in the Ileum. *Dig Dis Sci.* 2015;60(9):2677-2689.
34. Ratsika A, Codagnone MC, O'Mahony S, Stanton C, Cryan JF. Priming for Life: Early Life Nutrition and the Microbiota-Gut-Brain Axis. *Nutrients.* 2021;13(2).
35. Cusick SE, Georgieff MK. The Role of Nutrition in Brain Development: The Golden Opportunity of the "First 1000 Days". *J Pediatr.* 2016;175:16-21.
36. Willis KA, Ambalavanan N. Necrotizing enterocolitis and the gut-lung axis. *Semin Perinatol.* 2021:151454.
37. Jena A, Montoya CA, Mullaney JA, Dilger RN, Young W, McNabb WC, et al. Gut-Brain Axis in the Early Postnatal Years of Life: A Developmental Perspective. *Front Integr Neurosci.* 2020;14:44.
38. Rodríguez JM, Fernández L, Verhasselt V. The Gut–Breast Axis: Programming Health for Life. *Nutrients.* 2021;13(2).
39. Chetta KE, Schulz EV, Wagner CL. Outcomes improved with human milk intake in preterm and full-term infants. *Semin Perinatol.* 2021:151384.
40. Harder T, Bergmann R, Kallischnigg G, Plagemann A. Duration of breastfeeding and risk of overweight: a meta-analysis. *Am J Epidemiol.* 2005;162(5):397-403.
41. Bartz S, Freemark M. Pathogenesis and Prevention of Type 2 Diabetes: Parental Determinants, Breastfeeding, and Early Childhood Nutrition. *Curr Diab Rep.* 2012;12(1):82-87.
42. Xu L, Lochhead P, Ko Y, Claggett B, Leong RW, Ananthakrishnan AN. Systematic review with meta-analysis: breastfeeding and the risk of Crohn's disease and ulcerative colitis. *Aliment Pharmacol Ther.* 2017;46(9):780-789.
43. Güngör D, Nadaud P, LaPergola CC, Dreifelbis C, Wong YP, Terry N, et al. Infant milk-feeding practices and food allergies, allergic rhinitis, atopic dermatitis, and asthma throughout the life span: a systematic review. *Am J Clin Nutr.* 2019;109(Suppl_7):772s-799s.

Addendum

Nederlandse samenvatting

Abbreviations

Dankwoord

List of publications

Curriculum vitae

Nederlandse samenvatting

Vroeggeboorte, gedefinieerd als geboorte vóór een zwangerschapsduur van 37 weken, is wereldwijd een groot gezondheidsprobleem. Het is een belangrijke oorzaak van zowel neonatale mortaliteit als morbiditeit en veroorzaakt een aanzienlijke economische belasting voor de samenleving. Vroeggeboorte is vaak het gevolg van een ontsteking van de foetale vruchtvliezen (chorioamnionitis), die meestal ontstaat door microbiële invasie van de baarmoederholte vanuit het geboortekanaal. *Ureaplasma Parvum* (UP) is hierbij het meest geïsoleerde micro-organisme. Een chorioamnionitis kan leiden tot een systemisch inflammatoir responsyndroom bij de foetus (FIRS). Chorioamnionitis en FIRS zijn, onafhankelijk van vroeggeboorte, risicofactoren voor nadelige uitkomsten voor de neonaat, zoals de neonatale gastro-intestinale aandoening necrotiserende enterocolitis (NEC). NEC geeft een ernstige darmontsteking die vaak overgaat in necrose. Het is eveneens geassocieerd met aanzienlijke mortaliteit en morbiditeit op de lange termijn, waaronder vertragingen in de neurologische ontwikkeling. Hoewel verschillende factoren, zoals een onrijpe darmmotiliteit, microbiële dysbiose in de darm en een verminderde intestinale (mucus)barrièrefunctie duidelijk een rol spelen, is de pathofysiologie van NEC nog steeds niet volledig opgehelderd. De behandeling van NEC is tot op heden dan ook grotendeels gericht op symptoombestrijding. Het voeden van baby's met moedermelk is een belangrijke factor in het verminderen van het NEC-risico, vooral omdat moedermelk veel bioactieve componenten bevat die ziektemechanismen moduleren die betrokken zijn bij de NEC-pathogenese, zoals darmontsteking en verlies van darmbarrièrefunctie. Helaas is (eigen) moedermelk niet voor alle premature pasgeborenen beschikbaar en is donormelk geen volwaardig alternatief. Daarom is de ontwikkeling van voedingsinterventies die (combinaties van) bioactieve moedermelkcomponenten bevatten veelbelovend als nieuwe preventiestrategie om de incidentie en ernst van NEC te verminderen.

In dit proefschrift heb ik me gericht op verschillende elementen die bijdragen aan een nieuw raamwerk voor de verbetering van dergelijke preventieve voedingsinterventies. De focus ligt in het bijzonder op de multifactoriële pathofysiologie van NEC en het veronderstelde prenatale begin hiervan. Dit werd bereikt door:

1. het in kaart brengen van de huidige kennis over de effectiviteit en ziektemechanisme-specifieke effecten van enterale voedingsinterventies bij de preventie van NEC en het identificeren van manieren om het onderzoek naar dit onderwerp te verbeteren (**hoofdstuk 2**).
2. het vergroten van ons begrip van NEC-pathofysiologie door onderzoek te doen naar de effecten van chorioamnionitis en NEC op het enterisch zenuwstelsel en de intestinale mucusbarrière (**hoofdstuk 3-7**).
3. het onderzoeken van de effecten van een enterale voedingsinterventie (plant sterolen) in utero op de foetale darm die wordt aangetast door chorioamnionitis (**hoofdstuk 8**).
4. het ontwikkelen van een nieuw humaan darmorganoïde model voor het screenen van (combinaties van) voedingsinterventies in de context van door hypoxie geïnduceerde darmontsteking en het bestuderen van de effecten van voedingsinterventies in dit model. Hierbij zijn we gestart met (gehydrolyseerde) wei-eiwitten (**hoofdstuk 9**).

Enterale voedingsinterventies voor NEC-preventie: wat is er al bekend?

In **hoofdstuk 2** hebben we op systematische wijze de huidige wetenschappelijke kennis over enterale voedingsinterventies voor de preventie van NEC beoordeeld. We hebben laten zien dat experimentele dierstudies een grote hoeveelheid bewijs leveren over de gunstige effecten van specifieke enterale voedingsinterventies op de incidentie van NEC, op mortaliteit en op een breed scala van pathofysiologische mechanismen van NEC. In tegenstelling tot het uitgebreide bewijs uit dierstudies, zijn weinig enterale voedingsinterventies (probiotica en arginine) effectief gebleken in (meta-analyses van) klinische onderzoeken. Verschillende factoren kunnen ten grondslag liggen aan de moeizame translatie van diermodellen naar de klinische praktijk. Deze omvatten methodologische factoren gerelateerd aan dierexperimenten, zoals suboptimale beoordeling van bias, onduidelijke zekerheid van bewijs, suboptimale modellering van NEC en het starten van (preventieve) interventies gelijktijdig met experimentele NEC inductie. Ook factoren die verband houden met klinische studies spelen een rol; veel van deze studies hebben niet genoeg statistische power en NEC als klinische entiteit is niet altijd duidelijk gedefinieerd. Verschillende doseringen en toedieningsschema's worden zelden bestudeerd en het is onduidelijk hoe deze variabelen in dierstudies kunnen worden vertaald naar de neonaat. Ten slotte worden combinaties van verschillende voedingscomponenten slechts sporadisch bestudeerd, terwijl dit waarschijnlijk wél van cruciaal belang is in het licht van de complexe samenstelling van moedermelk en de multifactoriële aard van NEC-pathofysiologie.

Strategieën om de huidige tekortkomingen in NEC onderzoek te overbruggen zijn opgenomen in dit proefschrift en omvatten het verbeteren van ons begrip van NEC-pathofysiologie (**hoofdstuk 3-7**), het bestuderen van preventieve enterale voedingsinterventies op een vroeger moment (d.w.z. in utero) (**hoofdstuk 8**) en het ontwikkelen van een op menselijk weefsel gebaseerd experimenteel darmorganoïdenmodel dat medium- tot high-throughput screening van (combinaties) van voedingsinterventies mogelijk maakt (**hoofdstuk 9**).

Effecten van perinatale pro-inflammatoire hits op het enterische zenuwstelsel

In **hoofdstuk 3** hebben we in een schapen chorioamnionitismodel de effecten van intra-uteriene LPS-blootstelling op het foetale enterisch zenuwstelsel in de loop van de tijd bestudeerd. In deze studie zagen we dat de immunoreactiviteit van mature neuronen (PGP9.5) afnam in de myenterische plexus vier dagen na intra-uteriene blootstelling aan LPS, met een gelijktijdige afname van de immunoreactiviteit van enterische gliacellen (S100 β). Foetale darmontsteking en systemische ontsteking ging aan deze veranderingen vooraf en overlapte er mee. De structurele veranderingen van het enterisch zenuwstelsel waren 15 dagen na intra-uteriene blootstelling aan LPS genormaliseerd. In **hoofdstuk 4** vergeleken we de effecten van een acute blootstelling aan LPS in het vruchtwater (twee dagen of zeven dagen) met chronische blootstelling aan UP in het vruchtwater (42 dagen) of gecombineerde blootstelling (twee dagen of zeven dagen LPS en 42 dagen UP) op het foetale enterisch zenuwstelsel (ENS). Er werd voor deze studie opzet gekozen omdat chorioamnionitis vaak polymicrobieel is. Vergelijkbaar met de ENS-veranderingen die

werden waargenomen na vier dagen blootstelling aan LPS in het vruchtwater (**hoofdstuk 3**), veroorzaakte chronische blootstelling aan UP een vermindering van mature neuronen (PGP9.5) in de myenterische plexus en, in mindere mate, in de submucosale plexus. Ook werden de immunoreactiviteit van enterische gliacellen (S100 β) verlaagd in de myenterische plexus door chronische UP-blootstelling, terwijl acute (zeven dagen) LPS-blootstelling reactieve enterische gliosis veroorzaakte (verhoogde GFAP-immunoreactiviteit). Zowel acute LPS-blootstelling als chronische UP-blootstelling veroorzaakten zowel darmbeschadiging als mucosale en submucosale ontsteking, hoewel het patroon van darmontsteking verschilde tussen de groepen. In **hoofdstuk 5** hebben we postnatale veranderingen in het ENS longitudinaal bestudeerd in een muizen NEC-model. In tegenstelling tot onze bevindingen in utero, werd in deze studie een toename van mature neuronen (NeuN) waargenomen in zowel de submucosale als de myenterische plexus na 72 uur blootstelling aan het experimentele NEC-protocol, die gelijktijdig optrad met en voorafgegaan werd door een verhoogd aantal enterische gliacellen (S100 β). Daarnaast werden functionele veranderingen in het ENS bestudeerd; terwijl 24 uur blootstelling aan het NEC-protocol de darmpassage verhoogde, nam de passage af na 48 uur blootstelling aan het NEC-protocol.

Een gemeenschappelijke bevinding van de drie studies in **hoofdstuk 3, 4 en 5** is het feit dat de veranderingen van enterische gliacellen parallel liepen met die van mature enterische neuronen. Enterische gliacellen bieden niet alleen structurele ondersteuning aan enterische neuronen, maar zijn ook betrokken bij neuroprotectie en neuronaal onderhoud via mechanismen zoals afgifte van glutathion en afgifte van neurotrofe factoren. Naast hun goed gedocumenteerde beschermende rol, kunnen enterische gliacellen lokale ontstekingen versterken en neuronaal verlies veroorzaken. Of de enterische gliacellen een beschermende of nadelige rol spelen in de studies die in dit proefschrift zijn opgenomen en in de humane setting moet nog worden opgehelderd.

Belangrijk is dat zowel de acute als langetermijn functionele gevolgen van perinatale veranderingen van het enterisch zenuwstelsel op dit moment onbekend zijn. Aangezien een heel breed scala aan neuronale subtypes en neurotransmitters betrokken is bij de diverse functies van het enterisch zenuwstelsel, zijn functionele metingen zoals darmmotiliteitstesten onmisbaar om de functionele uitkomsten nauwkeurig te schatten. Deze zouden dan ook moeten worden opgenomen in toekomstige studies die ENS veranderingen bestuderen in de perinatale context. De langetermijngevolgen van perinatale veranderingen van het enterisch zenuwstelsel hangen niet alleen af van functionele veranderingen in het acute moment, maar ook van de mogelijkheden van het ENS om te herstellen van initiële schade. Het foetale en neonatale enterisch zenuwstelsel zijn nog in ontwikkeling en zijn daarmee potentieel plastischer dan dat in de volwassen setting. Er zijn dus aanvullende studies nodig om longitudinale en postnatale veranderingen van het enterisch zenuwstelsel na intra-uteriene ontsteking te beoordelen en om de invloed van microbiële trigger(s) en het moment van aanvang en duur van de ontsteking te bepalen.

Effecten van perinatale pro-inflammatoire hits op slijmbekercellen en de darmslijmbarrière

In **hoofdstuk 6** werden longitudinale veranderingen in slijmbekercellen in het terminale ileum bestudeerd in een schapen chorioamnionitismodel na blootstelling aan LPS in het vruchtwater. In deze studie hebben we een bifasische vermindering van het aantal slijmbekercellen waargenomen op 24 uur tot twee dagen en op 15 dagen na intra-uteriene LPS-blootstelling. De eerste reductie is zeer waarschijnlijk toe te schrijven aan slijmuitscheiding, terwijl de tweede reductie voorafgegaan werd door darmontsteking, verhoogde intestinale epitheliale endoplasmatisch reticulum (ER) stress (verhoogde BiP- en CHOP-immunoreactiviteit) in de crypten en apoptose in het lagere villusgebied, hetgeen impliceert dat deze afname het gevolg is van ER-stressgedreven apoptose van maturerende slijmbekercellen. In **hoofdstuk 7** hebben we de veranderingen in de slijmbarrière bestudeerd, inclusief slijmdikte als functionele maat, in het terminale ileum zeven dagen na intra-uteriene toediening van UP. Intra-uteriene blootstelling aan UP verhoogde de dikte van de slijmlaag, waarschijnlijk door mucushypersecretie. Deze veranderingen waren geassocieerd met verhoogde pro-apoptotische intestinale epitheliale ER-stress (verhoogd CHOP-positieve celltellingen) en secretore celorganelverstoringen, hetgeen aangeeft dat de veranderingen van de slijmbarrière plaatsvinden ten koste van de veerkracht van de slijmbekercellen. Dit concept wordt versterkt door de opmerkelijke overlap van onze gegevens met bevindingen van organelverstoring in het terminale ileum van zuigelingen met NEC.

Onze resultaten uit **hoofdstuk 6 en 7** laten zien dat slijmbekercellen in het terminale ileum intra-uterien reageren op microbiële triggers en al in staat zijn om de dikte van de slijmlaag in utero te vergroten. Hoewel dit op korte termijn gunstig kan zijn om te voorkomen dat microben het epitheel bereiken, suggereren onze bevindingen dat dit ten koste kan gaan van de veerkracht van slijmbekercellen en kan leiden tot verlies van slijmbekercellen. Bovendien geven onze bevindingen in **hoofdstukken 6 en 7** aan dat verhoogde intestinale epitheliale ER-stress, wat uiteindelijk kan leiden tot apoptose, waarschijnlijk een belangrijk mechanisme is dat bijdraagt aan grove verstoring van en verlies van slijmbekercellen in de in utero setting. Voor de netto barrièrefunctie is niet alleen de slijmdikte van belang, maar ook de slijmkwaliteit. Momenteel zijn de effecten van perinatale darmontsteking op de slijmkwaliteit onduidelijk; dit is een ander interessant onderwerp voor toekomstige studies en wordt momenteel meegenomen in lopend vervolgonderzoek.

Effecten van perinatale inflammatoire treffers op het foetale en neonatale darm

De collectieve bevindingen in **hoofdstukken 3-7** laten zien dat structurele veranderingen van het enterisch zenuwstelsel, verstoring en verlies van slijmbekercellen en mucusbarrièrerveranderingen al optreden in utero en in het vroege postnatale leven als reactie op pro-inflammatoire hits. Dit ondersteunt de hypothese dat schade aan het enterisch zenuwstelsel en slijmbekercellen bijdraagt aan NEC-pathofysiologie en deze bevindingen versterken het paradigma dat NEC-pathofysiologie al zijn oorsprong vindt in utero in ten minste een deel van de neonaten. Bovendien geeft dit aan dat vroege (d.w.z. in utero of vroeg-postnataal) preventieve behandelingen gericht op het verbeteren van de

uitkomst van het enterisch zenuwstelsel of slijmbekercellen mogelijk gunstig zijn voor NEC-preventie en een nuttige aanvulling kunnen zijn op, reeds uitgebreid bestudeerde, postnatale interventies.

Hoewel foetussen en pasgeborenen een grote ontwikkelingsplasticiteit hebben en na verloop van tijd waarschijnlijk zullen herstellen van initiële schade aan het ENS en slijmbekercellen, is er een onvermijdelijke periode van verhoogde kwetsbaarheid waarin initiële schade nog niet hersteld is. Gedurende deze tijdsperiode kunnen aanvullende pro-inflammatoire hits die een te vroeg geboren pasgeborene waarschijnlijk zal tegenkomen, zoals mechanische ventilatie en sepsis, en andere ingrijpende postnatale gebeurtenissen, zoals microbiële kolonisatie en introductie van enterale voeding, gemakkelijker de balans richting NEC-ontwikkeling doen doorslaan.

In utero voedingsinterventies als veelbelovende nieuwe preventiestrategie

Omdat de intestinale veranderingen die waarschijnlijk predisponeren voor postnatale NEC-ontwikkeling al plaatsvinden in utero na chorioamnionitis, zouden enterale voedingsinterventies idealiter zo vroeg mogelijk gestart moeten worden (d.w.z. in utero). Omdat de foetus tijdens de zwangerschap vruchtwater inslikt, hebben we in een proof-of-concept studie (**hoofdstuk 8**) onderzocht of (preventieve) verrijking van het vruchtwater met plantensterolen, door middel van toediening van plantensterolen in het vruchtwater, systemische ontsteking zou kunnen verminderen en de uitkomst van de darm zou kunnen verbeteren op dag zes na blootstelling aan UP in het vruchtwater. Er werd gekozen voor plantensterolen omdat deze eerder ontstekingsremmende effecten hebben laten zien in de darm en omdat deze voedingsstoffen de placenta passeren, waardoor verrijking van het vruchtwater via orale toediening aan de moeder mogelijk is. In de studie in **hoofdstuk 8** hebben we geobserveerd dat toediening van plantensterolen in het vruchtwater de plantensterolconcentraties in het vruchtwater verhoogde, zonder de foetale plasma-plantensterol- of cholesterolspiegels te veranderen. Dit suggereert dat de interventie veilig kan worden gebruikt. Bovendien ging deze therapie gepaard met vermindering van foetale systemische ontsteking, darmontsteking en slijmvliesbeschadiging. Daarmee hebben we laten zien dat in utero enterale voedingsinterventies de foetale gezondheid (van de darm) kunnen verbeteren. Bovendien hebben we plantensterolen geïdentificeerd als voedingsbestanddelen die klinisch relevant kunnen zijn voor de preventie of behandeling van FIRS.

Verrijking van het vruchtwater kan potentieel worden bereikt door aanpassing van het maternale dieet, aangezien veel voedingscomponenten de placenta passeren. Wel zijn preklinische veiligheidsonderzoeken noodzakelijk voordat naar klinische studies wordt overgegaan. Daarnaast zijn farmacokinetische studies nodig om te bepalen in welke dosis voedingscomponenten moeten worden toegediend om therapeutische concentraties in het vruchtwater te bereiken, rekening houdend met factoren zoals zwangerschapsduur en placentaire gezondheid. Inzicht in de dynamiek van darmontsteking en de gevolgen ervan na intra-uteriene ontsteking kan helpen bij het kiezen van het optimale moment van ingrijpen. Hoewel de bevindingen in **hoofdstukken 3, 4, 6 en 7** al zinvolle informatie opleveren, is aanvullend onderzoek nodig. Niet-invasieve markers voor het monitoren van

darmgezondheid kunnen helpen bij het bestuderen van het verloop van chorioamnionitis zonder gebruik te maken van grote hoeveelheden proefdieren en uitgebreide onderzoeksfondsen.

Menselijke darmorganoïden als in vitro screeningsmodel voor enterale voedingsinterventies

Om het screenen van de effecten van (combinaties van) voedingscomponenten op de darm in gezonde of zieke toestand te faciliteren, hebben we een nieuw humaan darmorganoïdenmodel ontwikkeld (**hoofdstuk 9**). In dit model hebben we hypoxie gebruikt als trigger voor darmontsteking, epitheliale apoptose en verlies van darmbarrière, aangezien hypoxie een belangrijke factor is die bijdraagt aan de pathofysiologie van verschillende darmziekten zoals NEC, inflammatoire darmziekten en ischemie-reperfusie schade van de darm. Om apicale toediening van voedingscomponenten mogelijk te maken, werden menselijke darmorganoïden in monolagen gekweekt. Bovendien werd het kweekmedium van de organoïden aangepast om crypt en villus structuren na te bootsen, waardoor het onderzoek naar het effect van voedingscomponenten langs de volledige crypte-villus-as mogelijk werd. Naast modelontwikkeling hebben we het effect van niet-gehydrolyseerd, matig gehydrolyseerd en uitgebreid gehydrolyseerd wei-eiwit getest als potentieel gunstige voedingsinterventies, zowel in het organoïdenmodel als bij vier relevante microbiële stammen en perifere immuuncellen. We vonden hierbij dat de hydrolysatiesstatus van de wei-eiwitmix belangrijk was voor de biologische functie. Matig gehydrolyseerde wei verbeterde de paracellulaire barrièrefunctie van de organoïden en verminderde gelijktijdig de mRNA-expressie van HIF1 α , terwijl niet-gehydrolyseerd wei-eiwit de CD4+-T-celproliferatie verminderde en op mRNA niveau de Th1-Th2-balans verschoof naar een Th1-fenotype. Gezamenlijk laten deze resultaten zien dat het nieuwe organoïdenmodel een snelle screening van (combinaties van) voedingscomponenten mogelijk maakt. Bovendien geven deze bevindingen aan dat wei-eiwitten biologisch relevante eigenschappen hebben om de darmgezondheid te bevorderen en dat de mate van hydrolysatie een factor is waarmee rekening gehouden moet worden gehouden tijdens de ontwikkeling van een voedingsinterventie.

Het huidige humane darmorganoïdenmodel biedt een goede basis voor screeningsdoeleinden met een medium- tot high-throughput. Toch kunnen een aantal aspecten van het model nog worden verbeterd. Zo zouden toekomstige experimenten met organoïden gekweekt uit neonatale of foetale darmweefsel de translationele waarde van onze huidige bevindingen naar de perinatale context kunnen vergroten. Belangrijk is hierbij dat de complexiteit van het in vitro-model goed in evenwicht moet zijn met de beheersbaarheid en kosten, om de toepassing ervan als screeningsmodel met medium- tot high-throughput te garanderen.

Conclusie

In dit proefschrift hebben we laten zien dat enterale voedingsinterventies veelbelovend zijn voor de preventie van NEC en dat nieuwe strategieën die zich richten op het gepostuleerde prenatale begin en de multifactoriële pathogenese ervan essentieel zijn voor het verbeteren van de ontwikkeling van dergelijke voedingsinterventies. We hebben aangetoond—in een schaapmodel—dat door chorioamnionitis geïnduceerde veranderingen van het ENS en grove slijmbekercelverstoreningen, waarvan wordt aangenomen dat ze predisponeren voor postnatale NEC-ontwikkeling, al in utero voorkomen. Deze veranderingen waren ingrijpender dan onderzoekers tot nu toe hebben aangetoond, en onderstrepen dat de effecten van intra-uteriene ontsteking op de foetale darm verder gaan dan alleen darmontsteking. Bovendien hebben we in een preklinische proof-of-concept-studie vastgesteld dat een intra-uteriene enterale voedingsinterventie met plantensterolen de foetale systemische- en darmuitkomst kan verbeteren. Dit geeft aan dat de schadelijke effecten van chorioamnionitis zo vroeg mogelijk (d.w.z. in utero) kunnen worden aangepakt. Ten slotte hebben we een humaan darmorganoïdenmodel ontwikkeld dat screening van (combinaties van) voedingscomponenten in zowel gezonde als in zieke toestand mogelijk maakt. Hoewel er meer onderzoek nodig is naar de synergetische effecten van voedingscomponenten, farmacodynamiek, farmacokinetiek en klinische veiligheid voordat nieuwe interventies in de klinische praktijk kunnen worden geïmplementeerd, zijn we ervan overtuigd dat de onderzoeken in dit proefschrift bijdragen aan een nieuw raamwerk voor de ontwikkeling van klinisch effectieve preventieve enterale voedingsinterventies voor NEC in de toekomst, door ons of door andere onderzoekers

Abbreviations

AA	arachidonic acid
AB-PAS	alcian blue-periodic acid–Schiff
ADMA	asymmetric dimethylarginine
AEC	3-amino-9-ethylcarbazole
AF	amniotic fluid
AMPs	antimicrobial peptides
ATCC	American type culture collection
AOS	acidic oligosaccharides
ARRIVE	Animal Research: Reporting of In Vivo Experiments
ATRA	all-trans retinoic acid
BA	bile acid
BCFA	branched chain fatty acids
BHI	brain heart infusion
BiP	binding immunoglobulin protein
BME	basement membrane extract
BrdU	bromodeoxyuridine
BSA	bovine serum albumin
CAT	catalase
CC3	cleaved caspase 3
CCL2	C-C motif chemokine ligand 2
CCR9	C-C motif chemokine receptor 9
CCU	color changing units
CD2	cluster of differentiation 2
CD3	cluster of differentiation 3
CD4	cluster of differentiation 4
CD8	cluster of differentiation 8
CD25	cluster of differentiation 25
CD28	cluster of differentiation 28
CD69	cluster of differentiation 69
CFSE	carboxyfluorescein diacetate succinyl ester
CHAT	choline acetyltransferase
CHOP	C/enhancer binding protein homologous protein
COX-2	cyclooxygenase 2
CGMP	caseinoglycomacropeptide
ChAT	choline acetyltransferase
CI	confidence interval
CXCL1	C-X-C motif chemokine 1
CXCL2	C-X-C motif chemokine 2
CXCL5	C-X-C motif chemokine 5
DA	discriminant analysis
DAB	3, 3'-diaminobenzidine
DF	discriminant function
DHA	docosahexaenoic acid

DM	differentiation medium
DPPI	dipeptidylpeptidase I
DPPIV	dipeptidylpeptidase IV
DSLNT	disialyllacto-N-tetraose
EGF	epidermal growth factor
EGR1	early growth response protein 1
EH	extensive hydrolysate
ELBW	extremely low birth weight
eNOS	endothelial nitric oxide synthase
ENS	enteric nervous system
EPA	eicosapentaenoic acid
EPO	erythropoietin
ER	endoplasmic reticulum
ESPGHAN	European Society for Pediatric Gastroenterology Hepatology and Nutrition
ET-1	endothelin-1
FBS	fetal bovine serum
FIRS	fetal inflammatory response syndrome
FITC	fluorescein isothiocyanate
2'-FL	2'-fucosyllactose
foxp3	forkhead box P3
GA	gestational age
GAPDH	glyceraldehyde 3-phosphate dehydrogenase
G-CSF	granulocyte colony-stimulating factor
GD3	ganglioside D3
GDNF	glial cell-line derived neurotrophic factor
GFAP	glial fibrillary acidic protein
GM	growth medium
GSH	glutathione
GSH-Px	glutathione peroxidase
GSSG	glutathione disulphide
HB-EGF	hemoglobin-binding EGF-like growth factor
H&E	hematoxylin and eosin
HIF1 α	hypoxia-inducible factor 1 α
HIO	human intestinal organoids
HMO	human milk oligosaccharides
HR	hazard ratio
IA	intra-amniotic
IAP	intestinal alkaline phosphatase
IBD	inflammatory bowel disease
IF	immunofluorescent
IFABP	intestinal fatty acid binding protein
IFN γ	interferon γ
IgA	immunoglobulin A
IGF1	insulin-like growth factor 1
IL1 α	interleukin 1 α

IL1 β	interleukin 1 β
IL1ra	interleukin 1 receptor antagonist
IL2	interleukin 2
IL4	interleukin 4
IL6	interleukin 6
IL8	interleukin 8
IL10	interleukin 10
IL12p70	interleukin 12 p 70
IL17	interleukin 17
IL18	interleukin 18
IL23	interleukin 23
I κ B α	nuclear factor kappa-light-chain-enhancer of activated B cells inhibitor α
I κ B β	nuclear factor kappa-light-chain-enhancer of activated B cells inhibitor β
iNOS	inducible nitric oxide synthase
IRAK1	interleukin 1 receptor-associated kinase 1
IRAK3	interleukin-1 receptor-associated kinase 3
IRE1 α	inositol-requiring protein 1 α
IRI	intestinal ischemia reperfusion injury
IQR	interquartile range
JAM	junctional adhesion molecules
LAT2	L-type amino acid transporter 2
LBW	low birth weight
LC-FOS	long chain fructo-oligosaccharides
LGR5	leucine-rich repeat-containing G-protein coupled receptor 5
LPS	lipopolysaccharides
LXR	liver-X-receptor
LYZ	lysozyme
MALDI-MSI	matrix-assisted laser desorption ionization mass spectrometry imaging
Math1	mouse atonal homolog 1
MD-2	myeloid differentiation factor 2
MDA	malonaldehyde
MFGM	milk fat globule membrane
MH	mild hydrolysate
MPL	milk polar lipids
MPO	myeloperoxidase
MRS	De Man, Rogosa and Sharpe agar
MS/MS	tandem mass spectrometry
Muc1	mucin 1
Muc2	mucin 2
Muc3	mucin 3
Muc5	mucin 5
NAC	N-acetylcysteine
NEC	necrotizing enterocolitis
NeuN	neuronal nuclear protein
NF κ β	nuclear factor kappa-light-chain-enhancer of activated B cells

NGS	normal goat serum
NiDAB	nickel-3, 3'-diaminobenzidine
NNT	number needed to treat
NOD	nucleotide-binding oligomerisation domain
NO	nitric oxide
NOS	nitric oxide synthase
nNOS	neuronal nitric oxide synthase
25-OHD	25-hydroxy vitamin D
8-OHdG	oxidized guanine
OLFM4	olfactomedin 4
OPN	osteopontin
OR	odds ratio
PAF	platelet-activating factor
PAF-AH	platelet-activating factor acetylhydrolase
PAFR	platelet-activating factor receptor
PBMC	peripheral blood mononuclear cell
PBS	phosphate buffered saline
PC	phosphatidyl choline
PCA	principle component analysis
PCNA	proliferating cell nuclear antigen
PDI	protein disulfide isomerase
PEPT1	peptide transporter 1
PGP9.5	protein gene product 9.5
PHD	prolyl-hydroxylase domain containing enzymes
PI	phosphatidylinositol
PLA2	phospholipase-A2-II
PPAR γ	peroxisome proliferator-activated receptor γ
PPIA	peptidylprolyl isomerase A
PRRs	pattern recognition receptors
PUFA	polyunsaturated fatty acids
qPCR	quantitative real-time polymerase chain reaction
RCT	randomized controlled trial
ROS	reactive oxygen species
RPS15	ribosomal protein S15
RR	relative risk
RT	room temperature
SCFA	short chain fatty acids
SC-GOS	short chain galacto-oligosaccharides
SD	standard deviation
SEM	scanning electron microscopy
SERT	serotonin transporter
SGLT1	sodium/glucose transporter 1
SIGIRR	single interleukin 1 receptor-related protein
SIRT1	sirtuin 1
SL	sialic acids

6'-SL	6'-sialyllactose
SM	sphingomyelin
Smad2	SMAD family member 2
SOD	superoxide dismutase
Sp1	specificity protein 1
SPDEF	SAM-pointed domain-containing ETS transcription factor
TCA	taurocholic acid
TCDA	taurodeoxycholic acid
TCDCa	taurochenodeoxycholic acid
TEM	transmission electron microscopy
TFF3	trefoil factor 3
TGF- β 2	transforming growth factor β
TIMP1	metallopeptidase inhibitor 1
TJ	tight junctions
TLR1	toll like receptor 1
TLR2	toll like receptor 2
TLR4	toll like receptor 4
TLR5	toll like receptor 5
TLR9	toll like receptor 9
TNF α	tumor necrosis factor α
TPH2	tryptophan hydroxylase 2
Treg	regulatory T cell
TUNEL	terminal deoxynucleotidyl transferase dUTP nick end labelling
UP	<i>Ureaplasma parvum</i>
UPR	unfolded protein response
VLBW	very low birth weight
WPI	whey protein isolate
XO	xanthine oxidase
YWHAZ	14-3-3 protein zeta/delta
ZO	zona occludens

Dankwoord

Met het einde van dit proefschrift komt een van de leukste onderdelen om te schrijven én een van de best gelezen hoofdstukken: het dankwoord. Zoals door zo velen voor mij gezegd, is een proefschrift altijd een teamprestatie; dit geldt zeker ook voor het mijne. Tijdens mijn promotietijd heb ik heel veel geleerd over onderzoek doen en het ontzettend goed naar mijn zin gehad. Daarnaast is mijn tijd als promovenda heel belangrijk geweest voor mijn persoonlijke ontwikkeling; ik heb veel over mijzelf geleerd en ben heel wat ervaringen rijker. Tijdens deze belangrijke periode in mijn leven heb ik van talloze mensen steun en praktische hulp ontvangen. Hoewel dit er te veel zijn om allemaal los te benoemen wil ik de belangrijkste mensen hier bedanken.

Allereerst mijn promotieteam:

Mijn promotor, **Dr. T.G.A.M. Wolfs**, beste Tim. Ik kan me nog levendig voor de geest halen hoe ik als tweedeaars student geneeskunde bij jou in het lab voor het eerst kennis mocht maken met het onderzoek, iets waar ik gelijk heel enthousiast van werd. Gedurende mijn verdere studie jaren hebben we contact gehouden en begin 2017 kwamen we samen met Wim tot het plan om een aanvraag in te dienen bij het *NUTRIM graduate programme* om mijn interesse in perinatale voedingsinterventies en darmgezondheid om te kunnen zetten in een promotietraject. Ik heb tijdens dit promotietraject veel van je geleerd over onderzoek doen, projectmanagement, wetenschappelijk schrijven en het 'verkopen van de auto'. Hoewel we in het begin regelmatig discussies hadden over of we nu naar een Fiat Panda keken of een Porsche Panamera, kwamen we uiteindelijk altijd op één lijn! Je was steunend tijdens de moeilijke periodes die er in deze vier jaar ook zijn geweest. Ik heb veel respect voor de manier waarop je het laboratorium kindergeneeskunde en onze onderzoeksgroep leidt en verbaas me er nog altijd over dat je in momenten van opperste concentratie snel de essentie van data weet te vatten. Ik kijk enorm uit naar onze samenwerking in de toekomst en al het moois dat deze hopelijk voort gaat brengen!

Mijn promotor, **Prof. dr. W.G. van Gemert**, beste Wim. Samen met Tim ben jij heel belangrijk geweest voor het mogelijk maken van mijn promotieonderzoek en daar ben ik je heel dankbaar voor! Je nam altijd uitgebreid de tijd voor onze meetings en had dan altijd veel enthousiaste verhalen, zowel over het onderzoek als over honderden één andere dingen waar jij je mee bezig houdt, zoals het opzetten van het Euregionaal Kinderchirurgisch Centrum. Je onderhield het contact met je klinische collega's van de kinderchirurgie en was van groot belang voor het verzamelen van de darmsamples van (NEC)patiënten die voor dit proefschrift essentieel waren. Heel veel dank!

Mijn copromotor, **Dr. J.P.M. Derikx**, beste Joep. Jij stroomde later in in mijn promotieteam toen ik voor mijn organoïdeproject op zoek was naar een 2D-model om apicale toediening van de voedingscomponenten mogelijk te maken. Je was direct enthousiast en hebt mij samen met Bruno met open armen ontvangen in Amsterdam. Met jullie hulp hadden we het monolayer model in enkele maanden lopend in Maastricht, iets wat van grote waarde is geweest voor mijn onderzoek! Je hebt daarnaast regelmatig scherp commentaar gegeven op mijn stukken en daarmee mijn proefschrift naar een hoger niveau getild. Ik hoop dat we in de toekomst nog vaak samen kunnen werken!

Daarnaast ben ik veel dank verschuldigd aan de leden van de beoordelingscommissie, **prof. dr. Gertjan Driessen, prof. dr. Daisy Jonkers, prof. dr. Torsen Plösch, prof. dr. Annemie Schols** en **prof. dr. Dick Tibboel**, die de tijd en moeite hebben genomen mijn proefschrift kritisch te beoordelen.

Speciale dank aan **prof. dr. Daisy Jonkers**, vanwege haar bijdrage aan het opzetten van het organoïdemodel met de tweewekelijkse organoïdmeetings die we in het begin van mijn promotieonderzoek hadden. Veel van de problemen waar we toen tegenaan liepen hebben we weten op te lossen. **Dr. Hendrik Niemarkt** en **dr. Veerle Melotte**, bedankt dat jullie plaats willen nemen in de corona.

Ik wil de leden van de NUTRIM Graduate Programme committee **prof. dr. Annemie Schols, dr. Roger Godschalk, dr. Harry Gosker, dr. Gijs Goossens** en **prof. dr. Daisy Jonkers** van harte bedanken omdat ze me de mogelijkheid gegeven hebben een promotietraject te doorlopen op een onderwerp dat ik écht interessant vind. Ik hoop nog vele jaren aan NUTRIM verbonden te blijven.

De verschillende co-auteurs waar ik mee samen gewerkt heb, wil ik bedanken voor hun hulp en de kritische feedback waarmee ze onze artikelen beter hebben gemaakt. Een aantal van hen wil ik specifiek benoemen. **Laurens Eeftinck Schattenkerk**, bedankt voor je hulp bij de review, in het bijzonder bij de kwaliteitsbeoordeling van een (groot!) aantal studies. **Dr. Werend Boesmans** en **dr. Veerle Melotte**, bedankt voor jullie hulp bij het ENS-werk, jullie brede en gedetailleerde kennis van het ENS heeft de verschillende artikelen naar een hoger niveau getild. **Dr. Isabelle De Plaen**, thank you for your work and constructive feedback on the mouse ENS paper! **Dr. Anne Bjørnshave** and **dr. Marie Stampe Ostenfeld**, thank you for the nice collaboration and your valuable input on the organoïd and whey protein paper. I look forward to our collaborations in the future! **Dr. Jan Damoiseaux**, bedankt voor je hulp en waardevolle feedback bij de FACS-experimenten en de organoïd paper. **Prof. dr. Jogchum Plat**, bedankt voor je waardevolle inbreng bij de plantsterolstudie!

Mijn paranimfen:

Charlotte, Charly, mijn 'partner in crime' bij Team Darm. Toen Tim ons voor het eerst aan elkaar voorstelde, schatte hij in dat wij wel een goed team zouden zijn, en wat heeft hij gelijk gehad! We vullen elkaar perfect aan. Ik ben je eigenlijk een eigen dankhoofdstuk verschuldigd, maar om wat papier te besparen heb ik het toch wat korter gehouden. We hebben tijdens onze beider promotietrajecten intensief samengewerkt, menig artikel samen geschreven en ook buiten het werk om veel plezier gehad met onder andere squashen, labuitjes en wandelen met Dorus. Waar ik meestal rustig ben kan men jou (met of zonder luchtalarm) van verre horen aankomen. Je bent een echte sfeermaker op het lab, staat altijd voor anderen klaar en was van grote steun voor mij door mijn projecten op te vangen toen ik tijdelijk niet kon werken. Ik bewonder je vermogen om creatief te denken, patronen in data te zien, de leiding te nemen en overzicht te houden over je projecten ondanks de chaos om je heen. Wat mij betreft op naar nog vele projecten samen!

Cathelijne, mijn dierbare collega en medepromovenda bij de kinderchirurgie. Ook met jou heb ik met heel veel plezier intensief samengewerkt. We hebben samen de projecten

rondom het ENS gedaan en daar een paar mooie hoofdstukken van gemaakt. Vliegenvlug organiseerde je een legertje studenten om te helpen met de histologische analyses en je behield hierbij een perfect overzicht over wat er al gedaan was en wat er nog te doen stond. Je bent een grote sfeermaker, met jou sprankelende lach (en gekakel) krijg je iedereen aan het lachen! We hebben enorm genoten van de labuitjes samen (één van de voordelen van het werken op twee afdelingen) en van diverse andere leuke activiteiten zoals de sinterklaasviering bij de heelkunde waar jij Sinterklaas was. Ik wens je heel veel succes met je opleiding tot anesthesioloog, we gaan elkaar vast nog tegenkomen in de kliniek!

De labetechnicians van de kindergeneeskunde: **Kimberly, Lilian, Nico, Daan en Teun.**

Kimberly, je bent en was een onmisbaar onderdeel van Team Darm. Je bent begonnen als student bij Charlotte en binnen hele korte tijd uitgegroeid tot een ervaren labtechnician. Je hebt me ontzettend geholpen met het darmwerk voor de schaapstudies, met de orgnoidkweken en nog veel meer. Je bent met recht de QuPath (en Qwin) Queen van de kindergeneeskunde. Jouw handigheid met deze software voor histologische analyses heeft ons heel veel tijdsinstaat en veel nauwkeurigere data opgeleverd. Dankjewel voor al je hulp!

Lilian, ook jij bent van onschatbare waarde geweest voor mijn promotietraject. Je hebt heel veel werk verricht, onder andere met het optimaliseren van immunohistochemische kleuringen, bij het meten van de mucus dikte, bij het prepareren van darmsamples voor organoidkweek en voor het organoidkweken zelf. Ik heb nog steeds heel veel bewondering voor jouw handigheid bij microscopisch werk en je hands-on mentaliteit. Bij de uitspraak 'Ik heb het nog nooit gedaan, dus ik denk dat ik het wel kan', moet ik altijd aan jou denken. Dankjewel!

Nico, ook jij was voor mij onmisbaar! Ik kon bij jou altijd terecht voor technische vragen over analysetechnieken, celkweken en labproducten. Je hebt mij begeleid toen ik zelf nog als student op het lab rondrende. Je hebt veel werk verricht voor met name het RNA/qPCR-werk dat een aanzienlijk deel van dit proefschrift beslaat en voor mijn celkweekexperimenten. Daarnaast heb je me uitstekend geholpen bij het begeleiden van een groot aantal studenten. Bedankt!

Daan V, hoewel je niet zo direct bij mijn projecten betrokken bent geweest, heb je veel van het schapenwerk op de LICU op je genomen waardoor ik de tijd en ruimte had om mijn proefschrift af te schrijven. Je bent een waardevolle aanvulling op het technicianteam. Dankjewel!

Teun, lieve Teun, we liepen tegelijkertijd stage op het lab kindergeneeskunde en zijn ongeveer tegelijk aan onze eerste baan begonnen. Ik kan me jou bulderende lach, blijdschap als er iets gelukt was en verontwaardigd 'hallo' nog levendig voor de geest halen. Je wordt nog steeds gemist!

Labtechnicians van de algemene heelkunde, in het bijzonder **Mo, Bas en Annemarie**. Hoewel ik vaker op het lab kindergeneeskunde dan op het lab heelkunde te vinden was, stonden jullie bij vragen altijd voor mij klaar. Jullie hebben mij geregeld geholpen met diverse praktische vragen en de ELISA's. Dankjulliewel!

Montserrat, lab technician from the gastroenterology department, thank you for helping me out with practical issues regarding the organoid cultures! **Pan**, thanks for your contribution to our organoid meetings!

Erwin, labtechnicus van de klinische immunologie, dankjewel voor alle hulp bij het opzetten en uitvoeren van de FACS-experimenten! Ik heb veel van je geleerd.

De kinderchirurgen uit het MUMC+, in het bijzonder **Ruben Visschers**, **Olivier Theeuws** en **Hamit Cakir**, dankjulliewel voor jullie hulp bij het verzamelen van darmsamples van neonaten! Heel fijn dat jullie mij (zelfs in de nacht!) gebeld hebben als er een operatie was met de mogelijkheid tot weefselverzameling. De NEC en humane controle samples zijn een essentieel onderdeel van dit proefschrift. **Mirjam Habex-Froidmont**, bedankt voor je praktische ondersteuning tijdens mijn promotieonderzoek!

Mijn andere collega's bij de kindergeneeskunde **Helene**, **Luise**, **Rob**, **Valéry**, **Lieke**, **Hyun Young/Hailey**, **Daan O**, **Matthias** en **Reint** en de collega's die net na mij gestart zijn met hun promotieonderzoek **Sophie** en **Tim**.

Helene, toen ik startte met mijn promotieonderzoek was jij één van mijn kamergenoten én de enige die ook een net bureau had en van opruimen houdt. Ik heb bewondering voor je organisatietalent, je doorzettingsvermogen en je groene vingers; waar mijn planten systematisch het loodje legden, had jij altijd een prachtige collectie vitale planten. Sorry voor de cactusstekels in je vinger toen je zo lief was te kijken of mijn planten voldoende water hadden gehad! Bedankt voor al je hulp en gezelligheid en heel veel succes met het afronden van jouw promotie!

Luise, ook voor lange tijd mijn kamergenote. Jij hebt mij fantastisch geholpen bij het opzetten van de FACS-experimenten, zowel bij het opzetten van de panels als bij het meten van de eerste run. Daarnaast heb je gezorgd voor een hoop gezelligheid, zo hebben we uitgebreid gelachen over het woord 'Eierschalensollbruchstellenverursacher'. Helaas kon ik mijn slappe thee nooit aan je slijten. Heel veel succes met jouw verdediging!

Rob, jij zorgde met je aprèsskimuziek en het organiseren van de nodige borrels voor een hoop gezelligheid. Helaas heb ik de skitrip naar Winterberg moeten missen; een volgende keer ga ik graag mee! Ik vind het knap hoe je, ondanks de nodige tegenslagen, je onderzoek combineert met je opleiding tot kinderarts én met je MRI-studies super innovatief onderzoek weet op te zetten. Heel veel succes!

Valéry, mijn kamergenote tijdens het laatste deel van mijn promotieonderzoek. Je wist Helene te vervangen als hoofd plant lady en hebt verscheidene dappere pogingen gedaan mijn planten te redden. Het was leuk om samen te sparren over de LICU en om te zien hoe je in korte tijd veel ervaring hebt opgedaan als PhD student. Ik wens je veel succes bij de rest van je onderzoek! Als je niet naar Groningen gaat, gaan we elkaar ook vast nog in het ziekenhuis zien.

Lieke, hoewel je niet zo vaak op het lab kan zijn, ben je echt een onderdeel van het lab kindergeneeskunde. Je hebt een aanstekelijk enthousiasme voor het onderzoek en de nieren. Ik heb goede herinneringen aan de wijnproeverij bij jou thuis. Heel veel succes met het afronden van je studies!

Hyun Young, Hailey, we were also roommates during the final stages of my PhD. I think it is very brave of you to switch to research with lab work; it's good to see that you get more and more comfortable with the topic. I enjoyed the moments of tea and snacks together (though I'm happy that I did not try the spicy noodles). Good luck with your future research! **Daan O**, bedankt voor alles wat je me geleerd hebt tijdens de schaapexperimenten en al het andere dat ik in de afgelopen jaren van je heb geleerd! We gaan elkaar vast de komende jaren nog tegenkomen.

Matthias en Reint, ook bedank voor jullie hulp! Ik heb er bewondering voor hoe jullie het drukke bestaan als neonatoloog kunnen combineren met een lopende carrière als wetenschapper. Matthias, bedankt voor je nuttige feedback op een groot aantal artikelen en alles wat je me op de LICU geleerd hebt!

Sophie en Tim, ik wens jullie heel veel succes met jullie promotieonderzoek! Het is leuk om te zien hoe jullie snel jullie draai in de groep en op de LICU hebben gevonden.

Mijn andere collega's bij de heelkunde, ik ga jullie niet allemaal bij naam noemen omdat ik over de jaren heen met heel veel van jullie heb samengewerkt, maar jullie hebben allemaal bijgedragen aan mijn werkplezier de afgelopen jaren! Ik herinner me vele labmeetings, labuitjes, Sinterklaasvieringen, het ambtenarencarnaval en verschillende borrels. Ik wil **Kaatje, Mirjam en Annet** graag nog specifiek bedanken. Jullie hebben me over de jaren enorm geholpen met het opzetten van het organoidmodel bij de kindergeneeskunde en met diverse praktische problemen waar ik tegen aan liep. Bedankt daarvoor!

Bruno, thank you for the warm welcome I got in Amsterdam and the help you gave me with the organoid monolayer experiments. I hope we can collaborate more in the future.

Tiny, bedankt voor je fantastische werk bij de opmaak van dit boekje!

De studenten die mij in de loop der jaren geholpen hebben: **Rui, Daniëlle, Tom, Elianne, Iris, Maurits, Moelong, Niky, Sophie en Tamara**. Jullie hebben een aanzienlijk deel van de voorbereidende experimenten en het praktische werk op het lab uitgevoerd en mij veel geleerd. Dankjulliewel!

Mijn huidige collega's in het Catharina Ziekenhuis Eindhoven, kinderartsen, arts-assistenten en verpleging. Bedankt voor het warme welkom dat ik in jullie groep heb gekregen. Jullie hebben ervoor gezorgd dat mijn terugkeer in het ziekenhuis na vier jaar onderzoek behoorlijk soepel is verlopen. Mede dankzij de goede sfeer die jullie weten te creëren, ga ik elke dag met veel plezier naar mijn werk!

Mijn middelbareschoolvriendinnen **Tessa, Iris, Irize, Anke, Laura en Sanne**. We kennen elkaar inmiddels al langer wél dan niet en we hebben al heel wat samen meegemaakt. Ik vind het bijzonder dat we nog steeds zo goed contact hebben. Ik kijk altijd uit naar onze uitjes en bankhangmiddagen samen. Bedankt voor alles! Mijn studievriendinnen **Marlou, Lisanne en Ayla**. Ik vind het leuk om te zien hoe we de afgelopen jaren allemaal onze eigen

weg zijn gegaan en toch nog altijd veel raakvlakken hebben. Hoewel het met de drukke agenda's niet zo vaak lukt om elkaar te zien, is het altijd weer gezellig! **Noortje** en **Mark**, bedankt voor alle gezelligheid bij onze gezamenlijke spelletjesmiddagen, hopelijk kunnen we deze nog lang voortzetten!

Thomas, Jan en **Heleen**, als onderdeel van de 'Buurheid' wil ik jullie ook van harte bedanken voor de gezelligheid, steun en interesse over de jaren heen.

Heel veel dank ben ik ook verschuldigd aan mijn (schoon)familie.

Lieve **Tim** en **Margret**. Vanaf het begin af aan heb ik me bij jullie altijd ontzettend welkom gevoeld en jullie betrokkenheid heeft me de afgelopen jaren enorm gesteund. Bedankt voor alle warmte en gezelligheid!

'**Opa**' **Jacques** en '**oma**' **Mies**. Ook jullie interesse, zowel in mijn werk als mijn algehele welzijn, heeft mij altijd gesteund. Ik mis de wekelijkse bezoeken op donderdag, hopelijk lukt het snel weer deze te hervatten. Jacques, hoewel je mijn verdediging helaas niet meer bij kunt wonen, weet ik zeker dat je beretrots op mij zou zijn geweest, zoals je op je hele familie altijd beretrots was. **Granny**, bedankt voor je betrokkenheid en belangstelling! **Ferry** en **Meryl**, ook jullie bedankt voor jullie interesse en steun. Als mijn promotie achter de rug is moeten we eens wat vaker afspreken! De rest van de schoonfamilie, **Peter** en **Veerle**, **Peter** en **Lea** en **tantoma Henny**, bedankt! Speciale dank voor **Peter** voor het ontwerpen van de prachtige kaft van dit boekje!

Lieve **opa Guus** en **oma Ilse**, bedankt voor de steun die ik de afgelopen jaren gekregen heb! De vele lieve kaartjes geschreven door oma (met heel veel uitroeptekens) waren voor mij een grote aanmoediging. Ik vind het heel feestelijk dat jullie mijn verdediging kunnen bijwonen en hoop dat jullie nog heel lang in mijn leven zullen zijn. Lieve **oma Hilligje**, wat bijzonder dat je mijn verdediging op deze hoge leeftijd nog mee kunt maken, we gaan samen de beelden zeker terugkijken. Je bent een ijzersterke vrouw. Bedankt voor alle steun en interesse!

Mijn tantes **Marjolein**, **Roos**, **Mariska** en **Godelief** en oom **Michiel**, bedankt voor jullie warme belangstelling.

Lieve **Pepijn** en **Emmie**. Pepijn, als broertje ben je me zeer dierbaar. Ik vind het fijn dat we de afgelopen jaren verder naar elkaar toe gegroeid zijn en ik verheug me altijd zeer op de momenten dat we samen zijn. Ik bewonder je taalgevoeligheid en ben altijd enorm trots als ik je stukken in de krant lees. Emmie, ik had me geen leukere schoonzus kunnen wensen! Ik verheug me er op om jullie beide vaker te zien wanneer jullie weer in Eindhoven wonen. Bedankt voor jullie steun!

Lieve **papa** en **mama**, naarmate ik ouder word realiseer ik me steeds meer hoe belangrijk jullie zijn geweest voor mijn ontwikkeling. Jullie hebben mij gevormd tot wie ik nu ben en hebben daarmee een niet te onderschatten bijdrage geleverd aan dit proefschrift en al het

andere wat ik tot nu toe heb bereikt. Jullie hebben me doorzettingsvermogen gegeven door te zeggen 'moeilijk gaat ook', jullie hebben mij liefde voor kunst en taal bijgebracht en hebben mij altijd gestimuleerd het beste uit mijzelf te halen. **Papa**, jij hebt me geleerd om met zelfvertrouwen de wereld tegemoet te treden en logisch te redeneren en staat nog altijd voor me klaar als ik tegen problemen aanloop. **Mama**, jij was als wetenschapper een voorbeeld voor me en hebt me met een warme kindertijd een solide basis gegeven voor de rest van mijn leven. Ik mis je ontzettend en had graag nog heel veel meer tijd met je doorgebracht. Ik hou van je.

Allerliefste **Yuri**, al ruim dertien jaar mijn geliefde en sinds drieëneenhalf jaar mijn man. Jij bent echt mijn betere helft. Je bent van onschatbare waarde voor mij geweest de afgelopen jaren. Je hebt me ondersteund en uitgedaagd en maakt me nog altijd aan het lachen. Je hebt waar nodig je best gedaan mij af te remmen en je hebt als taalpurist vrijwel al mijn manuscripten nagekeken. Dankjewel voor alle warmte en liefde die je me al jaren geeft. Ik kijk enorm uit naar de toekomst samen!

List of publications

1. **De Lange IH**, van Gorp C, Eeftinck Schattenkerk LD, van Gemert WG, Derikx JPM, Wolfs TGAM. Enteral Feeding Interventions in the Prevention of Necrotizing Enterocolitis: A Systematic Review of Experimental and Clinical Studies. *Nutrients*. 2021 May 19;13(5):1726.
2. Heymans C, den Dulk M, Lenaerts K, Heij LR, **de Lange IH**, Hadfoune M, van Heugten C, Kramer BW, Jobe AH, Saito M, Kemp MW, Wolfs TGAM, van Gemert WG. Chorioamnionitis induces hepatic inflammation and time-dependent changes of the enterohepatic circulation in the ovine fetus. *Sci Rep*. 2021 May 14;11(1):10331.
3. Van Gorp C, **de Lange IH**, Massy KRI, Kessels L, Jobe AH, Cleutjens JPM, Kemp MW, Saito M, Usada H, Newnham J, Hütten M, Kramer BW, Zimmermann LJ, Wolfs TGAM. Intestinal Goblet Cell Loss during Chorioamnionitis in Fetal Lambs: Mechanistic Insights and Postnatal Implications. *Int J Mol Sci*. 2021 Feb 16;22(4):1946.
4. Heymans C*, **de Lange IH***, Lenaerts K, Kessels LCGA, Hadfoune M, Rademakers G, Melotte V, Boesmans W, Kramer BW, Jobe AH, Saito M, Kemp MW, van Gemert WG, Wolfs TGAM. Chorioamnionitis induces enteric nervous system injury: effects of timing and inflammation in the ovine fetus. *Mol Med*. 2020 Sep 3;26(1):82.
5. Heymans C, **de Lange IH**, Hütten MC, Lenaerts K, de Ruijter NJE, Kessels LCGA, Rademakers G, Melotte V, Boesmans W, Saito M, Usuda H, Stock SJ, Spiller OB, Beeton ML, Payne MS, Kramer BW, Newnham JP, Jobe AH, Kemp MW, van Gemert WG, Wolfs TGAM. Chronic Intra-Uterine *Ureaplasma parvum* Infection Induces Injury of the Enteric Nervous System in Ovine Fetuses. *Front Immunol*. 2020 Mar 17;11:189.
6. Van Gorp C*, **de Lange IH***, Spiller OB, Dewez F, Cillero Pastor B, Heeren RMA, Kessels L, Kloosterboer N, van Gemert WG, Beeton ML, Stock SJ, Jobe AH, Payne MS, Kemp MW, Zimmermann LJ, Kramer BW, Plat J, Wolfs TGAM. Protection of the Ovine Fetal Gut against *Ureaplasma*-Induced Chorioamnionitis: A Potential Role for Plant Sterols. *Nutrients*. 2019 Apr 27;11(5):968.
7. **De Lange IH**, Van Oploo Roos FG, Bok LA. Parry Romberg syndrome presenting with a giant intracranial aneurysm: a case report. *Oxf Med Case Reports*. 2017 May 30;2017(5):omx017.

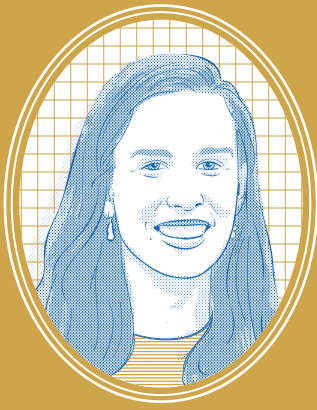
* authors contributed equally

Curriculum vitae English

Ilse de Lange was born on the 28th of July 1993 in Eindhoven, the Netherlands. She graduated from high school, Pleincollege Bisschop Bekkers in Eindhoven, with a gymnasium degree in 2011. Thereafter, she moved to Maastricht to start her bachelor study Medicine, which she finished in 2014 (cum laude). During her bachelor, Ilse was introduced to research, the pediatrics laboratory and dr. Tim Wolfs when she followed the Honours Programme Research. During her master Medicine at Maastricht University, she returned to the pediatrics laboratory for her scientific internship. During this internship she studied plant sterol signaling in the context of perinatal infections and inflammation, after which her thesis was awarded with the SWUM student award for the best master thesis of the Faculty of Health, Medicine and Life Sciences of Maastricht University. Enthused about research in general and intrigued about the possibilities of enteral feeding interventions for the prevention of adverse intestinal outcomes including necrotizing enterocolitis, Ilse successfully applied for the NUTRIM Graduate Programme that enabled her to design her own PhD project. After finishing her master in 2017 (cum laude), she subsequently started her PhD trajectory under the supervision of dr. Tim Wolfs, prof dr. Wim van Gemert and dr. Joep Derikx at the department of Pediatrics and the department of Surgery of Maastricht University Medical Center+ and in collaboration with the department of Pediatric Surgery at the Amsterdam University Medical Center and the Tytgat Institute for Liver and Intestinal Research. During her PhD trajectory, Ilse gave multiple oral and poster presentations at research meetings and was awarded with the Dutch Chiesi Fellow Award 2018 for the most innovative research in the field of neonatology, and the 1st prize for Improvement of Therapy at the Science Day of Maastricht University Medical Center. The results of her doctoral research are described in this thesis. In September 2021 Ilse was awarded with a ESPR Young Investigator Start-Up Grant, that supports a project in which the potential of exhaled VOC as biomarker for intra-amniotic infections (chorioamnionitis) will be investigated. From October 2021 onwards, she works as resident (not in training) Pediatrics at the Catharina Hospital in Eindhoven. In addition, she will continue her research as postdoctoral researcher at the department of Pediatrics of Maastricht University Medical Center + under supervision of dr. Tim Wolfs. Ilse lives in Maastricht with her husband Yuri Foreman.

Curriculum vitae Nederlands

Ilse de Lange werd geboren op 28 juli 1993 in Eindhoven, Nederland. Ze studeerde in 2011 af aan het Pleincollege Bisschop Bekkers in Eindhoven met een gymnasium diploma. Daarna verhuisde ze naar Maastricht om haar bachelor studie Geneeskunde te beginnen, die ze in 2014 cum laude afrondde. Tijdens haar bachelor kwam Ilse voor het eerst in aanraking met onderzoek, de onderzoeksgroep kindergeneeskunde en dr. Tim Wolfs toen ze het Honours Programme Research volgde. Tijdens haar master Geneeskunde aan de Universiteit Maastricht keerde Ilse terug naar het laboratorium Kindergeneeskunde voor haar wetenschappelijke stage. Tijdens deze stage heeft zij de signalering van plant sterolen bestudeerd in het kader van perinatale stress, waarna haar scriptie werd bekroond met de SWUM-studentenprijs voor de beste masterscriptie van de Faculty of Health, Medicine and Life Sciences van de Universiteit Maastricht. Enthousiast over onderzoek in het algemeen en geïntrigeerd door de mogelijkheden van enterale voedingsinterventies voor de preventie van necrotiserende enterocolitis, heeft Ilse zich met succes aangemeld voor het NUTRIM Graduate Program waarmee ze haar eigen PhD-project kon opzetten. Na het afronden van haar master in 2017 (cum laude), begon ze vervolgens aan haar promotietraject onder begeleiding van dr. Tim Wolfs, prof.dr. Wim van Gemert en dr. Joep Derikx op de afdeling Kindergeneeskunde en de afdeling Algemene Heelkunde van het Maastricht Universitair Medisch Centrum+ en in samenwerking met de afdeling Kinderchirurgie van het Amsterdam Universitair Medisch Centrum en het Tytgat Instituut voor Lever- en Darmonderzoek. Tijdens haar promotietraject heeft Ilse meerdere mondelinge en posterpresentaties gegeven op onderzoeksbijeenkomsten en werd zij bekroond met de Nederlandse Chiesi Fellow Award 2018 voor het meest innovatieve onderzoek op het gebied van neonatologie en de 1e prijs voor Verbetering van Therapie op de Wetenschapsdag van Maastricht Universitair Medisch Centrum. De resultaten van haar promotieonderzoek zijn in dit proefschrift beschreven. In September 2021 kreeg Ilse een ESPR Young Investigator Start-Up Grant, waarmee zij onderzoek zal doen naar het potentieel van VOC in uitademingslucht als biomarker voor intra-uterine infecties (chorioamnionitis). Vanaf oktober 2021 werkt zij als anios Kindergeneeskunde in het Catharina Ziekenhuis in Eindhoven. Daarnaast zal zij haar onderzoek voortzetten als postdoctoraal onderzoeker bij de afdeling Kindergeneeskunde van het Maastricht Universitair Medisch Centrum + onder begeleiding van dr. Tim Wolfs. Ilse woont in Maastricht met haar man Yuri Foreman.



Enteral feeding interventions for optimal fetal and neonatal health

Preterm birth, defined as birth before 37 weeks of gestation, is a major worldwide health concern. It is often caused by inflammation of the fetal membranes, i.e., chorioamnionitis, which can lead to a systemic inflammatory reaction in the fetus. Both are important independent risk factors for adverse postnatal outcomes, including the neonatal gastrointestinal emergency necrotizing enterocolitis (NEC). Breastmilk feeding is known to reduce NEC risk. This is mainly due to breast milk's many bioactive components that can modulate mechanisms involved in NEC pathogenesis, such as intestinal barrier function and gut inflammation. However, to date, preventive enteral feeding interventions have seldom been proven clinically effective. The present thesis contributes to a novel framework for improving such preventive nutritional interventions through the acknowledgement of the multifactorial pathophysiology of NEC and its postulated prenatal onset.

Ilse H. de Lange

